



St. Johns River Water Management District

Ann B. Shortelle, Ph.D., Executive Director

4049 Reid Street • P.O. Box 1429 • Palatka, FL 32178-1429 • 386-329-4500
On the internet at www.sjrwm.com.

DATE: May 15, 2020
TO: Interested Firms
FROM: Carol Miller, Senior Procurement Specialist
SUBJECT: Addendum 1 - Request for Information 35601, Lake Jesup: In-Lake Phosphorus Reduction Advanced Technology Review

This addendum provides prospective respondents a copy of the reports cited in the above referenced Request of Information.

The response due date and time remains the same (5:00 p.m., June 12, 2020).

NOTE: Please acknowledge receipt of this Addendum in your submittal.

If you have any questions regarding this addendum, contact Wendy Cox via email at wcox@sjrwm.com or at (386) 329-4118.

**Assessment of the Cycling and Compartmentalization of Nitrogen and Phosphorus
in Saturated Soils, Sediments and the Water Column in Lake Jesup, Florida**

Final Report

Contract # 25044

To:

St. Johns River Water Management District
4049 Reid St.
Palatka, FL 32177

Submitted by:

William Anderson^{1,2,‡}, Leonard Scinto^{1,2}, Shauna Nielsen^{1,2}, Serge Thomas⁴,
David Fugate⁴ and Reide Corbett⁵

¹Southeast Environmental Research Center, FIU, Miami, FL 33133

²Department of Earth and Environment, FIU, Miami, FL 33133

⁴Department of Marine Ecological Sciences, FGCU, Naples, FL 33965

Department of Geological Sciences, ECU, Greenville, NC 27858

[‡] (305)-348-2693 (ph), (305)-348-3877 (fax) andersow@fiu.edu

Administrative Contact:

Robert Gutierrez, Director
Office of Sponsored Research Administration
Florida International University, Miami, FL 33199
305-348-2494 (ph); 305-348-4117 (fax)

Date Submitted:

December 30, 2011

TABLE OF CONTENTS

	page
PROJECT SUMMARY	5
1.0 INTRODUCTION	6
2.0 GEOLIMNOLOGICAL SYSTEMS	10
2.1 Sediment Resuspension	11
3.0 SETTING	14
3.1 Regional Setting	17
3.2 Historical Changes	17
3.3 Geological Setting	23
3.4 Limnologic Formation	24
4.0 MATERIALS AND METHODS	26
4.1 Station Selection	28
4.2 Sediment Type	28
4.3 Sample Collection	29
4.3.1 Sediment Collection	29
4.3.2 Water Collection	29
4.4 Trap Systems	30
4.5 Other Instruments	31
4.6 Deployments and Recovery of Materials	32
4.6.1 Deployments	32
4.6.2 Recovery	32
4.7 Sample Preparation	32
4.8 Laboratory Biogeochemical Analysis	32
4.9 Radiometric Analysis	34
4.10 Sediment Oxygen Demand (SOD)	34
4.10.1 Core sampling	34
4.10.2 Sediment height adjustment	34
4.10.3 Core transportation	34
4.10.4 Incubating water	34
4.10.5 Incubations	34
4.10.6 SOD determinations	35
4.10.7 Water Oxygen Demand (WOD)	36
4.10.8 Floc Oxygen Demand (FOD) and floc characterization	36
4.11 Physical transport of suspended solids	38
4.11.1 Instruments used	38
4.11.2 Total Suspended Solids (TSS)	38
4.11.3 Calibration of acoustic instruments	39
4.11.4 Range correction	39
4.11.5 Settling velocity estimates using Reynolds Flux	40
4.11.6 Wave calculations	40
4.11.7 Wave, current and combined wave current shear stresses	41
4.12 Statistical Analysis	44
5.0 RESULTS	44

5.1 Sediment Type	44
5.2 Sediment Trap Analyses	45
5.2.1 Phosphorus	46
5.2.2 Nitrogen	46
5.2.3 Carbon	49
5.2.4 Bulk Density	51
5.2.5 pH	51
5.2.6 Organic Matter (%)	51
5.2.8 TP vs. TN vs. TC	51
5.3 Water Chemistry	52
5.3.1 Water Column Nutrients	52
5.3.2 Oxygen	52
5.3.3 Chlorophyll-a	53
5.3.4 Total Suspended Solids	53
5.4 Stable Isotopes	53
5.5 Weather	53
5.6 Current	54
5.7 Total Mass Accumulation	54
5.8 Nutrient Budget Calculations	54
5.9 Cores and Sediment Oxygen Demands	90
5.9.1 Pictures of the cores	90
5.9.2 Sediment oxygen demand including the floc layer (SOD)	90
5.9.3 Sediment oxygen demand without the floc layer (SedOD)	90
5.9.4 Comparison of sediment oxygen demand with (SOD) and without the floc layer (SedOD)	90
5.9.5 Comparison with previous SedOD ₂₀ data (Phase 1 vs. phase 2)	90
5.9.6 WOD, FOD and floc characteristics	91
5.10 Physical transport of suspended solids	99
5.10.1 November 2010 Deployment #7	99
5.10.2 January 2011 Deployment #8	100
5.10.3 April 2011 Deployment #9	101
5.11 Predictions of physical transport of suspended solids	123
5.11.1 The analytical method for predicting water column nutrient concentrations due to wind wave resuspension	123
5.12 Radiometric analysis of sediment trap material	133
5.12.1 Downcore Profiles	133
6.0 DISCUSSION	143
6.1 Sediment and Water Chemistry	143
6.2 Sediment Resuspension	144
6.3 Yearly Nutrient Water Column Flux Budget	145
6.3.1 Floc Recycling	145
6.4 Sediment Oxygen demand	153

	4
6.4.1 Sediment Oxygen demand, Floc Oxygen Demand, Water Oxygen Demand and actual dissolved oxygen in the water column	153
6.4.2 Comparison of Sediment oxygen demand with (SOD) and without the floc layer (SedOD): estimation of the contribution of the thickness of floc to SOD	154
6.4.3 Correlations of Sediment oxygen demands with the nutrients contents in the sediment, floc and water column as well as with water chlorophyll a concentration	155
6.4.4 Comparison of Sediment oxygen demands amongst various Florida Lakes	155
6.5 Physical transport of suspended solids	159
7.0 CONCLUSION	160
7.1 Future Work	161
7.1.1 Specific recommendations for radio isotope tracer work	161
8.0 REFERENCES	162
APPENDIX	A-1

PROJECT SUMMARY

Improved knowledge of sediment dynamics within a lake system is important for understanding lake water quality. This monitoring project was focused on an assessment of the vertical sediment flux in Lake Jesup, a shallow (1.3 m average depth) hypereutrophic lake of central Florida. Sediment dynamics were assessed at varying time scales (daily to weekly) to understand the transport of sediments from external forces; wind, waves, precipitation and/or runoff. Four stations were selected within the lake on the basis of water depth and the thicknesses of unconsolidated (floc) and consolidated sediments. At each of these stations, a 10:1 (length to diameter) high aspect ratio trap (STHA) was deployed over a two-year period to collect particulate matter for a one to two week period. The water and sediment samples were collected and analyzed for total carbon (TC), total phosphorus (TP) and total nitrogen (TN). Mass accumulation rates (MAR) collected by the traps varied from 77 to 418 g m⁻² d⁻¹ over seven deployments. TN, TP and TC sediment concentrations collected by the traps were consistently higher than the sediments collected by coring the lake bottom and is most likely associated with water column biomass. These sediments were also analyzed for sediment oxygen demand (SOD) over the same period. During this study the water column was always oxygenated. Supporting radionuclide data (⁷Be, ¹³⁷Cs and ²¹⁰Pb) were also collected from all trap material, floc and sediments to attempt to understand sediment mixing and potentially resuspension. Activities of ⁷Be were too low to be accurately used to create a mixing model, but ¹³⁷Cs and ²¹⁰Pb yielded consistently reliable data that indicated periods of erosion and deposition. A current meter (Acoustic Doppler Velocimeter – ADV) deployed at the most central location indicated that currents within the Lake Jesup are typically moving along the longest axis of the lake (longest length). Analysis determined that a wind speed at 2.24 m s⁻¹ (5 mph) is the lowest sustainable velocity required to resuspend sediments. This is significant, because the average wind speed for all deployments was 3.2 m s⁻¹ (7.1 mph). Prevailing winds that move in the north or south direction are most dominant in sediment transport. A yearly nutrient flux budget was determined from August 2009 to August 2010 with flux estimated as 2,033,882 mt yr⁻¹ total material cycling through the lake. Yearly flux of TP as estimated from our approach varied from 22 to 23 mt yr⁻¹. Assuming floc is the most readily resuspendable material in the system, our estimates indicate the Lake Jesup's floc resuspended 47 times per year from August 2009 to 2010 and from April 2010 to April 2011 38 times per year.

1.0 INTRODUCTION

Freshwater resources are critically important for life on Earth, however they only amount to approximately 0.017% of the total global water volume available (Wetzel 2001). Therefore, studying and understanding these freshwater sources are important for current and future populations. Florida has approximately 7,700 lakes that are over 4 km² in size and freshwater covers roughly 8% of the total area of the state (Ali et al. 1988). They are an extremely valuable natural resource, as lakes provide critical habitat for Florida's diverse communities of flora and fauna, as well as, our domestic, industrial, agricultural and recreational activities and in some cases are a source of drinking water. Therefore, it is necessary to understand lake processes and what affects these internal processes have on water quality.

Unfortunately, cultural eutrophication of many lakes in previous years has caused unnatural shifts to increasingly eutrophic conditions, changing from macrophyte dominated to phytoplankton-dominated communities, as observed in Lake Harney and Lake Monroe FL USA (Anderson et al. 2004, 2006). This shift in trophic level increases the lake's productivity potentially resulting in algal blooms, anoxic events and fish kills. Shallow (< 3 m) polymictic lakes are especially susceptible to these effects (Ali and Alam 1996).

A Eutrophic condition is defined as a nutrient-rich lake environment where planktonic activity is high, water clarity is low, dissolved oxygen (DO) often drops below levels needed to support fish and high amounts of sediments accumulate at the lake bottom (Ali and Alam 1996). A shift to an eutrophic environment can be natural, however in some cases this shift can be caused by increased nutrient supply into the lake by human activities, such as, urban or agricultural runoff (Phelps and German 1996). These nutrients, namely phosphorus and nitrogen, when present at high levels with in the water column cause eutrophication (via external loading).

Many Florida lakes and lakes around the world, have experienced increased nutrient loading over the recent century from the urban and agricultural runoff of the surrounding lands (Ali and Alam 1996). Lake Jesup FL USA is no exception. This type of eutrophication is often referred to as cultural eutrophication, where run off from human activities causes the lakes productivity to increase (Carpenter et al. 1998). In natural settings, eutrophication takes centuries to occur, but cultural eutrophication can cause the lake to become eutrophic in decades to years. Commonly intermittent algal blooms become more frequent in systems affected by cultural eutrophication (Henderson-Sellers and Markland 1987).

The Lake Jesup watershed has undergone intense urban development and agricultural activities since the 1920s (Cable et al. 1997), which has caused the lake to be hypereutrophic, because of external nutrient loading (Keesecker 1992). In 1977, the U.S. Environmental Protection Agency (U.S EPA) stated that Lake Jesup was one of the most eutrophic water bodies in the State of Florida. A major contributor of nutrients was associated with secondarily treated wastewater inputs into the lake for over 20 years, beginning in the 1960s (Keesecker 1992). These inputs and resultant algal production are

thought to have contributed to a thick, muddy, nutrient-rich, organic layer on the lake bottom.

Resuspended sediments of shallow lakes are a possible cause for poor water quality (Evans 1994; Lijklema et al. 1994; Bachmann et al. 2000). Wave action, water mixing, [bioturbation](#) and currents, especially in shallow lakes, can cause resuspension of sediments (Evans 1994; Bloesch 1995). Resuspension can cause a recycling of nutrients, such as, [sediment](#) phosphorus (Newman and Reddy 1992) and meroplankton cells (Carrick et al. 1993; Bachmann et al. 2000), which can decrease water transparency. The upper 10cm of sediments are thought to be the sediments involved in the resuspension process into the overlying water column, (Tessenow 1972; Schindler et al. 1977; Newman and Reddy 1992); however, this depth can vary depending on sediment type and shear stress (Lee 1970; Newman and Reddy 1992).

Sediment traps are an excellent way to collect suspended [solids](#), by measuring the gross sedimentation or downward flux as the settling suspended [solids](#) that deposit on the lake bottom (Kozerski 2003) and suspend materials such as phytoplankton are collected in the traps. High-aspect ratio traps are the most common traps used in lakes; however to achieve a differentiation between net and new sediment deposition, a second type of trap should be used (and was attempted in this study), such as a trap with a lower aspect ratio (Horppila and Nurminen 2005; Flower 1991), which can measure the horizontal (lateral) flux (Kozerski and Leuschner 1999). Plate sediment traps are ideal for measuring horizontal flux and are best for shallow environments, such as, lakes or streams with slow moving currents (Kozerski and Leuschner 1999). In this lake system, different trap systems and deployment methods were tested (Fig. 1.1, 1.2 and 1.3).

Ultimately, understanding nutrients by their cycling, sources and migration can help to identify the interaction between the bottom sediments and the water column of a lake, which can best be accomplished by a monitoring sample collection approach, from which an observational data base and time-series maybe constructed. This observational set of data then can be quantified (e.g. rate of flux through the system) for the nutrients within the water column and bottom sediment including: nitrogen; phosphorus; and carbon. This biogeochemical data can help establish relationships between the chemistry of the sediments and the overlying water column (Ali and Alam 1996).

Little research has taken place in shallow Florida lakes using sediment traps. This project deployed sediment traps (tested three types, Figs. 1.1 to 1.3) to help understand sediment resuspension in Lake Jesup and contribute to understanding the current conditions of the lake. Resuspended sediments (and solids) can potentially add to the internal recycling of important nutrients in lake systems. Using the data collected from this research effort, and previous work done by Cable et al. (1997), a comparison was made between current and previous lake conditions, contributing to an understanding of the current status of Florida lakes. The intended scope of this project included several defined goals, which were firstly based on a proof-of-concept effort with the creation of a sediment trap system for Lake Jesup. Once the proper system was selected and deployed in the lake, it was the project's goal to characterize the composition of the particulate material (biogeochemically) fluxing

downward and to understand the conditions (wind, currents, etc) that might cause resuspension and its effects on nutrient supply to the water column.

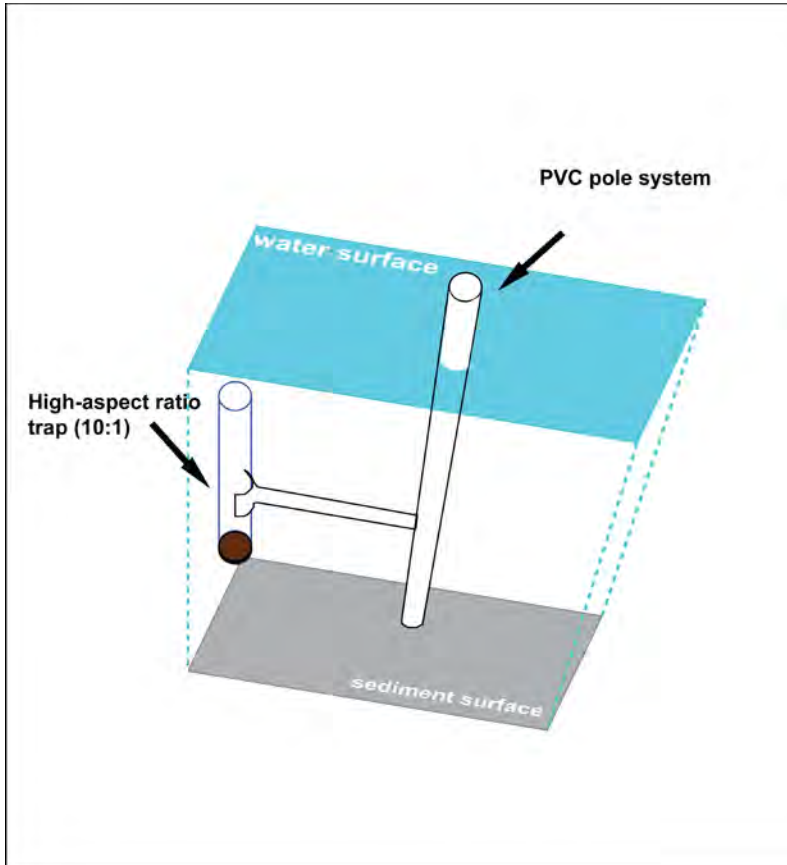


FIGURE 1.1 The original sediment trap - high aspect ratio (STHA) deployment method, which were deployed using PVC pipes. 10:1 aspect ratio refers to length of the tube relative to the width of the opening (inside diameter, ID) as discussed in Bloesch (1995). However, this approach proved to be un-workable as poles were never in the original position (e.g. hit by boat).

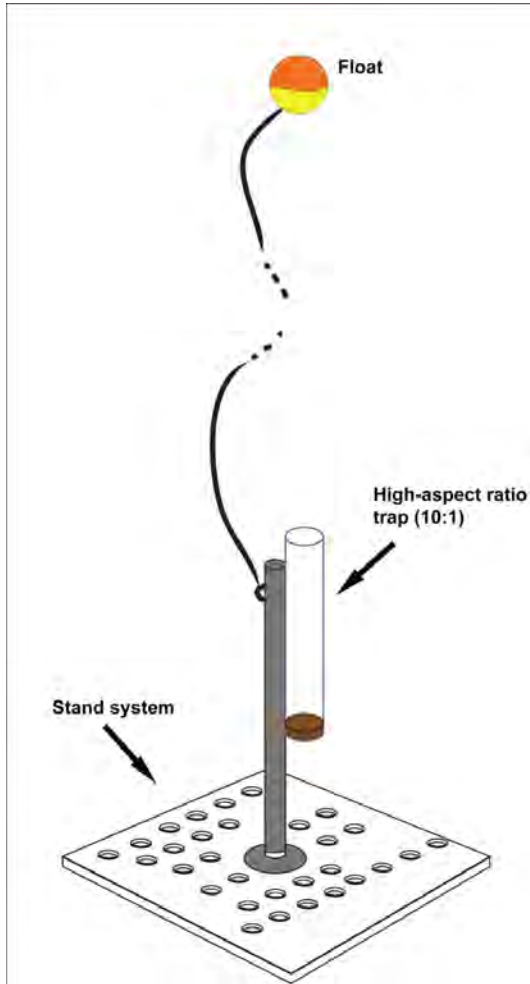


FIGURE 1.2 Sediment trap – high aspect ratio (STHA) system used for deployments 3 to 9. This version was the final design used for deployment.

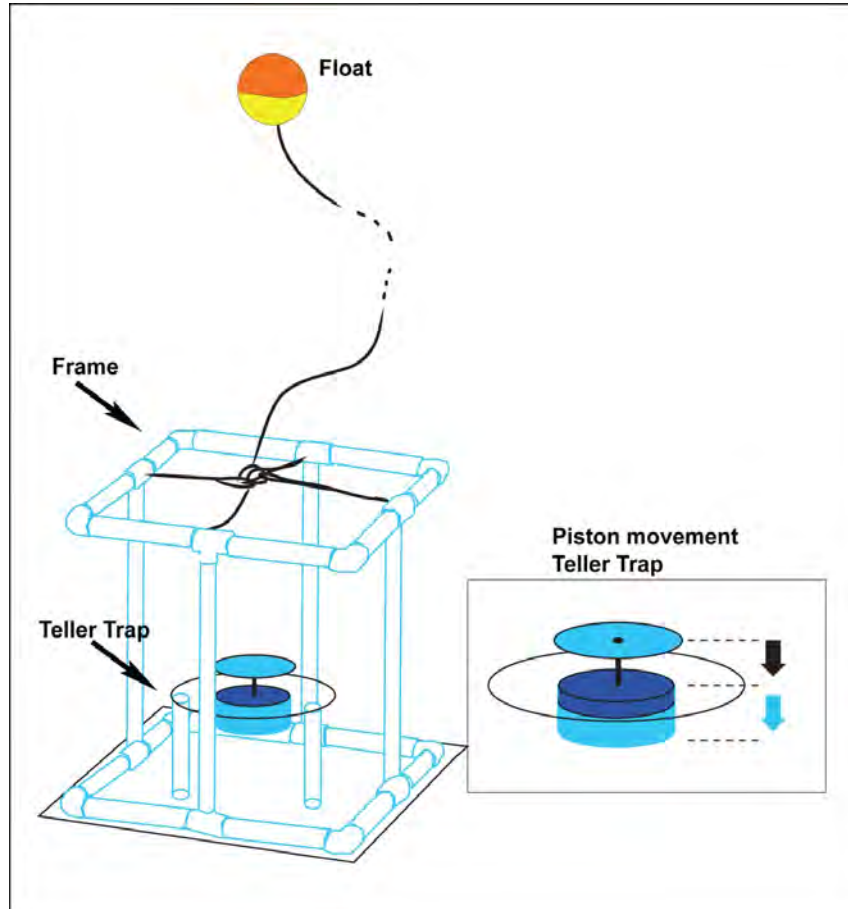


FIGURE 1.3 Sediment trap - Teller trap (STT) or plate trap system used for deployments 3 to 5. This was the final design used for deployment, although was not a successful method within Lake Jesup, because the sample was often lost during recovery.

2.0 GEOLIMNOLOGIC SYSTEMS

Lakes receive water from many sources: rainfall directly into the lake, inflow from the land surface, or by groundwater seepage. All of these are possible sources of inputs by which nutrients can enter into the system, which allow organisms to thrive in a lake environment. There are two types of nutrients: inorganic, which is found in an elemental state unassociated with carbon; and organic which is associated with carbon. Insufficient amounts of specific nutrients lead to a nutrient limited system, which restricts the growth of the lake biota. The most common limiting nutrients within a lake system are phosphorus and nitrogen.

Phosphorus is found in high concentrations within lake sediments, and can be 50 to 100 times greater in concentration than the overlying water (Henderson-Sellers and Markland 1987). Therefore, sediments can be a potentially “recycled” source of phosphorus and can affect a lake’s trophic state, especially in lake environments where sediment resuspension is high, such as shallow lakes. Human’s can cause phosphorus loading within the lake by use of phosphate fertilizers, ranching (ie. animal waste) or municipal sewage treatment plants that discharge waste into the system directly or via tributaries.

Nitrogen, in aquatic environments is found in many forms: ammonium (NH_4^+), nitrite (NO_2^-), nitrate (NO_3^-), organically bound nitrogen and as nitrogen gas (N_2). Atmospheric nitrogen (N_2 gas) is the main source of nitrogen into a lake system (N-fixaation), however dissolved inorganic nitrogen (DIN) and dissolved organic nitrogen (DON) can also enter the system through runoff. Humans have played an important role in increasing the amount of nitrogen in the aquatic system through the use of fertilizers, fossil fuels, ranching (ie. animal waste), sewage waste or septic tank leakage. The reality is, that any lake which is actively sedimenting, is a net sink for nutrients.

2.1 Sediment Resuspension

There are many factors that need to be considered in understanding sediment resuspension. First, it is important to realize that in extremely shallow lakes resuspension is a whole lake process (where entire water column is constantly mixed, with no or limited stratification), as sediment can easily be disturbed by external forcings (wind, wave and currents). Secondly, geographic location, surrounding topography, prevailing wind direction and speed, the lake size, morphometry and the lake depth must be taken into consideration (Bloesch 1995). Therefore, shallow lakes are especially susceptible to sediment resuspension (Luetlich et al. 1990; Kristensen et al. 1992; Lijklema et al. 1994).

In most shallow lake environments sediment resuspension is usually due to turbulence caused by wind or wave events (Bloesch 1995). Resuspension of nutrient rich bottom sediments from the disruption of the overlying water column may result in an algal bloom. An algal boom could then lead to low oxygen or even anoxic conditions within the water body, which may result in a lake-wide fish kill. This situation was observed in Lake Harney after Hurricane Charlie passed over the region in 2005, where fish kills and a surface bloom were observed after the wind event (Anderson et al, 2006). However, not all algal blooms can or will be attributed to wind driven sediment resuspension.

Lake bottom currents can apply current shear stress (τ) to the sediments forcing the uppermost layers to resuspend into the overlying water column. This can be quantified directly using the equation:

$$\tau = \rho_w \times C_d \times U^2 \quad [\text{N m}^{-2}]$$

where ρ_w is the water density (0.001 kg m^{-3}), C_d is a drag coefficient (1.1×10^{-3} ; Sternberg 1972) and U^2 is current speed (m s^{-1}) measured 1 meter above lake bottom (Bloesch 1995). Currents that are less than 0.02 m s^{-1} are not capable of resuspending non-cohesive particles $1 \text{ }\mu\text{m}$ in diameter (Bloesch 1995). Alternatively, current velocities greater than 0.07 m s^{-1} can resuspend non-cohesive particles up to $100 \text{ }\mu\text{m}$ in diameter. (Bloesch 1995).

Wind can be a driving force of sediment resuspension, creating large waves in depths shallower than one half their wavelength or wave base (Fig. 2.1 from Evans 1994). These waves can create a bottom scouring of the lake and cause sediments to resuspend. Wind speed sustained between 4.2 to 5.5 m s^{-1} (9.3 to 12.4 mph) is necessary before wind/wave induced resuspension can occur in most systems (Caper and Bachmann 1984).

The reintroduction of sediments into the water column is important, because it is a possible source of nutrients being released into the overlying water (Bloesch 1994; Qin et al. 2004). Figure 2.2 is a model of nutrient exchange between the sediments and the water column. This model is simplified to four sequential steps: 1) desorption, dissolution or decomposition of nutrients associated with solid particles into pore water, 2) diffusion of nutrients along concentration gradients through the sediment, 3) diffusion into the overlying water and 4) mixing into the water column (Brezonik et al. 1976). Alternatively, when water is turbulent the model in Figure 2.2b becomes a two-step process, 1) convection of sediment into the overlying water column and 2) release of nutrients into the water column (Brezonik et al. 1976).



FIGURE 2.1 The two regions of sediment resuspension within a lake. A) is the main area of resuspension and B) is less frequent or below the wave base (from Evans 1994). Shallow lakes are more likely to fall under the main zone of sediment resuspension.

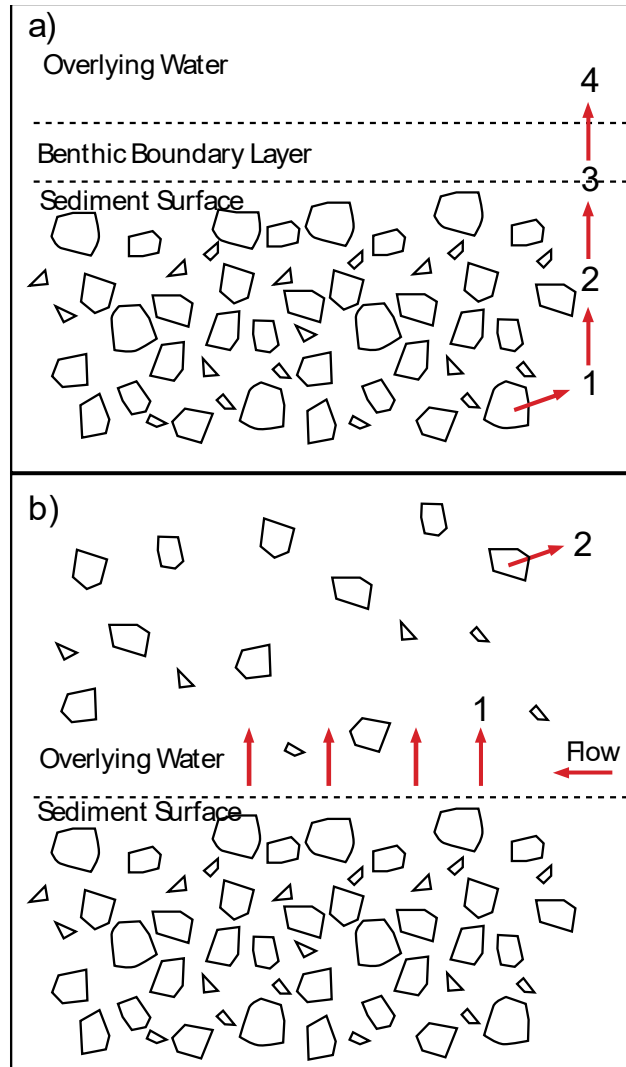


FIGURE 2.2 Model of nutrient release from sediments into the overlying water column. a) represents a simplified model of nutrient release with no turbulence, b) represents the release of nutrients from the sediment into the water column when resuspended by turbulence (from Brezonik et al. 1976). Processes include: 1) desorption, dissolution or decomposition of nutrients associated with solid particles into pore water; 2) diffusion of nutrients along concentration gradient through the sediment; 3) diffusion into the overlying water and; 4) mixing into the water column.

3.0 SETTING

The middle St. Johns River basin is located near Orlando, Florida and contains three large lakes: Lake Harney, Lake Jesup and Lake Monroe. These lakes are interconnected by the St. Johns River and are monitored by the St. Johns River Water Management District (SJRWMD). The SJRWMD is one of five water management districts in the state of Florida and is responsible for managing the water resources and groundwater in the northeast, north central region of the state. The St. Johns River is separated into three drainage basins: the upper, middle and lower St. Johns River. The upper St. Johns River is the area where the river begins in Indian River County and continues north to Lake Harney. The Middle St. Johns River contains the three-lake system previously stated and the Lower drainage basin, which extends from Lake Monroe towards Jacksonville where the river spills out into the Atlantic Ocean (Fig. 3.1).

Lake Jesup is located in the center of Seminole County, Florida (28°44'N, 81°14'W), 20 km northwest of the Orlando International Airport and is considered to be hypereutrophic (Cable et al. 1997). Average Lake Jesup total phosphorus (TP) from 1995 to 2002 was 0.16 mg L⁻¹ (Lake Jesup TMDL Basin Working Group, 2010). The St. John's River is connected with Lake Jesup in the northeastern part of the lake with limited connection to the river. The lake's temperature ranges between 12 °C to 27°C and the lake has a hydraulic residence time of 40 to 100 days (Kenney 2002). The lake has a surface area of 43 km² with an average depth of 1.3 m. Lake mixing regime is polymictic. Lake Jesup has limited flushing due to poor circulation by the ellipse-like shape of the lake, where the eastern and central regions of the lake are not mixed well with the western region (Cable et al. 1997). Another contributing factor affecting mixing could be associated with state road 46 (SR46), which cuts across the northeastern neck of the lake at its confluence with the St. Johns River. However, as of January 2010 SR46 has since been removed and an elevated bridge was built to take its place.

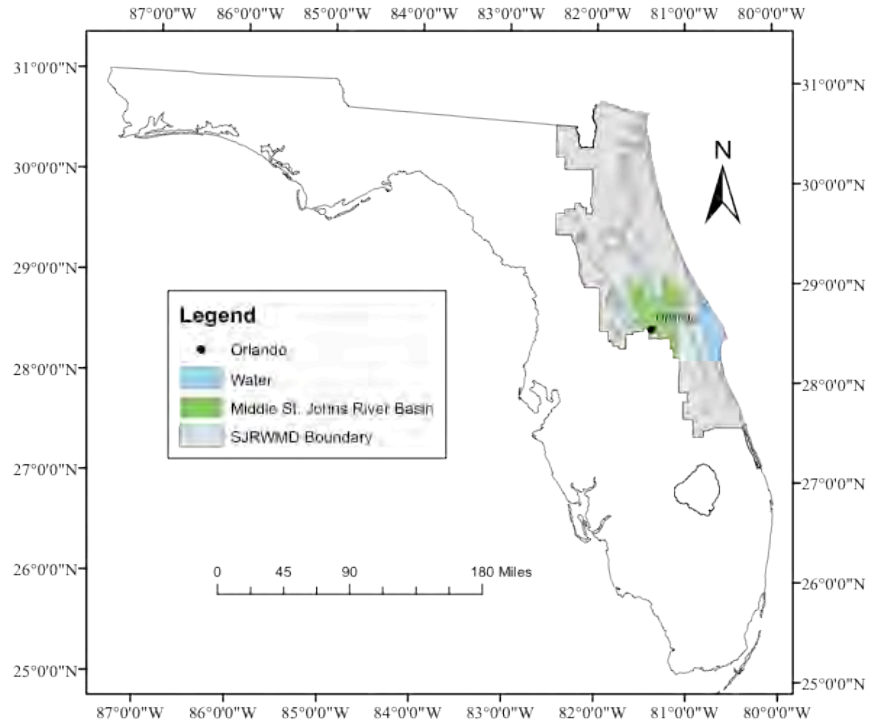


FIGURE 3.1 Location of study site depicting the St. Johns River Water Management District (SJRWMD) boundary and the middle St. Johns River Basin (MSJRB) relative to the St. Johns River (SJR) (image created in ArcGIS by data from SJRWMD).

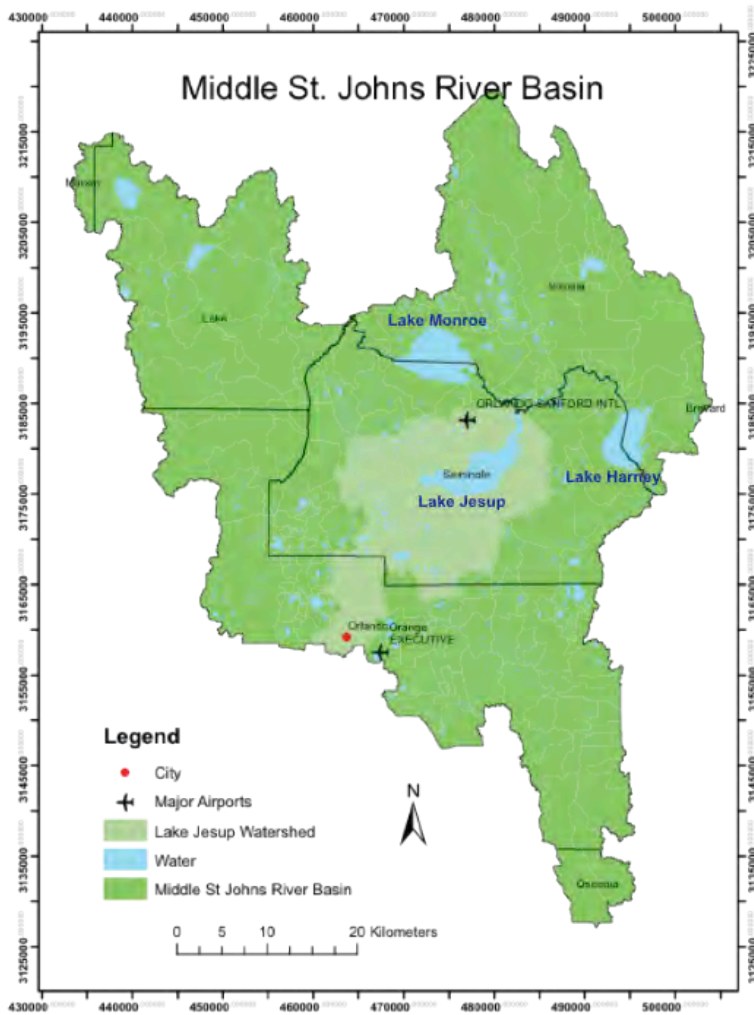


FIGURE 3.2 The MSJRB and Lake Jesup watershed relative to Orlando and the locations of the three lake system: Lake Monroe, Lake Jesup and Lake Harney (image created in ArcGIS by data from SJRWMD).

3.1 Regional Settings

The Middle St. Johns River Basin (MSJRB) contains three watersheds interconnected by the St. Johns River. These watersheds are named after the large lakes they embody: Lake Monroe, Lake Jesup and Lake Harney (Fig. 3.2). Lake Jesup has a poor connection with the St. Johns River, entering and exiting in the northeast portion of the lake. The St. Johns River is the main tributary into Lake Jesup, where Lake Harney drains into Lake Jesup and Lake Jesup drains into Lake Monroe all via the St. Johns River. There are many creeks and canals that drain into the lake within the Lake Jesup's 350 km² (Lake Jesup TMDL Basin Working Group, 2010) watershed, the three largest drain into the western part of the lake: Gee Creek, Howell Creek and Soldier Creek (Fig. 3.3).

3.2 Historical Changes

The climate in this area is humid subtropical with January having the coldest monthly average [temperature](#) of 14.8°C and July the hottest at 27.5°C, according to the National Climatic Data Center from 1971 to 2000 (Orlando Stanford station, 28°48'N, 81°16'W). The average total annual precipitation (from 1971 to 2000) is 130cm with the wettest months from May to October. The heaviest urbanized area within the Lake Jesup watershed is the city of Orlando, which is located in the southwest corner of the watershed. The population has steadily increased in the last century within the watershed. According to the United States Census Bureau, population from 1970 was almost 100,000 people and increased to almost 250,000 people by the year 2000 (Fig. 3.4).

The area surrounding the Lake Jesup watershed was first settled post Native-American colonization as early as the mid 1800s near the current town of Oviedo. Farming became one of the major economic factors during this time. Initially farms began growing cotton and sugar cane, but were unsuccessful. After these efforts, the planting of vegetables and citrus, [dawned](#) an agricultural explosion in the area. Before 1895, the town of Sanford was the largest shipper of citrus in the world, however, there was a big freeze in 1885 causing farmers to switch to vegetable crops, ferns and the raising of cattle. By 1950, almost one million crates of celery and 330,000 crates of citrus were being shipped annually with only 1,800 people populating Oviedo. Agriculture still takes place in this region, but has a much smaller role than in previous years. Besides the agricultural explosion that took place over the last century, there were also major modifications to Lake Jesup, particularly with the construction of roads and canal modifications. As early as the 1910s the area where the St. Johns River enters the lake was modified, by building a causeway now known as State Road 46 (SR46). Simultaneously two canals were built to allow for easy access for ferries and steamboats named the Old Ferry Canal and Government Cut Canal. These modifications are thought to have been the main cause for cutting off the circulation of inflow and outflow from the St Johns River into Lake Jesup. Thus these changes would have also affected the lake's trophic state by not allowing efficient water flux into and out of the lake into the main river. Since the 1960s, reports of four documented fish kills took place; 1960, 1968, 1981 and 1985 (Cable et al. 1997).

[The invasive exotic floating water hyacinth](#) caused major ecological problems for Lake Jesup (especially fisheries). Cable et al (1997) stated that hyacinths were first introduced to the St. Johns River in 1896 and reported to [have spread river-wide](#) by 1899. Before

1983, Lake Jesup had large amounts of secondary wastewater that for over 20 years was input into the lake from three of the lakes' tributaries (EPA 1977; Seminole County 1991; Gao 1996). There were a total of six discharge pipes and one effluent pipe that entered into Lake Jesup from Howell Creek, Gee Creek and Soldier Creek (Cable et al. 1996). Gee Creek and Howell Creek each had three drainage pipes that carried storm water and runoff from the surrounding urban communities into Lake Jesup. Soldier Creek was the site of a water treatment plant that discharged into the creek and thus Lake Jesup. By 1984, the pipes had been diverted away from Lake Jesup and its tributaries. This wastewater input, coupled with the rapid development of the watershed following waste diversion and poor circulation are thought to be the cause of an accumulated layer of soft flocculent unconsolidated organic-rich sediment, referred to as floc, on the bottom of the lake (Cable et al. 1997). Cable et al. (1997) also observed that the areas where wastewater was diverted into the lake had thicker floc layers relative to other regions of the lake.

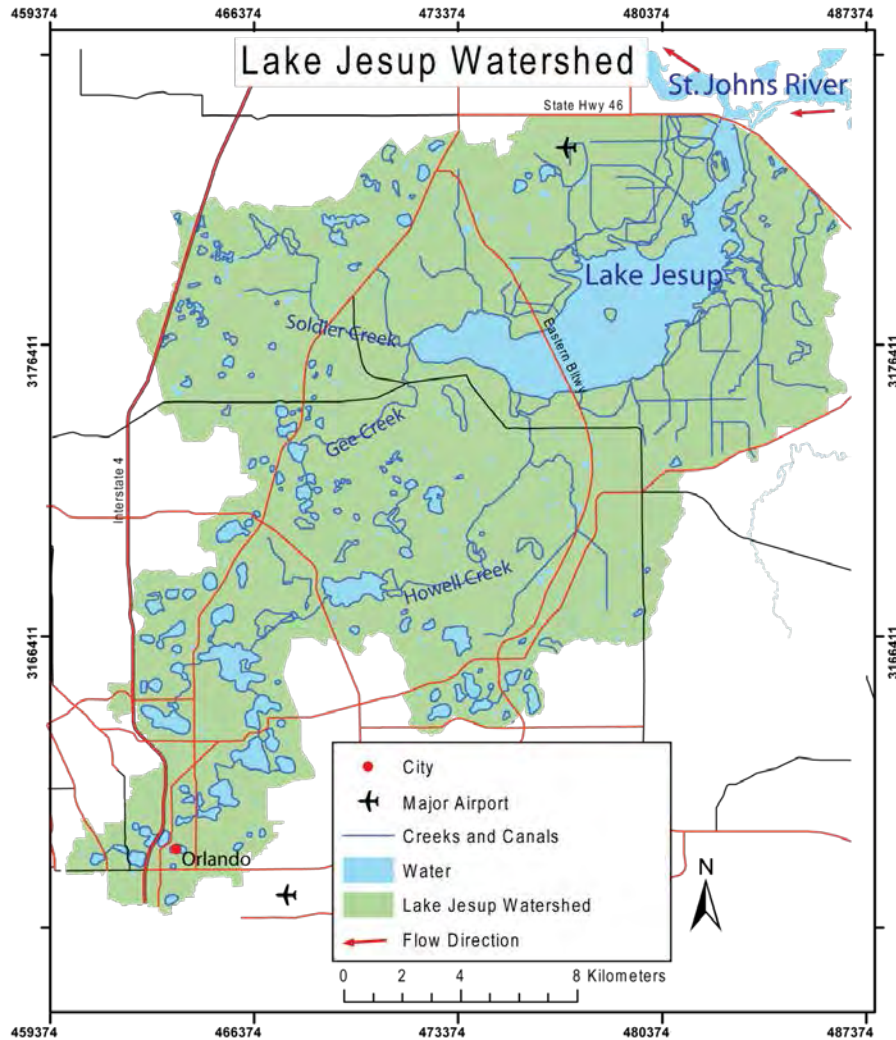


FIGURE 3.3 The Lake Jesup Watershed relative to the St. Johns River containing roads, canals and creeks (image created in ArcGIS by data from SJRWMD).

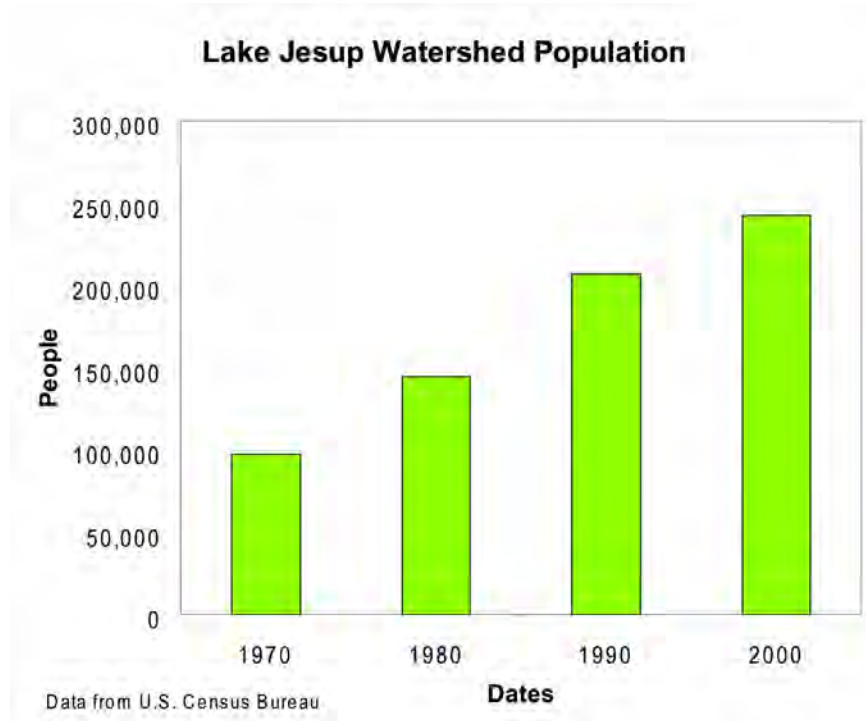


FIGURE 3.4 Population growth from 1970 to 2000.

The current land use within the Lake Jesup watershed (according to the SJRWMD) is roughly 50% Urban (including utilities and transportation) and 31% water and wetland areas. The remaining 19% is made up of open areas, pastures, rangelands, forests and agriculture (11% of the remaining 19%) (Fig. 3.5a, c). Historical land use suggests that the urban areas were smaller and agricultural, forests, rangelands, pastures and open lands were much larger. Using ArcGIS and data from SJRWMD a land use assessment was made from aerial photographs suggesting that the land use in 1973 was approximately 30% urban (including utilities and transportation), 15% water and wetlands and 55% remaining open areas, pastures, rangelands, forests and agriculture (22% of the remaining 55%) (Fig. 3.5b, d). By 2004, the remaining 31% of land previously used for agriculture in the past had been converted to urban (Fig. 3.5d).

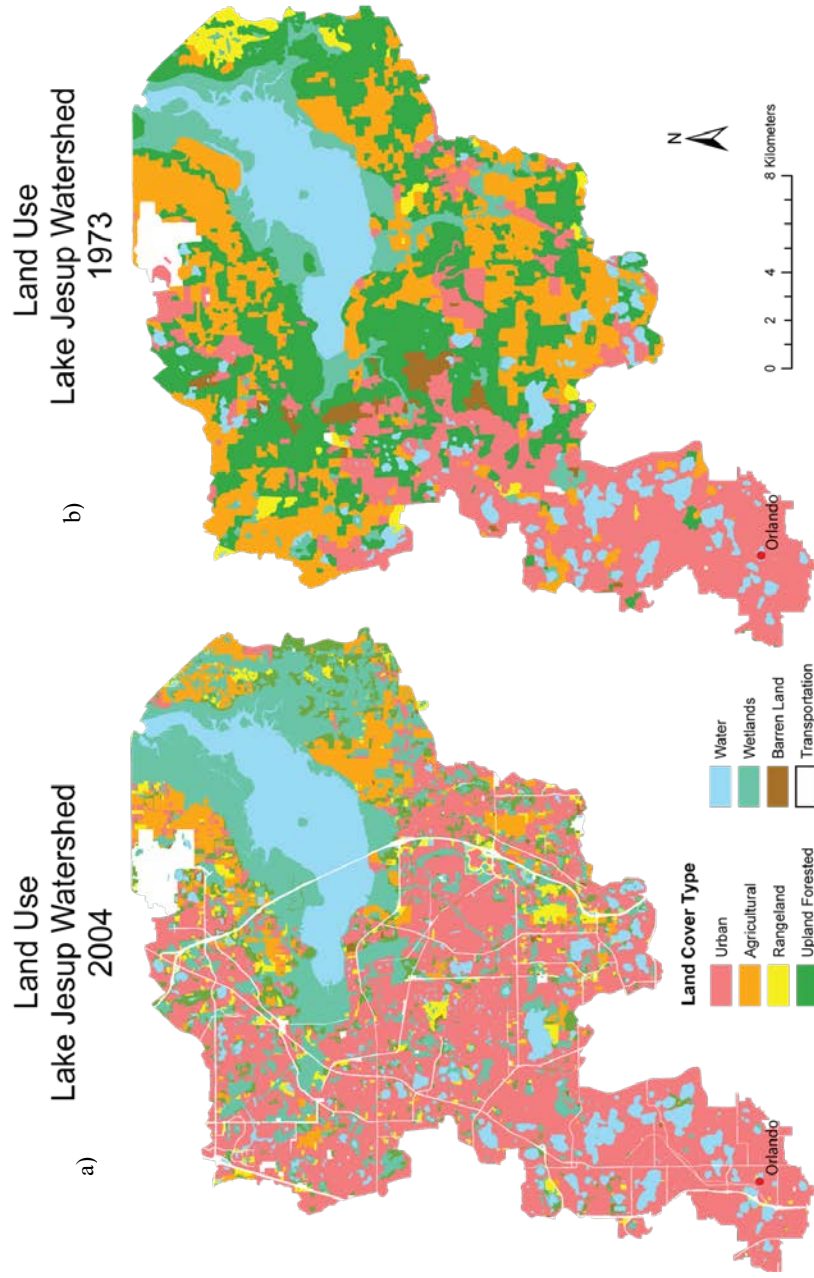


FIGURE 3.5 Land Cover use for 2004 (a) and 1973 (b) (image created in ArcGIS by data from SIRWMD).

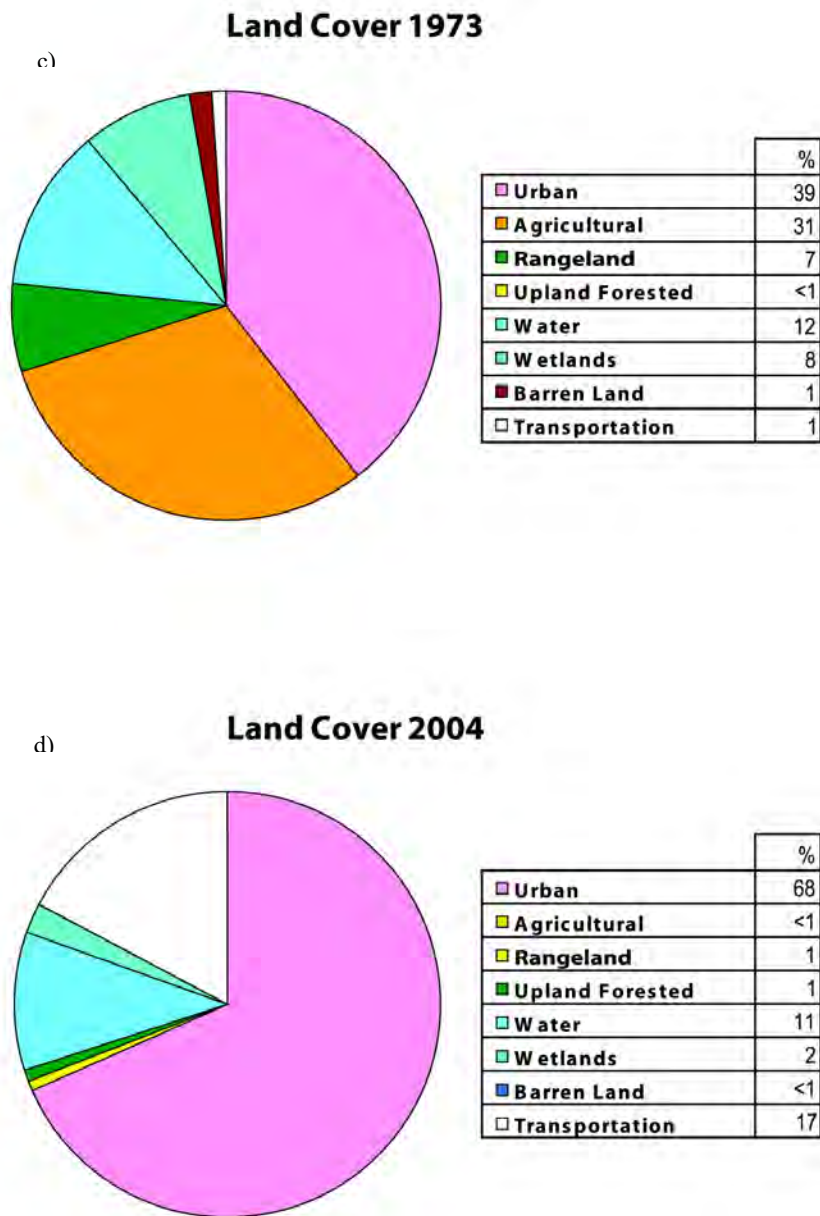


FIGURE 3.5 Percent Distribution of land cover area for the Lake Jesup watershed (calculated from SJRWMD data for land cover). c) 1973, d) 2004.

3.3 Geological Setting

The surrounding surface rock types within the MSJRB date back to as late as the Eocene (Approximately 35 million years old) with the deposition of the [Ocala](#) Limestone, which consists of skeletons of fossils in a silt to sand matrix. Massive chert nodules occur near the top and small spherical fossils are found at the base of this unit (Fig. 3.6). Within the basin, this outcrop is found west of Lake Jesup near the MSJRB border. Two different deposits of the Hawthorn Group are found here, taking up a third of the western portion of the basin aging back to the Miocene (Approximately 6 to 12 million years old). The older of the two deposits is from the Statenville Formation consisting of sand, silty sand and clay with phosphorite pebble and granule clasts. The younger Hawthorn Group deposits consist of interlaced quartz sand and quartzite gravel with a kaolinitic sandy clay basal unit. The central length of the basin consists of a Plio-Pleistocene aged deposit (2 to 3 Million years old) of deeply weathered sand and clayey sands. Located in the northeastern basin is the Fort Thompson Formation early to late Pleistocene in age (120 to 800 ka) consisting of clastic and shelly limestone deposits formed in fresh water and marine environments. The Anastasia Formation, late Pleistocene in age (12,000 to 126,000 years old), is also present in the basin located northeast of Lake Harney consisting of high-energy beach and bar deposits of shelly sands, dune sands and coquina limestone. The Princess Ann Formation, late Pleistocene in age (12,000 to 126,000 years old) is present along the St. Johns River cutting across the MSJRB consisting of sand silt and clay representing lagoonal and estuarine facies.

The physiographic divisions of Florida according to Brooks (1981) were characterized using the natural features associated with rock and soil type, geologic structures of the underlying rock, geomorphic processes and relief. Based on these principles, ten Districts (Apalachicola Delta, Central Lake, Dougherty Karst, Eastern Flatwoods, Gold Coast-Florida Bay, Ocala Uplift, Sea Island, Southern Pine Hills, Southwestern Flatwoods and Tifton Uplands) were established with each district being broken into several sub-districts. The St. Johns River and its tributaries run through the Eastern Flatwoods, Central Lake, Ocala Uplift and Sea Island districts (Fig. 3.7).

FIGURE 3.6 The geology of the Middle St. Johns River Basin (image created in ArcGIS by data from SJRWMD).

The Eastern Flatwoods District originated as barrier islands and lagoons and was formed during the Plio-Pleistocene era and recent times. The headwaters of the St. Johns Rivers can be found within the Eastern Flatwoods District in an area called the St. Johns Marsh (White 1970). To the east of the St. Johns River is the Central Atlantic Coastal Strip, which is a series of ridges predominantly made up of coquinas that runs parallel to the river in this area.

As the river flows north, it then moves into the Central Lake District where the MSJRB is located. A sub-district called the St. Johns Offset is a Pleistocene estuarine deposit (Brooks 1981). This area is also thought to be older than the southern headwater area (Pirkle 1969; White 1970), where deposits are a part of an older river valley with estuarine fill deposits possibly as far back as the Tertiary (Brooks 1966; 1968; White 1970) era. Finally, the St. Johns River flows into the Sea Island District near Jacksonville and into the Atlantic Ocean.

3.4 Limnologic Formation

The St. Johns River was thought to have been formed during the deposition of the Anastasia Formation around 125,000 years ago when sea level was high during the Pleistocene, where a series of shallow lagoons formed (Winn 1975). Over time, sea level dropped and the lagoons became valleys that were then connected by streams eroding the land surface, thus creating the now named St. Johns River (Winn 1975). It is believed that the lakes within

the MSJRB were formed during the Pleistocene from relics of former estuaries rather than depressions from the dissolution of limestone (White 1970).

FIGURE 3.7 The physiographic districts within the SJRWMD boundary (image created in ArcGIS by data from SJRWMD).

4.0 MATERIALS AND METHODS

Various geolimnologic approaches were used to determine the interactions between the water and the sediments. Samples of the unconsolidated sediment/flocculent organic matter (floc), lake bottom sediments (consolidated sediments), solids from the water column (total suspended solids, TSS) and water samples were taken at various periods throughout the year ranging between one to two week intervals at three to four different sites in the lake. All sediment samples for this study were collected by hand coring from a flat bottom skiff anchored at each sampling site.

Lake Jesup's sample collection took place over nine deployment periods spanning two years from April 2009 to April 2011. Each deployment period lasted from one to two weeks and required a deployment and recovery of materials at each of the four sites. Lake level played a factor when deployment or recovering samples (limited boat access when stage was low) because of various shallow locations on the lake (Fig. 4.1). All sediments (grab and trap samples) were analyzed for total nitrogen (TN), total phosphorus (TP), total carbon (TC), total inorganic carbon (TIC), $\delta^{15}\text{N}$, $\delta^{13}\text{C}$, %Ash, %OM, %Water, pH and bulk density. Piston (at depths less than 90cm) and short cores (at depth less than 36cm) were taken and split every 4cm and analyzed for ^{210}Pb , ^{137}Cs , ^{234}Th , and ^7Br at each of the four sites. Beginning in August of 2010, the high aspect ratio traps were also analyzed for ^{210}Pb , ^{137}Cs , ^{234}Th , and ^7Br . The surface water chemistry was analyzed at all four sites for TN, TP, chlorophyll-*a* (CHL-*a*), dissolved oxygen (DO) and total organic carbon (TOC). An ISCO auto water sampler collected samples daily during deployment periods and analyzed for TN, TOC and TP (Table 4.1).

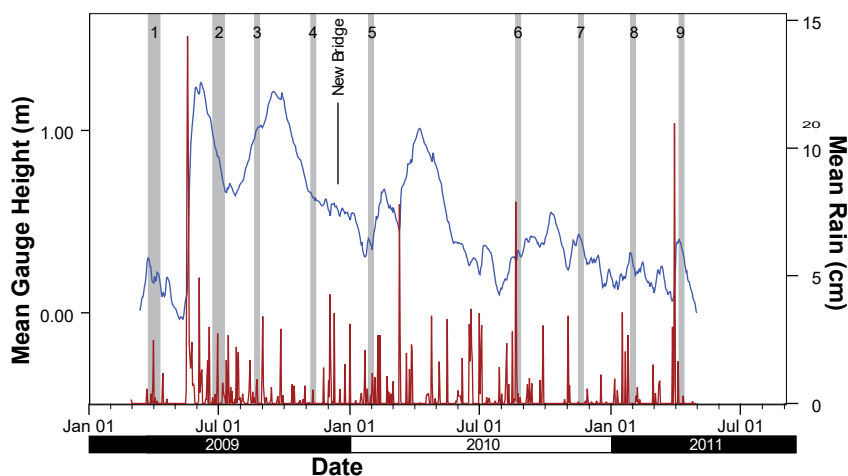


FIGURE 4.1 Daily mean lake level (blue) and total precipitation NCDC – Sanford Airport (red) from April 2009 to April 2011. Highlighted grey areas designate each deployment.

TABLE 4.1 Deployment dates and successful samples collected for Grab samples (water and sediment), YSI (D = deployed, P = profile), current, weather (S1 = Station 1, " barge," S2 = Station 2, by SR-46), STHA, STT (plate trap), STM8 (Mark8 trap) and Radiometric coring.

Deployment	Deployment Date	Grab	ISCO	YSI	Current	Weather		STHA		STT	STM8	Radiometric analysis
						S1	S2	LJ14	LJ22			
1	04/25/2009 to											
	05/08/2009	X	X		X	X	X	X	X			
2	06/26/2009 to											
	07/09/2009	X	X	X	X	X	X	X	X			
3	08/21/2009 to											
	08/28/2009	X	X	X		X	X	X	X			
4	11/06/2009 to											
	11/13/2009	X	X	X		X	X	X	X		X	
5	01/29/2010 to											
	02/05/2010	X	X	X	X	X	X	X	X	X	X	
6	08/20/2010 to											
	08/27/2010	X	X		X	X	X	X	X	X		X
7	11/11/2010 to											
	11/19/2010	X	X		X	X	X	X	X			X
8	01/28/2011 to											
	02/04/2011	X	X	X	X	X	X	X	X	X		X
9	04/08/2011 to											
	04/15/2011	X	X	X	X	X	X	X	X	X		X

4.1 Station Selection

Four stations were selected based on preliminary coring following data using the previous work done by Cable et al. (1997), who selected stations using an equal area grid of Lake Jesup. The four stations for this study were selected based on varying depth, location, floc thickness and accessibility with District consultation and approval. Stations LJ-14, LJ-22 and LJ-28 were selected at the beginning of the sampling cycle and LJ-44 was added in August of 2010. Sample site LJ-28 was selected as the barge location, because the thin floc layer, lake depth (deepest of the stations selected) and central location eased the deployment of equipment (Fig 4.2). All instrumentation was deployed at this site.

Lake Jesup and Study Sites



FIGURE 4.2 Sampling stations on Lake Jesup for the two year sampling period. Coordinates (decimal degrees): LJ22, = 28.7169, -81.2694, LJ14 = 28.7147, -81.2478, LJ28 = 28.7317, -81.2014 and LJ44 = 28.7597, -81.1844.

4.2 Sediment Type

Three main types of sediments were found in Lake Jesup: a) the top-most was floc (unconsolidated sediment), b) followed by gyttja and c) below that peat. Additionally, dependent on location, other sediment types we encountered including pink marl, blue clay and sands. All of these additional types, except the blue clay, were found at depths (15 cm to 58 cm), most likely exceeding the depth of resuspension. The blue clay layer was exposed at the sediment surface near Bird Island, where no floc was present (as similarly observed by Cable, 1995). Shells can be found in any of the sediment layers within the lake, but are rarely found in the floc layer. The floc layer is highly organic (33.28%). Gyttja is more consolidated than floc and peat is more consolidated than gyttja, all types contain

relatively high amounts of organic matter (OM), low OM reflects samples that contained many shell fragments similar to what was observed in Lakes Monroe and Harney (Anderson et al, 2004 and 2006).

4.3 Sample Collection

4.3.1 Sediment Collection

Initial sampling periods lasted for two weeks, but were found to be problematic, because samples were lost either by theft, boats or alligators disrupting the sediment traps. After repeated trips where samples were lost a one-week sampling period was established. The shorter deployment times would limit the time the equipment would be in the field, but we had a better chance of recovering the equipment (less exposure to potential threats or damage).

Sediments were collected in three ways: grab samples, sediment traps and cores. The grab samples and cores taken for radiometric analysis were collected by using a coring device (push core), made of PVC piping with a detachable clear polycarbonate “barrel” roughly 10cm in diameter for the radiometric samples and 5cm for the grab samples. The coring device allows water to flow only one way with a check valve, as the core is pushed into the sediment. After the core was pulled upwards, the one-way flow created suction that allowed the sediment to be brought to the surface. For the grab samples, the unconsolidated top sediments (floc) and the surficial 5cm of consolidated sediments (immediately underlying the floc) were collected separately in whirl-pak bags and placed on ice. The remaining sediments in the core were discarded. The cores collecting the samples for radiometric analysis were split into 4cm increments for the entire length of the collected core (between 20 to 32 cm depth), immediately following recovery from the lake bottom, in the boat. After sub-sampling, these samples were sent to Eastern Carolina University (ECU) for radiometric analysis.

Sediment traps were used to collect particle flux for time-series analysis. Three different trap systems were used to collect suspended solids in the water column: 10:1 (length to diameter) high aspect ratio sediment trap (STHA), modified plate or “teller” trap (originally developed by I.G.B. Berlin, pat.-Nr. 19737448.4) and the Mark8 autosampler (made by McLane Research Laboratories inc. located in East Falmouth, Massachusetts).

4.3.2 Water Collection

Water samples were collected by two different approaches: 1) surface “grab” and 2) with an automated water sampler (ISCO) daily. The water grab samples were collected at the same time as the sediment grab samples at all four sites during a deployment period. The collected water was split immediately following fieldwork at the dock, into filtered (0.45µm nitrocellulose membrane filters), unfiltered samples, and, chlorophyll-a filtration (25mm GF/F glass microfiber filters) samples and placed on ice. An ISCO water sampler located on a floating stationary barge at site LJ-28 (Fig. 4.3), were set to collect daily water samples at 13:30 during each deployment period. These unfiltered samples were collected

at the time of recovery. All water samples were frozen, until analysis, at the Soil/sediment Biogeochemistry Laboratory (SBL) at Florida International University (FIU).



FIGURE 4.3 Photograph of the barge located at LJ28 with deployed ISCO water sampler and Weather Station 1.

4.4

Trap Systems

The sediment trap high-ratio (STHA) had a ratio of 10:1 (Bloesch and Burns, 1979) made of polycarbonate with an inside diameter of 5.3cm and a length of 53cm and measures vertical flux by trapping suspended solids over a period of time. This trap was established as the primary TSS trap system for this research effort and underwent a modification in August of 2009. The initial deployment design had the trap secured to a PVC pole that was visible at the water surface (see Fig. 4.3), this design was changed after poles were tilted or missing upon retrieval. The new system allowed the trap to rest on the lake bottom and was attached to a rope and float that was visible on the surface. The rope and float design was used for the high aspect ratio trap beginning August of 2009 and continued through April of 2011. Therefore the data presented and analyzed in this report does not include any of the earlier traps placed on poles due to their perturbed nature (as to not skew the data).

The plate trap system had an outer ring diameter of 35cm and an inner collection area of 14cm and was designed to simulate sedimentation rates in moving waters with the consideration of gravity and bottom shear (Kozerski and Leuschner 1999). The trap functioned as a vertical moving piston, which presents the collection area when open and secures the sample when closed. The outer ring of the plate trap represents the boundary layer and the shear stress conditions of the lake bottom (Kozerski and Leuschner 2000).

Particles then settle into the collection area based on shear stress and sinking velocities. Unfortunately, the plate trap system was not appropriate for the Lake Jesup environment, where lake water clarity is low and deployment procedures did not allow us to enter the water to effectively collect the sample. It is suggested that a redesign of the trap be implemented to close the trap and collect the sample more effectively or new collection procedures that involve diving.

The Mark8 autosampler has a funnel design that empties into bottles that rotate every 12 to 24 hours. The trap has a height of 116cm with a funnel diameter of 53.7cm that collects into 250mL bottles. The trap is similar to the high aspect ratio trap, except it collects the daily flux of settling particles. Attached to the Mark8 at the same height was a high aspect ratio trap that allowed comparison of materials collected and to understand the settling particles at this height with in the water column. Unfortunately, the instrument was lost during sampling in November of 2010. Efforts to locate the Mark8 with side scan SONAR were not successful.

4.5 Other Instruments

To understand the dynamics of the interactions between the water and the sediments other data collection instruments were used. An Aquadopp current meter (2MHz, P22042, Probe ID: APK 33942) was used to measure the water current and wave height. The current meter was attached to a mount and set to rest at the bottom of the lake around 0.75 meters above lake sediments and was recovered at the end of a deployment period. The data was then downloaded to a laptop.

Two weather stations were used to understand the effects that wave intensity and wind velocity have on sediment resuspension. One weather station was fixed in place on a constructed platform near the SR46 Bridge and the other was on the barge with the ISCO water autosampler. The weather stations collected wind velocity and direction, air temperature and precipitation, every 15 minutes continuously over the course of a deployment period. Of the two weather stations, the weather station on the barge (Station 1, 2 meters above water surface) collected wind velocity, precipitation and temperature and the weather station near SR46 collected wind direction (Station 2, around 4 meters above water surface).

Lastly, two YSI units were used: an auto sampling YSI (Model: 600QS-ORP-M) and a YSI (Model: ProODO) that profiled the water column at 25 cm intervals. The Auto-sampling YSI unit was placed on the barge to collect dissolved oxygen (DO), pH and temperature in the water column every half hour during a deployment period. This system was used to potentially understand the effects of sediment resuspension on the DO and pH within a meter of the water surface. The YSI used for profiling collected the water temperature and DO every 25 cm from the lake surface to the top of the soft flocc layer (measured immediately before trap deployment and again during trap recovery at all four sites).

4.6 Deployments and Recovery of Materials

4.6.1 Deployments

During the deployments all instruments and traps were prepared for collection over a week to two week period. The AquaDopp current meter, YSI autosampler and ISCO autosampler were programmed to collect data over the course of the deployment period. The plate (only at three sites, did not deploy plate traps after January 2010), STHA traps (deployed at all four sites) and AquaDopp (deployed at LJ28 only) were deployed by lowering the systems over the side of the boat and left on the lake bottom. The YSI and ISCO autosampler were set up to operate from the barge at LJ28. Also, during the deployments sediment (floc and 5cm consolidated samples), water grab samples and DO profile were taken at all four sites and the weather data was downloaded from the two weather stations.

4.6.2 Recovery

During recovery all traps, samples and instruments were collected (except for the weather stations and ISCO autosampler, which were affixed to the barge or permanent platform). The AquaDopp and YSI autosampler were collected and the data were downloaded. Both weather stations data were downloaded, ISCO water samples and/or Mark8 samples were collected. Beginning in August of 2010, coring samples for radioisotope analysis were collected, during the recovery, at each of the four sites and split on the boat every 4cm. These samples were placed in whirl-pak bags and put in a cooler on ice. Once back at FIU, these samples were refrigerated until they were shipped to ECU for radiometric analysis.

4.7 Sample Preparation

All sediment samples, except the radioisotope samples, were prepared and analyzed at the SBL/FIU. TSS sample were processed and analyzed at FGCU. All water samples were frozen until they were sent to SERC Water Quality Lab (NELAC – E76930-12-07/01/2010) for analysis.

Removal of the sediments in the traps took place within 5 days after they were collected from the lake. Before the sediments were removed the sediment height within the traps was measured. The grab samples were weighed in the whirl-pak bags and in cups where the volume was measured. After fresh weights were collected all sediment samples were dried (80°C until constant weight), cooled in a desiccators, ground using a mortar and pestle and weighed prior to geochemical analysis.

4.8 Laboratory Biogeochemical Analysis

The Samples were analyzed by FIU, at several labs by using standard analytical methods. Lake water was analyzed for soluble reactive orthophosphate (SRP; USEPA method 365.1) and total dissolved phosphorus (TDP; EPA 365.1), soluble nitrate, nitrite (NO₃, NO₂; USEPA 353.2) and ammonium (NH₄; USEPA 350.1) on a Technicon Autoanalyzer II System (Pulse Instrument Ltd.) total dissolved nitrogen (TDN; ASTM D5176) and dissolved organic carbon (DOC; USEPA 415.1) was determined on a Shimadzu TOC-VCSH fitted with Shimadzu TNM-1 Total Nitrogen Analyzer.

Total phosphorus in sediments was determined using the ashing/acid hydrolysis method of Solorzano and Sharp (1980) with the resulting soluble reactive phosphorus (SRP) being measured as above. Sediments were processed for dry weight (80°C), field bulk densities

(g dry weight cm⁻³), fractional water content and percent organic matter by loss on ignition (LOI) at 550 °C (as % ash) (ASTM D2974-87). Sediment total C and N were analyzed using Perkin Elmer Series II 2400 CHNS/O Analyzer (Nelson and Sommers 1996). Radiometric analysis was analyzed at ECU under the methods used by Dail et al. (2007).

Carbon and nitrogen isotopes of the sediments were determined by standard elemental analyzer isotope ratio mass spectrometry (EA-IRMS) procedures. Carbon isotopes were measured using decarbonated samples, where they were reacted with 1M HCl for 24 hours, whereas, nitrogen analysis were measured on the untreated sample.

4.9 Radiometric Analysis

Sediment cores and sediment trap material were collected to evaluate short-term processes via short-lived nuclides. Cores were collected by push core from the boat. Extruded subsamples for radiochemical analysis of ⁷Be, ¹³⁷Cs, and ²¹⁰Pb were stored and sent to East Carolina University. Samples from all sediment cores were analyzed for ⁷Be (t_{1/2} = 53.3 days), ²¹⁰Pb (t_{1/2} = 22.1 years), and ¹³⁷Cs (t_{1/2} = 30.2 years) by direct gamma counting. Samples were initially dried homogenized and packed into standardized vessels before counting for approximately 24h. Gamma counting was conducted on one of four low-background, high-efficiency, high-purity, Germanium detectors coupled with a multi-channel analyzer. Calibration of the detectors was calculated using several natural matrix standards (IAEA-300, 315, 314) at each energy of interest (except ⁷Be) in the standard counting geometry for the associated detector. The counting efficiency of ⁷Be was determined by linear regression of calculated efficiencies for energies beyond 200 keV and activity was measured using the net counts at the 477 keV photopeak. Activities were corrected for the radioactive decay that had occurred between sample collection and analysis. Inventories were calculated by integrating the activity of each subsample according to the following equation (after Canuel et al., 1990):

$$I = \sum X_i(1 - \Phi_i)\rho_s(xsA_i),$$

Where: I is the total inventory of the sediment core (dpm cm⁻²); X_i is the subsection thickness (cm); Φ is the porosity of the subsection (unitless); ρ_s is the sediment density (g cm⁻³); and xsA_i is the activity above the level supported by the radioactive parent (dpm g⁻¹). Sediment dry-bulk density was calculated by gravimetrically determining water content and correcting for salt residue. ⁷Be inventories at each site were then separated into two components, residual and new inventory (see Corbett et al., 2007). Residual inventory is the decay-corrected inventory of the previous cruise. Residual inventory is then subtracted from the total inventory giving the new inventory. New inventory indicates the net change of inventory between each sampling event (Corbett et al., 2007). Although many erosional and/or depositional events may occur at any point between sampling intervals, only the net result is obtained.

4.10 Sediment Oxygen Demand (SOD)

4.10.1 Core sampling

Two sediment cores were sampled at each station. Coring was performed with a hand-held corer (cf. Appendix 1 for design) onto which was attached a clear acrylic core (62cm x 6.35cm, length x I.D.) which wall was 0.635cm thick. About $\frac{3}{4}$ of the acrylic core was pushed through the floc and sediment to prevent the sediment core from sliding out during retrieval. The acrylic core was then retrieved and, before it was removed from the water, its bottom was plugged with a rubber stopper size #13 to prevent losing cored materials. Once at the deck level, the acrylic core was disengaged from the corer and plugged with a foam stopper at its apex. The rubber stopper #13 was finally duck taped onto the acrylic core and the intact core was stored in the dark in its upright position.

4.10.2 Sediment height adjustment

Before leaving Lake Jesup, the sediment inside the core was adjusted underwater so that 13cm of headspace filled with L. Jesup water ($\sim 0.4\text{L}$) remained on top of the floc or sediment if a floc layer was lacking. The sediment was pushed upward with a 3cm thick piston so that interface water-floc (or sediment if not floc was present) was positioned $\sim 13\text{cm}$ below the apex of the acrylic core. The piston was then locked into place with a $\frac{1}{2}$ " thick PVC tube to proper length. The $\sim 0.4\text{L}$ of L. Jesup water above the floc/sediment interface was calculated so that: the volume of water above the floc (in liters L divided by the core surface area (in m^2) was 126 L m^{-2} (similar to the 132 L m^{-2} as recommended in Bowman and Delfino, 1980). The core was then capped at both ends as described in the "core sampling section" above.

4.10.3 Core transportation

All 8 cores were tightly encapsulated between two 5-gallon buckets with their openings facing to each other (\sim dark conditions) and transported in an air conditioned vehicle to FGCU (Fort Myers, FL) where they were incubated.

4.10.4 Incubating water

Surface water was sampled from the subsurface at the LJ28 station and kept in two 3-gallon thermo insulated kegs (Bubba®). The water temperature in the keg remained at 25°C until incubation.

4.10.5 Incubations

Two sets of incubations were performed within 24-48h of sediment core collection. The first incubation was performed 24h after the core collection with the intact sediment core including the floc layer overlying the consolidated sediment (= determination of Floc + Sediment Oxygen Demand = SOD). The second incubation was performed 48h after the core collection and involved only the consolidated sediment (= determination of sediment oxygen demand = S_{edOD}). The floc was removed after measuring its volume (cm^3) with a turkey baster. The overlying water was also removed before floc removal. The turkey baster was unable to remove the sediment underlying the floc. All incubations took place in a dark room at $\sim 25^\circ\text{C}$. The cores were placed in their upright position and organized in a rosette fashion in a core rack (Fig. 4.4). L. Jesup water overlaying the floc/sediment was removed and replaced with station LJ28 air saturated water. Air saturation (100%) was reached after one hour of air bubbling in LJ28 water. Each core was then capped tightly with a modified rubber stopper #13 (Fig. 4.5). The modified rubber stopper included i) a

2" long 5/16" thick magnetic stir bar (Fisher®) mounted on a fluorocarbon swivel and positioned at 6.5cm above the floc/sediment, ii) a low flow, low oxygen consumption DO probe which tip was positioned ~1cm above the stir bar and iii) a pin hole (obstructed by a pin after insertion of the stopper) to evacuate the excessive water pressure occurring during the stopper insertion (Fig. 4.5). Two types of DO probes were used. For LJ14, LJ22 and LJ28 cores, an ORION 083010A DO polarographic probe connected to an ORION 835A meter/logger was used while for LJ44 cores, a Hach LDO 101 luminescent DO probe connected to a Hach HQ40d meter/logger was used. A stir bar was spun at 20 rpm to prevent strong DO gradients from building in the incubated volume of water as the sediment depleted its DO. The stir bar was rotated through the use of a strong earth magnet mounted on the shaft of 12V gear head DC rotary motor (model GH35GM, HSIANG®). Twenty rpm was found to be ideal to mix the water in the chamber without creating any resuspension (based on a preliminary "dye study" – not shown). The DO was recorded every 10 minutes (15 minutes for the Hach probes) for 24h.

4.10.6 SOD determinations

DO concentrations in the chambers were plotted as a function of time in hours and the slope was determined (mg O₂/L/h). Since the organisms present in the incubated water respire, WOD (cf. WOD in methods below) was withdrawn from the absolute value of the slope (assuming that the respiration rate was a positive value). SOD or S_{ed}OD could then be computed as follow:

$$SOD_T \text{ or } S_{ed}OD_T = 24 |S| V/A,$$

in gO₂/(m²day) Where T is the temperature in °C of the incubation, S is the slope WOD corrected in mgO₂/L/h, V is the volume of incubated water in m³, A is the surface area of core in m² (0.00317 m²) and 24 is the unit conversion constant. In order to compare with other SODs available in the literature, SOD_T and S_{ed}OD_T rates were corrected to 20 °C using a Q₁₀ (Van't Hoff) equation (Butts and Evans, 1978):

$$SOD_{20} = SOD_T/1.065^{(T-20)} \text{ and } S_{ed}OD_{20} = S_{ed}OD_T/1.065^{(T-20)}.$$

Since incubations were conducted at ~ 25 °C, 1/1.065⁽²⁵⁻²⁰⁾ = ~3/4.

4.10.7 Water Oxygen Demand (WOD)

Water oxygen demand (WOD) of L. Jesup was assessed within 24h and in triplicate at 25°C in three ~295ml dark BOD borosilicate bottles (Wheaton® 300mL bottle). LJ-28 water was first air saturated and then poured into the bottle. Dissolved oxygen and temperature were assessed before and after a 24h incubation period with a Hach LDO BOD self-stirring probe connected to an HQ40d meter (www.hach.com). WOD was expressed in mgO₂ /L/h.

4.10.8 Floc Oxygen Demand (FOD) and floc characterization

FOD was measured within 48h of core collection. Once the floc was removed from the acrylic tube, its volume was recorded to the nearest ml and 10ml was subsampled and incubated at 25 °C in a ~295ml dark BOD borosilicate bottle (Wheaton® 300mL bottle) filled with air-saturated LJ28 water. DO changes within a 4h period were recorded the same way as for the WOD. After the WOD correction, FOD was expressed in $\text{mgO}_2/(\text{h ml_floc})$ or $\text{mgO}_2/(\text{h g_floc})$ using the following equation:

$$\text{FOD} = [(\Delta\text{O}_2/\Delta t) - \text{WOD}](v/10)$$

if expressed in $\text{mgO}_2/(\text{h ml_floc})$ - this number was divided by the floc bulk density (g/ml_floc) to express FOD in $\text{mgO}_2/(\text{h g_floc})$. Where $(\Delta\text{O}_2/\Delta t)$ is the change in DO over 4h in $\text{mgO}_2/\text{L/h}$, v in L is the volume of the BOD bottle minus 10 ml of floc and 10 is the volume of floc added to the bottle (ml). The determination of the bulk density of floc (g/ml_floc), its inorganic as assessed by the ratio of ash weight/dry weight (AW/DW) and deducted organic fractions ($[\text{ash free DW}]/\text{DW}$) were determined gravimetrically in aluminum pre-weighed pans. A recorded floc volume was dried in an oven set at 80°C until constant weight to determine DW. The dried floc was then combusted at 450 °C for 4 hours and the ashes were weighed to determine ash weight (AW). The AFDW was deducted from the difference between DW and AW.

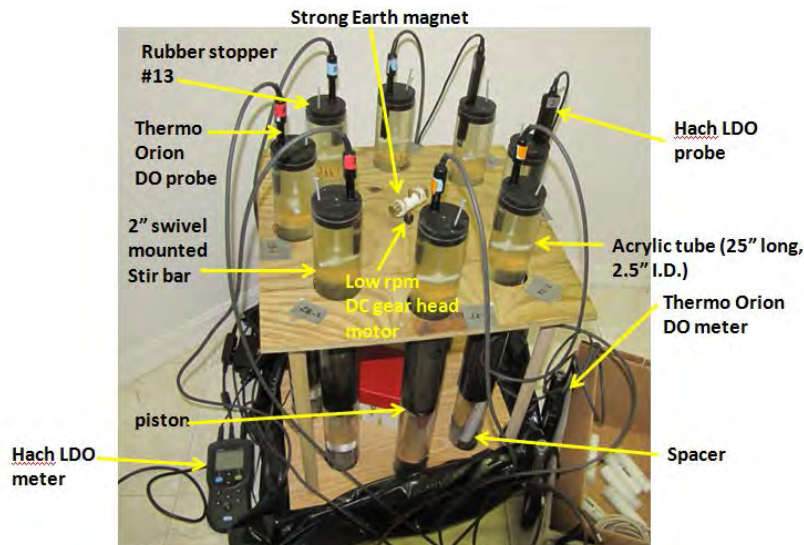


FIGURE 4.4 Picture showing the 8 incubated cores arranged in a rosette around a strong earth magnet mounted onto a low rpm DC gear head rotary motor. The interface sediment-water or floc-water is kept 13cm below the apex of each core. Incubated water (0.4L) is encapsulated in the core with a rubber stopper #13 onto which a DO probe (polarographic = Thermo Orion probe, LDO = Hach probe) and a 2" long 5/16" thick swiveling magnetic stir bar are mounted. The stir bar maintained slow mixing in the incubated water while DO probes readings were transmitted to the meters every 10 (Thermo Orion) or 15 minutes (Hach). The incubations were performed in the dark at a room temperature set at 25°C. See text for more details about this setup.

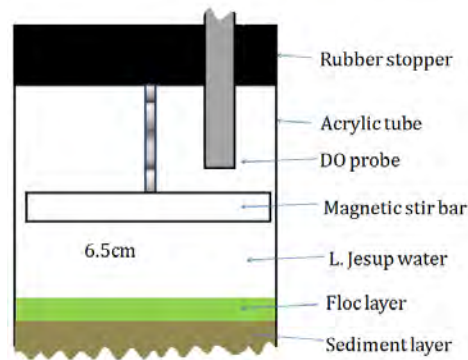


FIGURE 4.5 Diagram showing the top of each acrylic core during the incubation of the sediment and floc. The interface was kept 13cm below the apex of the core so that 0.4L of L. Jesup (station LJ-28 water) would be encapsulated. The magnetic stir bar slowly rotated at 20rpm to provide a uniform mixing in the water without creating sediment resuspension. Mixing allows for representative measurement of DO in the water made with the DO probe at every 10-15 minutes. See text for more details.

4.11 Physical transport of suspended solids

The physical transport of suspended solids and their associated nutrients in Lake Jesup, is determined by a complex suite of interacting processes in shallow eutrophic waters. Shallow waters are especially subject to wind and wave forcing.

4.11.1 Instruments used

The suspended solid transport dynamics at the site were explored using acoustic and optical instruments. A 10Mhz Sontek Acoustic Doppler Velocimeter (ADV) measured the 3 components of velocity in a small volume ($1/3 \text{ cm}^3$) as well as the pressure. In addition to estimation of current speed and directions, the magnitude of the acoustic return from many acoustic current meters such as the ADV may be used as a proxy for suspended solids concentrations. The acoustic return in dB (called acoustic backscatter, or echo amplitude), can be linearly related to the log of the suspended solids concentration (e.g. Fugate and Friedrichs, 2002 and references therein). The ADV was coupled with a D & A Optical Back Scatterer (OBS). The ADV was configured to sample 10 minute bursts every hour at a sampling rate of 15 Hz, thus providing 9000 current measurements per burst. In the deployments from November 2010 to April 2011, a 2MHz Aquadopp profiler with high resolution capabilities was also deployed. The Aquadopp measured the water column from 5 cm above the sensor to around 1.5 meters above the bottom at a 5 cm bin resolution. The 3 components of velocity as well as the acoustic backscatter are measured at each vertical bin. The data from the Aquadopp and from the ADV in these later deployments were much better and more useful for examining the suspended solids dynamics of the lake, compared to the earlier deployments. The focus of this report is therefore on the latter deployments. The ADV, Aquadopp, and OBS were mounted on a platform and deployed on the bottom at the site (Fig. 4.6). A Sequoia Science Laser *In Situ* Scatterer and Transmissometer 100X

(LISST) measures particle size distributions ranging from 5 to 500 microns in the water column using laser diffraction methods. However, because calibrations of the LISST show a bias that indicates high concentrations of large particles which did not exist in the calibration standards, the top four size bins were dropped. This narrowed the range of measured particles to 5 to about 250 microns. The LISST was hung from a floating platform higher in the water column to measure the more variable sediment properties above the floc layer.

4.11.2 Total Suspended Solids (TSS)

Bulk water samples were collected with an ISCO sampler from the water column, and stored in a refrigerator after transporting to lab. Total suspended solids concentrations were determined gravimetrically from the bulk water samples. First, 47 μm glass filters were baked at 525C then pre-weighed. Approximately 100 ml of the bulk water sample was filtered, then dried at 80° C for 24 hours, weighed, then dried another 24 hours and weighed again. Once the weight stabilized (another drying cycle was performed if necessary), these values were used to derive the TSS concentration. In order to estimate the organic content of the suspended sediment, the filters were then baked in a muffle furnace at 525° C for four hours. Subsequently, the filters were weighed to determine the loss on ignition of volatile matter.

4.11.3 Calibration of acoustic instruments

There was a generally very good correlation between the OBS and the acoustic backscatter. However, on some deployments, there appeared to be random deviations in the OBS return, perhaps due to electrical noise or interference by fish. Because the amplitude appeared to be more consistent than the OBS readings, the amplitude was used as a more reliable proxy for suspended sediment in this report.

Mass concentrations that were measured gravimetrically from pumped water samples were used to calibrate the acoustic backscatter for both the ADV and Aquadopp. Acoustic backscatter from the profiles had to first be adjusted for near field spreading and range correction (see below). Since these calibrations are based on *in situ* samples, the adjustments were not necessary for the ADV, which samples only one discrete point rather than a profile. The near field range corrected backscatter from the 10th bin (0.75 meters above the bottom (mab) from each deployment was calibrated with the concentrations from pumped samples that were measured at the same time, or interpolated between measurements if the pumped sample was taken between bursts measured by the Aquadopp. Because the acoustic instruments are more sensitive to the inorganic (i.e. denser) portion of the suspended sediments, the calibrations were performed on the TSS concentration minus the total organic carbon (TOC) concentration. This produced much better calibrations than just using the TSS alone (Fig. 4.7).

Although the strong correlation between the independent OBS and acoustic backscatter measures suggest that they are indeed sensing real variations in suspended matter (for example the Feb 2011 deployment), calibrations with bulk water sample gravimetric analyses were generally poor for the ADV (although June/July 2009, August 2009 were reasonable, excluding a few outliers). This may be because of the relatively low variability

of TSS concentrations compared to higher energy environments, and the occasional lack of contemporaneous bulk water sampling and ADV sampling. Also, the wide range and high percentage of organic matter may have caused significant variations in aggregate density so that there were too few bulk water samples to get a robust calibration curve for such a small range in variation. Particle size distributions from the LISST suggest that during periods when resuspension is high, a population of aggregates around 90-140 μm are resuspended. These populations of aggregates or sediment particles have higher inorganic content. This change in particle population densities and sizes may also contribute to calibration error. A final contributing factor may be that the acoustic frequency of the ADV (10 MHz) was not as sensitive to the dominate particle sizes as the Aquadopp (2 MHz). Consequently, a conservative ad hoc calibration of the ADV was performed separately for the 2nd Jan 2011 and 3rd April 2011 deployment (the ADV malfunctioned in the first November 2011 deployment) by calibrating the minimum acoustic backscatter with the minimum measure from the pumped samples and the maximum acoustic backscatter with the maximum measure from the pumped samples.

4.11.4 Range correction

Acoustic backscatter from the Nortek Aquadopp was range corrected for acoustic spreading, and water absorption using the relationship established in (Lohrmann, 2001):

$$EL = \text{Amp} * 0.43 + 20 \log_{10} R + 2 \alpha_w * R + 0$$

where Amp is the measurement from the sensor, R is the range, and 0 is assuming that particle attenuation is negligible and less than errors associated with gravimetric sampling.

Near the transducer the acoustic signal spreads in a complex non-spherical manner (e.g. Hill et al. 2003). The near field correction for this may be expressed according to Thorne et al. (1993):

$$\begin{aligned} \psi &= 1 && \text{for } r > \epsilon r_n, \\ \psi &= \frac{1}{3} \left(2 + \epsilon \frac{r_n}{R} \right) && \text{for } r < \epsilon r_n, \end{aligned}$$

where ϵ is set to 2, $r_n = \pi a_t^2 / \lambda$, and a_t is the radius of the transducer, $\lambda = c/f$ is the wavelength of the transmitted pulse, with c the speed of sound and f the frequency. For the 2 MHz Nortek Aquadopp, r_n is 0.821 m and the region where the near field correction needs to be made is 1.64 m (Kawanisi and Yokoyama, 2008).

4.11.5 Settling velocity estimates using Reynolds Flux

In a steady state condition near the bed, there is a balance between the degree of mixing away of the vertical gradient in TSS concentration created by the settling of particles:

$$-w_s C = K \partial C \partial z$$

where w_s is the settling velocity of the particles, C is the concentration of particles, K is the eddy diffusivity, and z is in the vertical direction. The left side of the equation represents the downward flux by settling, and the right side represents the upward flux by turbulent

mixing and resuspension. The vertical diffusive flux on the right side can be measured using the ADV and Reynolds averaging:

$$K \frac{\partial C}{\partial z} = \overline{w'C'}$$

where w' is deviations of the vertical velocity from the burst mean and C' is deviations of the concentration from the burst mean. This is called the Reynolds sediment flux and is a measure of the degree of turbulent dispersion, or turbulent flux of sediment. During steady state periods, the settling velocity and background concentrations may then be estimated (Fugate and Friedrichs, 2002, 2003).

4.11.6 Wave calculations

Wave period spectra were calculated using along-beam velocities from the highest highest bin above the bottom measured by the Aquadopp. . The spectra were calculated using a Welsch spectral estimator with a Hanning window of 256 (provided in Matlab ©). Bursts from the Aquadopp were measured either at 4 or 8 Hz, depending on the deployment, capable of resolving 1 second waves. This period was the dominant period and corresponds well to the mean of expected waves using the shallow water wave theory in shore protection manual method for shallow water waves (USACE, 1984).

Wave analyses using PUV algorithms did not seem consistent with concentrations, and appeared to be affected by the same within-burst noise of current data. However wind speed and direction from nearby weather stations were used to estimate the wave activity. Significant wave height and periods at the site location were estimated using the shore protection manual method (SPMSWG) for shallow water waves (USACE, 1984). The adjustment velocity used in the SPMSWG method underestimates the low wind speeds that are typically found over the site, therefore the adjust velocity factor was set to one, rather than 0.71. For waves that are not fetch limited, the average period would be about 1.2 seconds in the lake, and therefore, travel about 1.9 m s^{-1} (associated wavelengths are about 2.25 m). Maximum fetch is about 6700 meters, so it will take about one hour for a wave to travel the fetch distance at that speed. Thus, wind speed and direction need to be constant for about one hour for the wave to become fetch limited and hourly averages should provide the necessary time interval to estimate fetch limited waves. Wind speed and direction were smoothed using a running average with an hour window, and wave heights and periods were determined from these speeds. The fetch was determined by the wind direction using the distances in Table 4.2. Fetches for directions not in Table 4.2 were determined by linear interpolation between the two nearest available fetches.

4.11.7 Wave, current and combined wave current shear stresses

Mean currents were generally low at the site, and resuspension events were dominated by waves. The critical shear stress caused by combined wave and currents are a subject of much investigation (e.g. Wiberg, 1995; Soulsby 1993; Grant-Madsen, 1979). The combined shear stress may be much greater than the simple addition of the two separate stresses, and its magnitude depends upon the angle between the waves and mean current. Soulsby's (1997) method for calculating the combined shear stress was used for this study. For this calculation, the direction of the waves was assumed to be the same as that of the

wind, and the direction and speed of the current was measured by the Aquadopp. Significant wave heights and periods were determined from SPMSWG. Wave orbital velocities were estimated by:

$$u_b = \frac{H\omega}{2\sinh(kh)}$$

where H is the significant wave height, ω is the wave angular frequency, k is the wave number, and h is the height of the water column. The bottom roughness height was assumed to be a Nikuradse height of 0.001 m. For wave orbital velocities less than 0.01 m s^{-1} , maximum wave friction velocity and the combined wave current friction velocity were set to the same as the current friction velocity.

TABLE 4.2 Fetch calculation as a function of the distance over which the wind blows from site LJ28 and the wind direction.

Direction	angle (°)	fetch (m)
N	0	1767
NNE	22.5	4064
NE	45	2995
ENE	67.5	2021
E	90	1393
ESE	112.5	898
SE	135	1135
SSE	157.5	981
S	180	1173
SSW	202.5	3169
SW	225	4762
WSW	247.5	6702
W	270	1330
WNW	292.5	3084
NW	315	2177
NNW	337.5	1324

10MHz Sontek Acoustic Doppler Velocimeter (ADV)

- Measures pressure, 3 components of velocity
- Measures acoustic backscatter, a proxy for TSS
- Small measurement volume (1/3 cm³)
- High frequency sampling (15 Hz)
- OBS attached

2MHz Aquadopp profiler with high resolution capabilities

- Measures pressure
- Measures profiles of 3 components of velocity (cell size 0.05 m)
- Measures profiles of acoustic backscatter, a proxy for TSS
- Sampling Frequency (8 and 4 Hz)

Sequoia Science Laser In Situ Scatterer and Transmissometer 100X (LISST)

- Measures particle size distributions ranging (5 to 500 microns) in the water column using laser diffraction methods
- Hung in upper water column

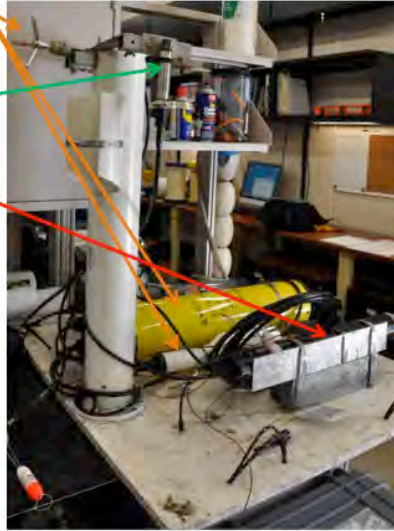


FIGURE 4.6 Instruments deployed to measure physical sedimentology.

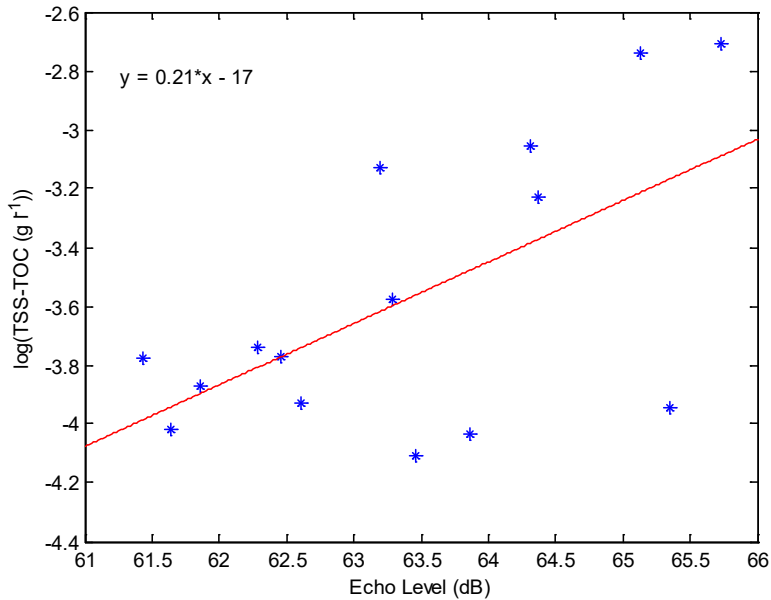


FIGURE 4.7 Calibration of Aquadopp range-corrected acoustic echo to inorganic fraction of TSS ($R=0.60$, with a $p<0.05$).

4.12 Statistical Analysis

Correlations were made using Pearson 2-tailed correlations to understand the relationships of the various data collected. One-way ANOVA's were conducted for all data with either Dunnett's C or Tukey – REGWQ Post Hoc test used depending on the homogeneity of variance tests. Box and whiskers were conducted from the results and labeled (a, b, c, etc.) representing significant differences at $p < 0.05$. All statistical analysis was done using SPSS version 18.

5.0 RESULTS

5.1 Sediment Type

Sediment recovered by grab samples and cores were predominantly flocculent and gyttja (Fig. 5.1). Peat, sand, pink marl and blue clay were also observed in the lake sediments, but were

not sampled or analyzed, because they exceeded the sampling depth or were not present at the sample location.

Floc within Lake Jesup was observed to be an organic-rich material (7.57% to 42.59%), unconsolidated and dark brown in color with a mean OM content of 33.28%. Floc is a unconsolidated sediment, and in this report, we use the field definition, which is “floc flows” (Anderson et al., 2004). Floc was found at all sites during most deployments, except for deployment 8 (January, 2011) at sampling station LJ28. Thickness of the floc varied with each deployment and location, ranging from 0.0 cm to 5.0 cm (Average of 3.2cm for deployments 6 to 9; Table 5.1). Floc thickness was not measured for deployments 1 through 5, but samples were collected.

Gyttja is a semi-consolidated sediment that is organic rich and dark brown to black in color with organic carbon <50% (Wetzel 2001). Fresh gyttja is very soft and hydrous containing organic matter, mineral matter and inorganic precipitates. Hansen (1961) observed that gyttja is present in large eutrophic lakes where phytoplankton productivity dominates. In Lake Jesup, Gyttja is found directly below the floc layer when present and had a black-greenish color and often times contained whole and fragmented mollusk shells.

5.2 Sediment Trap Analyses

Total C, N and P were analyzed in all TSS samples. In total, 114 samples (Floc = 30, Sediments = 31, STHA = 33, STM8 = 20) were collected and analyzed. Teller trap samples (STT) did not collect sufficient material and therefore, in most cases, could not be analyzed for TC, TN and TP (STT = 9 samples). Samples were also analyzed for bulk density, pH, %OM and %Water.

Gyttja nutrient concentrations (TN, TC and TP) were lower than floc and trap solids. This difference was observed for organic matter, %Water and with gyttja having higher values for bulk density. It is clear from box and whisker plots in this section (e.g. Figs 5.2 etc.) that there is a distinct separation between the floc, sediments (gyttja) and trap samples with some potential mixing between floc and trap samples and floc and sediment (gyttja) samples.

TP concentrations for all solids, including floc, trap material, and sediments, were significantly correlated with TN, TC, %OM, and %Water and inversely correlated for bulk density, TIC and pH (Table 5.2). TN for all solids has a significant correlation with TC, %OM, and %Water and inversely correlates with TIC, bulk density and pH. TC shows significant correlations between %OM and %Water and inversely correlated with TIC, bulk density and pH. TIC has an inverse correlation with %OM, %Water and bulk density and correlates significantly with $\delta^{15}\text{N}$ and pH. $\delta^{15}\text{N}$ significantly correlates with $\delta^{13}\text{C}$ and bulk density and inversely correlates with %Water. $\delta^{13}\text{C}$ inversely correlates with %Water. %OM correlates with %Water and inversely correlates with bulk density and pH. %Water is inversely correlated with bulk density and pH and bulk density correlates well with pH.

5.2.1 Phosphorus

Total phosphorus (TP) concentrations, of the lake sediments (floc and gyttja) and trap material, varied by each deployment, site and sediment type ranging from 212 to 2721 $\mu\text{g g}^{-1}$ dw with a mean of 1,496 $\mu\text{g g}^{-1}$ dw for the entire sampling period (Fig. 5.2). Floc grab samples ranged from 285 to 2,209 $\mu\text{g g}^{-1}$ dw with a mean of 1,282 $\mu\text{g g}^{-1}$ dw (Table 5.3). Sediment grab samples collected below the floc layer had a relatively lower mean of 663 $\mu\text{g g}^{-1}$ dw with a range of 212 to 1,923 $\mu\text{g g}^{-1}$ dw. All trap sample solids were relatively higher than the sediment types collected. High aspect ratio traps (SHTA) had a range from 982 to 2652 with a mean of 2,028 $\mu\text{g g}^{-1}$ dw and Mark8 autosampler (STM8) had a range from 991 to 2,720 $\mu\text{g g}^{-1}$ dw with a mean of 2,199 $\mu\text{g g}^{-1}$ dw (deployments 4 and 5 only). The Teller traps, (STT) did not have much success collecting a viable sample in almost all cases. Of the samples we collected the range was 1,014 to 2,078 $\mu\text{g g}^{-1}$ dw with a mean of 1,699 $\mu\text{g g}^{-1}$ dw (deployment 5 only). STT traps were not consistently reliable during the course of this study however, deployment 5 was successful in collecting samples for three sites (LJ14, LJ22 and LJ28). This is the only consistent data collected during the two-year study period for the plate traps and results may prove valuable for future work.

Over the course of the nine deployments the TP concentrations of the different lake components fluctuated in a cyclical pattern with winter months having the higher TP concentrations and the summer months having the lower concentrations (Fig. 5.3). Also, during the course of the deployments there is a well-defined variability between the sediment types per each deployment for TP. The trap samples have a relatively higher concentration of TP (982 to 2,652 $\mu\text{g g}^{-1}$ dw), followed by the floc (385 to 2,209 $\mu\text{g g}^{-1}$ dw), with the grab sediments (212 to 1,923 $\mu\text{g g}^{-1}$ dw) having the lowest concentrations (Fig. 5.4).

5.2.2 Nitrogen

Total nitrogen (TN) concentration analysis had similar results to TP with trap samples having the higher relative concentrations, followed by floc and then grab sediments having the lowest, ranging from 0.0 (or below detection) to 20.8 mg g^{-1} (Fig. 5.5). The floc samples had a range from 7.7 to 23.6 mg g^{-1} and a mean of 17.1 mg g^{-1} . Sediment grab samples had a mean of 8.5 mg g^{-1} , ranging from mean of 24.9 mg g^{-1} (deployment 4 and 5 only) with a range of 20.0 to 28.27 mg g^{-1} and STT trap concentration ranged from 24.5 to 24.9 with a mean of 24.7 (deployment 5 only).

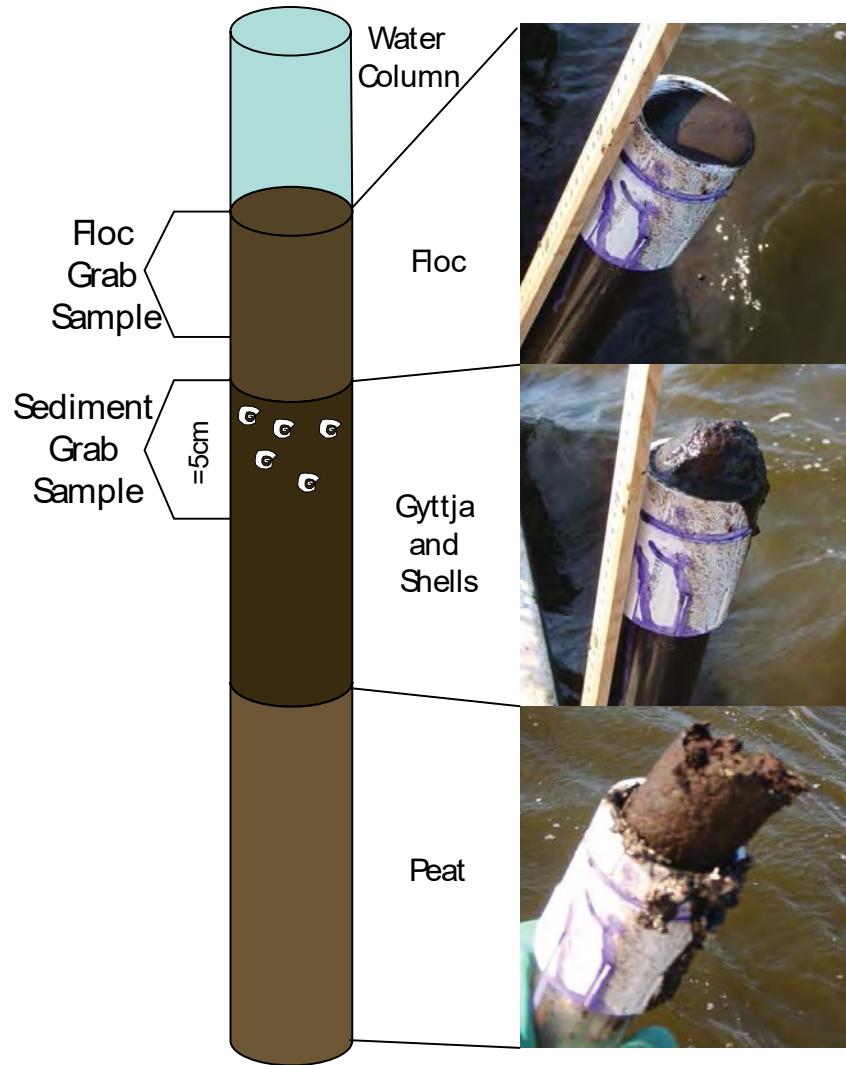


FIGURE 5.1 Representative layering at depth of sediment within Lake Jesup with pictures. Top photo is representative of floc (a type of consolidated sediment), middle photo is representative of gyttja and the bottom photo is typical of peat. The core [drawing](#) is not to scale.

Table 5. 1 Mean and standard deviation of floc thickness for deployments 6, 7, 8 and 9. Deployments 1 to 5 were not measured.

Site	Trip	Mean(cm)	Std. Dev. (+/-)	N
LJ14	6	3.03	0.13	2
	7	4.51	0.49	2
	8	4.64	0.04	2
	9	3.11	0.24	2
	Total	3.82	0.83	8
LJ22	6	4.02	0.06	2
	7	3.34	0.08	2
	8	3.25	0.31	2
	9	3.20	0.06	2
	Total	3.45	0.37	8
LJ28	6	2.21	0.00	2
	7	2.51	0.02	2
	8	.00	0.00	2
	9	1.51	0.00	2
	Total	1.55	1.03	8
LJ44	6	3.36	0.06	2
	7	4.26	0.22	2
	8	4.38	0.04	2
	9	3.61	0.69	2
	Total	3.90	0.54	8
All stations	6	3.15	0.70	8
	7	3.65	0.87	8
	8	3.07	1.97	8
	9	2.86	0.90	8
	Total	3.18	1.20	32

0.0 (or below detection) to 15.7 mg g⁻¹ (Table 5.4). STHA traps had TN concentrations ranging from 7.0 to 28.7 mg g⁻¹ with a mean of 24.0 mg g⁻¹. STM8 concentrations have a

TN values over the course of the period varied by deployment, although with less variation than TP. The concentrations between sediment type is well defined, with sediment trap solids having the higher concentrations of TN, grab sediments had the lower relative concentrations and floc somewhere between the sediment grab samples and the trap samples (Fig. 5.6).

5.2.3 Carbon

Carbon analysis consisted of total carbon (TC) and total inorganic carbon (TIC). TC concentrations had similar results to TN showing less variation in sample fluctuation than TP with TC concentrations ranging from 29.7 to 277.1 mg g⁻¹ (Fig. 5.7). Floc TC concentrations ranged from 77.8 to 209.2 mg g⁻¹ with a mean of 164.4 mg g⁻¹. Sediments had the lowest relative TC concentrations ranging from 29.7 to 174.8 mg g⁻¹ with a mean of 118.7 mg g⁻¹ (Table 5.5). Trap solids had the highest TC concentrations, with STHA traps having a mean of 226.0 mg g⁻¹, ranging from 68.5 to 277.1 mg g⁻¹. STM8 had TC concentrations ranging from 189.7 to 253.6 mg g⁻¹ and a mean of 224.2 mg g⁻¹ and STT concentrations ranging from 220.9 to 225.2 mg g⁻¹ with a mean of 223.5 mg g⁻¹.

%OM	%Water	Bulk Density	pH
785**	0.574**	-0.532**	-0.630**
935**	0.704**	-0.632**	-0.666**
932**	0.645**	-0.575**	-0.590**
.390**	-0.473**	-0.447**	0.308**
0.022	-0.458**	0.433**	-0.144
0.001	-0.228**	0.146	0.101
-	0.663**	-0.616**	-0.627**
	-	-0.938**	-0.522**
		-	0.497**

TABLE 5.2 Correlation matrix of **solids** analysis with n = 117 (except for pH, n = 116 and bulk density, n = 128), for all **solids** (floc, sediments, STHA, STM8 and STT). ** = significant at p < 0.01.

TC concentrations varied through the course of the nine deployment periods. There was a similar relationship what was previously observed with TP, with floc having the highest concentrations of TC and grab sediments with the least. In some cases the grab sediment and the floc layer are slightly similar in their concentrations, much more so then TN. The trap samples have much higher concentrations of TC then the floc or grab sediments (Fig. 5.8). TIC was relatively low through the course of the study. The average TIC concentration for all samples was 1.44 mg g^{-1} but a majority of the samples were 0, or below detection limits. Sediments collected by grab sampling had a TIC with a mean of 5.1 mg g^{-1} .

5.2.4 Bulk Density

Bulk density of the sediments ranged widely from 0.018 to $0.707 \text{ g dw cm}^{-3}$ with a mean of $0.087 \text{ g dw cm}^{-3}$ ($n=128$) (Fig. 5.9 & 5.10 and Table 5.6). Floc and all trap samples had a bulk density less than $0.10 \text{ g dw cm}^{-3}$ with floc, in most cases, having a slightly higher bulk density then STHA and STM8 traps. Floc ranged from 0.021 to $0.082 \text{ g dw cm}^{-3}$ with a mean of $0.049 \text{ g dw cm}^{-3}$. STHA had a mean of $0.035 \text{ g dw cm}^{-3}$ ranging from 0.018 to $0.075 \text{ g dw cm}^{-3}$. STM8 had a similar mean to STHA trap samples of $0.034 \text{ g dw cm}^{-3}$ ranging from 0.021 to $0.046 \text{ g dw cm}^{-3}$. STT trap samples had a mean of $0.076 \text{ g dw cm}^{-3}$, ranging from 0.075 to $0.079 \text{ g dw cm}^{-3}$.

5.2.5 pH

The pH of the sediments ranged from 6.47 to 8.23 with a mean of 7.31 . Floc had the lowest pH, while grab sediments had the highest (Fig. 5.11). Floc had a mean pH of 7.40 , grab sediments a mean of 7.71 and STHA sediments 7.18 (Table 5.7). STM8 and STT had the lowest pH mean values at 6.95 and 6.88 . The pH of the sediments fluctuated by each deployment, but without an apparent seasonal pattern.

5.2.6 Organic Matter (%)

Organic matter content (%OM) had the highest mean percent in the trap solids and the lowest in the grab sediments (Fig. 5.12). %OM of floc ranged from 7.6 to 42.6% with a mean of 33.3% , while grab sediments ranged from 2.9 to 43.2% with a mean of 21.7% (Table 5.8). Trap samples ranged from 28.4 to 65.5% OM with STHA traps having a mean of 47.2% , STM8 44.7% and STT 44.9 . During the course of the study the %OM showed a fluctuation between sediment types and deployments. August, 2009 (deployment 3) had the highest mean %OM for STHA, January, 2011 (deployment 8) had the highest %OM mean for floc and August, 2010 (deployment 6) had the highest %OM mean for grab sediments, but in most cases by deployment STHA had the higher percents and sediments had the lower %OM (Fig. 5.13).

5.2.8 TP vs. TN vs. TC

Correlations between TP, TN and TC are very high for all sediments (Table 5.8 and Figs. 5.14 and 5.15) Trap material/sediments had the highest concentrations of TP, TN, and TC followed by floc and grab sediments. TN and TC correlate extremely well for all sediment samples. Correlations were also made for TN, TC and TP for floc, grab sediments and STHA samples (Table 5.8). The TN, TC and TP contents all fall on a mixing line. However, without a well defined end member for primary material formed in the lake, it is

not possible to create a mixing model at this time (future work can supply such information).

5.3 Water Chemistry

Surface water grab samples and daily samples of water were automatically collected and analyzed at all nine deployments and are presented in the following sections. Analysis of TP, TN, TOC, dissolved oxygen (DO), chlorophyll-a (Chl-a) and total suspended solids (TSS) were investigated. Correlation analysis for TP, TN, TOC and TSS for the ISCO water samples revealed a significant correlation between TP and TSS and between TN and TOC (Table 5.9).

5.3.1 Water Column Nutrients

Water column total phosphorus (TP) concentrations fluctuated through the course of this study by deployment with a range of 40 to 489 $\mu\text{g L}^{-1}$ and a mean of 150 $\mu\text{g L}^{-1}$ (Table 5.10). Site LJ44 had the lowest mean of 71 $\mu\text{g L}^{-1}$ for TP within the water with a range of 40 to 100 $\mu\text{g L}^{-1}$ (Fig 5.16). LJ28 had the highest mean TP concentrations with a mean of 124 $\mu\text{g L}^{-1}$ and a range of 75 to 215 $\mu\text{g L}^{-1}$ for the water grab samples. Also, for LJ28 the daily autosampler (ISCO) concentrations were higher than the water grab samples with a mean of 169 $\mu\text{g L}^{-1}$ and a range of 44 to 489 $\mu\text{g L}^{-1}$. Over the course of the study the TP concentrations within the water column, based on grab samples decreased (Fig. 5.17).

Water column total nitrogen (TN) fluctuated through the two-year period of this project, concentrations ranged from 0.50 to 7.67 mg L^{-1} with a mean of 1.65 mg L^{-1} (Table 5.10). LJ28 had the highest mean of 1.81 mg L^{-1} for water grab samples, while LJ22 had the least at a mean of 1.108 mg L^{-1} (Fig. 5.18).

Total organic carbon (TOC) for the two-year sampling period reflects a slight decrease over time with a mean of 16.56 mg L^{-1} with a range from 9.60 to 39.53 mg L^{-1} (Table 5.10). Grab water samples for LJ28 had the highest mean of 15.96 mg L^{-1} and LJ22 had the lowest mean TOC concentration of 14.42 mg L^{-1} (Fig. 5.19).

5.3.2 Oxygen

Continuous dissolved oxygen (DO) was only available for a few of the deployments, because the instrument used to measure the DO often times failed to collect or log data. Deployments 2, 3, 4 and 5 collected data by YSI successfully every 30 minutes for the majority of the deployment which resulted in diurnal variations for DO concentrations (Fig. 5.20). Deployments 6, 7, 8, and 9 collected water column DO profiles (with an optical YSI DO meter), twice per trip, once on deployment and once on recovery of instruments and samples. Refer to Table 5.11 for the results of DO by the available deployments.

Profiles of daytime DO for Deployments 6, 7, 8 and 9 for each site (within a 2 hour period) showed that DO concentrations, in most cases, had a slight decrease with depth, until it reached the sediment or lake bottom. At the sediment-water interface oxygen concentrations declined rapidly, reaching nearly 0 mg L^{-1} ; however, it was observed that the lake was oxygenated throughout the water column during the day (Fig. 5.21). DO concentrations could be at 15 mg/L at one site within the lake and 10 mg/L at another, suggesting that lake mixing is not always uniform laterally. This difference could be

associated with the western half of the lake not mixing well with the eastern half of Lake Jesup (Cable et al. 1997).

5.3.3 Chlorophyll-a

Chlorophyll-a (Chl-a) results showed that there was a large fluctuation in concentrations over the two-year long study with a mean of $49.0 \mu\text{g L}^{-1}$, ranging from 6.9 to $138.3 \mu\text{g L}^{-1}$. LJ28 had the highest mean concentrations of Chl-a with a mean of $56.4 \mu\text{g L}^{-1}$ and a range from 8.6 to $103.6 \mu\text{g L}^{-1}$, while LJ14 had the lowest concentrations with a mean of $25.6 \mu\text{g L}^{-1}$, ranging from 7.4 to $79.0 \mu\text{g L}^{-1}$ (Fig. 5.22).

5.3.4 Total Suspended Solids

Total suspended solids (TSS) for Lake Jesup were analyzed from the ISCO water samples for each deployment by Florida Gulf Coast University. These data were used to calibrate the ADV system. April, 2009 (deployment 1) had the highest average TSS amounts at 0.08 g L^{-1} with a range of 0.048 to 0.111 g L^{-1} (Table 5.12). Deployment 3 had the least average TSS amounts of 0.023 g L^{-1} with a range of 0.009 to 0.039 g L^{-1} (Fig. 5.23).

5.4 Stable Isotopes

Results from $\delta^{15}\text{N}$ and $\delta^{13}\text{C}$ indicate that there isn't a clear distinction between the sediment types, although, sediment grab samples had the largest range for both $\delta^{15}\text{N}$ and $\delta^{13}\text{C}$. $\delta^{15}\text{N}$ ranged from 0.94 to 4.94 ‰ with a mean of 2.61 ‰ , while $\delta^{13}\text{C}$ ranged from -24.05 to -18.53 ‰ with a mean of -22.37 ‰ (Fig. 5.24). Grab sediments for $\delta^{15}\text{N}$ ranged from 1.24 to 4.94 ‰ with a mean of 2.67 ‰ , while $\delta^{13}\text{C}$ had a range of -23.77 to -18.53 ‰ with a mean of -22.40 ‰ (Table 5.13).

5.5 Weather

The wet season for the Lake Jesup region generally begins in June and ends in September, while the dry season lasts from November to February. Prevailing winds in fall and winter move in a northerly direction and southerly direction in the spring and summer (Cable et al. 1997). Over the course of this study (from April 2009 to April 2011) the total precipitation for the two-year period was 229.3 cm (data from NCDC- Sanford Airport), with April 2009 to April 2010 (142.0 cm) having close to twice the amount of precipitation then between May 2010 to April 2011 (87.3 cm) (Fig. 5.25 and 5.26). The average wind velocities for the two-year study period were around 3.1 m s^{-1} (7 mph) with wind direction towards the south-southeast. The months with the highest average velocities occurred in the winter months while the lower average velocities were in the summer with an average monthly prevailing wind direction towards the south (NCDC – Sanford Airport and Stations 1 and 2 on the Lake) (Fig. 5.26 and 5.27).

Weather data collected on Lake Jesup was collected every 15 minutes during each deployment. November 2009 had a download error for weather station 1 (located on the barge at LJ28) therefore; data was used from weather station 2 (located near SR46). Table 5.14 shows the averages collected by the weather stations by deployment (wind velocities, precipitation and temperature from weather station 1 and wind direction from weather station 2).

5.6 Current

Lake current within Lake Jesup at LJ28 resulted in currents that moved predominately in a southerly direction (Fig. 5.27). Two deployments (3 and 4) did not collect any data, because of instrument failure or theft. Velocities during deployment averages were, as far east as, 133 degrees or the southeastern direction (April, 2009; deployment 1) and as far west as 230 degrees or southwestern direction (June, 2009; deployment 2). August, 2010 (deployment 6) had the highest deployment average at 0.099 m/s, while January, 2011 (deployment 8) had the slowest deployment average at 0.046 m/s (Table 5.15).

5.7 Total Mass Accumulation

Total mass accumulation rates (MAR) was calculated using STHA trap samples for Total MAR, TP MAR, TN MAR and TC MAR. Deployments 1 and 2 were removed from the data, because the trap design for those deployments was flawed. Total MAR varied by deployment with deployment 4 at LJ22 having the highest ($419 \text{ g dw m}^{-2} \text{ d}^{-1}$) and Deployment 3 at LJ28 having the least ($87 \text{ g dw m}^{-2} \text{ d}^{-1}$; Figure 5.28). MAR TP, TN and TC reflected that of the results from total MAR (Figure 5.29 to 5.31).

5.8 Nutrient Budget Calculations

The nutrient budget for Lake Jesup was calculated using the mass accumulation rates calculated from the sediment trap data. The mass was converted into mass accumulation rate (MAR; $\text{g m}^{-2} \text{ day}^{-1}$). The sediment traps were deployed for a week to two week long period, therefore calculations were made for MAR values weekly for the entire two- year study. The MAR for each week was then summed for a yearly total and the nutrient budget was calculated from August, 2009 to August, 2010 and from April, 2010 to April, 2011.

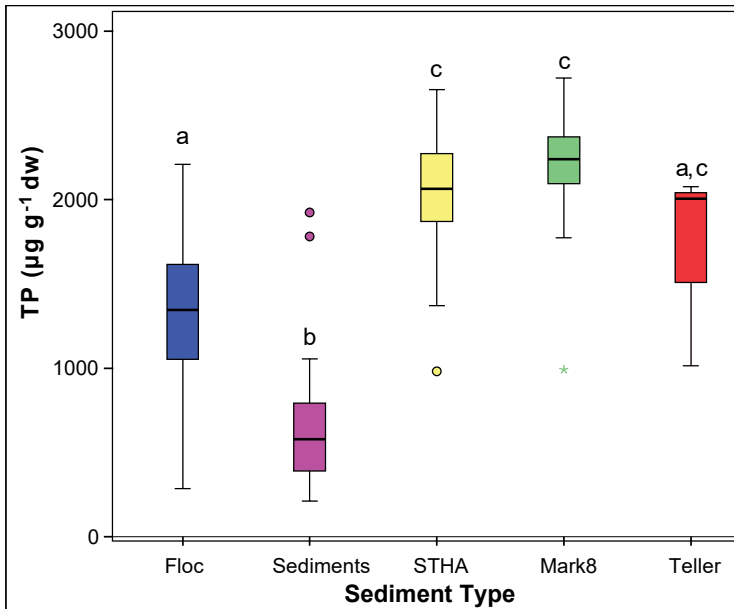


FIGURE 5.2 Box and whisker plots for total phosphorus by sediment type. Significant differences ($p < 0.05$) as determined by ANOVA are denoted by differing letters. Box and Whisker plots show the median value (mid-line) the upper and lower bounds to the middle quartiles (shaded areas of boxes representing 50% of all sample values) and the upper and lower quartiles (whiskers). Symbols represent samples greater or less than 1.5 times the box length and asterisk are considered extreme values. All other box plots have been analyzed in a similar fashion.

TABLE 5.3 Mean, standard deviation and range of total phosphorus ($\mu\text{g g}^{-1}\text{dw}$) for floc, sediments and traps..

Sediment Type	Mean +/- Std. Dev.	Range	n
Floc	1282 +/- 465	285 - 2209	30
Sediments	663 +/- 390	212 - 1923	31
STHA	2028 +/- 392	982 - 2652	31
Mark8	2199 +/- 355	991 - 2721	20
Teller	1699 +/- 594	1014 - 2078	3
All Sediments	1496 +/- 724	212 - 2721	117

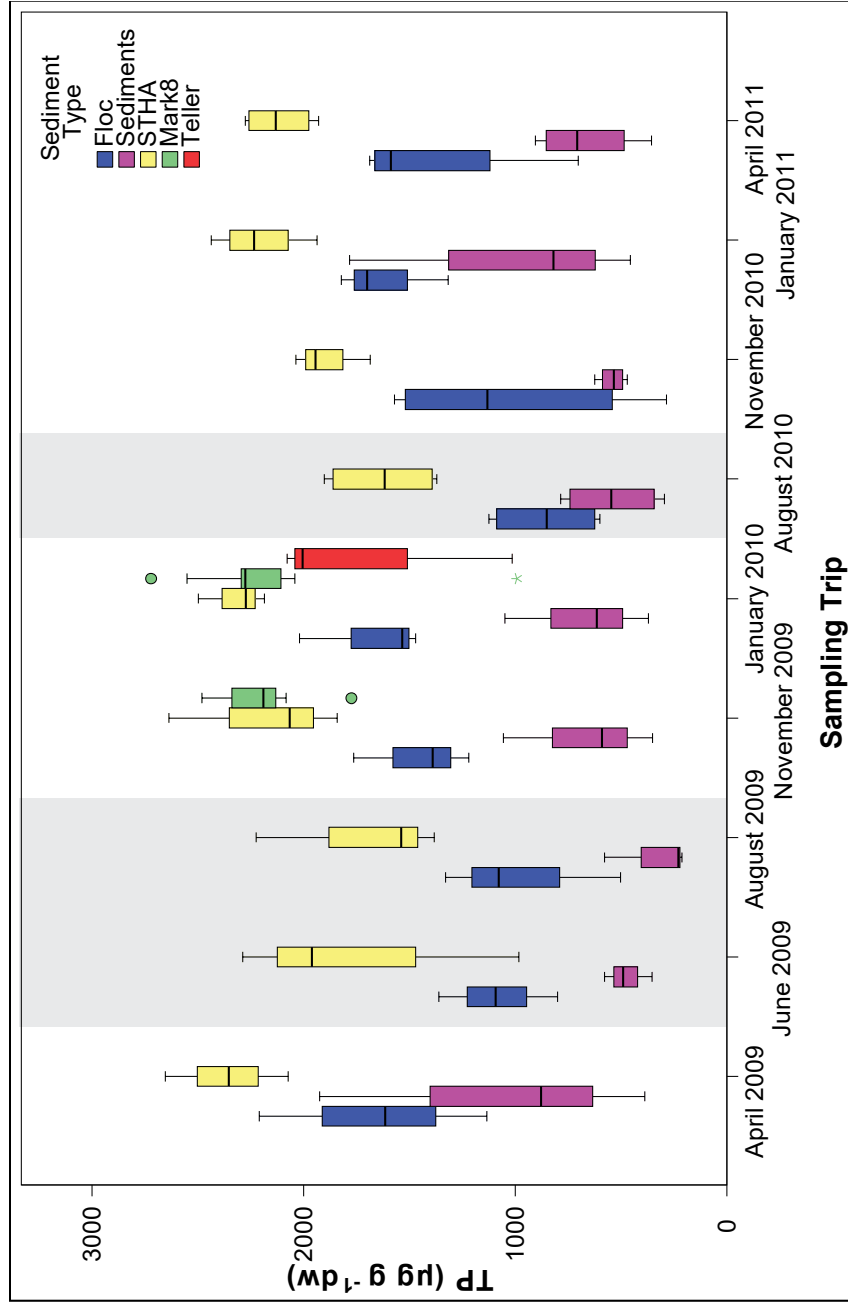


Figure 5.3 Box and whisker plot for total phosphorus by deployment and sediment type. Shading indicates summer periods.

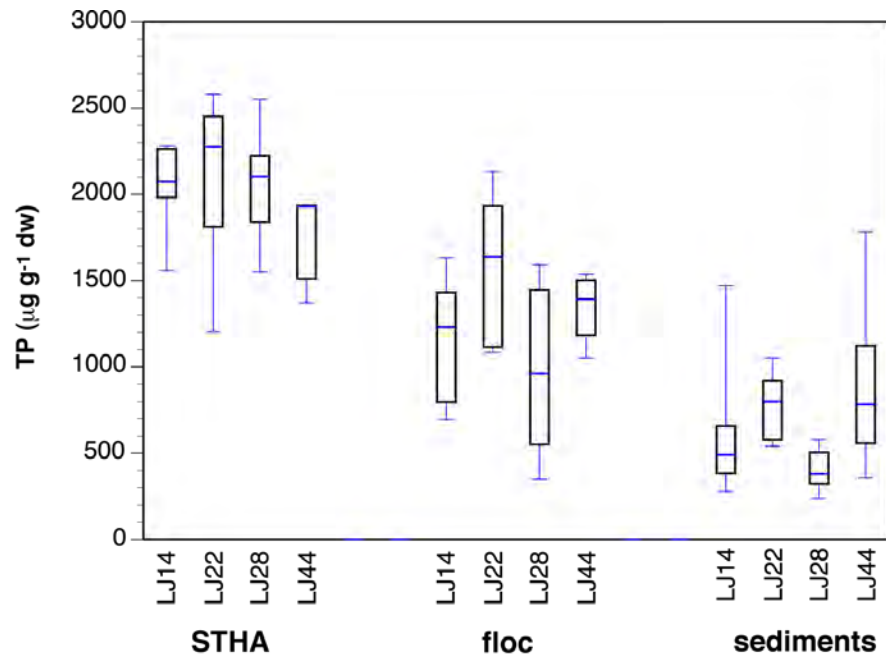


FIGURE 5.4 Variations for total phosphorus for sediment trap – high aspect ratio, floc and sediments.

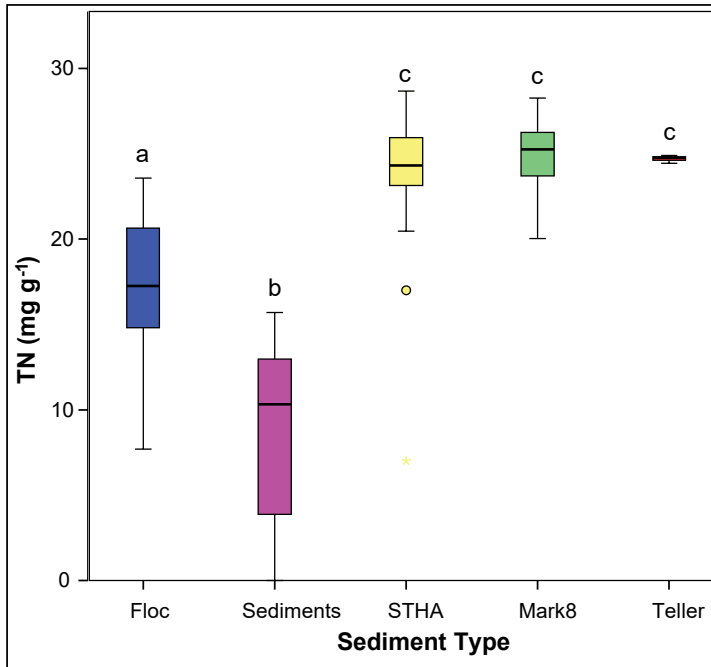


FIGURE 5.5 Box and whisker for total nitrogen by sediment type. Refer to figure 5.2 for explanation of box plot details.

TABLE 5.4 Mean, standard deviation and range of total nitrogen (mg L⁻¹) by sediment type. Refer to figures 5.8 to 5.9 for additional graphs.

Sediment Type	Mean +/- Std. Dev.	Range	n
Floc	17.07 +/- 4.15	7.70 - 23.56	30
Sediments	8.50 +/- 5.34	0.00 - 15.70	31
STHA	23.96 +/- 4.02	7.00 - 28.67	31
Mark8	24.88 +/- 1.89	20.04 - 28.27	20
Teller	24.70 +/- 0.23	24.45 - 24.89	3
All Sediments	18.29 +/- 7.77	0.00 - 28.67	117

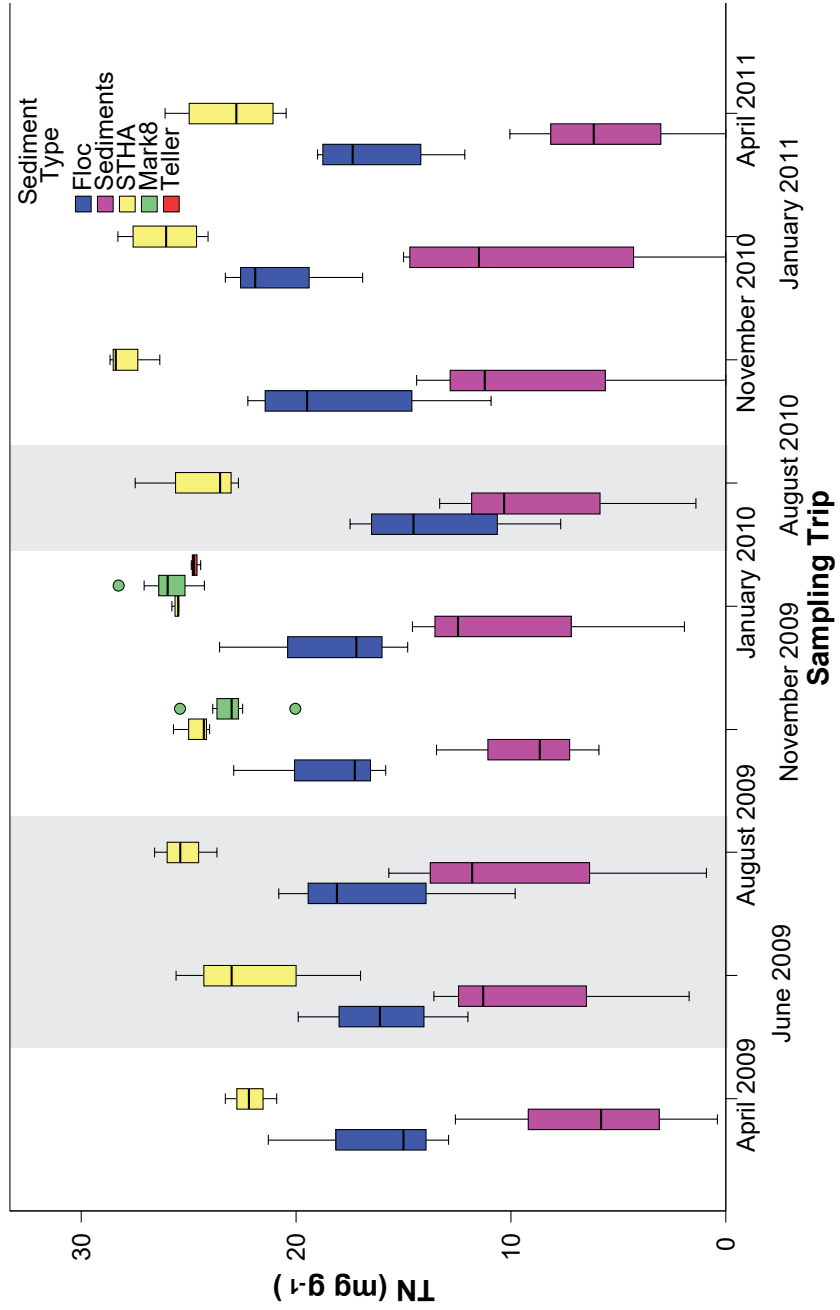


FIGURE 5.6 Box and whisker plot for total nitrogen by deployment and sediment type, refer to figure 5.2 for explanation of box plot details.

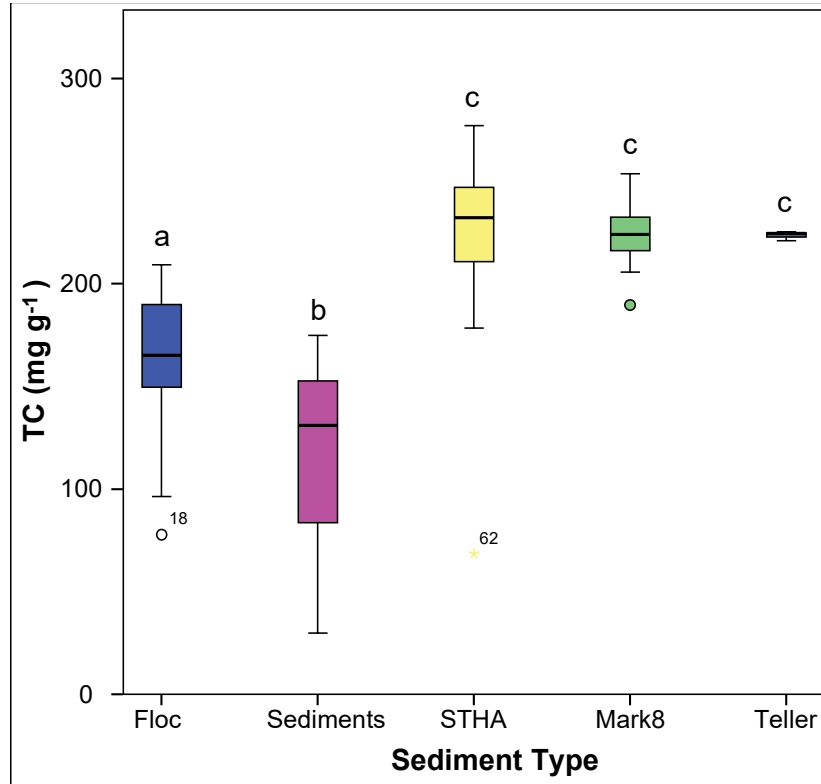


FIGURE 5.7 Box and whisker for total carbon by sediment type. refer to figure 5.2 for explanation of box plot details.

TABLE 5.5 Mean, standard deviation and range of total carbon (mg L^{-1}) by sediment type. Refer to figures 5.12 and 5.13 for additional graphs.

Sediment Type	Mean +/- Std. Dev.	Range	n
Floc	164.40 +/- 33.47	77.80 - 209.24	30
Sediments	118.73 +/- 43.29	29.70 - 174.76	31
STHA	225.98 +/- 36.61	68.50 - 277.06	31
Mark8	224.18 +/- 15.03	189.65 - 253.62	20
Teller	223.53 +/- 2.32	220.88 - 225.21	3
All Sediments	181.33 +/- 56.52	29.70 - 277.06	117

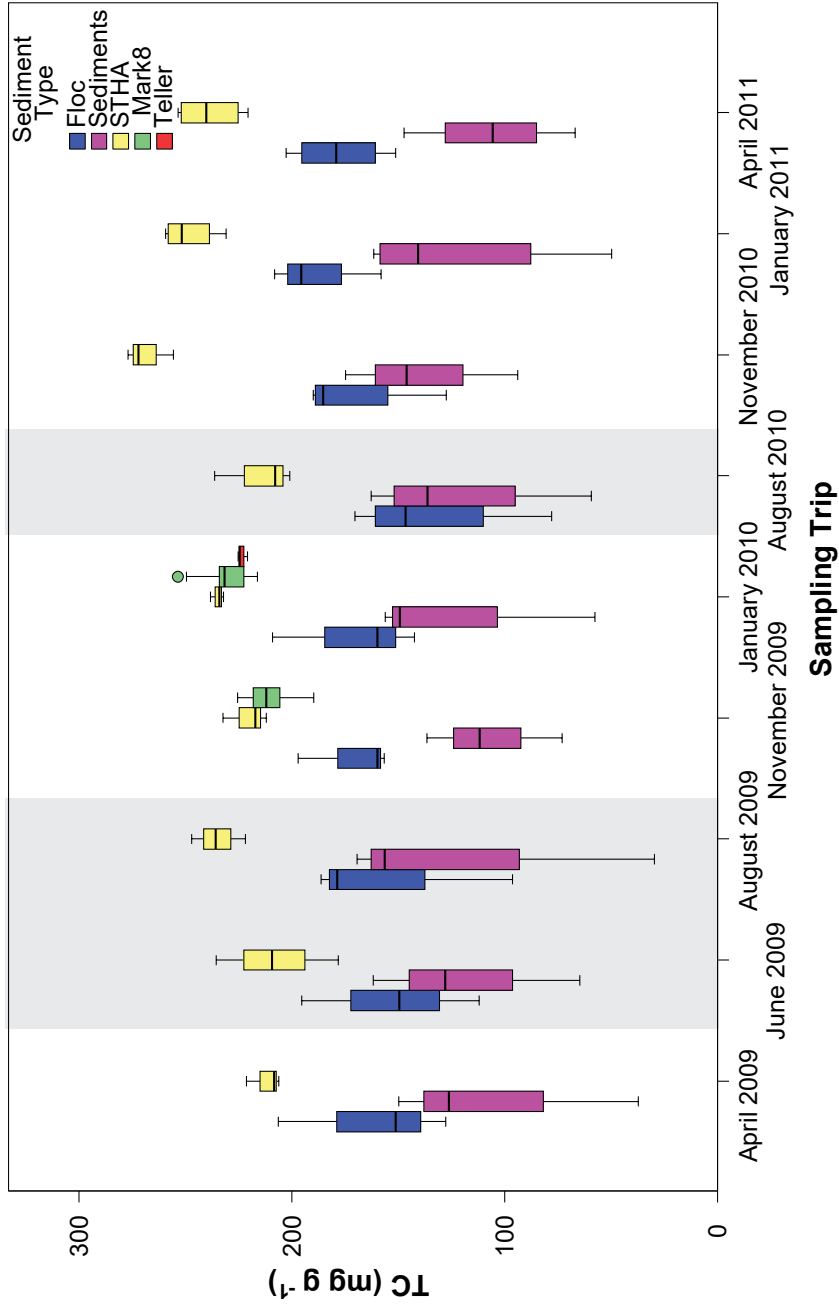


FIGURE 5.8 Box and whisker for total carbon by deployment and sediment type. refer to figure 5.2 for explanation of box plot details.

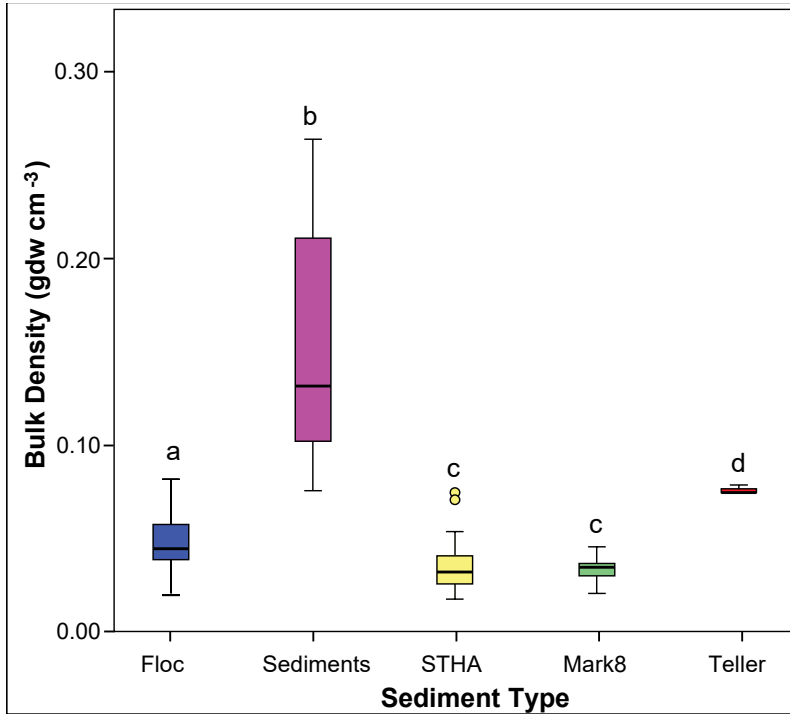


FIGURE 5.9 Box and whisker for bulk density by sediment type, seven outliers for sediments were removed (six from LJ28 and one from LJ22). Refer to figure 5.2 for explanation of box plot details.

TABLE 5.6 Mean, standard deviation and range of bulk density (g dw cm^{-3}) by sediment type. Refer to figures 5.17 and 5.18 for additional graphs

Sediment Type	Mean +/- Std. Dev.	Range	n
Floc	0.049 +/- 0.015	0.021 - 0.082	30
Sediments	0.232 +/- 0.211	0.076 - 0.707	31
STHA	0.035 +/- 0.013	0.018 - 0.075	42
Mark8	0.034 +/- 0.006	0.021 - 0.046	20
Teller	0.076 +/- 0.002	0.075 - 0.079	3
All Sediments	0.087 +/- 0.132	0.018 - 0.707	128

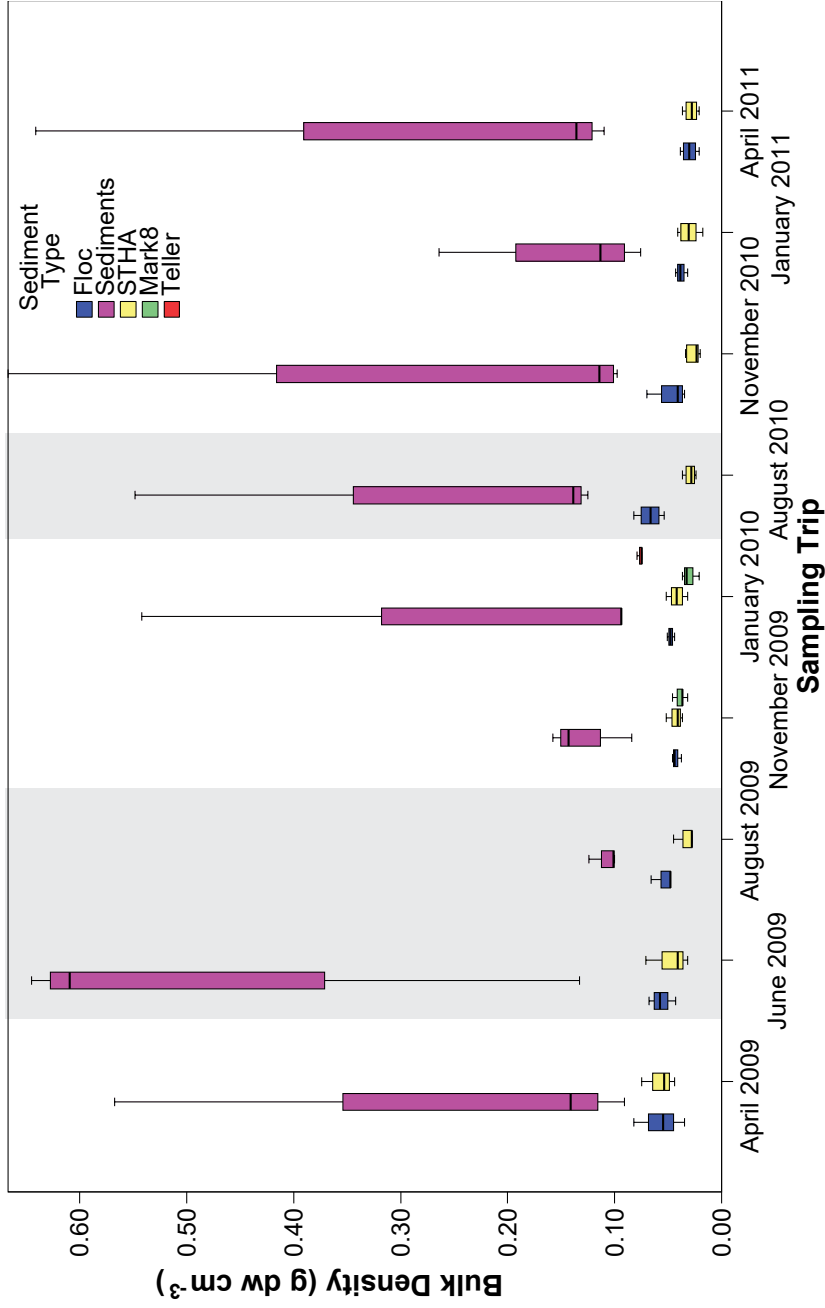


FIGURE 5.10 Box and whisker for bulk density by deployment and sediment type. refer to figure 5.2 for explanation of box plot details.

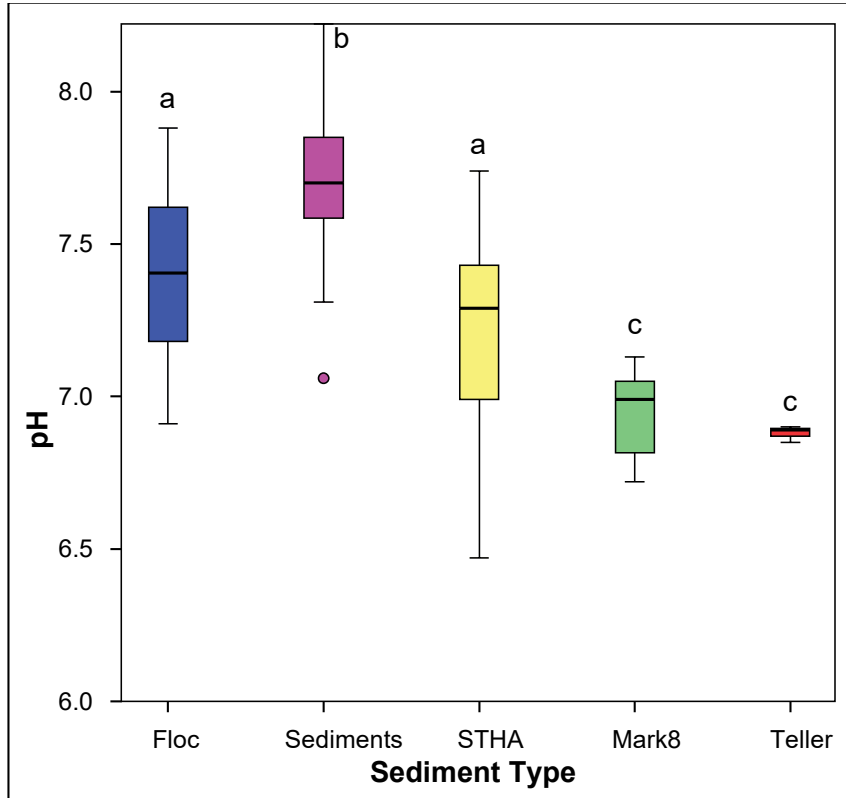


FIGURE 5.11 Box and whisker for total in pH by sediment type. Refer to figure 5.2 for explanation of box plot details.

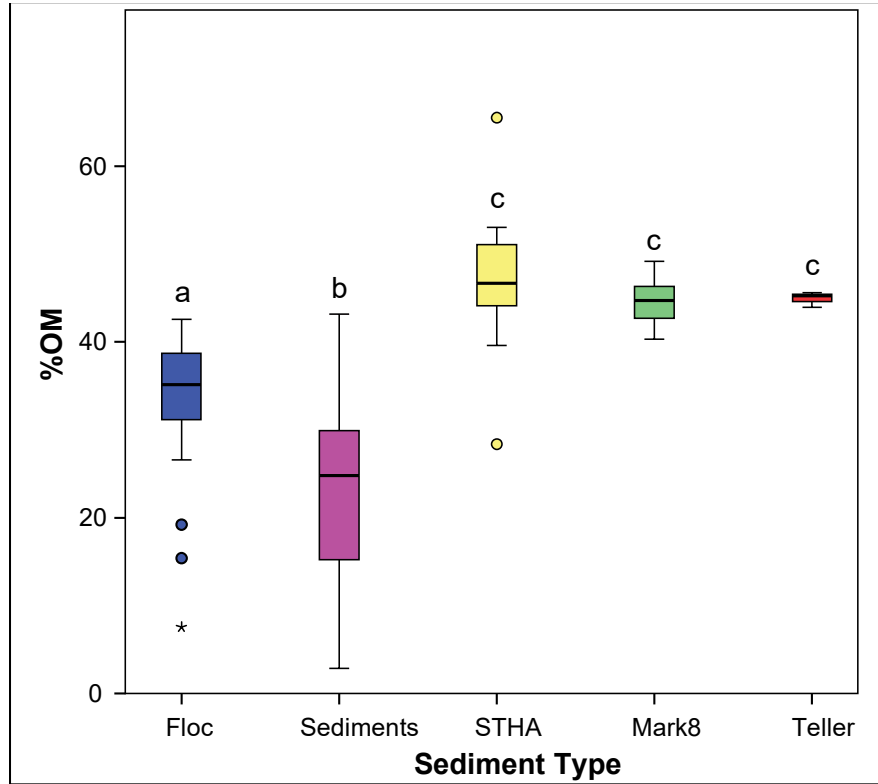


FIGURE 5.12 Box and whisker for percent organic matter by sediment type. Refer to figure 5.2 for explanation of box plot details.

TABLE 5.7 Mean, standard deviation and range of percent organic matter by sediment type. Refer to figures 5.21 to 5.22 for additional graphs.

Sediment Type	Mean +/- Std. Dev.	Range	n
Floc	33.28 +/- 7.96	7.57 - 42.59	30
Sediments	21.73 +/- 10.67	2.86 - 43.17	31
STHA	47.16 +/- 6.22	28.38 - 65.51	31
Mark8	44.65 +/- 2.38	40.34 - 49.17	20
Teller	44.94 +/- 0.86	43.97 - 45.62	3
All Sediments	36.34 +/- 12.74	2.86 - 65.51	117

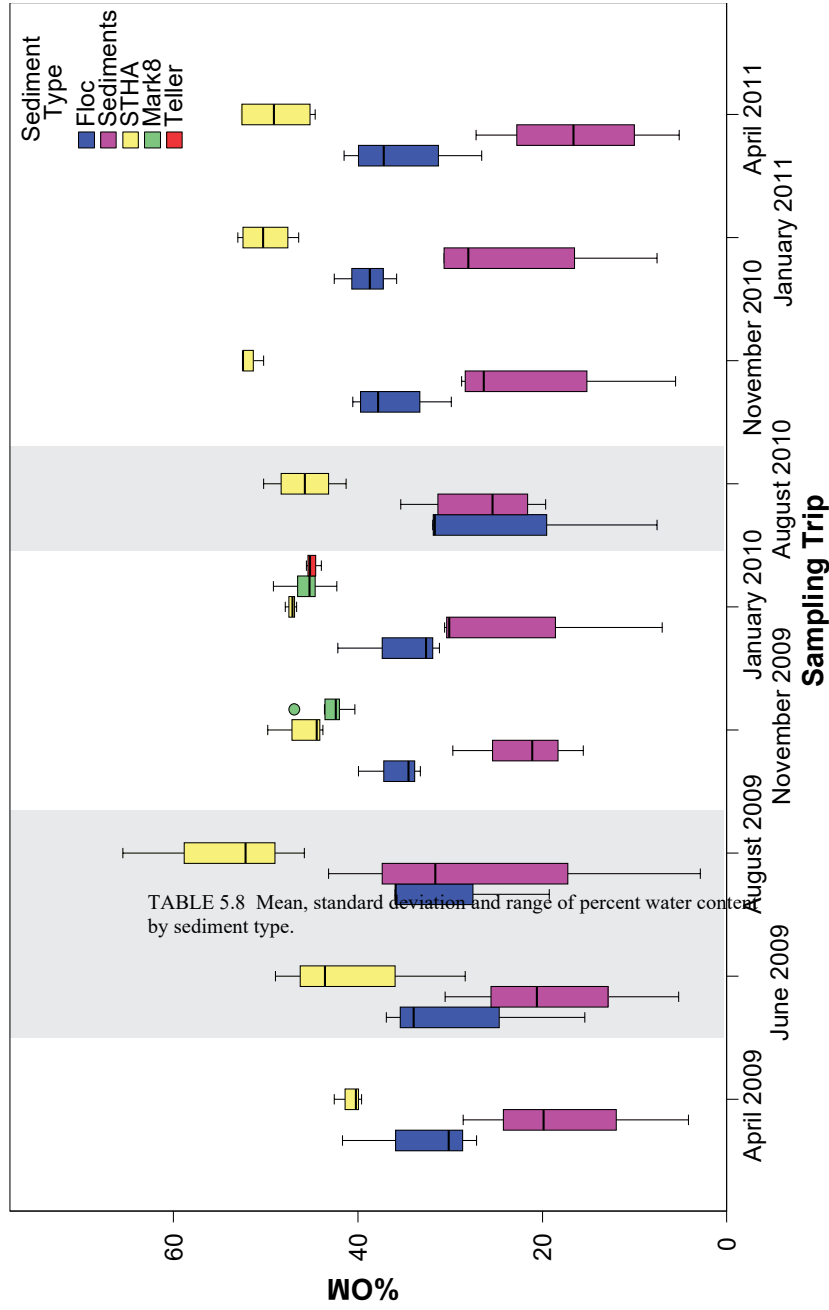


FIGURE 5.13 Box and whisker for percent organic matter by deployment and sediment type. Refer to figure 5.2 for explanation of box plot details.

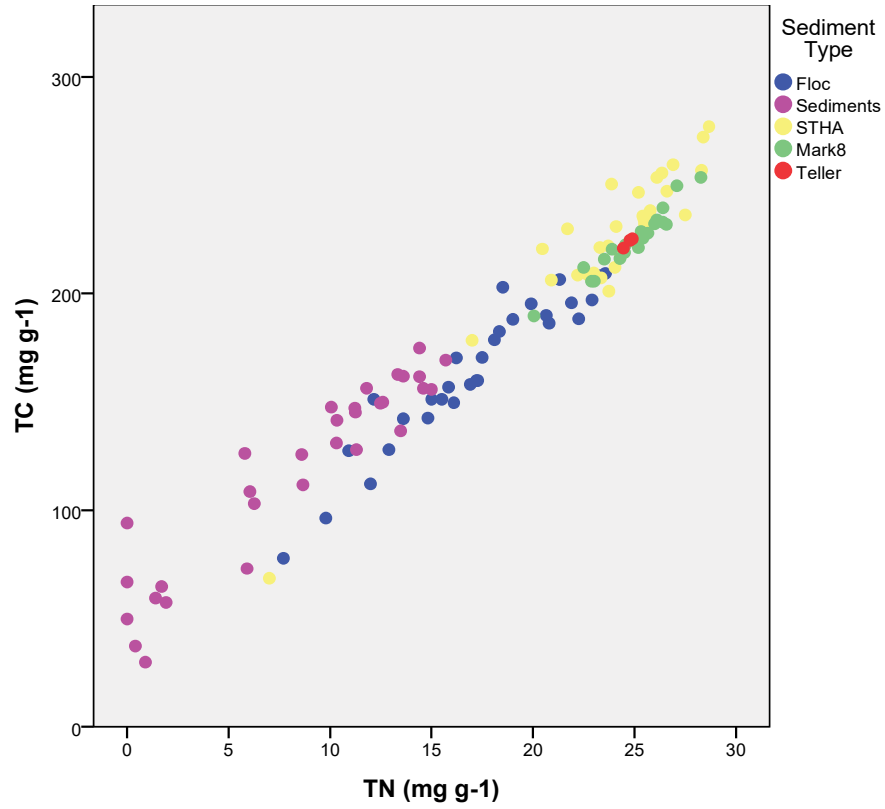


FIGURE 5.14 Total carbon vs. total nitrogen for all sediments types and trap material.

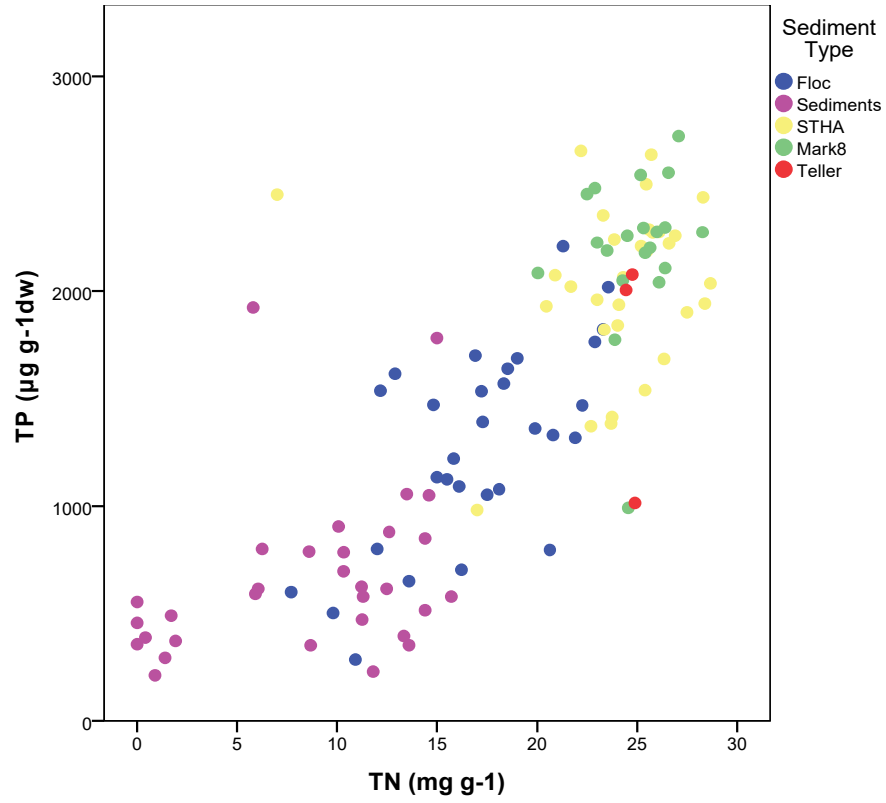


FIGURE 5.15 Total phosphorus vs. total nitrogen for all sediments types and trap material.

TABLE 5.8 Pearson Product Moment correlations between the water and different solids types and their nutrient concentrations where n = 30 or 31 (* indicate p<0.05, and ** indicate p<0.01).

	TP - water	TN - water	TOC - water	TP - flocc	TN - flocc	TC - flocc	TP - STHA	TN - STHA	TC - STHA
TP - water	-	-0.086	0.276	0.078	-0.103	-0.092	0.204	-0.389*	0.343
TN - water		-	0.127	-0.244	-0.437*	-0.453*	-0.244	-0.122	-0.180
TOC - water			-	-0.306	-0.402*	-0.299	-0.033	-0.269	-0.233
TP - flocc				-	0.668**	0.670**	0.393*	0.012	0.033
TN - flocc					-	0.948**	0.067	0.135	0.148
TC - flocc						-	0.117	0.108	0.219
TP - STHA							-	0.415*	0.432*
TN - STHA								-	0.849**
TC - STHA									-

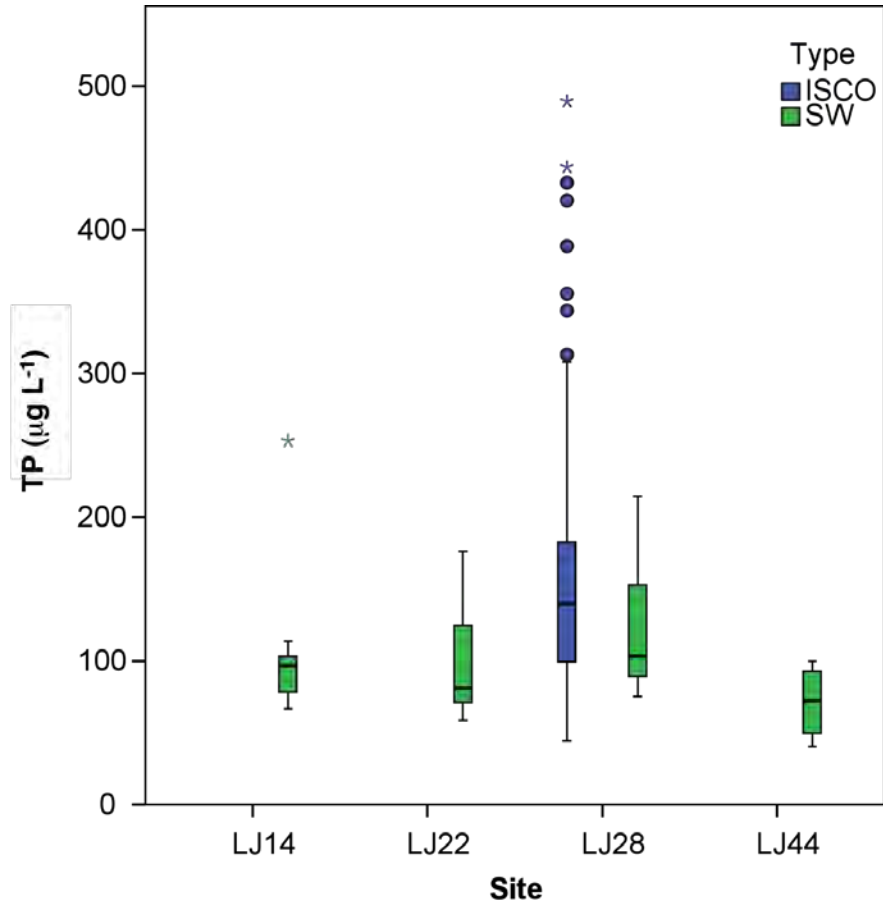


FIGURE 5.16 Box and whisker for total phosphorus in the water column by site location. Refer to figure 5.2 for explanation of box plot details.

TABLE 5.9 Water nutrient correlation matrix for ISCO water samples where $n = 73$ (except for TP, $n = 72$). ** = significant at $p < 0.01$.

	TP	TN	TOC	TSS
TP	-	-0.004	-0.008	0.636**
TN		-	0.318**	0.052
TOC			-	0.155
TSS				-

Table 5.10 Mean, standard deviation and range for total phosphorus, nitrogen, organic carbon and chlorophyll-a by site location and sampling type. Refer to figures 5.29 to 5.31 for additional graphs.

Sample Type	Site		TP ($\mu\text{g/L}$)	TN ($\mu\text{g/L}$)	TOC ($\mu\text{g/L}$)	Chlr-a ($\mu\text{g/L}$)
ISCO	28	Mean	169	1713	17234	
		Std. Dev.	102	1015	4716	
		Minimum	44	496	11710	
		Maximum	489	7670	39528	
		N	72	72	72	
SW	14	Mean	107	1442	15248	45.6
		Std. Dev.	57	546	2348	24.7
		Minimum	66	623	10620	7.4
		Maximum	253	2374	18390	79.0
		N	9	9	9	9
	22	Mean	99	1108	14419	50.3
		Std. Dev.	40	387	2501	31.4
		Minimum	59	558	10340	6.9
		Maximum	176	1765	17200	103.6
		N	9	9	9	9
	28	Mean	124	1811	15961	56.4
		Std. Dev.	49	1831	2705	41.7
		Minimum	75	648	10960	8.6
		Maximum	215	6851	20020	138.3
		N	10	10	10	10
	44	Mean	71	1847	13729	35.1
		Std. Dev.	27	523	4096	19.4
		Minimum	40	1191	9601	8.2
		Maximum	100	2363	18188	51.3
		N	4	4	4	4

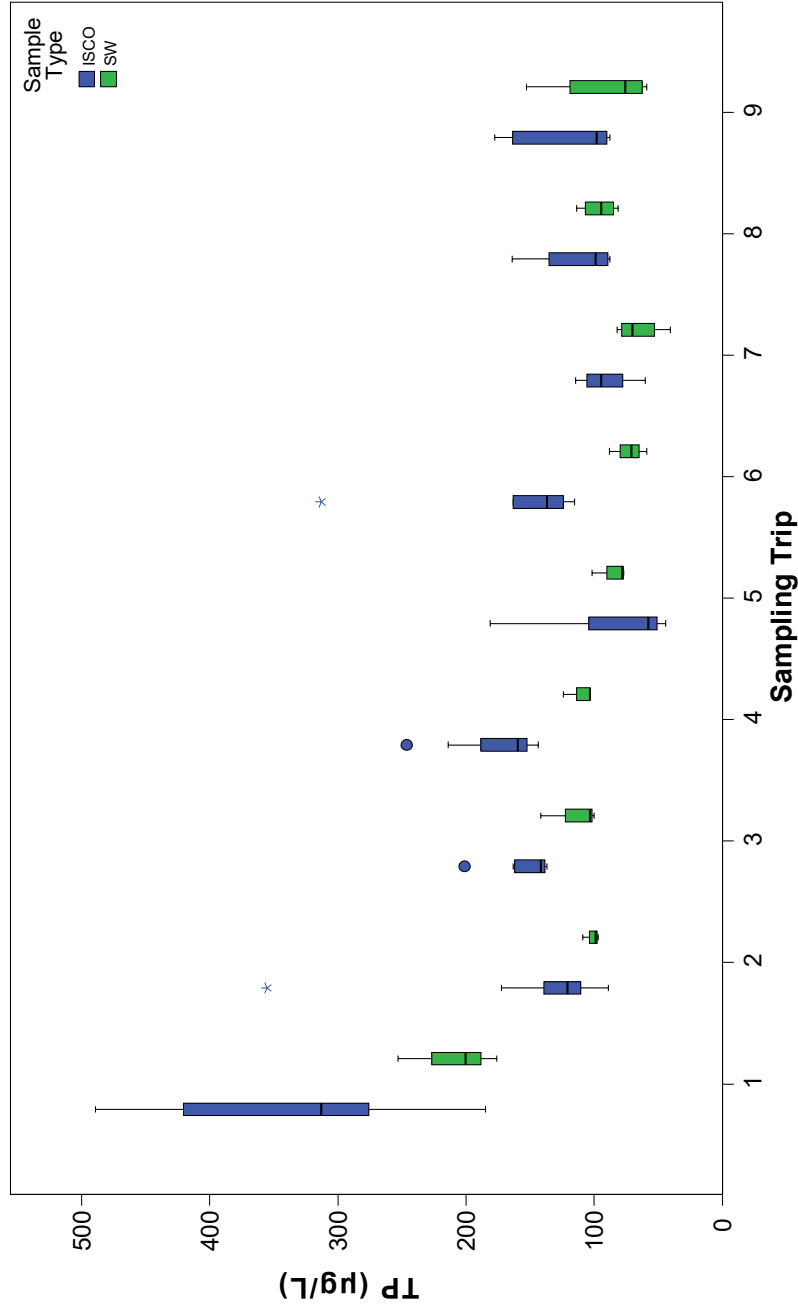


Figure 5.17 Box and whisker for total phosphorus in the water column by deployment and sampling type. Refer to figure 5.2 for explanation of box plot details.

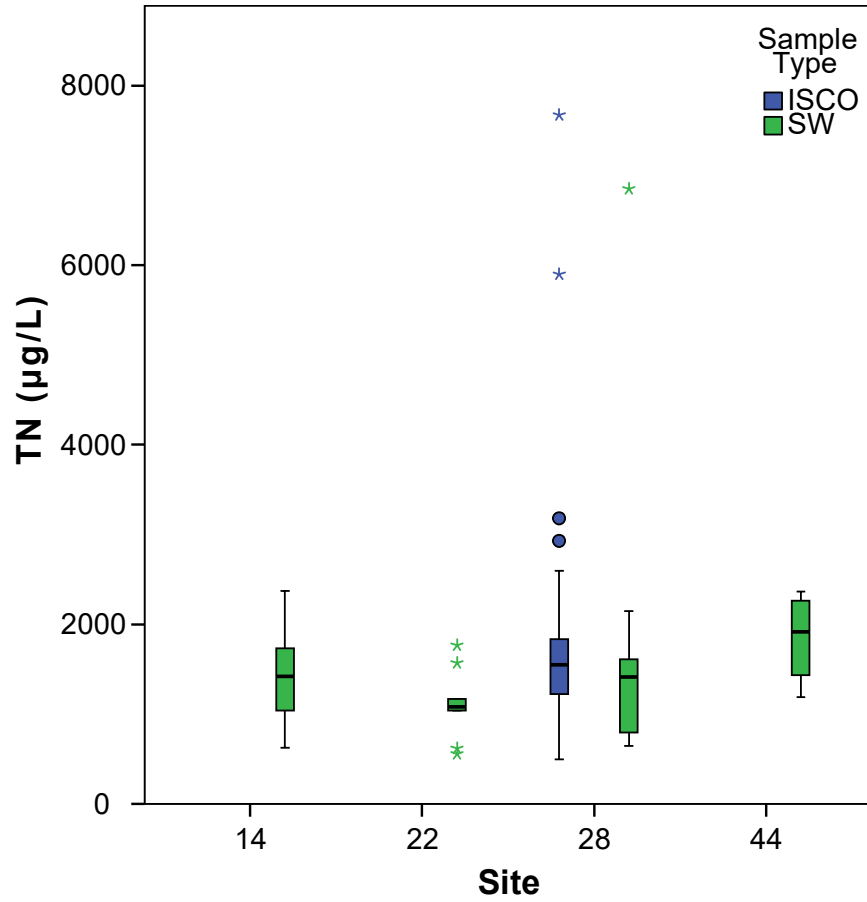


FIGURE 5.18 Box and whisker for total nitrogen in the water column by site location. Refer to figure 5.2 for explanation of box plot details.

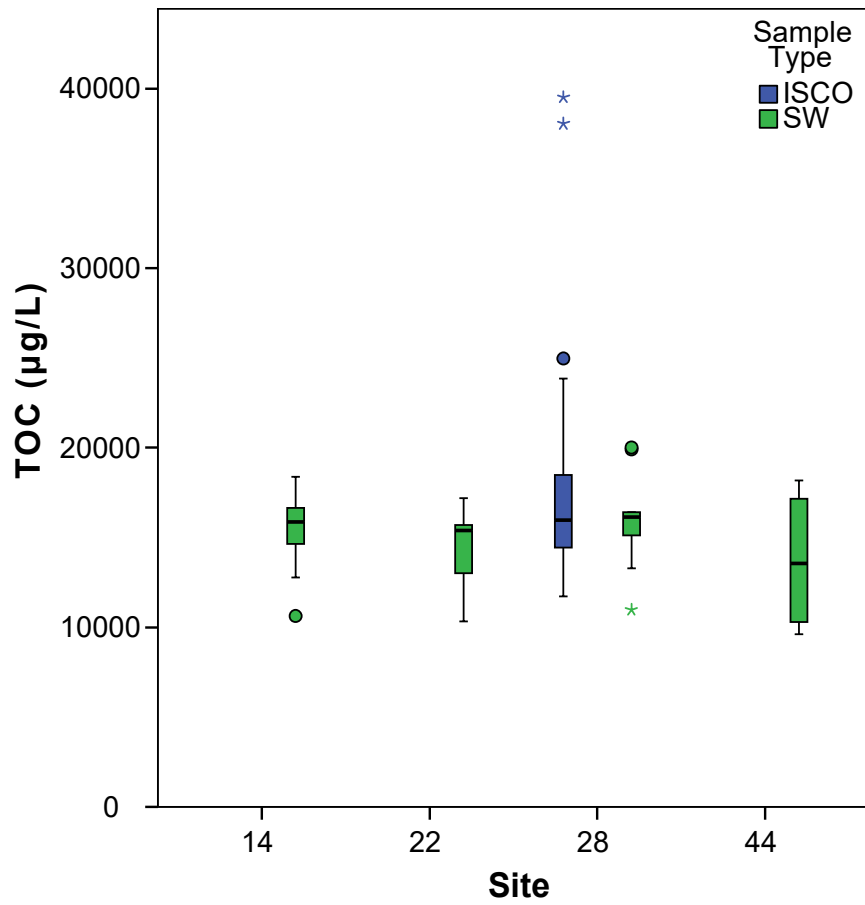


FIGURE 5.19 Box and whisker for total organic carbon in the water column by site location.

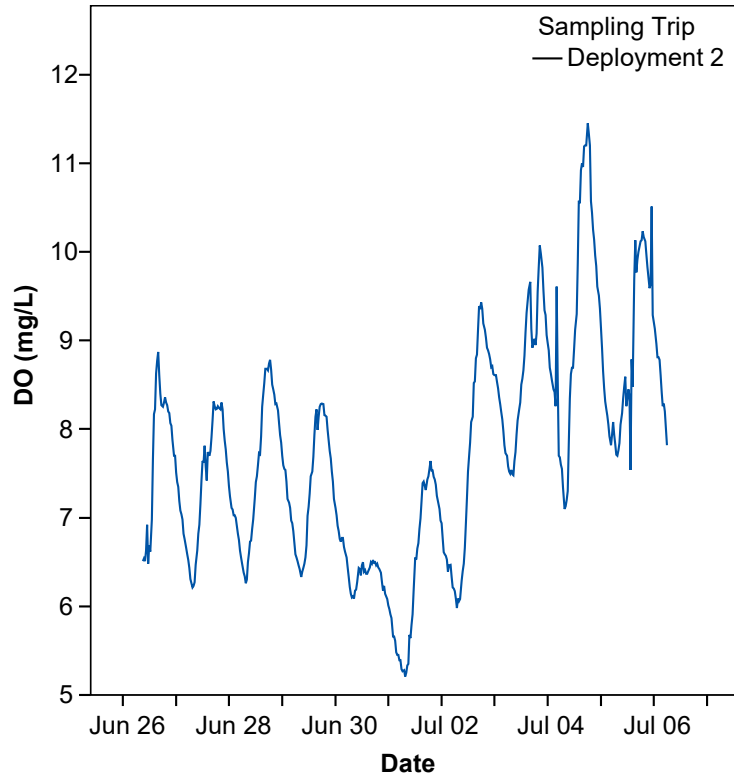


FIGURE 5.20 Time series analysis for dissolved oxygen during deployment 2 within the water column at 0.5 meter depth.

TABLE 5.11 Mean, standard deviation and range of dissolved oxygen in the surface water (depth around 0.5 m) by deployment.

Sampling Trip	Mean +/- Std. Dev.	Range	n
Deployment 2	7.73 +/- 1.26	5.21 - 11.45	475
Deployment 3	1.22 +/- 0.62	0.67 - 8.42	334
Deployment 4	9.41 +/- 0.68	7.87 - 10.51	78
Deployment 5	16.50 +/- 1.87	13.01 - 20.62	334
All Deploy	8.46 +/- 5.83	0.67 - 20.62	1221

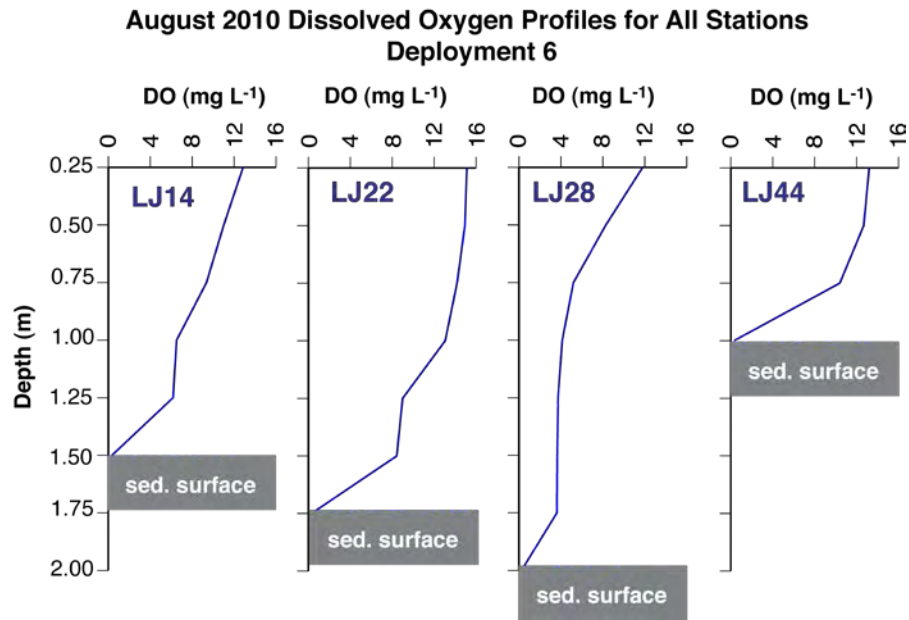


FIGURE 5.21 Lake wide profiles for dissolved oxygen from all four stations. Each station has a different depth, and is illustrated on each profile. Note the water column is oxygenated throughout expect near the sediment water interface.

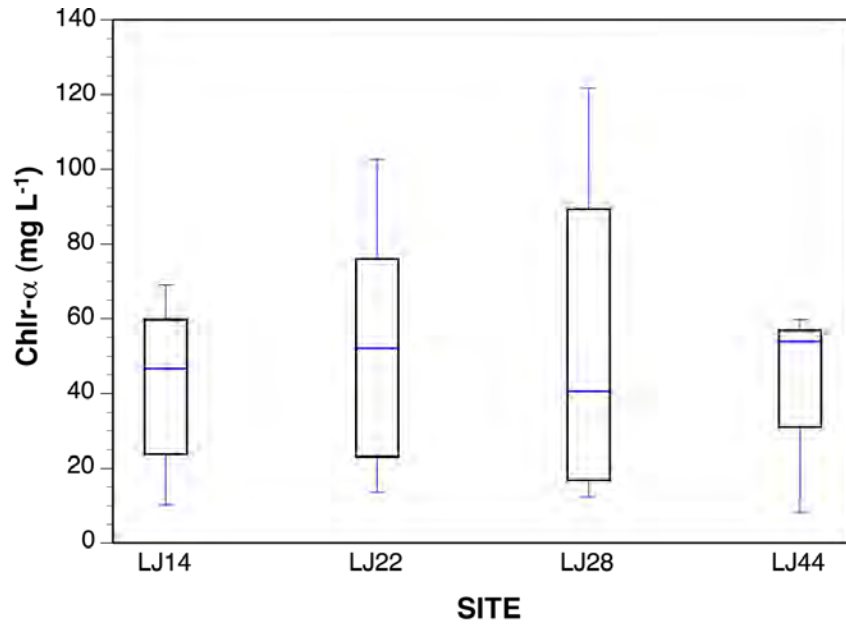


FIGURE 5.22 Box and whisker for chlorophyll-*a* in the water column by site location. Refer to figure 5.2 for explanation of box plot details.

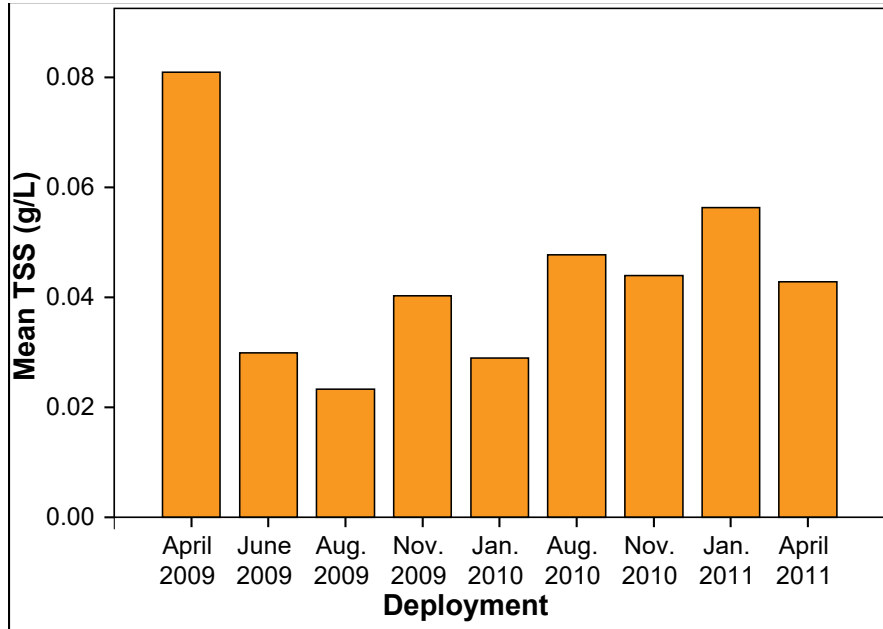


FIGURE 5.23 Bar graph of total suspended solids within the water column at a depth around 0.5 meters.

TABLE 5.12 Mean, standard deviation and range of the total suspended solids within the water column (depth around 0.5 m) by deployment.

Deployment	Mean +/- Std. Dev.	Range	n
1	0.08 +/- 0.02	0.05 - 0.11	13
2	0.03 +/- 0.01	0.02 - 0.05	13
3	0.02 +/- 0.01	0.01 - 0.04	7
4	0.04 +/- 0.02	0.01 - 0.05	7
5	0.03 +/- 0.01	0.02 - 0.04	7
6	0.05 +/- 0.01	0.03 - 0.07	7
7	0.04 +/- 0.01	0.03 - 0.06	8
8	0.06 +/- 0.03	0.03 - 0.08	4
9	0.04 +/- 0.02	0.02 - 0.06	7
All Deploy	0.05 +/- 0.02	0.01 - 0.11	73

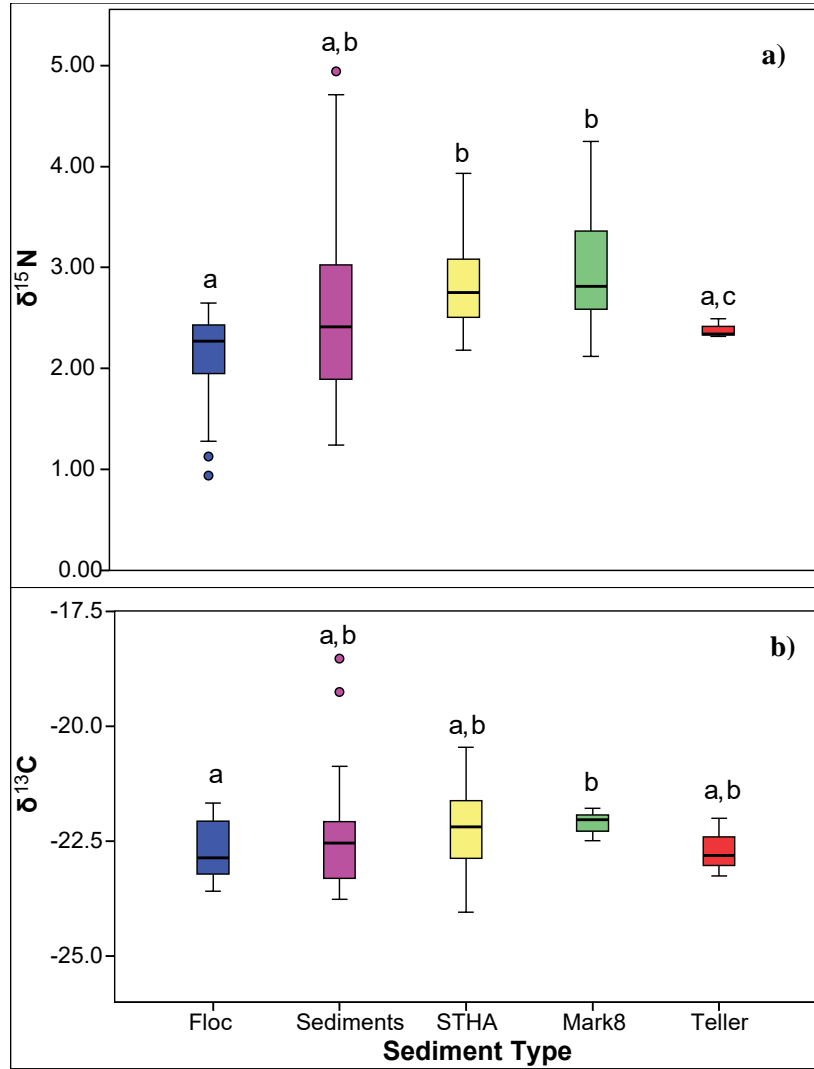


FIGURE 5.24 Box and whisker of stable isotopes, $\delta^{15}\text{N}$ (a) and $\delta^{13}\text{C}$ (b) within the bottom sediments of Lake Jesup by sediment type. Refer to figure 5.2 for explanation of box plot details.

Sediment Type		N15	C13
Floc	Mean	2.11	-22.70
	Std. Dev.	0.45	0.60
	Minimum	0.94	-23.59
	Maximum	2.65	-21.67
	N	30	30
Sediments	Mean	2.67	-22.40
	Std. Dev.	1.03	1.20
	Minimum	1.24	-23.77
	Maximum	4.94	-18.53
	N	31	31
STHA	Mean	2.82	-22.18
	Std. Dev.	0.43	0.85
	Minimum	2.18	-24.05
	Maximum	3.93	-20.46
	N	31	31
Mark8	Mean	2.94	-22.09
	Std. Dev.	0.57	0.21
	Minimum	2.12	-22.49
	Maximum	4.25	-21.79
	N	20	20
Teller	Mean	2.38	-22.69
	Std. Dev.	0.09	0.64
	Minimum	2.32	-23.26
	Maximum	2.49	-22.00
	N	3	3
Total	Mean	2.61	-22.37
	Std. Dev.	0.73	0.85
	Minimum	0.94	-24.05
	Maximum	4.94	-18.53
	N	117	117

TABLE 5.13 Mean, standard deviation and range of stable isotopes, $\delta^{15}\text{N}$ and $\delta^{13}\text{C}$ within the sediments by sediment

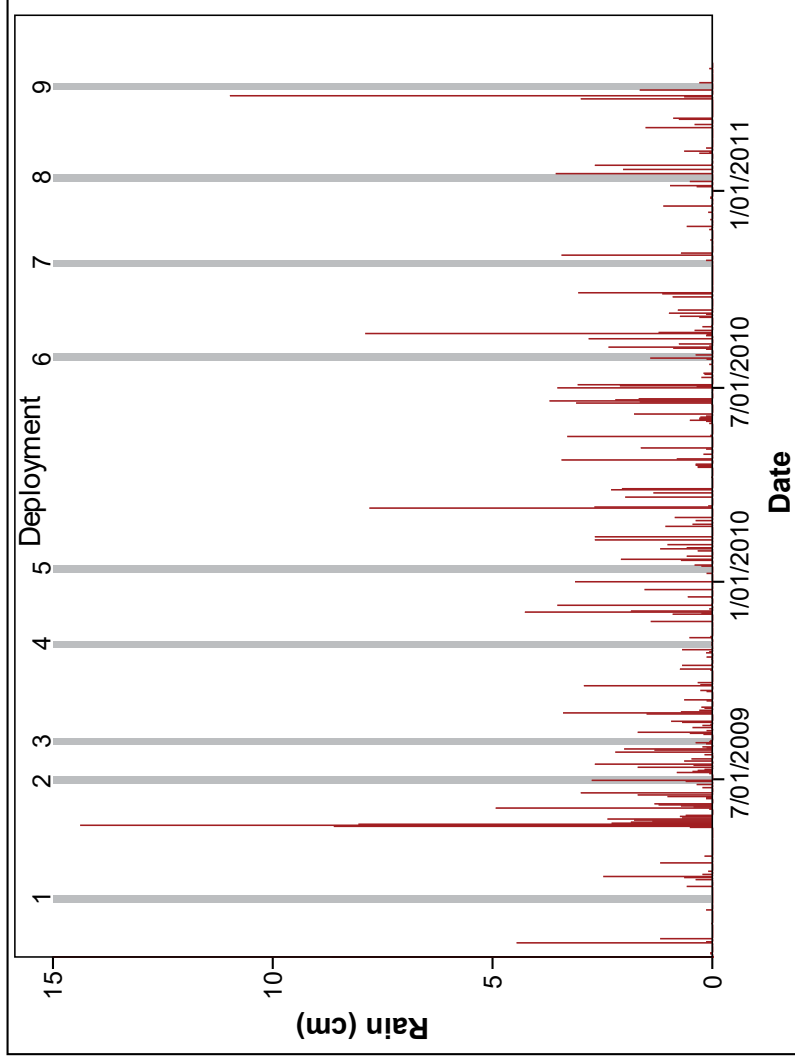


FIGURE 5.25 Bar graph of daily precipitation from the National Climatic Data Center from Sanford Airport over the two-year sampling period.

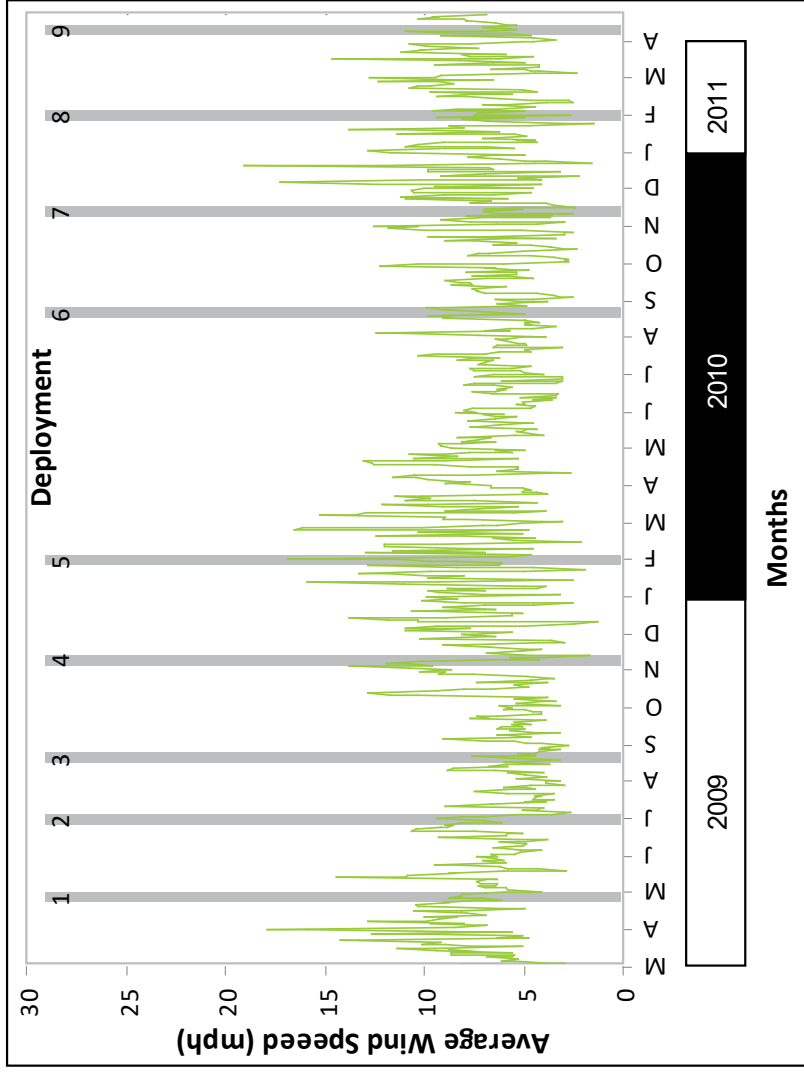


FIGURE 5.26 time series analysis of hourly wind speeds from the National Climatic Data Center from Sanford Airport over the two-year sampling period.

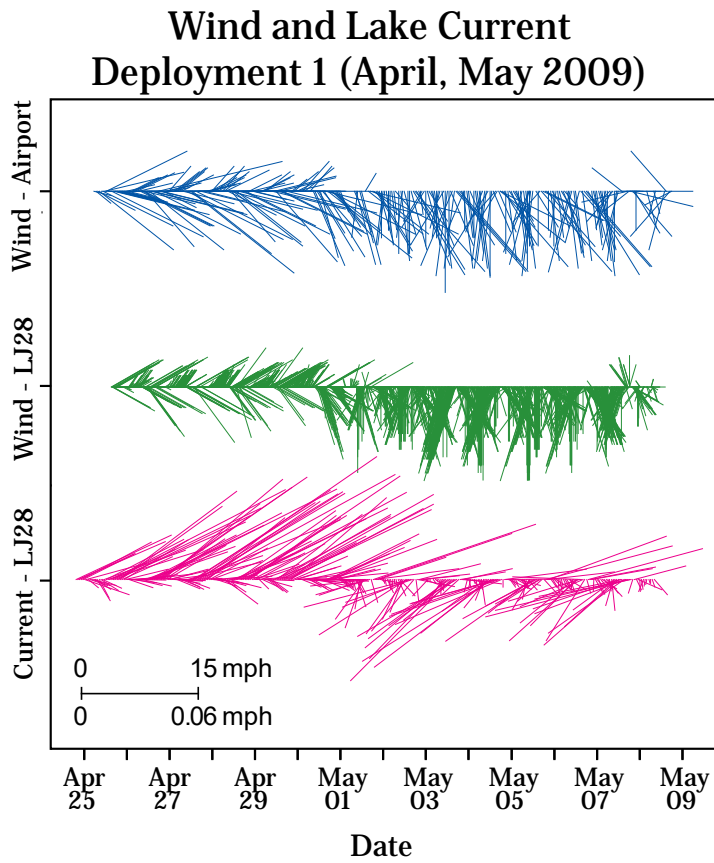


FIGURE 5.27 Stick plots for deployment 1, the top plot is wind data from Sanford Airport, the middle plot is from the weather stations on the lake, and the bottom plot is current (0.75 m above the lake bottom) measured on the lake over time.

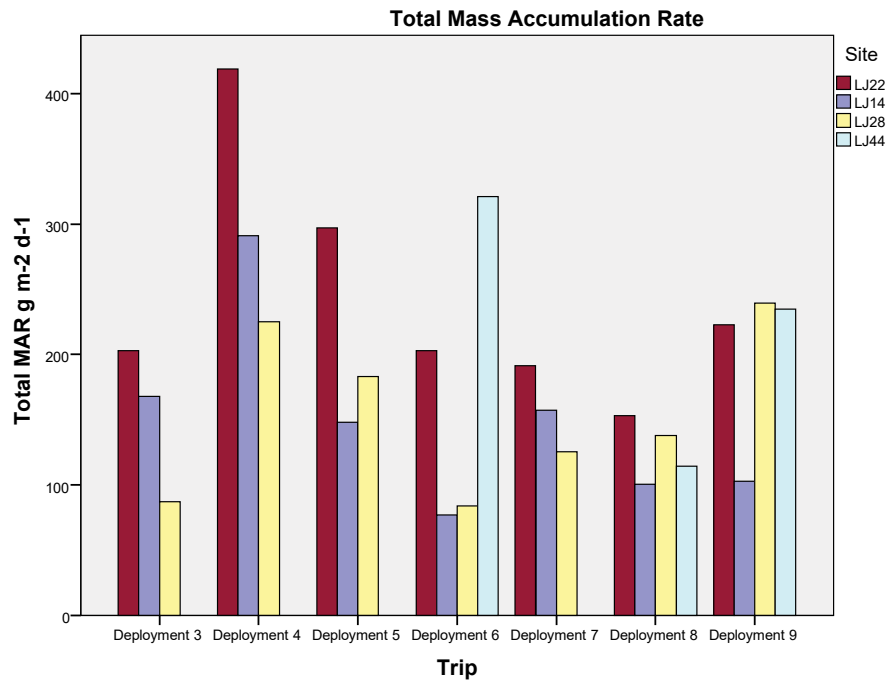


FIGURE 5.28 Total daily mass accumulation rates (MAR) from deployments 3 to 9.

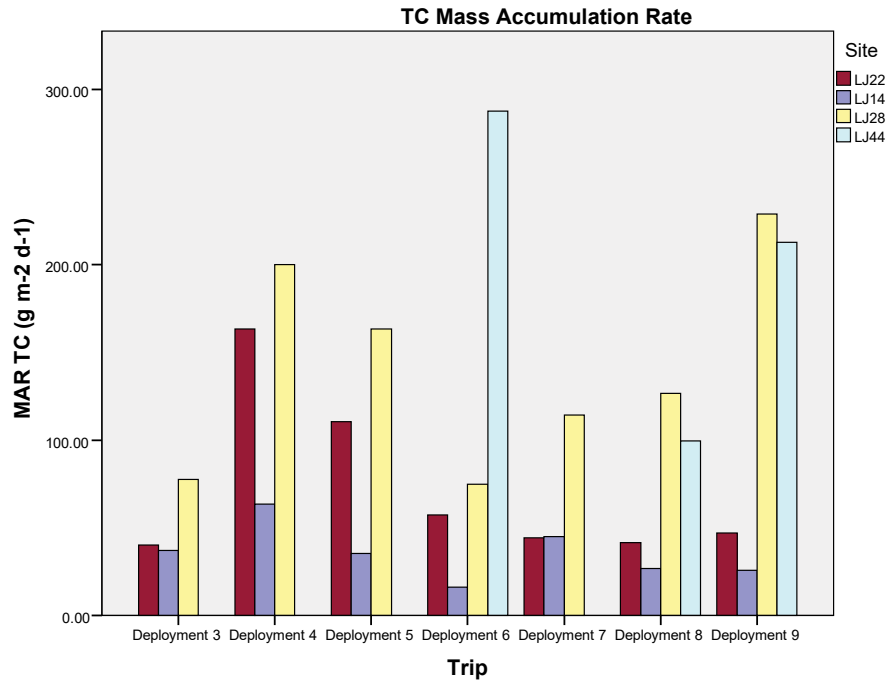


FIGURE 5.29 Variations in mass accumulation rate (MAR) for TC from deployments 3 to 9.

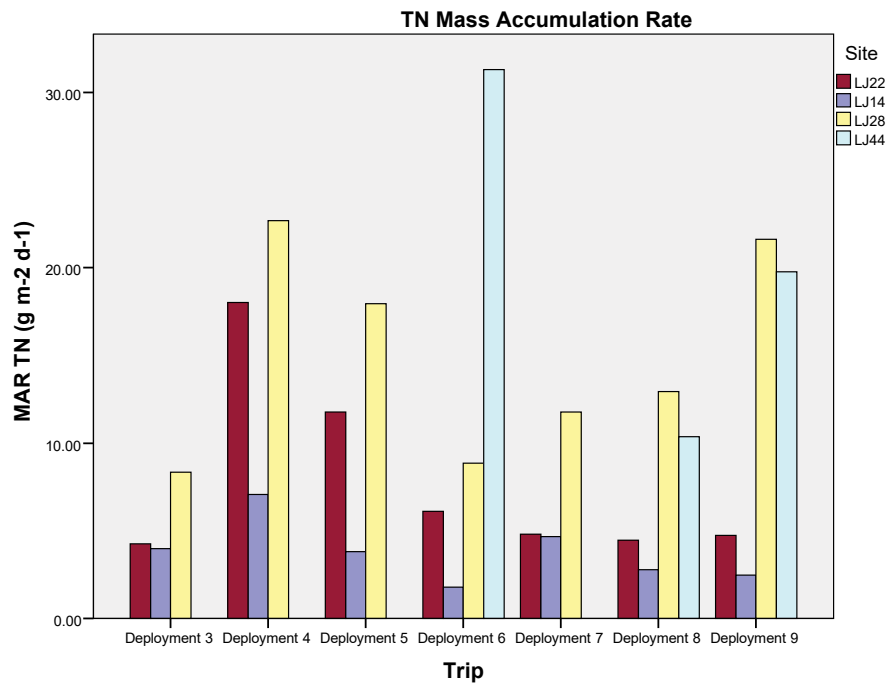


FIGURE 5.30 Variations in mass accumulation rate (MAR) for TN from deployments 3 to 9.

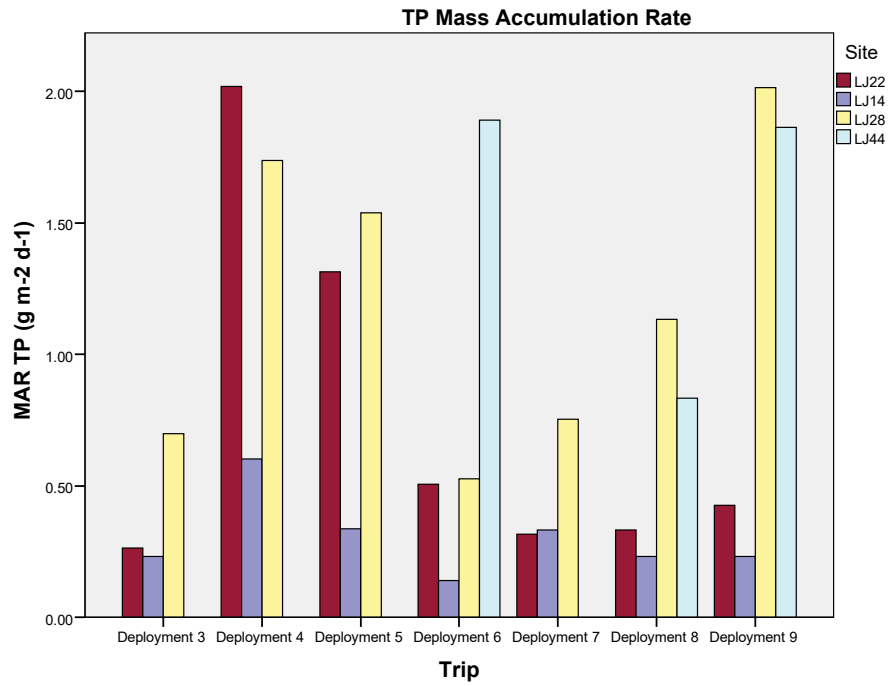


FIGURE 5.31 Variations in mass accumulation rate (MAR) for TP from deployments 3 to 9.

TABLE 5.14 Mean, standard deviation and range of wind velocity, direction temperature and rain by deployment from weather stations 1 and 2 (wind direction).

Deployment	Temperature (C)	Wind Velocity (mph)	Wind Direction (Degrees)	Rain (cm)	
April 2009	Mean	24	9	133	0
	Std. Deviation	3	4	64	0
	Range	18 - 33	0 - 20	0 - 360	0 - 2
	n	1257	1257	1202	1257
June 2009	Mean	28	11	150	0
	Std. Deviation	2	4	117	1
	Range	24 - 34	0 - 28	0 - 360	0 - 22
	n	1257	1257	1257	1257
Aug. 2009	Mean	28	4	60	0
	Std. Deviation	2	4	97	1
	Range	24 - 34	0 - 21	0 - 360	0 - 20
	n	681	681	681	681
Jan. 2010	Mean	16	8	168	0
	Std. Deviation	4	5	127	0
	Range	10 - 22	0 - 22	0 - 360	0 - 2
	n	681	681	681	681
Aug. 2010	Mean	28	7	207	0
	Std. Deviation	2	5	80	2
	Range	24 - 35	0 - 22	0 - 360	0 - 34
	n	681	681	681	681
Nov. 2010	Mean	20	5	149	0
	Std. Deviation	3	4	133	0
	Range	14 - 29	0 - 16	0 - 360	0 - 1
	n	777	777	777	777
Jan. 2011	Mean	17	6	149	0
	Std. Deviation	4	4	109	0
	Range	9 - 25	0 - 15	0 - 360	0 - 0
	n	681	681	681	681
April 2011	Mean	25	5	181	0
	Std. Deviation	3	4	113	0
	Range	18 - 32	0 - 18	0 - 360	0 - 0
	n	681	681	681	681

Deployment	Velocity (m/s)	Direction	
1	Mean	0.07	133
	Std. Dev	0.08	62
	Minimum	0.03	52
	Maximum	0.81	272
	N	330	330
2	Mean	0.06	230
	Std. Dev	0.04	25
	Minimum	0.03	131
	Maximum	0.77	267
	N	317	317
5	Mean	0.05	140
	Std. Dev	0.02	62
	Minimum	0.03	54
	Maximum	0.11	300
	N	162	162
6	Mean	0.10	208
	Std. Dev	0.18	43
	Minimum	0.03	60
	Maximum	0.85	267
	N	174	174
7	Mean	0.05	143
	Std. Dev	0.01	52
	Minimum	0.03	50
	Maximum	0.09	268
	N	189	189
8	Mean	0.05	181
	Std. Dev	0.01	47
	Minimum	0.03	74
	Maximum	0.10	255
	N	169	169
9	Mean	0.05	186
	Std. Dev	0.02	51
	Minimum	0.00	59
	Maximum	0.12	267
	N	163	163

TABLE 5.15 Mean, standard deviation and range of lake current velocity and direction by deployment.

Deployment	Velocity (m/s)	Direction
All Mean	0.06	175
Std. Deviation	0.08	62
Minimum	0.00	50
Maximum	0.85	300
N	1504	1504

TABLE 5.15 (continued) Mean, standard deviation and range of lake current velocity and direction by deployment.

5.9 Cores and Sediment Oxygen Demands

5.9.1 Pictures of the cores

All cores contained visible zooplankton (e.g. cladocerans and copepods) and phytoplankton at the interface floc or sediment - water interface. Invertebrate dwellers such as *Chironomus* sp. as well as leeches (Annelida, Hirudinae) were also found in the cores. The pictures of the cores are displayed for events 6, 7, 8 and 9 (Figs. 5.32 to 5.35).

5.9.2 Sediment oxygen demand including the floc layer (SOD)

The average temperature during the incubations was $24.1 \pm 2.8^\circ\text{C}$ and $24.2 \pm 1.3^\circ\text{C}$ for the SOD_T and SedOD_T incubations, respectively. SOD_T was $0.66 \pm 0.38 \text{ gO}_2/(\text{m}^2 \text{ day})$ and SOD_{20} was $0.52 \pm 0.31 \text{ gO}_2/(\text{m}^2 \text{ day})$ for events 6 through 9 (Figs. 5.36 and 5.37). No correlation was found between either SOD_T or SOD_{20} and TN, TP, TC, TIC, %C or %TN in the floc ($r^2 < 0.1$ and regression p values > 0.05). Similarly, with the exception of a negative correlation with water DOC ($r^2 = 0.25$, $p < 0.05$), no noticeable correlation was found with water nutrient and chl a concentrations. Additionally, no correlation was found between the SOD_T or SOD_{20} and the volume of floc in the core ($r^2 < 0.01$).

5.9.3 Sediment oxygen demand without the floc layer (SedOD)

SedOD_T was $1.57 \pm 1.44 \text{ gO}_2/(\text{m}^2 \text{ day})$ and SedOD_{20} was $1.24 \pm 1.37 \text{ gO}_2/(\text{m}^2 \text{ day})$ for events 6 through 9 (Figs. 5.38 and 5.39). Without the outlier values determined for station LJ28 on event 8, SedOD_T was $1.23 \pm \text{S.D } 0.49 \text{ gO}_2/(\text{m}^2 \text{ day})$ and SedOD_{20} was $0.91 \pm 0.41 \text{ gO}_2/(\text{m}^2 \text{ day})$ for the same aforementioned period. No correlation was found between either SedOD_T or SedOD_{20} and TN, TP, TC, TIC, %C or %TN in the sediment ($r^2 < 0.1$ and regression p values > 0.05). Similarly, no correlation was found with water nutrient and chl a concentrations.

5.9.4 Comparison of sediment oxygen demand with (SOD) and without the floc layer (SedOD)

The difference $\text{SedOD}_{20} - \text{SOD}_{20}$ (same station and event) was very largely positive (with the exception of two occurrences) and averaged $0.42 \pm 0.31 \text{ gO}_2/(\text{m}^2 \text{ day})$.

5.9.5 Comparison with previous SedOD₂₀ data (Phase 1 vs. phase 2)

SedOD_T from phase 1 were incubated at 19.7 ± 0.7 °C, so SedOD₂₀ was selected to compare phase 1 and 2 (T test). When the SedOD₂₀ were compared for each station (LJ14, LJ22, LJ28), no difference was found between phase 1 and phase 2 ($P > 0.05$, $\alpha = 0.05$). SedOD₂₀ from phase 1 and 2 of the project were thus combined in the same graph (Fig. 5.40). These tests were performed without the outlier LJ28 of event 8.

5.9.6 WOD, FOD and floc characteristics

WOD averaged 0.097 ± 0.022 mg O₂/L/h for all events and changed significantly over time ($p < 0.05$, Fig. 5.41). WOD was positively correlated with water TN ($r^2 = 0.42$, $p < 0.05$), TON ($r^2 = 0.43$, $p < 0.05$), Chl_a ($r^2 = 0.15$, $p = 0.04$), and DOC ($r^2 = 0.17$, $p = 0.03$) and negatively correlated with NH₄⁺ ($r^2 = 0.24$, $p = 0.01$) and TDN ($r^2 = 0.42$, $p < 0.05$). No correlation was found with water phosphorus (TP, DP or SRP). FOD averaged 0.013 ± 0.002 mgO₂/(h.ml_floc) or 0.53 ± 0.48 mgO₂/(h.g_floc) for events 6 through 9 (Figs. 5.42 & 5.43). When reported per ml of floc, FODs at the various stations were similar for each event and FODs were the same for events 6 through 8. Event 9 had significantly lower FODs than for the other events ($p < 0.05$). FOD was positively correlated with floc TN ($r^2 = 0.19$, $p = 0.02$) and %TN ($r^2 = 0.19$, $p = 0.02$). FOD was also positively correlated with water TDN ($r^2 = 0.23$, $p < 0.05$) and negatively correlated with TOC ($r^2 = 0.45$, $p < 0.05$). No correlation was found with phosphorus.

Floc bulk density was 0.037 ± 0.018 g/cm³_floc, while floc thickness and floc % organic were 3.19 ± 1.20 cm and 36 ± 7 % respectively (Figs. 5.44, 5.45 and 5.46). Floc thickness changed over time and was different amongst the stations. LJ28 floc had a lower thickness and organic content and had a higher bulk density ($p < 0.05$). No correlation between the amount of downward particulate flux collected in the high aspect ratio traps and the thickness of floc was found.

Commented [A1]: Statistical?

I DID NOT TEST THIS BECAUSE IT IS OVIOUS ON THE GRAPH 5.59 THAT LJ28 HAD MUCH LESS FLOC (ERROR BARS DO NOT OVERLAP WITH THE OTHER CORES FOR THE OTHER SITES). If so, provide stats.

In these figures it is difficult to see differences in floc, would it be possible to put an arrow next to each core indicating the interface between floc and consolidated sediment? IT IS INDEED IMPOSSIBLE TO DELINEATE THE FLOC/SEDIMENT INTERFACE ON THE PICTURES. THE READER WILL HAVE TO RELY ON THE FLOC THICKNESS DEDUCTED FROM THE VOLUME OF FLOC EXTRACTED FOR THE CORES. LOOK AT FIG. 5.59 FOR FLOC THICKJNESS.

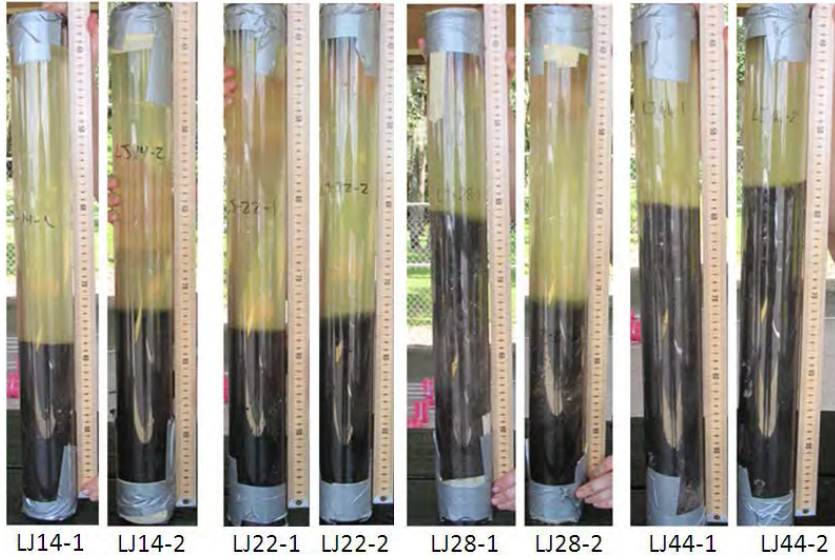


FIGURE 5.32 Pictures of the cores sampled during Event 6.

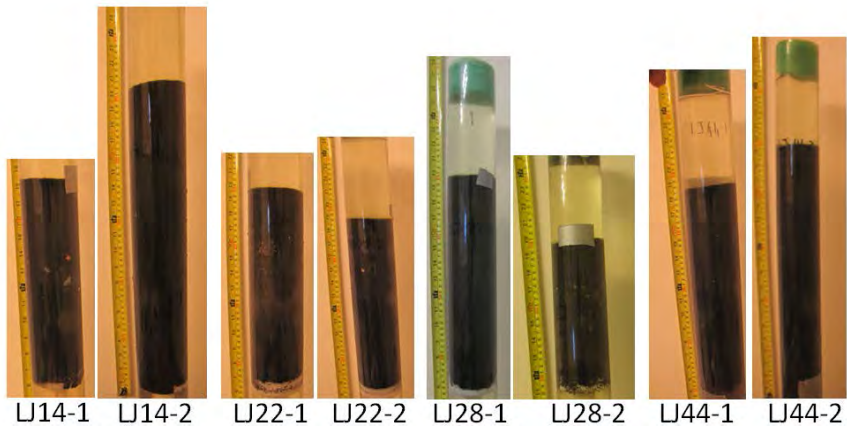


FIGURE 5.33 Pictures of the cores sampled during Event 7.

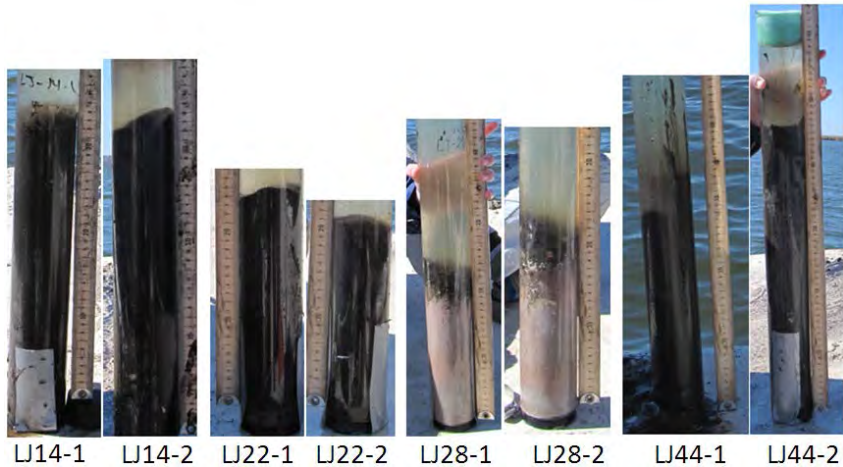


FIGURE 5.34 Pictures of the cores sampled during Event 8.

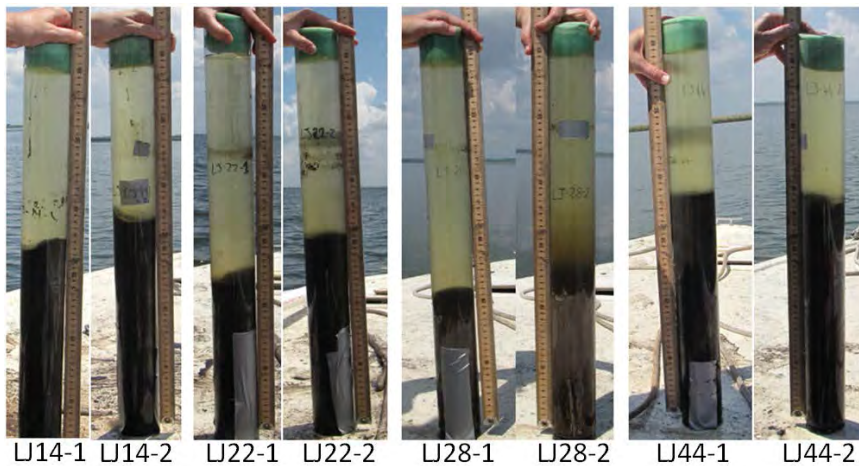


FIGURE 5.35 Pictures of the cores sampled during Event 9.

Commented [A2]: The title or legend should define acronyms. I HAVE FIXED THIS PROBLEM IN ALL THE GRAPHS.

Define error bars.
I HAVE DEFINED THE ERROR BARS

Are differences statistically significant?
IT WOULD NOT BE WISE TO DO SEVERAL T TESTS FOR EACH EVENT BECAUSE OF INCREASE OF TYPE I ERROR. I TRIED TO RUN AN ANOVA WITH TIME AS BLOCKING THAT I COULD NOT RUN BECAUSE I VIOLATE THE HOMOSCEDASTICITY ASSUMPTION. I DID RUN SEVERAL ANOVAS ON RANKS FOR EACH EVENT AND I DID NOT GET ANYTHING BECAUSE THERE IS MUCH VARIANCE WITH ONLY TWO REPLICATES.

I THUS RATHER FOCUSED ON THE LAST COMMENT.

Can differences be related to any sediment characteristic? %TOC, TOC mass, etc? Apply to next several figures also.

I HAVE RUN SEVERAL CORRELATIONS WHICH GAVE ME A FEW WEAK CORRELATIONS SOMETIMES POSITIVE, SOMETIMES NEGATIVE. EVEN THOUGH THE P VALUE IS <0.05, I FIND THE SCATTERPLOT QUITE NOISY TO DRAW REALLY STRONG CONCLUSIONS IN THE DISCUSSION.

CF RESULTS APPROPRIATE AND CONCLUSION SECTIONS.

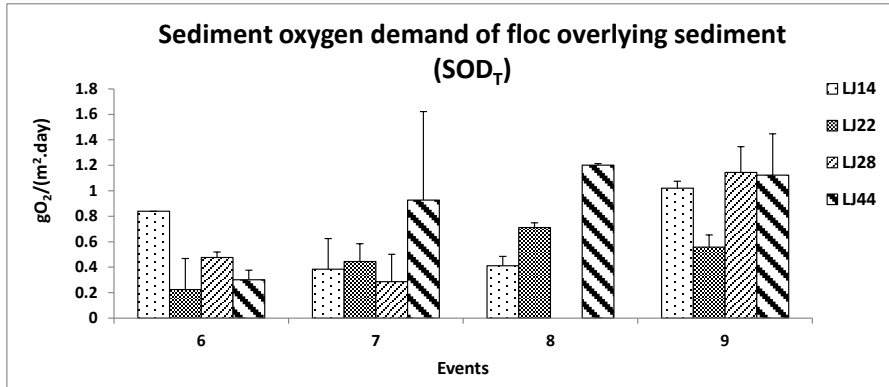


FIGURE 5.36 Change in SOD_T from events 6 to 9. There is no value for LJ28, event 8 because no floc was present for this particular event. Error bars represent the standard deviation (n=2).

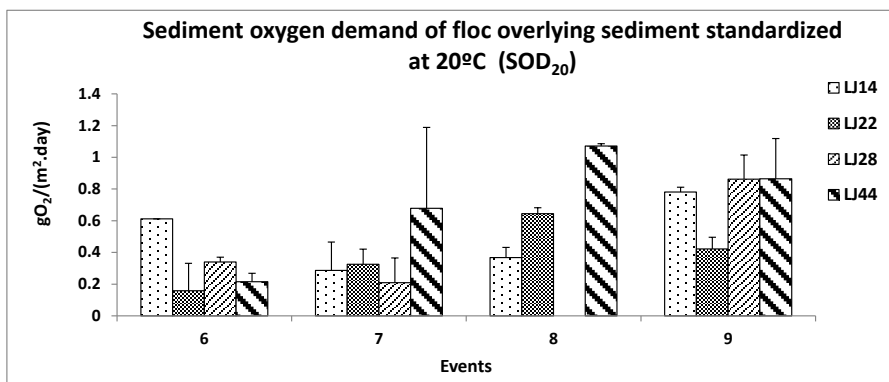


FIGURE 5.37 Change in SOD₂₀ from events 6 to 9. There is no value for LJ28, event 8 because no floc was present for this particular event. Error bars represent the standard deviation (n=2).

Commented [A3]: Provide more details on what makes outlier "atypical" Why would such a short distance make such are large difference.
IT IS UNKNOWN WHY THIS SAMPLE HAD SUCH A HIGH SEDOD. BESIDE NOT HAVING ANY OVERLYING FLOC, THE SEDIMENT APPEARED "NORMAL".

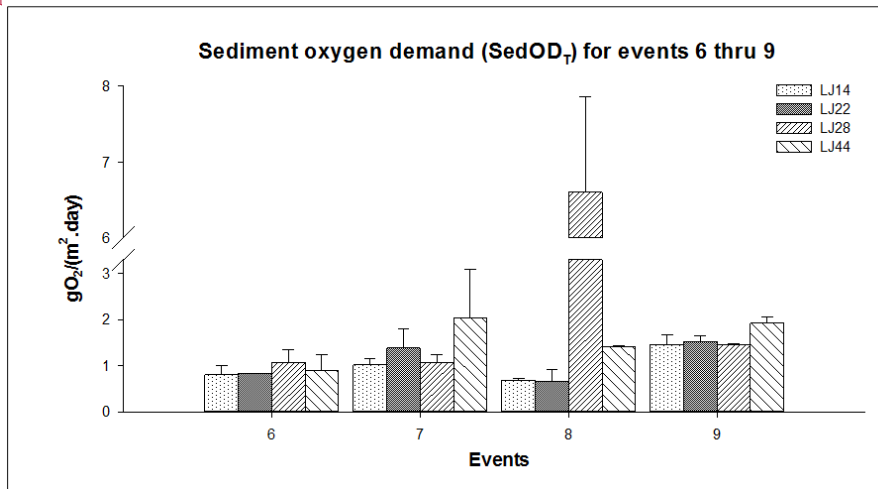


FIGURE 5.38 Change in SedOD_T from events 6 to 9. The high value for LJ28, event 8 is due to an outlier core collected 200m east of the regular LJ28 location. It is not known what caused this high SedOD_T. Error bars represent the standard deviation (n=2).

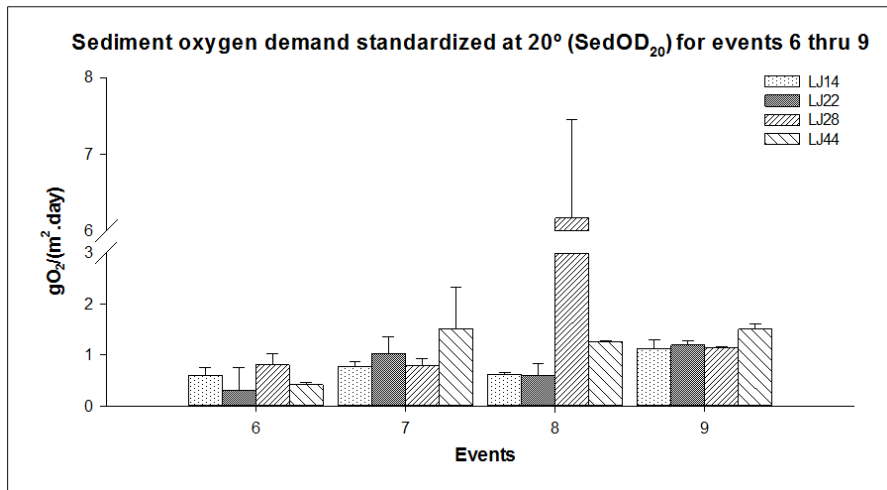


FIGURE 5.39 Change in SedOD₂₀ from events 6 to 9. The high value for LJ28, event 8 is due to an outlier core collected 200m east of the regular LJ28 location. It is not known what caused this high SedOD₂₀. Error bars represent the standard deviation (n=2).

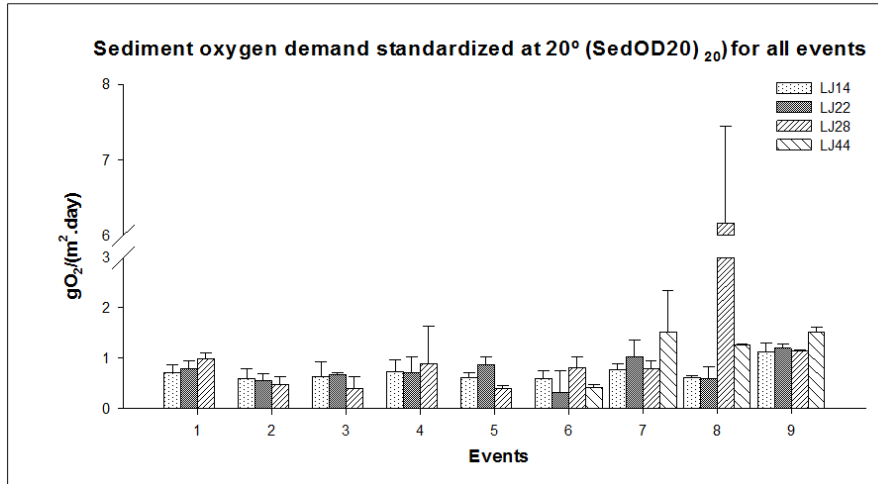


FIGURE 5.40 Comparison of SOD₂₀ between phase 1 and 2 of the study. No differences were found when the outlier LJ28, event 8 was removed (see text for more detail). Error bars represent the standard deviation (n=2).

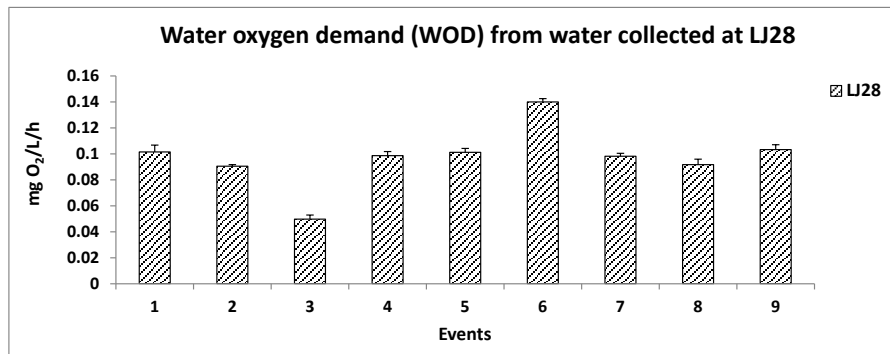


FIGURE 5.41 Change in WOD. Error bars represent the standard deviation (n=3).

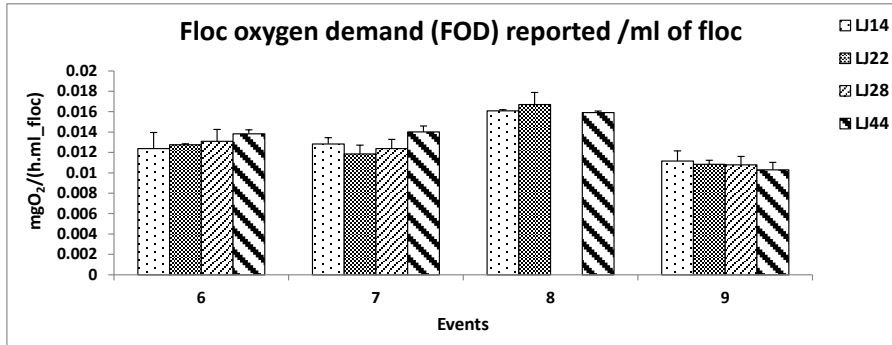


FIGURE 5.42 Change in FOD expressed in $\text{mg O}_2/(\text{h.ml_floc})$ from events 6 to 9. Error bars represent the standard deviation ($n=2$).

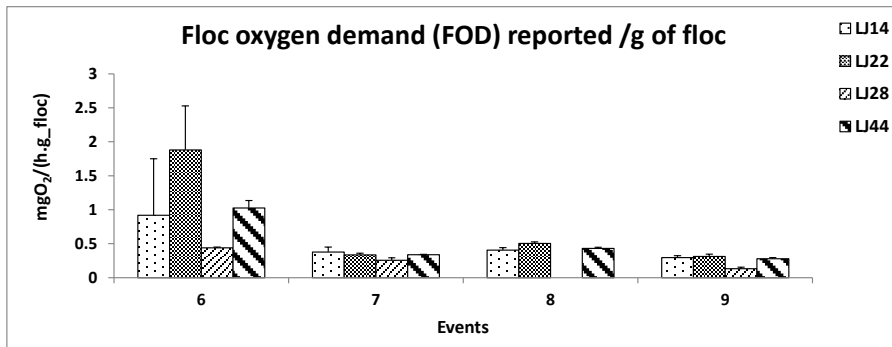


FIGURE 5.43 Change in FOD expressed in $\text{mg O}_2/(\text{h.g_floc})$ from events 6 to 9. Error bars represent the standard deviation ($n=2$).

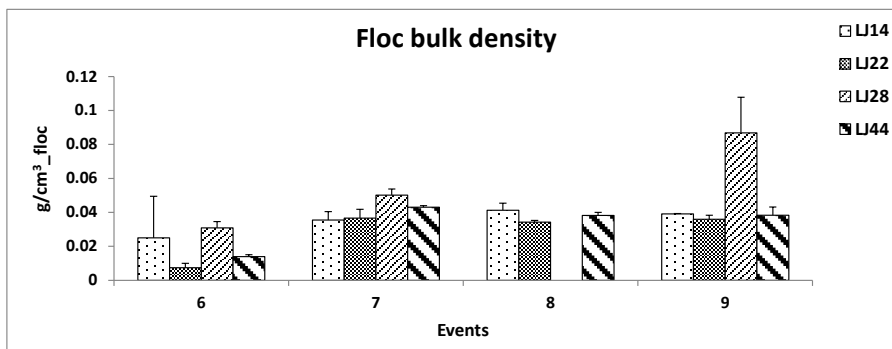


FIGURE 5.44 Change in floc bulk density from events 6 to 9. Error bars represent the standard deviation ($n=2$).

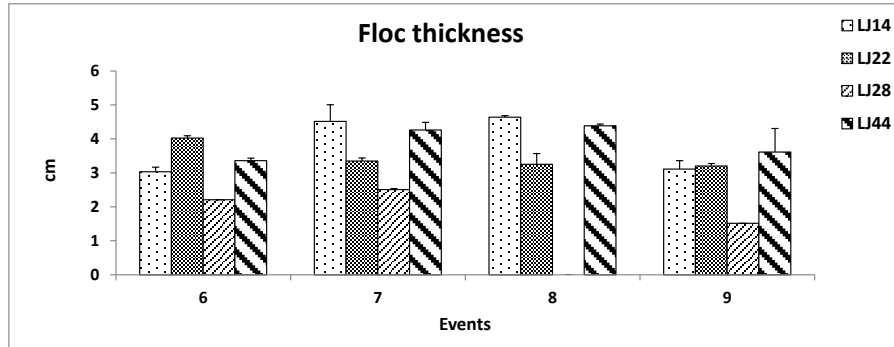


FIGURE 5.45 Change in floc thickness from events 6 to 9. Error bars represent the standard deviation (n=2).

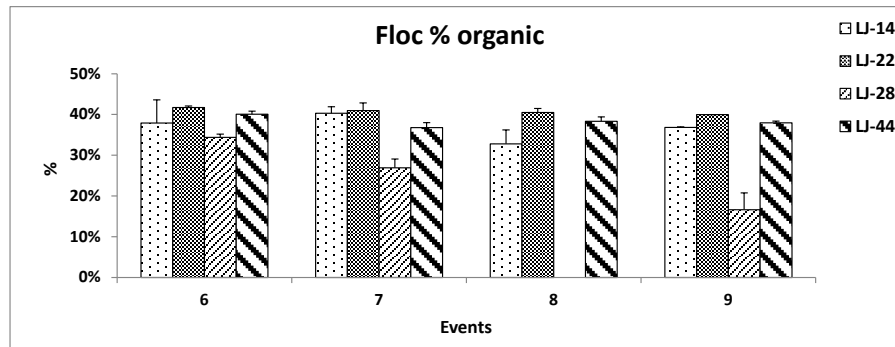


FIGURE 5.46 Change in % organic in floc from events 6 to 9. Error bars represent the standard deviation (n=2).

5.10 Physical transport of suspended solids

One objective of this project was to estimate settling velocities by using measures of the turbulent flux of suspended solids. These are termed Reynolds fluxes and are measured by calibrating the acoustic backscatter to TSS and calculating the covariance of within-burst fluctuations about the mean TSS value and the mean vertical velocity component value as described in the Methods section (see 4.11). Quantitative estimates of the Reynolds flux of sediment failed for the 2009 year of deployments because burst values of acoustic backscatter varied hugely from burst average means. The exponential relationship of the calibration curve for values outside of the range of the burst average means in the calibration curve estimated enormous and impossible values of TSS. Nevertheless, the generally good correlation between OBS and acoustic backscatter which are independent, one being an optical instrument and the other an acoustic instrument, suggest that both were sensing real variations in the amount of suspended matter. In order to take advantage of this and draw some insight from the results, a qualitative measure of the Reynolds sediment flux was made by calculating the covariance between fluctuations of the vertical component of velocity and the acoustic backscatter (rather than the calibrated acoustic backscatter). These measurements of qualitative Reynolds flux (w'Amp') are shown in the results of selected early deployments and provide some insights into the sediment dynamics of the lake. Later deployments in which the velocity range configuration on the ADV was reduced, produced more reasonable, but noisy estimates of settling velocities. In general, the results from the last year (i.e. Phase 2 or the second year of the project) of deployments were more consistent and produced the best data. Therefore, the focus of this report will be on the results and analyses of these latter deployments. The earlier deployment results are included as appendices for completeness, but their analyses are not presented to the same extent.

5.10.1 November 2010 Deployment #7

Time series of water elevation as recorded by the pressure sensor in the Aquadopp show semidiurnal tidal oscillations of a few centimeters overlaying larger synoptic variations of up to 15 cm (Fig. 5.47a). Water temperature exhibited an initial diurnal oscillation but then a more continuous heating from about 17.5 up to about 21 °C (Fig. 5.47b). Time series of profiles of north and east components of velocity show that currents are generally weak ($<0.2 \text{ m s}^{-1}$), and that occasionally near bottom currents are stronger than surface currents (Figs. 5.48, 5.49). This may occur when pressure gradients from the water slope are in the opposite direction from the wind. Scatter plots of the current components at two levels in the water column show that the near bed currents are somewhat more rectilinear than the surface currents (Fig. 5.50). The general orientation of the currents is along the same northeast-southwest axis as the geometry of Lake Jesup. While the north south component of current reached over 0.10 m s^{-1} , profiles of the net current movement show that there is little net movement along the north-south axis, on the order of a few millimeters per second. In contrast, there is a significant movement of water towards the east that reaches almost 0.25 m s^{-1} in the middle of the water column (Fig. 5.51). This suggests that the LJ28 site may be located within a subtidal eddy.

A Welsch type spectral estimator was applied to the along beam velocity signal from the Aquadopp. Although this analysis does not provide estimates of wave heights, it does show the dominant wave periods and their intensity. Typical wave periods are about one

second or slightly longer during this deployment, and wave energy peaks correspond well with wind measurements taken from a nearby weather station (Fig. 5.52). A scatter plot of wind speeds and wave energy density at 1 Hz shows that significant wave activity generally does not occur until the wind reaches about 5 mi hr^{-1} (about 2.2 m s^{-1} , Fig. 5.53). At higher wind speeds, waves develop with their energy being dependent upon both the wind speed and the fetch. The longest fetches are from winds from the northeast and southwest directions, so winds from these directions create the largest waves for a given wind speed (Fig. 5.54).

Time series of profiles of the inorganic fraction of total suspended solids from calibration of the range corrected acoustic backscatter show distinct resuspension events (Fig. 5.55a). Concentrations of inorganic sediments near the bed range from around 0.03 to 0.06 g L^{-1} . The peak resuspension events, in which sediment was resuspended most of the way to the surface, correlate well with the high wind and wave energy events (Fig. 5.55 a,b). Comparison of the direction and magnitude of sediment transport (Fig. 5.56a) with the wind directions (Fig. 5.56b) and wave intensities (Fig. 5.54) show that sediment transport is generally forced by wind and waves from the northeast and southwest, when fetches are longest and resuspension of sediments is greatest. The friction velocity, $U_* = \sqrt{\tau/\rho}$ is a function of the shear stress, τ , and the water density ρ , and is commonly used to represent the amount of shear stress. While wind and wave shear stresses at the bottom were correlated, maximum wave friction velocities were generally over twice the magnitude of the current friction velocity (Fig. 5.57). Comparison of combined wave current friction velocities shows a good correlation with inorganic TSS from the highest bin of the Aquadopp (Fig. 5.58). The comparison also demonstrates that very little shear stress is required to resuspend sediment and that exact determination of the critical shear stress is below the measurement capabilities. Combined wave current friction velocities were set to zero for wave orbital velocities less than 0.01 m s^{-1} ; the spread around friction velocities equal to zero in Fig. 5.58 show that there is no obvious critical shear stress above which the amounts of sediment per increased shear (represented by the slope of the line in Fig. 5.58) are resuspended. Note, the ADV did not work properly during this deployment so results from this instrument are omitted.

5.10.2 January 2011 Deployment #8

Time series of pressure and temperature during the January and February, 2011 deployment show the same general characteristics as in the first deployment (Fig. 5.59). Small semidiurnal oscillations overlay a larger synoptic change in elevation of around 15 cm. North and east components of velocity are somewhat stronger than during the first deployment, reaching 0.3 m s^{-1} (Figs. 5.60, 5.61). The general northeast to southwest orientation of the current is also maintained (Fig. 5.62), although there is a somewhat more easterly at the lowest bin of the sensor. Examination of the profiles of net current movement shows that there was insignificant movement in the east west axis ($<0.02 \text{ m s}^{-1}$), but about a 0.07 m s^{-1} net movement to the south near the bottom (Fig. 5.63).

Wave events as calculated by spectral analysis of the along beam velocity of the Aquadopp correlated well with time series of wind speeds (Fig. 5.64ab) as in the first deployment. And as before, significant wave activity was only initiated at wind speeds of about 5 mi hr^{-1} (mph) or higher (Fig. 5.65). Wave intensities were stronger during this deployment and

resuspended higher amounts of inorganic sediment (Fig. 5.66). In addition to resuspended sediment, there were episodes of suspended sediment advected in surface plumes. These events tended to occur at the same time as resuspension by waves, but the acoustic backscatter from the event on February 1st clearly shows the slow settling of sediment downwards from the surface. As before, the majority of sediment transport was in the northeast and southwest directions (Fig. 5.67). The friction velocity due to currents was very low and not well correlated with either the inorganic TSS or the friction velocity due to waves, which was of much higher magnitude (not shown). In contrast, the combined wave-current friction velocity was well correlated with inorganic TSS (Fig. 5.68). Figure 5.68 shows two scatter plots, one for the data before February 3rd, 4:00 am, and another afterwards. This deployment had much higher levels of suspended solids both in the water column, and apparently much more mobile sediment near the bed. The slope of these two time periods within this deployment are very similar, indicating that a given increase in wave-current friction velocity resuspends a proportionally greater amount of sediment. However, the change in intercept indicates that there was a much larger background level of suspended solid concentration during the last resuspension event. These high levels of suspended sediment appear to have been advected into the region, and have disappeared by the next deployment in April 2011.

The settling velocity was estimated using the Reynolds flux determined by the ADV. Only observations in which the suspended sediment concentration was at a relatively steady state were used ($\text{abs}(dC/dt) < 0.0001 \text{ g L}^{-1} \text{ s}^{-1}$). The relationship is noisy, but produces a realistic settling velocity estimate of 0.0002 m s^{-1} and a background suspended sediment concentration of 0.037 g L^{-1} (Fig. 5.69).

5.10.3 April 2011 Deployment #9

Pressure and temperature measurements were comparable with the previous two deployments (Fig. 5.70). Time series of north and east components of velocities are shown in Figures 5.71 and 5.72. The Aquadopp configuration was slightly different during this deployment and may have contributed to the apparently much more rectilinear currents than in the previous deployments (Fig. 5.73). Profiles of net currents show a trend toward the northeast with net currents more towards the north at the bottom and more towards the east at the surface (Fig. 5.74).

Wave spectra from the along beam velocities from the Aquadopp were relatively dampened compared to the first two deployments, perhaps due to the slightly different configuration (Fig. 5.75). Nevertheless, maximum wave intensities were still around waves with about a 1 s period, and wave intensities are still well correlated with wind speeds. The relationship between wave intensity and wind speed is noisier than previous deployments, but still shows clear increases around wind speeds of 5-7 mi hr^{-1} (Fig. 5.76). There were several small resuspension events during the deployment (Fig. 5.77). They do not seem to correspond as well to the wave intensities as in previous deployments; although there is a positive relationship between combined wave current shear stress and TSS (Fig. 5.78). As in previous deployments, the direction of sediment transport was in the northeast and southwest directions (Fig. 5.79).

Using the criterion for steady state from the previous deployment ($\text{abs}(dC/dt) < 0.0001 \text{ g L}^{-1} \text{ s}^{-1}$) did not give a good correlation for estimates of settling velocity. An order of magnitude higher criterion ($\text{abs}(dC/dt) < 0.00001 \text{ g L}^{-1} \text{ s}^{-1}$) gives the same estimate for settling velocity ($w_s = 0.00002 \text{ m s}^{-1}$) as in the previous deployment. This estimate may be fortuitous, however, since the total number of bursts that qualify is small (Fig. 5.80). Particle size distributions from the LISST suggest that during periods when resuspension is high, a population of aggregates around 90-140 μm are resuspended (Fig. 5.81).

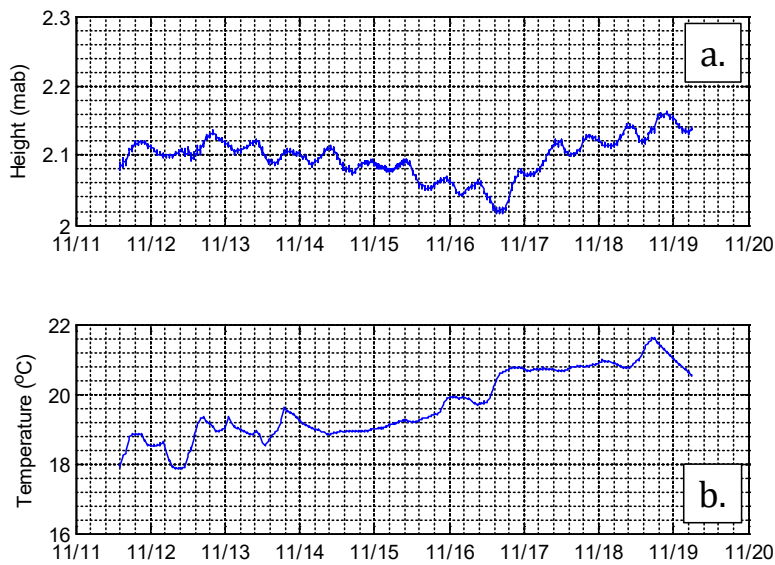


FIGURE 5.47 (a) Time series of water height 9 (m) above bed (mab) and (b) water temperature during the Nov 2010 deployment at site LJ28

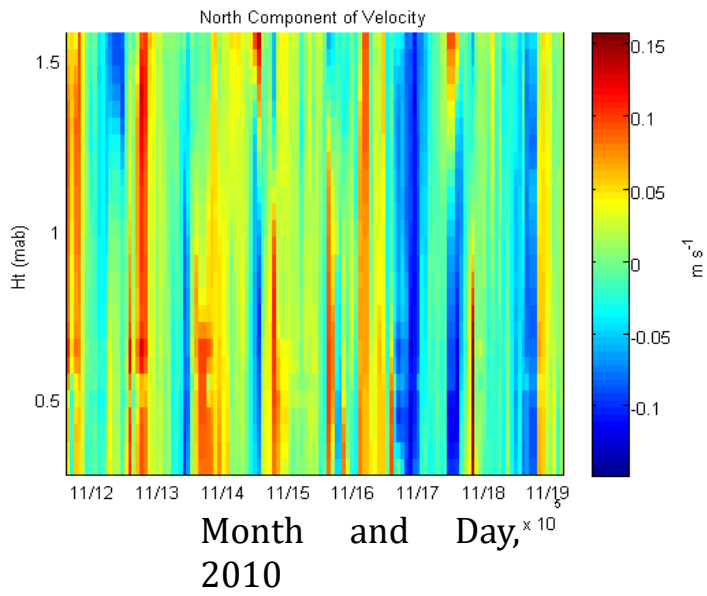


FIGURE 5.48 Time series of profiles of north component of velocity, Nov 2010 deployment.

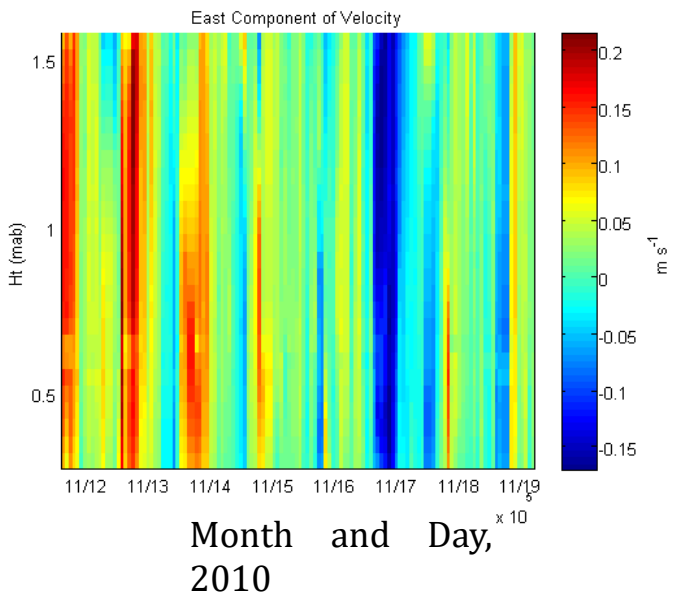
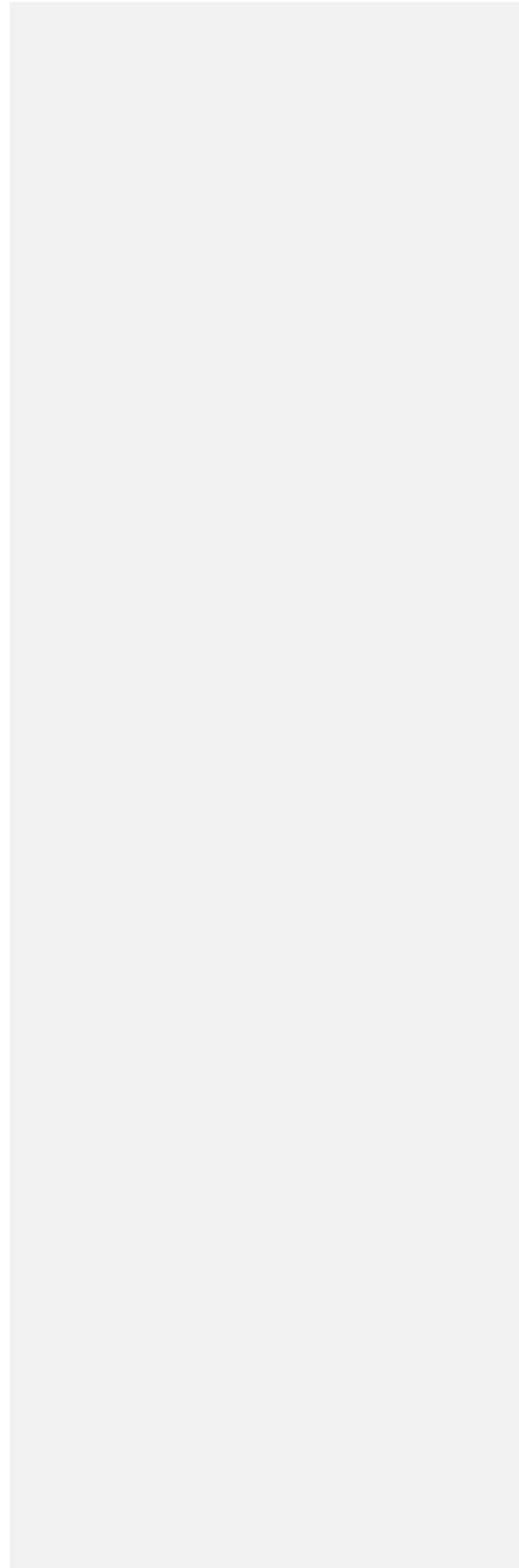


FIGURE 5.49 Time series of profiles of north component of velocity, Nov 2010 deployment.



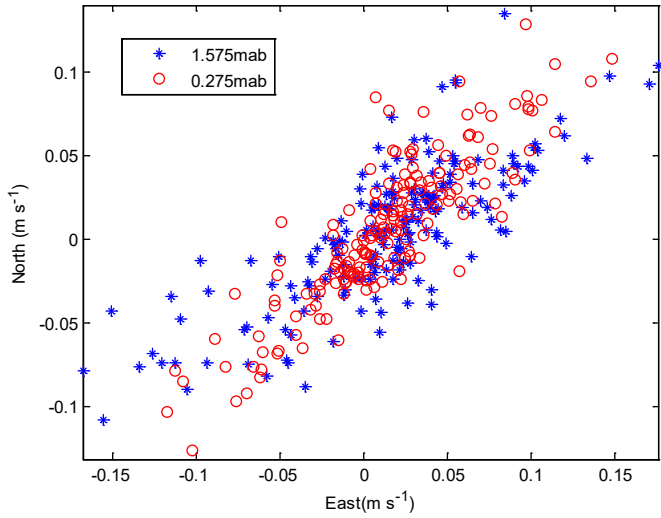


FIGURE 5.50 Velocities at about 0.27 and 1.6 meters above the bed (mab), Nov 2010 deployment.

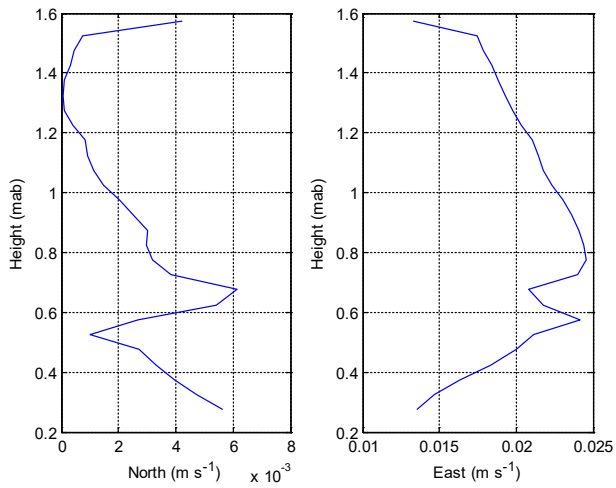


FIGURE 5.51 Profiles of net currents over entire deployment , Nov 2010.

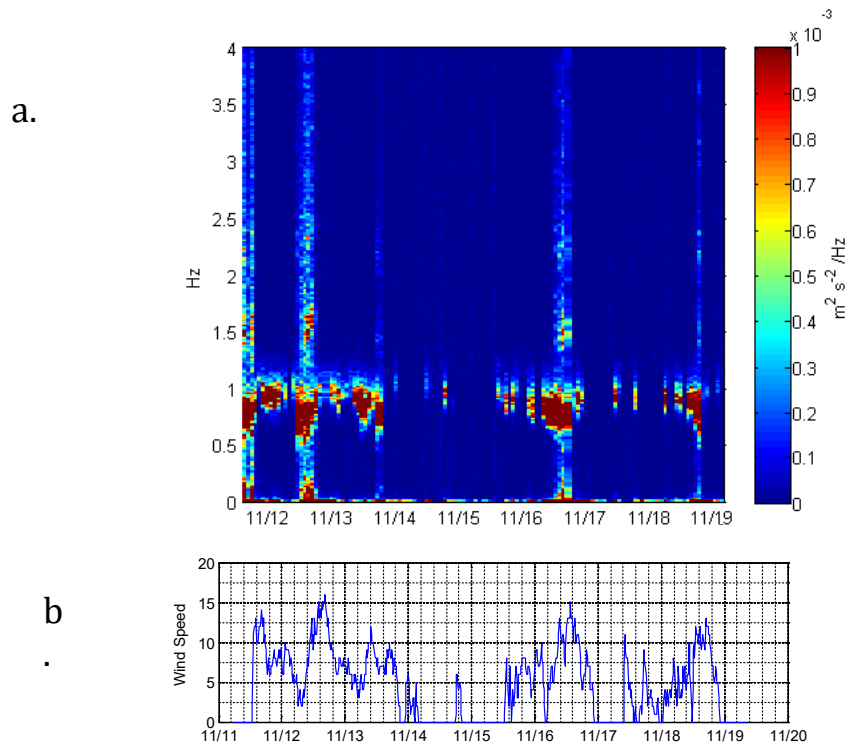


FIGURE 5.52 Time series of wave energy spectra from the along beam velocity of the (a) Aquadopp and (b) windspeed (mph), Nov 2010 deployment.

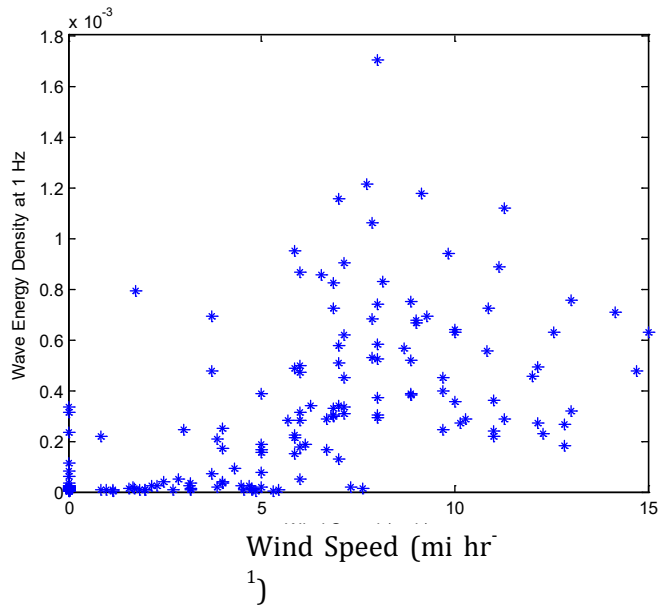


FIGURE 5.53 Wave energy density at 1 Hz by wind speed.

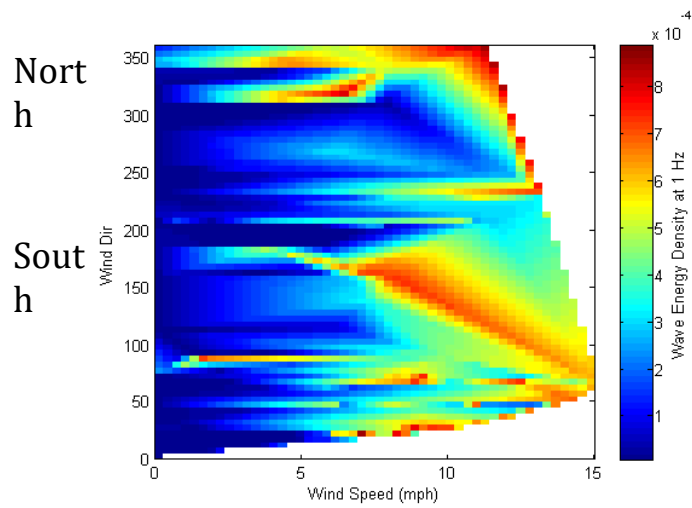


FIGURE 5.54 Wave energy at 1 Hz by wind speed and wind direction, Nov 2010 Deployment

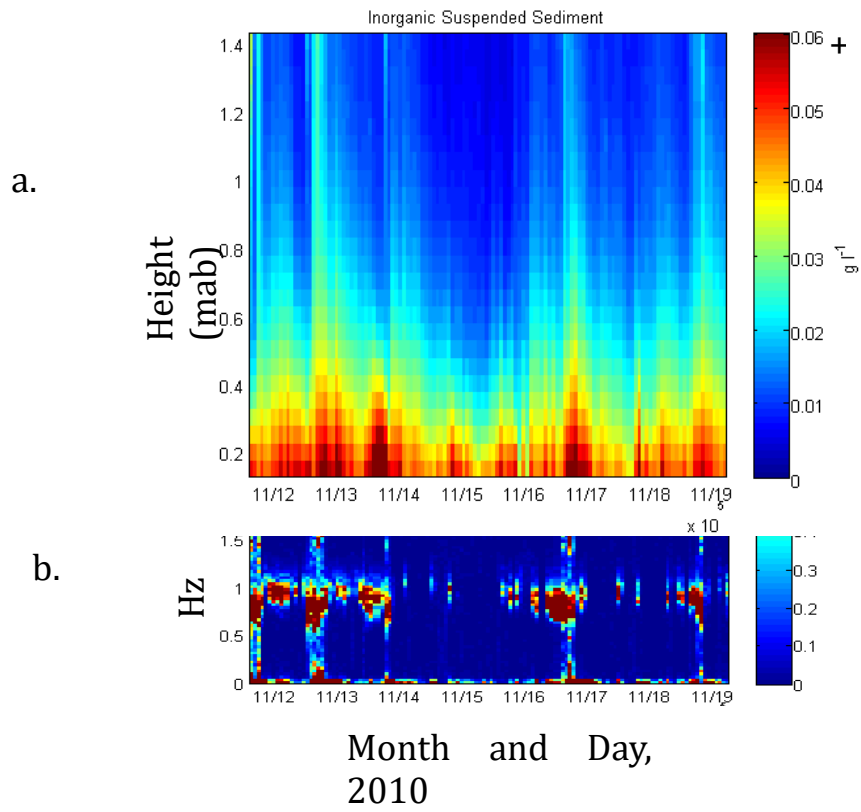


FIGURE 5.55 (a) Time series of profiles of inorganic fraction of TSS ($g\ l^{-1}$). (b) inset of Fig. 25a, showing wave intensities around 1 Hz.

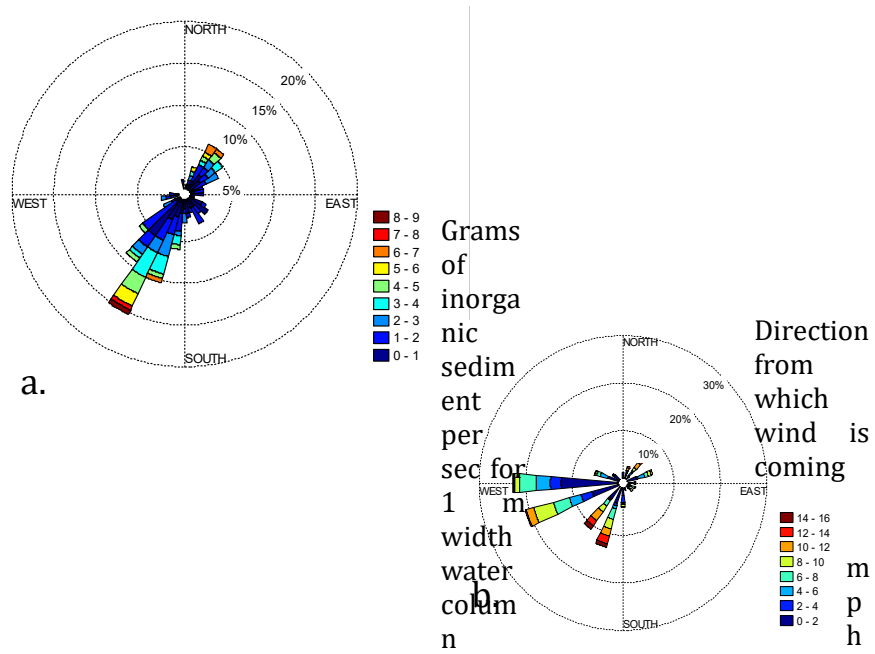


FIGURE 5.56 (a) Direction and magnitude distribution of hourly inorganic suspended solid transport ($\text{g s}^{-1} \text{m}^{-1}$), Nov 2010 (b) Wind speed and direction distribution (showing direction from which wind is coming).

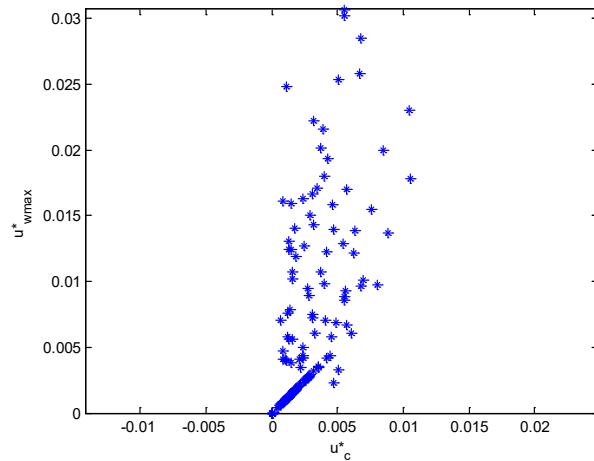


FIGURE 5.57 Maximum wave friction velocity by current friction velocity (m s^{-1}), Nov 2010.

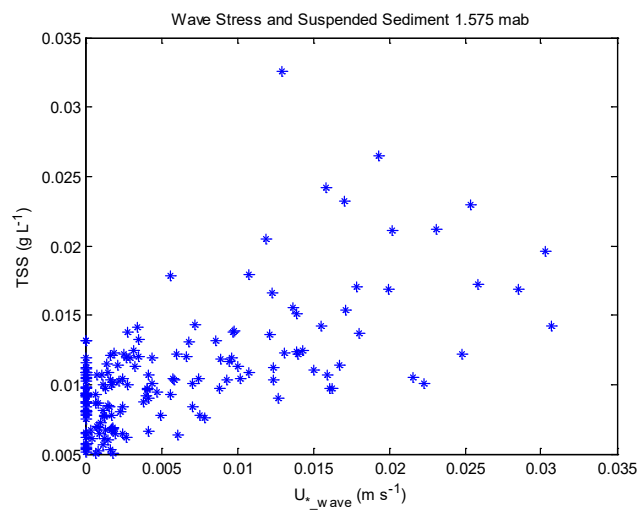


FIGURE 5.58 Relationship between combined wave – current friction velocity and inorganic TSS, Nov 2010.

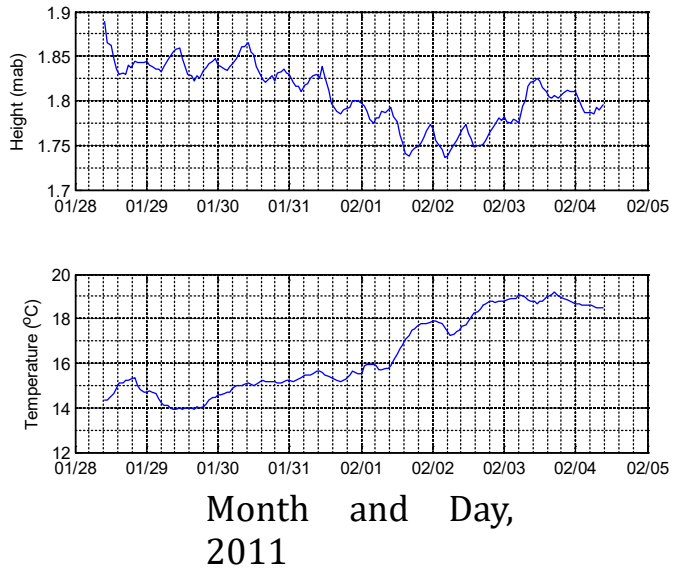


FIGURE 5.59 Time series of water height above bed (mab) and water temperature during the Feb 2011 deployment.

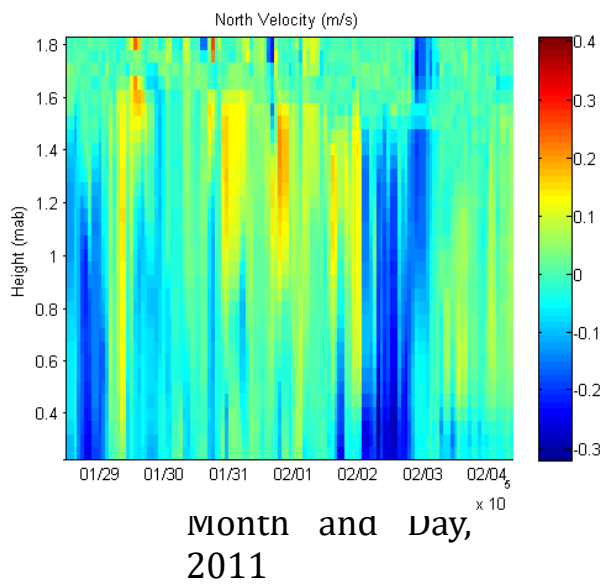
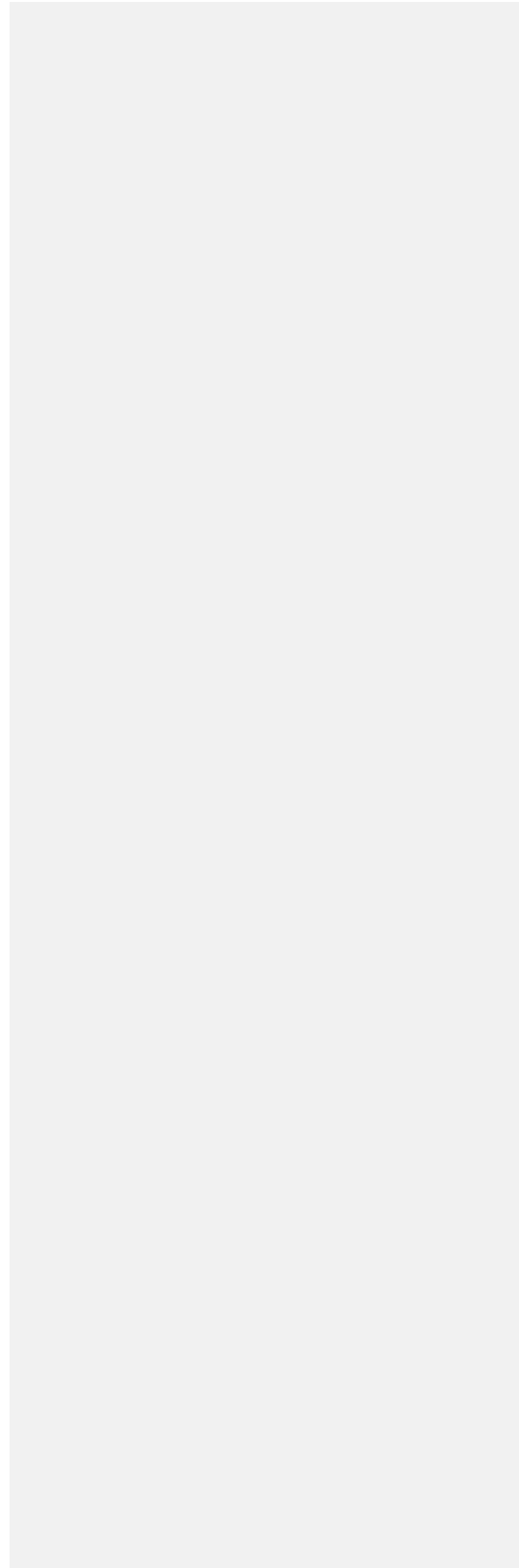


FIGURE 5.60 Time series of profiles of north component of velocity, February 2011 deployment.



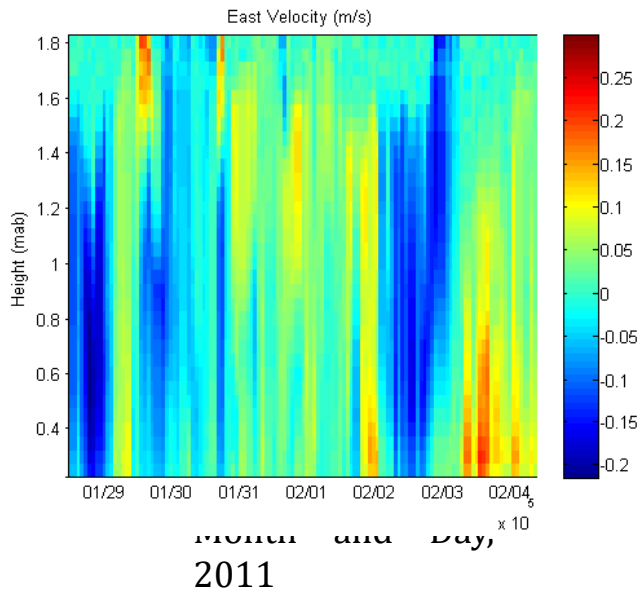


FIGURE 5.61 Time series of profiles of east component of velocity, February 2011 deployment.

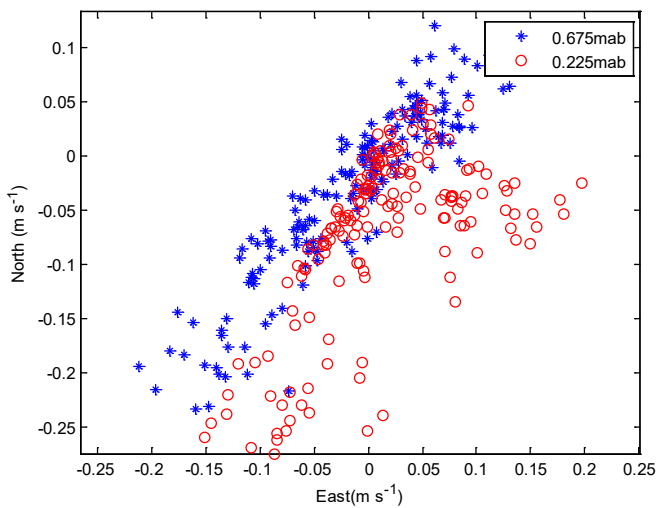


FIGURE 5.62 Velocities at about 0.68 and 0.22 meters above the bed (mab), Feb 2011 deployment.

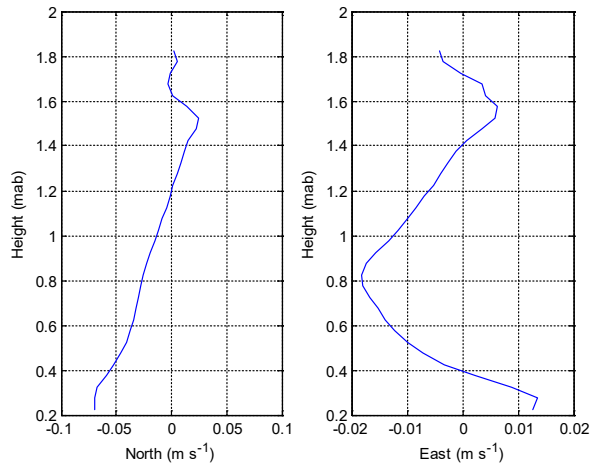
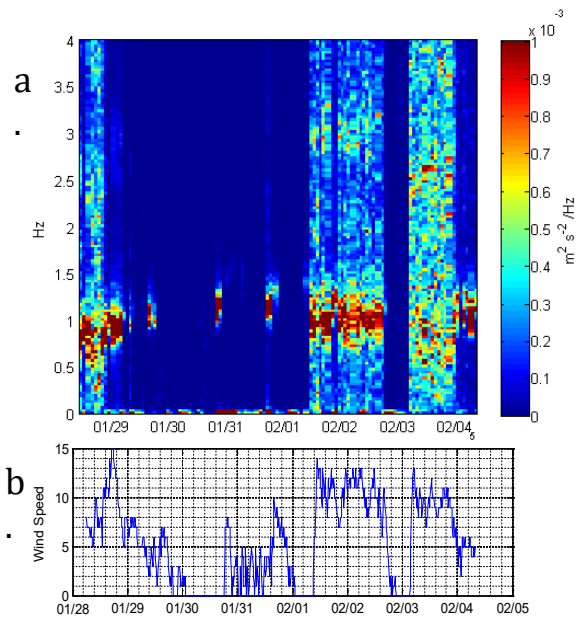


FIGURE 5.63 Profiles of net currents over entire deployment , Feb 2011.



Month and Day,
2011

FIGURE 5.64 Time series of wave energy spectra from the along beam velocity of the (a) Aquadopp and (b) windspeed (mps), Feb 2011 deployment.

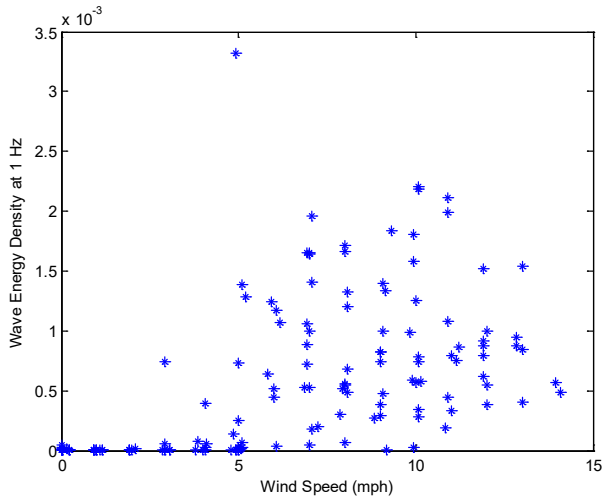


FIGURE 5.65 Wave energy density at 1 Hz by wind speed, Feb 2011 deployment.

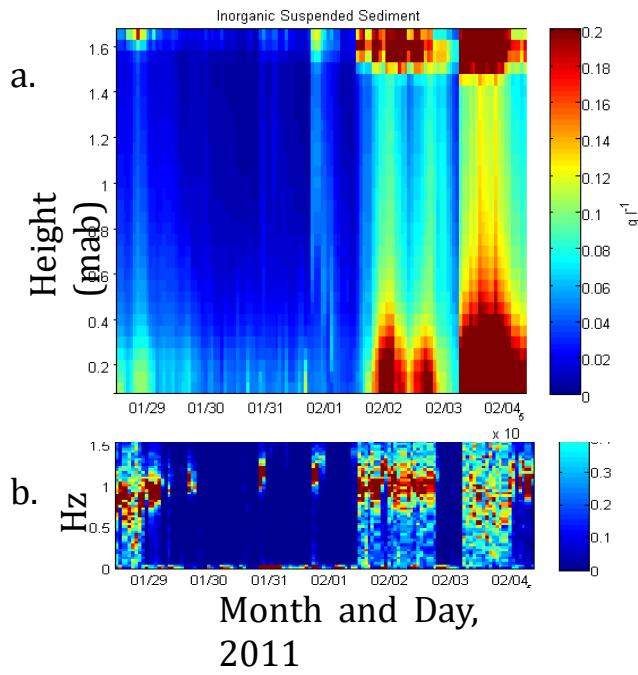


FIGURE 5.66 (a) Time series of profiles of inorganic fraction of TSS (g l^{-1}). (b) inset of Fig. 20a, showing wave intensities around 1 Hz. All from Feb. 2001 deployment

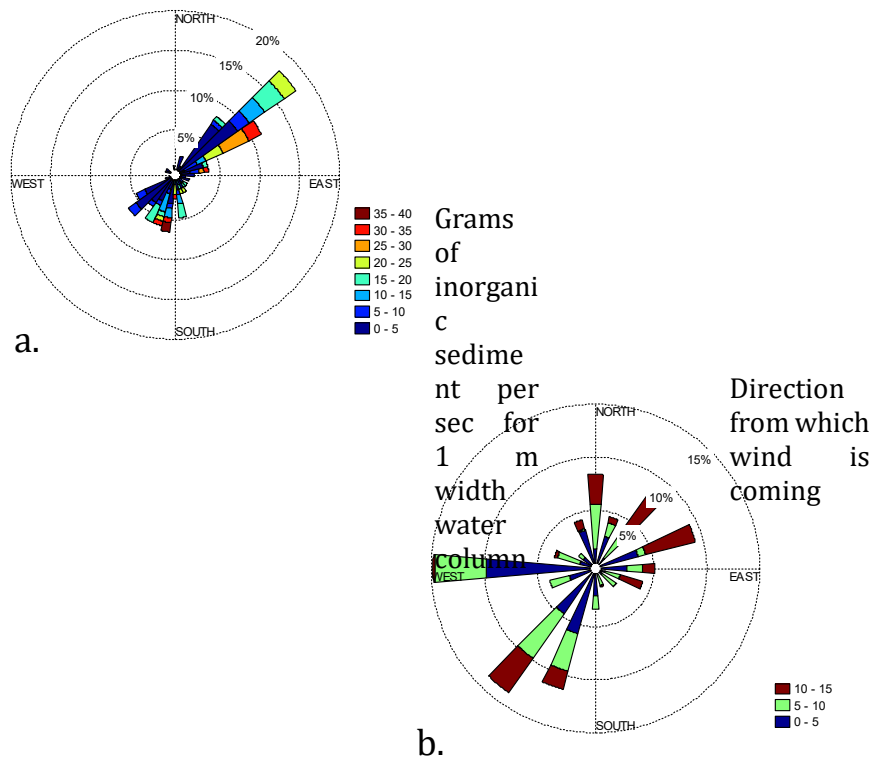


FIGURE 5.67 (a) Direction and magnitude distribution of hourly inorganic suspended solid transport ($\text{g s}^{-1} \text{m}^{-1}$), Feb 2011. (b) Wind speed and direction distribution (showing direction from which wind is coming)

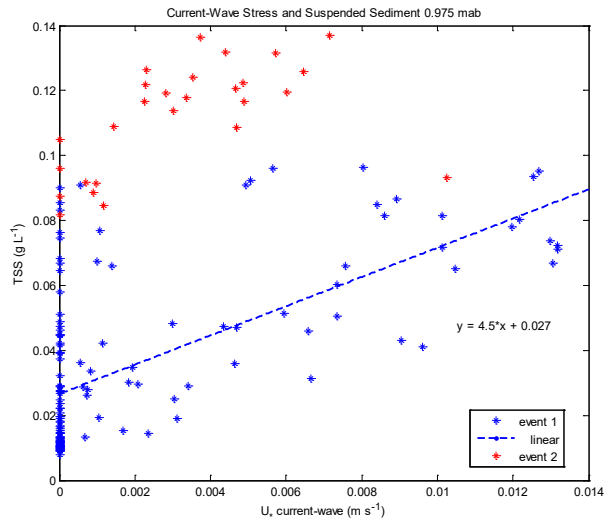


FIGURE 5.68 Relationship between combined wave – current friction velocity and inorganic TSS, Feb 2011. Blue markers are before Feb 3, 2011, 4:00 a.m., red markers are for the resuspension event afterwards.

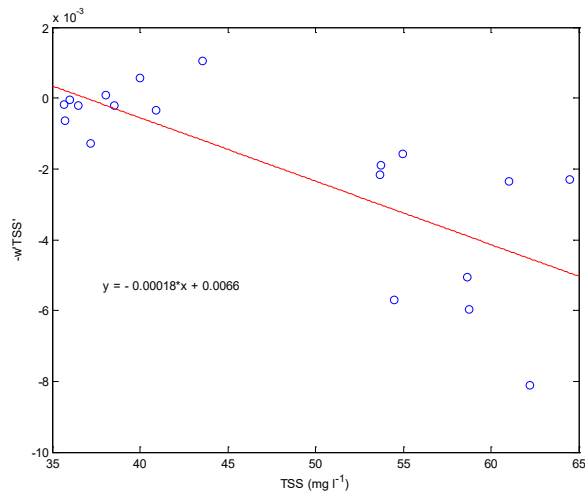


FIGURE 5.69 ADV estimate of settling velocity, $w_s = 0.2 \text{ mm s}^{-1}$ and background suspended sediment concentration = 37 mg l^{-1} , Feb 2011 deployment.

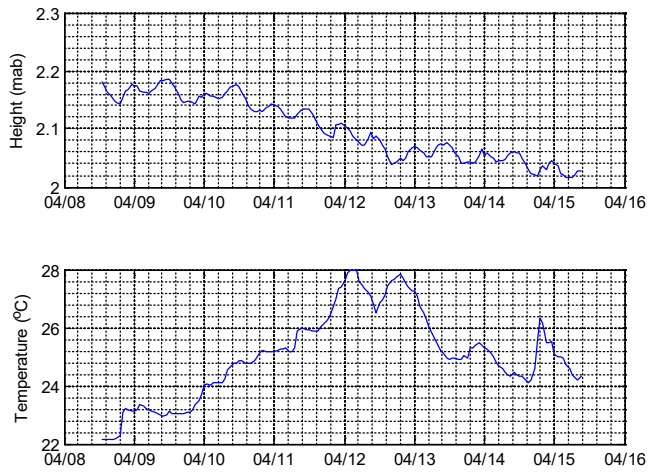


FIGURE 5.70. Time series of water height above bed (mab) and water temperature during the Apr 2011 deployment.

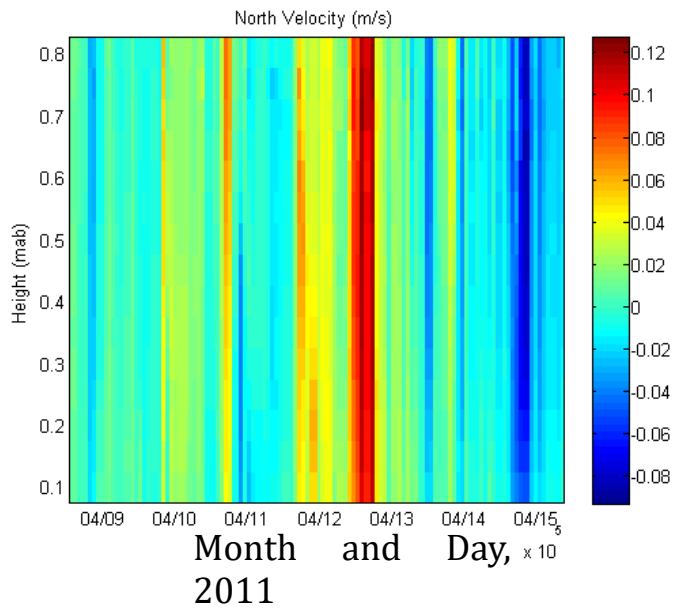
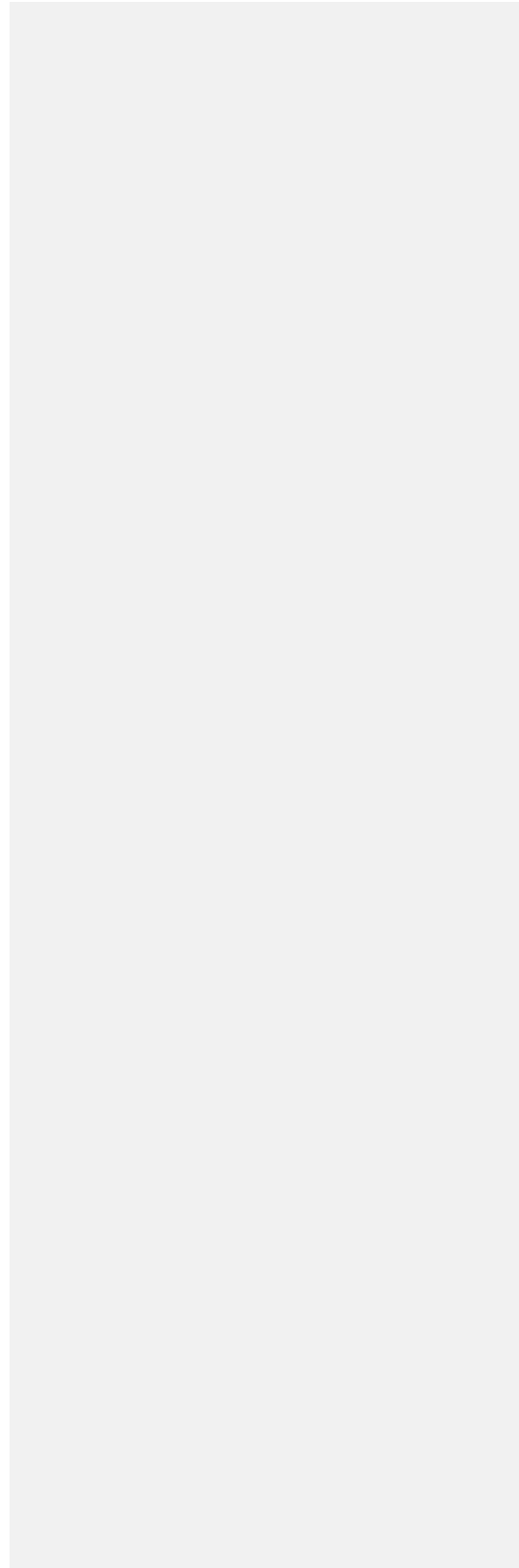


FIGURE 5.71. Time series of profiles of north component of velocity, Apr 2011 deployment.



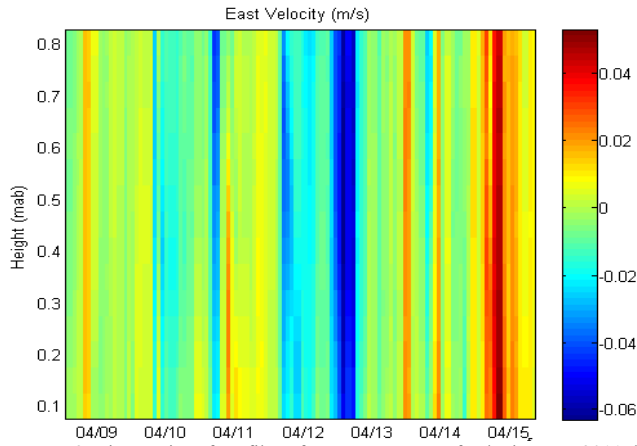


FIGURE 5.72 Time series of profiles of east component of velocity, Apr 2011 deployment.

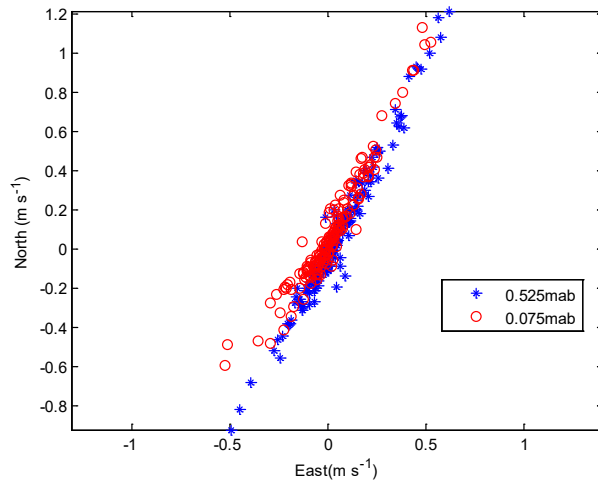


FIGURE 5.73 Velocities at about 0.07 and 0.5 meters above the bed (mab), Apr 2011 deployment.

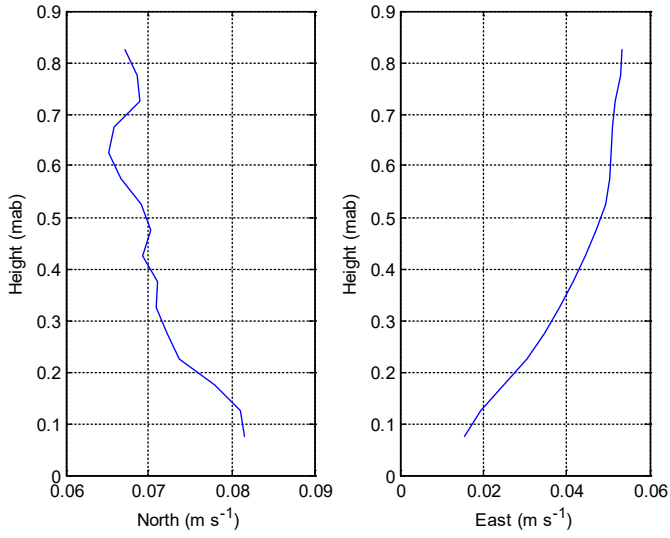


FIGURE 5.74 Profiles of net currents over entire deployment , Apr 2011.

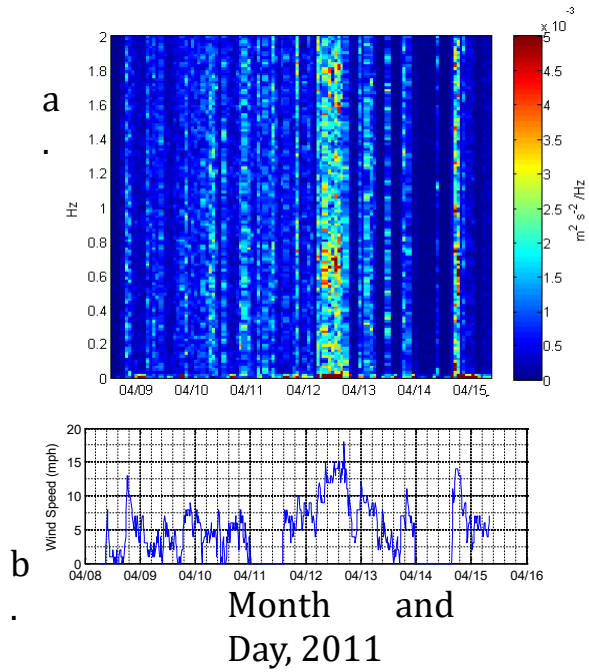


FIGURE 5.75 Time series of wave energy spectra from the along beam velocity of the (a) Aquadopp and (b) windspeed (mps), Apr 2011 deployment.

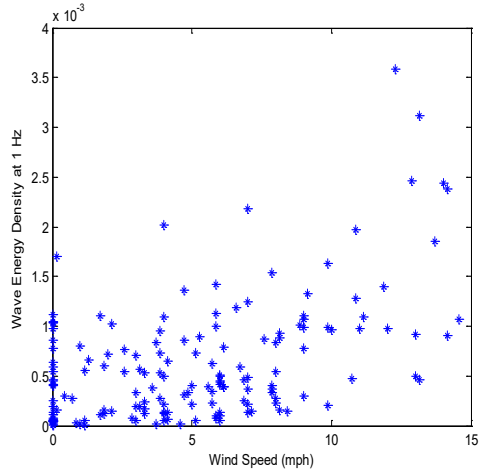


FIGURE 5.76 Wave energy density at 1 Hz by wind speed, Apr 2011 deployment.

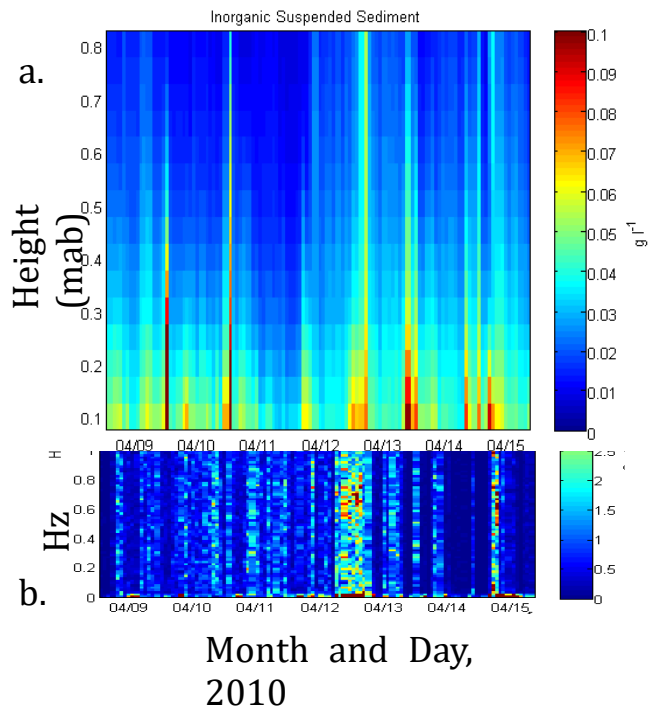


FIGURE 5.77 (a) Time series of profiles of inorganic fraction of TSS (g l^{-1}). (b) inset of Fig. 48a, showing wave intensities around 1 Hz.

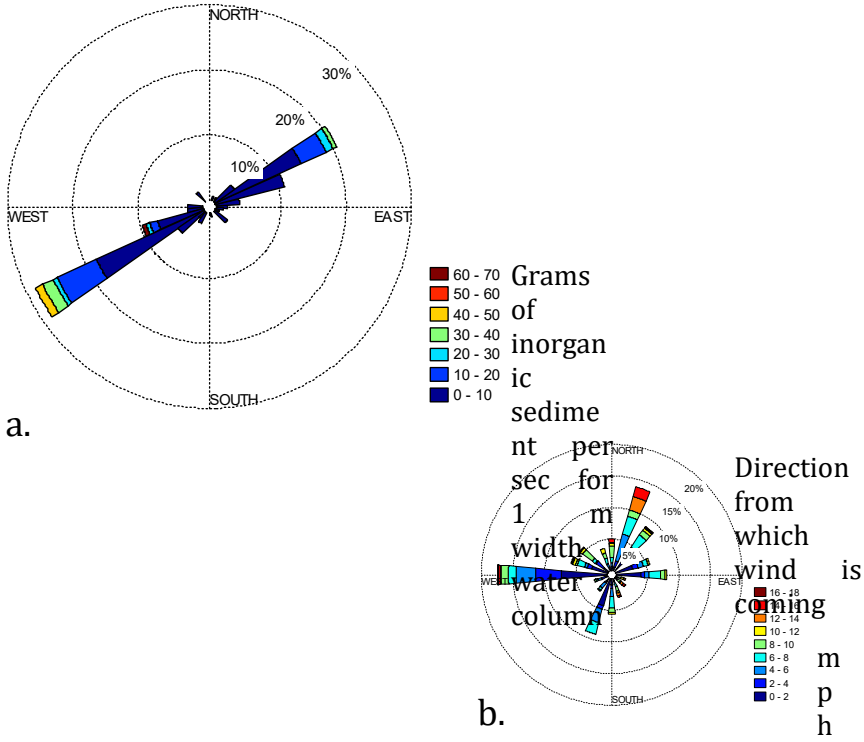


FIGURE 5.79 (a) Direction and magnitude distribution of hourly inorganic suspended solid transport ($\text{g s}^{-1} \text{m}^{-1}$), Apr 2011. (b) Wind speed and direction distribution (showing direction from which wind is coming).

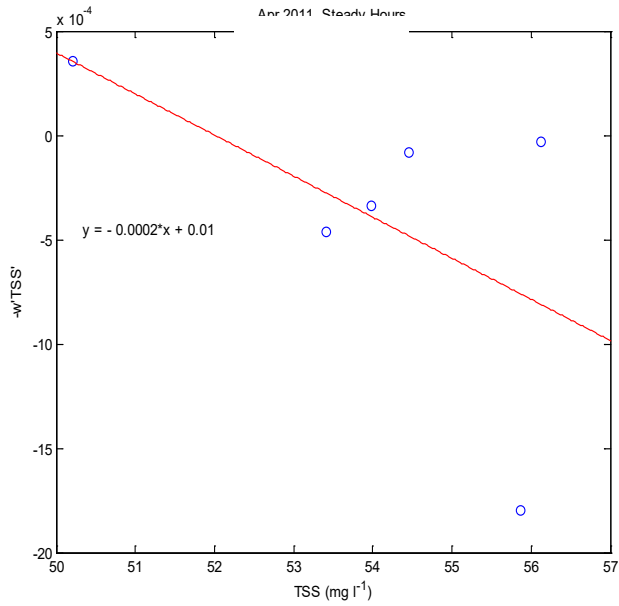


FIGURE 5.80 ADV estimate of settling velocity, $w_s = 0.2 \text{ mm s}^{-1}$ and background suspended sediment concentration = 50 mg l^{-1} , Apr 2011 deployment.

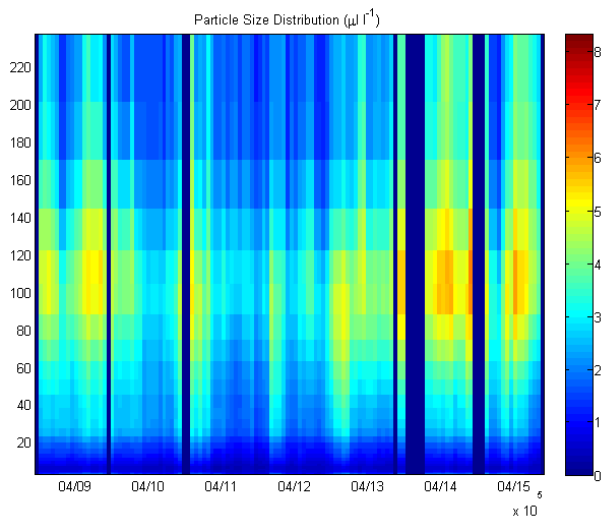


FIGURE 5.81 Time series of particle size distribution, Apr 2011 deployment.

5.11 Predictions of physical transport of suspended solids

The previous results and theoretical relationships may be combined to develop analytical expressions to predict the effect of a given wind speed and direction on suspended sediment concentrations due to wave resuspension. These, in turn, can be combined with the nutrient analyses to develop relationships between wind speed and direction, and total nitrogen and total phosphorous concentrations in the water column. One important caveat is that although the dominant process related to variations in the sediment concentration is related to wind and wave events, these predictions cannot account for the increase in suspended sediment due to advection through exchange with the St. Johns River. Nor is it able to account for resuspension due to biota or boats, etc. The advection of high concentrations of sediment was important to increasing the overall background concentration and the available pool of resuspendable sediment in the February 2011 deployment. During this time, much larger amounts of sediment were resuspended for the same amount of wave-current friction velocity than were in the November 2010 and April 2011 deployment. These two deployments, however, were very consistent with each other, and there was no evidence for significant advection. Therefore, these predictions are based on the data from the November 2010 and April 2011 deployments and are conservative estimates.

5.11.1 The analytical method for predicting water column nutrient concentrations due to wind wave resuspension

The drag of the wind creates a mean current as well as producing waves. The combination of the mean current and wave orbitals near the bottom generate a shear stress that is greater than the addition of each component. In order to predict the wave-current shear stress, current speeds and wave orbital velocities are needed. Wind speeds are used to predict mean current speed for wind speeds over 2.5 m s^{-1} . A quadratic relationship is fitted to the wind and current data from the April 2011 deployment (Fig. 5.82). The other deployments were noisier.

Wave characteristics were determined using the SPMSWG method (USACE, 1984). The fetch was determined for a suite of wind directions around the compass as described earlier. Predictions of wave height and wave period were made for these wind directions and wind speeds of 1 to 14 m s^{-1} , which are typical for Lake Jesup (Figs. 5.83, 5.84). At 2 meter depth, such as the deployment site, these predicted waves would generate the orbital velocities shown in Fig 5.85. All of the above calculations were used to generate current and wave - current friction velocities using Soulsby's (1997) method described in the methods section (section 4.11 and Figs 5.86 and 5.87).

Combining the data from the November 2010 and April 2011 deployments produced a good relationship between observed wave-current friction velocities and the inorganic fraction of TSS (Fig. 5.88). Typical errors are less than 0.005 g l^{-1} .

Inorganic fractions of suspended sediment were used to calibrate the acoustic sensors. Nutrient concentrations were determined from the dry weight of combined inorganic and organic sediment fractions from the sediment grabs, floc layer and sediment traps. These values represent the range of observed nutrient mass per solids mass in all of the pools of solids. The TSS from Lake Jesup exhibited a typical relationship between total suspended

solids and percentage of organic content (Fig. 5.89). A typical organic percentage of 50% was used to estimate the total suspended solids from the predicted resuspended inorganic fraction. Total phosphorous concentrations ranged from low values around $200 \mu\text{g g}^{-1}$ of dry sediment to high values around $2700 \mu\text{g g}^{-1}$ of dry sediment (Fig. 5.90). These two values and a mean value of $1450 \mu\text{g g}^{-1}$ were used to provide upper and lower bounds, and medium values of predicted nutrient concentration in the suspended sediment of Lake Jesup for the given suite of wind speeds and directions. Total nitrogen concentrations were estimated using the linear relationship found between TP and TN (Fig. 5.90). Predicted TP concentrations ranged from 6.5 to $10.0 \mu\text{g L}^{-1}$ depending on the wind speed and direction for the low concentration scenario (Fig. 5.91) and 85 to $135 \mu\text{g L}^{-1}$ in the high concentration scenario (Fig. 5.92). Medium predicted values of total phosphorous ranged from 45 to $60 \mu\text{g L}^{-1}$ (Fig. 5.93). Predicted total nitrogen concentrations ranged from 0.22 to 0.36 mg L^{-1} depending on the wind speed and direction for the low concentration scenario (Fig. 5.94) and 0.9 to 1.4 mg L^{-1} in the high concentration scenario (Fig. 5.95). Medium predicted values of total nitrogen ranged from 0.55 to 0.90 mg L^{-1} (Fig. 5.96). These predictions should be considered conservative prediction of the actual values. Additional factors such as a mean current unrelated to wind, advection of sediment, or underestimate of percent organic content will significantly increase the concentrations in the water column.

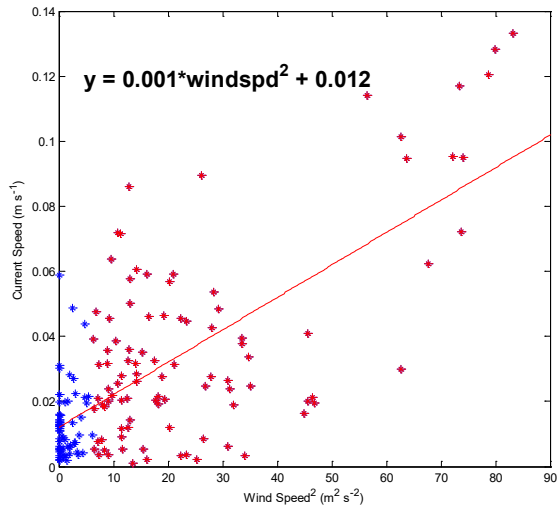


FIGURE 5.82 Apr 2011: Relationship between wind speed and mean current for wind speeds > 2.5 m s⁻¹ ($R^2=0.41$, $p<0.05$). Blue markers are ≤ 2.5 m s⁻¹, red markers are > 2.5 m s⁻¹

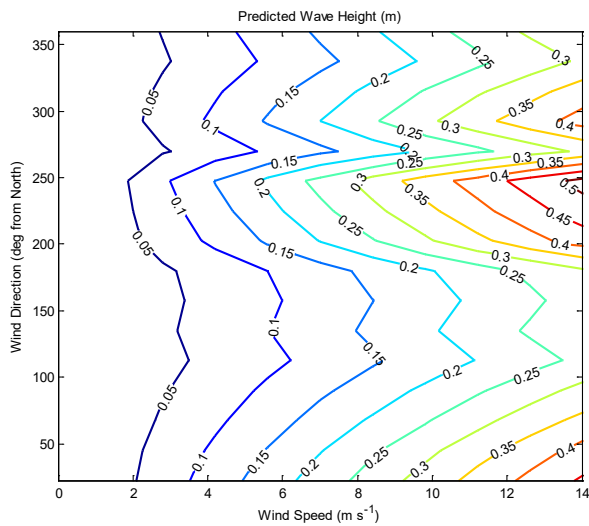


FIGURE 5.83 Predicted wave heights.

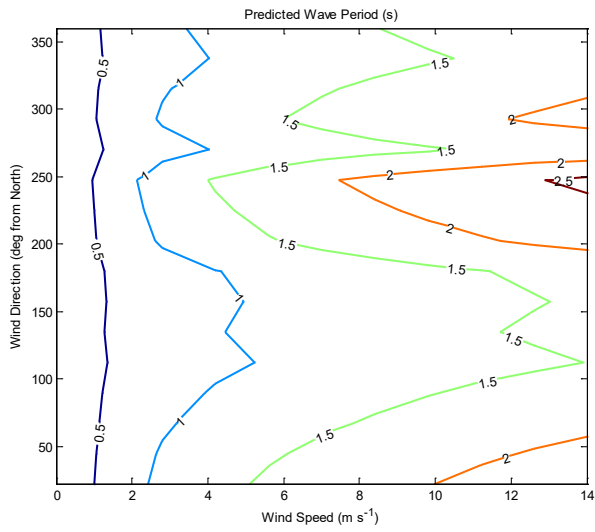


FIGURE 5.84 Predicted wave periods.

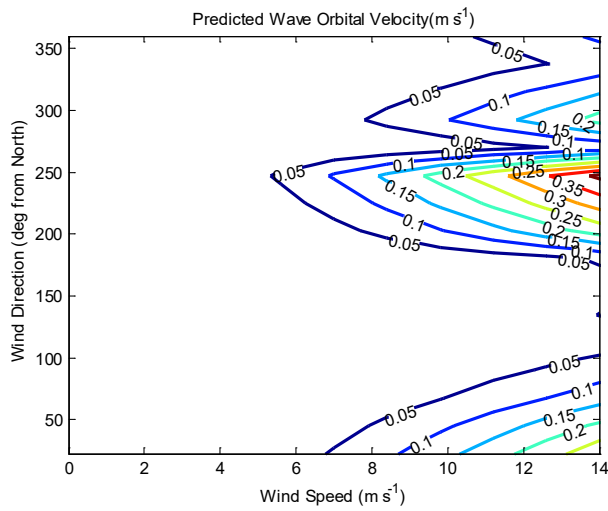


FIGURE 5.85 Predicted wave orbitals.

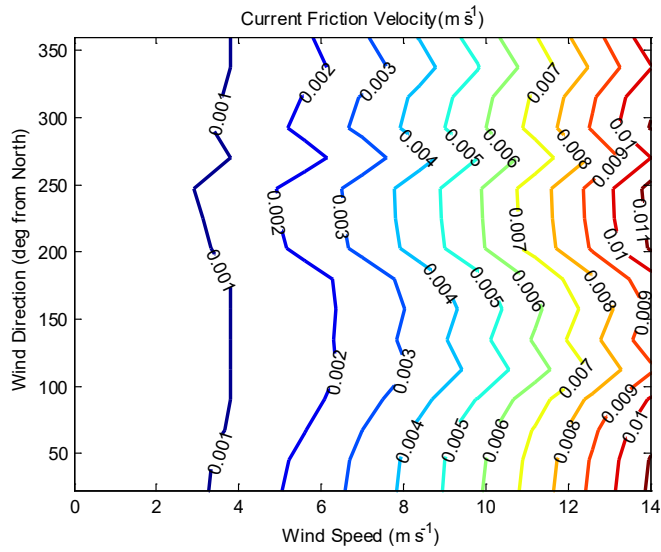


FIGURE 5.86 Predicted current friction velocities

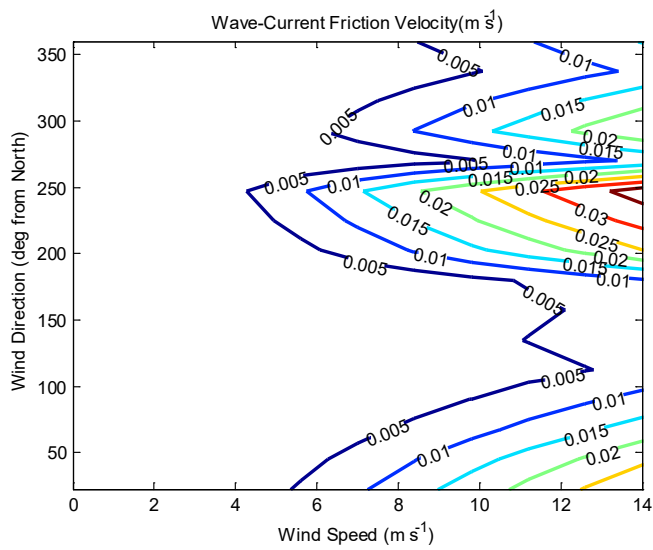


FIGURE 5.87 Predicted wave-current friction velocities

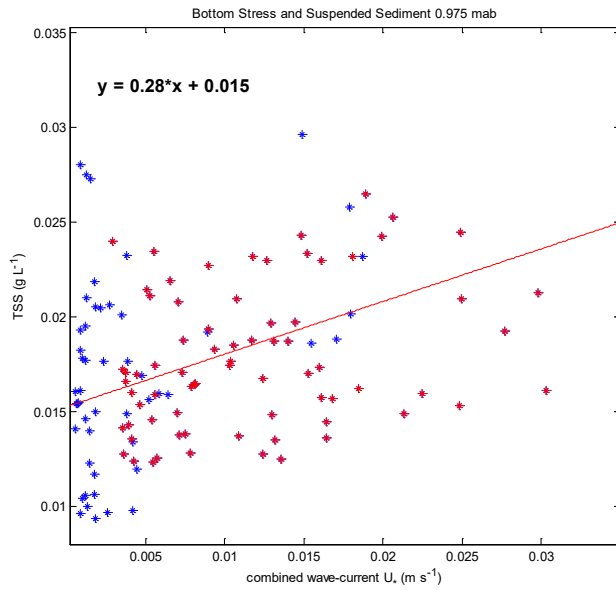


FIGURE 5.88 Nov 2010 (blue) and Apr 2011 (red), 5 outliers from Nov 2010 excluded from plot, ($R^2=0.14$).

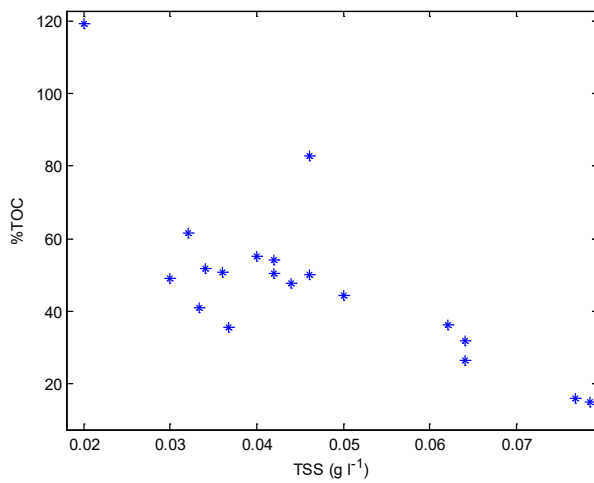


FIGURE 5.89 Relationship between total suspended solids (TSS) and percentage of organic content (TOC). Values over 100% occur from measurement error associated with small concentrations of TSS.

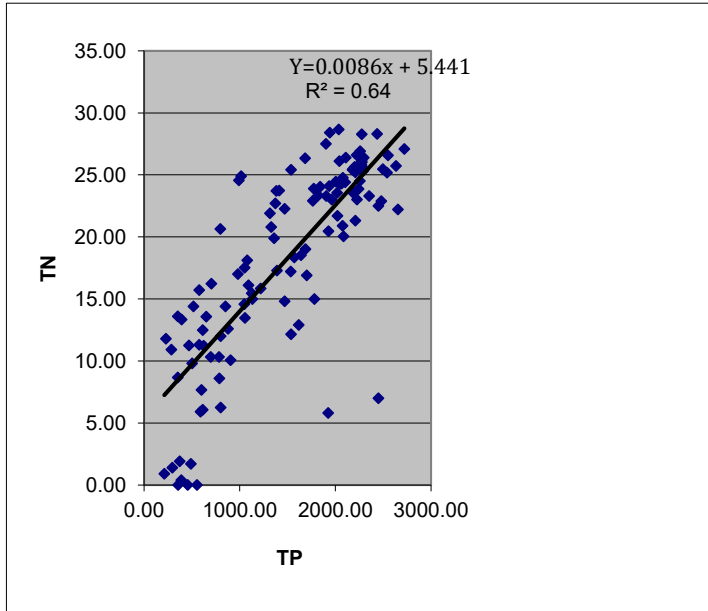


FIGURE 5.90 Relationship between total nitrogen (TN, mg g⁻¹ dry weight) and total phosphorous (TP, μg g⁻¹ dry weight) from floc samples, sediment traps, and sediment grabs.

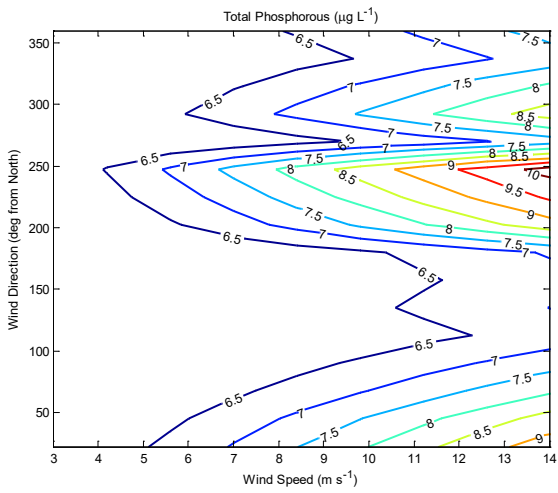


FIGURE 5.91 Predicted lower bound of water column concentrations of total phosphorous (μg L⁻¹) for the low TP scenario, TP=200 μg g⁻¹ dry sediment

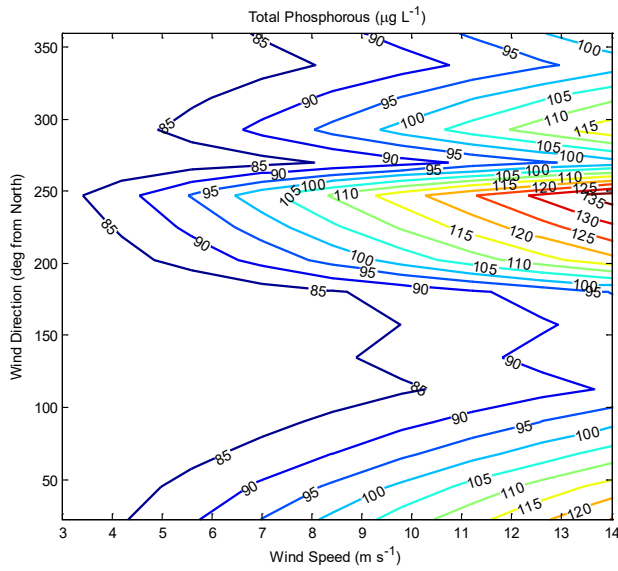


FIGURE 5.92 Predicted upper bound of water column concentrations of total phosphorous ($\mu\text{g L}^{-1}$) for the high TP scenario, $\text{TP}=2750 \mu\text{g g}^{-1}$ dry sediment

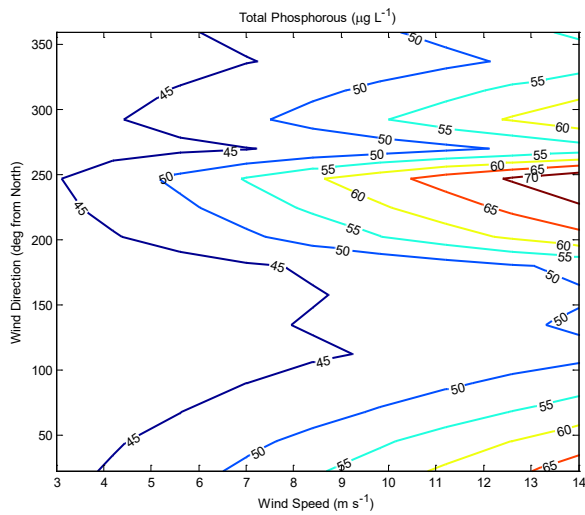


FIGURE 5.93 Predicted medium levels of water column concentrations of total phosphorous ($\mu\text{g L}^{-1}$) for the medium TP scenario, $\text{TP}=1450 \mu\text{g g}^{-1}$ dry sediment

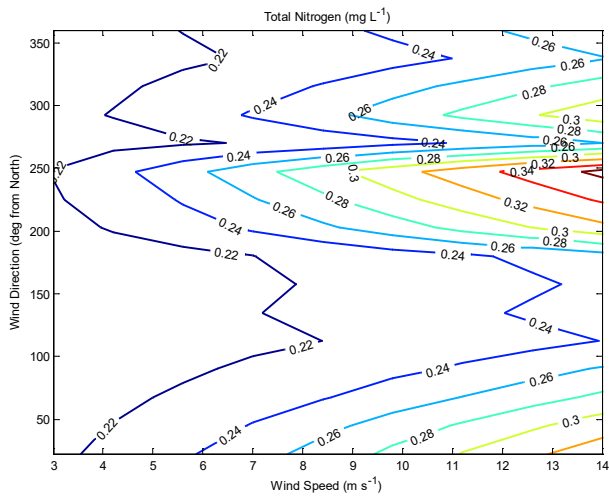


FIGURE 5.94 Predicted lower bound of water column concentrations of total nitrogen (mg L^{-1}) for the low TP scenario, $\text{TP}=200 \mu\text{g g}^{-1}$ dry sediment

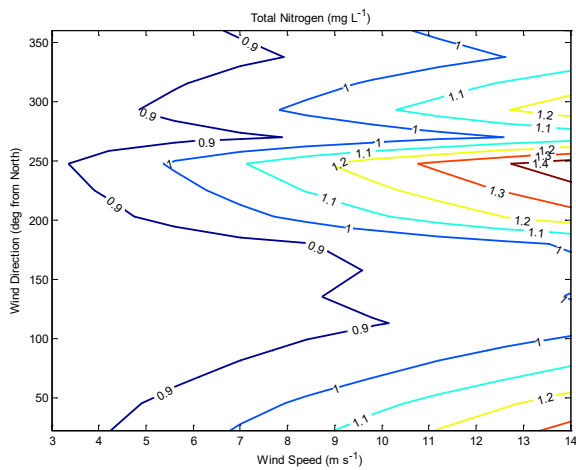


FIGURE 5.95 Predicted upper bound of water column concentrations of total nitrogen (mg L^{-1}) for the high TP scenario, $\text{TP}=2750 \mu\text{g g}^{-1}$ dry sediment

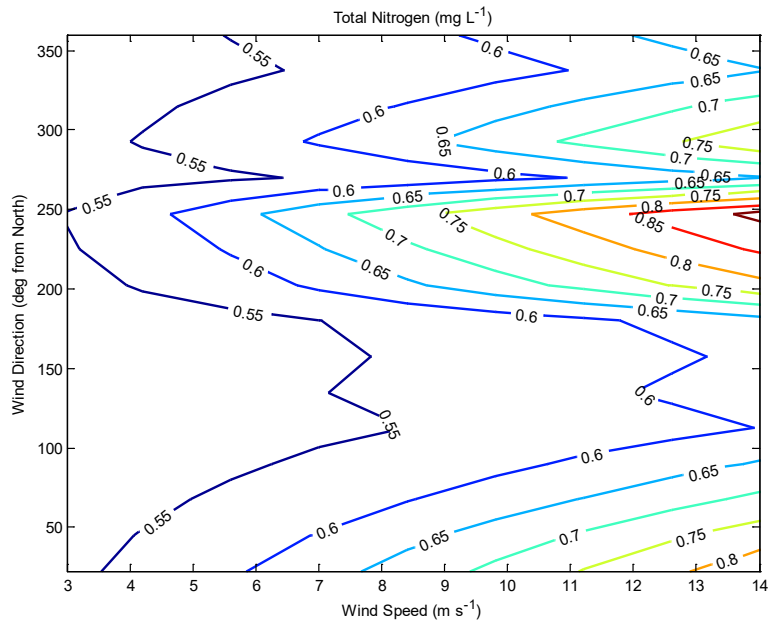


FIGURE 5.96 Predicted medium levels of water column concentrations of total nitrogen (mg L⁻¹) for the medium TP scenario, TP=1450 $\mu\text{g g}^{-1}$ dry sediment

5.12 Radiometric analysis of sediment trap material

Material collected in water column, just above the sediment bed, provides some insight into the possible utility of radioisotopes as tracers of sediment dynamics (Table 5.16). Trap material was not available from the first sampling event (June, 2010). The activities of ^{137}Cs and ^{210}Pb were the most consistent across space and time and these likely represent erosion of material off the surrounding landscape. ^7Be showed the greatest variability across space and time. All sites showed the greatest change between August and November, decreasing by as much as 3 times (LJ14). However, the general changes (+ versus -) in ^7Be activity magnitude were consistent across all sites with time (all sites either decreased or increased across space and time). Due to these large variations in ^7Be activities associated with source material, it is difficult to use this isotope as a tracer without additional input data (atmospheric deposition over time). Variations in ^7Be downcore activities and/or inventories at each site may simply be a product of source activity rather than sediment dynamics (erosion/deposition). There was much less variability found in the longer-lived nuclides. Site LJ28 seemed to have the greatest consistency in long-lived radionuclide activities over time, which may be related to its location in the widest area of the lake. In contrast, LJ14 had the greatest variability of all the nuclides over time.

5.12.1 Downcore Profiles

The downcore profiles (Fig. 5.97 – 5.99) have been used directly, as well as the inventory of the top 20-cm (Figure 5.100), to interpret changes in deposition and resuspension over the course of the study period. ^{210}Pb profiles typically show a non-steady state profile (Fig. 5.97). In addition, no cores (except possibly LJ44, June 2010) had a defined ^{137}Cs peak that could be used to evaluate a rate of accumulation (Fig. 5.98). The highest activity of ^{137}Cs is typically found at the sediment-water interface of cores. Together, these two nuclide profiles are suggested of an environment dominated by physical and/or biological mixing (Christiansen and Emelyanov, 1995; Dellapenna et al., 2003; Corbett et al., 2007b). ^7Be activities are low at most sites throughout much of the sampling period (Fig. 5.99).

Integrating the individual profiles with depth provides a total inventory, a single value, for the site with time (Fig. 5.100). As expected based on the profiles and sediment trap data, LJ14 appeared to have the greatest variability of inventory for most nuclides. All sites showed considerable variation in ^7Be inventories, likely driven by significant changes in source material. ^{210}Pb was fairly consistent with time in all but LJ14. Although an assessment of deposition and erosion is provided based on the changes in ^7Be inventory, it is likely that much of this change is driven by large fluctuations in material input (source). Additional measurements (both temporal and spatial) needed to better constrain this method is likely necessary to accurately determine the dynamics based on this method (see next section for measurements needed).

Using the downcore profiles and, to a lesser extent, inventories at each site, interpretations of the short-term dynamics were constructed (Figure 5.101-5.105). Most sites showed consistency in interpretation between ^{210}Pb and ^{137}Cs . Only site LJ14 had conflicting interpretations in the middle of the sampling period. Like the other data sets presented, LJ14 also showed the greatest variability in this interpretation (Figure 5.101). The most significant and consistent event that occurred was an erosional event between June and August 2010 at all sites. This erosional event ranged between 4 and 15 cm. Sites LJ22

Commented [A4]: I would think the widest spot might have more variable depositional conditions since at low stage the high fetch might expose the bottom to sufficient shear stress to make the area erosional, while at higher stages the waves might exert less energy and allow deposition. However I'm assuming that at low stages the waves are not self dampening, which may not be correct.

Reply:

We would have to deploy ADVs at more than one site to be sure – those conditions can not be predicted with the radiometric approach. A future proposal we intend to write will include deploying up to four ADVs.

and LJ28 did not show any additional change throughout the study period. This was evident through all three radio-tracers, with little change in the ^{210}Pb and ^{137}Cs downcore profiles and little to no deposition of ^7Be (Figure 5.102-5.103). LJ44 was the only site that showed significant deposition (total of ~10 cm between November and April), and consistent across all tracers, during the study period (Figure 5.105).

TABLE 5.16 Summary of sediment trap activities (dpm g^{-1}) over time at each station.

<i>Site</i>	<i>Radionuclide</i>	<i>August</i>	<i>November</i>	<i>February</i>	<i>April</i>
LJ14	Pb-210	8.1 ± 1.4	8.4 ± 1.4	11.4 ± 1.8	15.6 ± 2.4
	Cs-137	0.8 ± 0.1	0.7 ± 0.1	0.9 ± 0.1	1.1 ± 0.1
	Be-7	10.4 ± 2.5	3.5 ± 0.9	3.9 ± 1.0	12.9 ± 3.0
LJ22	Pb-210	8.1 ± 1.3	15.3 ± 2.5	15.4 ± 2.3	16.5 ± 2.4
	Cs-137	0.5 ± 0.1	1.4 ± 0.1	1.1 ± 0.1	1.2 ± 0.1
	Be-7	8.8 ± 1.9	4.9 ± 1.1	5.5 ± 1.2	8.5 ± 2.0
LJ28	Pb-210	12.6 ± 2.2	12.5 ± 2.0	13.3 ± 2.0	11.4 ± 1.7
	Cs-137	1.1 ± 0.1	1.1 ± 0.1	0.9 ± 0.1	0.8 ± 0.1
	Be-7	15.3 ± 3.4	5.7 ± 1.3	4.8 ± 1.1	6.9 ± 1.6
LJ44	Pb-210	12.8 ± 2.1		8.8 ± 1.4	11.1 ± 1.7
	Cs-137	1.2 ± 0.1		0.8 ± 0.1	1.0 ± 0.1
	Be-7	21.6 ± 4.6		3.9 ± 1.0	6.0 ± 1.4

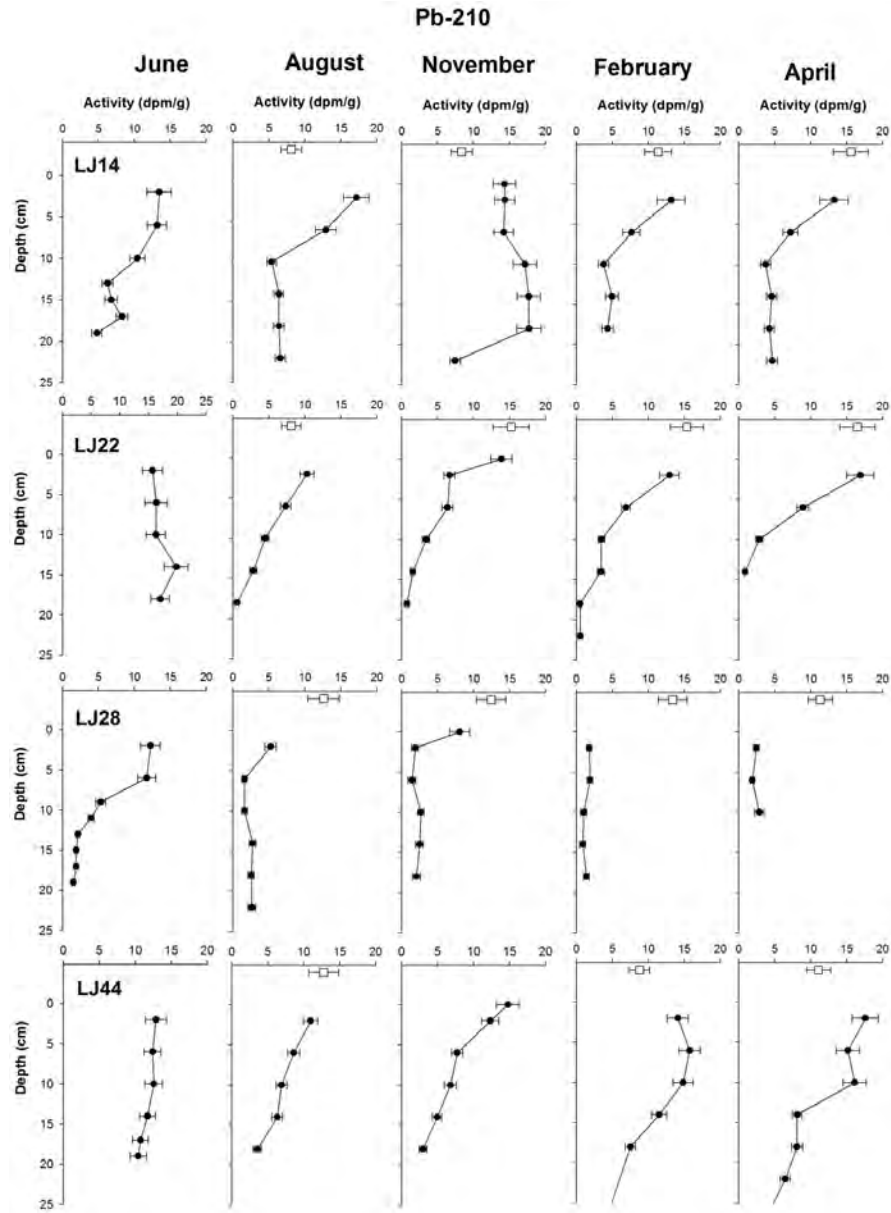


FIGURE 5.97 Summary time series of Total ^{210}Pb downcore activity from all sites sampled from June 2010 through April 2011. Open square represents sediment trap material. Note that the top core sample (closed circle) in November represents the “floc” material and was assigned a depth of 0-cm.

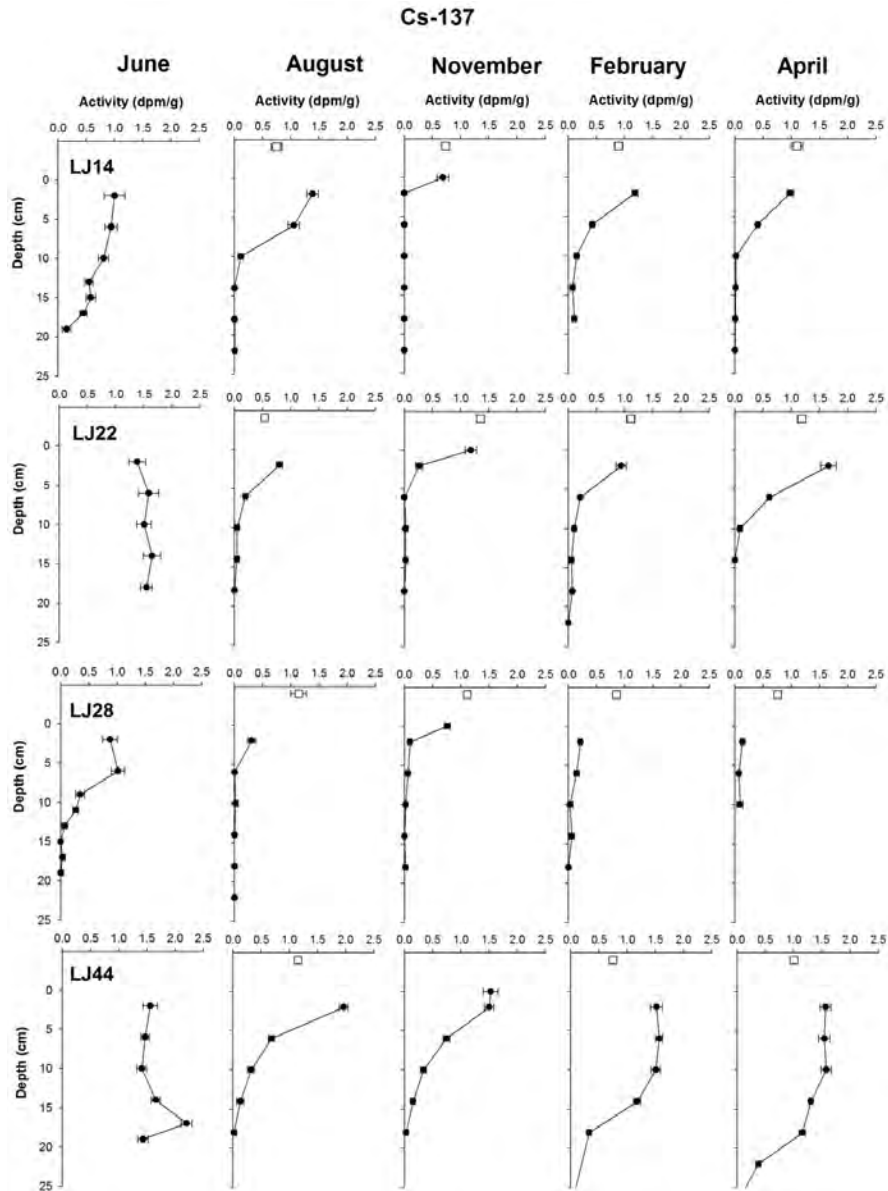


FIGURE 5.98 Summary time series of ^{137}Cs downcore activity from all sites sampled from June 2010 through April 2011. Open square represents sediment trap material. Note that the top core sample (closed circle) in November represents the “floc” material and was assigned a depth of 0-cm.

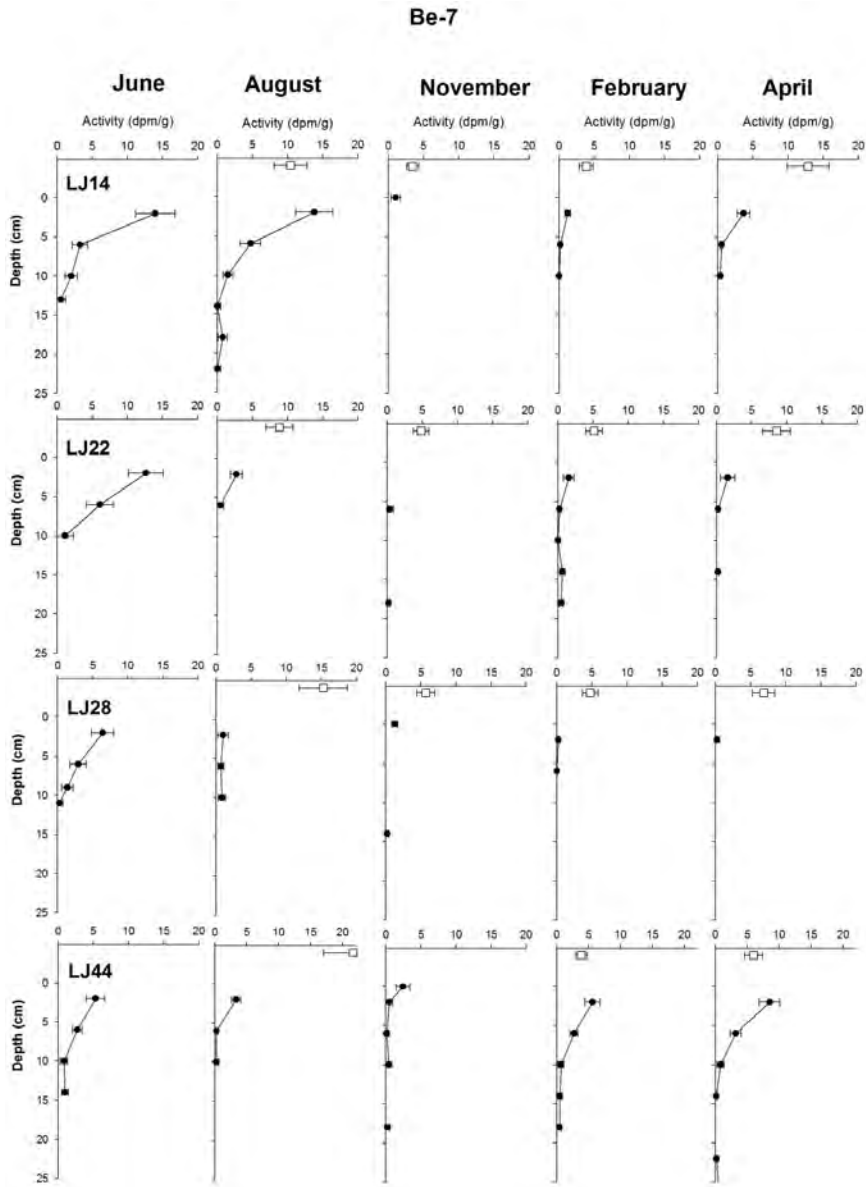


FIGURE 5.99 Summary time series of ^7Be downcore activity from all sites sampled from June 2010 through April 2011. Open square represents sediment trap material. Note that the top core sample (closed circle) in November represents the “floc” material and was assigned a depth of 0-cm.

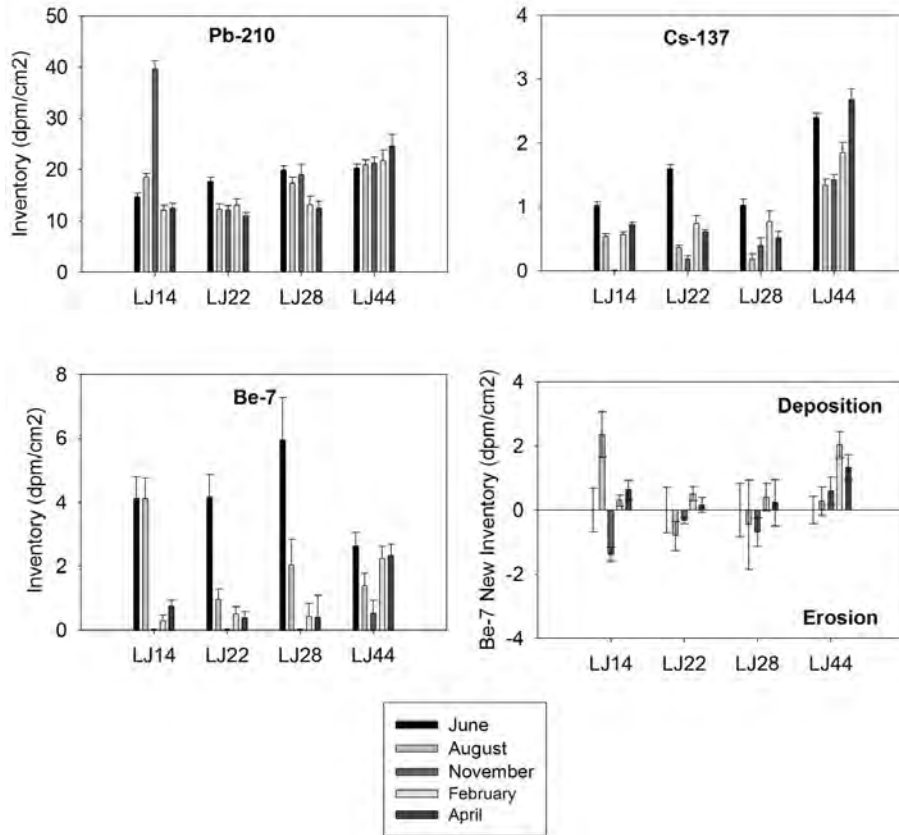


FIGURE 5.100 Summary of radionuclide inventories. A preliminary assessment of erosion versus deposition is made for each site based on “New Be-7 Inventory” (from the upper 20 cm of surface sediments), accounting for decay of material between sampling events (see Corbett et al., 2007).

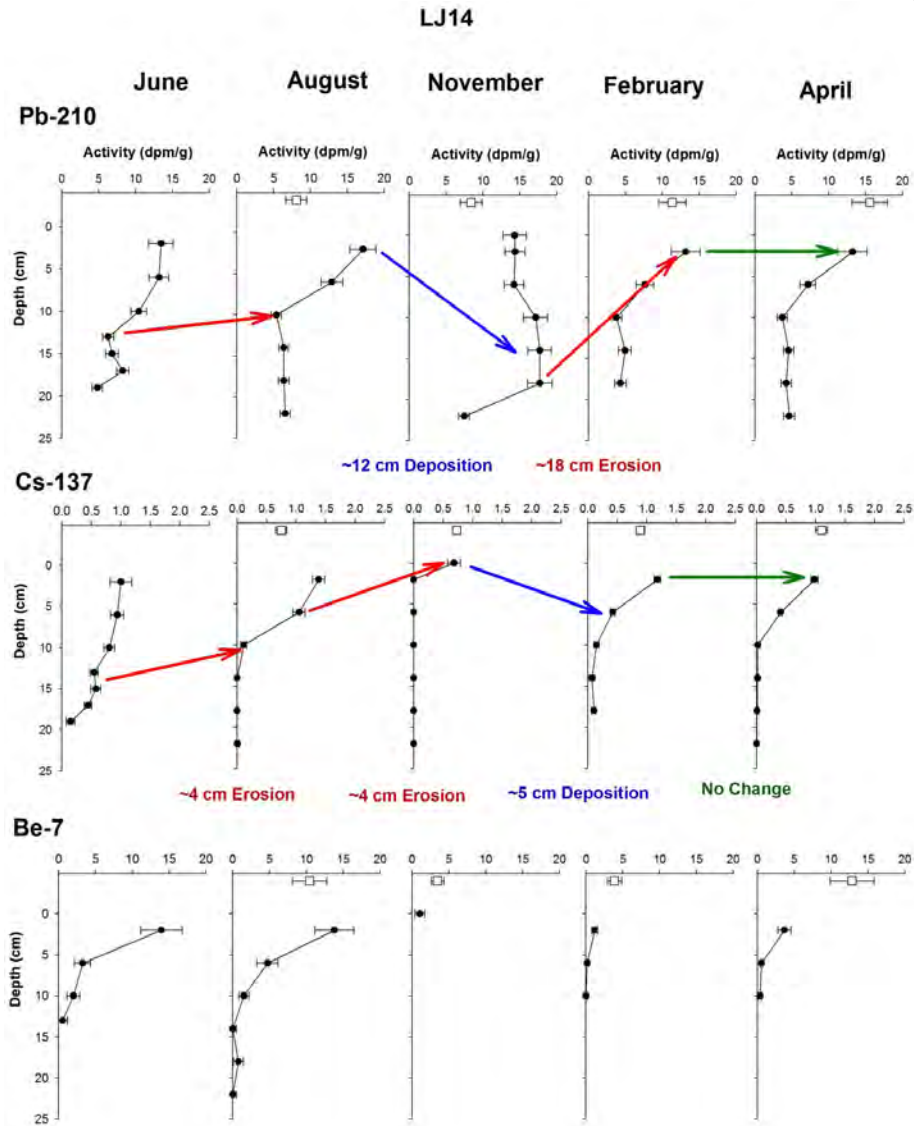
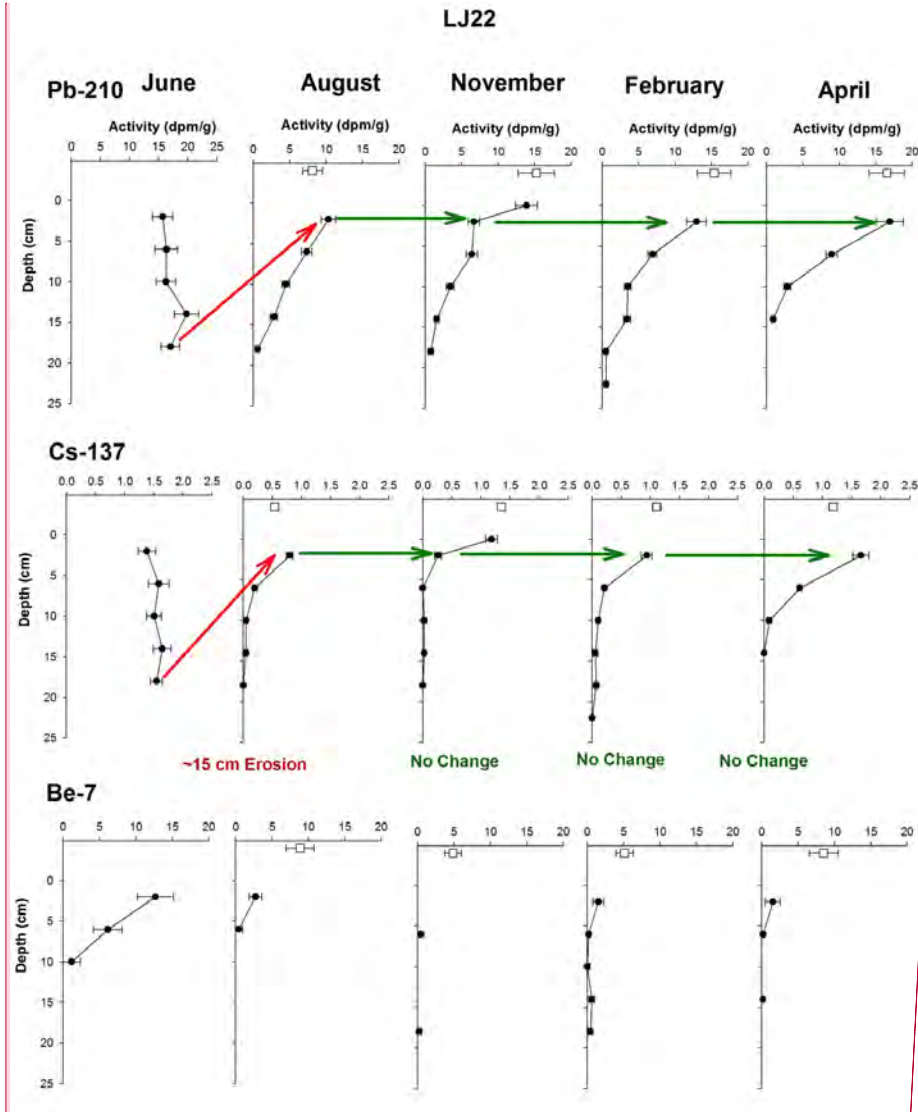


FIGURE 5.101 Time series of down core radionuclide profiles at LJ14. Sediment bed changes are interpreted based on depth variations of the profile. Note that ^{210}Pb and ^{137}Cs do not always agree at this site, as ^{137}Cs can be mobile in OM rich anoxic sediments such as found in adjacent Lake Monroe (Anderson et al, 2004).



Commented [A5]: Is there a way to compare the predicted erosional events to the observed change in TSS. Does the magnitude of resuspension match the observed change in TSS? If not, why? I suspect that erosion of large particles is very short-lived since they settle rapidly.

Not really, as this is a temporal issue, the sediments integrate over a different time period, and this approach did not correlate with the sediment trap data. However, we know the event happened and material moved.

FIGURE 5.102 Time series of down core radionuclide profiles at LJ22. Sediment bed changes are interpreted based on depth variations of the profile.

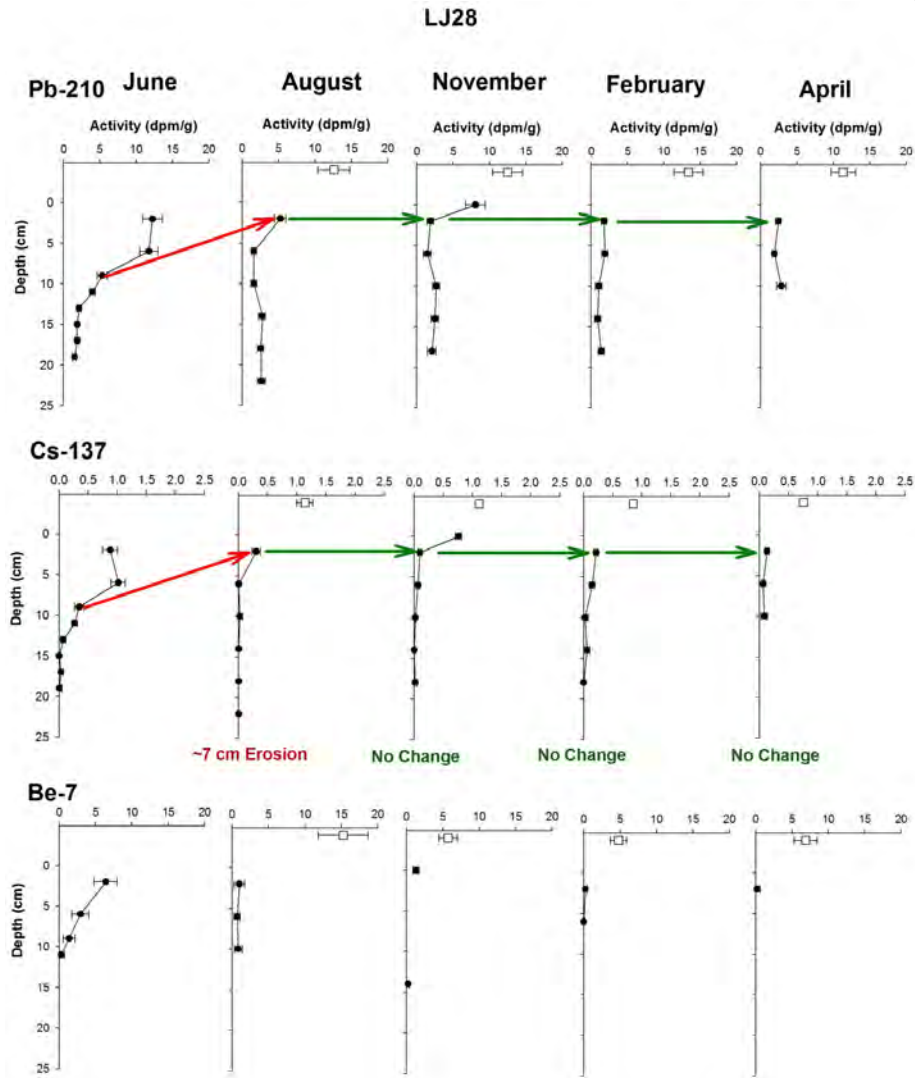


FIGURE 5.103 Time series of down core radionuclide profiles at LJ28. Sediment bed changes are interpreted based on depth variations of the profile.

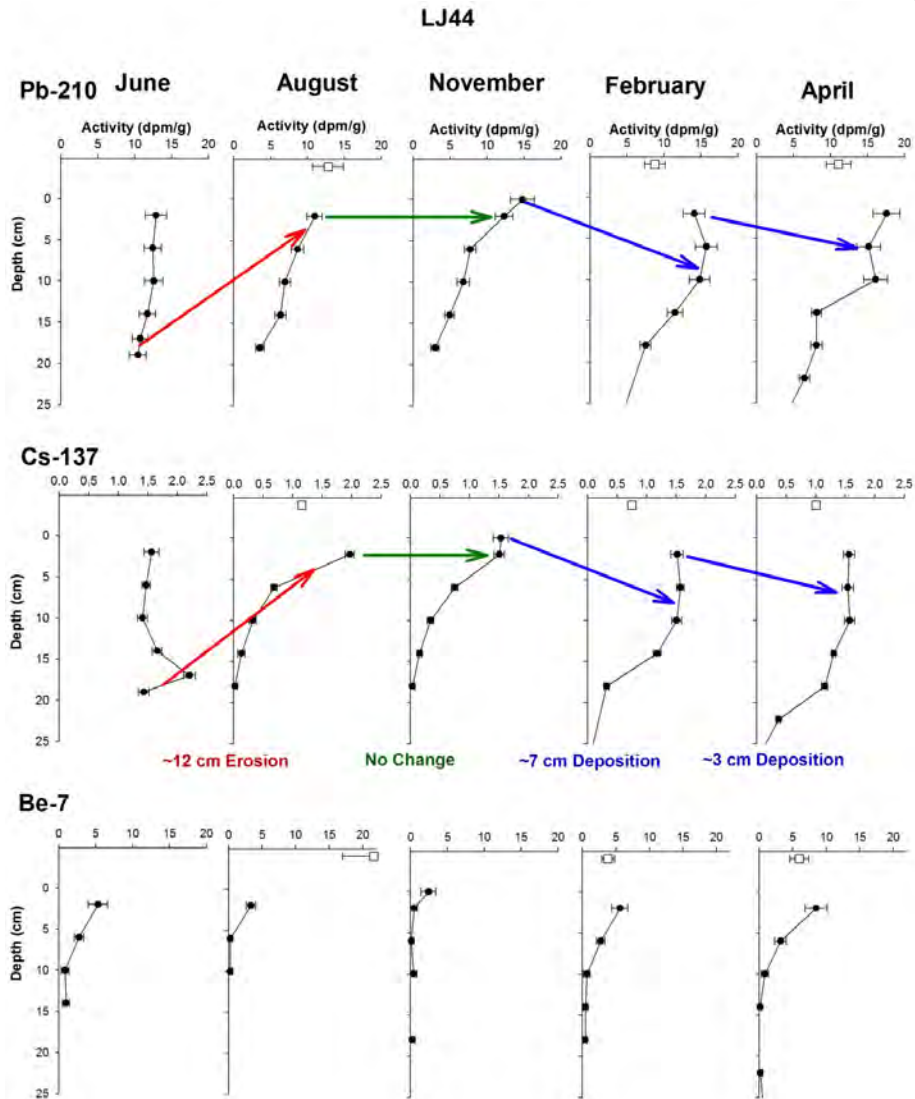


FIGURE 5.104 Time series of down core radionuclide profiles at LJ44. Sediment bed changes are interpreted based on depth variations of the profile.

6.0 DISCUSSION

Understanding sediment resuspension in a lake environment is an important internal process, because it further enhances our understanding of nutrient cycling and its potential affects on the aquatic environment (Bloesch, 1994). Evans (1994) categorized two zones for sediment resuspension: the main zone or shallow areas of resuspension and deep or episodic areas of resuspension. Shallow lake environments fall into the first category where continuous mixing occurs over the entire volume of the lake (Bloesch 1995). Mixing of a shallow lake is caused by mechanisms involving turbulence within the water column that applies enough shear stress to bottom sediments for suspension to occur (Lund-Hansen et al. 1999). In shallow lakes, the dominant mechanisms for sediment resuspension are waves and currents (Bloesch, 1994).

6.1 Sediment and Water Chemistry

From this two-year study, sediment concentrations were quantified for time-series analysis. The sediment traps, floc, sediments, ISCO water samples and grab water samples showed variations by deployment for each nutrient (TN, TP and TC). Interactions between of the floc layer with the water column were observed through correlation analysis.

The upper most sedimentary layer in Lake Jesup is composed of floc, described as, a dark brown to black, , organic-rich and unconsolidated sediment that are the most recent sediments being deposited and, most likely resuspended, within the lake. Located directly below the floc layer is gyttja, which is slightly less organic-rich than floc and still relatively young in age (Cable et al. 1997). Nutrient concentrations within the sediment were correlated resulting in sediments that are highly influenced by their organic matter content (OM). Water chemistry was also analyzed for total suspended solids (TSS), which correlated with TP water concentrations. This relationship is significant in that TSS concentrations influences the TP concentrations within the water column due to resuspension of sediments, similar to Kristensen et al.'s (1992) results on Lake Arreso in Denmark, although, a higher frequency of sampling would improve the resolution of these findings. Most likely there is a lag between the suspension of particles and the release of nutrients from the particles into the water column, however, in this study, sampling took place once per day, therefore a lag time could not be established (Brezonik et al. 1976).

Correlations between the water column nutrients and sediments (floc, grab sediments and STHA traps) were analyzed. Significant inverse correlations were found between TN water concentrations and floc concentrations for TN ($r = -0.437$, $p < 0.05$, $n = 30$) and TC ($r = -0.453$, $p < 0.05$, $n = 30$) and TOC water concentrations with floc TN concentrations ($r = -0.403$, $p < 0.05$, $n = 30$). These correlations determined that TN and TOC water nutrients increase as TN within the floc decreases and TOC water nutrients increase as TN of the floc decrease. TP correlations did not reflect interactions between the water and floc layer, perhaps there is another mechanism controlling TP particles. Further more there is a positive correlation between TP floc and TP STHA, most likely caused by the traps collecting the floc material. Another indicator that sediments are influenced by OM from

Commented [A6]: What fractions is bioturbation? It would be useful to discuss the difference in energetic requirements between keepings particles in suspension vs resuspending the same size particle.

Reply:
We have not quantified Bioturbation, that would require a separate experiment.

Commented [A7]: Need to discuss how you separate our effects of algae from resuspended sediments on particulate phosphorus measurements in water column.

Reply:
We did not quantify the algae proportion of material, and perhaps a pigment approach would work in the future – a much needed component for future work

primary lake production is provided by the stable isotope analysis of $\delta^{15}\text{N}$ and $\delta^{13}\text{C}$ of the sediments (Fig. 6.1). When $\delta^{13}\text{C}$ and C/N ratios are plotted against a Meyers plot the sediments are shifted up and to the right, suggesting this lake is highly productive (Meyers and Lallier-Vergès 1999).

Bulk density of the floc inversely correlated very highly with TSS ($r = -0.938$, $p < 0.01$, $n=8$), suggesting that there is an inverse relationship between floc and TSS. Lastly, TP for STHA and OM for STHA show a correlation, which suggests that TP concentrations for traps are mostly made of OM, possibly another indicator that TP from STHA traps are receiving additional OM from the water column algal contributions and not just from resuspension.

6.2 Sediment Resuspension

Sediment resuspension in shallow lakes is a whole lake process, but not necessarily uniform (Evans 1994). One area of a lake could be more affected by dominant wind directions resulting in more sediments that resuspend. Lateral movement of bottom sediments is another interest when examining resuspension. Cable et al. (1997) describes that Lake Jesup has thick flocculent layers in the southern part of the lake then in other areas. They further explain that the dominant wind direction is to the south. Weather data from weather stations 1 and 2 on Lake Jesup agree with these observations. Furthermore, currents within Lake Jesup are predominantly towards the south, which can produce a build up of unconsolidated sediments in the southern region of the lake (Cable et al. 1997). For Lake Jesup, this sediment transport to the south influences the nutrients that become suspended by current shear stress (CSS). TN water concentrations within the lake correlate with CSS that moves towards the south ($r = 0.754$, $p < 0.01$, $n = 43$), where CSS towards the north inversely correlates with TP ($r = -0.689$, $p < 0.05$, $n=11$). Comparing TN and TP with CSS disregarding direction TP ($r = 0.275$, $p < 0.05$, $n=54$) and TN ($r = 0.733$, $p < 0.01$, $n = 54$) show a positive correlation (Table 6.1). It was hypothesized that sediment resuspension is caused predominantly by storms, which create higher wind and wave events, but there were no significant storm events (e.g. tropical storm) during the two year sampling period. A major storm event could have caused an increase in sediment resuspension and particles that collect in the traps.

Sediment resuspension correlates with the process by which sediments resuspend (Qin 2004), meaning that sediment resuspension will correlate with the mechanism that causes the resuspension. By assuming TSS will directly correlate with a resuspension processes; correlations were made for TSS versus lake level, lake currents and wave heights. Wave analysis for each deployment (deployments 6 and 8 were unavailable) was supplied by Florida Gulf Coast University, where they used the weather data from weather stations 1 and 2 located at Lake Jesup using the Shore Protection Manual - Shallow Wave Growth Model (SPMSWG. 1984) in Matlab. Through out the deployments wave height correlated with current velocities (Table 6.2).

Mentioned previously, TSS and TP water concentrations were correlated for the entire two-year lake analysis. Alternatively, comparing the TSS and TP and current shear stress shows there does appear to be a positive relationship. TSS inversely correlates well with lake

level ($r = -0.718$, $p < 0.01$, $n = 73$), suggesting that bottom sediments are more easily disturbed by lower lake level coupled with winds or currents (and potentially biota – bioturbation).

Depositional environments can be categorized using particle grain size and current velocities from the Hjulstrom Curve model. Hjulstrom (1935) created a model based on particle grain size and stream flow velocity. He then categorized three environments acting on the bottom sediments: erosional, depositional and transitional (Fig. 6.2). Cable et al. (1997) described the grain sizes through out Lake Jesup as having 5.0% sand, 76.6% silt and 18.4% clay. Radiochemical tracers of ^{210}Pb , ^{137}Cs and ^7Br were analyzed to evaluate the depositional, erosional and transport of sediments by East Carolina University (deployments 6, 7, 8 and 9). These results are comparable to the Hjulstrom model, where Deployment 7 had the slowest maximum velocity, which resulted in a depositional phase for one of the stations (LJ14). LJ22 and LJ28 resulted in sediments that were constantly being transported for deployments 7 through 9; Fig. 6.3.

6.3 Yearly Nutrient Water Column Flux Budget

A nutrient budget was developed from the STHA trap data for the two-year sampling period for the material cycling through the water column. Note, the traps collect downward flux, and this model shows how much material and nutrients is fluxed through the system, as not all of this material is sedimented/deposited but it is being continually subjected to resuspension. Ultimately, this nutrient budget will express the mass of nutrients loading into the lake system from sediment resuspension. Deployments 1 and 2 were removed when developing the budget, because of a trap redesign. Initially, traps were deployed by sticking a PVC pipe in the soft sediment and left for the duration of that deployment, this was found to have flaws and was redesigned.

To develop a budget, traps were deployed at 3 or 4 sites through out the lake. Using previous work by Cable et al. (1997), zones were modified to encompass 1 trap per zone (Figs. 6.4 and 6.5). Flux was calculated for each deployment at each site. The area for each zone was established using ArcGIS and calculations were tallied to create the yearly flux for total sediment, TP, TN and TC. Total sediment flux for Lake Jesup is 2,033,882 mt (dw)/yr for August 2009 to August 2010 (Table 6.3).

6.3.1 Floc Recycling

Calculations were made to understand and estimate how often the floc layer recycles in Lake Jesup during an annual cycle. The average floc thickness was used from deployments 6 to 9 for each site along with bulk density to obtain the mass per area. Mass per area was then multiplied for the calculated areas created in ArcGIS from Figure 6.5 to determine the mass of floc for each zone. The calculated masses for each zone were summed to arrive at the average total mass of floc (42,922 dw mt) within Lake Jesup. The total flux for Lake Jesup was then divided by the average total mass of floc to determine the frequency of resuspension per year. For August 2009 to 2010 the floc resuspended 47 times per year and from April 2010 to April 2011 38 times per year.

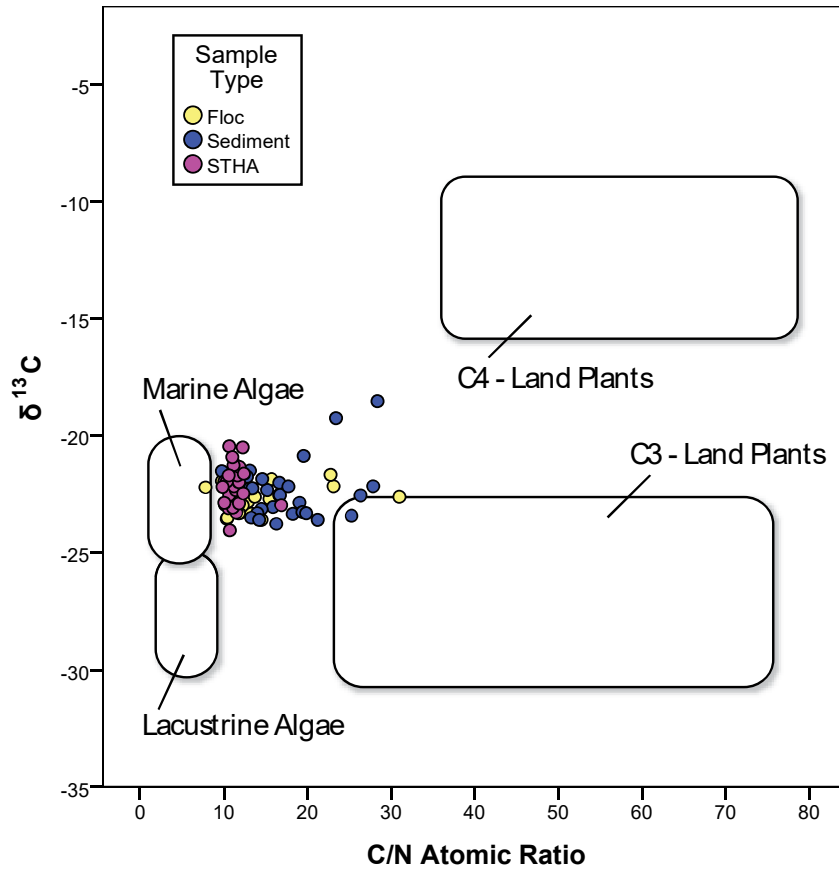


FIGURE 6.1 $\delta^{13}\text{C}$ vs. C/N ratio for all sediments. Points plot slightly higher and to the right due to the high productivity within the lake (from Meyers 1999).

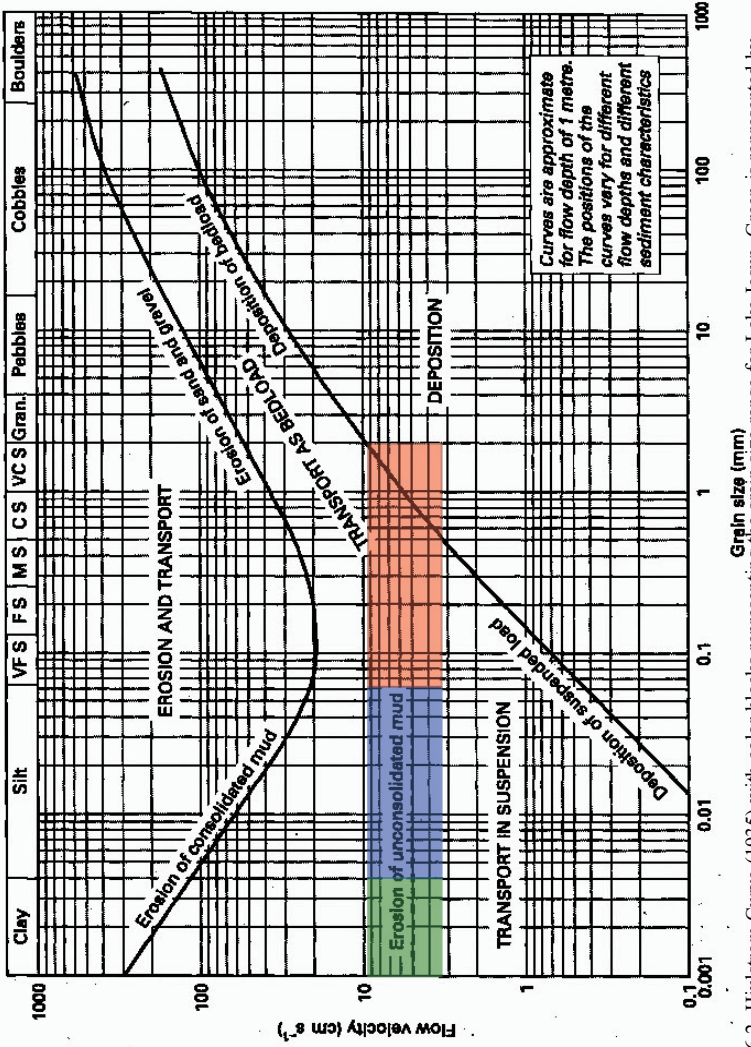


FIGURE 6.2 Hjulstrom Curve (1935) with color blocks representing the grain size range for Lake Jesup. Green is represented by clay, blue is silt and red is sands. The shaded area represents the range in current velocities for Deployment 7.

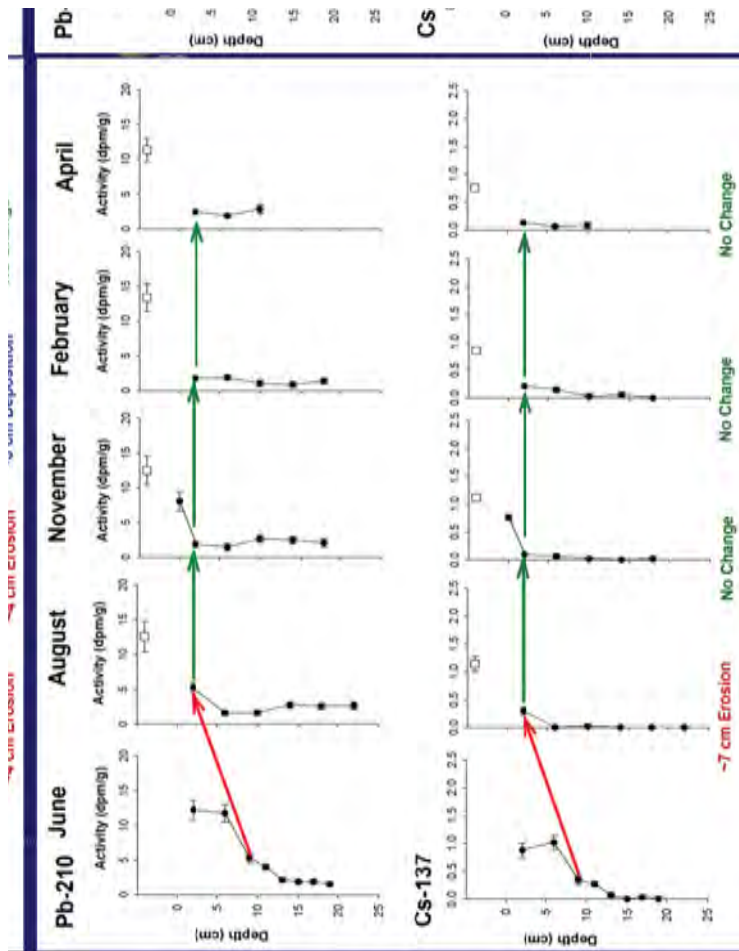


FIGURE 6.3 Pb-210 and Cs-137 inventories for down core changes through time for L.J28. This figure represents no net change for deployments 6 to 9.

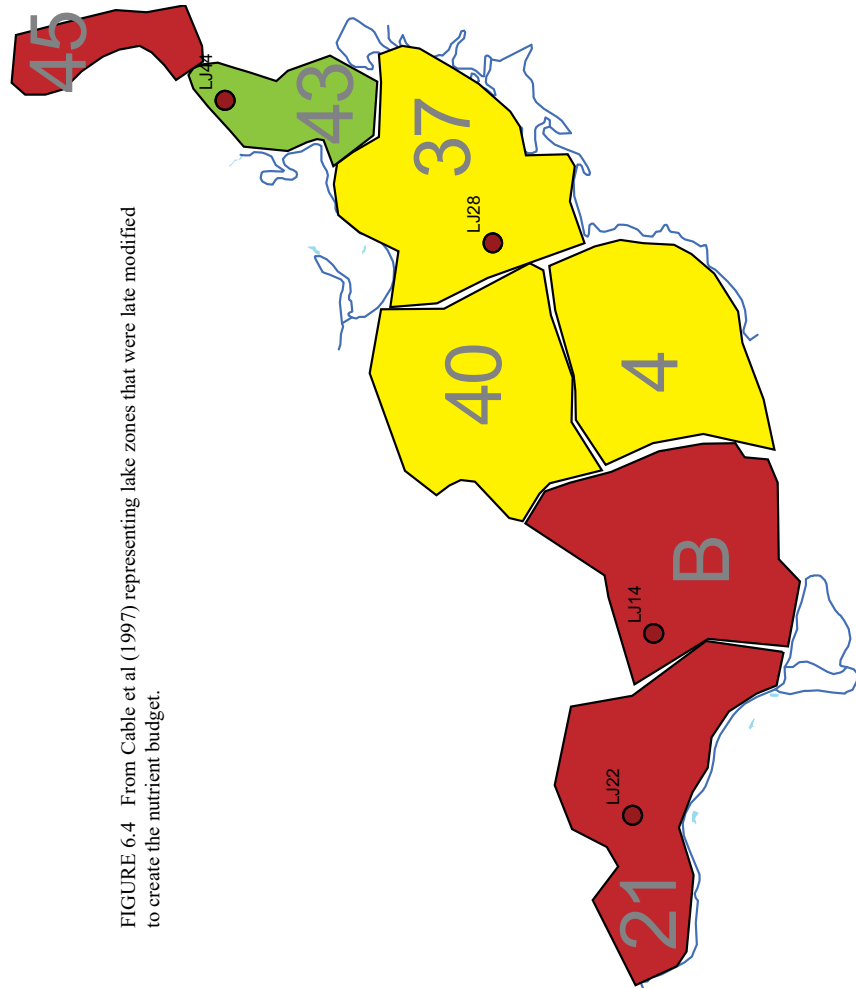


FIGURE 6.4 From Cable et al (1997) representing lake zones that were late modified to create the nutrient budget.

FIGURE 6.5 Zoning areas for the nutrient budget. a) represents the zoning when data is not available for LJ44, b) is the zoning with all four locations.

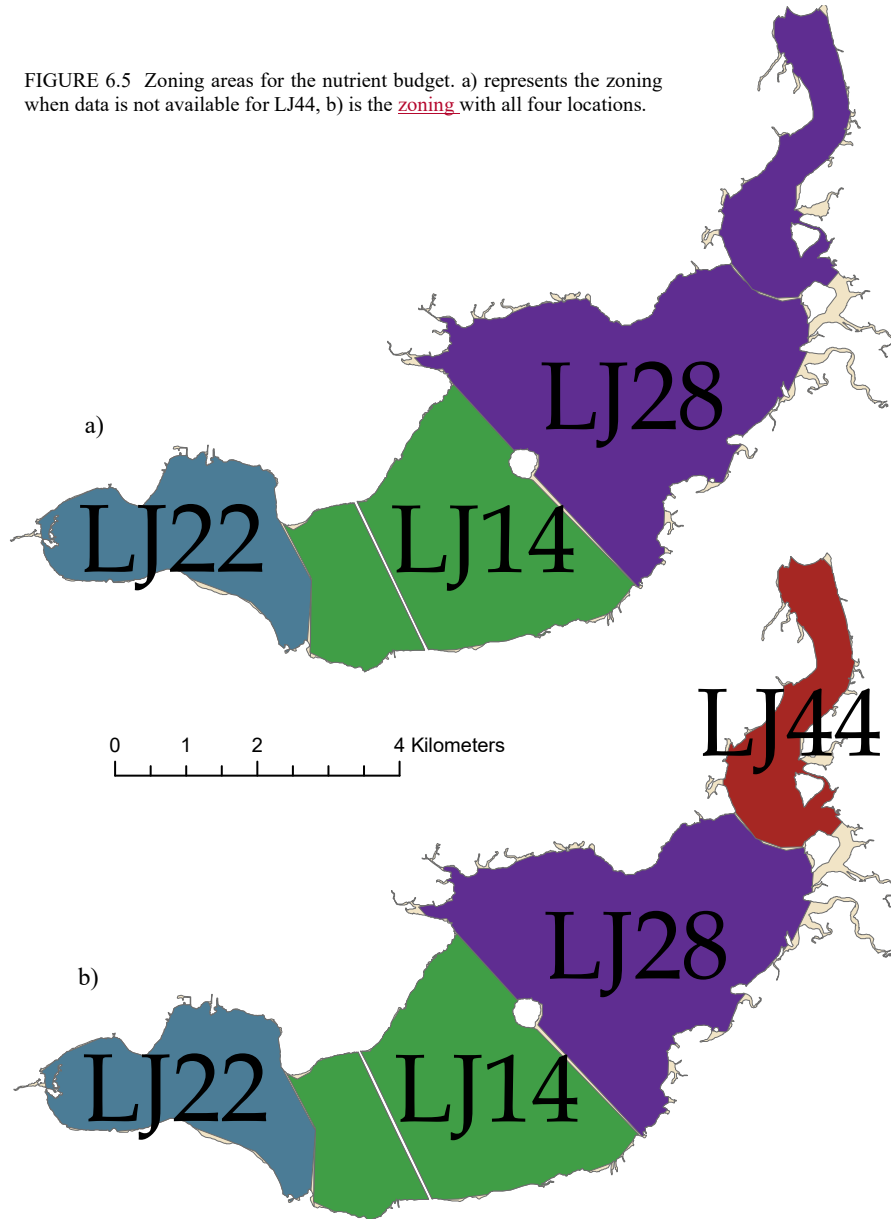


TABLE 6.1 Matrix correlation between the ISCO water and the turbulent mechanisms. CSS, current shear stress from entire study period. (n=40 to 72). Note, p<0.05 = *, and p<0.01 = **.

	TP	TN	TOC	TSS	CSS	Lake Level	Wave Height
TP	-	0.324**	0.123	0.628**	0.275	-0.423**	0.051
TN		-	0.318**	0.050	0.733**	-0.014	0.001
TOC			-	0.148	-0.193	-0.292*	-0.307*
TSS				-	0.230	-0.716**	0.010
CSS					-	-0.040	0.386*
Lake Level						-	0.114
Wave Height							-

TABLE 6.2 Matrix correlation between ISCO water samples and the turbulent mechanism with directional correlations (n= 11 to 44). Note, $p < 0.05 = *$, and $p < 0.01 = **$.

	TP	TN	TOC	TSS	Lake Level	Wave Height
CSSn	-0.689*	0.421	-0.012	0.236	0.804**	-0.185
CSSs	-0.047	0.754**	0.064	0.586**	-0.254	-0.161
CSSw	0.079	0.529**	-0.214	0.638**	-0.051	-0.053
CSSe	0.367	0.233	-0.128	0.130	0.103	-0.008

TABLE 6.3 Estimate of nutrient budget results for Lake Jesup, water to sediment flux.

	August 2009 to 2010	April 2010 to 2011
Total Flux (mt/yr)	2,033,882	1,609,672
TP (mt/yr)	23	22
TN (mt/yr)	284	287
TC (mt/yr)	2,549	2,676

6.4 Sediment Oxygen demand

6.4.1 Sediment Oxygen demand, Floc Oxygen Demand, Water Oxygen Demand and actual dissolved oxygen in the water column

Part of this study aimed to assess the extent SOD can deplete oxygen levels in the water column. This oxygen depletion can occur through i) slow molecular diffusion of DO to the sediment when no resuspension occurs and ii) when there is resuspended sediment in the water column. By examining the morning water column profiles of temperature and DO as well as the diurnal mid-water temperature and DO changes at station LJ28, it clearly appears that the lake is polymictic (ie. well mixed) and well oxygenated most days. A previous study reports that the water is supersaturated in oxygen during the day because of the high algal photosynthesis in the 0.6m deep euphotic zone (Scinto et al. 2008). Since the lake is polymictic, this excess of dissolved oxygen is advected underneath the euphotic zone and counteracts the WOD and the SOD. The oxygen supply through advection under the euphotic zone is however not strong enough to prevent anoxia at the vicinity of the sediment. The observed oxycline at all the stations located just above the sediment is likely linked to the SOD which locally depletes the oxygen, thus creating a steep oxygen decrease above the lake bed during the day. This pattern is amplified at night but does not create anoxia in the water column (Scinto et al. 2008).

It is not known whether the oxycline position was overlapping the floc/water interface because water and floc indeed exert the same resistance to the DO probe as it is lowered towards the lake bed. The use of an optical infrared device to find the boundary between the floc-water column would have been beneficial to alleviate this problem (Thomas, 2009). It would be possible that, because of the different densities of the floc and water, the floc/water interface would limit advection and as such, molecular diffusion of oxygen would be the main process of gas exchange. This assertion would support the fact that, at least at the time when the DO profiles were performed, there was no current strong enough to disturb (resuspend) the floc or sediment. However, our results also indicate that there is a steady concentration of large ($\geq 400 \mu\text{m}$) highly organic aggregates suspended in the water column in L. Jesup. These aggregates are likely floc aggregates, which are suspended when the water column is mixed and would stay suspended in the water column. With an estimated settling velocity of 0.0002 m s^{-1} , a suspended particle located a meter above the lake bed would take about 1.4h to settle if there was no additional mixing (since this is the

Commented [A8]: Is this an average depth, how much does it vary?

I DO NOT HAVE THIS DATA WITH ME AT FGC. THE PROFILES OF OXYGEN ARE NOT FORMATTED TO GET THIS INFORMATION YET.

Commented [A9]: What about fluxes of CO₂, methane, H₂S from deeper sediments.

OK. BUT OXYGEN IS THE FOCUS HERE>

And we did not measure these in the project.

assumption used to measure the settling velocity). Since the lake is polymictic, it is assumed that the 1.4 h would be a minimal residence time in the water column and a suspended particle would likely remain in the water column longer than this. Moreover, results suggest that large aggregates would break down into smaller fragments ($\sim 100 \mu\text{m}$) during more turbulent events, thus reducing settling. During resuspension, our results indicate that the resuspended material reaches $0.035\text{-}0.200 \text{ g O}_2 \text{ L}^{-1}$ within the water column. If we assume that this resuspended material is i) mostly floc, ii) is located under the euphotic zone (i.e. $< 0.6\text{m}$, Scinto et al. 2008), and iii) has lost its photosynthetic capability if the material is found within the euphotic zone (i.e. $> 0.6\text{m}$); then we can assume that the floc is responsible for an oxygen depletion of $0.019\text{-}0.106 \text{ mg O}_2 \text{ L}^{-1} \text{ h}^{-1}$. It was not tested whether some of the floc components would still be able to photosynthesize (although they can, Thomas, unpublished) but the median oxygen demand linked to the resuspended floc ($0.063 \text{ mg O}_2 / (\text{L}\cdot\text{h})$) is of the same order of magnitude as the WOD ($0.097 \text{ mg O}_2 \text{ L}^{-1} \text{ h}^{-1}$). This adds up to the assumption that floc is, at times, resuspended and contributes, for an extended amount of time, to the **WOD**.

6.4.2 Comparison of Sediment oxygen demand (SOD) with and without the floc layer (SedOD): estimation of the contribution of the thickness of floc to SOD

SOD being technically a combination of FOD and SedOD, it was anticipated that SedOD be lower. However, the contrary was found. This discrepancy can be explained by a lack of adequate oxygen diffusion from the water to the sediment or a lack of mixing in the overlying water bringing dissolved oxygen to the sediment. Thus, it is hypothesized that only the floc actually contributed to the SOD measured and that the floc isolated the sediment from the water column dissolved oxygen.

Furthermore, because there was no correlation between FOD and the floc volume, it is assumed that only a fraction of the floc contributed to the resulting SODs measured in the chamber. The very low mixing in the chamber did not create enough mixing to bring dissolved oxygen deep enough through the floc layer and reach the sediment. This stresses the importance of adequate mixing mimicking the natural conditions occurring at the sediment vicinity to generate realistic SOD results. On the other hand, the FOD calculated are likely maximized because dissolved oxygen was determined after 4 hours subsequent to thorough mixing of the water in the bottle. This assertion can however be used to estimate what thickness of floc actually contributed to a change in the dissolved oxygen content in the core during incubation. This was done by i) using the change in dissolved oxygen concentration in the core ($\text{mg O}_2 \text{ L}^{-1} \text{ h}^{-1}$), ii) correcting this change by the WOD ($\text{mg O}_2 \text{ L}^{-1} \text{ h}^{-1}$), iii) dividing this resulting change by the volume of incubated water (L) and iv) dividing this value which unit is “ $\text{mg O}_2/\text{h}$ ” by the FOD ($\text{mg O}_2/(\text{h ml_floc})$). Thus, this very roughly estimated the volume of floc (ml_floc) responsible of the SOD_T in the chamber. By dividing this volume of floc by the surface area of core (cm^2), it was found that the thickness of floc involved in the SOD_T was $0.9 \pm 0.6\text{cm}$, $0.5 \pm 0.4\text{cm}$, $1.35 \pm 1.5\text{cm}$ and $1.18 \pm 0.9\text{cm}$ for stations LJ14, LJ22, LJ28 and LJ44 respectively.

6.4.3 Correlations of Sediment oxygen demand with the nutrients contents in the sediment, floc and water column as well as with water chlorophyll a concentration

The nutrient contents in the consolidated sediment and in the water column did not explain the variation in SedOD or even SOD over time. However, the FOD was correlated with

Commented [A10]: I don't think algae should be assumed to lose their photosynthetic ability during short departures out of the photic zone. There are many meroplanktonic species which persist at the sediment-water interface and become photosynthetically active when brought into the photic zone. See http://www.aslo.org/lo/toe/vol_38/issue_6/1179.pdf for one local example.

I AGREE TOTALLY, AND I ALSO CAME TO THE SAME CONCLUSION THAT ALGAE, EVEN BURIED INTO THE SEDIMENTS STILL ARE ABLE TO PHOTOSYNTHESIZE ONCE THEY ARE EXPOSED TO LIGHT. MY POINT IS THAT THE ORDER OF MAGNITUDE IS CORRECT, WHICH SEEMS TO VALIDATE OUR FINDINGS.

TN in the floc and TDN in the water. No correlation with phosphorus was found and this seems to imply a limitation in N. WOD was logically correlated with the amount of algae present in the water column (chl_a) and their nitrogen content (TN and TON). Here again, there was a lack of correlation with phosphorus suggesting an environment limited in N, but not in P.

6.4.4 Comparison of Sediment oxygen demands amongst various Florida Lakes

To compare the SODs gathered during this study, it is central to understand what factors control SOD. SOD is the result of two main processes: the biological respiration from the heterotrophs/autotrophs (= Biological Sediment Oxygen Demand or BSOD) and the chemical oxidation of reduced compounds (e.g. divalent iron, sulfide and manganese, Chemical Sediment Oxygen Demand or CSOD). Several factors affect the SOD. Through their respiration, the biomass and metabolism of decomposers in the sediment regulate the amount of SOD yield. Since the physiology of poikilothermic organisms is temperature-dependent, temperature is logically an important factor controlling SOD. Some authors report that a 10°C increase in temperature doubles SOD ($Q_{10}=2$, e.g. McDonnell and Hall, 1969). More recently, it is found that the relationship is not linear but follows a Van't Hoff law (Butts and Evans, 1978). It is thus important that to compare different SODs, the temperature be adjusted to a common temperature – usually 20°C. In addition to temperature, the DO availability in the overlaying water above the sediment is also an important controlling factor. More oxygen available at the vicinity of the sediment yields a larger sediment aerobic respiration. It is then central, when comparing SODs to have incubations begin with similar DO supplies. The DO saturation of the water is often performed (such as with this study), as well as maintaining an adequate V/L ratio and water mixing in the chamber (see below). The presence of invertebrates in the sediment would also decrease DO availability *a fortiori* if some of these organisms can create bioturbation (e.g. Hargrave, 1969). It is not often mentioned whether dwelling invertebrates are found in the sediment core samples, but the presence of such organisms in most of the cores likely have increased measured SODs. Water mixing and thus advective DO input and eventually sediment resuspension are also regarded as factors increasing SOD. SOD increases linearly as water velocity increases when the velocities are low. However, beyond a threshold, usually linked to resuspension occurring, SOD increases exponentially (e.g. James, 1974 ; Mackenthun, 1988). Thus, accurately measuring SOD without altering most of the factors controlling it is a difficult task. As such, there are as many systems to measure SOD as there are studies (cf. Bowman and Delfino, 1980). Since all of the SOD data compiled in this report and the comparison SOD data rely on the “batch” method, this method is solely discussed here.

SOD determination commonly involves the use of a chamber which seals a certain area of sediment and volume of overlaying water (batch system). Within the chamber, the DO is then measured over time and corrected from the WOD to assess SOD. Although the principle of the method seems simple, several variations exist. The SOD determinations can be done *in situ* at ambient temperature or in the laboratory under controlled temperature (generally 20 to 25°C). Moreover, the chamber's size (especially the volume to surface area of sediment ratio or V/S; Bowman and Delfino, 1980), shape (round tube and dome), opacity and material build (soft to hard plastic or metal) are quite variable. Stirring with either a paddle or a water pump which circulates the water in the chamber is also normally

Commented [A11]: ??

More SOD is indeed yield subsequent to an increase of DO availability.

I MEANT THAT THE MORE OXYGEN AVAILABLE, THE MORE OXIC RESPIRATION POSSIBLE. THIS IS WHY SOME SCIENTISTS SATURATE THE WATER WITH OXYGEN PRIOR TO DETERMINING SOD.

Commented [A12]: Decrease?? YES

(though not always) used. Stirring is done to prevent the steep DO gradient formation at the interface between the sediment and the water since, if not performed; such a gradient would limit the DO availability to the sediment and reduce aerobic respiration and thus measured SOD. Stirring is also done to allow uniform DO concentration in the water within the chamber so that DO measurement at the tip of the DO probe measures DO changes in the chambers as closely as possible. As a general rule, mixing should always be similar to the *in situ* conditions but not be strong enough to create resuspension and artificially increase SOD. Furthermore, the pacing of DO measurements over time can greatly vary among authors. The time allowed to assess SOD is quite variable among studies since it ranges from an hour to several hours and even days. DO is then measured at the beginning and at the end of the incubations, or at constant intervals over time so that the oxygen depletion slope can be determined with better precision. Several SODs were gathered from the literature and summarized below. This table generalizes the main characteristics of the methods used (Table 6.4) and column graphs depict the average SODs gathered from the Floridian literature (= white columns) and how they compare to the SODs of this (=black column) and previous studies in L. Jesup (= grey columns). SOD_T and SOD₂₀ are presented, but because temperature is an important factor, the actual comparison is only done with SOD₂₀ (Figs. 6.6 and 6.7).

Commented [A13]: How were SOD20 calculations made from raw data? Any discussion of the implications of these measurements?

I HAVE NOT BEEN ABLE TO GET A HOLD OF THE RAW DATA DESPITE SOME EMAILS SENT TO THE AUTHORS. THE ONLY RAW DATA GATHERED WERE FROM HYDRO2 INC. THE REST WAS THE RESULT OF COMPUTATIONS MADE FROM THE PUBLISHED PAPERS.

I AM RELUCTANT TO INCLUDE ANY IMPLICATIONS OF THESE COMPARISONS BECAUSE OF THE METHODS ARE VERY DIFFERENT FROM EACH OTHER.

A RECOMMENDATION WOULD BE TO COME UP WITH A SINGLE METHOD TO USE TO MEASURE SODS IN THE REGION.

Paper	Location	type of chamber	V/S (L/m ²)	Surface area of sediment (m ²)	Incub. period	DO measured every	Inc. temp (mean °C)	Mixing with
This report	L. Jesup	Plexiglas tube, lab	126	0.00317	4h	10-15'	24	paddle
HydrO ₂ , Inc., 2006	L. Jesup	Al. tube, <i>in situ</i>	232	0.22480	1.5h - 3h	10-20'	30 (estimate)	pump
Fisher et al. 2005	L. Okeechobee	Polycarbonate tube, lab	156	0.00385	12h	0 & 12h	25	none
DBEnv, 2007	L. Blue Cypress	Acrylic tube (open at the apex), lab	104-320	0.00385	48h	0, 2, 8-10, 24, 36 and 48h	25	none
	L. Hell 'n Blazes						24	
	L. Poinsett						25	
	L. Sawgrass						24	
	L. Washington						26	
L. Winder	24							
Belanger, 1981	L. Apopka	Plexiglas tube, lab	329	0.00114	2-3 h	5-10'	25	none

TABLE 6.4 Principal characteristics of the SOD methods used by various authors dealing with Florida lakes. Note that the adequate V/S is supposed to be 132 L/m² (Bowman and Delfino, 1980) and that mixing without creating resuspension is required for good DO measures. Furthermore, higher number of DO measurements over time (collected) is better than a measurement at the beginning and at the end of the incubation. NOTE: It appears evident that no common method to measure SOD is in place. Therefore, the SOD20 comparisons must be interpreted with caution. As a general rule, *in situ* incubations yield higher SOD, than laboratory ones for a given standardized temperature (Murphy and Hicks, 1986). Furthermore, *in situ* incubations are generally preferred because there is i) limited sediment disruption during sampling and transportation as well as ii) mimic the natural conditions in the laboratory. However, laboratory methods are easier to setup and control the incubation conditions and are cheaper to implement (Bowman and Delfino, 1980).

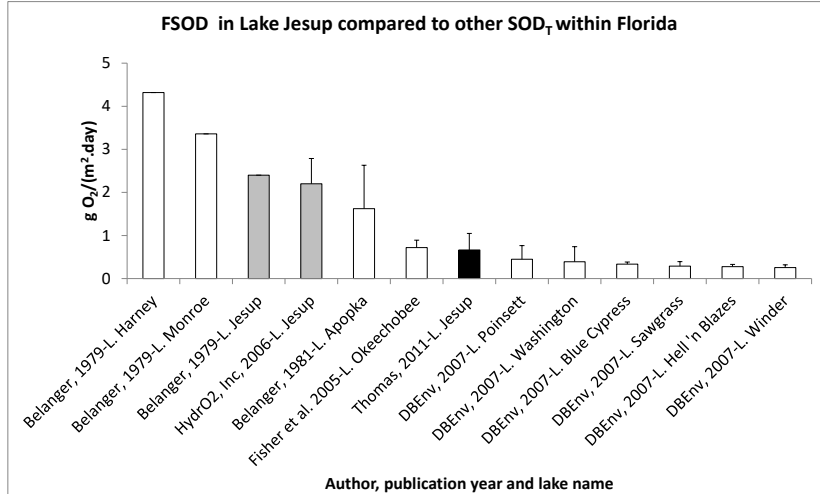


FIGURE 6.6 Comparisons of the average SOD_T ±S.D. from this study and from others. Average SOD_T from this study is depicted as a black column, the two other SOD_T from L. Jesup are depicted as grey columns. Note that some error bars could not be computed because of lack of data available in the papers gathered.

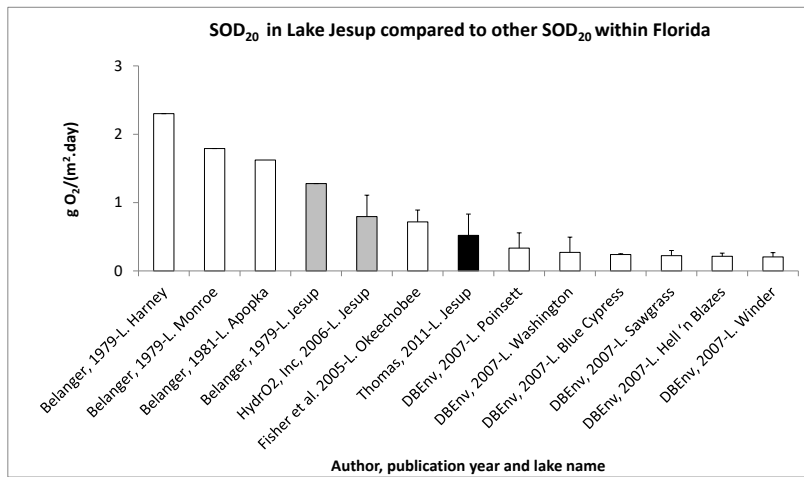


FIGURE 6.7 Comparisons of the average SOD₂₀ ±S.D. from this study and from others. Average SOD₂₀ from this study is depicted as a black column, the two other SOD₂₀ from L. Jesup are depicted as grey columns. Note that some error bars could not be computed because of lack of data available in the papers gathered.

6.5 Physical transport of suspended solids

The currents that were observed in Lake Jesup were generally weak ($<0.15 \text{ m s}^{-1}$) diurnal oscillating currents that tend to move in a northeast to southwest direction and are likely due to afternoon peaks in wind speed. Although far from the ocean, there is a semi-diurnal tide with a range of only a few centimeters. The semi-diurnal variations in water height do not produce significant currents, which are dominated by changes in discharge and the daily wind regime noted above.

Resuspension events in Lake Jesup are relatively common and driven by wind wave forcing. Suspended solid concentrations reached up to 0.200 g L^{-1} near the bottom during the January 2011 deployment and were as low as 0.035 g L^{-1} between resuspension events during the November 2010 deployment. These observations were consistent with estimates made by the ADV of background concentrations of 0.037 and 0.050 g L^{-1} at the measuring height of the ADV sensor of about 1 meter above the bed. During resuspension events a population of $\sim 100 \mu\text{m}$ sized aggregates with higher inorganic content are input into the water column and available for transport by the mean currents. Sediment transport is generally in the direction of the axis of Lake Jesup. Although winds often blow across main axis of the Lake, the fetch is not sufficient to develop waves large enough to resuspend significant amounts of sediment. The critical friction velocity necessary to resuspend sediment into the water column is relatively small, perhaps only 0.0025 m s^{-1} (e.g. Fig. 5.58). The acoustic instruments were calibrated to the inorganic fraction of sediment, however all of these mass transport estimates would be larger if the organic sediment fraction were included. The relationship between total suspended solids (TSS) and total organic content (TOC) in Lake Jesup is typical, with higher levels of TSS associated with lower percentages of TOC (Fig. 5.89).

Distinct periods of advection of surface plumes of sediment were discovered during the January 2011 deployment. These surface plumes deserve more investigation as they may be evidence of new sediment input into the Lake, either from the shores or inlets at the head of the Lake.

The presence of significant net currents and vertical current structures (Figs. 5.51, 5.63, 5.74) suggest that there are complex three-dimensional currents in Lake Jesup that change over the time scale of a few months. These currents are not likely the simple result of filling or emptying of the lake through changes of discharge. A back of the envelope calculation of the current speed due to discharge into the lake and past the site for a relatively rapid water level change can be made, for example, for the later part of the Nov 2010 deployment when the water level rose approximately 0.10 m in about 19 hours. The total volume of water that went past the site would be approximately 0.10 m change in height * 3000 m width * 8000 m in extent southwest of the site. This volume of water, passed through a cross section roughly 2.5 m deep by 3000 m wide in 19 hours, yielding a mean current of about 0.0047 m s^{-1} , an order of magnitude smaller than the observed net velocities of 0.0250 m s^{-1} . Currents from a seiche within the Lake should have roughly canceled out in a net flow. The complex currents are likely caused by bathymetry and geometry of the Lake interacting with discharge and wind caused currents that result in eddies within the lake or small channel deflections of the current or both. Three

dimensional numerical modeling may be necessary to capture all of these complexities, and an expanded number of sites within the lake would be required to validate the model.

7.0 CONCLUSIONS

Sediment and TSS nutrient concentrations and analysis of the internal processes that affect Lake Jesup were performed to better understand the relationship between sediment resuspension and water column nutrient concentrations. Sediments in Lake Jesup are frequently being resuspended (on a near daily basis), because the bottom sediments are in constant interaction with the overlying water column. As indicated by the amount of solids collected in our traps (and the Hjulstrom curve diagrams), and sediments are constantly undergoing erosion, transportation and deposition. An inverse correlation between bulk density of the floc layer and TSS suggests that the floc layer is slightly denser when TSS is low; meaning when TSS is high, floc thickness is relatively less or decreased. As the floc is suspended, and becomes part of the TSS, its amount (thickness) decreases. Lake level has a direct effect on sediment resuspension and TSS. Therefore when lake level is relatively high, currents, wind and waves have a slightly reduced affect on the system. Conversely when lake levels are low, TSS were often found to be high.

Currents within the Lake Jesup are typically moving along the longest axis of the lake (longest length) as interpreted by the current stick plots and analysis (Florida Gulf Coast University, Dr. Fugate). Dr. Fugate's analysis determined that a wind speed at 2.24 m s^{-1} (5 mph) is the lowest sustainable velocity, to cause sediment resuspension. This is significant, because the average wind speed for all deployments was 3.2 m s^{-1} (7.1 mph) from wind data collected by weather station 1. Prevailing winds that move in the north or south direction are most dominant in sediment transport (Dr. Fugate, FGCU).

Directional shifts in the lake bottom currents may change how the sediment nutrient concentrations are distributed into the water column. Current directions influence the nutrient concentrations with TP concentrations lower when currents move northward and TN concentrations higher when current moves southward by current shear stress. This connection between current direction and nutrient concentrations suggests that nutrients within the lake sediments are not uniform and may play an important role in the distribution of the nutrients. These spatial differences are also seen in the DO profiles of the water column.

This study concentrated on creating an annual nutrient flux budget to understand the magnitude of sediment resuspension and deposition. The estimated flux budget calculated from the sediment traps was extremely high; roughly two billion kg per year of material was cycled through the lake system (from sediment layer to upper water column). This mass of material is an extremely high amount and if all of this material were not from resuspended sediments, then the lake basin would completely fill up within weeks to a year. At the same time, the lake does have net deposition of sediments (which include OM), but

Commented [A14]: Deployments 1-6 were not discussed in much detail at all. Please include their discussion in results if they are to be included in conclusions.

Reply,

The trap material was included from all deployments (except the first two where the traps were messed with by boaters or animals), and is discussed, only the early deployments of the ADV, LISST and OBS had issues with the first batch deployments and were recalibrated for the conditions of Lake Jesup.

some sites within the basin will export sediment to other sites, as was observed by Cable et al. (1997).

7.1 Future Work

This work revealed many interesting relationships such as, TP versus TSS, bulk density of the floc versus TSS and directional current shear stress versus nutrient water concentrations; however, an increase in frequency of sampling would help to improve our understanding of these relationships within the water column. Perhaps a model can be analyzed for bulk density of the floc and TSS, by sampling at a high resolution, predicting the amount of sediment that is being resuspended. Additionally, as noted earlier, an investigation of surface plumes might yield important data on non-suspended sources of nutrients and TSS, such as bioturbation. This goal might be obtained by deploying more than one auto sampler (ISCO) on the barge, in order to capture discrete events, or an automated system that collects during a high-TSS event (so that nutrient analyses maybe carried out on these samples).

Another interesting aspect of Lake Jesup is its possible influence from tidal variations and seiches with Lake Monroe. These tidal influences may have an effect on the current direction and velocities that ultimately would have an effect on sediment resuspension and the transport of nutrients within Lake Jesup. It is hypothesized that Lake Jesup's internal flushing of the entire lake could be due to higher than normal tides that pull water out of the lake and down the St. Johns River. Tides could be another mechanism controlling Lake Jesup's complex lake current structure, however diurnal wind variations could mimic tidal variations. However, the diurnal changes in wind direction and current can also appear to be "tidal".

7.1.1 Specific recommendations for radio isotope tracer work

Radionuclide activities of the particle-reactive tracers used here can vary as a function of grain size. Therefore, a better interpretation could be made with additional grain size information. Down core grain size data over space and time should be considered.

The variability of the ^7Be activity found in the sediment trap material suggests significant changes in the source material delivered to the sites over time. To better use this radio-tracer in the future, both wet and dry deposition of ^7Be should be monitored over time, near the center of the site. Additional measurements of suspended sediments should also be made at the major inlets and outlets of the system. This sampling will help constrain the fluctuation of material, as well as the activity variability of the radiotracers on these sediments prior to deposition.

Although the number of samples generated in a study like this can be large, it is important in future approaches to have higher temporal resolution to better assess changes in sediment resuspension and deposition. These tracers can only evaluate the **net** change at the site between two sampling events. There may be multiple resuspension and deposition events that occur between sampling, the net change or the most recent event is all that is recorded in the tracers. Higher temporal resolution together with continuous *in situ* measurements of currents, waves, and turbidity would provide a much more robust assessment of sediment dynamics in the system. Lastly, a better assessment of intra-site variability should be completed to better determine the tracer variability with space so that changes over time

(or stage) are better quantified. For example, during the period where radioisotopes were measured the lake was at a relatively low stage, and higher stages may generate different results.

8.0 REFERENCES

- Ali, A. and Alam, M.K. 1996. Nutrient levels at the sediment-water interface in Lake Jesup, Florida. *Florida Science*. 50(1): 20-29.
- Anderson, W.T., Gaiser, E.E., and Scinto, L.J. 2006. Lake Harney sediment accumulation and past water quality – Final Report. St. Johns River Water Management District (SH45213), 132p.
- Anderson, W.T., Scinto, L.J., Gaiser, E.E., Carroll, B., Quillen, A. and Haberer, J. 2004. Lake Monroe sediment accumulation and past water quality – Final Report. St. Johns River Water Management District (SG452AA), 196p.
- Appleby, P.G. and Oldfield, F. 1983. The assessment of ^{210}Pb data from sites with varying accumulation rates. *Hydrobiologia*. 103: 29-35.
- Bachmann, R.W., Hoyer, M.V., Vinzon, S.B. and Canfield Jr., D.E. 2005. The origin of the fluid mud layer in Lake Apopka, Florida. *Limnol. Oceanogr.* 50(2): 629-635.
- Bachmann, R.W., Hoyer, M.V. and Canfield Jr., D.E. 2000. The potential for wave disturbance in shallow Florida lakes. *Lake and Res. Manage.* 16(4): 281-291.
- Belanger, T. V. 1981. Benthic oxygen demand in Lake Apopka, Florida. *Water Research* 15:267-274.
- Belanger, T.V. 1979. Benthic oxygen demand in selected Florida aquatic systems. Ph.D. dissertation. University of Florida, Gainesville, FL, USA. 210p.
- Bloesch, J. 1994. Editorial: Sediment resuspension in lakes. *Hydrobiologia* 284: 1-3
- Bloesch, J. 1995. Mechanisms, measurement and the importance of sediment resuspension in lakes. *Mar. Freshwater Res.* 46: 295-304
- Bloesch, J. and Burns, N.M. 1979. A critical review of sediment trap technique. *Swiss Journ. Of Hydrobiol.* 42: 15-55.
- Bowman, G. T. and J. J. Delfino. 1980. Sediment Oxygen Demand Techniques: A review and comparison of laboratory and *in-situ* systems. *Water Research* 14: 491-499.

- Brezonik, P.L. and Engstrom, D.R. 1998. Modern and historic accumulation rates of phosphorus in Lake Okeechobee, Florida. *J. Paleolim.* 20: 31-46.
- Brezonik, P.L., Fox, J.L. Carriker, N.E., Hand, J.G. Nisson, J.D. and Belanger, T.V. 1976. Analysis of eutrophication and water quality factors in the middle St. Johns River Basin. Report for Department of Environmental Engineering Sciences, University of Florida, Gainesville, FL.
- Brooks. H.K. 1981. Guide to the physiographic division of Florida. Institute of Food and Agriculture Sciences. Gainesville, Florida.: University of Florida.
- Brooks. H.K. 1981. Guide to the physiographic division of Florida (map). Institute of Food and Agriculture Sciences. Gainesville, Florida.: University of Florida.
- Brooks, H.K., 1968, The Plio-Pleistocene of Florida with special reference to the strata outcropping on the Caloosahatchee River., *in* Perkins, R.D., ed., Late Cenozoic stratigraphy of south Florida: Miami, Miami Geological Society, p. 3-42.
- Butts, T.A. and L.R. Evans. 1978. Sediment oxygen demand studies of selected northeastern Illinois streams. ISWS/CIR. Circular 129, 177p.
- Cable, J.E., Schelske, C.L., Hansen, P.S., Kenney, W.F. and Whitmore, T.J. 1997. Sediment and nutrient deposition in Lake Jesup, Florida (USA) – Final Report. Department of Fisheries and Aquatic Sciences. Univ. of Florida.
- Canuel, E., Martens, C., Benninger, L., 1990. Seasonal variations in Be-7 activity in the sediments of Cape Lookout Bight, North Carolina. *Geochimica Cosmochimica Acta* 54, 237–245.
- Carpenter, S.R., Caraco, N.F., Correll, D.L., Howarth, R.W., Sharply, A.N. and Smith, V.H. 1998. Nonpoint pollution of surface waters with phosphorus and nitrogen. *Issues in Ecology* No. 3.
- Carper, G.L. and Bachmann, R.W. 1984. Wind resuspension of sediments in a prairie lake. *Canadian Journal of Fisheries and Aquatic Sciences.* 41:1763-1767.
- Carrick, H.J., Aldridge, F.J. and Schelske, C.L. 1993. Wind influences phytoplankton biomass and composition in a shallow productive lake. *Limnol. Oceanogr.* 38:1179-1192.
- Christiansen, C., Emelyanov, E., 1995. Nutrients and organic matter in southern Kattegat-western Baltic Sea sediments: effects of resuspension. *Danish Journal of Geography* 95, 19-27.
- Corbett, D.R., *Dail, M.D.*, McKee, B.A., 2007a. High frequency time-series of the dynamic sedimentation processes on the western shelf of the Mississippi River delta. *Continental Shelf Research*, 27, 1600-1615.

- Corbett, D.R., D. Vance, E. Letrick, D. Mallinson, S. Culver, 2007b. Decadal-scale sediment dynamics and environmental change in the Albemarle estuarine system, North Carolina. *Estuarine, Coastal, and Shelf Science*. 71 (3-4) 717-729.
- Dail, M.D., Corbett, D.R., Walsh, J.P., 2007. Assessing the Importance of a Major Hurricane on Continental Margin Sedimentation in the Mississippi Delta Region. *Continental Shelf Research*, 27, 1857-1874.
- DB Environmental, Inc. 2007. Sediment Oxygen Demand in Six Lakes of the Upper St. Johns River Basin. SJRWMD report. 80p.
- Dellapenna, T.M., Kuehl, S.A., Schaffner, L.C., 2003. Ephemeral deposition, seabed mixing and fine-scale strata formation in the York River estuary, Chesapeake Bay. *Estuarine, Coastal and Shelf Science* 58, 621-643
- Durham, R.W. and Joshi, S.R. 1980. Recent sedimentation rates, ^{210}Pb fluxes and particle settling velocities in Lake Huron, Laurentian Great Lakes. *Chem. Geol.* 31: 53-66.
- Evans, R.D. 1994. Empirical evidence of sediment resuspension in lakes. *Hydrobiologia* 317:5-12.
- Fisher, M.M., K.R. Reddy and R.T. James. 2005. Internal, nutrient loads from sediments in a shallow, subtropical lake. *Lake and Reservoir Management* 21:338-349.
- Flower, R.J. 1991. Field calibration and performance of sediment traps in a eutrophic holomictic lake. *J. Paleolimnology* 5:157-188.
- Fugate, D.C., and Friedrichs, C.T., 2002. Determining concentration and fall velocity of estuarine particle populations using ADV, OBS and LISST. *Continental Shelf Research*, 22: 1867-1886.
- Fugate, D.C., and C.T. Friedrichs, 2003, Controls on Suspended Aggregate Size in Partially Mixed Estuaries, *Estuarine Coastal and Shelf Science* 58:389-404.
- Gao, X. 1996. Nutrient and Unionized Ammonia TMDLs for Lake Jesup. Division of Water Resource Management, Bureau of Watershed Management. Florida Department of Environmental Protection.
- Goldberg, E.D. 1963. Geochronology with Pb-210. In radioactive dating. Internat. Energy Agency. 121-131.
- Grant, W.D. and O.S. Madsen. 1979. Combined wave and current interaction with a rough bottom. *Journal Geophysical Research* 84: 1797-1808.
- Henderson-Sellers, B. and Markland H.R. 1987. Decaying lakes: the origins and control of cultural eutrophication. Chichester [West Sussex] ; New York : Wiley.

- Hargrave, B.T. 1969. Similarity of oxygen uptake by benthic communities. *Limnology and Oceanography* 14:801-805.
- Hill, D.C., S.E. Jones and D. Prandle. 2003. Derivation of sediment resuspension rates from acoustic backscatter time-series in tidal waters. *Continental Shelf Research* 23: 19-40.
- Hjulstrom, F. (1935). "The Morphological Activity of Rivers as Illustrated by River Fyris," *Bulletin of the Geological Institute*, Uppsala, vol. 25, ch. 3.
- Horppila, J. and Nurminen, L. 2005. Effects of calculation procedure and sampling site on trap method estimates of sediment resuspension in a shallow lake. *Sedimentology* 52: 903-913.
- HydO₂, Inc. 2006. *In situ* assessment of sediment nutrient flux assessment and sediment oxygen demand. SJRWMD report. 32p.
- James, A. 1974. The measurement of Benthic respiration. *Water Research* 8:955-959.
- Kawanisi ,K. and T. Yokoyama. 2009. Transport characteristics of suspended sediment on mud flat in a tidal channel. *Advances in water resources and hydraulic engineering III*:809-814.
- Keesecker, D.H. 1992. Lake Jessup restoration, diagnostic evaluation, water budget and nutrient budget. Water and air research, inc. Gainesville, FL.
- Kenney, W.F., Waters, M.N., Schelske, C.L. and Brenner, M. 2002. Sediment records of phosphorus-driven shifts to phytoplankton dominance in shallow Florida lakes. *Journal of Paleolimnology*. 27: 367-377.
- Kozerski, H.P. 2003. More about plate sediment trap measurements – Reply to comment of Sukhodolov et al. *Water Research*. 37: 2796-2801.
- Kozerski, H.P and Leuschner, K. 2000. A plate sediment trap: design and first experiences. *Verh. Intern. Verein. Limnol.* 27: 242-245.
- Kozerski, H.P., Behrendt, H. and Kohler, J. 1999. The N and P budget of the shallow, flushed lake Muggelsee retention, external and internal load. *Hydrobiologia*. 408/409: 159-166.
- Kozerski, H.P and Leuschner, K. 1999. Plate sediment traps for slow moving waters. *Water Res.* 33(13): 2913-2922.
- Krishnaswami, S., Lal, D. Martin, J.M. and Meybeck, M. 1971. Geochronology of lake sediments. *Earth Planate. Sci. Letters*. 11: 407-414.

Kristensen, P., Sondergaard, M. and Jeppesen, E. 1992. Resuspension in shallow eutrophic lakes. *Hydrobiologia*. 228: 101-109.

Lee, G.F. 1970. Factors affecting the transfer of materials between water and sediments. Univ. of Wisconsin. Eutrophication Information Program, Literature Review No. 1 Madison, Wisconsin.

Lijklema, L., Aalderink, R.H., Blom, G. and VanDuin, E.H.S. 1994. Sediment transport in shallow lakes – two case studies related to eutrophication. P. 235-280. *In*: J.V. DePinto, W. Lick, and J.F. Paul. (eds.) Transport and transformation of contaminants near the sediment-water interface. Lewis Publ. Boca Raton, FL.

Lohrmann, A. 2001. Monitoring Sediment Concentration with acoustic backscattering instruments. Nortek Technical Note No.:003, 5p.

Luetlich, R.A., Harlman, D.R.F., Sonlyody, L. 1990. Dynamic behavior of suspended sediment concentrations in a shallow lake perturbed by episodic wind events. *Limnol. Oceanogr.* 35: 1050-1067.

Lund-Hansen, L.C., Peterson, M. and Nurjaya, W. 1999. Vertical sediment fluxes and wave-induced sediment resuspension in a shallow-water coastal lagoon. *Estuaries*. 22(1): 39-46.

McDonnell, A.J. and S.D. Hall. 1969. Effects of environmental factors on benthic oxygen uptake. *Journal of Water Pollution Control. Fef.* 41:R353-R363.

Mckenthum, A.A. 1998. Effect of Flow Velocity on Sediment Oxygen Demand: Experiments. *Journal of Environmental Engineering* 124:222-230.

Meyers, P.A and Lallier-Vergès, E. 1999. Lacustrine sedimentary organic matter records of Late Quaternary paleoclimates. *Journal of Paleolimnology*. 21: 345-372.

Murphy, P.J. and D.B. Hicks. 1986. *In situ* method for measuring sediment oxygen demand. *In*: Hatcher, K.J., Eds. Sediment Oxygen Demand: Processes, Modeling, and Measurement. University of Georgia Institute of Natural Resources, Athens, pp. 307-330. Nelson, D.W. and Sommers, L.E., 1996. Total carbon, organic carbon, and organic matter. *In*: Methods of Soil Analysis, Part 2, 2nd ed., A.L. Page et al., Ed. Agronomy. 9:961-1010. Am. Soc. of Agron., Inc. Madison, WI.

Newman, S. and Reddy, K.R. 1992. Sediment resuspension effects on alkaline phosphate activity. *Hydrobiologia* 245:75-86.

Qin, B., Hu, W., Gao, G., Luo, L. and Zhang, J. 2004. Dynamics of sediment resuspension and the conceptual schema of nutrient release in the large shallow Lake Taihu, China. *Chinese Science Bulletin*. 49(1): 54-64.

Schindler, D.W., Hesslein, R., and Kipphur, G. 1977. Interactions between sediments and overlying waters in an experimentally eutrophied Precambrian Shield Lake. *In*: H.L. Golterman (ed.), Interactions between sediments and freshwater. Dr. W. Junk, The Hague: 235-243.

Scinto, L.J., S. Thomas, Anderson W., Ikenaga M., and C. Sinigalliano. 2008. Assessment of N₂-fixation in Lakes Jesup and Monroe, Florida. 2008. SJRWMD report, SK42812. 80p.

Seminole County. 1991. *Sanitary Sewer Element*. Seminole County 1991 Comprehensive Plan. Seminole County Planning Office, Sanford, Florida.

Thomas, S. (2009). Lake Apopka sediment analyses. SJRWMD report # 25378.

Solorzano, L and Sharp, J.H., 1980. Determination of Total Dissolved Phosphorus and Particulate Phosphorus in Natural Waters. *Limnology and Oceanography*, 25(4): 754-758.

Soulsby, R.L, L. Hamm, G. Klopman, D. Myrhaug, R.R Simons, and G.P. Thomas. 1993. Wave-current interaction within and outside the bottom boundary layer. *Coastal Engineering* 21: 41-69.

Soulsby, D.H. 1997. "Dynamics of marine sands. A manual for practical applications," Thomas Telford Publications, London, England, 249 p.

Sternberg, R.W. 1972. Predicting initial motion and bedload transport of sediment particles in the shallow marine environments, p. 61-82. In Swift, D.J.P. and Pikey, O.H. (eds), *Shelf Sediment Transport: Process and Pattern*. Dowden, Hutchinson and Ross, Stroudsburg, PA.

Tassenow, U., 1972 Losungs-, Diffusions- und sorption-sprozesse in der Oberschicht von Seesedimenten. 1. Ein Langzeitexperiment unter aeroben end anaeroben Bedingungen in Fleibgleichgewicht. *Arch. Hydrobiol. Suppl.* 38: 353-398.

Thorne, P.D., P.J. Hardcastle, and R. L. Soulsby. 1993, Analysis of acoustic measurements of suspended sediments. *Journal of Geophysical Research* 98(C1): 899-910.

U.S. Army Corps of Engineers, 1984, *Shore Protection Manual*, Publisher: Vicksburg, Miss. : Dept. of the Army, Waterways Experiment Station, Corps of Engineers, Coastal Engineering Research Center ; Washington, DC : For sale by the Supt. of Docs., U.S. G.P.O.

Wetzel, R.G. 2001. *Limnology: Lake and River Ecosystems*, 3rd ed. Academic Press. San Diego, CA. p.2

White, W.A., 1970, *The Geomorphology of the Florida Peninsula*: Tallahassee, Bureau of Geology, p. 147.

Wiberg, P.L. 1995. A theoretical investigation of boundary layer flow and bottom shear stress for smooth, transitional, and rough flow under waves. *Journal of Geophysical Research* 100(C11): 22667-22679.

Winn, E. rev. 2003. *Early History of the St. Johns River*. Winn's Books, Maitland, Florida.

APPENDIX

TABLE A1 List of sediment nutrient analysis.

Sample Type	Sample ID	Site	Deployment	Collection Date	UTM North	UTM East
SF	LJ280508SF	28	1	5/8/2009	480334	3178274
SF	LJ140514SF	14	1	5/14/2009	475800	3176405
SF	LJ220514SF	22	1	5/14/2009	473685	3176656
SF	LJ140626SF	14	2	6/26/2009	475800	3176405
SF	LJ220626SF	22	2	6/26/2009	473685	3176656
SF	LJ280626SF	28	2	6/26/2009	480334	3178274
SF	LJ140821SF	14	3	8/21/2009	475800	3176405
SF	LJ220821SF	22	3	8/21/2009	473685	3176656
SF	LJ280821SF	28	3	8/21/2009	480334	3178274
SF	LJ221106SF	22	4	11/6/2009	473685	3176656
SF	LJ281106SF	28	4	11/6/2009	480334	3178274
SF	LJ141106SF	14	4	11/6/2009	475800	3176405
SF	LJ140129SF	14	5	1/29/2010	475800	3176405
SF	LJ220129SF	22	5	1/29/2010	473685	3176656
SF	LJ280129SF	28	5	1/29/2010	480334	3178274
SF	LJ140820SF	14	6	8/20/2010	475800	3176405
SF	LJ220820SF	22	6	8/20/2010	473685	3176656
SF	LJ280820SF	28	6	8/20/2010	480334	3178274
SF	LJ440820SF	44	6	8/20/2010	481994	3181379
SF	LJ221111SF	22	7	11/11/2010	473685	3176656
SF	LJ141111SF	14	7	11/11/2010	475800	3176405
SF	LJ281111SF	28	7	11/11/2010	480334	3178274
SF	LJ441111SF	44	7	11/11/2010	481994	3181379
SF	LJ140128 SF	14	8	1/28/2011	475800	3176405
SF	LJ220128 SF	22	8	1/28/2011	473685	3176656
SF	LJ440128 SF	44	8	1/28/2011	481994	3181379
SF	LJ140408 SF	14	9	4/8/2011	475800	3176405
SF	LJ220408 SF	22	9	4/8/2011	473685	3176656
SF	LJ280408 SF	28	9	4/8/2011	480334	3178274
SF	LJ440408 SF	44	9	4/8/2011	481994	3181379

TABLE A1 cont. List of sediment nutrient analysis.

Sample Type	Sample ID	Site	Deployment	Collection Date	UTM North	UTM East
SS	LJ280508SS	28	1	5/8/2009	480334	3178274
SS	LJ140514SS	14	1	5/14/2009	475800	3176405
SS	LJ220514SS	22	1	5/14/2009	473685	3176656
SS	LJ140626SS	14	2	6/26/2009	475800	3176405
SS	LJ220626SS	22	2	6/26/2009	473685	3176656
SS	LJ280626SS	28	2	6/26/2009	480334	3178274
SS	LJ140821SS	14	3	8/21/2009	475800	3176405
SS	LJ220821SS	22	3	8/21/2009	473685	3176656
SS	LJ280821SS	28	3	8/21/2009	480334	3178274
SS	LJ141106SS	14	4	11/6/2009	475800	3176405
SS	LJ281106SS	28	4	11/6/2009	480334	3178274
SS	LJ221106SS	22	4	11/6/2009	473685	3176656
SS	LJ280129SS	28	5	1/29/2010	480334	3178274
SS	LJ140129SS	14	5	1/29/2010	475800	3176405
SS	LJ220129SS	22	5	1/29/2010	473685	3176656
SS	LJ140820SS	14	6	8/20/2010	475800	3176405
SS	LJ220820SS	22	6	8/20/2010	473685	3176656
SS	LJ280820SS	28	6	8/20/2010	480334	3178274
SS	LJ440820SS	44	6	8/20/2010	481994	3181379
SS	LJ441111SS	44	7	11/11/2010	481994	3181379
SS	LJ141111SS	14	7	11/11/2010	475800	3176405
SS	LJ221111SS	22	7	11/11/2010	473685	3176656
SS	LJ281111SS	28	7	11/11/2010	480334	3178274
SS	LJ140128 SS	14	8	1/28/2011	475800	3176405
SS	LJ220128 SS	22	8	1/28/2011	473685	3176656
SS	LJ280128 SS	28	8	1/28/2011	480334	3178274
SS	LJ440128 SS	44	8	1/28/2011	481994	3181379
SS	LJ140408 SS	14	9	4/8/2011	475800	3176405
SS	LJ220408 SS	22	9	4/8/2011	473685	3176656
SS	LJ280408 SS	28	9	4/8/2011	480334	3178274
SS	LJ440408 SS	44	9	4/8/2011	481994	3181379

TABLE A1 cont. List of sediment nutrient analysis.

Sample Type	Sample ID	Site	Deployment	Collection Date	UTM North	UTM East
STHA	LJ280329STHA	28	0	3/29/2009	480334	3178274
STHA	LJ280425 STHA	28	1	4/25/2009	480334	3178274
STHA	LJ140514STHA	14	1	5/14/2009	475800	3176405
STHA	LJ220514STHA	22	1	5/14/2009	473685	3176656
STHA	LJ140709STHA	14	2	7/9/2009	475800	3176405
STHA	LJ220709STHA	22	2	7/9/2009	473685	3176656
STHA	LJ280709STHA	28	2	7/9/2009	480334	3178274
STHA	LJ140828STHA	14	3	8/28/2009	475800	3176405
STHA	LJ220828STHA	22	3	8/28/2009	473685	3176656
STHA	LJ280828STHA	28	3	8/28/2009	480334	3178274
STHA	LJ221113STHA	22	4	11/13/2009	473685	3176656
STHA	LJ141113STHA	14	4	11/13/2009	475800	3176405
STHA	LJ281113STHA	28	4	11/13/2009	480334	3178274
STHA	LJ280205STHA	28	5	2/5/2010	480334	3178274
STHA	LJ220205STHA	22	5	2/5/2010	473685	3176656
STHA	LJ140205STHA	14	5	2/5/2010	475800	3176405
STHA	LJ140827STHA	14	6	8/28/2010	475800	3176405
STHA	LJ220827STHA	22	6	8/28/2010	473685	3176656
STHA	LJ280827STHA	28	6	8/28/2010	480334	3178274
STHA	LJ440827STHA	44	6	8/28/2010	481994	3181379
STHA	LJ22B1119STHA	22	7	11/19/2010	473685	3176656
STHA	LJ28B1119STHA	28	7	11/19/2010	480334	3178274
STHA	LJ22A1119STHA	22	7	11/19/2010	473685	3176656
STHA	LJ28A1119STHA	28	7	11/19/2010	480334	3178274
STHA	LJ14B1119STHA	14	7	11/19/2010	475800	3176405
STHA	LJ14A1119STHA	14	7	11/19/2010	475800	3176405

TABLE A1 cont. List of sediment nutrient analysis.

Sample Type	Sample ID	Site	Deployment	Collection Date	UTM North	UTM East
STHA	LJ44B0204 STHA	44	8	2/4/2011	481994	3181379
STHA	LJ28B0204 STHA	28	8	2/4/2011	480334	3178274
STHA	LJ44A0204 STHA	44	8	2/4/2011	481994	3181379
STHA	LJ22B0204 STHA	22	8	2/4/2011	473685	3176656
STHA	LJ14B0204 STHA	14	8	2/4/2011	475800	3176405
STHA	LJ28A0204 STHA	28	8	2/4/2011	480334	3178274
STHA	LJ14A0204 STHA	14	8	2/4/2011	475800	3176405
STHA	LJ22A0204 STHA	22	8	2/4/2011	473685	3176656
STHA	LJ14A0415 STHA	14	9	4/15/2011	475800	3176405
STHA	LJ14B0415 STHA	14	9	4/15/2011	475800	3176405
STHA	LJ22A0415 STHA	22	9	4/15/2011	473685	3176656
STHA	LJ22B0415 STHA	22	9	4/15/2011	473685	3176656
STHA	LJ28A0415 STHA	28	9	4/15/2011	480334	3178274
STHA	LJ28B0415 STHA	28	9	4/15/2011	480334	3178274
STHA	LJ44A0415 STHA	44	9	4/15/2011	481994	3181379
STHA	LJ44B0415 STHA	44	9	4/15/2011	481994	3181379

TABLE A1 cont. List of sediment nutrient analysis.

Sample Type	Sample ID	Site	Deployment	Collection Date	UTM North	UTM East
--------------------	------------------	-------------	-------------------	------------------------	------------------	-----------------

STM8	LJ281107STM8	28	4	11/7/2009	480334	3178274
STM8	LJ281108STM8	28	4	11/8/2009	480334	3178274
STM8	LJ281109STM8	28	4	11/9/2009	480334	3178274
STM8	LJ281110STM8	28	4	11/10/2009	480334	3178274
STM8	LJ281111STM8	28	4	11/11/2009	480334	3178274
STM8	LJ281112STM8	28	4	11/12/2009	480334	3178274
STM8	LJ281113STM8	28	4	11/13/2009	480334	3178274
STM8	LJ280205STM8	28	5	2/5/2010	480334	3178274
STM8	LJ280204bSTM8	28	5	2/4/2010	480334	3178274
STM8	LJ280204aSTM8	28	5	2/4/2010	480334	3178274
STM8	LJ280203bSTM8	28	5	2/3/2010	480334	3178274
STM8	LJ280203aSTM8	28	5	2/3/2010	480334	3178274
STM8	LJ280202bSTM8	28	5	2/2/2010	480334	3178274
STM8	LJ280202aSTM8	28	5	2/2/2010	480334	3178274
STM8	LJ280201bSTM8	28	5	2/1/2010	480334	3178274
STM8	LJ280201aSTM8	28	5	2/1/2010	480334	3178274
STM8	LJ280131bSTM8	28	5	1/31/2010	480334	3178274
STM8	LJ280131aSTM8	28	5	1/31/2010	480334	3178274
STM8	LJ280130bSTM8	28	5	1/30/2010	480334	3178274
STM8	LJ280130aSTM8	28	5	1/30/2010	480334	3178274
STT	LJ280508STT	28	1	5/8/2009	480334	3178274
STT	LJ220514STT	22	1	5/14/2009	473685	3176656
STT	LJ140828STT	14	3	8/28/2009	480334	3178274
STT	LJ220828STT	22	3	8/28/2009	480334	3178274
STT	LJ280828STT	28	3	8/28/2009	480334	3178274
STT	LJ141113STT	14	4	11/13/2010	475800	3176405
STT	LJ280205STT	28	5	2/5/2010	480334	3178274
STT	LJ220205STT	22	5	2/5/2010	473685	3176656
STT	LJ140205STT	14	5	2/5/2010	475800	3176405

TABLE A1 cont. List of sediment nutrient analysis.

Sample ID	BD ²	pH	Dry	H ₂ O	OM	Ash
-----------	-----------------	----	-----	------------------	----	-----

	gdw cm ⁻³		%	%	%	%
LJ280508SF	0.055	7.64	5.47	94.53	27.13	72.87
LJ140514SF	0.082	7.48	7.73	92.27	30.13	69.87
LJ220514SF	0.035	7.30	3.44	96.56	41.69	58.31
LJ140626SF	0.043	7.14	4.27	95.73	15.38	84.62
LJ220626SF	0.058	6.91	5.54	94.46	33.94	66.06
LJ280626SF	0.068	7.21	7.12	92.88	36.94	63.06
LJ140821SF	0.048	6.96	4.68	95.32	35.89	64.11
LJ220821SF	0.048	7.01	4.97	95.03	36.00	64.00
LJ280821SF	0.066	7.15	6.80	93.20	19.22	80.78
LJ221106SF	0.038	7.03	3.84	96.16	39.92	60.08
LJ281106SF	0.044	7.18	4.24	95.76	33.24	66.76
LJ141106SF	0.046	7.04	4.55	95.45	34.50	65.50
LJ140129SF	0.044	7.73	4.77	95.23	32.60	67.40
LJ220129SF	0.048	7.72	4.39	95.61	42.20	57.80
LJ280129SF	0.051	7.57	5.30	94.70	31.15	68.85
LJ140820SF	0.064	7.41	7.69	92.31	31.90	68.10
LJ220820SF	0.069	7.38	6.54	93.46	31.52	68.48
LJ280820SF	0.082	7.40	7.98	92.02	7.57	92.43
LJ440820SF	0.054	7.36	6.51	93.49	31.78	68.22
LJ221111SF	0.043	7.35	4.14	95.86	36.72	63.28
LJ141111SF	0.039	7.45	3.92	96.08	38.91	61.09
LJ281111SF	0.070	7.50	6.10	93.90	29.89	70.11
LJ441111SF	0.035	7.33	3.60	96.40	40.54	59.46
LJ140128 SF	0.043	7.54	4.46	95.54	35.79	64.21
LJ220128 SF	0.032	7.62	3.20	96.80	42.59	57.41
LJ440128 SF	0.039	7.53	3.94	96.06	38.70	61.30
LJ140408 SF	0.033	7.78	3.80	96.20	38.42	61.58
LJ220408 SF	0.021	7.77	2.68	97.32	41.49	58.51
LJ280408 SF	0.028	7.88	3.39	96.61	26.57	73.43
LJ440408 SF	0.039	7.67	4.18	95.82	36.02	63.98

TABLE A1 cont. List of sediment nutrient analysis.

Sample ID	BD ² gdw cm ⁻³	pH	Dry %	H ₂ O %	OM %	Ash %
-----------	---	----	----------	-----------------------	---------	----------

LJ280508SS	0.567	8.23	43.55	56.45	4.13	95.87
LJ140514SS	0.141	7.38	13.15	86.85	19.86	80.14
LJ220514SS	0.091	7.44	9.56	90.44	28.60	71.40
LJ140626SS	0.133	7.82	10.45	89.55	5.19	94.81
LJ220626SS	0.609	7.83	12.11	87.89	20.61	79.39
LJ280626SS	0.645	7.98	44.52	55.48	30.56	69.44
LJ140821SS	0.100	7.31	9.03	90.97	31.61	68.39
LJ220821SS	0.124	7.63	11.67	88.33	43.17	56.83
LJ280821SS	0.101	7.56	9.11	90.89	2.86	97.14
LJ141106SS	0.143	7.41	11.55	88.45	21.10	78.90
LJ281106SS	0.158	7.52	15.03	84.97	15.54	84.46
LJ221106SS	0.084	7.06	8.21	91.79	29.71	70.29
LJ280129SS	0.542	8.03	39.83	60.17	6.98	93.02
LJ140129SS	0.094	7.85	9.43	90.57	30.12	69.88
LJ220129SS	0.094	7.89	8.59	91.41	30.61	69.39
LJ140820SS	0.125	7.56	10.55	89.45	23.51	76.49
LJ220820SS	0.140	7.65	11.93	88.07	35.37	64.63
LJ280820SS	0.548	7.61	52.11	47.89	19.65	80.35
LJ440820SS	0.138	7.67	12.89	87.11	27.33	72.67
LJ441111SS	0.125	7.69	12.03	87.97	24.80	75.20
LJ141111SS	0.098	7.73	9.54	90.46	28.77	71.23
LJ221111SS	0.104	7.67	10.04	89.96	27.95	72.05
LJ281111SS	0.707	7.99	49.02	50.98	5.56	94.44
LJ140128 SS	0.121	7.71	11.56	88.40	25.53	74.47
LJ220128 SS	0.106	7.78	9.66	90.34	30.68	69.32
LJ280128 SS	0.264	7.86	23.81	76.19	7.54	92.46
LJ440128 SS	0.076	7.70	7.17	92.83	30.59	69.41
LJ140408 SS	0.110	7.85	10.87	89.13	14.86	85.14
LJ220408 SS	0.132	7.85	12.36	87.64	18.41	81.59
LJ280408 SS	0.641	8.01	46.54	53.46	5.14	94.86
LJ440408 SS	0.140	7.69	12.06	87.94	27.19	72.81

TABLE A1 cont. List of sediment nutrient analysis.

Sample ID	Trap Days Collecting days	STHA height cm	Volume cm ³	BD ¹ gdw cm ⁻³	Dry Weight g	MAR g m ⁻² d ⁻¹
-----------	---------------------------------	----------------------	---------------------------	---	--------------------	--

LJ280329STHA	16	11	235.59	0.043	10.100	295
LJ280425 STHA	14	28.5	610.39	0.054	32.660	1089
LJ140514STHA	18	13	278.42	0.075	20.791	539
LJ220514STHA	18	47.5	1017.32	0.044	44.826	1163
LJ140709STHA	13	55	1177.95	0.071	83.730	3007
LJ220709STHA	13	10	214.17	0.032	6.942	249
LJ280709STHA	13	10	214.17	0.041	8.833	317
LJ140828STHA	7	2.6	55.68	0.045	2.511	168
LJ220828STHA	7	5	107.09	0.028	3.037	203
LJ280828STHA	7	2.2	47.12	0.028	1.298	87
LJ221113STHA	7	8	171.34	0.037	6.275	419
LJ141113STHA	7	5	107.09	0.041	4.370	291
LJ281113STHA	7	3	64.25	0.052	3.368	225
LJ280205STHA	7	4	85.67	0.032	2.741	183
LJ220205STHA	7	5	107.09	0.042	4.450	297
LJ140205STHA	7	2	42.83	0.052	2.222	148
LJ140827STHA	7	2	42.83	0.027	1.156	77
LJ220827STHA	7	6	128.50	0.024	3.040	203
LJ280827STHA	7	2	42.83	0.030	1.264	84
LJ440827STHA	7	6	128.50	0.037	4.812	321
LJ22B1119STHA	8	7	149.92	0.022	3.319	194
LJ28B1119STHA	8	3	64.25	0.033	2.131	124
LJ22A1119STHA	8	6	128.50	0.025	3.234	189
LJ28A1119STHA	8	3	64.25	0.034	2.171	127
LJ14B1119STHA	8	6	128.50	0.020	2.601	152
LJ14A1119STHA	8	6	128.50	0.022	2.788	163

TABLE A1 cont. List of sediment nutrient analysis.

Sample ID	Trap Days Collecti ng days	STHA height cm	Volume cm ³	BD ¹ gdw cm ⁻³	Dry Weight g	MAR g m ⁻² d ⁻¹
LJ44B0204 STHA	7	2	42.83	0.041	1.771	118

LJ28B0204 STHA	7	2.5	53.54	0.038	2.020	135
LJ44A0204 STHA	7	2	42.83	0.039	1.659	111
LJ22B0204 STHA	7	3.5	74.96	0.029	2.173	145
LJ14B0204 STHA	7	3	64.25	0.023	1.462	98
LJ28A0204 STHA	7	3	64.25	0.033	2.108	141
LJ14A0204 STHA	7	4	85.67	0.018	1.542	103
LJ22A0204 STHA	7	4.5	96.38	0.025	2.419	161
LJ14A0415 STHA	7	3.5	74.96	0.021	1.550	103
LJ14B0415 STHA	7	3.5	74.96	0.021	1.543	103
LJ22A0415 STHA	7	5	107.09	0.030	3.229	215
LJ22B0415 STHA	7	6	128.50	0.027	3.458	231
LJ28A0415 STHA	7	6	128.50	0.029	3.790	253
LJ28B0415 STHA	7	6	128.50	0.026	3.395	226
LJ44A0415 STHA	7	4.5	96.38	0.037	3.518	235
LJ44B0415 STHA	7	4.5	96.38	0.037	3.525	235

TABLE A1 cont. List of sediment nutrient analysis.

Sample ID	Trap Days Collecting days	Volume cm ³	BD ² gdw cm ⁻³	Dry Weight g	MAR g m ⁻² d ⁻¹	pH
LJ281107STM8	1	285	0.032	9.210	37	6.81
LJ281108STM8	1	245	0.041	10.139	41	6.72
LJ281109STM8	1	260	0.037	9.694	39	6.77
LJ281110STM8	1	290	0.037	10.588	42	6.82
LJ281111STM8	1	275	0.037	10.201	41	6.84

LJ281112STM8	1	250	0.046	11.614	46	6.81
LJ281113STM8	1	145	0.042	6.106	24	7.05
LJ280205STM8	0.5	200	0.035	6.979	56	7.11
LJ280204bSTM8	0.5	180	0.036	6.481	52	7.13
LJ280204aSTM8	0.5	210	0.035	7.346	59	7.13
LJ280203bSTM8	0.5	140	0.036	5.026	40	7.13
LJ280203aSTM8	0.5	190	0.037	7.072	57	7.02
LJ280202bSTM8	0.5	95	0.021	1.983	16	7.05
LJ280202aSTM8	0.5	160	0.027	4.261	34	7.00
LJ280201bSTM8	0.5	180	0.035	6.225	50	6.99
LJ280201aSTM8	0.5	210	0.031	6.465	52	6.99
LJ280131bSTM8	0.5	75	0.027	2.036	16	6.99
LJ280131aSTM8	0.5	115	0.033	3.807	30	6.96
LJ280130bSTM8	0.5	145	0.030	4.394	35	6.91
LJ280130aSTM8	0.5	160	0.027	4.275	34	6.78
LJ280508STT						
LJ220514STT						
LJ140828STT	7		NO	DATA		
LJ220828STT	7					
LJ280828STT	7					
LJ141113STT	7	10	0.742	7.422	638	--
LJ280205STT	7	150	0.075	11.229	965	6.90
LJ220205STT	7	128	0.079	10.142	872	6.89
LJ140205STT	7	130	0.075	9.811	843	6.85

TABLE A1 cont. List of sediment nutrient analysis.

Sample ID	TP ^a µg g ⁻¹ dw	TP mg g ⁻¹	TN ^a mg g ⁻¹	TN ^a %	TC mg g ⁻¹	TIC mg g ⁻¹
LJ280508SF	1615.26	1.62	12.90	1.29	127.80	0.00
LJ140514SF	1132.98	1.13	15.00	1.50	151.20	0.00
LJ220514SF	2208.75	2.21	21.30	2.13	206.50	0.00
LJ140626SF	799.22	0.80	12.00	1.20	112.00	0.03
LJ220626SF	1091.74	1.09	16.10	1.61	149.50	0.00

LJ280626SF	1359.77	1.36	19.90	1.99	195.30	0.00
LJ140821SF	1329.11	1.33	20.80	2.08	186.20	0.00
LJ220821SF	1077.22	1.08	18.10	1.81	178.60	0.00
LJ280821SF	501.90	0.50	9.80	0.98	96.20	0.00
LJ221106SF	1764.14	1.76	22.90	2.29	197.03	0.48
LJ281106SF	1220.00	1.22	15.83	1.58	156.75	0.00
LJ141106SF	1390.68	1.39	17.28	1.73	159.81	3.90
LJ140129SF	1471.26	1.47	14.81	1.48	142.52	0.00
LJ220129SF	2018.73	2.02	23.56	2.36	209.24	0.00
LJ280129SF	1533.59	1.53	17.21	1.72	159.77	0.80
LJ140820SF	650.59	0.65	13.6	1.36	142.1	0.00
LJ220820SF	1123.84	1.12	15.5	1.55	151.2	0.00
LJ280820SF	599.34	0.60	7.7	0.77	77.8	0.00
LJ440820SF	1051.52	1.05	17.5	1.75	170.4	0.00
LJ221111SF	1569.38	1.57	18.33	1.83	182.39	0.00
LJ141111SF	796.08	0.80	20.64	2.06	189.92	0.00
LJ281111SF	285.06	0.29	10.92	1.09	127.39	0.00
LJ441111SF	1468.42	1.47	22.26	2.23	188.22	0.00
LJ140128 SF	1700.59	1.70	16.90	2.33	158.00	0.00
LJ220128 SF	1903.33	1.90	23.30	2.19	208.20	0.00
LJ440128 SF	1316.26	1.32	21.90	1.69	195.60	0.00
LJ140408 SF	1687.09	1.69	19.01	1.90	188.02	0.00
LJ220408 SF	1639.07	1.64	18.52	1.85	202.86	8.14
LJ280408 SF	702.42	0.70	16.22	1.62	170.25	0.00
LJ440408 SF	1535.76	1.54	12.16	1.22	151.22	0.00

TABLE A1 cont. List of sediment nutrient analysis.

Sample ID	TP ^a µg g ⁻¹ dw	TP mg g ⁻¹	TN ^a mg g ⁻¹	TN ^a %	TC mg g ⁻¹	TIC mg g ⁻¹
LJ280508SS	387.80	0.39	0.40	0.04	37.30	2.72
LJ140514SS	1923.24	1.92	5.80	0.58	126.20	3.81
LJ220514SS	878.54	0.88	12.60	1.26	149.80	0.54
LJ140626SS	489.85	0.49	1.70	0.17	64.70	2.58
LJ220626SS	577.79	0.58	11.30	1.13	127.90	0.02
LJ280626SS	351.99	0.35	13.60	1.36	161.70	0.01
LJ140821SS	229.06	0.23	11.80	1.18	156.30	0.00
LJ220821SS	577.62	0.58	15.70	1.57	169.30	0.00

LJ280821SS	211.71	0.21	0.90	0.09	29.70	0.00
LJ141106SS	351.33	0.35	8.67	0.87	111.68	1.21
LJ281106SS	590.00	0.59	5.90	0.59	73.00	1.09
LJ221106SS	1055.51	1.06	13.48	1.35	136.51	0.16
LJ280129SS	371.07	0.37	1.92	0.19	57.43	38.90
LJ140129SS	614.73	0.61	12.48	1.25	149.29	0.00
LJ220129SS	1049.00	1.05	14.59	1.46	156.11	0.00
LJ140820SS	393.72	0.39	13.33	1.33	162.69	0.00
LJ220820SS	696.33	0.70	10.32	1.03	130.89	0.30
LJ280820SS	294.17	0.29	1.40	0.14	59.37	4.33
LJ440820SS	784.13	0.78	10.33	1.03	141.49	0.34
LJ441111SS	623.60	0.62	11.22	1.12	147.10	0.00
LJ141111SS	470.69	0.47	11.25	1.13	145.12	0.06
LJ221111SS	514.69	0.51	14.40	1.44	174.76	0.00
LJ281111SS	552.97	0.55	0.00	0.00	93.95	4.58
LJ140128 SS	787.60	0.79	8.60	1.50	125.70	0.00
LJ220128 SS	849.16	0.85	14.40	0.86	161.60	0.00
LJ280128 SS	456.01	0.46	0.00	0.00	49.70	1.84
LJ440128 SS	1781.58	1.78	15.00	1.44	155.70	0.00
LJ140408 SS	614.44	0.61	6.05	0.61	108.48	43.14
LJ220408 SS	800.00	0.80	6.26	0.63	103.00	0.00
LJ280408 SS	355.84	0.36	0.00	0.00	66.84	45.24
LJ440408 SS	904.27	0.90	10.06	1.01	147.43	7.36

TABLE A1 cont. List of sediment nutrient analysis.

Sample ID	pH	Dry %	H ₂ O %	OM %	Ash %
LJ280329STHA	6.99	4.28	95.72	41.23	58.77
LJ280425 STHA	6.82	4.77	95.23	40.25	59.75
LJ140514STHA	7.00	4.68	95.32	39.59	60.41
LJ220514STHA	7.17	4.16	95.84	42.55	57.45
LJ140709STHA	7.05	7.03	92.97	48.97	51.03
LJ220709STHA	7.08	3.24	96.76	28.38	71.62
LJ280709STHA	--	3.74	96.26	43.57	56.43
LJ140828STHA	6.55	3.02	96.98	45.84	54.16
LJ220828STHA	6.47	2.97	97.03	65.51	34.49
LJ280828STHA	6.88	2.71	97.29	52.19	47.81
LJ221113STHA	6.57	3.25	96.75	49.81	50.19
LJ141113STHA	6.59	3.29	96.71	43.83	56.17
LJ281113STHA	6.75	3.30	96.70	44.46	55.54

LJ280205STHA	6.64	2.22	97.78	46.67	53.33
LJ220205STHA	6.71	2.26	97.74	47.09	52.91
LJ140205STHA	6.71	1.92	98.08	47.90	52.10
LJ140827STHA	7.67	2.19	97.81	46.42	53.58
LJ220827STHA	7.16	2.44	97.56	50.22	49.78
LJ280827STHA	7.60	2.67	97.33	45.12	54.88
LJ440827STHA	7.49	3.68	96.32	41.31	58.69
LJ22B1119STHA	7.14	2.06	97.94		
LJ28B1119STHA	7.43	2.11	97.89		
LJ22A1119STHA	7.33	2.06	97.94	52.49	47.51
LJ28A1119STHA	7.39	2.29	97.71	50.25	49.75
LJ14B1119STHA	7.09	1.91	98.09		
LJ14A1119STHA	6.99	1.86	98.14	52.49	47.51

TABLE A1 cont. List of sediment nutrient analysis.

Sample ID	pH	Dry %	H ₂ O %	OM %	Ash %
LJ44B0204					
STHA	7.09	2.81	97.19		
LJ28B0204					
STHA	7.56	2.33	97.67		
LJ44A0204					
STHA	7.43	2.66	97.34	46.42	53.58
LJ22B0204					
STHA	7.34	2.20	97.80		
LJ14B0204					
STHA	7.41	1.85	98.15		
LJ28A0204					
STHA	7.36	2.42	97.58	48.79	51.21
LJ14A0204					
STHA	7.29	1.88	98.12	53.06	46.94
LJ22A0204					
STHA	7.38	1.98	98.02	51.85	48.15

LJ14A0415					
STHA	7.54	1.93	98.07	52.67	47.33
LJ14B0415					
STHA	7.37	2.04	97.96		
LJ22A0415					
STHA	7.38	2.08	97.92	52.51	47.49
LJ22B0415					
STHA	7.4	2.15	97.85		
LJ28A0415					
STHA	7.46	2.59	97.41	45.76	54.24
LJ28B0415					
STHA	7.62	2.65	97.35		
LJ44A0415					
STHA	7.74	3.11	96.89	44.65	55.35
LJ44B0415					
STHA	7.71	3.01	96.99		

TABLE A1 cont. List of sediment nutrient analysis.

Sample ID	Dry %	H ₂ O %	OM %	Ash %	TP ^a µg g ⁻¹ dw
LJ281107STM8	3.38	96.62	43.65	56.35	2178.51
LJ281108STM8	3.85	96.15	46.91	53.09	2188.99
LJ281109STM8	4.03	95.97	41.69	58.31	2450.71
LJ281110STM8	4.04	95.96	43.54	56.46	1773.69
LJ281111STM8	4.04	95.96	42.31	57.69	2478.79
LJ281112STM8	4.69	95.31	42.39	57.61	2225.92
LJ281113STM8	4.23	95.77	40.34	59.66	2083.69
LJ280205STM8	3.40	96.60	45.26	54.74	2551.02
LJ280204bSTM8	3.21	96.79	44.73	55.27	2540.63
LJ280204aSTM8	3.46	96.54	44.66	55.34	2202.34
LJ280203bSTM8	3.28	96.72	43.03	56.97	991.09
LJ280203aSTM8	3.33	96.67	44.78	55.22	2293.63
LJ280202bSTM8	2.18	97.82	47.74	52.26	2040.42
LJ280202aSTM8	2.53	97.47	48.57	51.43	2720.90
LJ280201bSTM8	3.06	96.94	46.07	53.93	2274.78
LJ280201aSTM8	2.94	97.06	45.82	54.18	2107.15
LJ280131bSTM8	2.56	97.44	43.60	56.40	2049.38

LJ280131aSTM8	3.22	96.78	42.27	57.73	2256.73
LJ280130bSTM8	2.71	97.29	46.53	53.47	2295.82
LJ280130aSTM8	2.37	97.63	49.17	50.83	2274.38
LJ280508STT	2.86	97.14			
LJ220514STT	1.96	98.04			
LJ140828STT	27.85	72.15			
LJ220828STT	19.95	80.05			
LJ280828STT	13.17	86.83			
LJ141113STT	1.48	98.52	49.39	50.61	2103.48
LJ280205STT	2.28	97.72	43.97	56.03	2004.63
LJ220205STT	2.17	97.83	45.62	54.38	1013.78
LJ140205STT	2.12	97.88	45.22	54.78	2077.85

TABLE A1 cont. List of sediment nutrient analysis.

Sample ID	%N	$\delta^{15}\text{N}$	$\delta^{13}\text{C}$	
			%C	Decarbonated
LJ280508SF	1.15	2.61	15.54	-21.87
LJ140514SF	1.29	2.47	17.14	-22.70
LJ220514SF	2.18	2.62	20.68	-23.26
LJ140626SF	1.67	2.25	17.23	-22.93
LJ220626SF	1.93	2.47	19.90	-23.29
LJ280626SF	0.47	2.18	12.43	-22.62
LJ140821SF	1.75	2.30	19.36	-22.82
LJ220821SF	1.52	2.35	18.92	-23.59
LJ280821SF	0.81	2.43	6.86	-21.96
LJ221106SF	2.39	2.36	21.26	-23.55
LJ281106SF	1.61	2.65	17.47	-22.19
LJ141106SF	1.91	2.52	19.24	-23.17
LJ140129SF	1.73	2.33	17.39	-23.06
LJ220129SF	2.47	1.95	22.05	-23.51
LJ280129SF	1.51	2.58	10.13	-22.21
LJ140820SF	1.47	1.13	17.31	-22.62
LJ220820SF	1.73	1.32	17.89	-23.13
LJ280820SF	0.66	0.94	13.17	-22.16

LJ440820SF	1.75	1.28	18.69	-21.91
LJ221111SF	1.77	2.31	20.23	-23.33
LJ141111SF	1.90	1.86	19.94	-22.98
LJ281111SF	1.51	2.28	14.75	-21.98
LJ441111SF	2.10	2.00	17.67	-21.94
LJ140128 SF	1.98	1.77	19.12	-22.95
LJ220128 SF	2.26	1.96	22.89	-23.31
LJ440128 SF	2.13	1.79	20.14	-21.97
LJ140408 SF	2.09	2.08	20.85	-22.91
LJ220408 SF	2.27	2.26	22.38	-23.22
LJ280408 SF	0.83	2.06	16.20	-21.67
LJ440408 SF	2.06	2.28	19.02	-22.07

TABLE A1 cont. List of sediment nutrient analysis.

Sample ID	%N	$\delta^{15}\text{N}$	%C Decarbonated	$\delta^{13}\text{C}$
LJ280508SS	0.21	4.03	1.77	-21.52
LJ140514SS	0.68	1.78	11.17	-22.86
LJ220514SS	1.20	2.30	14.49	-23.52
LJ140626SS	1.26	1.55	17.21	-23.05
LJ220626SS	0.82	1.93	12.87	-23.35
LJ280626SS	0.18	4.15	1.62	-22.13
LJ140821SS	1.47	2.09	16.61	-22.24
LJ220821SS	1.21	2.50	16.92	-23.77
LJ280821SS	0.11	2.92	1.26	-22.25
LJ141106SS	0.99	1.50	16.47	-23.27
LJ281106SS	0.50	2.52	5.64	-21.50
LJ221106SS	1.48	2.57	18.38	-23.14
LJ280129SS	0.24	4.07	4.01	-20.87
LJ140129SS	1.34	1.77	12.85	-22.50
LJ220129SS	1.51	2.68	18.14	-23.31
LJ140820SS	1.33	1.24	17.35	-22.32
LJ220820SS	0.99	1.61	16.85	-23.32
LJ280820SS	0.20	4.06	4.88	-18.53
LJ440820SS	1.06	2.89	15.08	-22.02

LJ441111SS	1.11	3.03	15.74	-22.54
LJ141111SS	1.10	1.87	15.74	-22.54
LJ221111SS	1.36	1.92	15.48	-23.51
LJ281111SS	0.17	4.94	3.73	-23.43
LJ140128 SS	1.04	1.54	15.83	-22.18
LJ220128 SS	1.40	2.27	17.13	-23.60
LJ280128 SS	0.33	4.32	6.72	-19.25
LJ440128 SS	1.52	2.41	16.72	-21.76
LJ140408 SS	0.68	2.02	15.37	-22.55
LJ220408 SS	0.74	2.39	13.54	-23.60
LJ280408 SS	0.17	4.71	4.17	-22.16
LJ440408 SS	1.20	3.02	15.07	-21.85

TABLE A1 cont. List of sediment nutrient analysis.

Sample ID	TP ^a µg g ⁻¹ dw	TP mg g ⁻¹	TN ^a mg g ⁻¹	TN ^a %	TC mg g ⁻¹	TIC mg g ⁻¹
LJ280329STHA	2449.12	2.45	7.0	0.70	68.5	0.27
LJ280425 STHA	2652.36	2.65	22.20	2.22	208.50	0.00
LJ140514STHA	2073.75	2.07	20.90	2.09	206.20	0.14
LJ220514STHA	2352.57	2.35	23.30	2.33	221.30	0.00
LJ140709STHA	2286.71	2.29	25.60	2.56	235.70	0.00
LJ220709STHA	982.08	0.98	17.00	1.70	178.30	0.05
LJ280709STHA	1960.84	1.96	23.00	2.30	209.40	0.00
LJ140828STHA	1382.53	1.38	23.70	2.37	221.90	0.00
LJ220828STHA	1537.94	1.54	25.40	2.54	235.80	0.00
LJ280828STHA	2223.28	2.22	26.60	2.66	247.20	0.00
LJ221113STHA	2635.00	2.64	25.72	2.57	232.33	0.04
LJ141113STHA	2065.02	2.07	24.31	2.43	217.33	1.30
LJ281113STHA	1840.16	1.84	24.03	2.40	212.09	0.00
LJ280205STHA	2185.50	2.19	25.49	2.55	232.07	0.00
LJ220205STHA	2496.41	2.50	25.46	2.55	234.20	0.00
LJ140205STHA	2271.91	2.27	25.78	2.58	238.23	0.05
LJ140827STHA	1820.73	1.82	23.35	2.34	207.19	0.00
LJ220827STHA	1901.81	1.90	27.50	2.75	236.27	0.00
LJ280827STHA	1414.00	1.41	23.74	2.37	201.06	0.00
LJ440827STHA	1371.34	1.37	22.70	2.27	208.66	0.00

LJ22B1119STHA						
LJ28B1119STHA						
LJ22A1119STHA	1942.59	1.94	28.39	2.84	272.17	0.00
LJ28A1119STHA	1684.05	1.68	26.35	2.63	255.70	0.00
LJ14B1119STHA						
LJ14A1119STHA	2035.06	2.04	28.67	2.87	277.06	0.00

TABLE A1 cont. List of sediment nutrient analysis.

Sample ID	TP ^a µg g ⁻¹ dw	TP mg g ⁻¹	TN ^a mg g ⁻¹	TN ^a %	TC mg g ⁻¹	TIC mg g ⁻¹
LJ44B0204 STHA						
LJ28B0204 STHA						
LJ44A0204 STHA	1935.67	1.94	24.10	2.41	231.00	0.07
LJ22B0204 STHA						
LJ14B0204 STHA						
LJ28A0204 STHA	2210.28	2.21	25.20	2.52	246.60	0.31
LJ14A0204 STHA	2258.40	2.26	26.90	2.69	259.50	0.00
LJ22A0204 STHA	2436.25	2.44	28.30	2.83	256.80	0.00
LJ14A0415 STHA	2241.17	2.24	23.86	2.39	250.46	0.00
LJ14B0415 STHA						
LJ22A0415 STHA	2275.43	2.28	26.10	2.61	253.49	0.00
LJ22B0415 STHA						
LJ28A0415 STHA	2021.20	2.02	21.69	2.17	229.84	7.27
LJ28B0415 STHA						
LJ44A0415 STHA	1929.31	1.93	20.46	2.05	220.56	0.00
LJ44B0415 STHA						

TABLE A1 cont. List of sediment nutrient analysis.

Sample ID	TP mg g ⁻¹	TN ^a mg g ⁻¹	TN ^a %	TC mg g ⁻¹	TIC mg g ⁻¹
LJ281107STM8	2.18	25.41	2.54	225.52	0.22
LJ281108STM8	2.19	23.5	2.35	215.75	0.00
LJ281109STM8	2.45	22.49	2.25	212.00	0.02
LJ281110STM8	1.77	23.89	2.39	220.42	4.10
LJ281111STM8	2.48	22.89	2.29	205.64	0.80
LJ281112STM8	2.23	23.01	2.30	205.76	0.03
LJ281113STM8	2.08	20.04	2.00	189.65	0.31
LJ280205STM8	2.55	26.57	2.64	231.79	0.00
LJ280204bSTM8	2.54	25.18	2.83	221.08	0.00
LJ280204aSTM8	2.20	25.65	2.43	227.83	0.00
LJ280203bSTM8	0.99	24.56	2.45	222.57	0.00
LJ280203aSTM8	2.29	25.32	2.60	228.66	0.00
LJ280202bSTM8	2.04	26.10	2.64	234.02	0.00
LJ280202aSTM8	2.72	27.08	2.61	249.63	0.00
LJ280201bSTM8	2.27	25.99	2.71	232.16	0.00
LJ280201aSTM8	2.11	26.40	2.46	232.90	0.00
LJ280131bSTM8	2.05	24.28	2.53	216.22	0.00
LJ280131aSTM8	2.26	24.51	2.52	218.93	0.00
LJ280130bSTM8	2.30	26.40	2.56	239.51	0.00
LJ280130aSTM8	2.27	28.27	2.66	253.62	0.00
LJ280508STT					
LJ220514STT					
LJ140828STT					
LJ220828STT					

LJ280828STT					
LJ141113STT	2.10	24.40	2.45	221.28	0.00
LJ280205STT	2.00	24.45	2.49	220.88	0.00
LJ220205STT	1.01	24.89	2.48	225.21	0.00
LJ140205STT	2.08	24.77	2.44	224.51	0.00

TABLE A1 cont. List of sediment nutrient analysis.

Sample ID	%N	$\delta^{15}\text{N}$	%C	$\delta^{13}\text{C}$ Decarbonated
LJ280329STHA	2.52	3.08	21.71	-21.97
LJ280425 STHA	2.23	3.40	20.30	-22.25
LJ140514STHA	2.19	3.08	21.08	-22.73
LJ220514STHA	2.38	2.79	23.04	-23.15
LJ140709STHA	1.23	2.59	17.85	-22.97
LJ220709STHA	2.66	3.93	24.40	-24.05
LJ280709STHA	2.42	3.39	22.22	-22.52
LJ140828STHA	2.58	3.06	23.59	-22.53
LJ220828STHA	2.98	3.58	25.83	-22.95
LJ280828STHA	2.38	2.94	23.34	-22.33
LJ221113STHA	2.58	3.20	25.40	-23.30
LJ141113STHA	2.47	3.12	22.38	-23.10
LJ281113STHA	2.47	2.92	23.79	-22.16
LJ280205STHA	2.62	2.51	23.31	-21.97
LJ220205STHA	2.63	2.75	25.01	-23.08
LJ140205STHA	2.69	2.96	23.21	-22.87
LJ140827STHA	2.26	2.20	22.91	-22.89
LJ220827STHA	2.59	3.28	27.33	-22.47
LJ280827STHA	2.32	2.18	22.66	-21.55
LJ440827STHA	2.25	2.44	22.30	-21.61
LJ22B1119STHA				
LJ28B1119STHA				
LJ22A1119STHA	2.75	2.36	27.89	-21.99
LJ28A1119STHA	2.74	2.49	26.56	-21.24
LJ14B1119STHA				
LJ14A1119STHA	2.78	2.50	27.80	-21.71

TABLE A1 cont. List of sediment nutrient analysis.

Sample ID	%N	$\delta^{15}\text{N}$	%C	$\delta^{13}\text{C}$ Decarbonated
LJ44B0204 STHA				
LJ28B0204 STHA				
LJ44A0204 STHA	2.42	2.70	24.62	-21.35
LJ22B0204 STHA				
LJ14B0204 STHA				
LJ28A0204 STHA	2.43	2.63	25.53	-20.50
LJ14A0204 STHA	2.65	2.54	28.14	-21.63
LJ22A0204 STHA	2.73	2.77	23.09	-22.19
LJ14A0415 STHA	2.76	2.22	26.41	-21.27
LJ14B0415 STHA				
LJ22A0415 STHA	2.92	2.69	26.55	-21.70
LJ22B0415 STHA				
LJ28A0415 STHA	2.48	2.61	22.69	-20.46
LJ28B0415 STHA				
LJ44A0415 STHA	2.37	2.39	22.40	-20.92
LJ44B0415 STHA				

TABLE A1 cont. List of sediment nutrient analysis.

Sample ID	%N	$\delta^{15}\text{N}$	%C Decarbonated	$\delta^{13}\text{C}$
LJ281107STM8	2.58	3.44	22.67	-22.29
LJ281108STM8	2.46	3.59	23.48	-22.09
LJ281109STM8	2.22	3.61	22.75	-22.49
LJ281110STM8	2.45	3.28	23.12	-22.27
LJ281111STM8	2.37	4.25	22.54	-22.43
LJ281112STM8	2.32	3.05	22.58	-22.35
LJ281113STM8	2.17	3.86	22.02	-22.29
LJ280205STM8	2.68	2.79	22.25	-22.18
LJ280204bSTM8	2.67	2.76	23.34	-22.02
LJ280204aSTM8	2.70	2.66	22.93	-21.94
LJ280203bSTM8	2.69	2.87	22.56	-22.01
LJ280203aSTM8	2.71	2.70	23.17	-22.00
LJ280202bSTM8	2.75	2.47	23.84	-21.82
LJ280202aSTM8	2.86	2.70	24.06	-21.88
LJ280201bSTM8	2.75	2.51	23.54	-21.83
LJ280201aSTM8	2.84	2.85	24.02	-21.98
LJ280131bSTM8	2.57	2.21	21.93	-22.17
LJ280131aSTM8	2.71	2.84	21.18	-22.05
LJ280130bSTM8	2.79	2.23	23.82	-21.79
LJ280130aSTM8	3.06	2.12	22.50	-21.92
LJ280508STT				
LJ220514STT			20.20	-22.76
LJ140828STT				
LJ220828STT				
LJ280828STT				
LJ141113STT	2.55	1.78	23.06	-22.97
LJ280205STT	2.52	2.32	21.60	-22.00
LJ220205STT	2.56	2.34	23.45	-23.26
LJ140205STT	2.56	2.49	22.88	-22.81

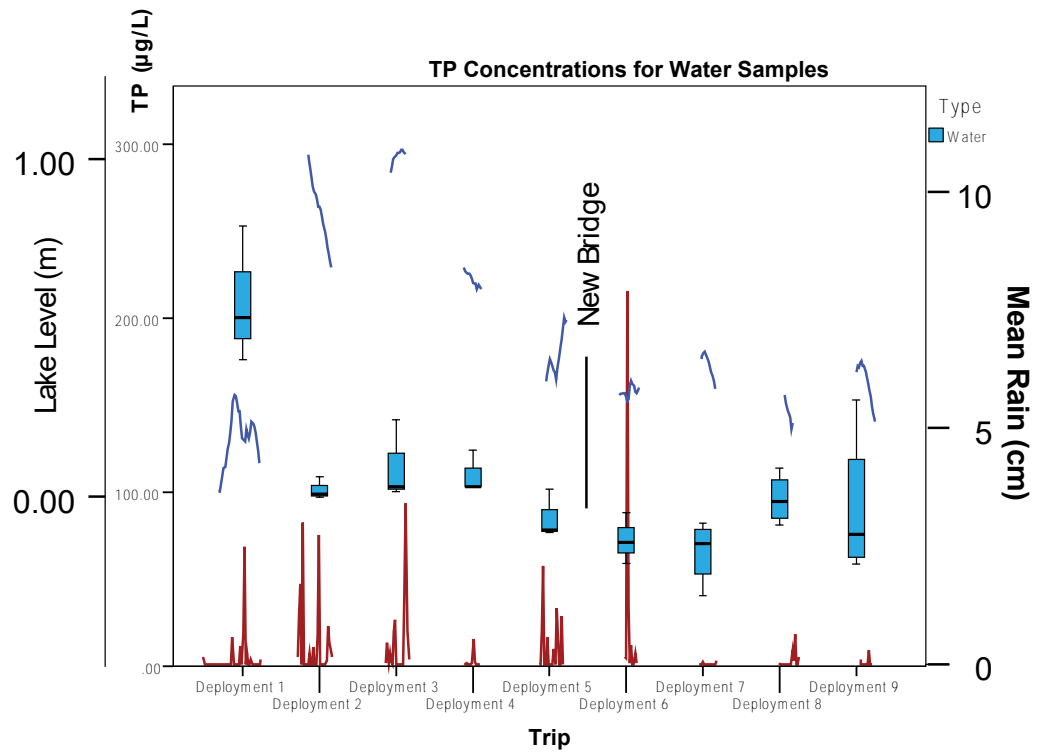


FIGURE A1. Precipitation, TP and Lake level for all 9 Deployments.

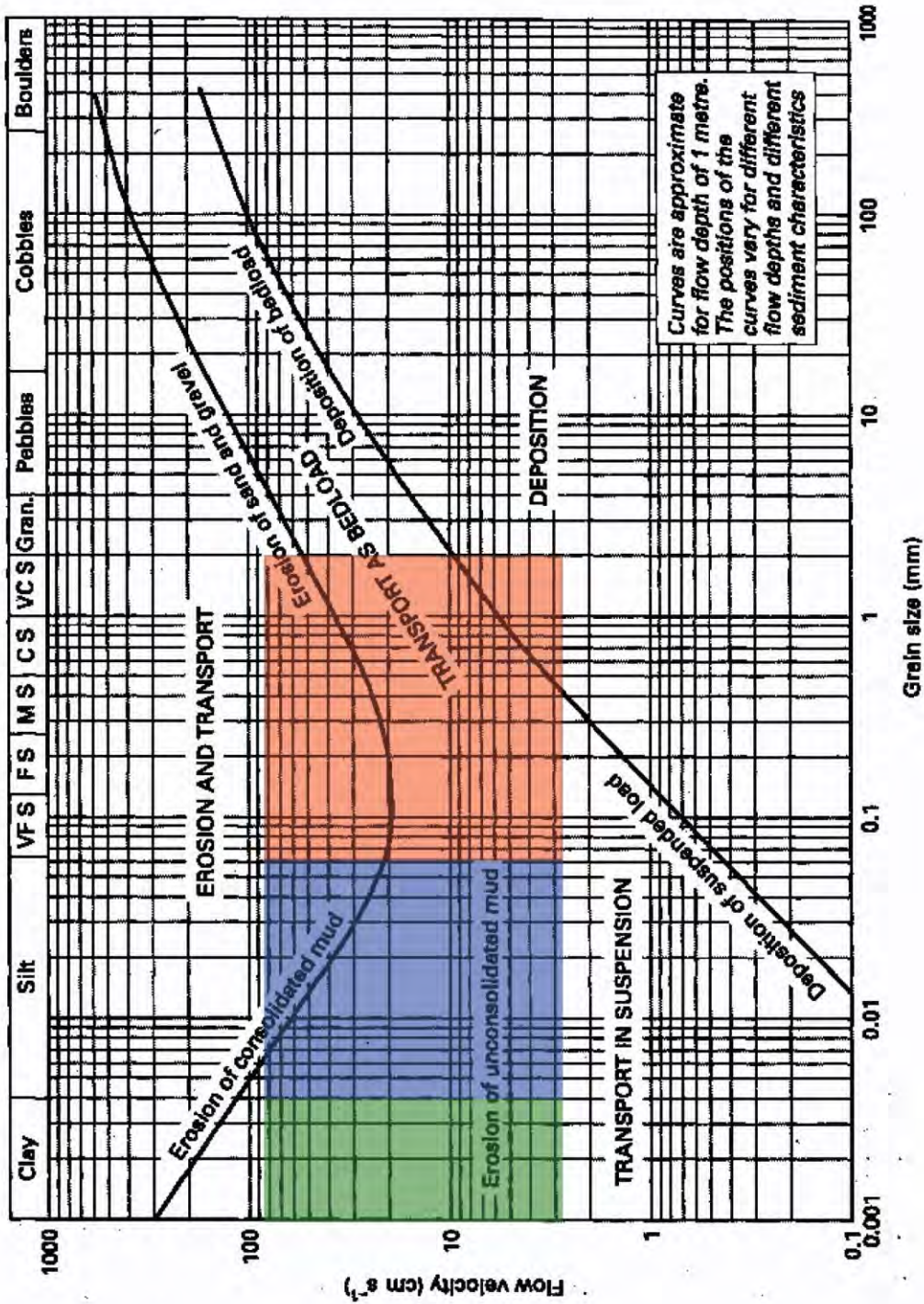


FIGURE A2. Hjulstrom Curve (1935) with color blocks representing the grain size range for Lake Jesup. Green is represented by clay, blue is silt and red is sands. The shaded area represents the range in current velocities for Deployment 1.

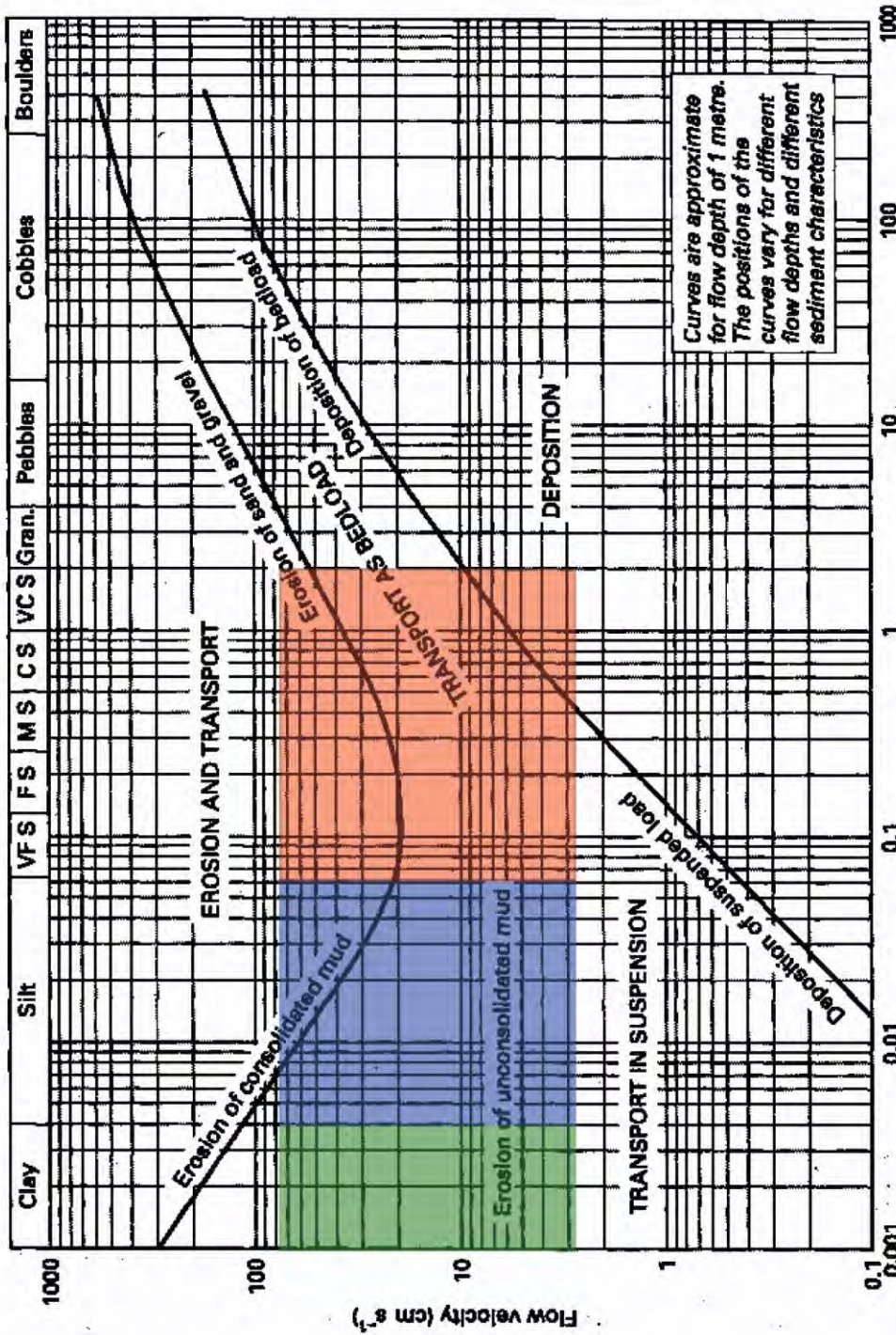


FIGURE A3. Hjulstrom Curve (1935) with color blocks representing the grain size range for Lake Jesup. Green is represented by clay, blue is silt and red is sands. The shaded area represents the range in current velocities for Deployment 2.

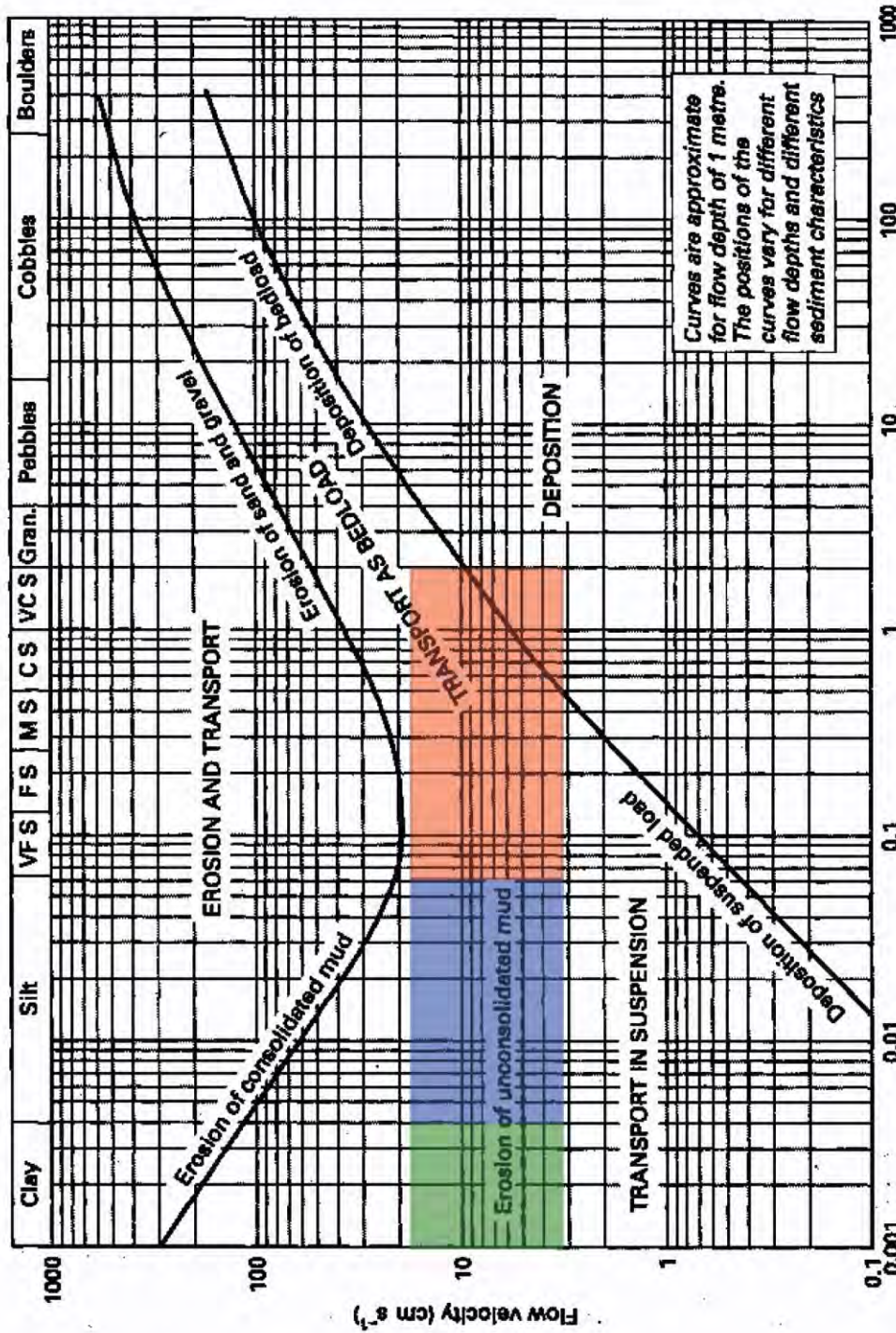


FIGURE A4. Hjulstrom Curve (1935) with color blocks representing the grain size range for Lake Jesup. Green is represented by clay, blue is silt and red is sands. The shaded area represents the range in current velocities for Deployment 5.

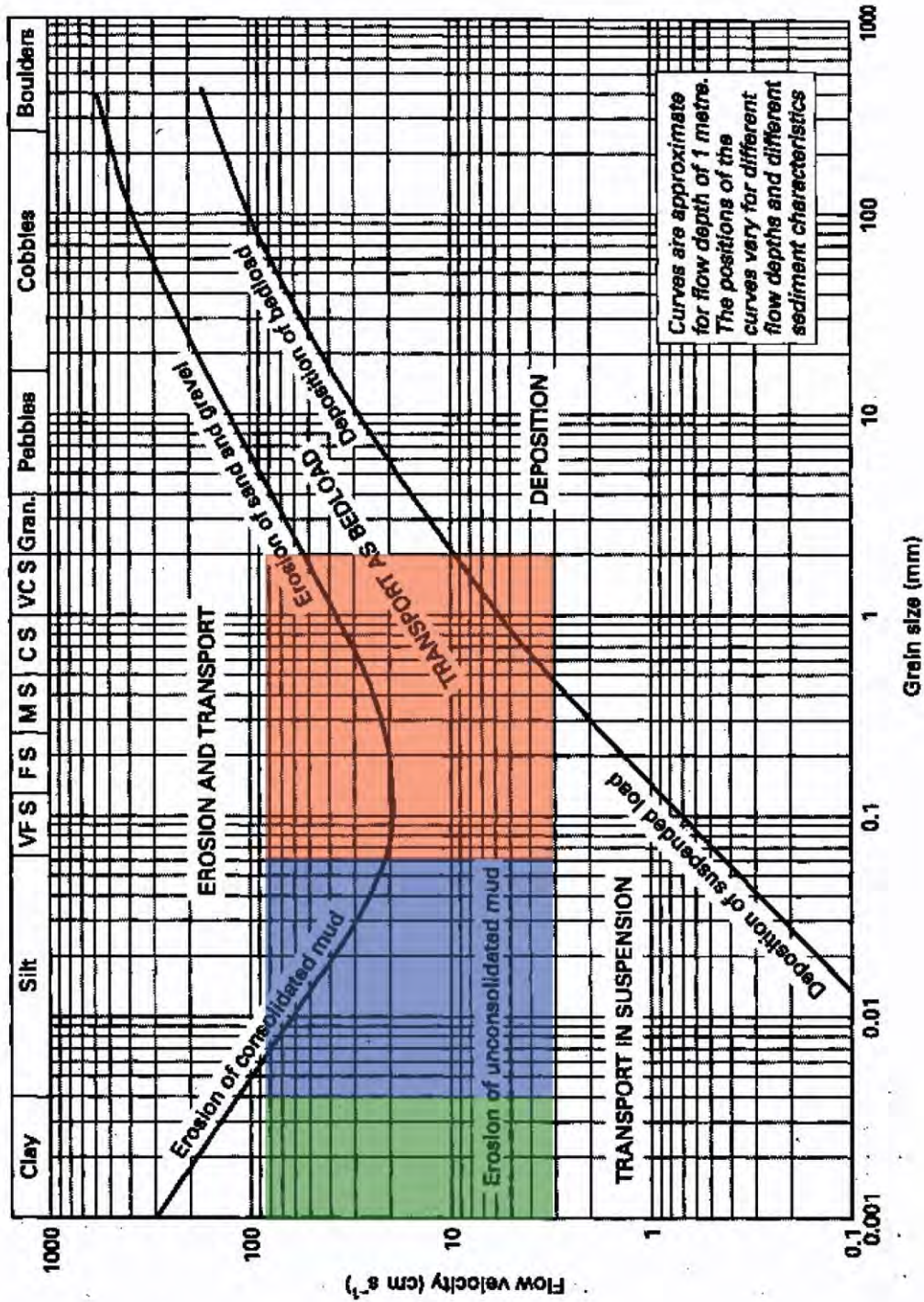


FIGURE A5. Hjulstrom Curve (1935) with color blocks representing the grain size range for Lake Jesup. Green is represented by clay, blue is silt and red is sands. The shaded area represents the range in current velocities for Deployment 6.

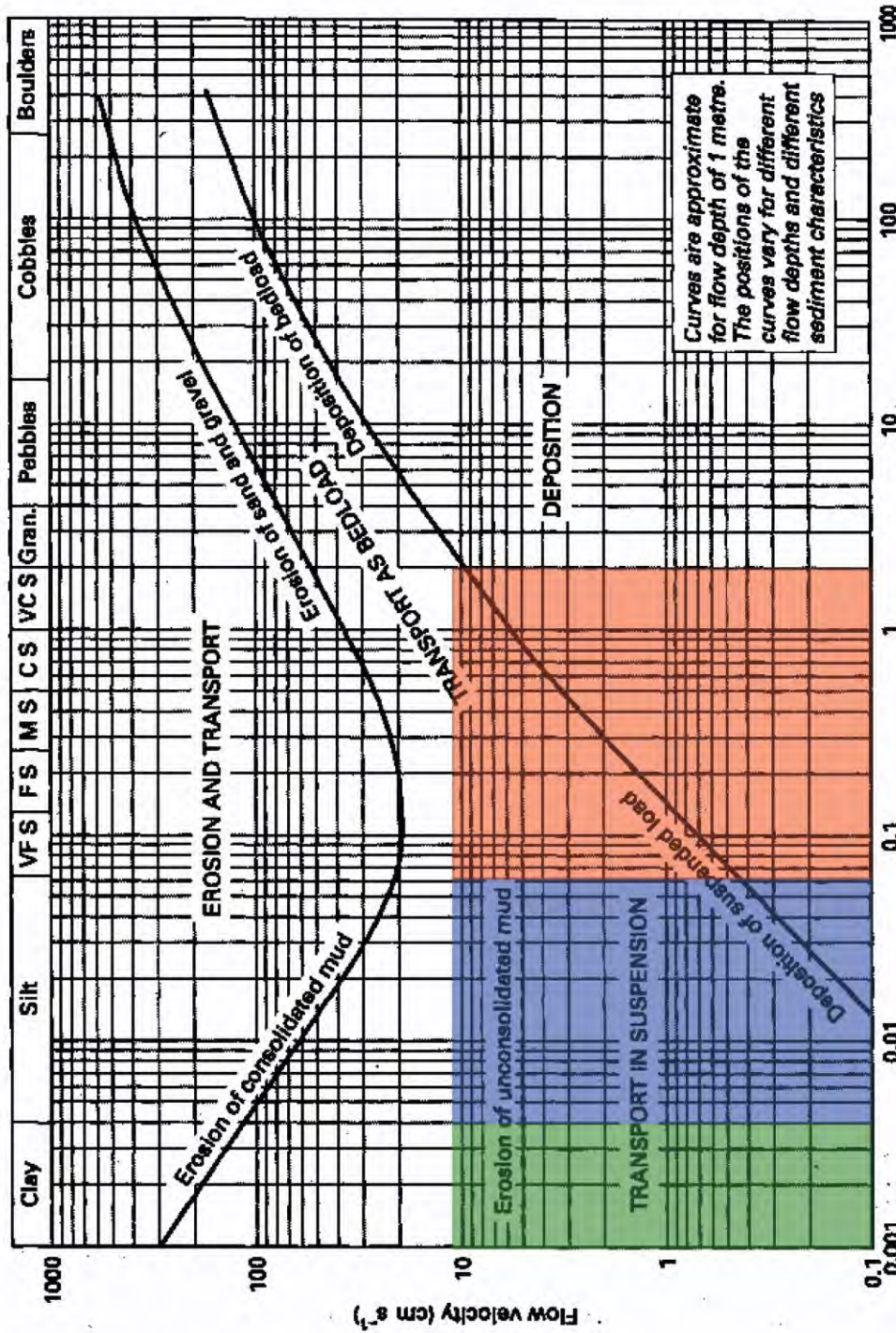


FIGURE A6. Hjulstrom Curve (1935) with color blocks representing the grain size range for Lake Jesup. Green is represented by clay, blue is silt and red is sands. The shaded area represents the range in current velocities for Deployment 8.

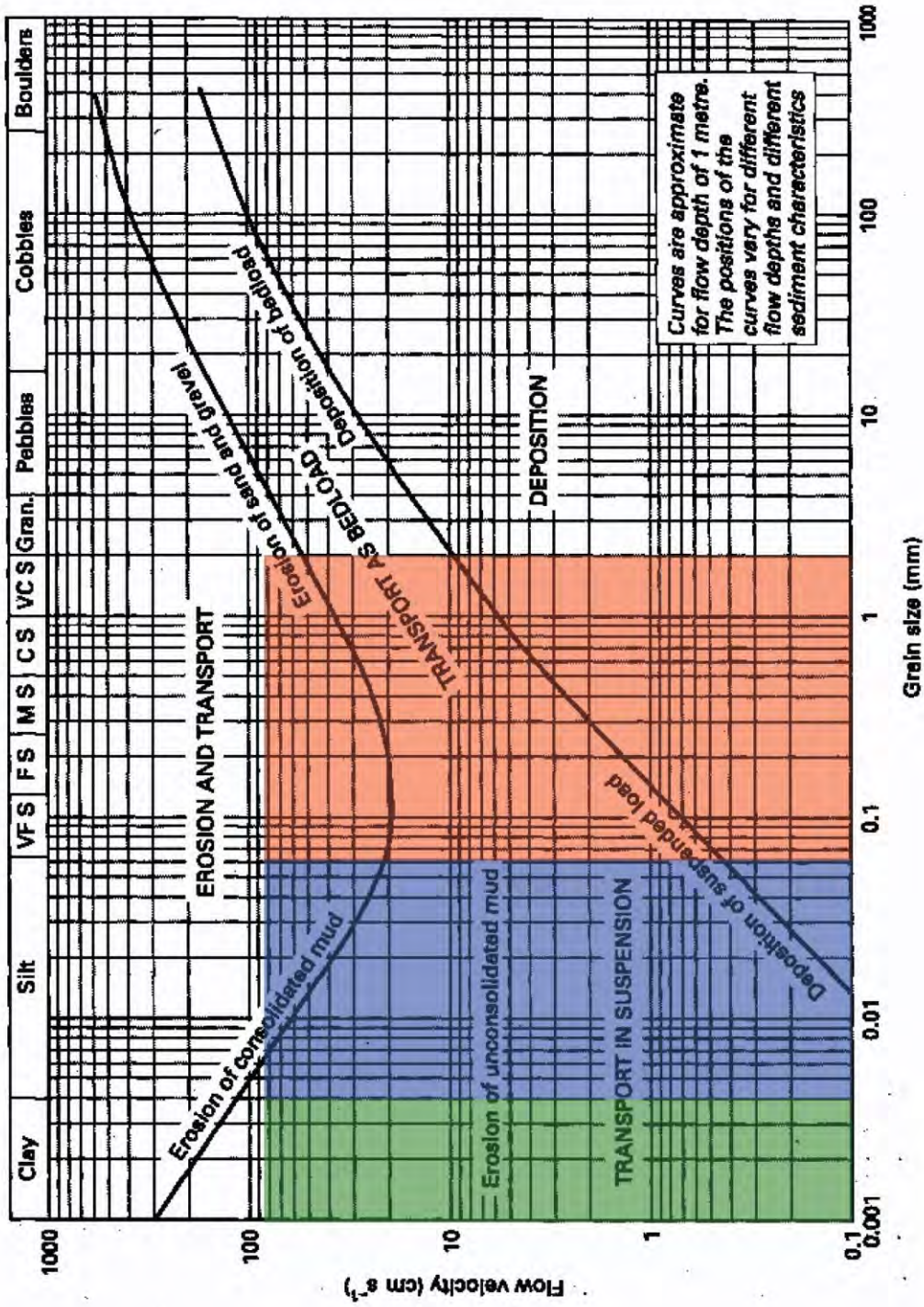


FIGURE A7. Hjulstrom Curve (1935) with color blocks representing the grain size range for Lake Jesup. Green is represented by clay, blue is silt and red is sands. The shaded area represents the range in current velocities for Deployment 8.

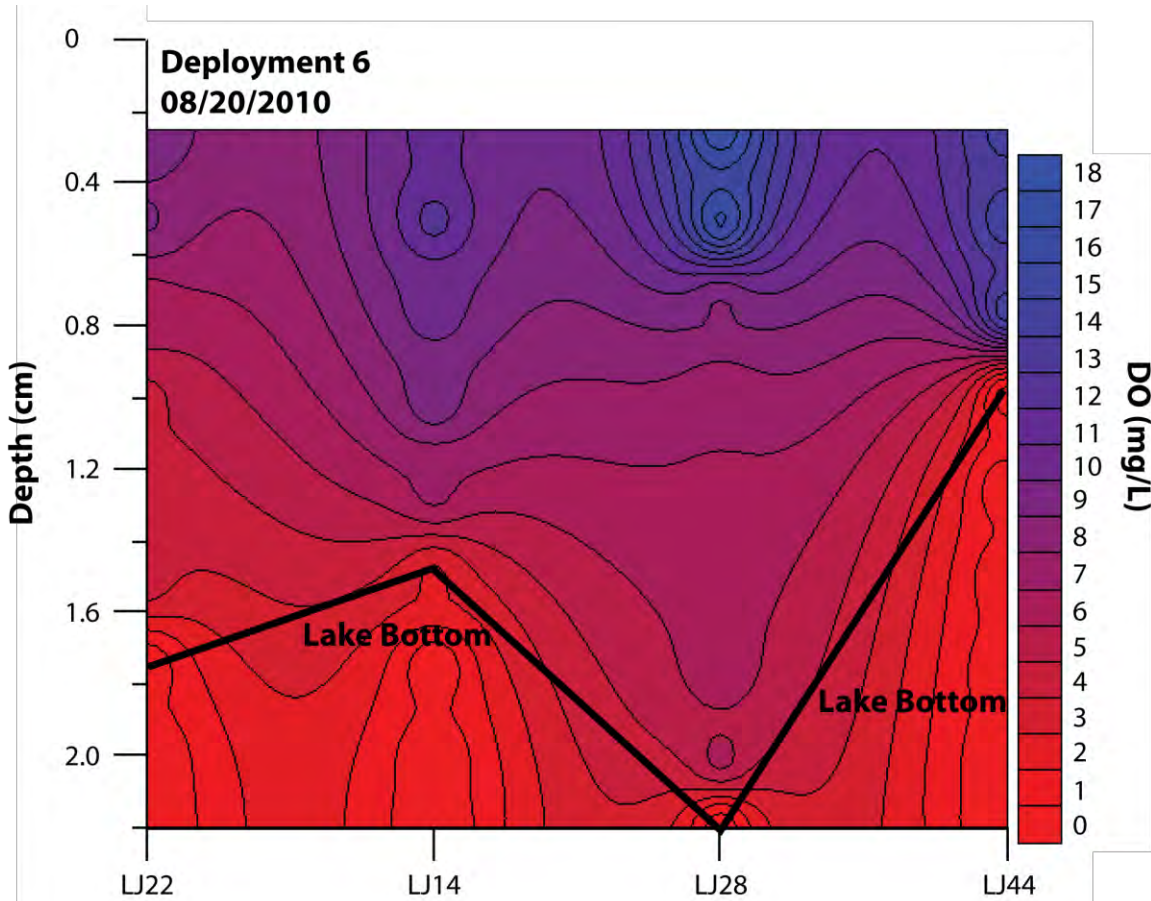


FIGURE A8. Lake wide DO profile for from West to East for Deployment 6.

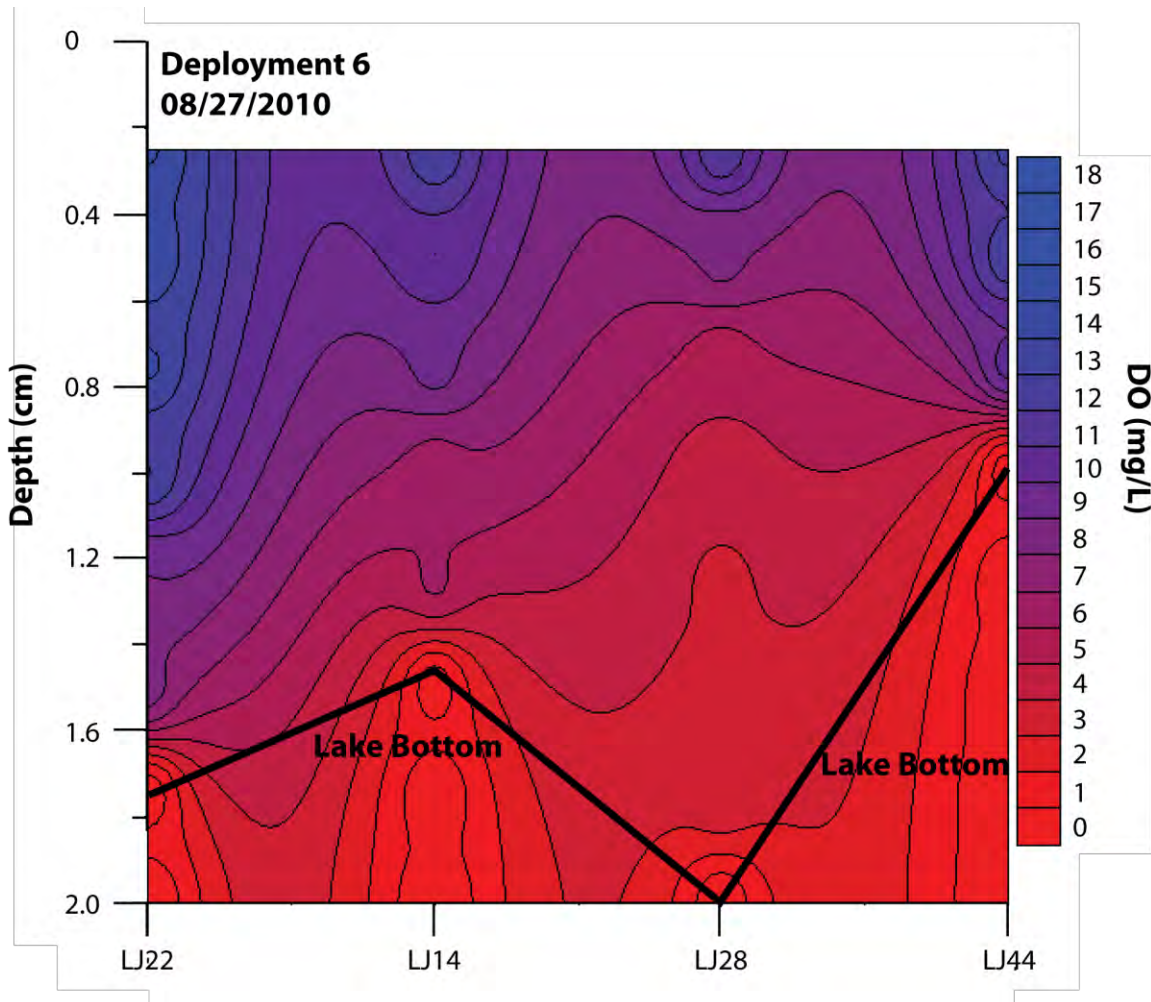


FIGURE A9. Lake wide DO profile for from West to East for Deployment 6.

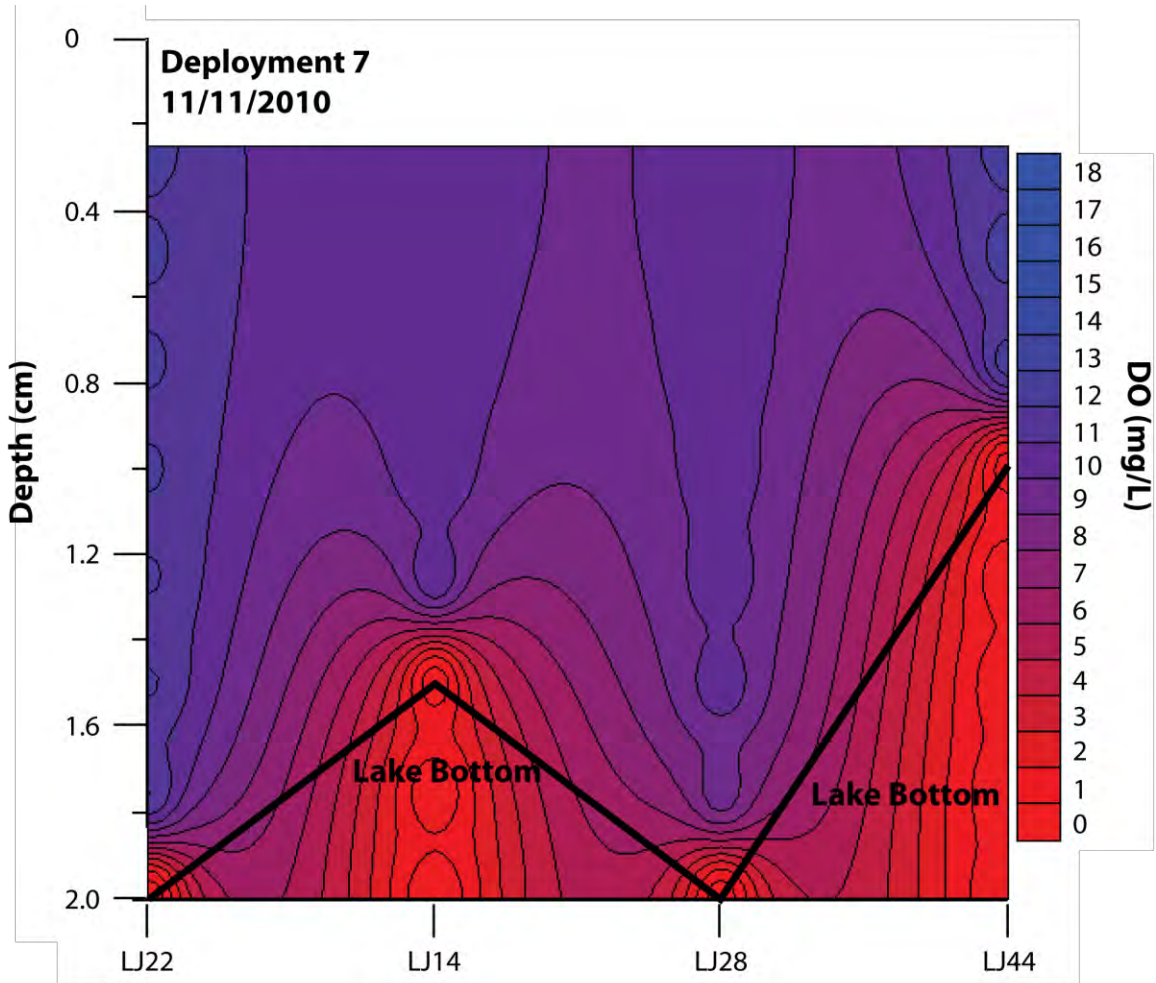


FIGURE A10. Lake wide DO profile for from West to East for Deployment 7.

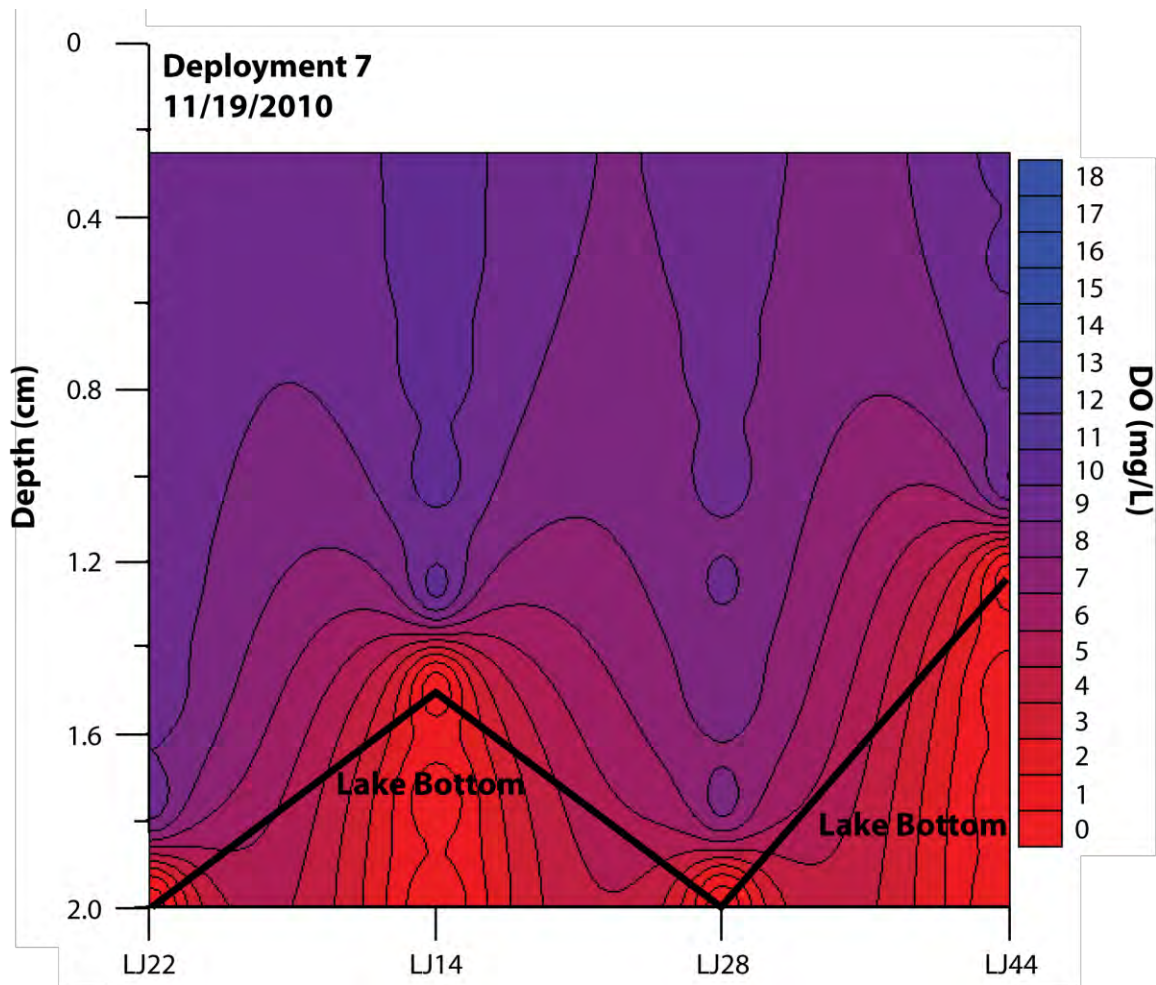


FIGURE A11. Lake wide DO profile for from West to East for Deployment 7.

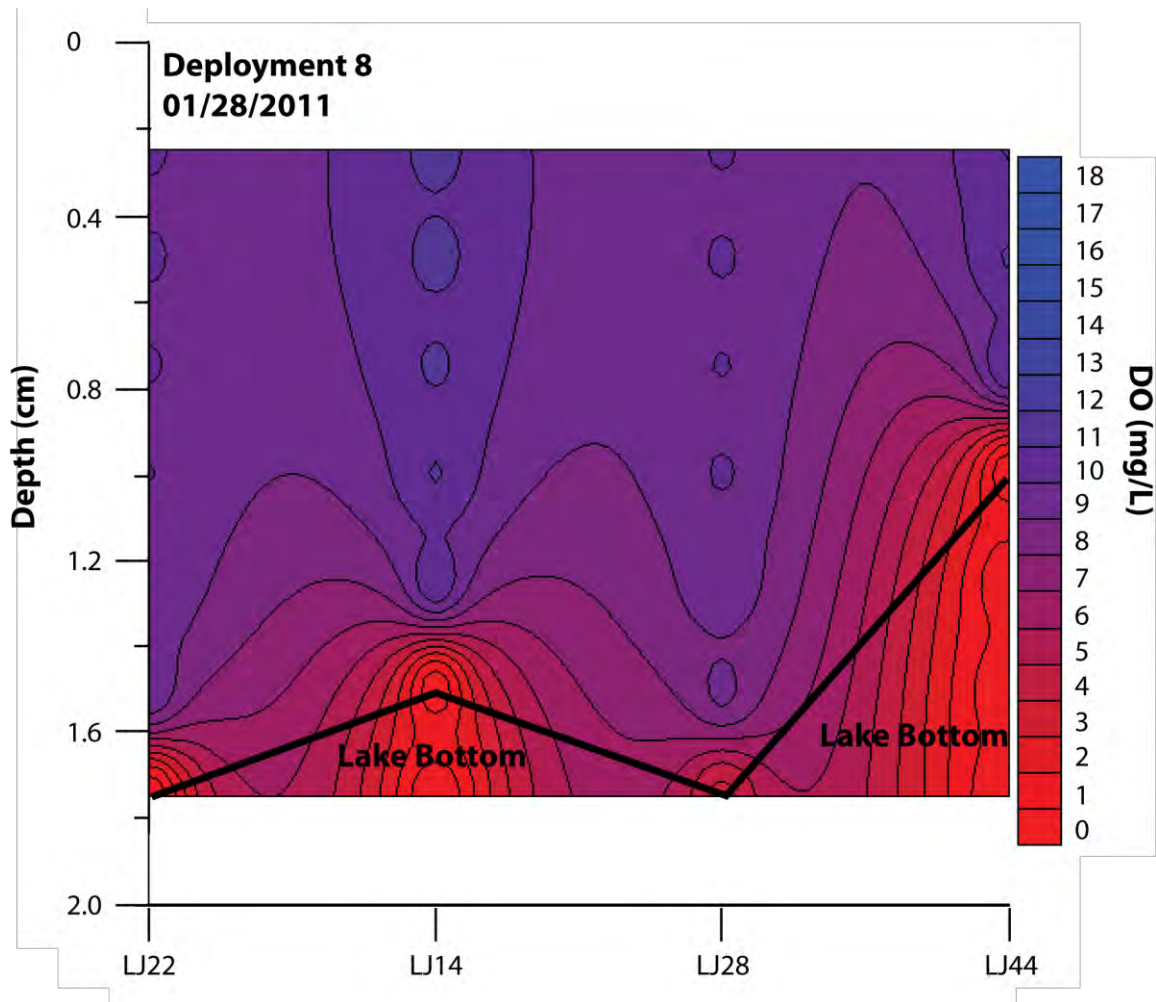


FIGURE A12. Lake wide DO profile for from West to East for Deployment 8.

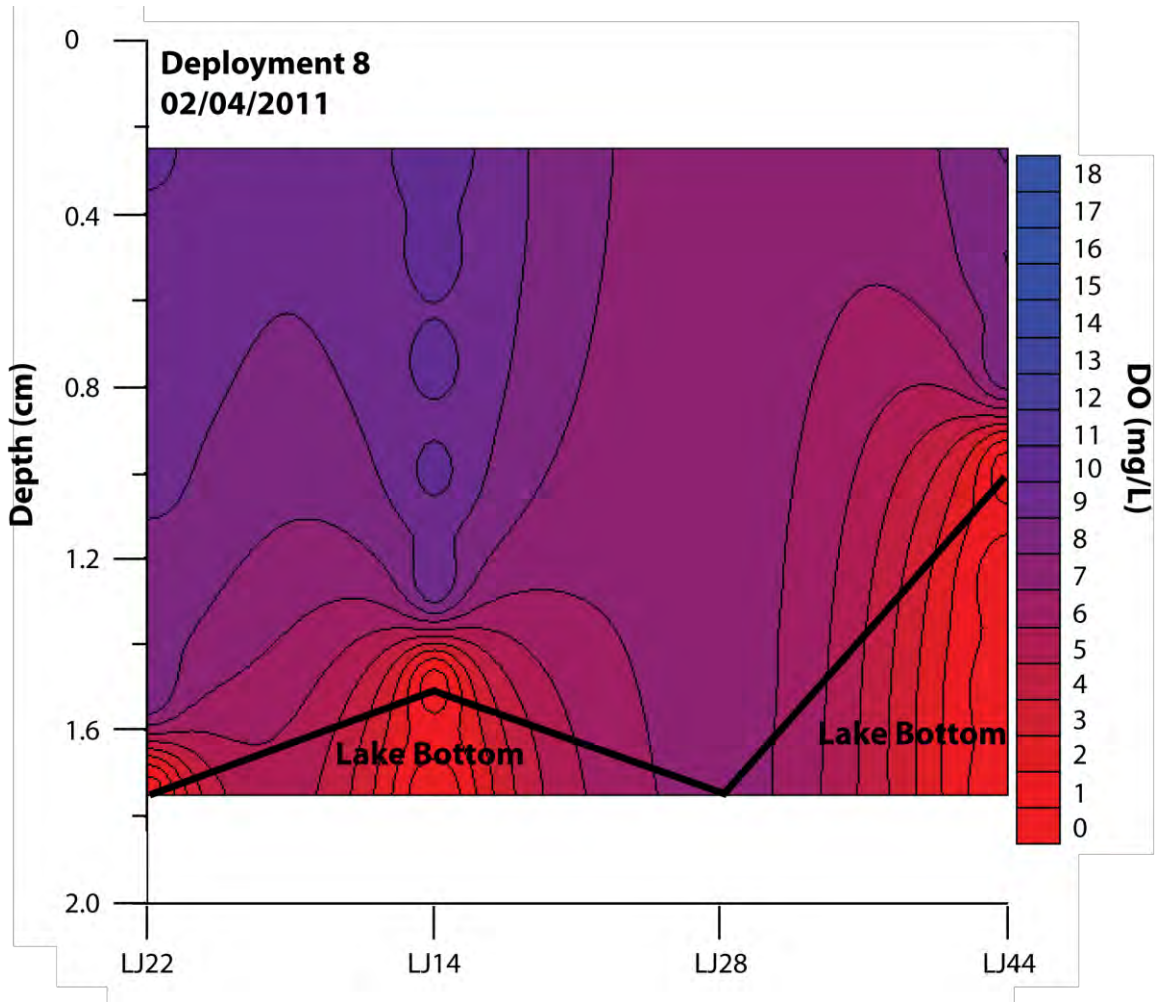


FIGURE A13. Lake wide DO profile for from West to East for Deployment 8.

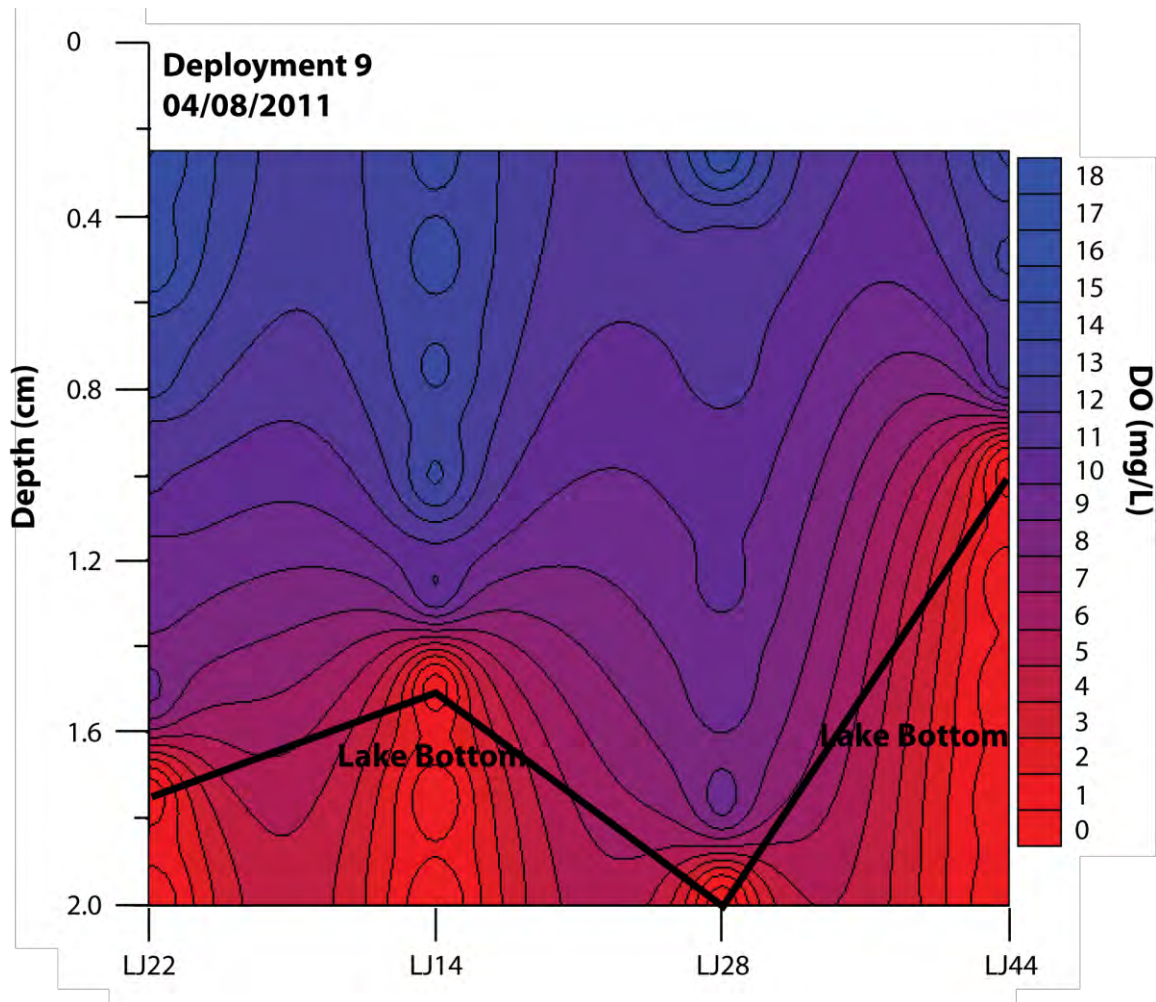


FIGURE A14. Lake wide DO profile for from West to East for Deployment 9.

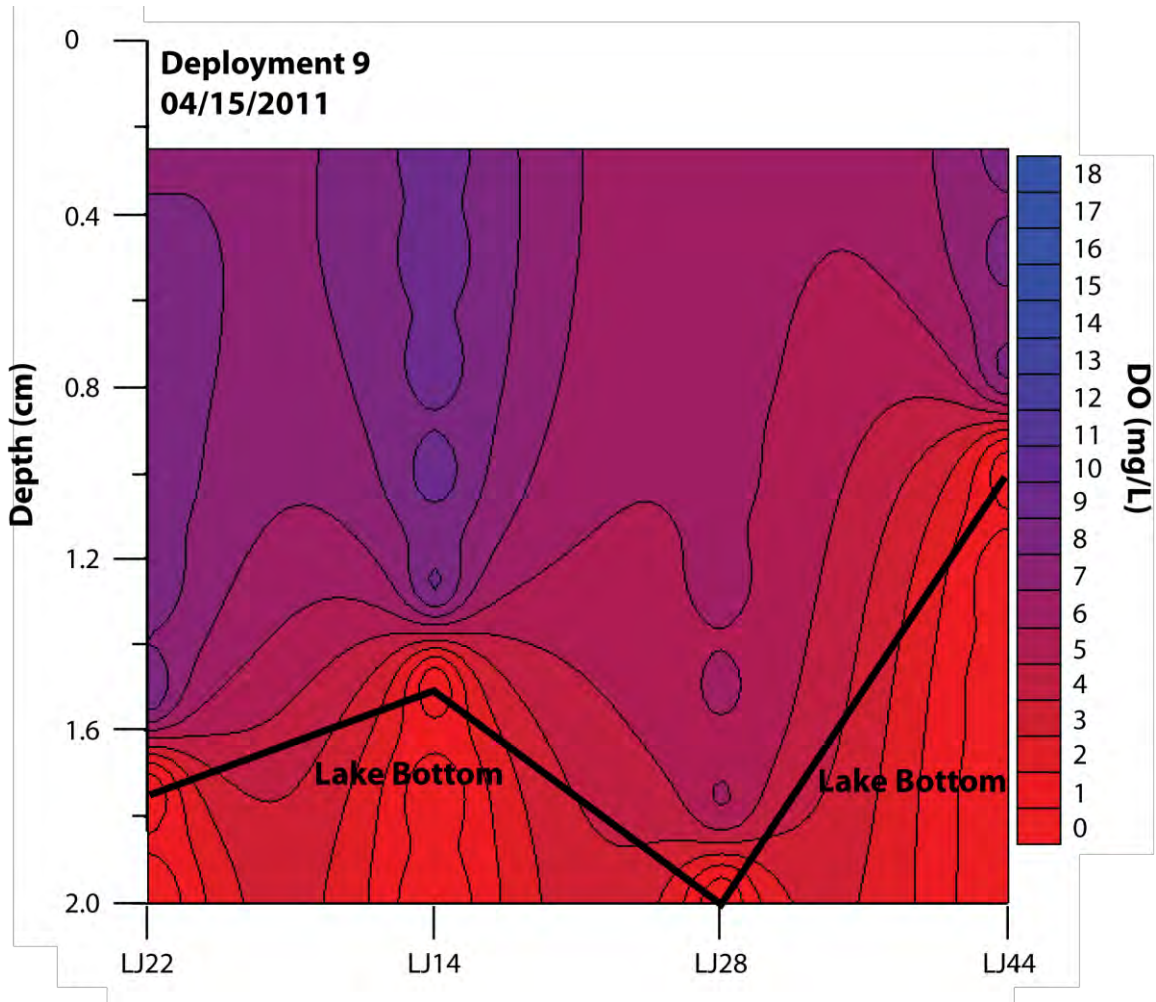


FIGURE A15. Lake wide DO profile for from West to East for Deployment 9

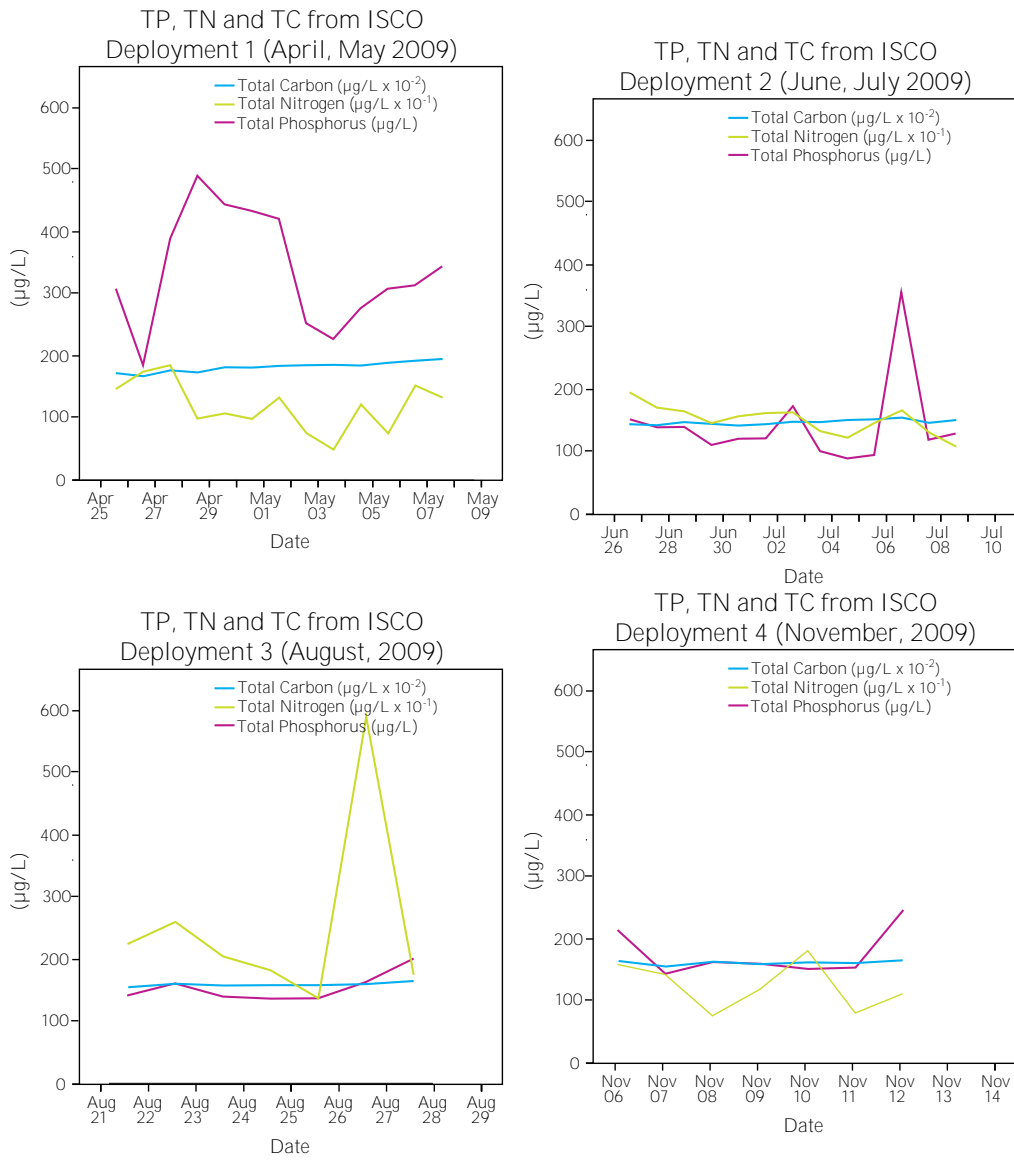


FIGURE A16. Daily nutrient concentrations for TP, TN and TOC for Deployments 1 to 4.

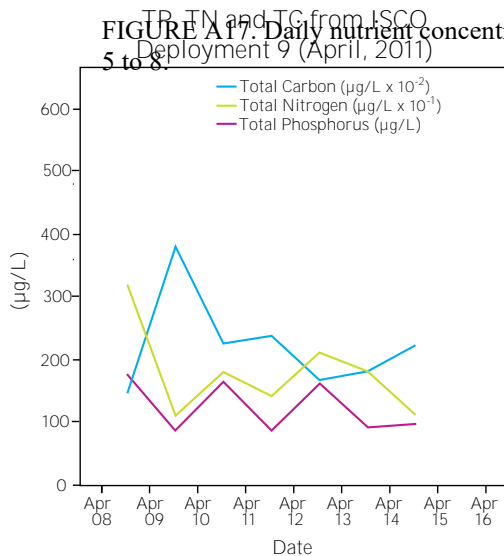
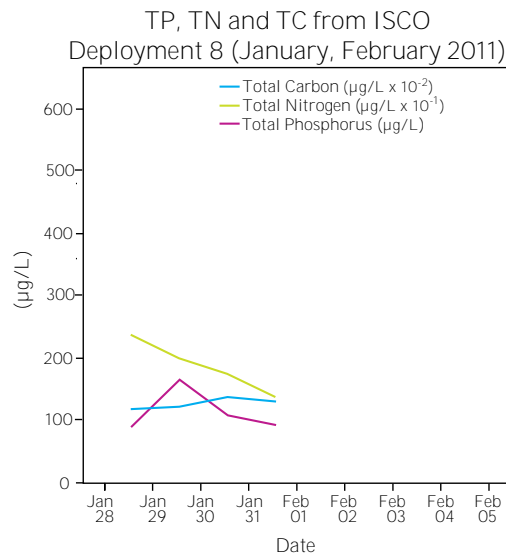
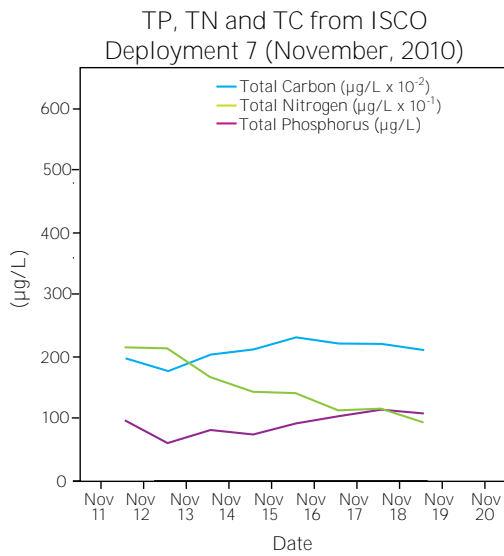
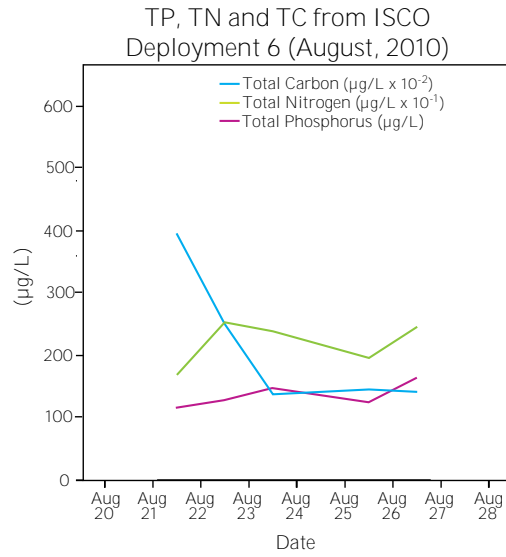
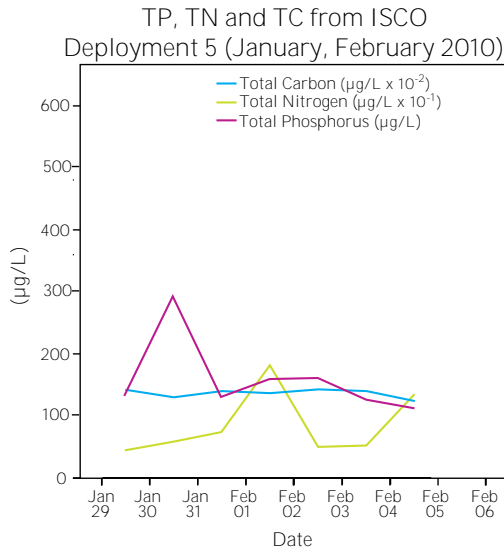


FIGURE A17. Daily nutrient concentrations for TP, TN and TOC for Deployments 5 to 9.

FIGURE A18. Daily nutrient concentrations for TP, TN and TOC for Deployment 9.

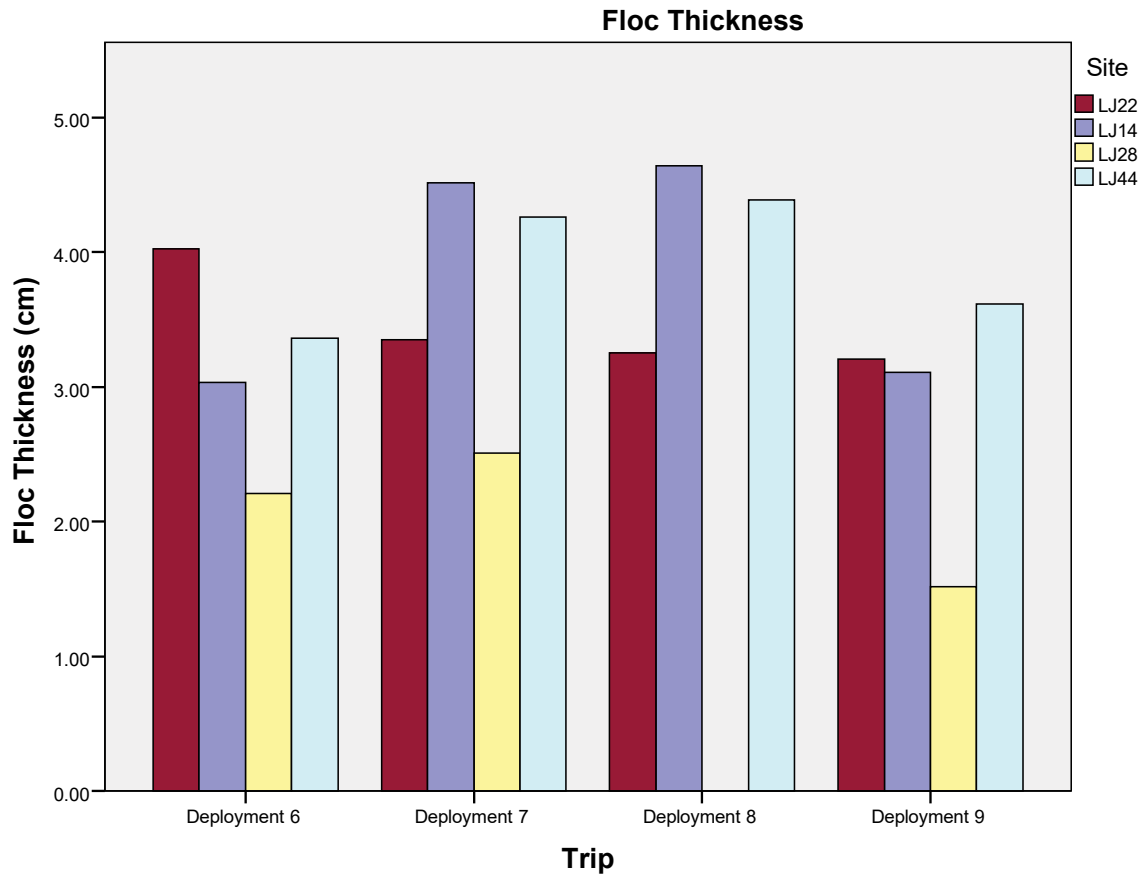


FIGURE A19. Floc thickness for deployments 6 to 9.

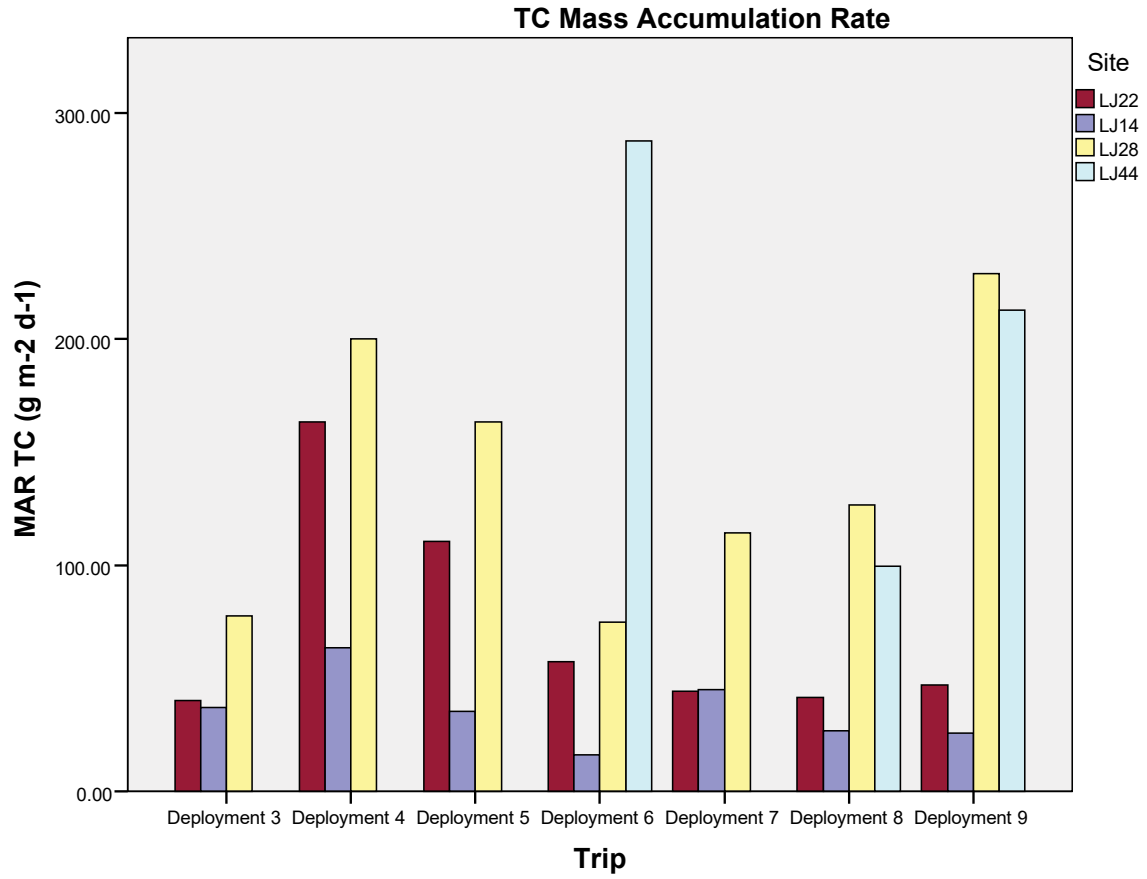


FIGURE A20. TC Mass accumulation rates for Deployments 3 to 9.

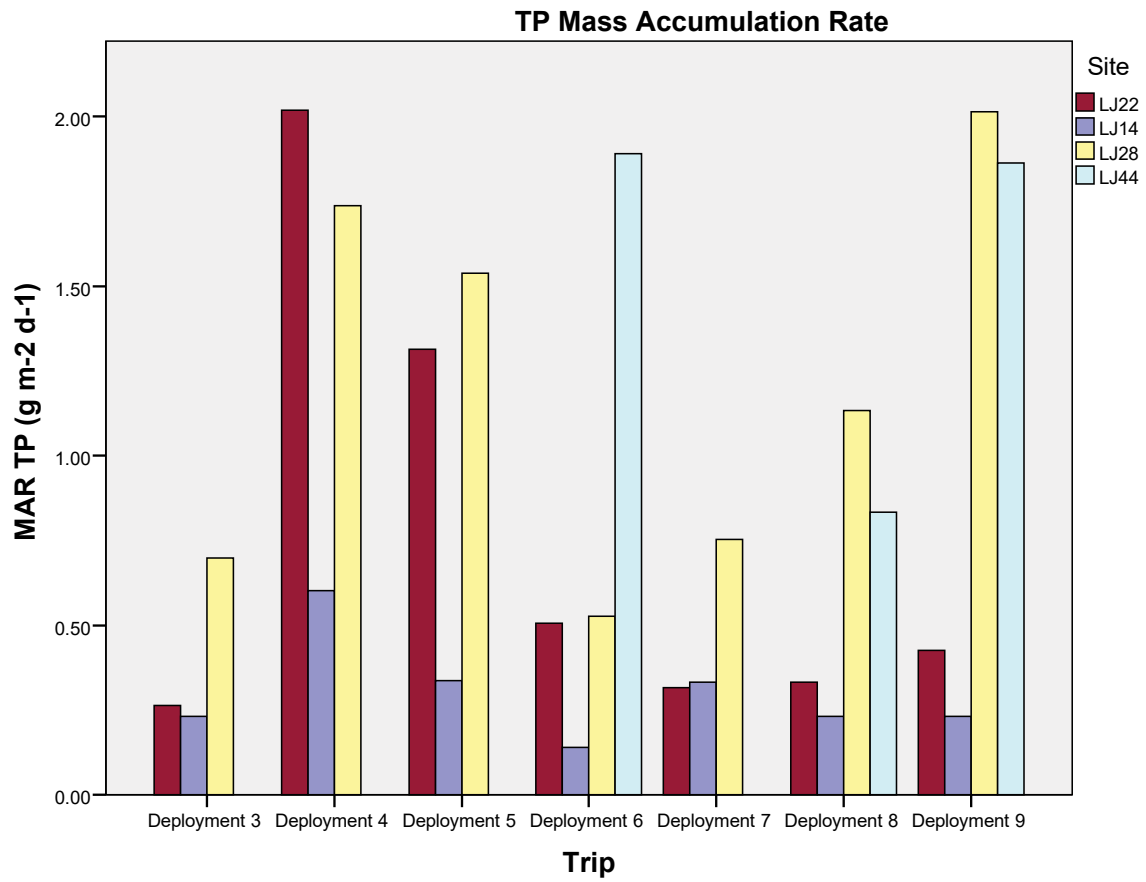


FIGURE A21. TP Mass accumulation rates for Deployments 3 to 9.

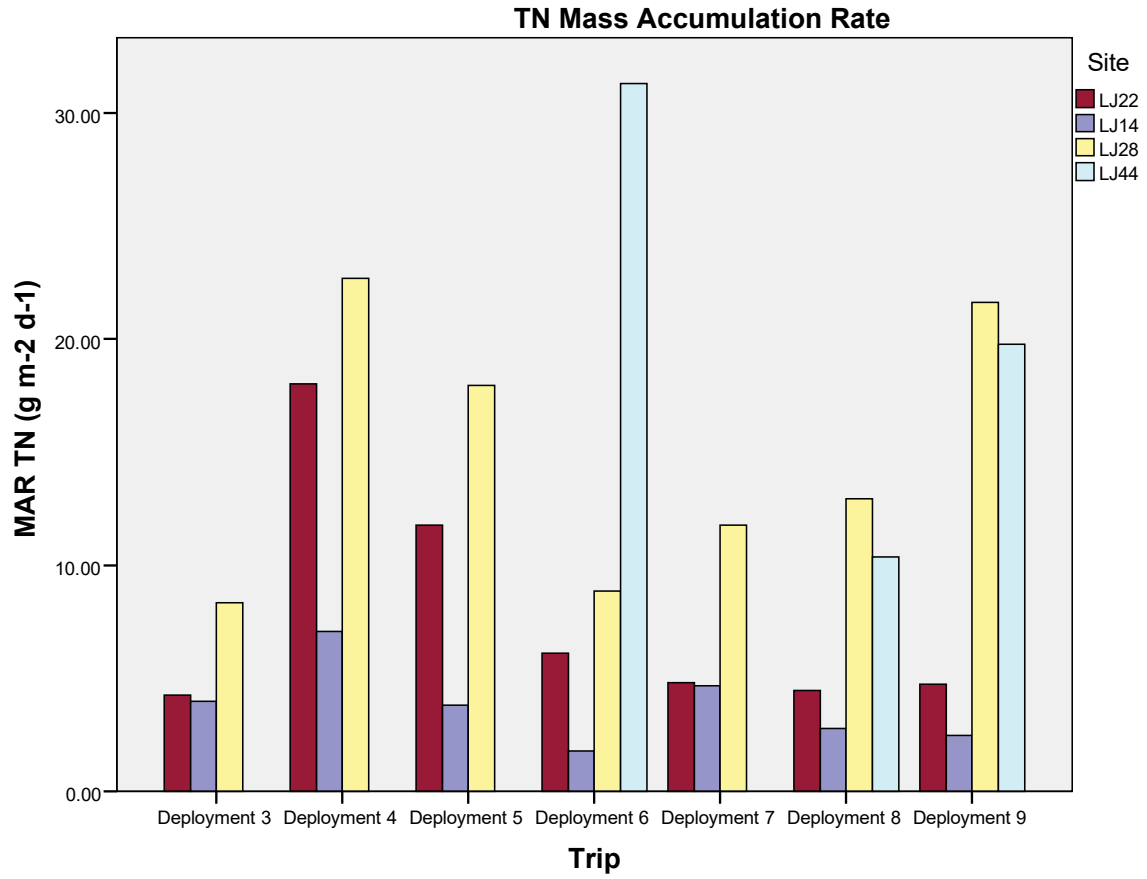


FIGURE A22. TN Mass accumulation rates for Deployments 3 to 9.

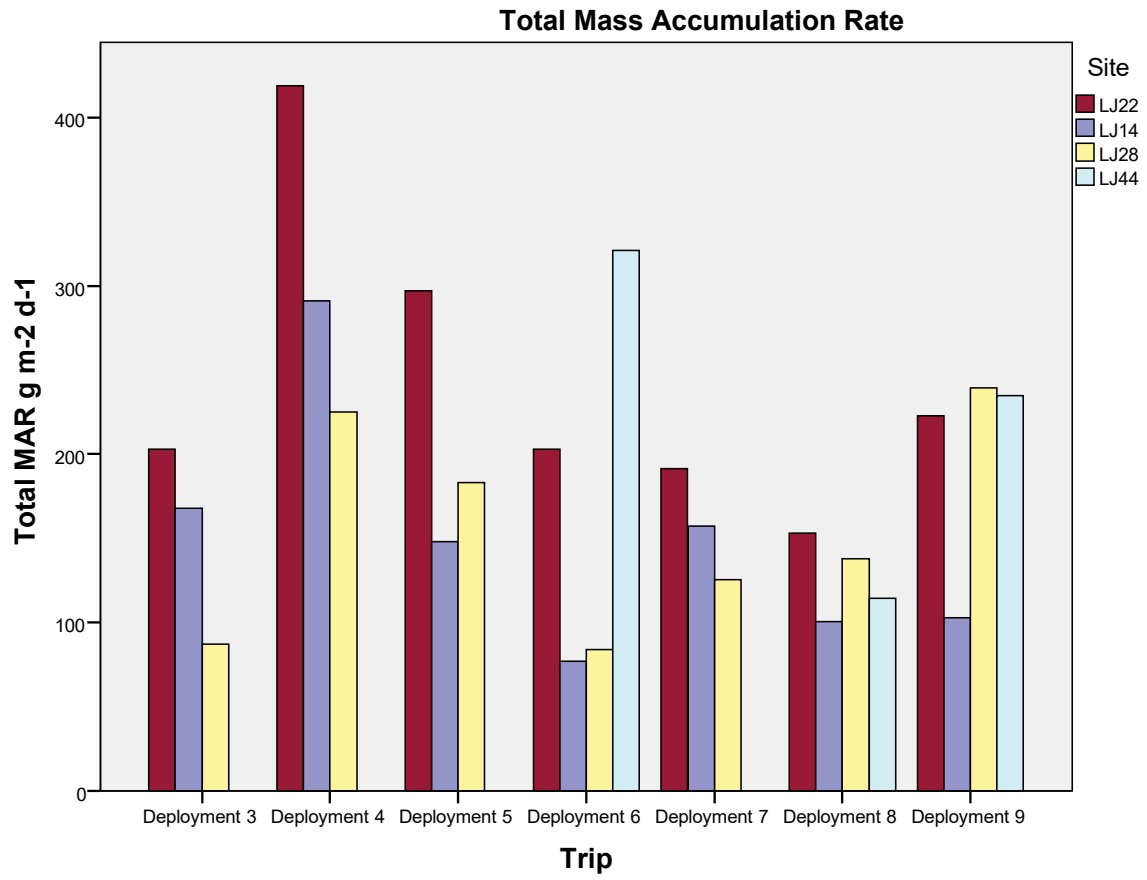


FIGURE A23. Total Mass accumulation rates for Deployments 3 to 9.

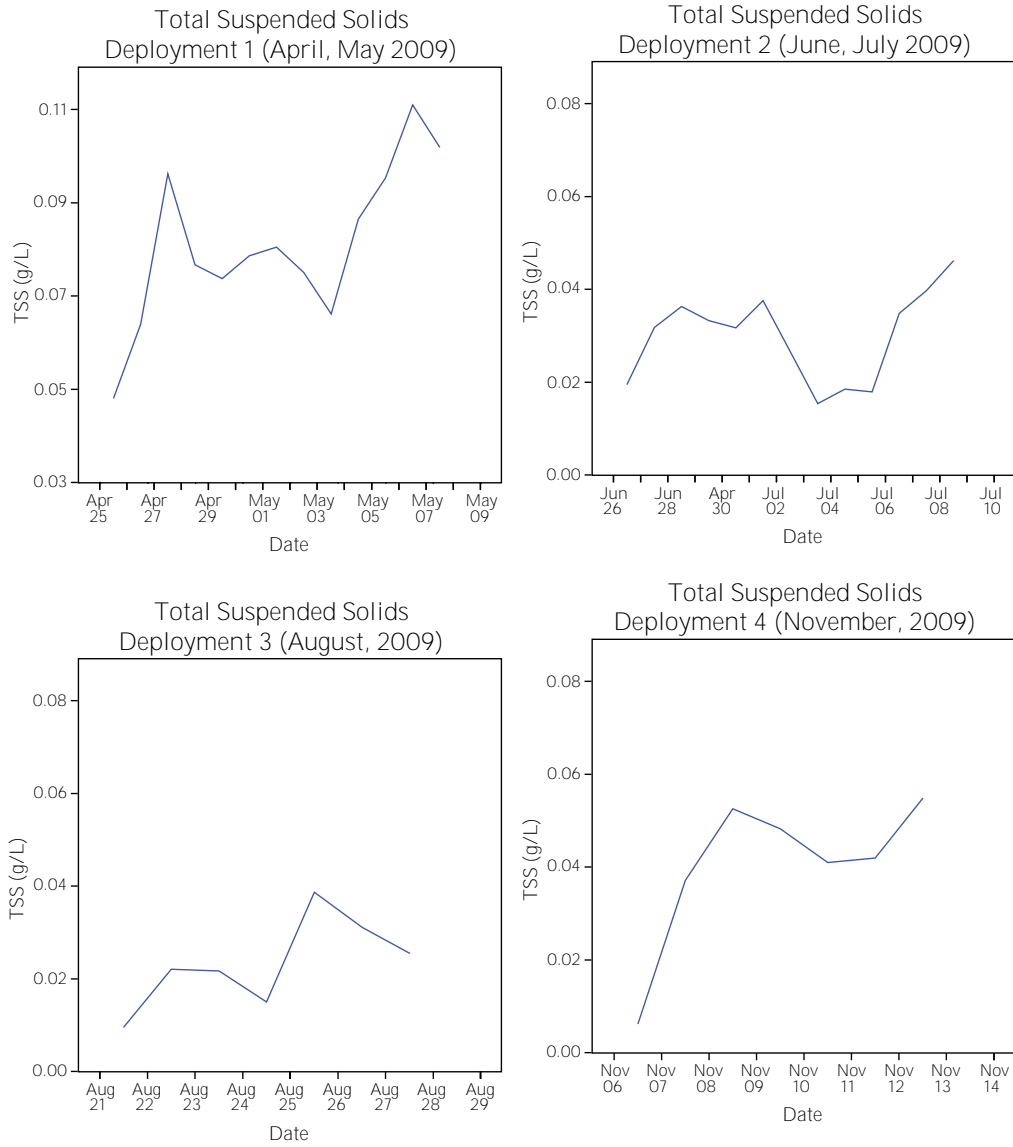


FIGURE A24. Total suspended solids for Deployments 1 to 4.

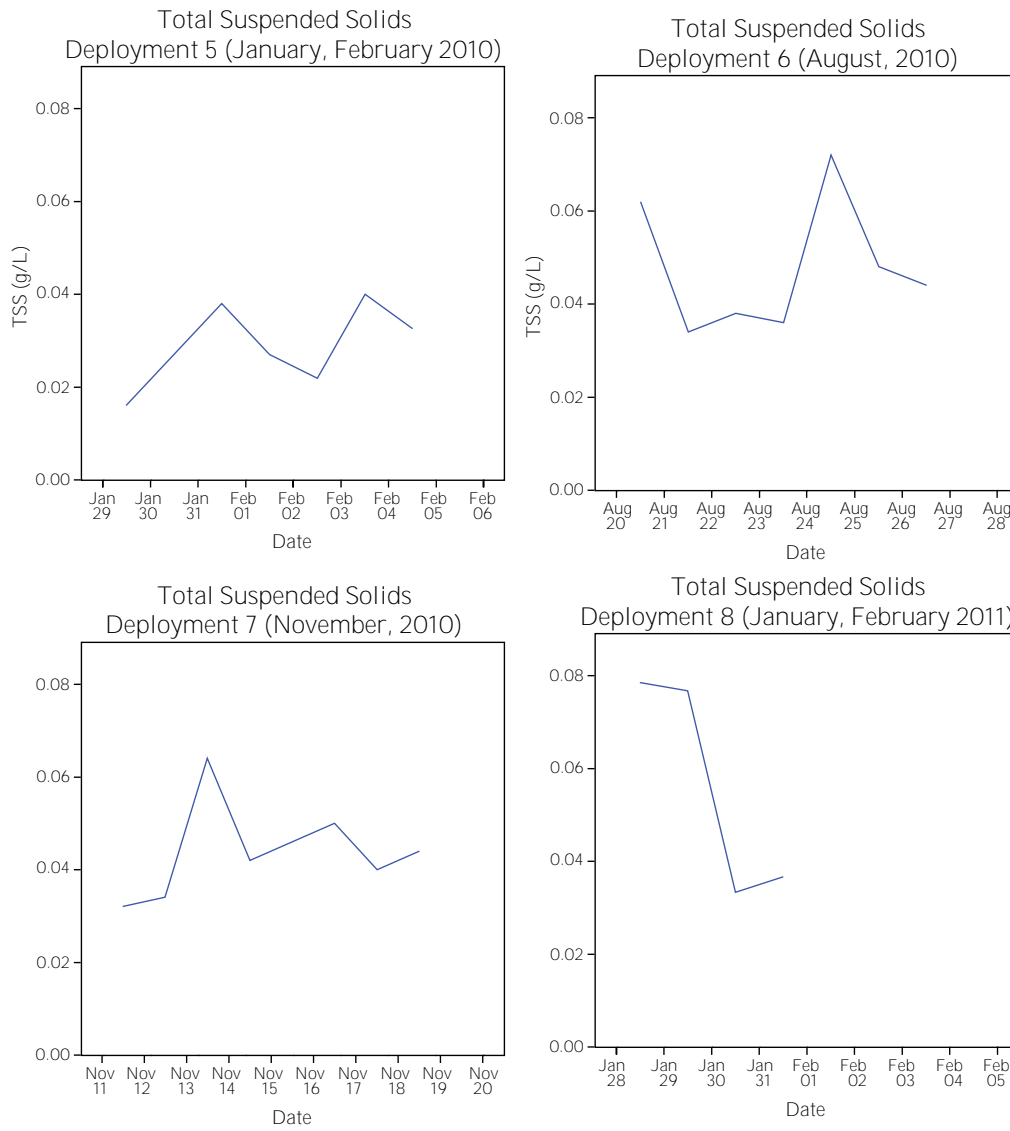


FIGURE A25. Total suspended solids for Deployments 5 to 6.

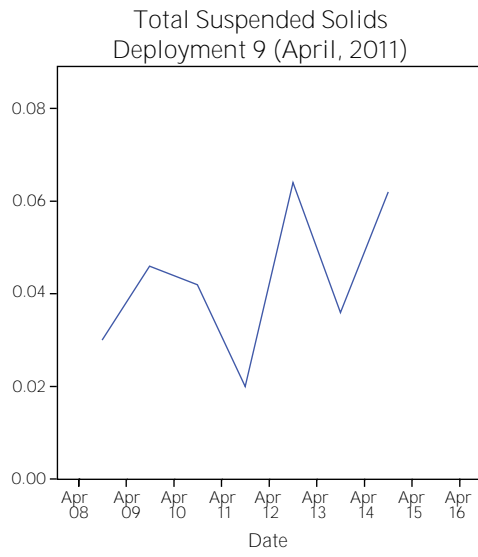


FIGURE A26. Total suspended solids for Deployment 9.

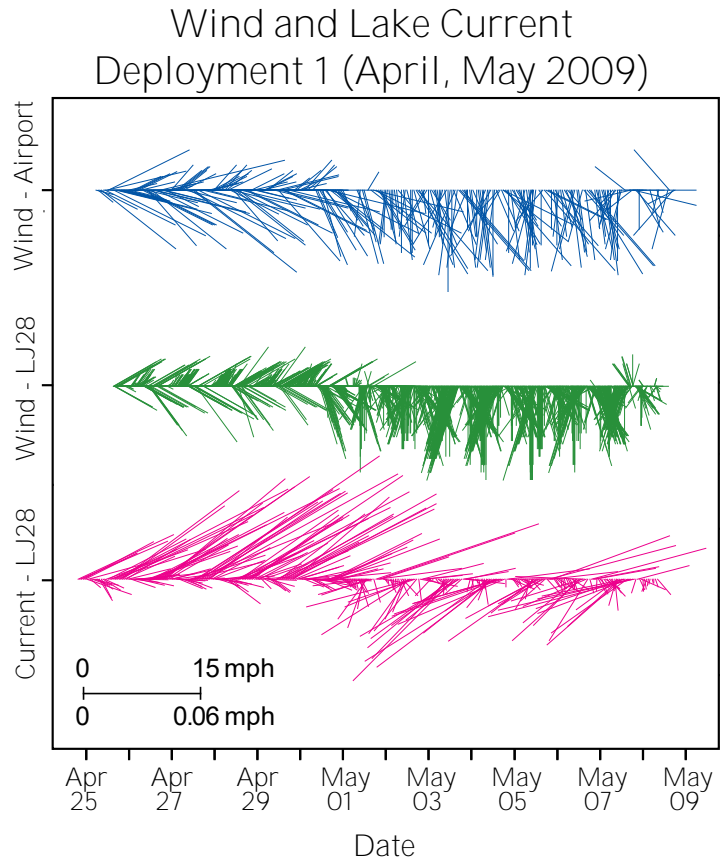


FIGURE A27. Stick plots of wind (LJ28 and Sanford Airport) and current for Deployment 1.

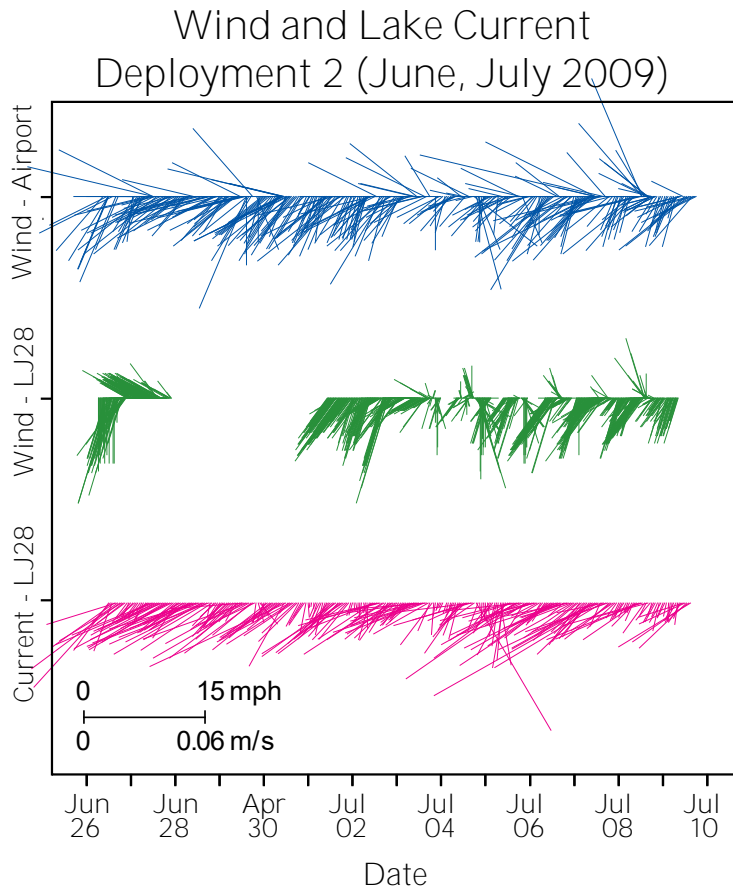


FIGURE A28. Stick plots of wind (LJ28 and Sanford Airport) and current for Deployment 2.

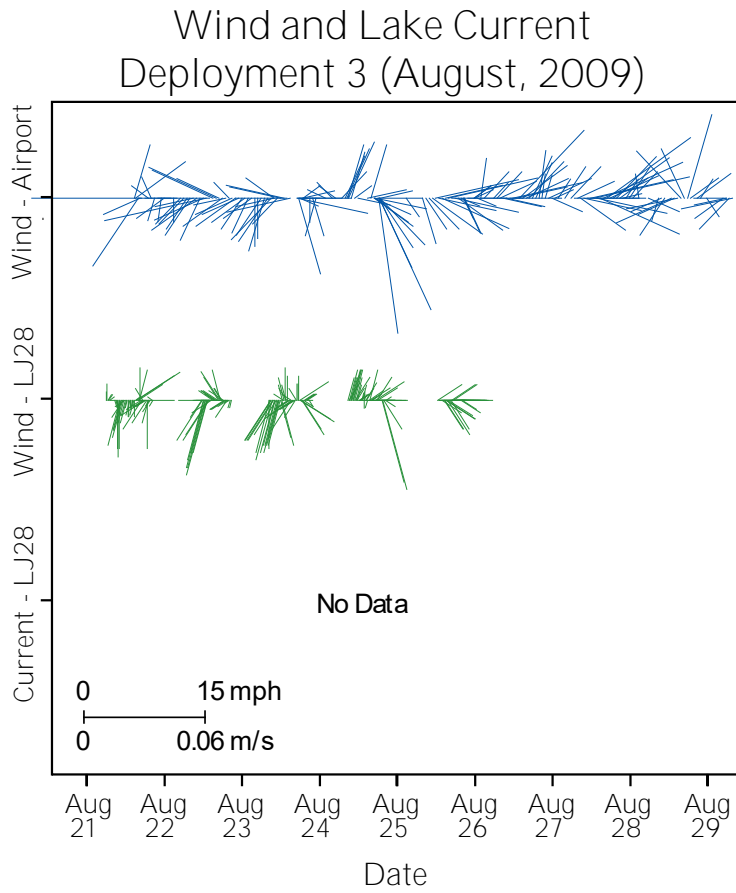


FIGURE A29. Stick plots of wind (LJ28 and Sanford Airport) for Deployment 3.

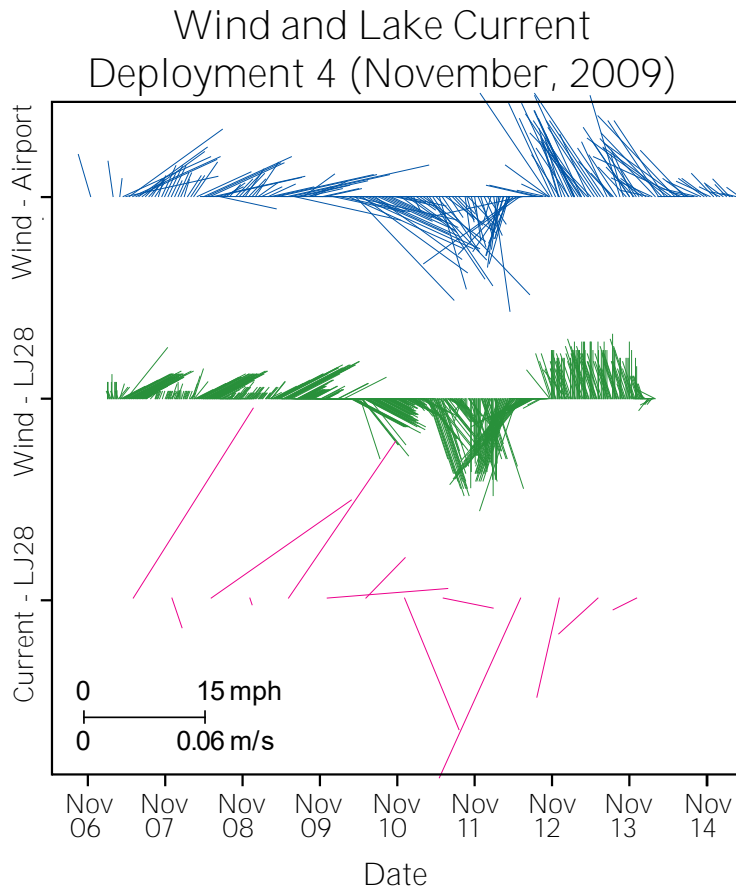


FIGURE A30. Stick plots for wind (LJ28 and Sanford Airport) and current for Deployment 4.

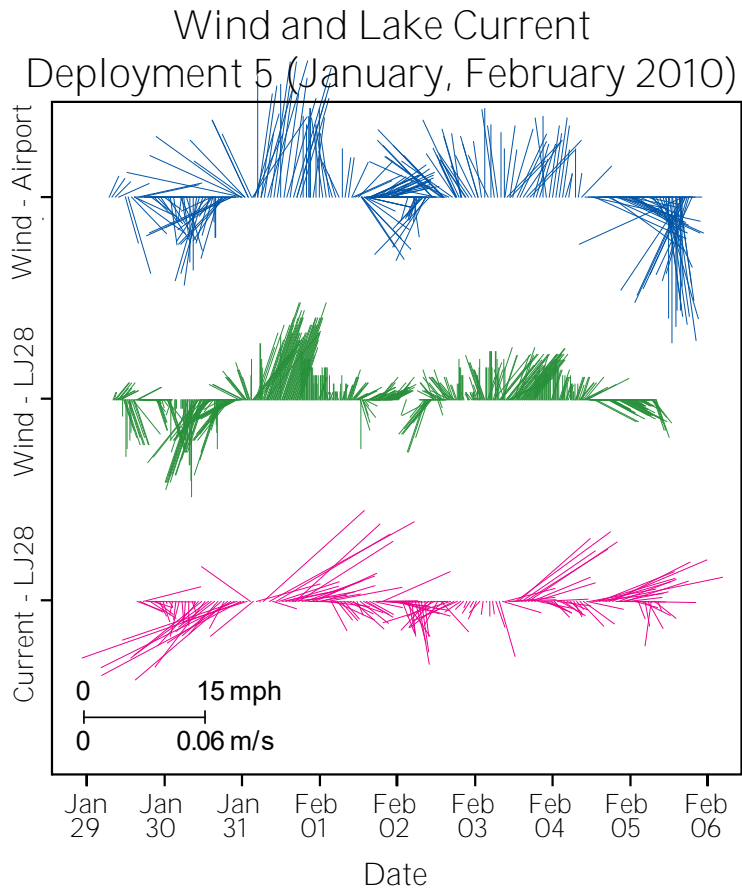


FIGURE A31. Stick plots of wind (LJ28 and Sanford Airport) and current for Deployment 5.

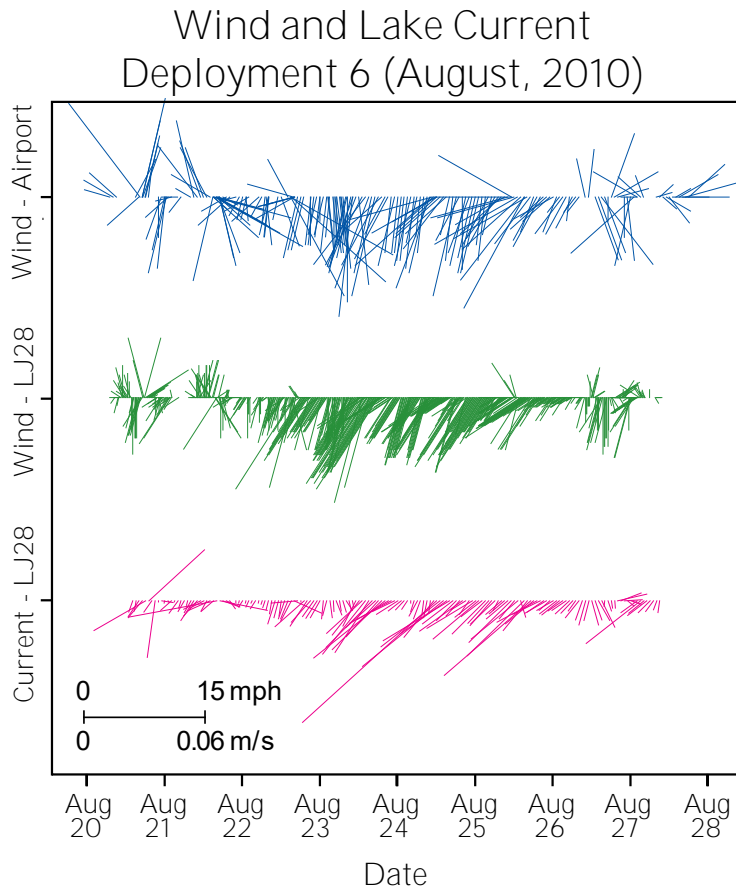


FIGURE A32. Stick plots of wind (LJ28 and Sanford Airport) and current for Deployment 6.

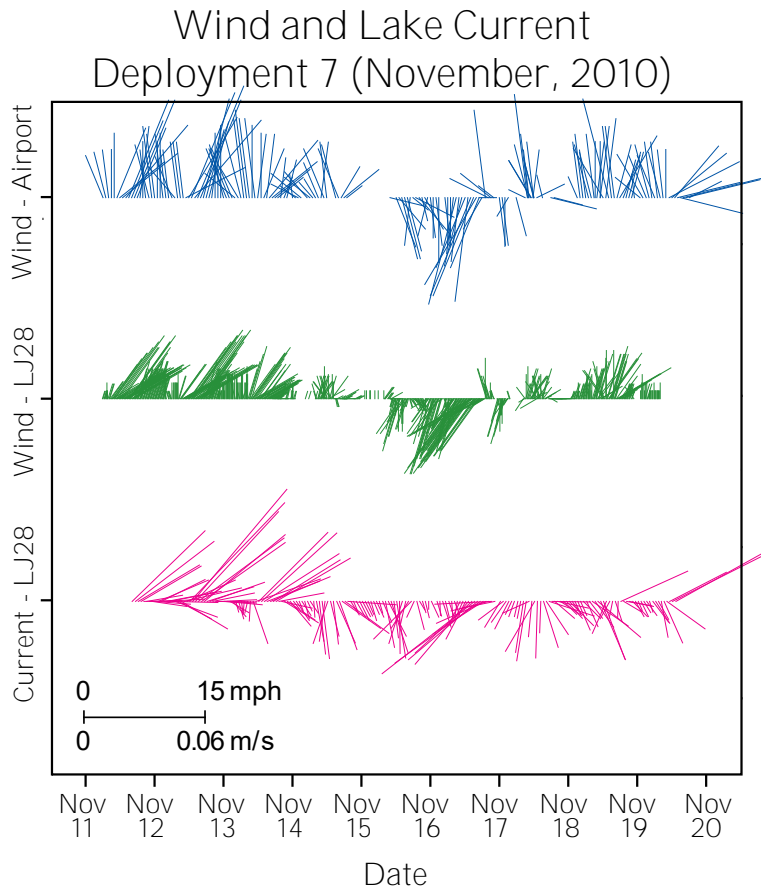


FIGURE A33. Stick plots of wind (LJ28 and Sanford Airport) and current for Deployment 7.

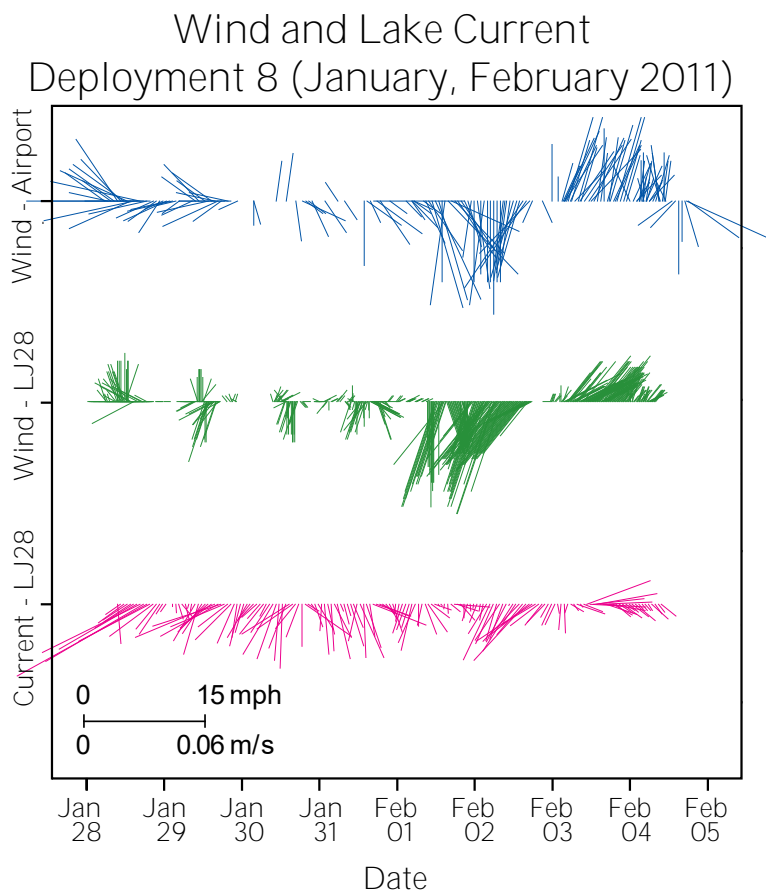


FIGURE A34. Stick plots of wind (LJ28 and Sanford Airport) and current for Deployment 8.

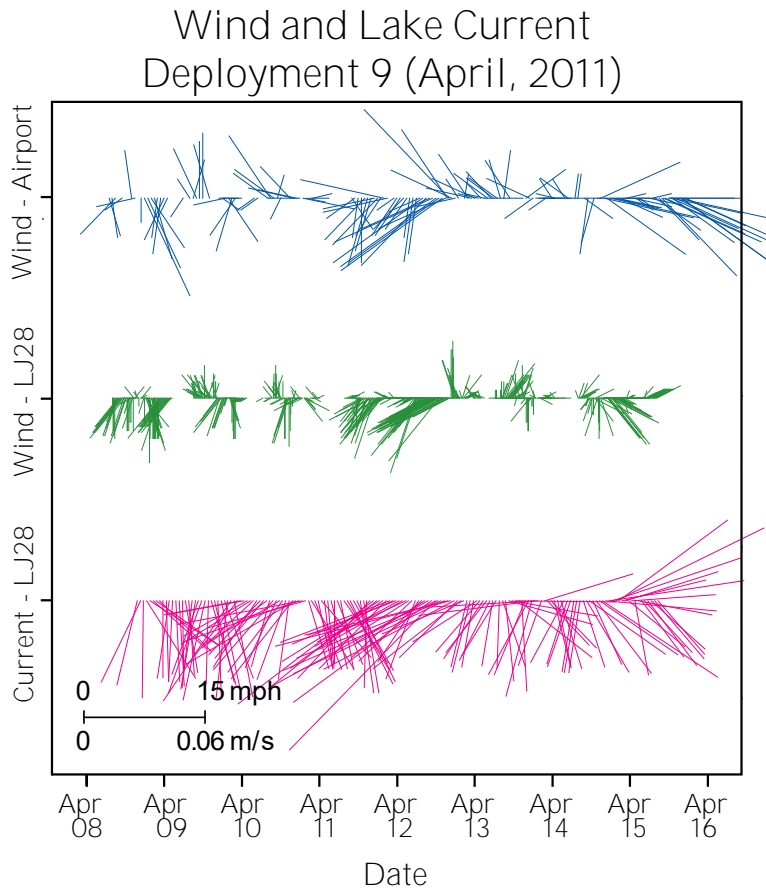


FIGURE A35. Stick plots of wind (LJ28 and Sanford Airport) and current for Deployment 9.

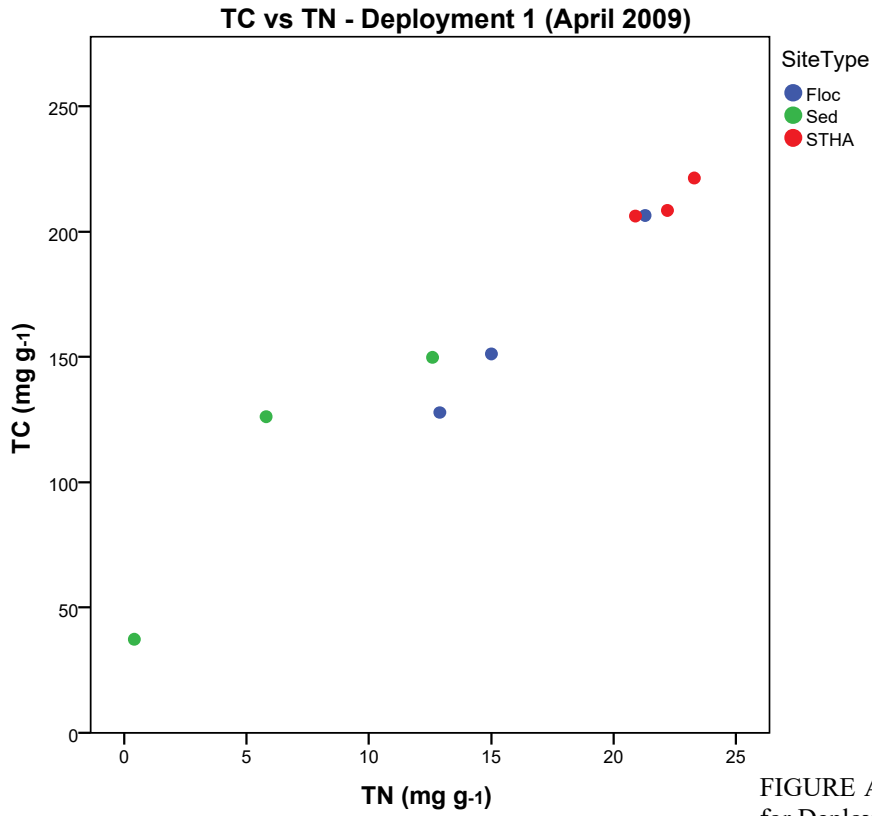
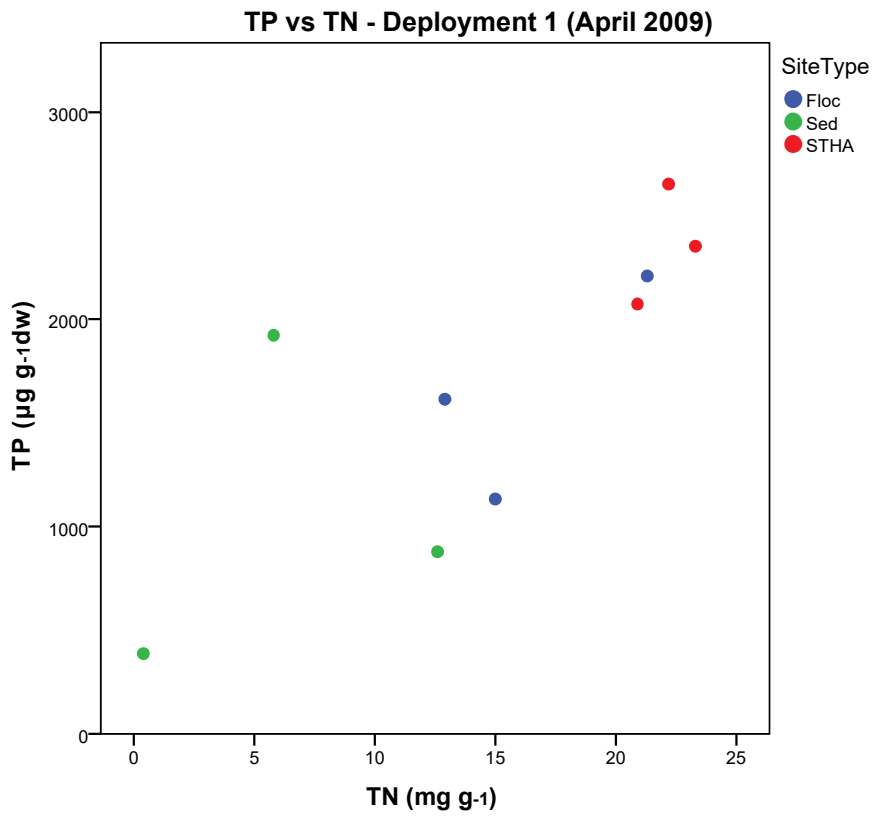


FIGURE A36. TC vs. TN vs TP for Deployment 1.



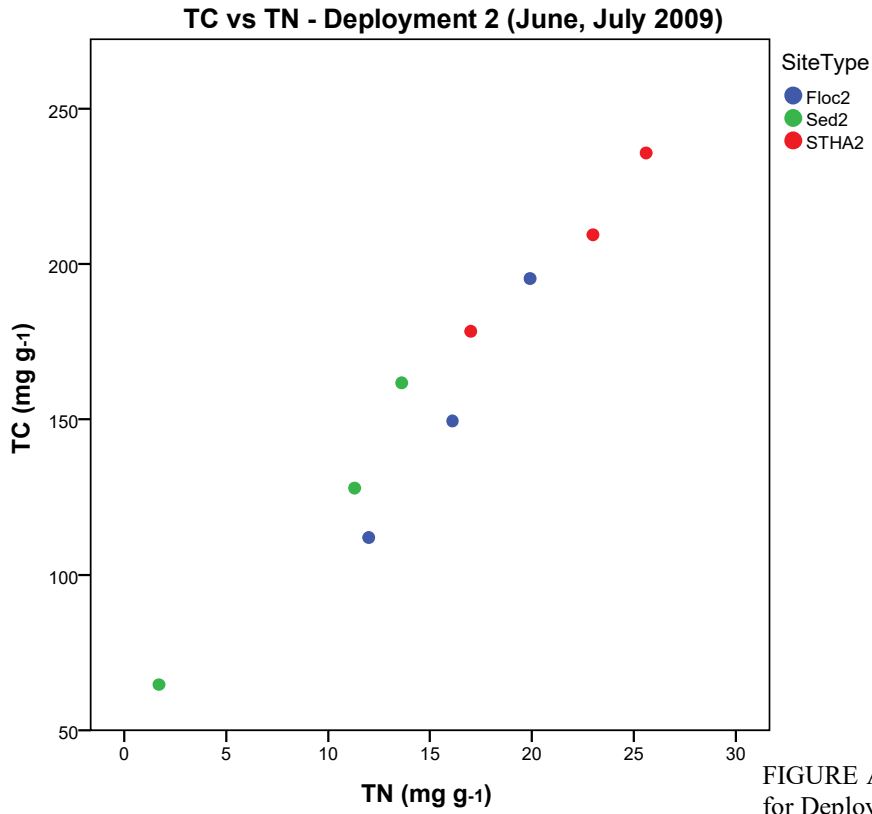
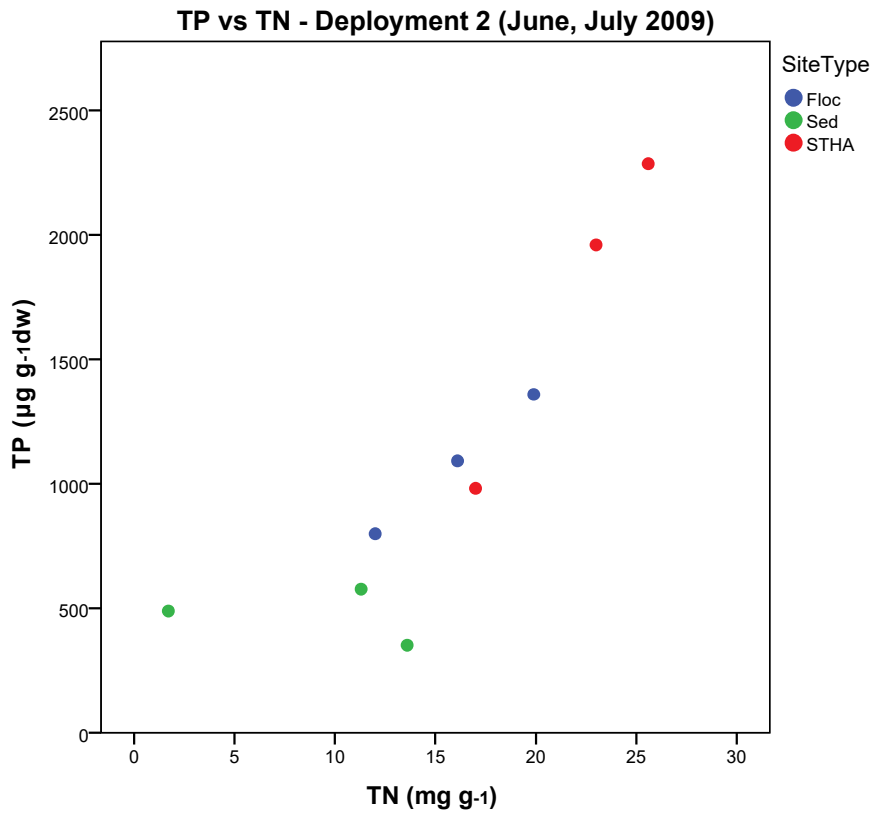


FIGURE A37. TC vs. TN vs TP for Deployment 2.



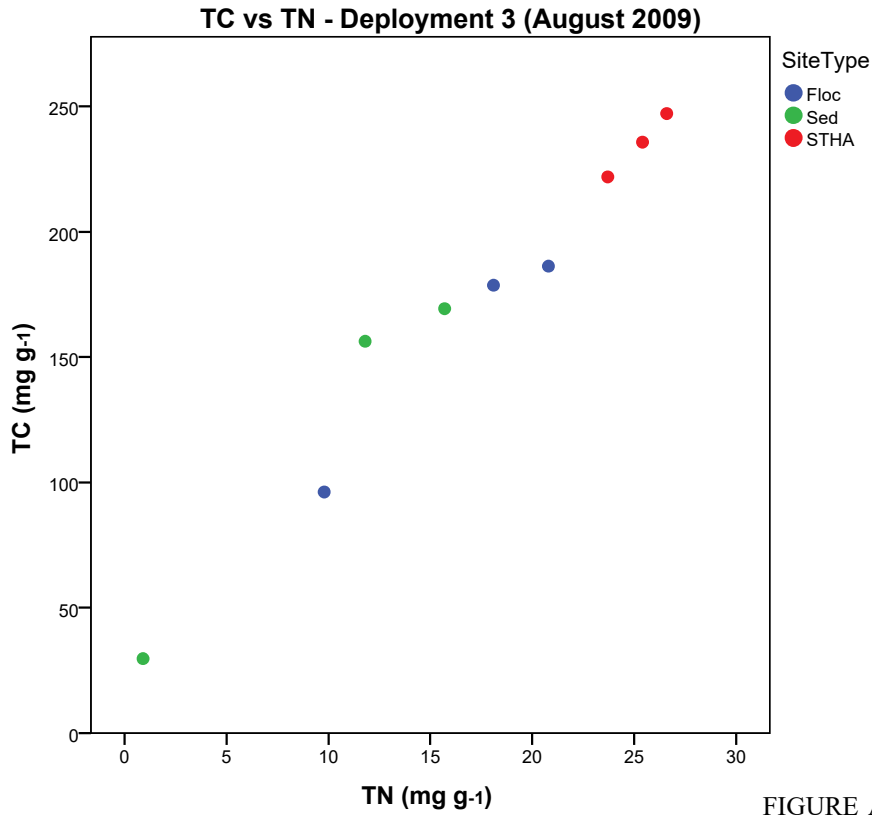
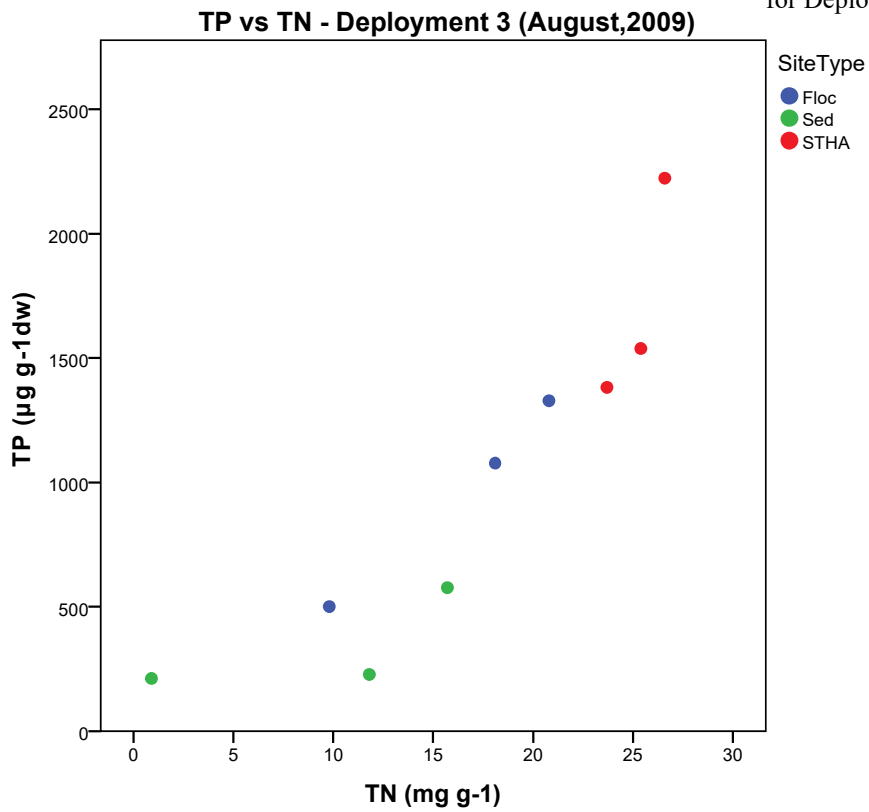


FIGURE A38 TC vs. TN vs TP for Deployment 3.



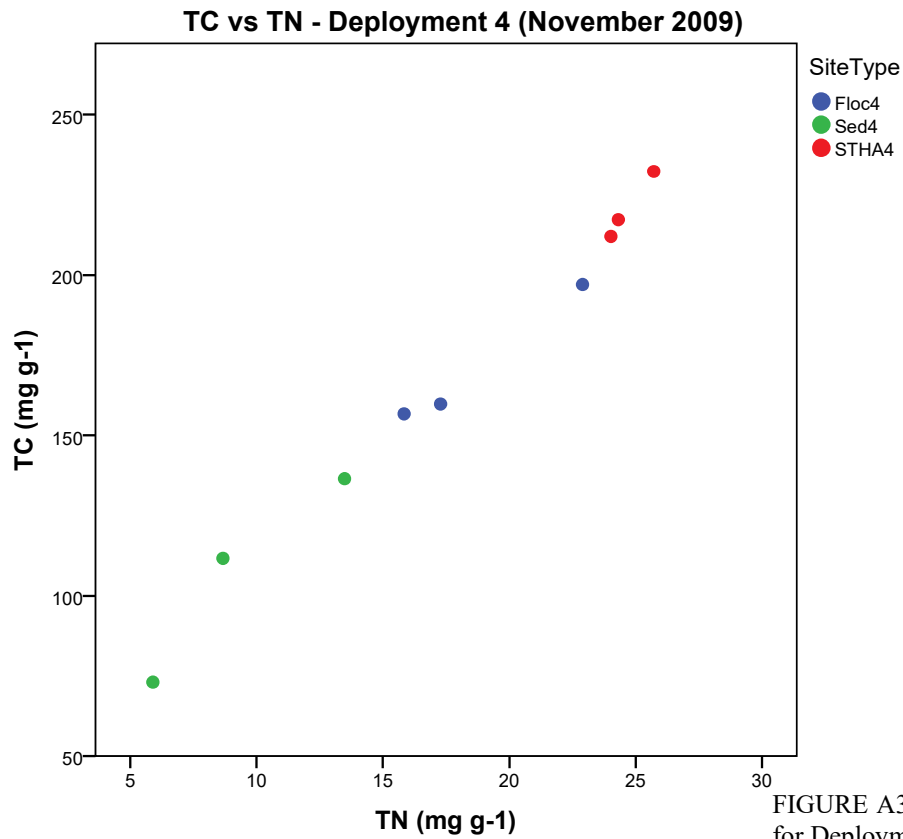
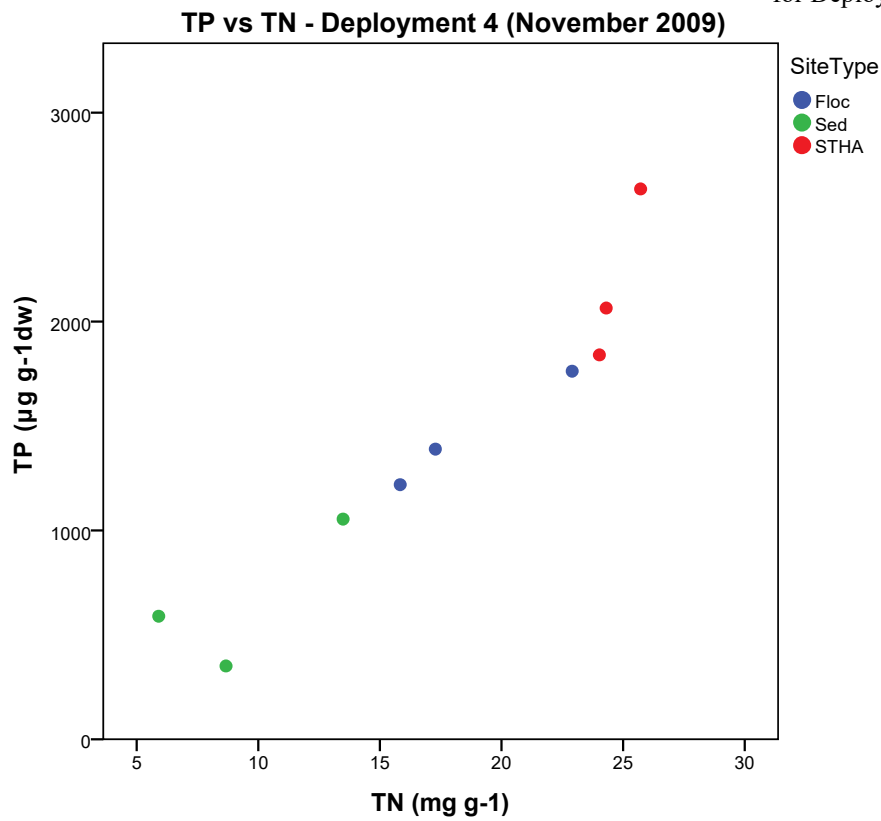


FIGURE A39. TC vs. TN vs TP for Deployment 4.



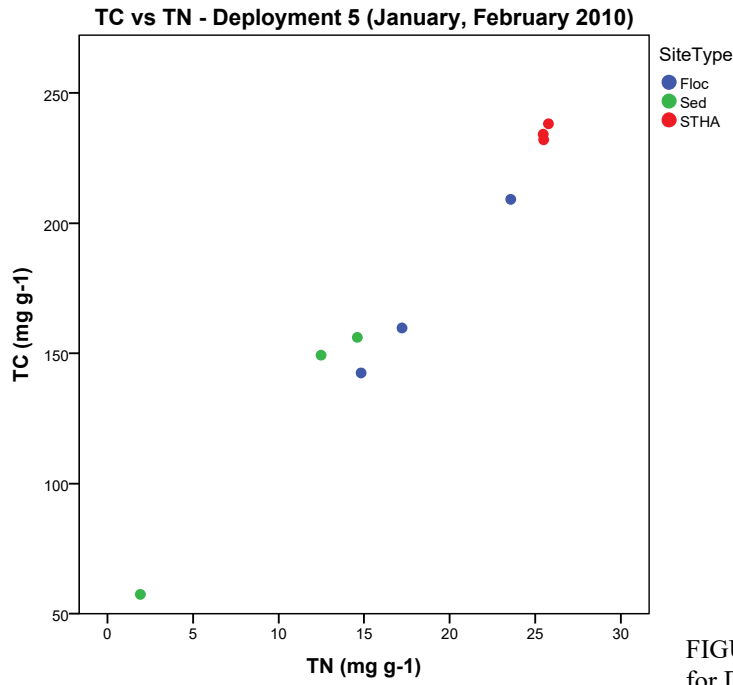
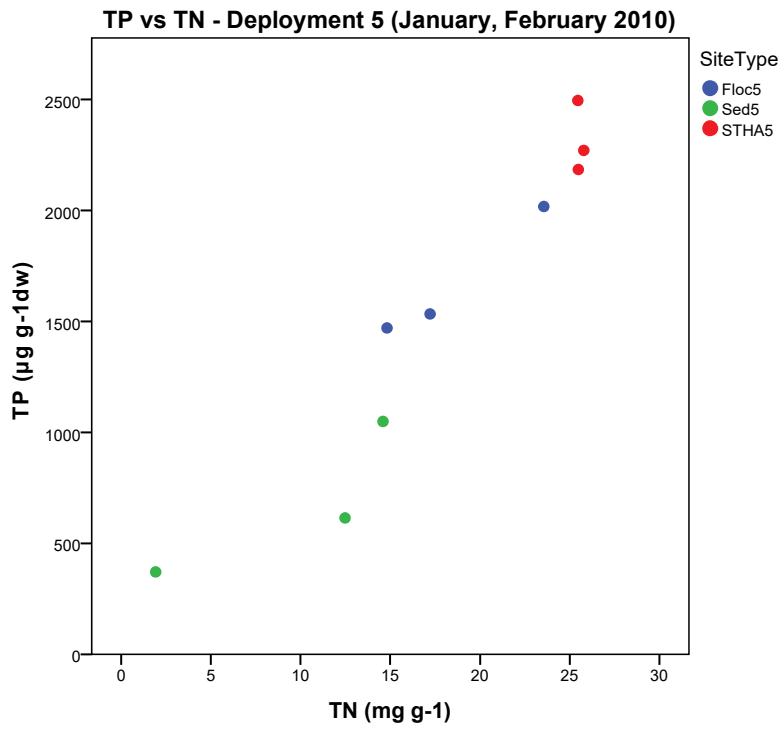


FIGURE A40. TC vs. TN vs TP for Deployment 5.



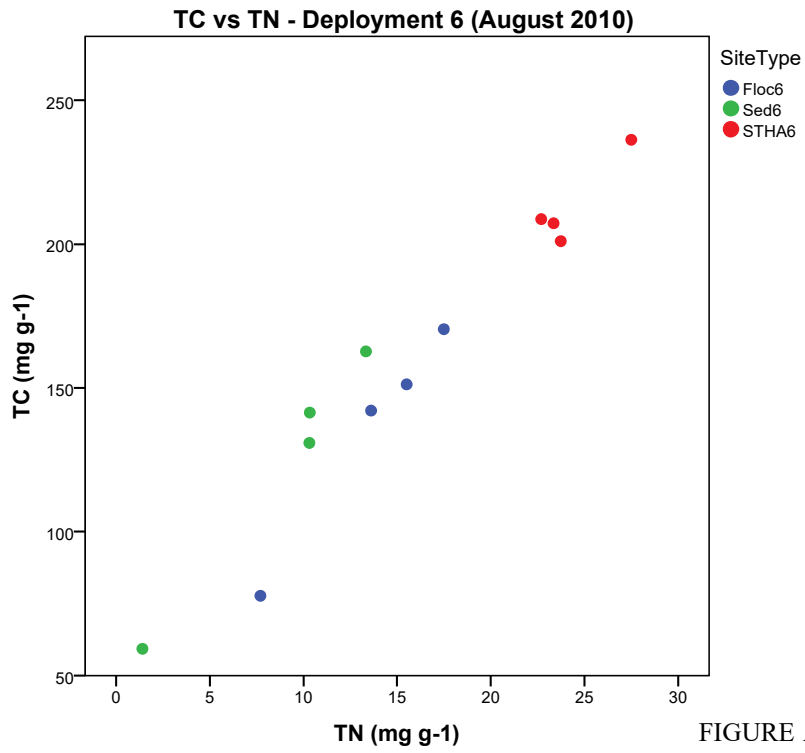
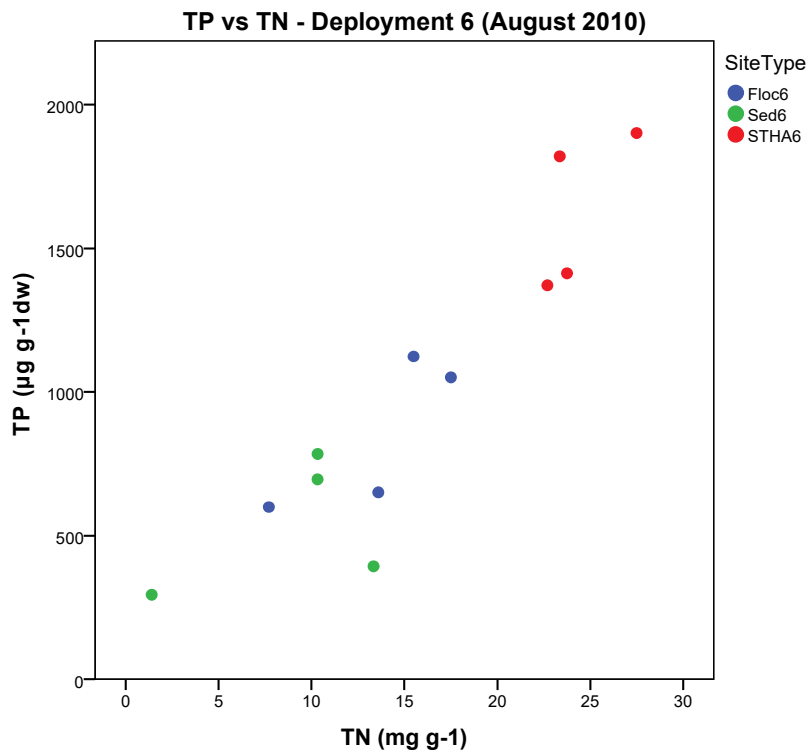


FIGURE A41. TC vs. TN vs TP for Deployment 6.



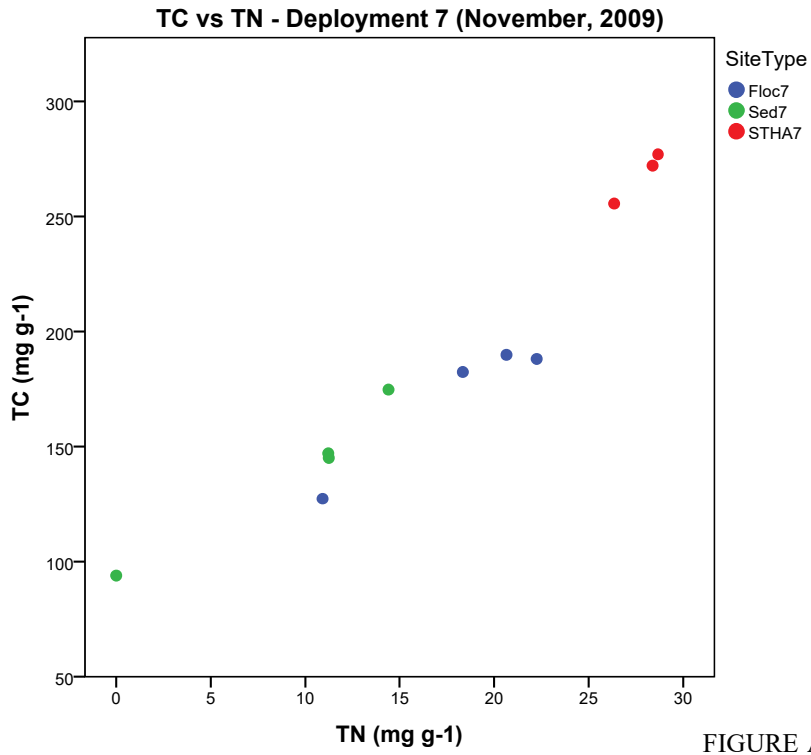
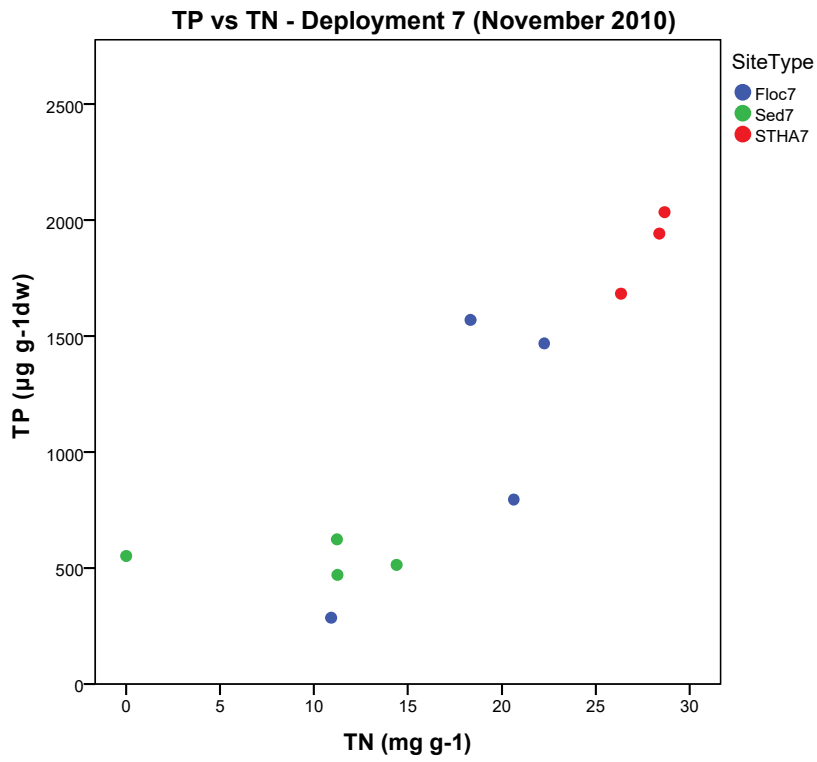


FIGURE A42. TC vs. TN vs TP for Deployment 7.



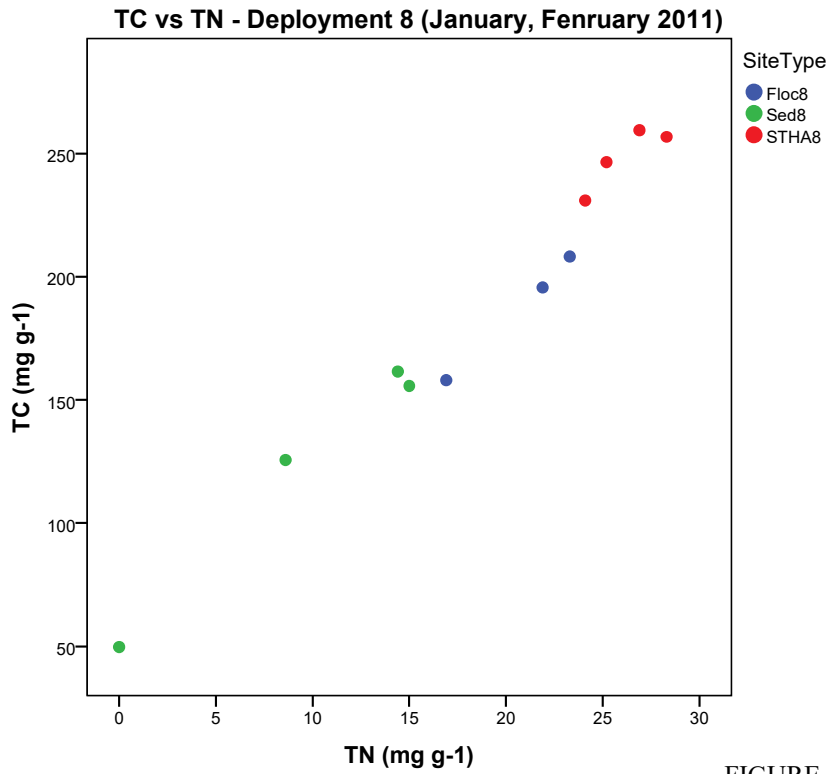
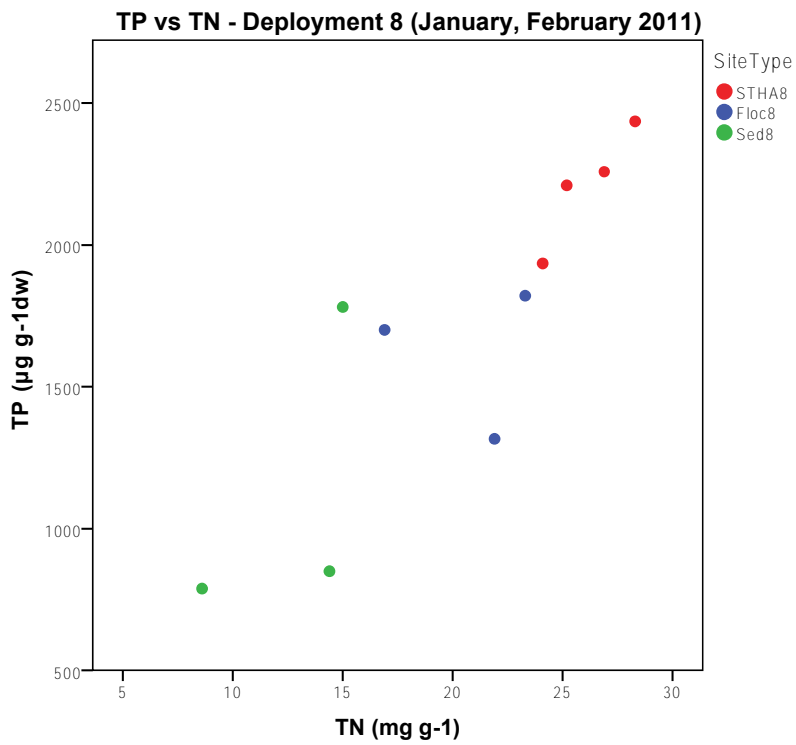


FIGURE A43. TC vs. TN vs TP for Deployment 8.



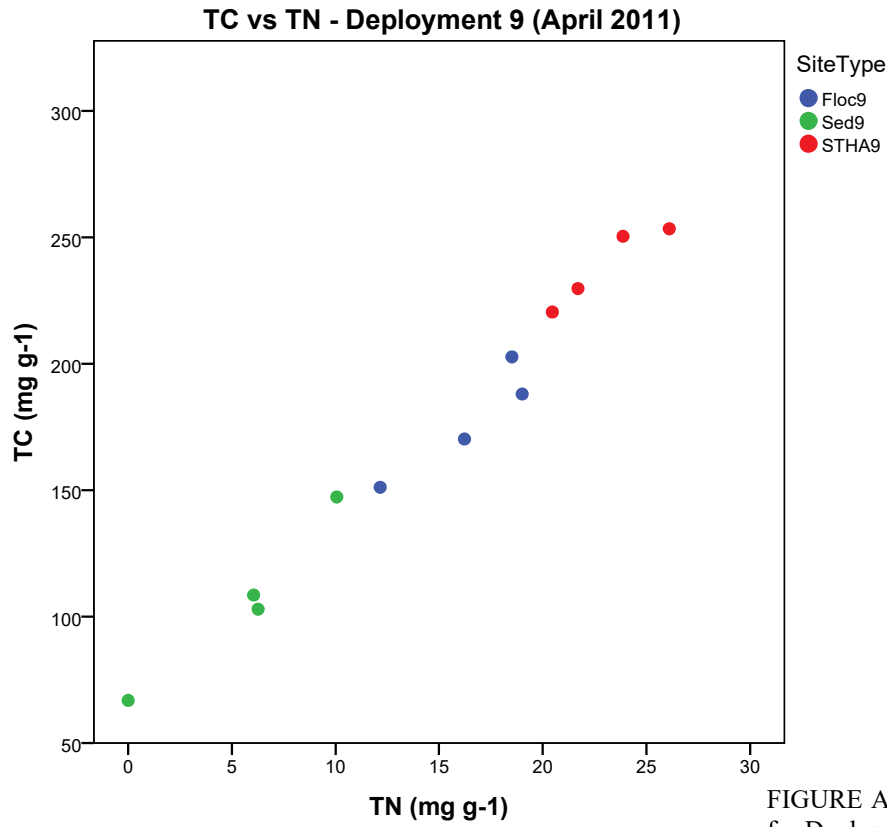
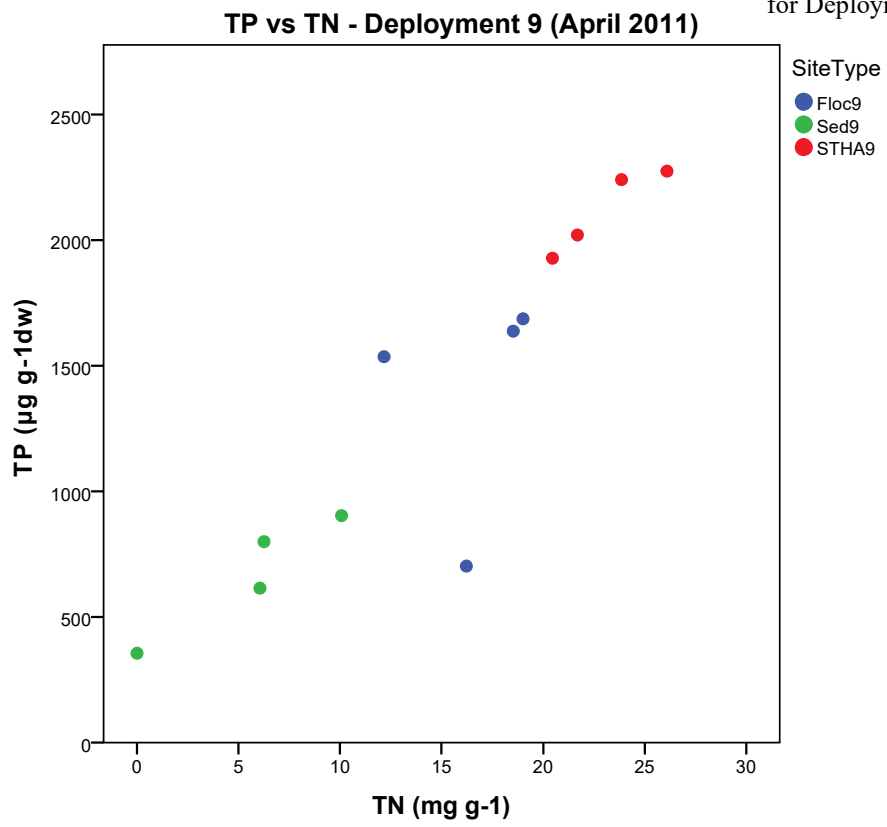


FIGURE A44. TC vs. TN vs TP for Deployment 9.



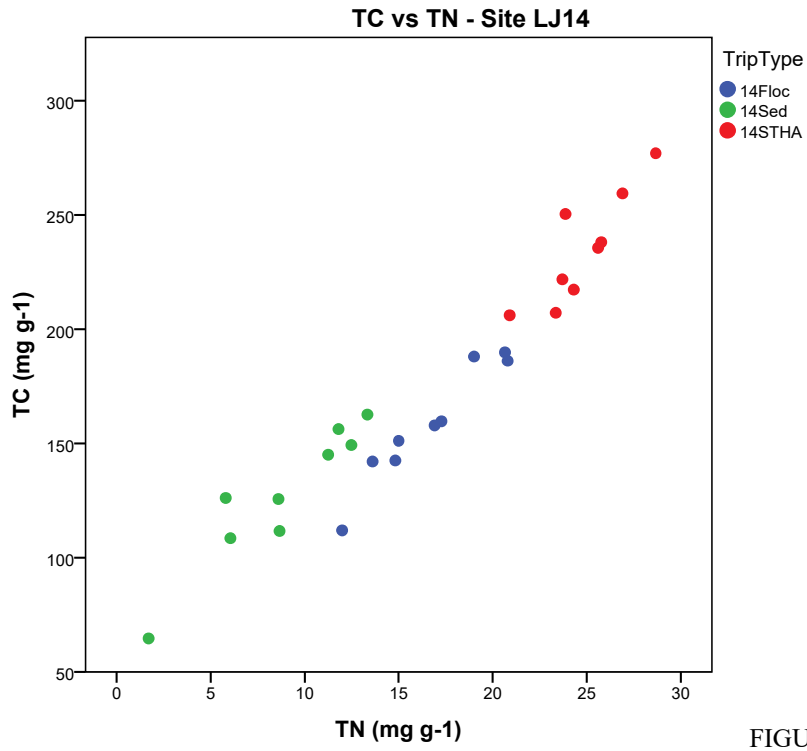
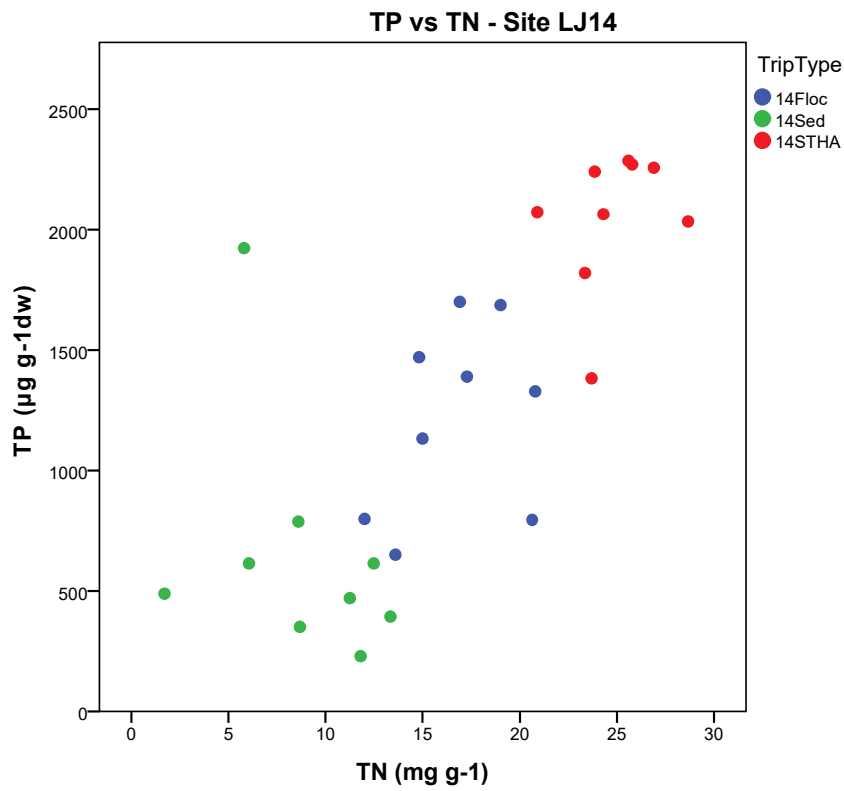


FIGURE A45. TC vs. TN vs TP for site LJ14.



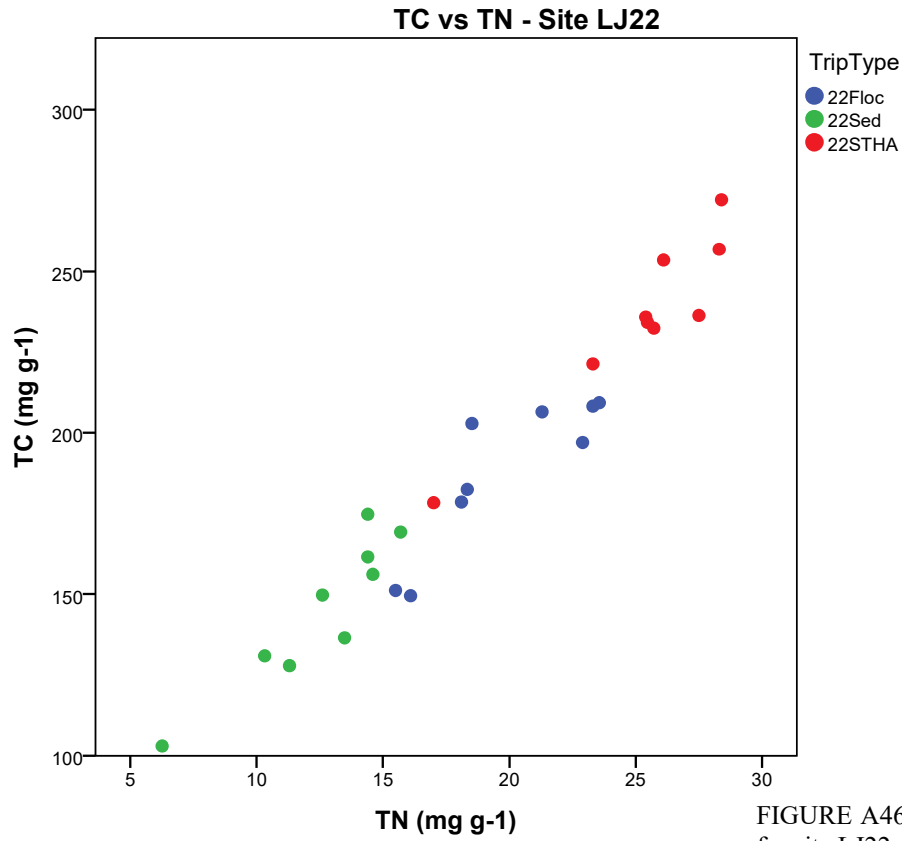
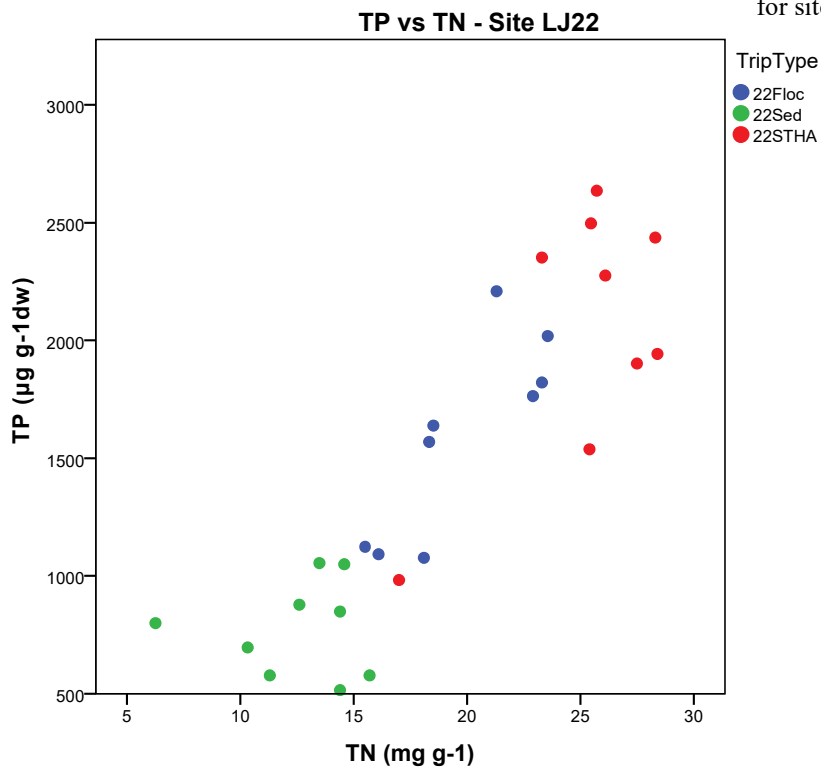


FIGURE A46. TC vs. TN vs TP for site LJ22.



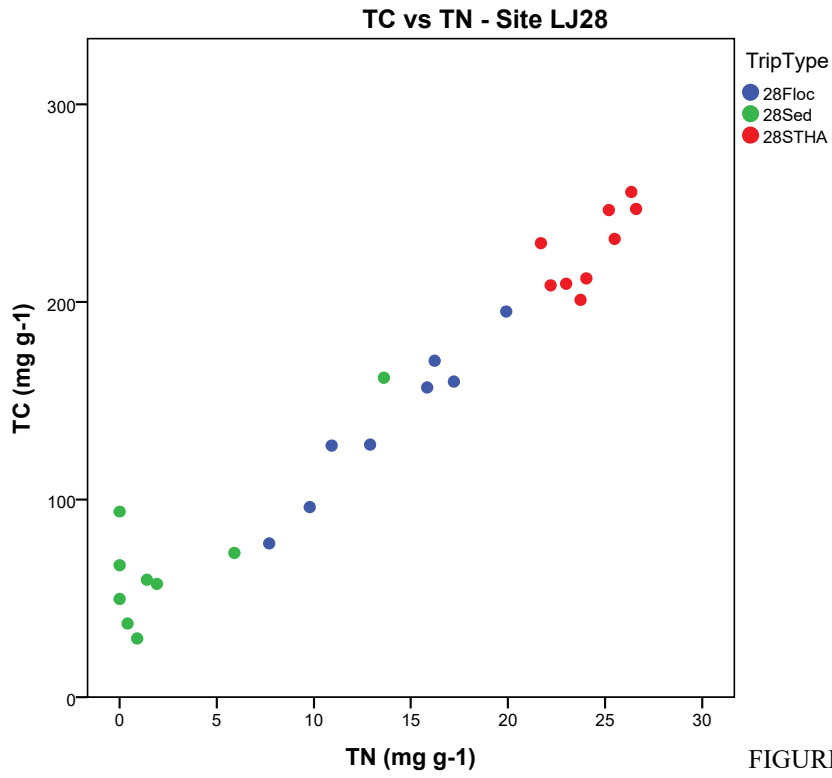
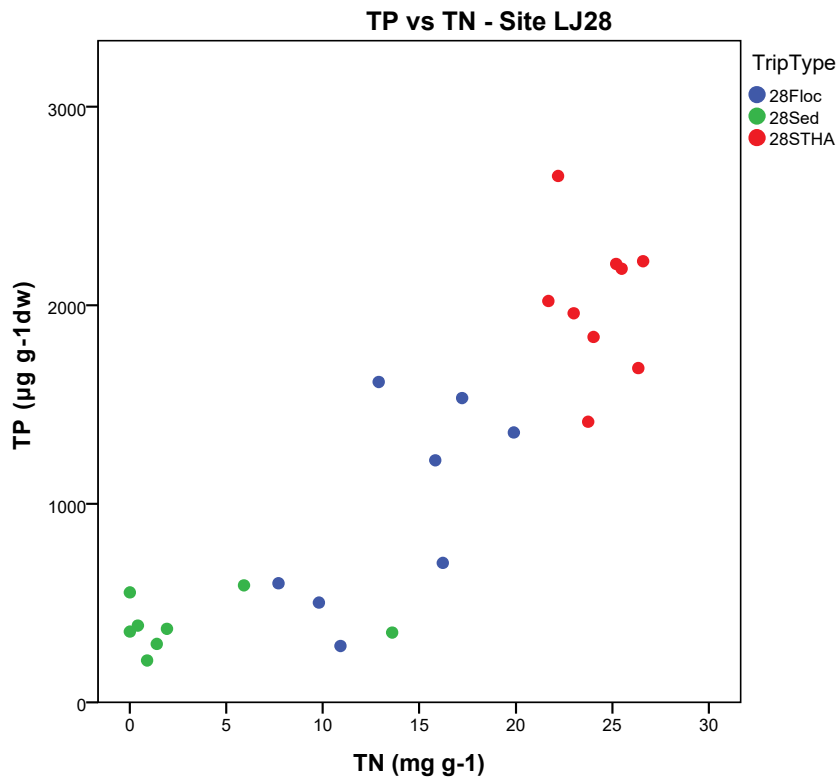


FIGURE A47. TC vs. TN vs TP for site LJ28.



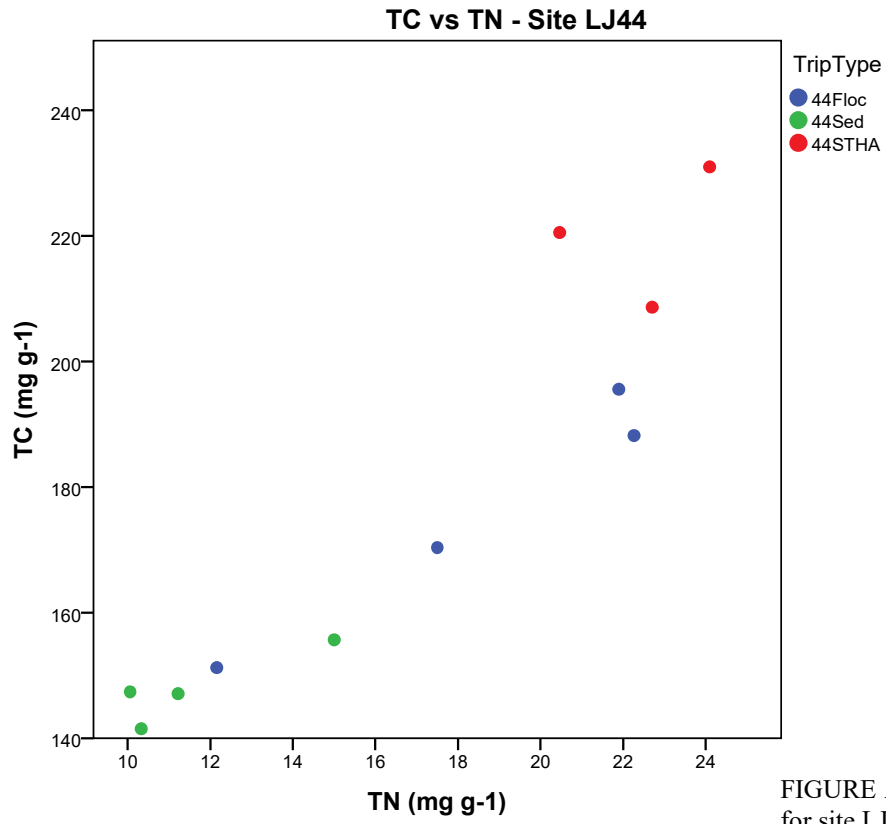
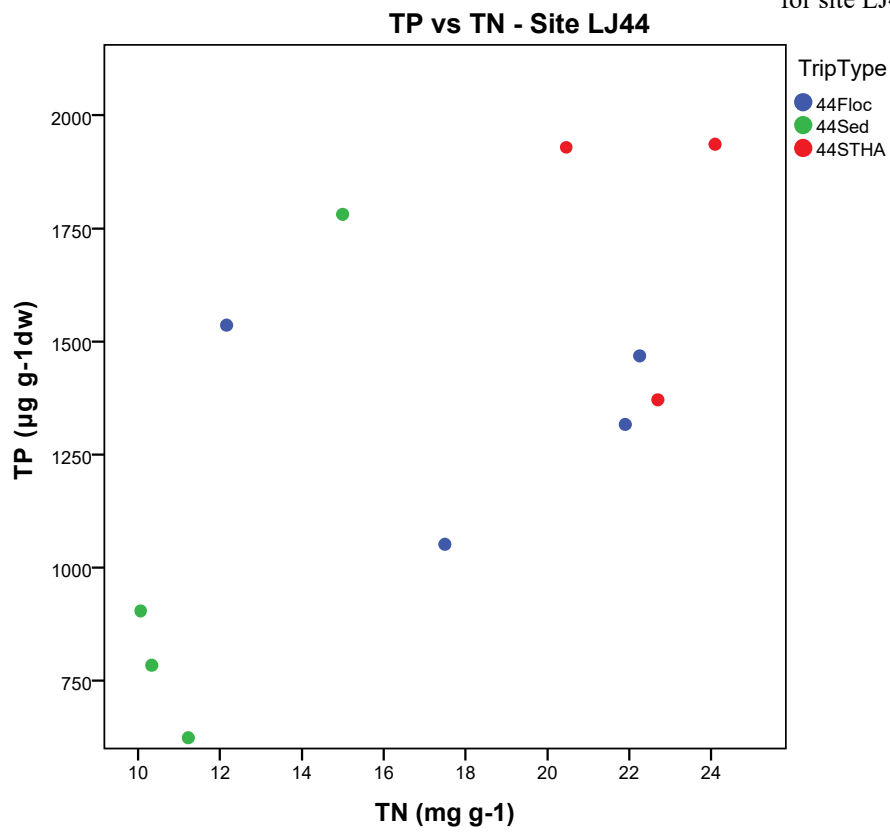


FIGURE A48. TC vs. TN vs TP for site LJ44.



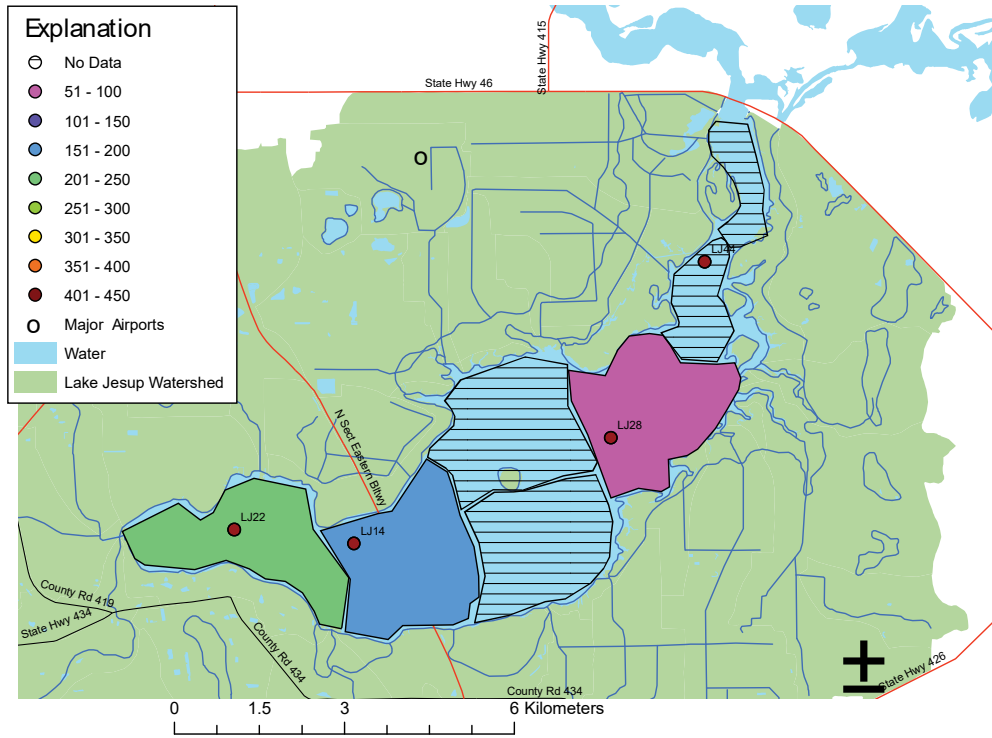


FIGURE A49. Spatial variations of MAR for Deployment 3.

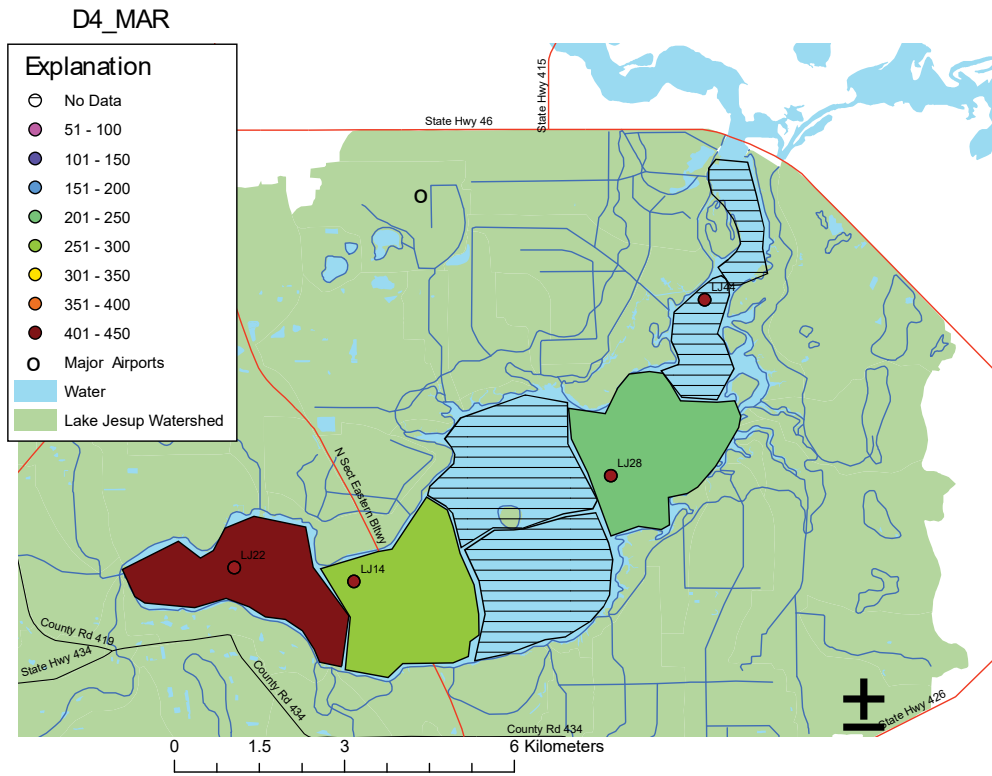


FIGURE A50. Spatial variations of MAR for Deployment 4.

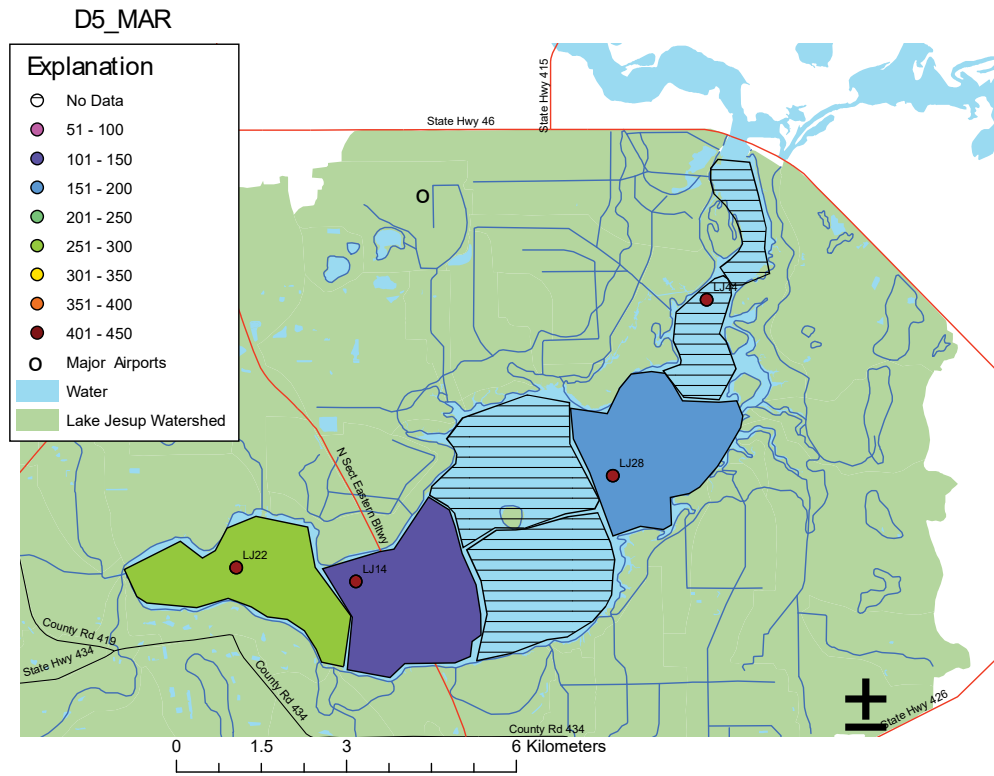


FIGURE A51. Spatial variations of MAR for Deployment 5.

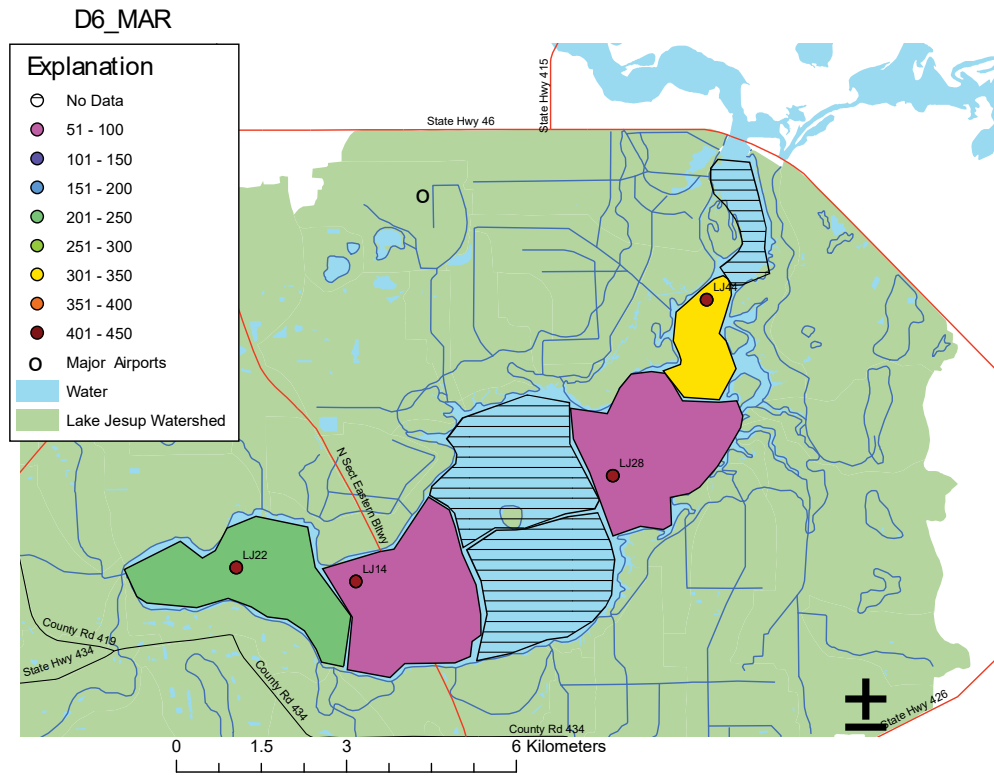


FIGURE A52. Spatial variations of MAR for Deployment 6.

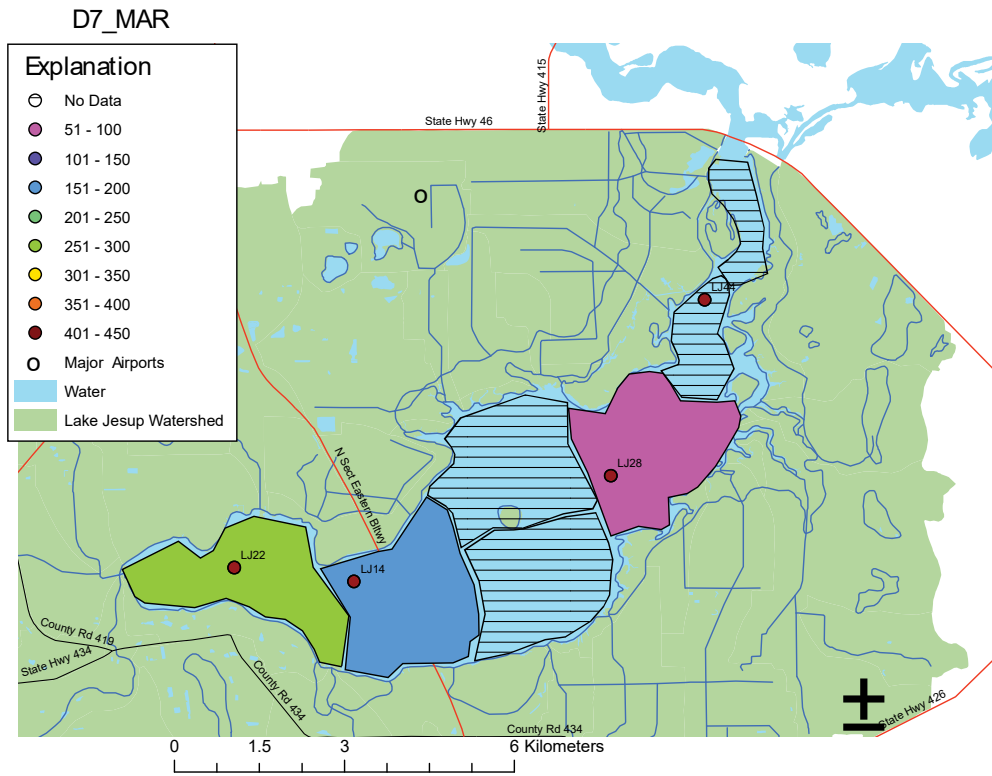


FIGURE A52. Spatial variations of MAR for Deployment 7.

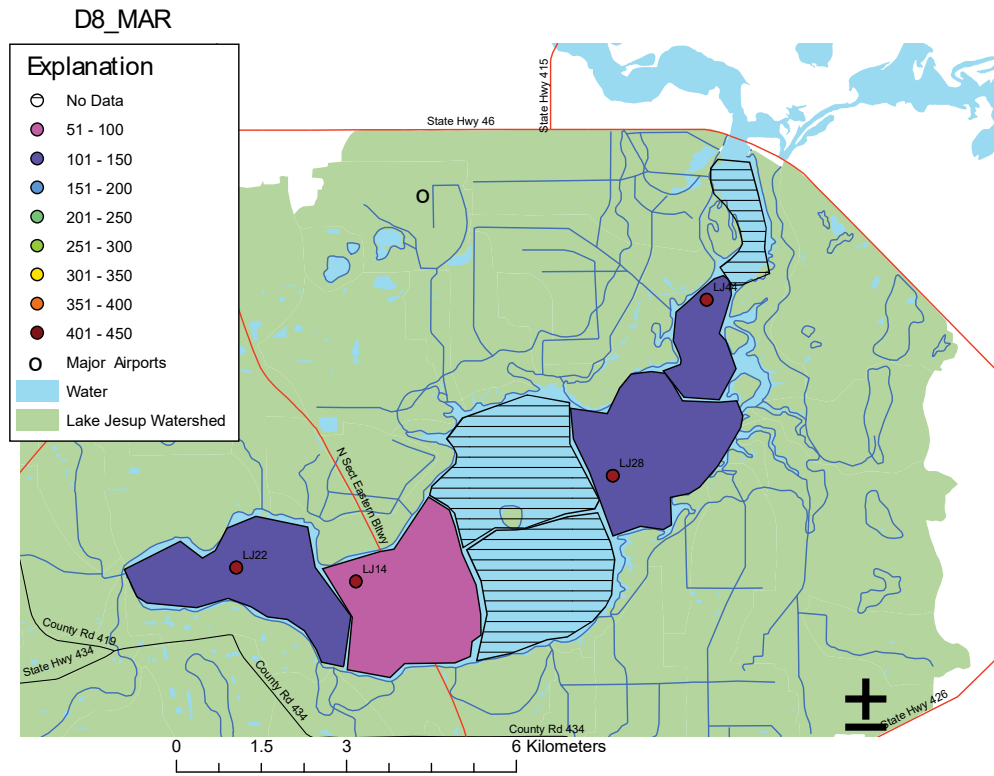


FIGURE A53. Spatial variations of MAR for Deployment 8.

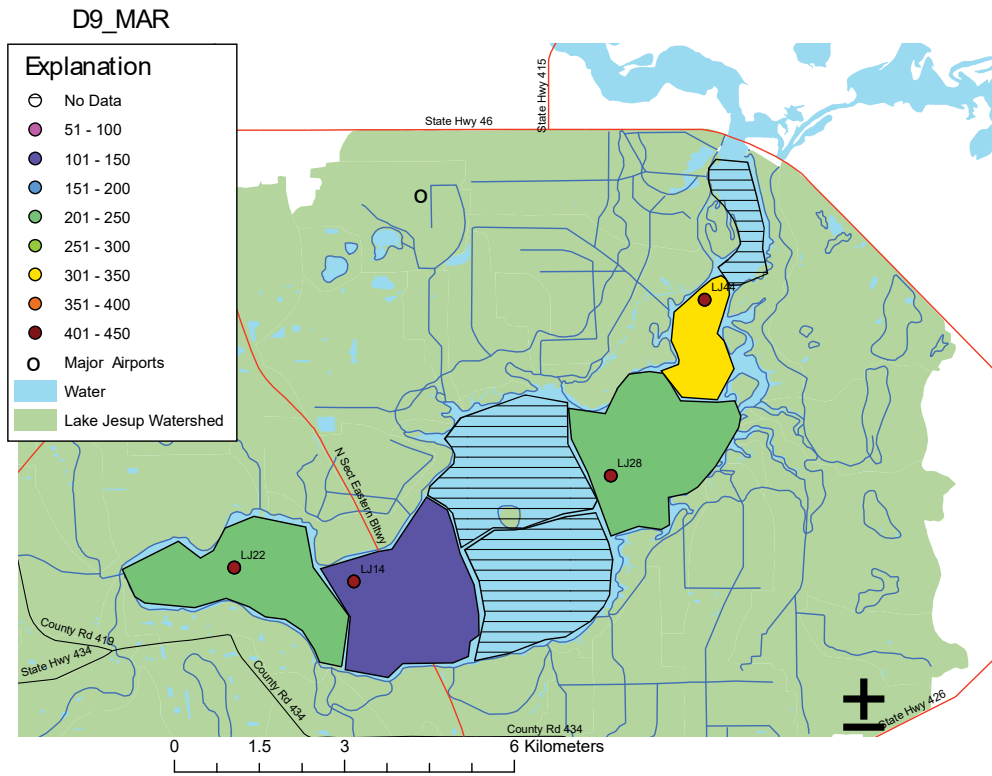


FIGURE A54. Spatial variations of MAR for Deployment 8.

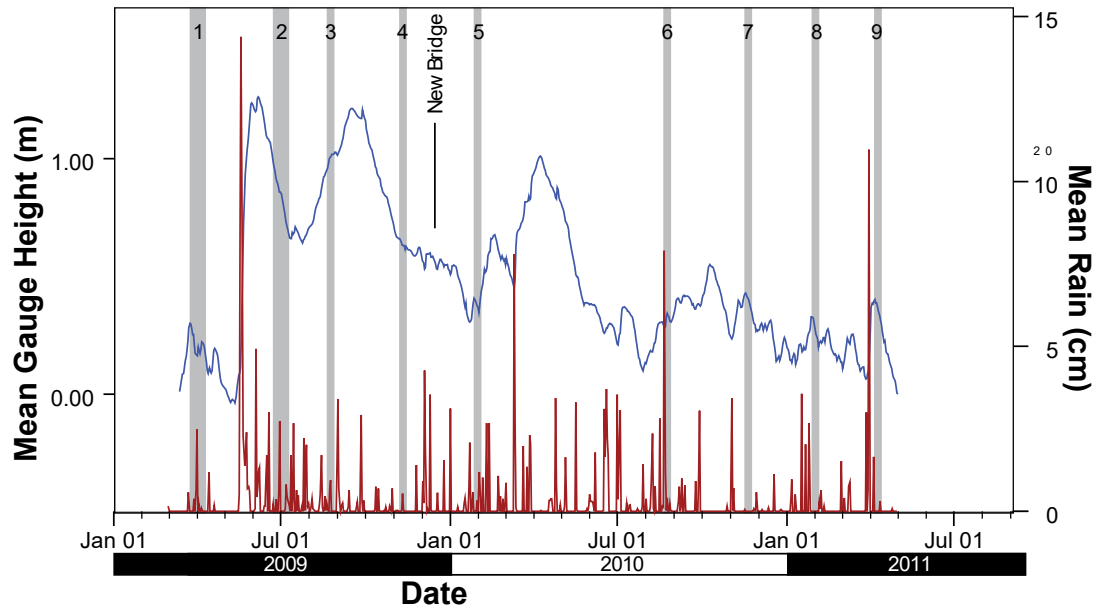


FIGURE A55. Lake level (blue) and precipitation (red) for the two year period of project sampling.

Lake Current vs TN and TP from ISCO Deployment 1 (April, May 2009)

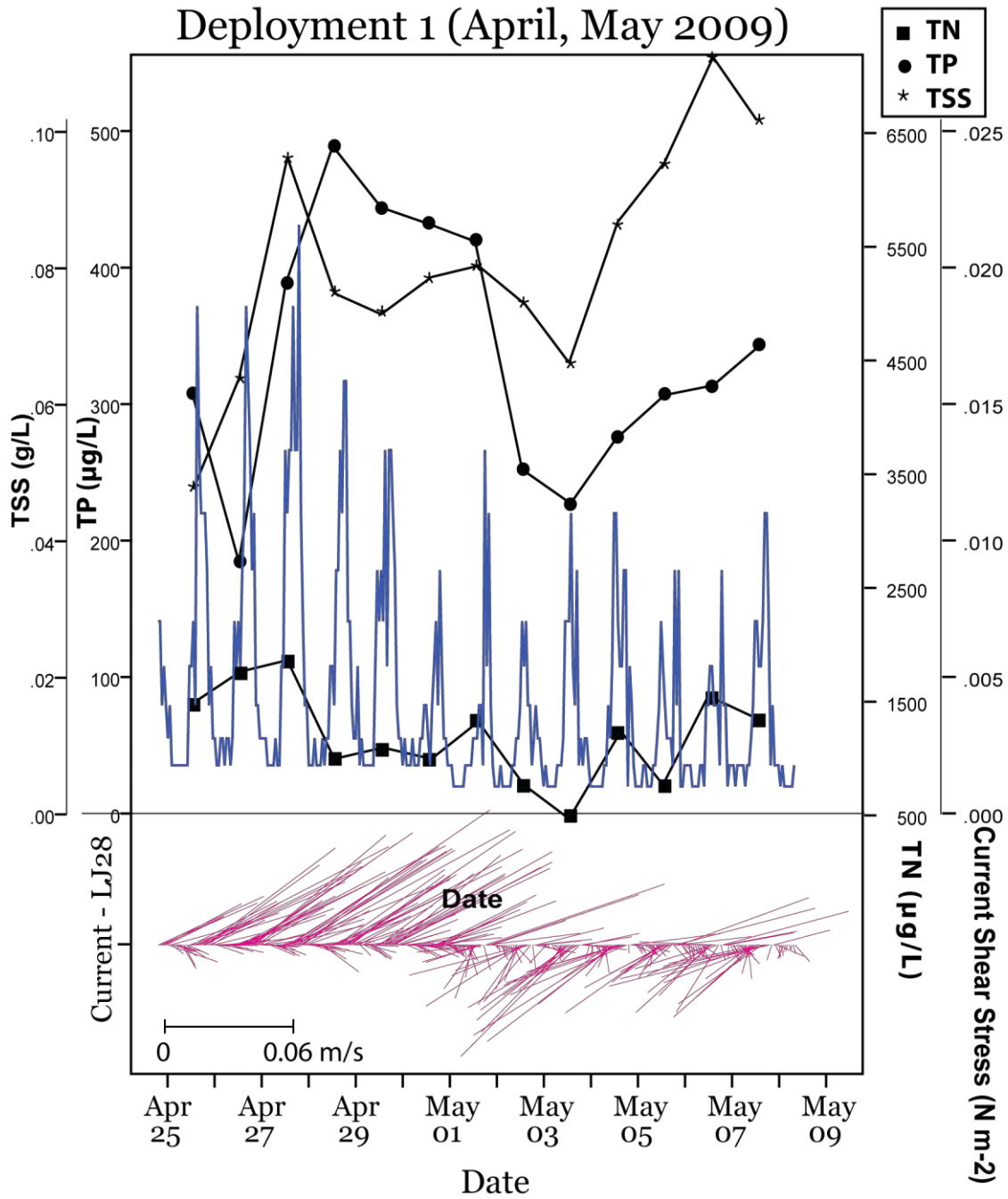


FIGURE A56. Time-series of current shear stress (blue), current stick plots (pink), TP, TN and TSS for Deployment 1.

Lake Current vs TN and TP from ISCO Deployment 2 (June, July 2009)

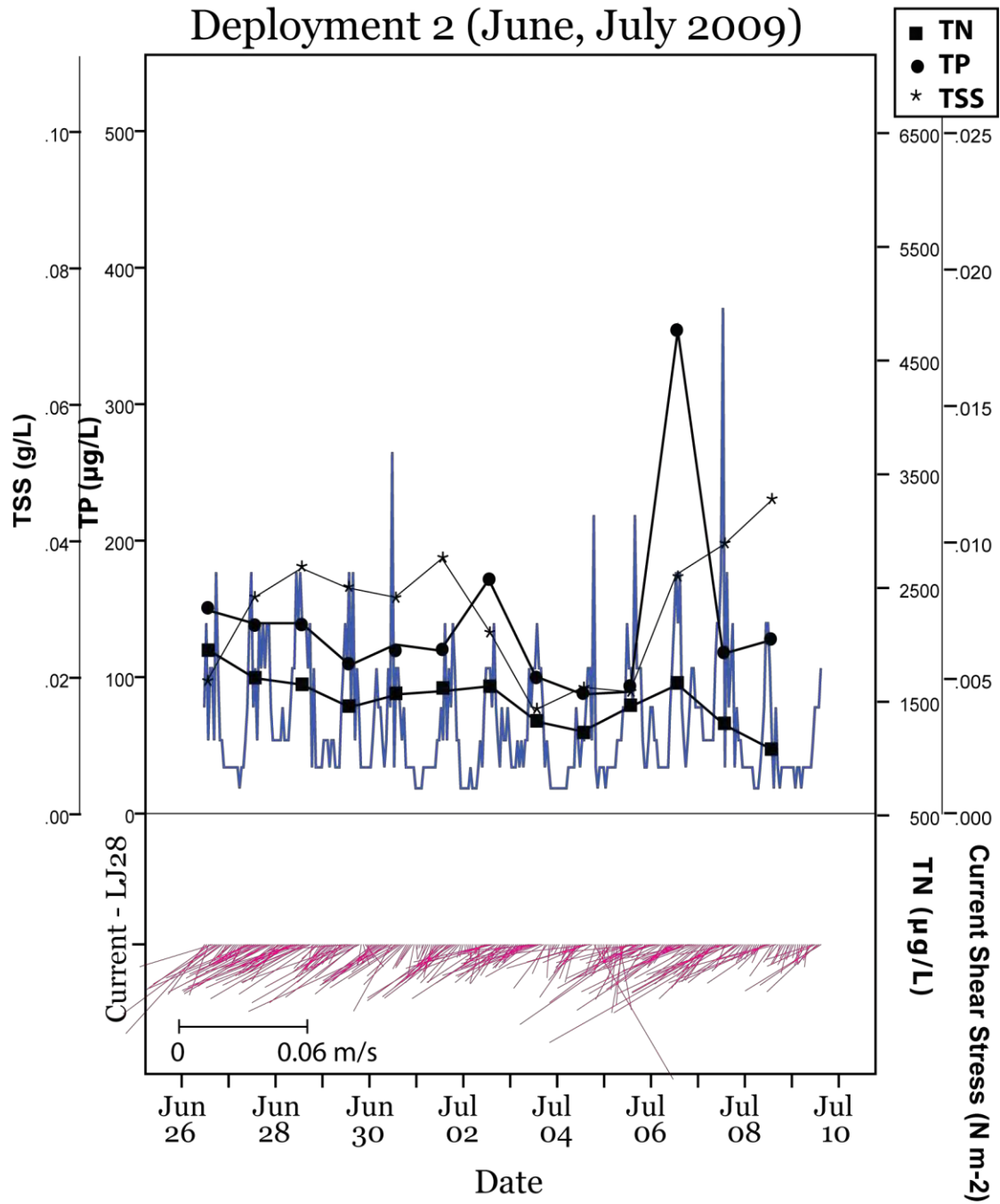


FIGURE A57. Time-series of current shear stress (blue), current stick plots (pink), TP, TN and TSS for Deployment 2.

Lake Current vs TN and TP from ISCO Deployment 5 (January. February 2010)

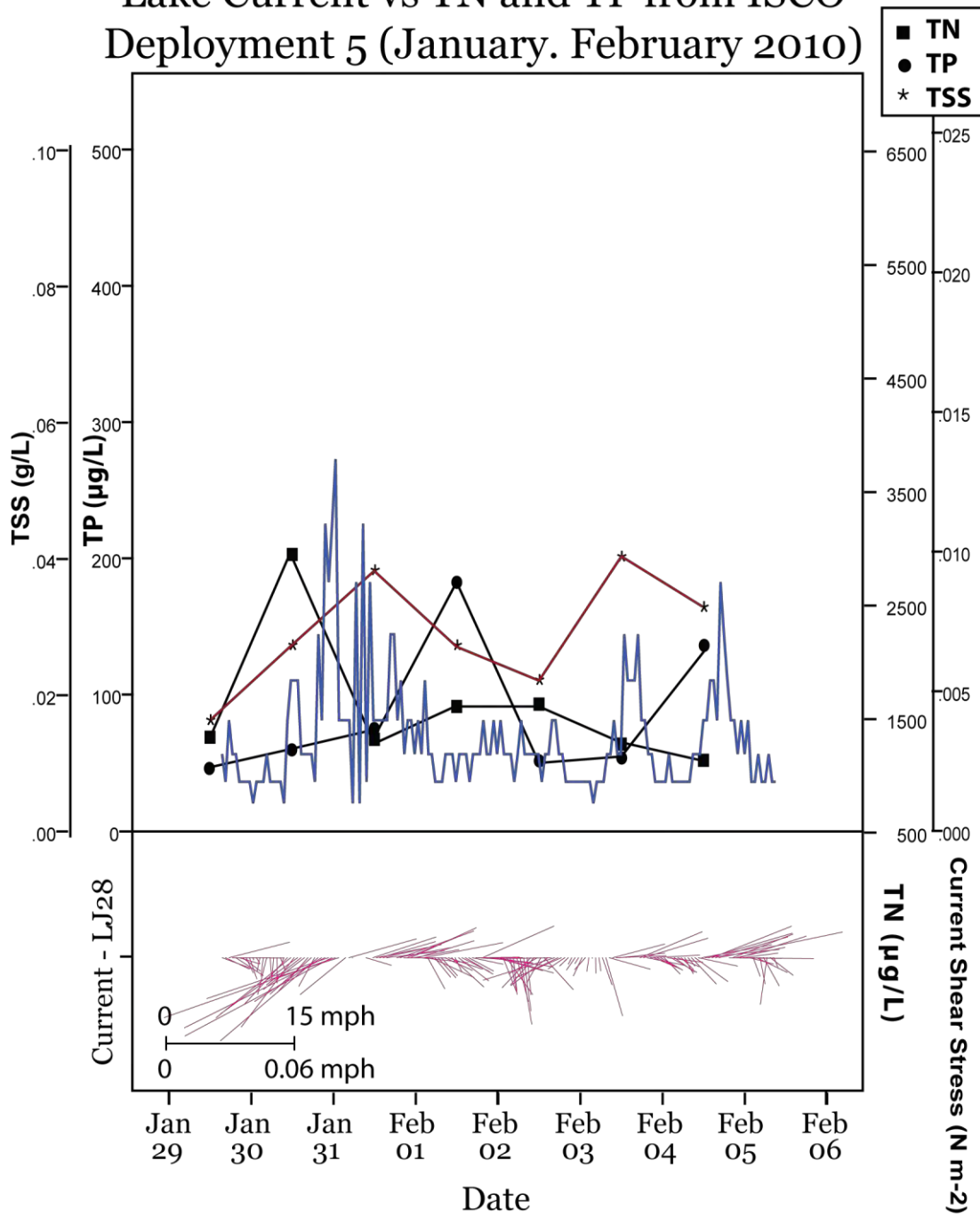


FIGURE A58. Time-series of current shear stress (blue), current stick plots (pink), TP, TN and TSS for Deployment 5.

Lake Current vs TN and TP from ISCO Deployment 6 (August 2010)

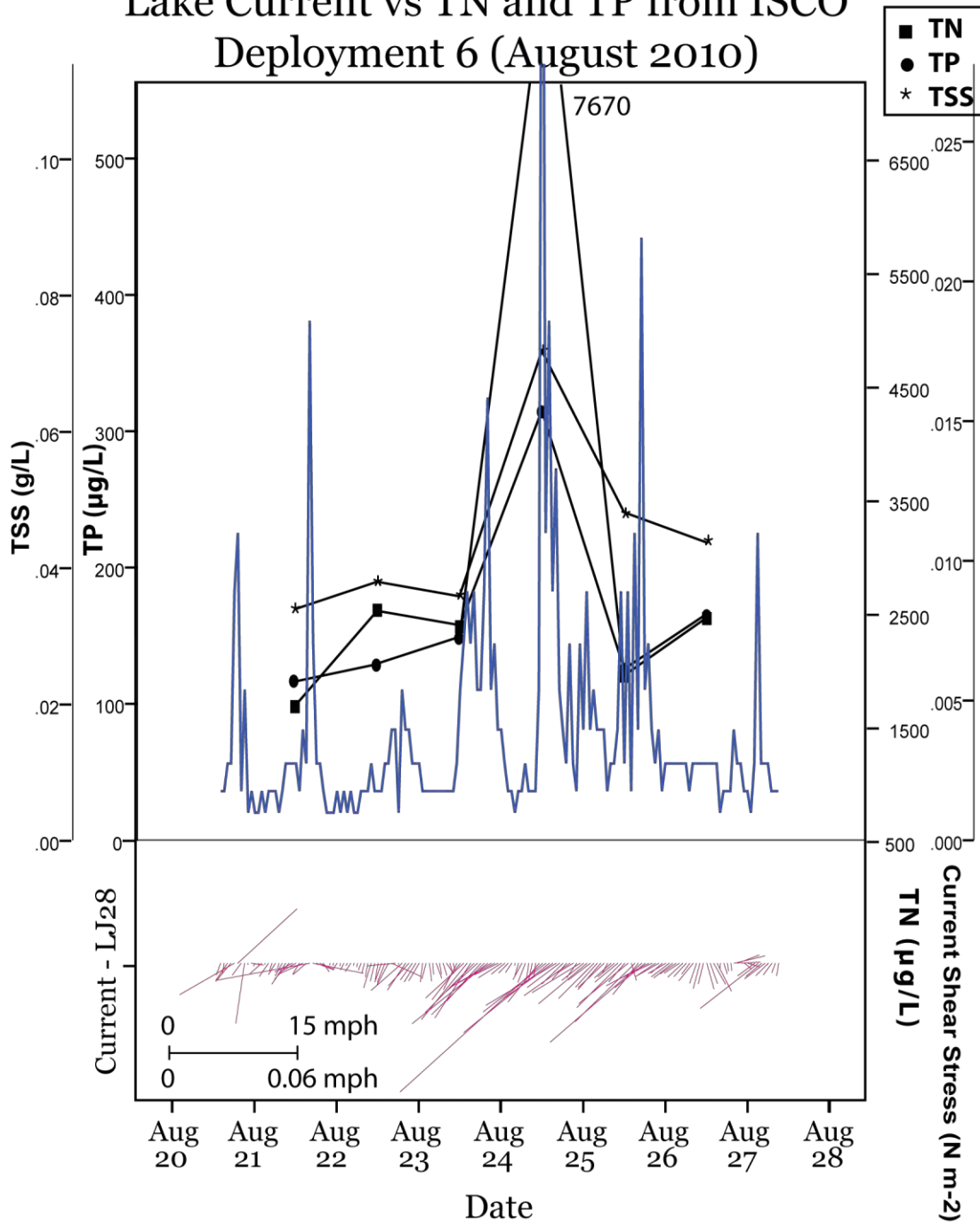


FIGURE A59. Time-series of current shear stress (blue), current stick plots (pink), TP, TN and TSS for Deployment 6.

Lake Current vs TN and TP from ISCO Deployment 7 (November 2010)

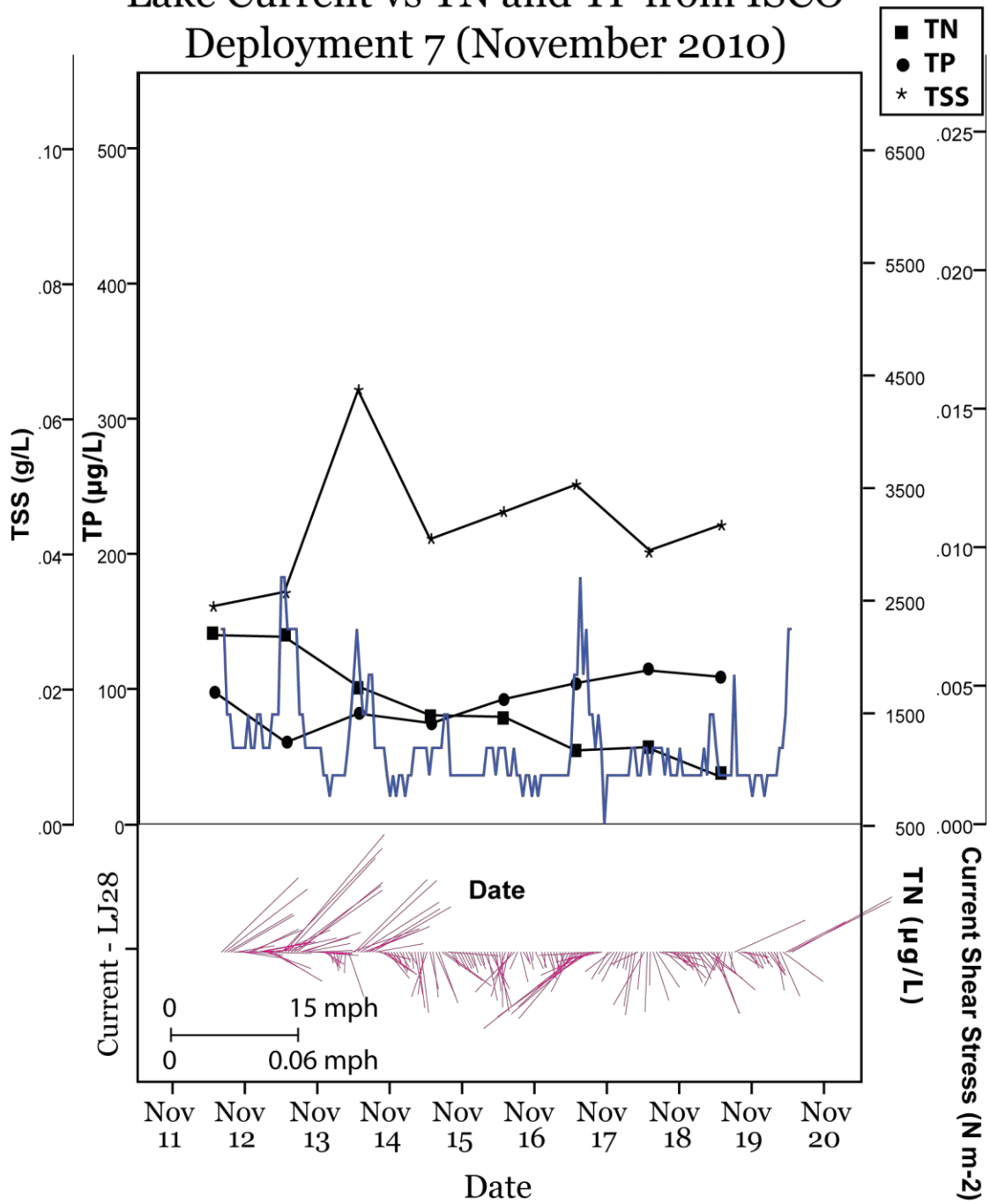


FIGURE A60. Time-series of current shear stress (blue), current stick plots (pink), TP, TN and TSS for Deployment 7.

Lake Current vs TN and TP from ISCO Deployment 8 (January, February 2011)

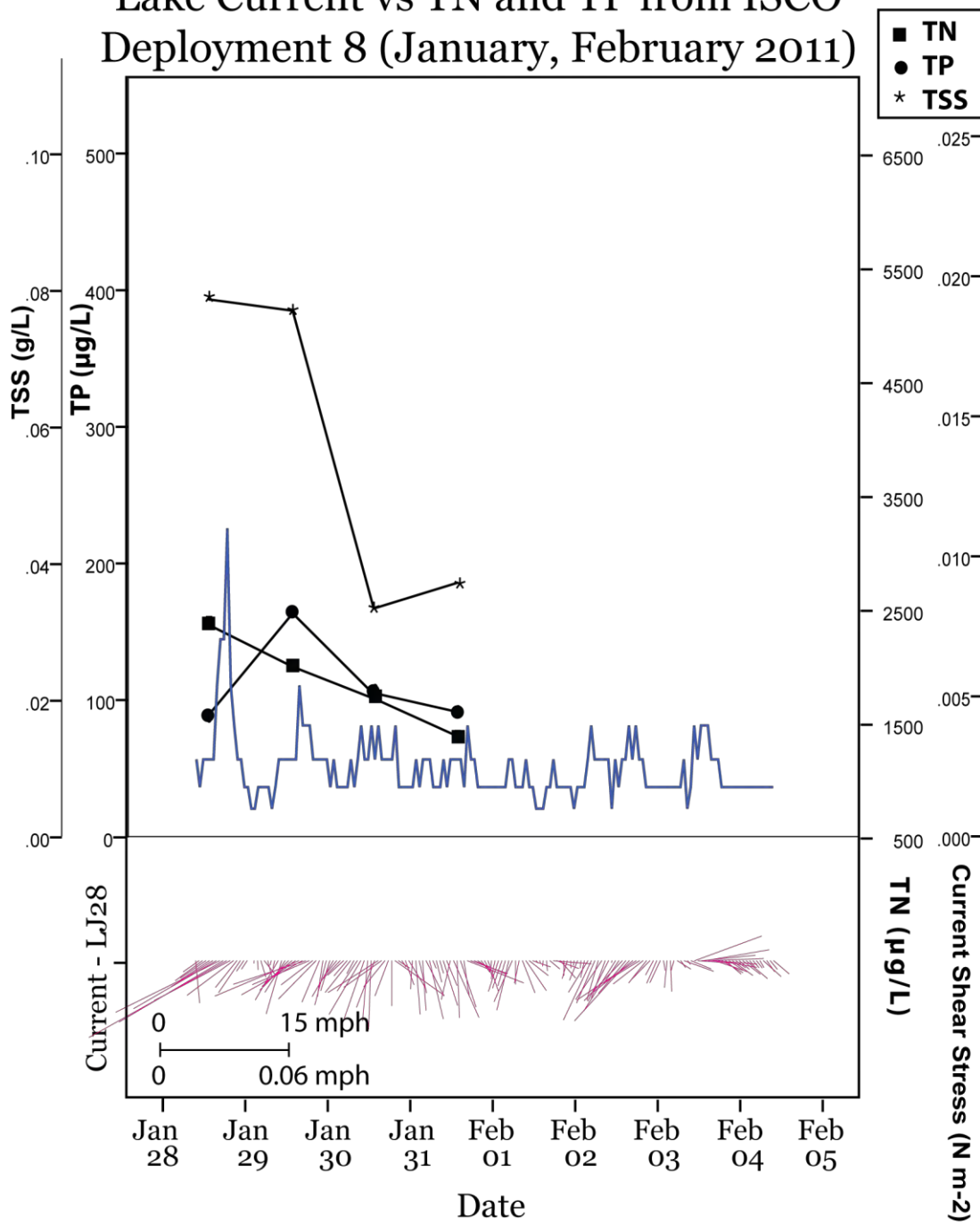


FIGURE A61. Time-series of current shear stress (blue), current stick plots (pink), TP, TN and TSS for Deployment 8.

Lake Current vs TN and TP from ISCO Deployment 9 (August 2011)

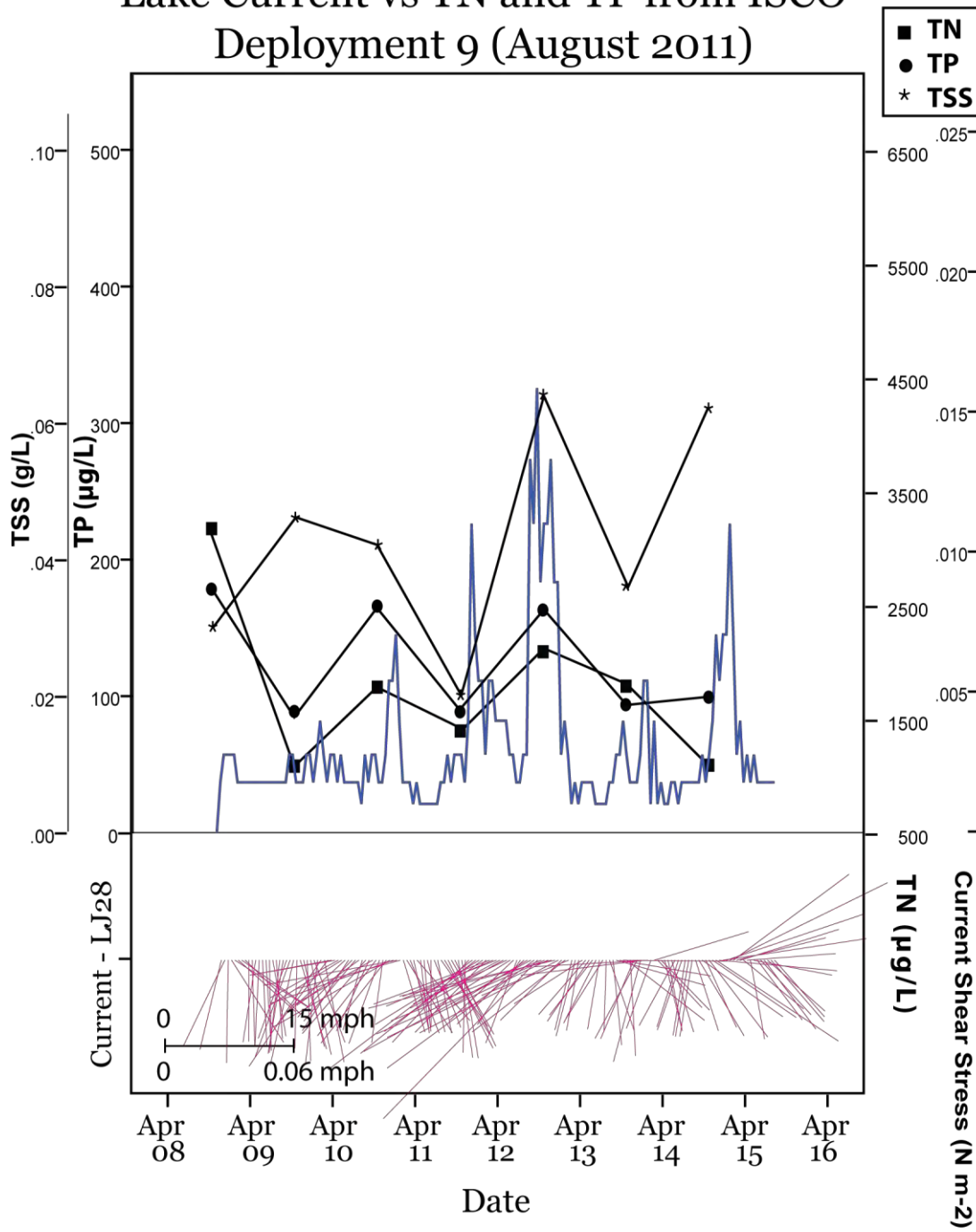


FIGURE A62. Time-series of current shear stress (blue), current stick plots (pink), TP, TN and TSS for Deployment 9.

APPENDICES

Appendix 2- Physical Measurement Results from July 2009 - February 2010

GENERAL SUMMARY:

Near bed currents at the station were very weak, along flow current speeds were less than 10 cm s^{-1} , and across flow and vertical currents were less than 2 cm s^{-1} . Suspended sediment concentrations were relatively low, usually between 20 and 50 mg l^{-1} , and of a highly organic content. Sediment dynamics at the station were primarily governed by mechanisms operating over a synoptic scale. Wind speed and direction were not available for several of these early deployments, so could not be evaluated well. Horizontal advection of material is a likely mechanism for some of the larger variations in sediment concentrations as the current switched directions. A secondary mechanism was local resuspension from current shear, increased currents were likely accompanied by waves and an increased shear stress over that by current velocity alone, although this could not be evaluated for these deployments because of lack of complete wind data. The very low velocities ($2.5 - 5 \text{ cm s}^{-1}$) that were necessary to resuspend sediment suggest that the particles have a very low settling velocity, as might be expected from highly organic aggregates. The slow settling velocity also requires much more time for an equilibrium or steady state concentration profile to develop. Instead, forcing factors changed on a much shorter time scale, preventing indirect measures of the settling velocity using the ADV. Nevertheless, the qualitative measure of the Reynolds flux of sediment provided insight into the vertical concentration profiles. When the qualitative Reynolds flux is positive, a typical resuspension profile was created with higher concentrations near the bottom. During periods when advection by surface currents moved sediment across the station, concentrations were higher near the surface as they settled towards the bottom. In either condition, the vertical sediment concentration profile was rarely at a steady state

June / July 2009 - The ADV probe became dislodged on the morning June 30, 2009 and velocity correlations were poor afterwards and so were not used for analyses. The signal conditioner of the ADV was also deployed such that the compass headings were not correct; nevertheless, the current components were rotated successfully and provided useful data. Current flow along the major axis (called "along flow" direction in this report) was generally rectilinear and mostly in one direction, but ranged from around -0.07 m s^{-1} to 0.02 m s^{-1} , "across flow" current (perpendicular to the major axis) and vertical current magnitudes were generally less than 0.02 m s^{-1} (Fig A.2.1).

The relationship between acoustic backscatter and total suspended solid (TSS) concentrations measured from the bulk water samples was generally good (Fig A.2.2). Three outliers were excluded in calculation of the calibration curve. The relationship between TSS concentrations and percent organic is variable, percentage organic ranging from 75 to 100% (Fig A.2.3)

Water level exhibited semidiurnal oscillations imposed on a generally decreasing water level from about 2.5 m at the beginning of the period to about 2.4 meters minimum, with a slight general rise afterwards (Fig. A.2.4). Suspended sediment concentration peaks were diurnal and generally coincided with the diurnal peaks in velocity. Peaks in water velocity and TSS exhibited a diurnal signal, with peaks generally in mid-afternoon during this period when wind and waves were probably at a maximum. There is a generally positive relationship, although noisy, between velocity squared, which is proportional to near bed shear stress. This suggests that variations in TSS are due to local resuspension (Fig.A.2.5).

August 2009 - Along flow currents ranged from -0.06 to 0.04 m s^{-1} and the cross flow currents ranged from -0.03 to 0.02 m s^{-1} (Fig. A.2.6). As in the previous deployment, water level variations exhibit a slight semidiurnal signal (amplitude ~ 0.01 m) superimposed upon a synoptic scale variation of about 0.05 m over a 2 day period (Fig. A.2.7).

The relationship between acoustic backscatter and TSS was generally good; the calibration of the acoustic backscatter excluded one outlier (Fig. A.2.8). Estimates of percentage organic were all near 100%.

Suspended sediment concentrations exhibited a strong diurnal variation during the first few days then a relatively low and dampened variation of concentration near the end of the deployment (Fig. A.2.7). The diurnal concentration peaks coincide with velocity peaks. Comparison of the velocity squared with TSS shows a reasonable relationship, with larger concentrations associated with larger bottom shear, although there is a fair amount of noise (Fig. A.2.9). Local resuspension appears to occur once currents reach the relatively low speed of about 0.015 m s^{-1} .

The plot of qualitative Reynolds sediment flux (w' Amp') against the acoustic backscatter show that the general condition of the vertical profile of sediment concentration throughout the deployment was not at a steady state and so it is impossible to get an indirect estimate of the settling velocity with this method (Fig. A.2.10). Instead, time series plots show that there were intervals of both negative and positive values (Fig. A.2.11). The sign of w' Amp' during periods of resuspension is expected to be positive. The consistent intervals of negative values suggest a nonequilibrium profile in which surface values of TSS were higher than regions near the bottom, likely an indication of advection of material by faster surface currents and subsequent mixing down of the material towards the bed. This can be seen more clearly by examining the net qualitative Reynolds flux, where positive values of the slope of the line indicate periods of resuspension and negative values of the slope show mixing downward of suspended material (Fig. A.2.12). Note that the change in the sign of the slope occurs around the same time that the water level begins to increase and the sediment velocity changes direction, consistent with the advection of new material over the sampling station.

Much of the wind speed and direction was missing for this deployment.

November 2009 - Along flow water velocity was somewhat larger than previous deployments, ranging from -9 to about 10 cm s^{-1} . Across flow and vertical flows were similar, usually less than 2 cm s^{-1} (Fig. A.2.13).

The calibration of acoustic backscatter calibrations with TSS from bulk water samples was bad (not shown). Bulk water samples had high organic content and little variation in concentration, between 35 and 55 mg l^{-1} (Fig. A.2.14). Likewise, there was little variation in burst average acoustic backscatter (41.2 - 42.2 dB). These two results were probably the main source of the calibration problem. For this deployment, a calibration curve was constructed by assigning the minimum and maximum bulk TSS concentrations to the

minimum and maximum burst averaged amplitudes to get a rough estimate of suspended sediment concentrations throughout the deployment.

Flow exhibited a strong diurnal variation for the first 3 days of the deployment (although always in the same direction), then held steady at a low flow, finally reversing to a stronger flow in the opposite direction (Fig. A.2.15a). The cessation of the diurnal variation in flow was accompanied by a reduction in the water level. Water level elevations had very slight semidiurnal signal superimposed upon a steadily falling water level from about 2.4 to 2.15 m throughout the deployment (Fig. A.2.15b). The abrupt change in water level on 11/7 was apparently due to movement of the instrument.

Time series of TSS show diurnal peaks as in the previous deployments. The spike in concentration on 11/8 was associated with the highest velocities of the deployment (Fig. A.2.15c). Comparison of the velocity squared with TSS shows a reasonable relationship, with larger concentrations associated with larger bottom shear, although there is a fair amount of noise likely related to variations in wave energy (Fig. A.2.16). Local resuspension appears to occur once currents reach the speed of about 5 cm s^{-1} , somewhat higher than in the previous deployment. The highest levels of suspended sediment occurred at the beginning of the deployment when the velocities were positive and the water level was relatively high.

Qualitative estimates of Reynolds sediment flux show distinct pattern of mostly negative during first part of deployment and then more positive after the current switched and the lake levels became lower (Fig. A.2.17). At beginning of deployment, when currents are higher, concentrations are higher, and the Reynolds sediment flux varies with the currents. Higher values occurred during higher concentrations, when the vertical gradient in concentration is presumably higher because of surface advection. The overall trends can be seen more clearly by looking at the cumulative net Reynolds sediment flux, where the negative slope at the beginning of the deployment suggests advection and downward mixing, followed by a change in slope and return to upward mixing by resuspension (Fig. A.2.18).

Wind speed and direction data were not available for this deployment.

January / February 2010 - Along flow water velocity was similar to the previous deployment, ranging from -9 to about 8 cm s^{-1} . Across flow velocities were usually less than 2 cm s^{-1} and vertical flows were very low, less than 1 cm s^{-1} (Fig. A.2.19).

The calibration of acoustic backscatter calibrations with TSS from bulk water samples was bad (not shown). Bulk water samples had high organic content and varied between 15 and 40 mg l^{-1} (Fig. A.2.20). The relationship between percent organic and TSS was more representative of higher energy environments where higher TSS is associated with lower percent organic. As in the last deployment, a calibration curve was constructed by assigning the minimum and maximum bulk TSS concentrations to the minimum and maximum burst averaged amplitudes to get a rough estimate of suspended sediment concentrations throughout the deployment.

Along flow velocities varied during the first 4 days of the deployment, only returning to the regular diurnal pattern that was exhibited in previous deployments during the last 2 days (Fig. A.2.21a). Water height also did not exhibit the diurnal pattern of the previous deployments (Fig. A.2.21b).

TSS was showed a generally increasing trend over the period from 1/30 to 2/03, then a sharp drop (Fig. A.2.21c). In contrast to the other deployments, there was little relationship between near bottom shear stress and TSS concentration (Fig. A.2.22).

Qualitative estimates of Reynolds sediment flux show no distinct pattern (Fig. A.23). Cumulative net Reynolds flux does not show a consistent relationship with current direction as in other deployments (Fig A.2.24).

Although wind speed reached up to 20 m s^{-1} during this deployment, it did not seem to be related to the variations in sediment concentration (Fig. A.2.25).

Observations from the LISST show small variations in the mean particle diameter (D_{50}) and total volume concentration. The concentrations appear to peak in a regular fashion from one to two times a day in the earliest part of the deployment. In general, larger volume concentrations are associated with larger size particles, as might be expected from a dynamic population of particles aggregating and disaggregating. This is also indicated for the first part of the deployment because there is not a close association between volume concentration and mass concentration. This suggests that the same population of particles were changing size but not changing their mass concentration. The last half of the deployment has a generally lower volume concentration, but a larger mass concentration, suggesting that a different population of particles has become dominant that has a higher density than those during the first part of the deployment.

Despite the pattern observed from comparing particle size, volume concentration, and mass concentration, it is unclear what the physical mechanism is for these changes. They do not seem to be associated with water level, current speed or direction, wind direction, or waves (Fig. A.2.26) and therefore is likely due to advection.

Appendix 2: Corer design

This piston corer works well in 3-4 m deep lakes. The piston consists of a 2" one-way check valve (Mfg# 101-108HC). This piston features spring-loaded poppet and stainless steel spring with O-ring seal. The arrow on the check valve shows that water can move only in one direction (upward in our case).

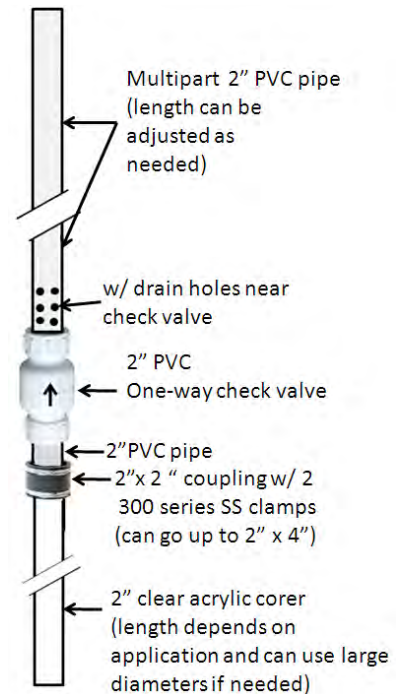
The length of the clear acrylic core used depends on the intended depth of the core. Retrieving 2-m cores with this system is not a problem.

Depending on the water depth, the length of pipe above the check valve can be adjusted.

Once the corer is assembled, it is lowered until the sediment is reached, then pushed down to the desired depth, then pulled up to the surface. The water inside the pipe above the check valve is drained through the drain holes.

With the clear acrylic (or CAB) corer still in the water, a rubber is inserted at the open end, then the corer is lifted outside the water.

The acrylic core is separated from the coupling using an electric screwdriver.



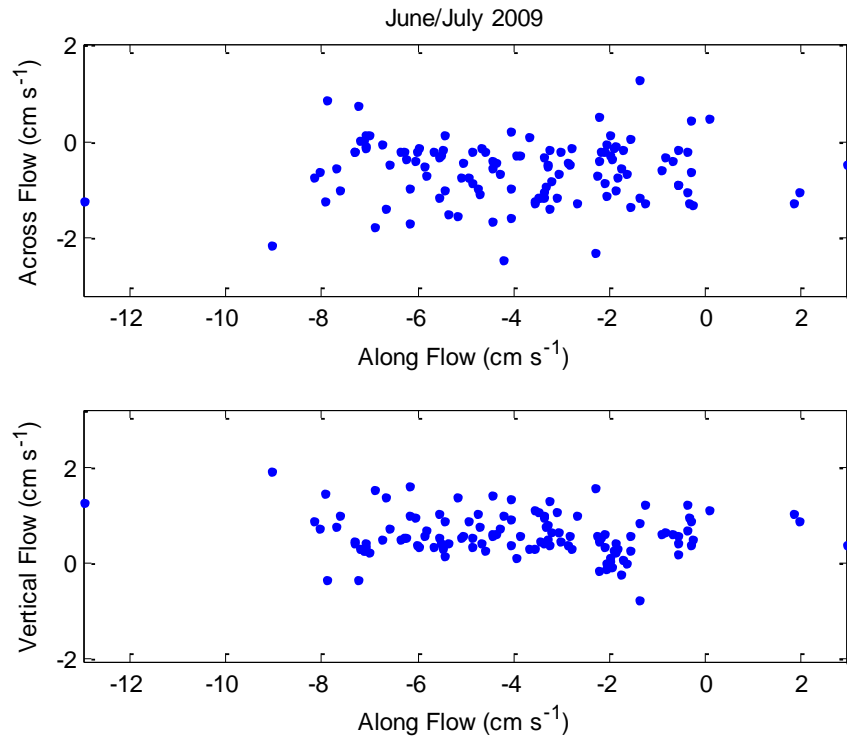


Fig. A 2.1. June/July 2009 , Rotated current measurements from ADV

Calibration

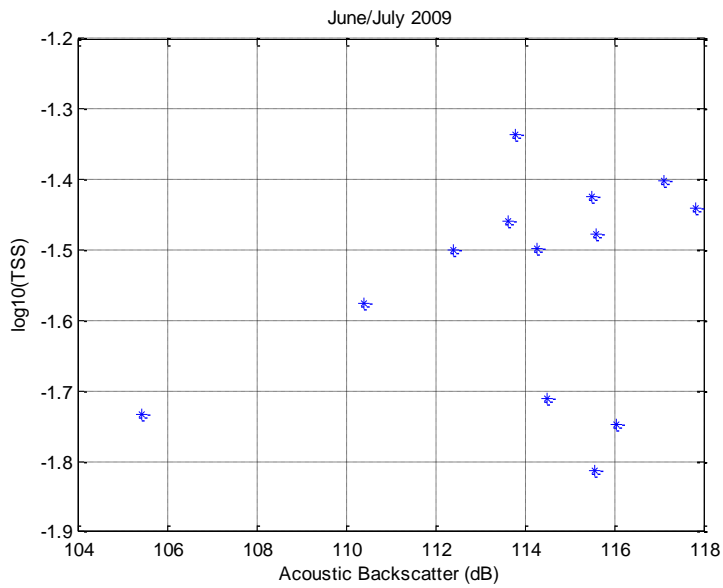


Fig. A 2.2. June/July 2009, Calibration of ADV backscatter to total suspended solids, outliers circled

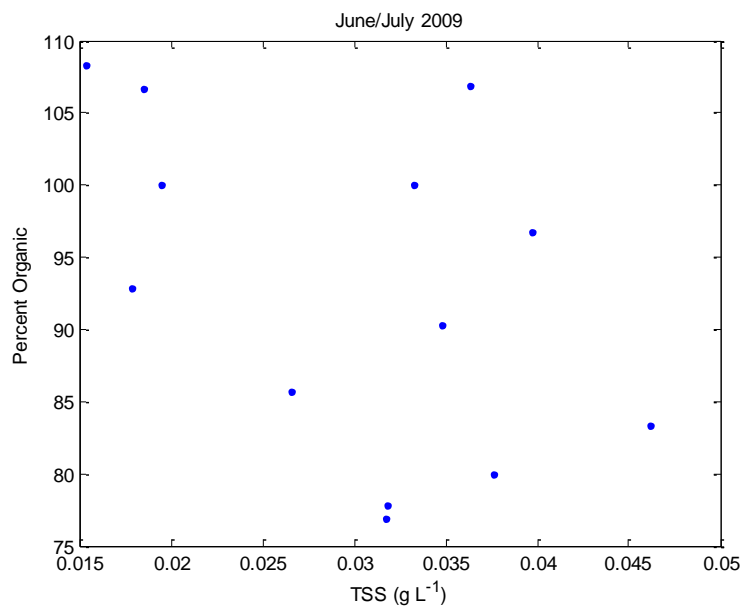


Fig. A 2.3. June/July 2009, Percentage of organic material by TSS concentration

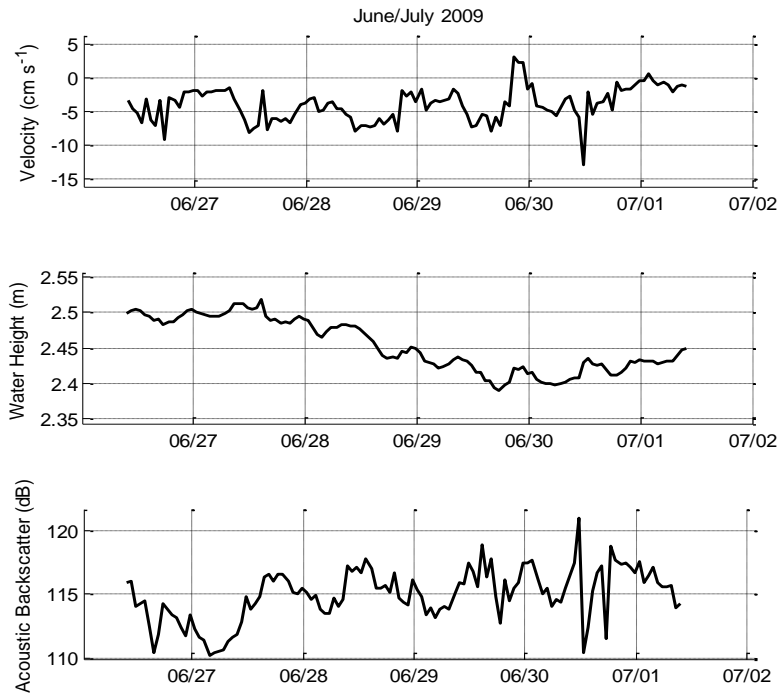


Fig. A 2.4. June/July 2009, Time series of along channel velocity, water height, and acoustic backscatter.

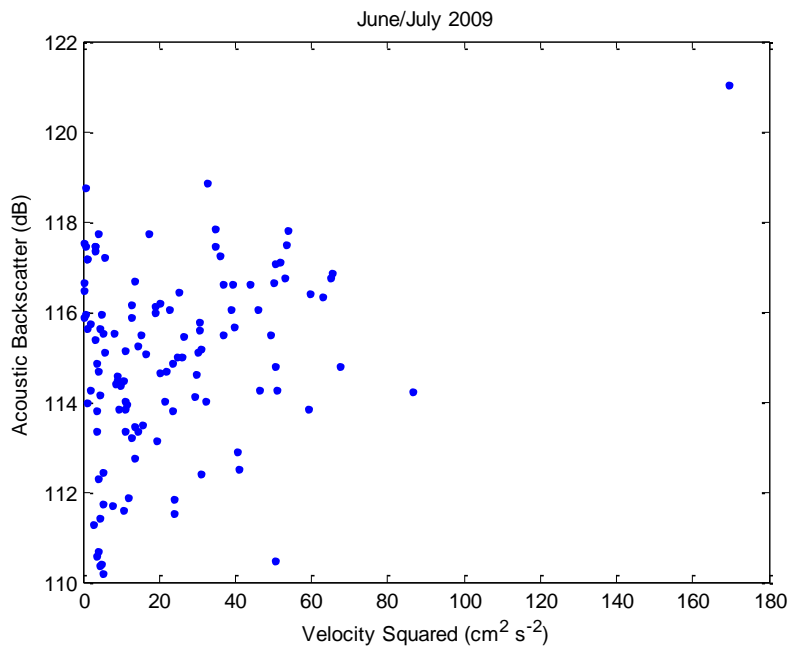


Fig. A 2.5. June/July 2009, Acoustic backscatter by the square of velocity

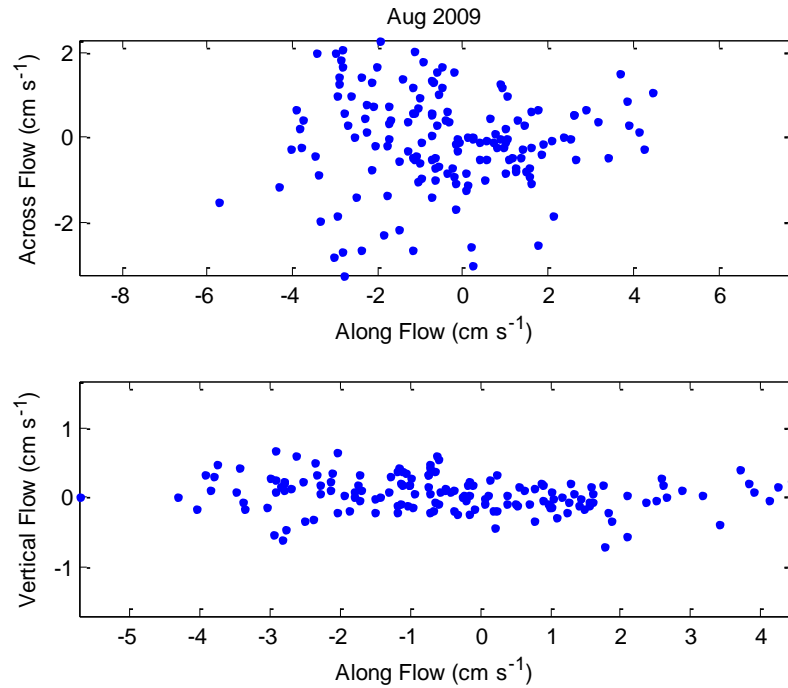


Fig. A 2.6. August 2009, Rotated current measurements from ADV

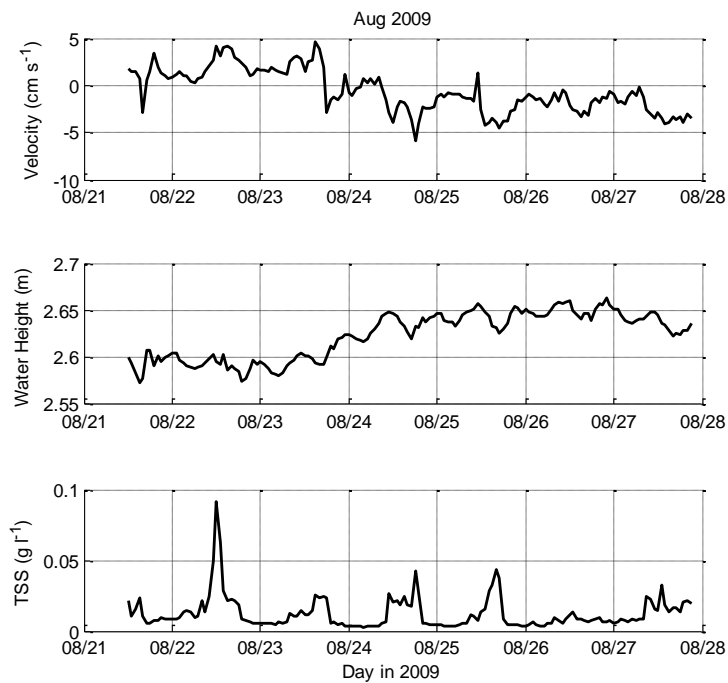


Fig. A 2.7. August 2009, Time series of along channel velocity, water height, and calibrated acoustic backscatter.

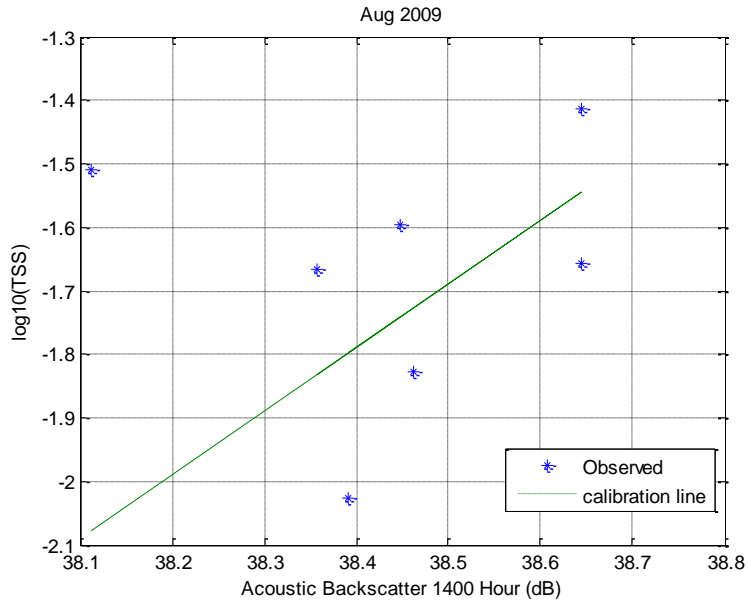


Fig. A 2.8. August 2009, Calibration of ADV backscatter to total suspended solids, outlier circled.

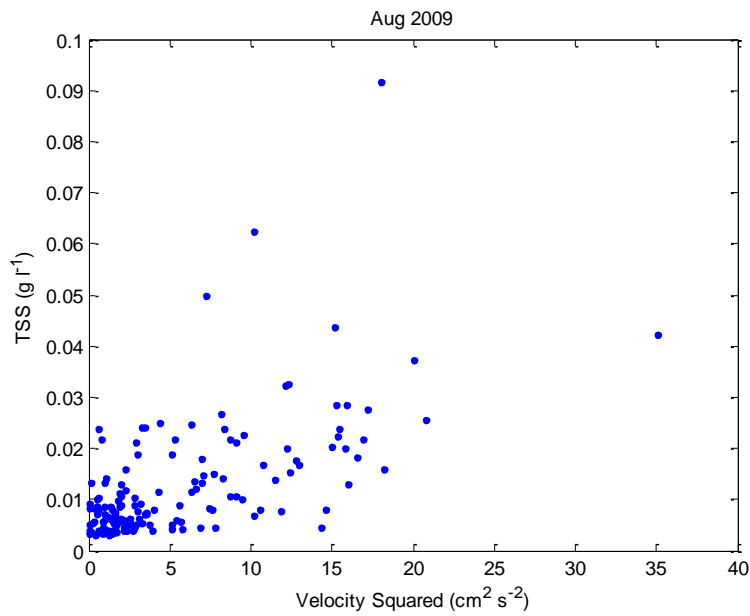


Fig. 2.9. August 2009, Calibrated acoustic backscatter by the square of velocity.

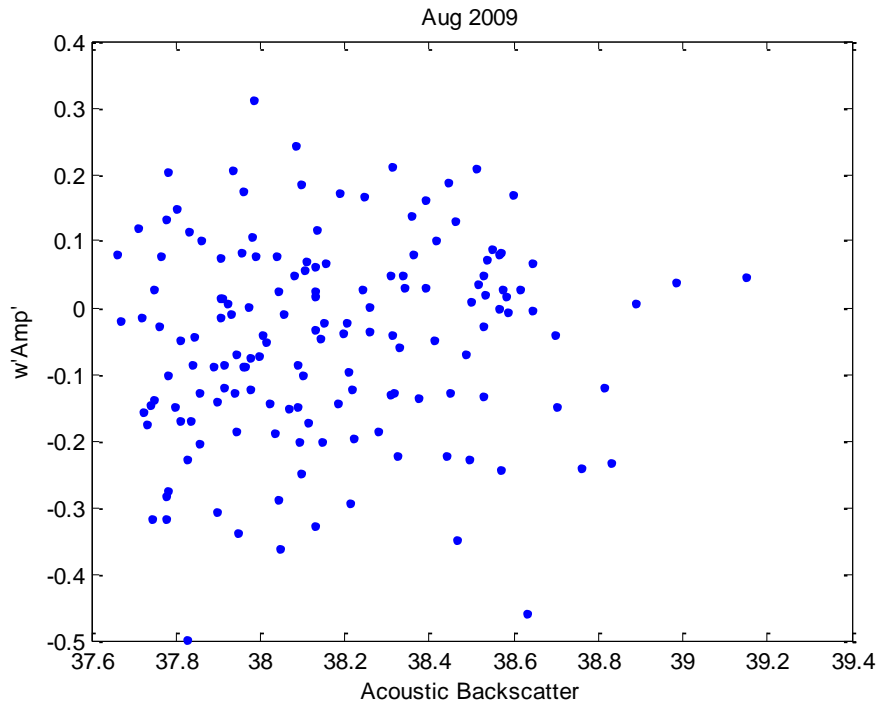


Fig. 2.10. August 2009, Qualitative Reynolds flux by acoustic backscatter.

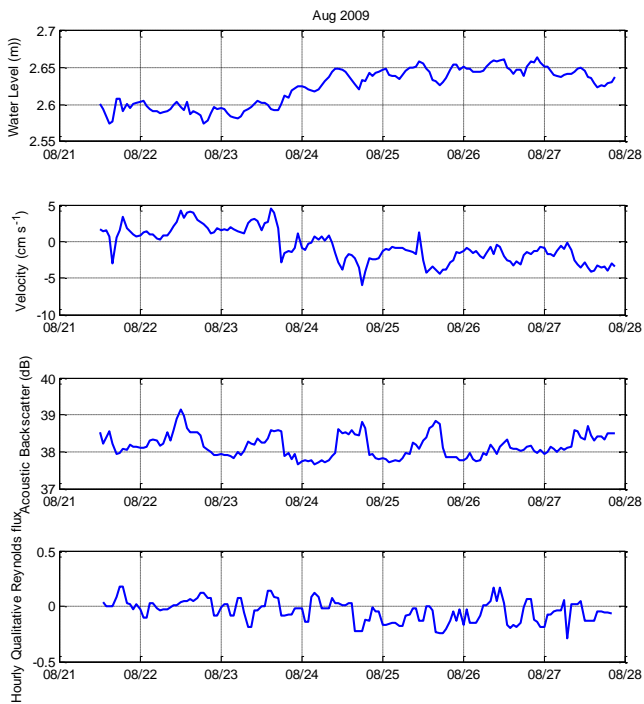
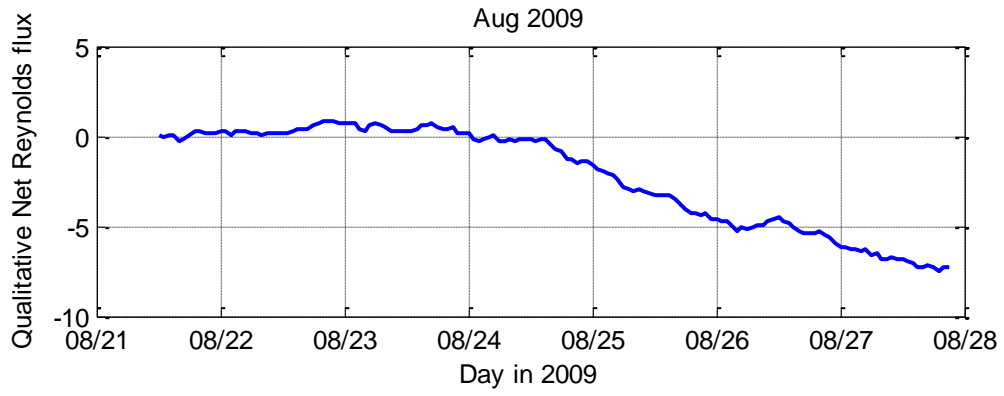


Fig. 2.11. August 2009, Time series of water level, along channel velocity, acoustic backscatter and hourly qualitative Reynolds flux

Fig. A2.12. August 2009, Time series of net qualitative Reynolds flux. Positive values of the slope of the line indicate periods of resuspension and negative values of the slope show mixing downward of suspended material



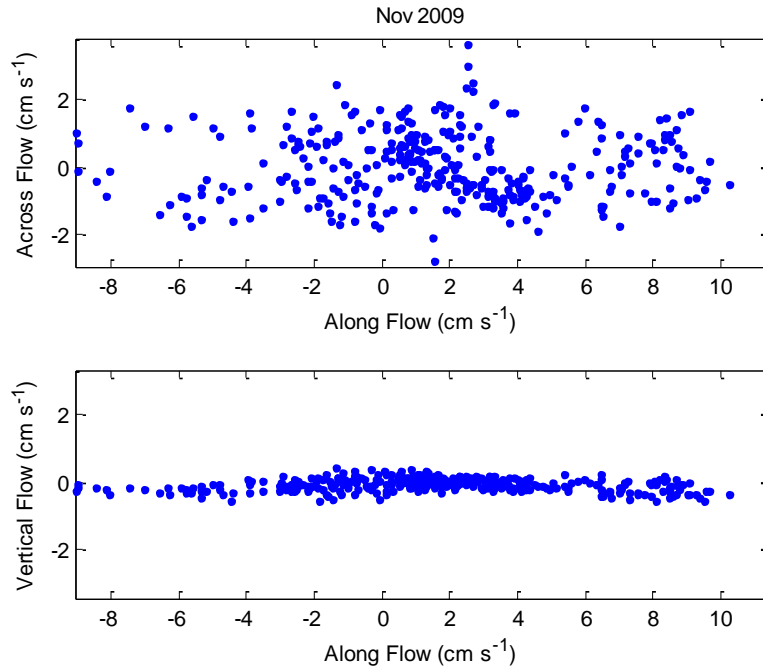


Fig. A 2.13. November 2009, Rotated current measurements from ADV.

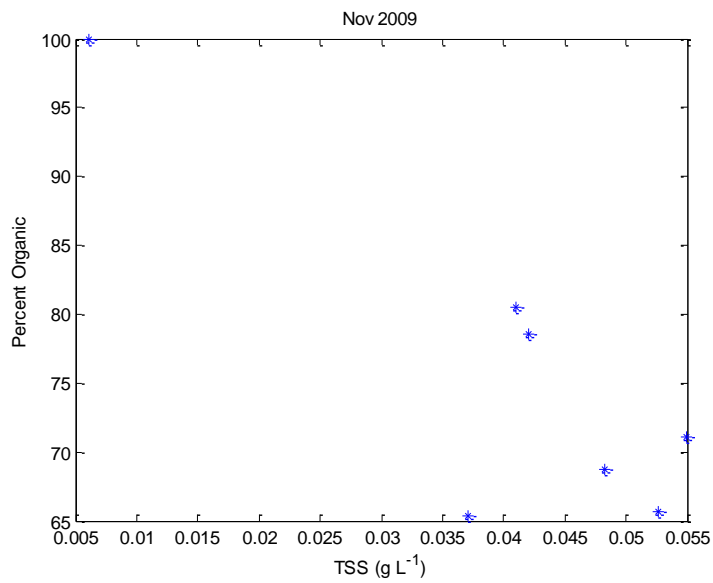


Fig. A 2.14. November 2009, Percentage organic content of total suspended solids.

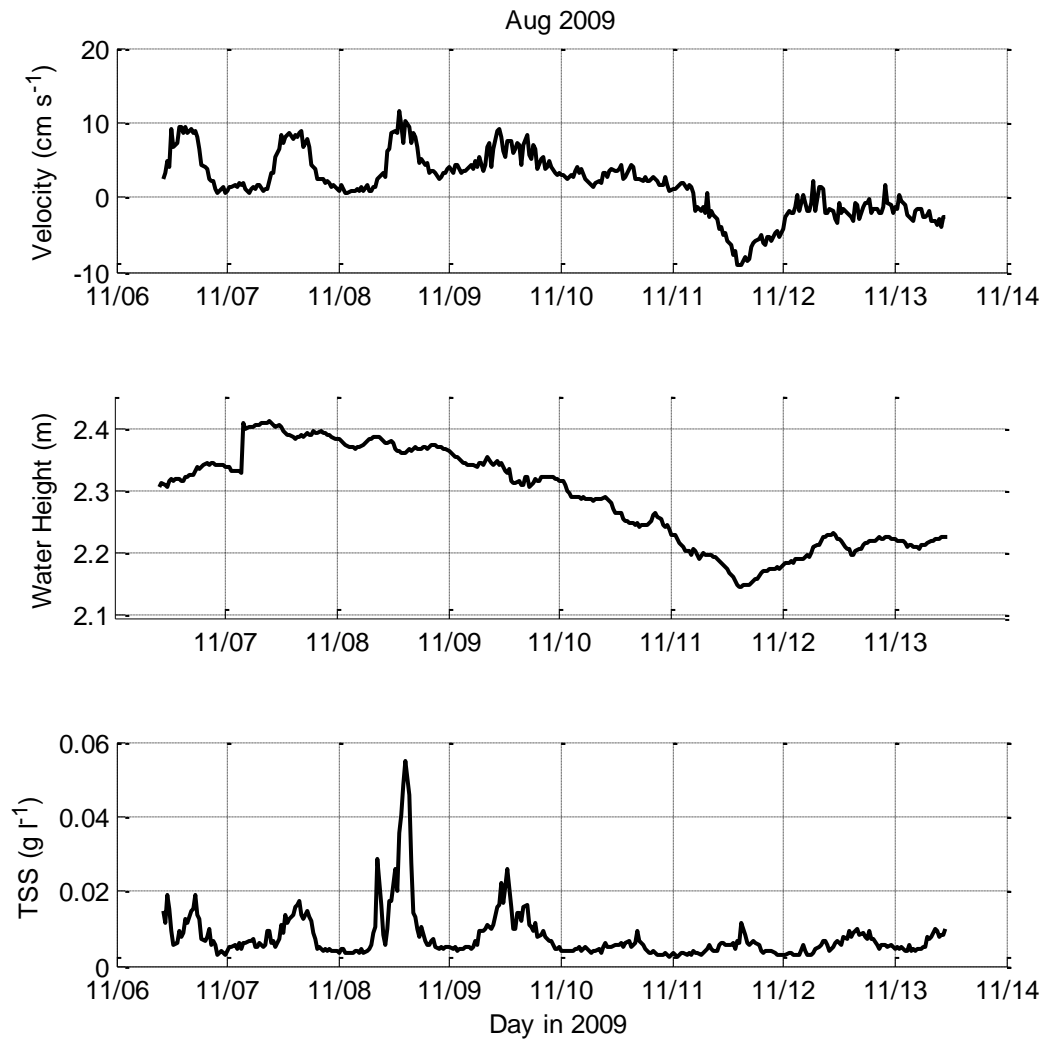


Fig. A 2.15. November 2009, Time series of along channel velocity, water height, and calibrated acoustic backscatter.

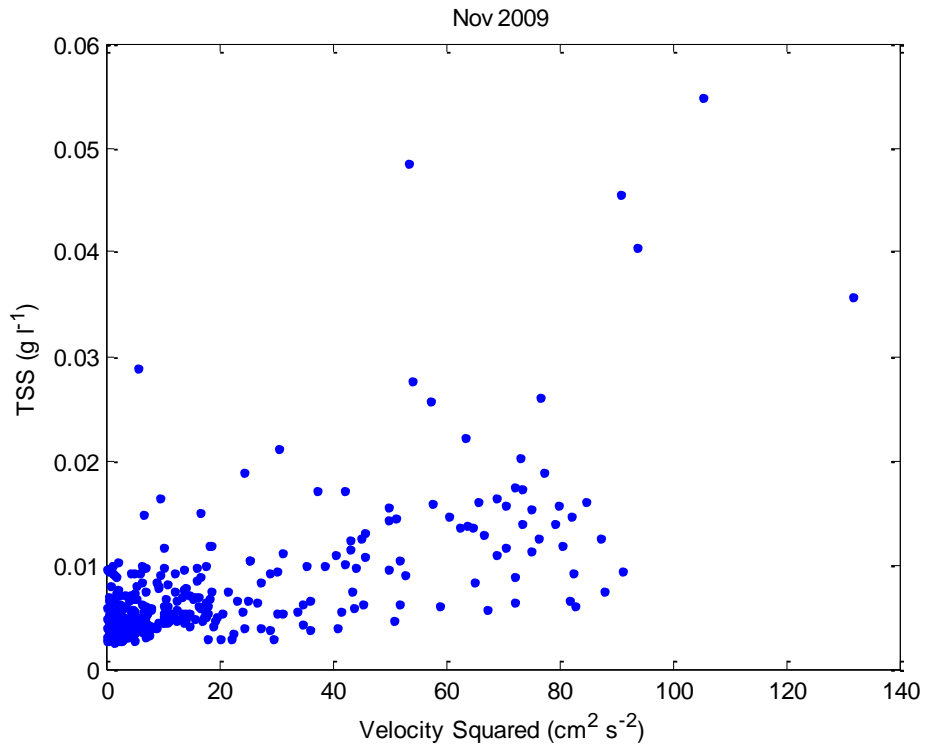


Fig. A 2.16. November 2009, Calibrated acoustic backscatter by the square of velocity.

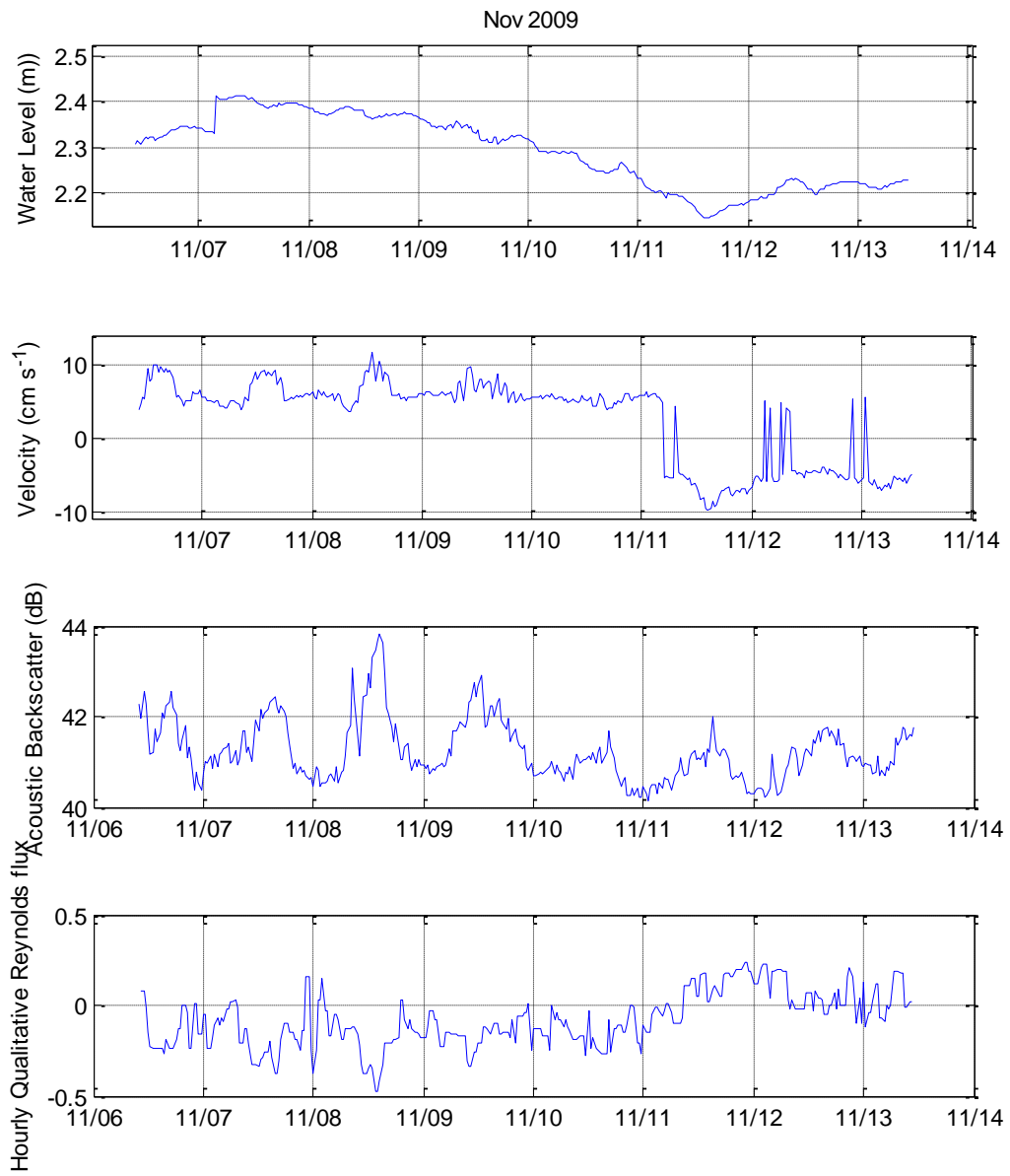
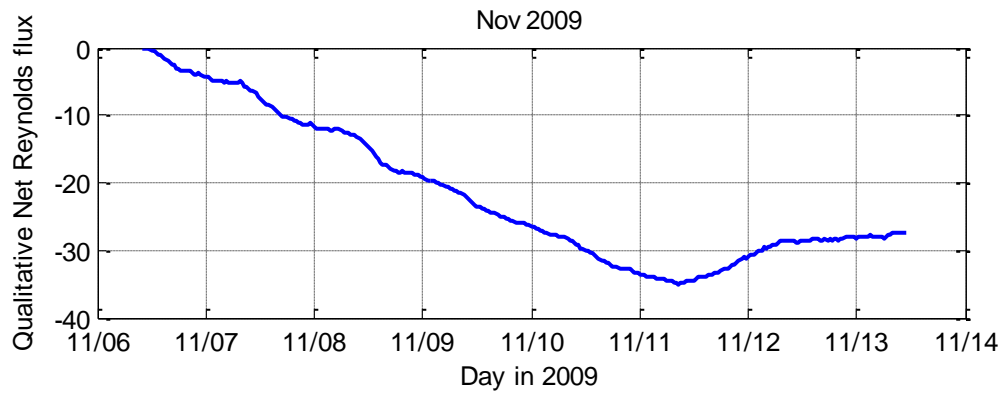


Fig. A 2.17. November 2009, Time series of water level, along channel velocity, acoustic backscatter and hourly qualitative Reynolds flux.

Fig. A.2.18. November 2009, Time series of net qualitative Reynolds flux. Positive values of the slope of the line indicate periods of resuspension and negative values of the slope show mixing downward of suspended material .



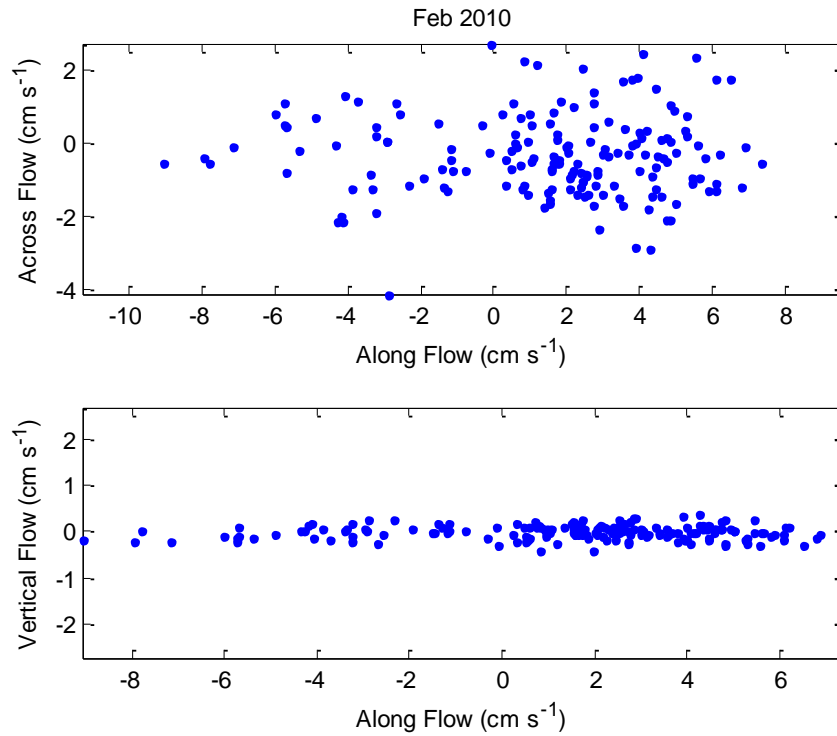


Fig. A 2.19. February 2010, Rotated current measurements from ADV

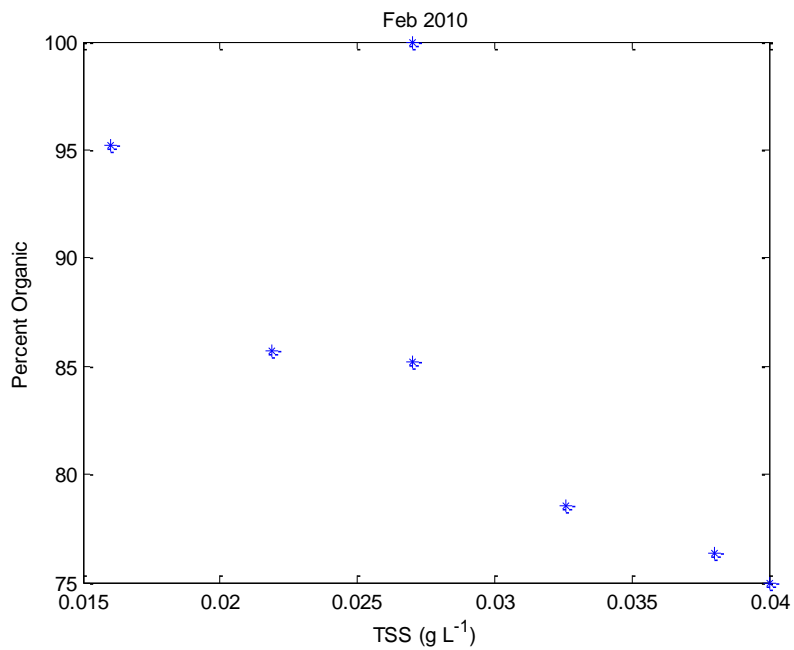


Fig. A 2.20. February 2010, Percentage of organic material by TSS concentration

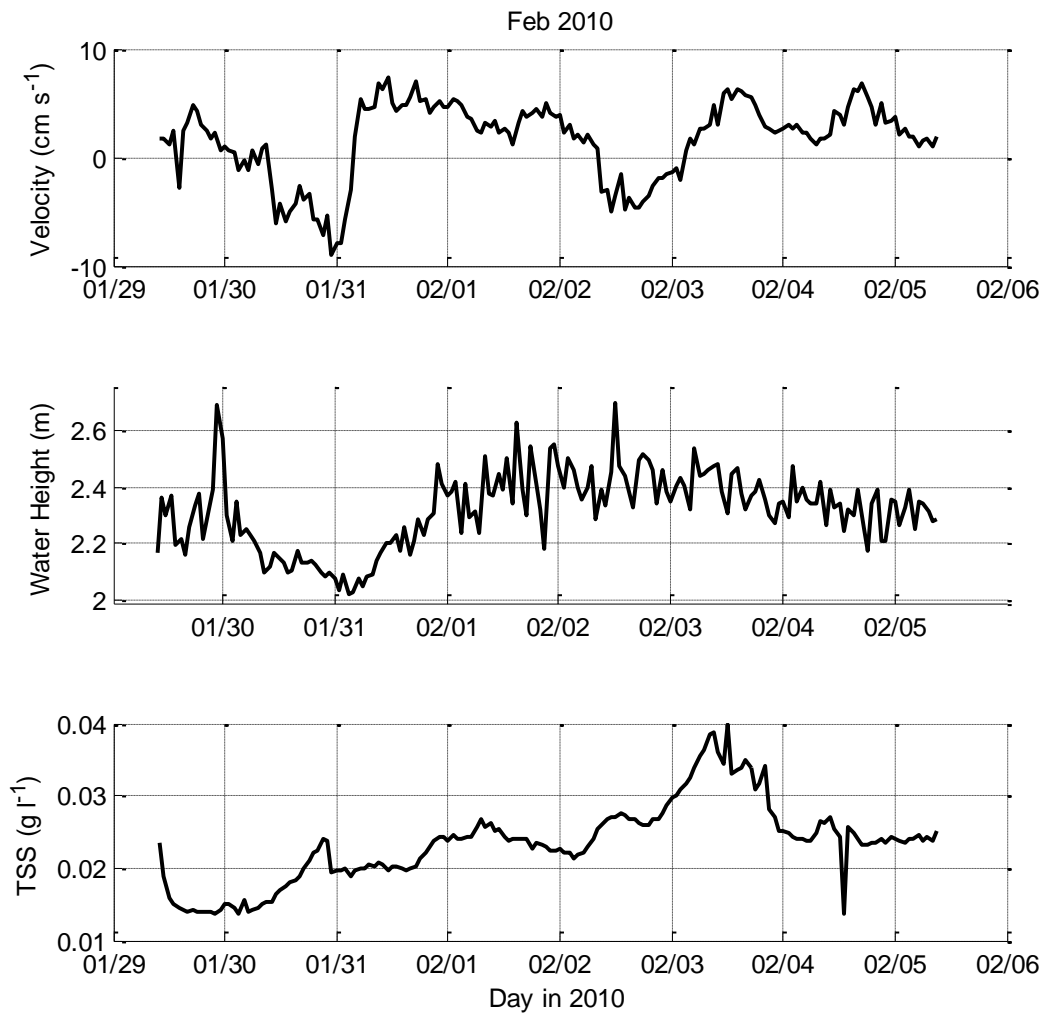


Fig. A 2.21. February 2010, Time series of along channel velocity, water height, and calibrated acoustic backscatter.

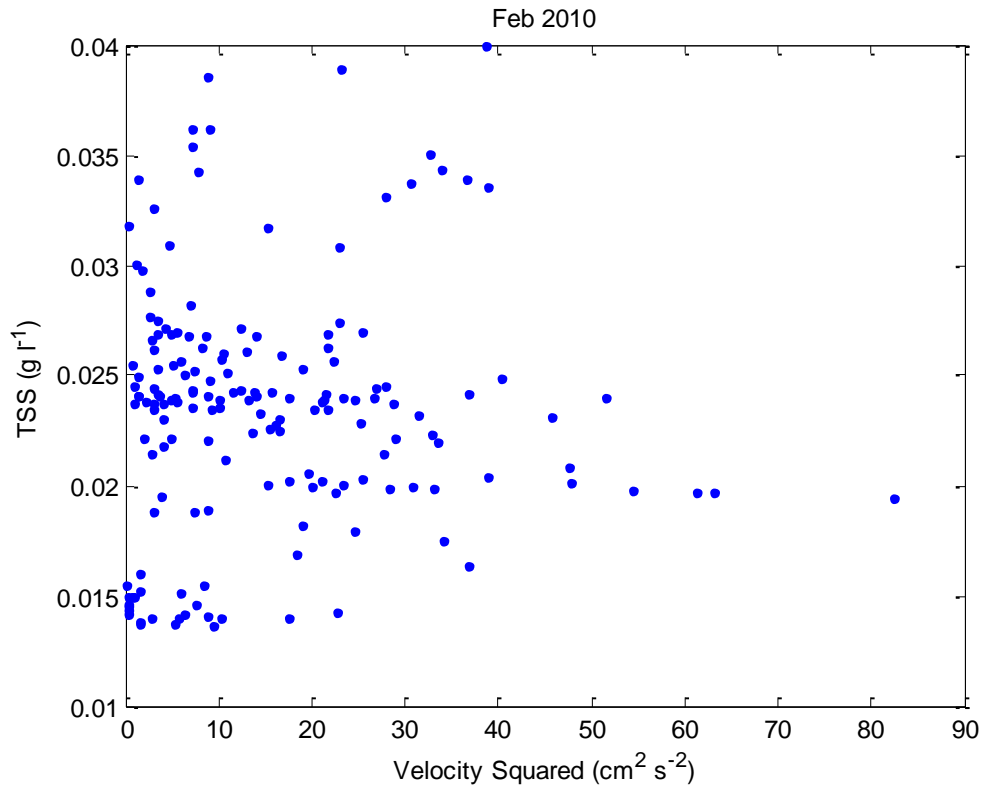


Fig. A 2.22. February 2010, Acoustic backscatter by the square of velocity.

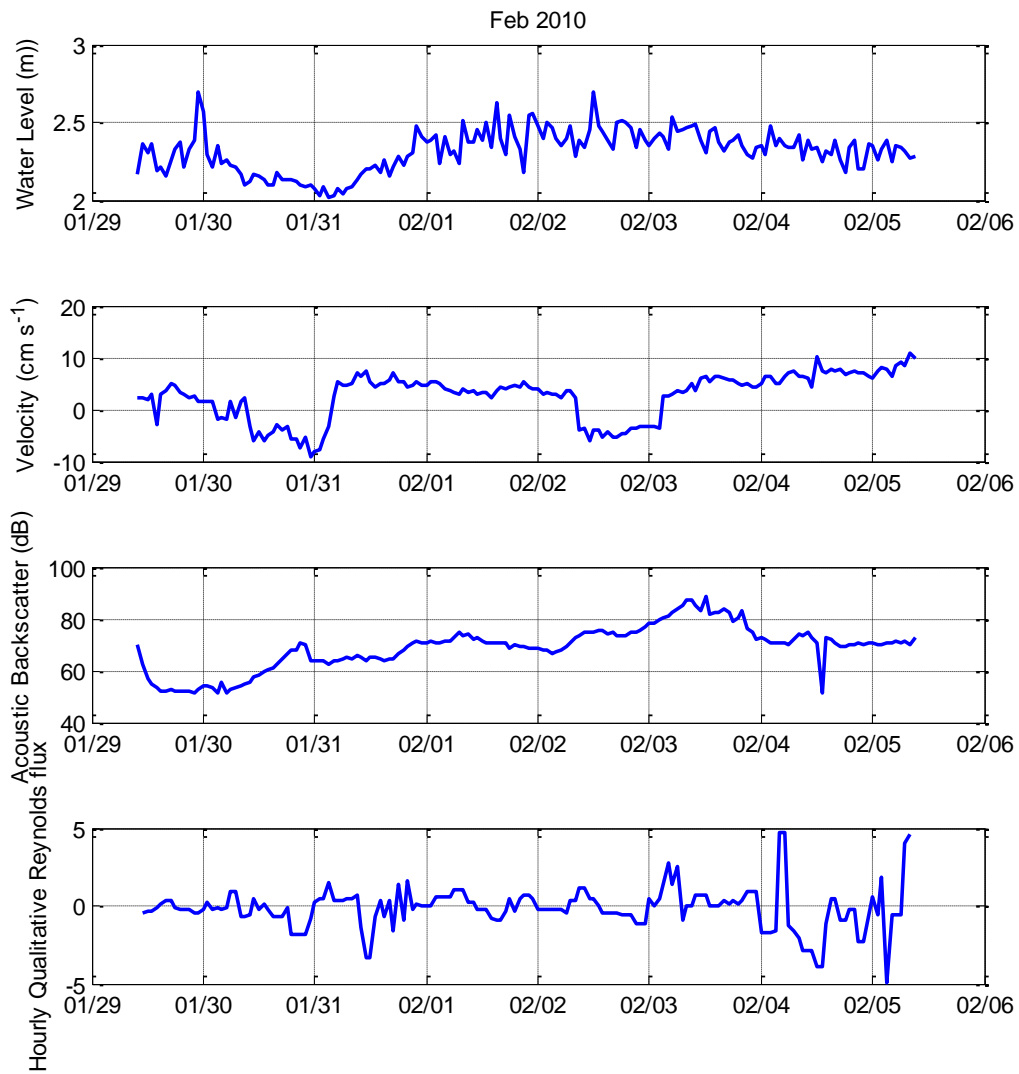
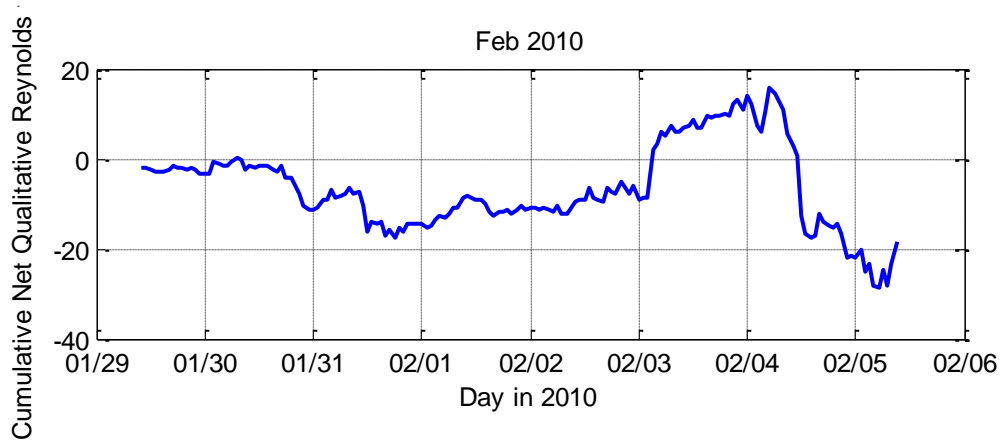


Fig. A 2.23. February 2010, Time series of water level, along channel velocity, acoustic backscatter and hourly qualitative Reynolds flux.

Fig. A 2.24. February 2010, Time series of net qualitative Reynolds flux. Positive values of the slope of the line indicate periods of resuspension and negative values of the slope show mixing downward of suspended material .



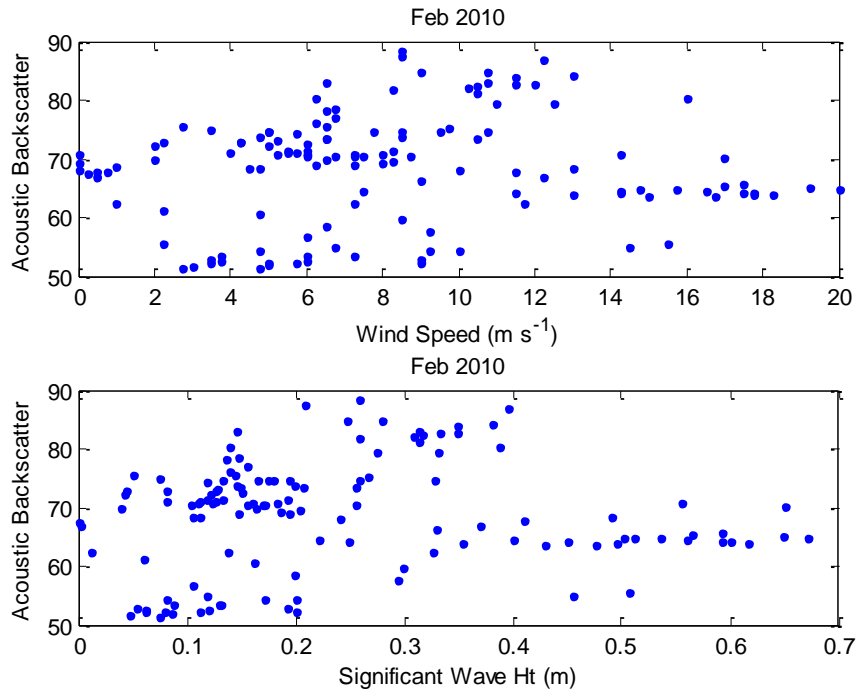


Fig. A 2.25. February 2010, Relationship between wind and waves, and acoustic backscatter.

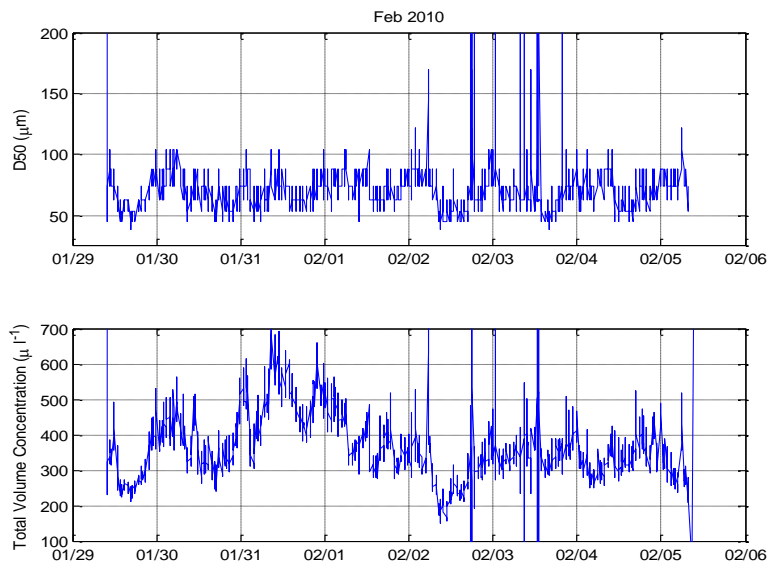


Fig. A 2.26. February 2010, Time series of median particle size (D50) and total volume concentration from the LISST.

Evaluation of Sediment Impacts on Hydrologic and Nutrient Loadings from Groundwater Seepage to Lake Jesup

Final Report



June 2013



Prepared for:



Seminole County, Florida

Kim Ornberg, Project Manager

Prepared by:



Environmental Research & Design, Inc.

Harvey H. Harper, Ph.D., P.E.
3419 Trentwood Blvd., Suite 102
Belle Isle (Orlando), FL 32812-4864
407 855-9465

TABLE OF CONTENTS

Section / Description	Page
LIST OF TABLES	LT-1
LIST OF FIGURES	LF-1
1. INTRODUCTION	1-1
1.1 Background	1-1
1.2 Work Efforts Conducted by ERD	1-5
2. FIELD AND LABORATORY ACTIVITIES	2-1
2.1 Introduction	2-1
2.2 Field Activities	2-2
2.2.1 Seepage Meter Construction and Installation	2-2
2.2.2 Seepage Meter Monitoring	2-7
2.3 Laboratory Analyses	2-12
3. RESULTS	3-1
3.1 Rainfall Characteristics	3-1
3.2 Hydrologic Inputs	3-4
3.2.1 Data Collection	3-4
3.2.2 Seepage Inflow	3-6
3.2.3 Seasonal Variability in Seepage Rates	3-10
3.2.4 Error Evaluation	3-12
3.3 Chemical Characteristics of Seepage Samples	3-12
3.4 Horizontal Variability in Seepage Characteristics	3-28
3.5 Comparison with Previous Studies	3-32
4. SUMMARY AND CONCLUSIONS	4-1
4.1 Summary	4-1
4.2 Conclusions	4-3

Appendices

- A. Field Measurements of Seepage Inflow Volumes in Lake Jesup from January 2012-March 2013
- B. Chemical Characteristics of Groundwater Seepage Samples Collected in Lake Jesup from January 2012-March 2013

LIST OF TABLES

Number / Title	Page
2-1 Analytical Methods and Detection Limits for Laboratory Analyses	2-13
3-1 Summary of Measured and Historical Rainfall in the Vicinity of Lake Jesup	3-3
3-2 Summary of Measured Seepage Inflows to Lake Jesup from January 2012-March 2013	3-7
3-3 Summary of Mean Seepage Inflows at the Lake Jesup Monitoring Sites	3-8
3-4 ANOVA Comparison of Seepage Inflow Rates in Lake Jesup With and Without Sediment Contact	3-10
3-5 Mean Seepage Inflows to Lake Jesup by Collection Date	3-11
3-6 Mean Characteristics of Groundwater Seepage Collected at the Lake Jesup Seepage Monitoring Sites from January 2012-March 2013	3-13
3-7 ANOVA Comparison of Non-Transformed Seepage Characteristics in Lake Jesup With and Without Existing Sediments	3-25
3-8 ANOVA Comparison of Log-Transformed Seepage Characteristics in Lake Jesup With and Without Existing Sediments	3-25
3-9 Summary of Significant Differences in Seepage Characteristics (Non-Transformed) With and Without Sediment Contact by Monitoring Site	3-26
3-10 Summary of Significant Differences in Seepage Characteristics (Log-Transformed) With and Without Sediment Contact by Monitoring Site	3-27
3-11 Comparison of Mean Measured Seepage Characteristics at Similar Monitoring Sites During the 2011 and Current Seepage Study	3-33

LIST OF FIGURES

Number / Title	Page
1-1 Location Map for Lake Jesup	1-2
1-2 Lake Jesup Watershed and Sub-basin Areas	1-3
2-1 Hydrologic Cycle Illustrating Groundwater Seepage to Surface Waters	2-1
2-2 Typical Seepage Meter Installation	2-3
2-3 Typical Seepage Meter Used in Lake Jesup	2-4
2-4 Photographs of Installation of the Aluminum Cylinders and Sediment Removal	2-5
2-5 Photographs of the Seepage Sample Collection Process	2-6
2-6 Locations for Seepage Meter Pairs Installed in Lake Jesup	2-8
2-7 Expanded Location Map for Seepage Monitoring Site 1	2-9
2-8 Expanded Location Map for Seepage Monitoring Site 2	2-9
2-9 Expanded Location Map for Seepage Monitoring Site 3	2-10
2-10 Expanded Location Map for Seepage Monitoring Site 4	2-10
2-11 Expanded Location Map for Seepage Monitoring Site 5	2-11
2-12 Expanded Location Map for Seepage Monitoring Site 6	2-11
3-1 Locations of Identified Rainfall Recording Stations in the Vicinity of Lake Jesup	3-2
3-2 Comparison of Measured and Historical Rainfall in the Vicinity of Lake Jesup	3-4
3-3 Number of Useable Groundwater Seepage Inflow Samples Collected in the 6 Monitoring Sites	3-5
3-4 Resuspended Sediments During Collection of Seepage Samples	3-6
3-5 Statistical Comparison of Measured Seepage Inflow Rates at the 6 Monitoring Sites With and Without Sediment Contact	3-9
3-6 Temporal Variability in Mean Seepage Inflow Rates to Lake Jesup During the Field Monitoring Program	3-11

LIST OF FIGURES -- CONTINUED

Number / Title	Page
3-7 Statistical Comparison of pH Values in Seepage Samples Collected With and Without Sediment Contact	3-15
3-8 Statistical Comparison of Alkalinity Values in Seepage Samples Collected With and Without Sediment Contact	3-17
3-9 Statistical Comparison of Conductivity Values in Seepage Samples Collected With and Without Sediment Contact	3-18
3-10 Statistical Comparison of Ammonia Values in Seepage Samples Collected With and Without Sediment Contact	3-19
3-11 Statistical Comparison of NO _x Values in Seepage Samples Collected With and Without Sediment Contact	3-20
3-12 Statistical Comparison of Total Nitrogen Values in Seepage Samples Collected With and Without Sediment Contact	3-21
3-13 Statistical Comparison of SRP Values in Seepage Samples Collected With and Without Sediment Contact	3-23
3-14 Statistical Comparison of Total Phosphorus Values in Seepage Samples Collected With and Without Sediment Contact	3-24
3-15 Comparison of Seepage Nutrient Concentrations in Lake Jesup With and Without Sediments and Seepage Concentrations Measured in Other Central Florida Lakes	3-28
3-16 Flow-Weighted Mean Concentrations of Alkalinity in Lake Jesup Seepage Samples With and Without Sediment Contact	3-29
3-17 Flow-Weighted Mean Concentrations of Ammonia in Lake Jesup Seepage Samples With and Without Sediment Contact	3-30
3-18 Flow-Weighted Mean Concentrations of Total Nitrogen in Lake Jesup Seepage Samples With and Without Sediment Contact	3-30
3-19 Flow-Weighted Mean Concentrations of SRP in Lake Jesup Seepage Samples With and Without Sediment Contact	3-31
3-20 Flow-Weighted Mean Concentrations of Total Phosphorus in Lake Jesup Seepage Samples With and Without Sediment Contact	3-32

SECTION 1

INTRODUCTION

1.1 Background

Lake Jesup is a 10,660-acre shallow, hypereutrophic lake located in northern-central Seminole County. A general location map for Lake Jesup is given on Figure 1-1. The lake is currently included on the Verified List, developed by the Florida Department of Environmental Protection (FDEP), as impaired for nutrients and unionized ammonia. Lake Jesup (WBID 2981) is also a priority waterbody as part of the State of Florida's Surface Water Improvement and Management (SWIM) Program. The mouth of Lake Jesup (WBID 2981A) is hydraulically connected to the St. Johns River at the northern end by a narrow channel near the SR 46 bridge and causeway. The SR 417 bridge, completed in 1993, crosses the lake near the western end. A small island, commonly referred to as Bird Island, is located near the center of Lake Jesup.

Lake Jesup is an extremely shallow waterbody with a mean depth ranging from approximately 3-4 ft, depending upon water elevation. The average water stage in Lake Jesup is approximately 1.8-2.0 ft (NGVD). In general, net water movement occurs from Lake Jesup into the St. Johns River, although flow reversal is observed periodically during periods of differential rainfall in adjacent sub-basin areas.

The drainage basin for Lake Jesup covers an area of approximately 87,331 acres (FDEP, 2006). An overview of the Lake Jesup watershed and sub-basin areas is given on Figure 1-2. The vast majority of the watershed is located within Seminole County, with a small portion of the southwest end extending into Orange County. The watershed area includes 11 separate municipalities, including Sanford, Lake Mary, Oviedo, Winter Springs, Longwood, Casselberry, Altamonte Springs, Maitland, Winter Park, Eatonville, and Orlando. Large portions of the watershed are highly urbanized, consisting of a combination of residential, commercial, and transportation land uses. The mean hydraulic residence time for Lake Jesup has been estimated from 82-99 days, depending upon the source.

A final TMDL report for Lake Jesup was issued by FDEP on April 14, 2006 which establishes total maximum daily loads (TMDLs) for nutrients and unionized ammonia in Lake Jesup. The TMDL report provides estimates of annual total phosphorus loadings from various sources into Lake Jesup, calibrated for the period from 1995-2002, which include surface runoff, baseflow, septic tanks, artesian input, atmospheric deposition, and inflow from the St. Johns River. Nutrient loadings from septic tanks are included based upon the number of septic tanks within 200 meters of any waterbody connected to Lake Jesup. The input referred to as "artesian inputs" reflects contributions from upwelling of the Floridan Aquifer from two springs (Clifton Springs and Lake Jesup Springs) which is separate from shallow groundwater seepage.



Figure 1-1. Location Map for Lake Jesup.

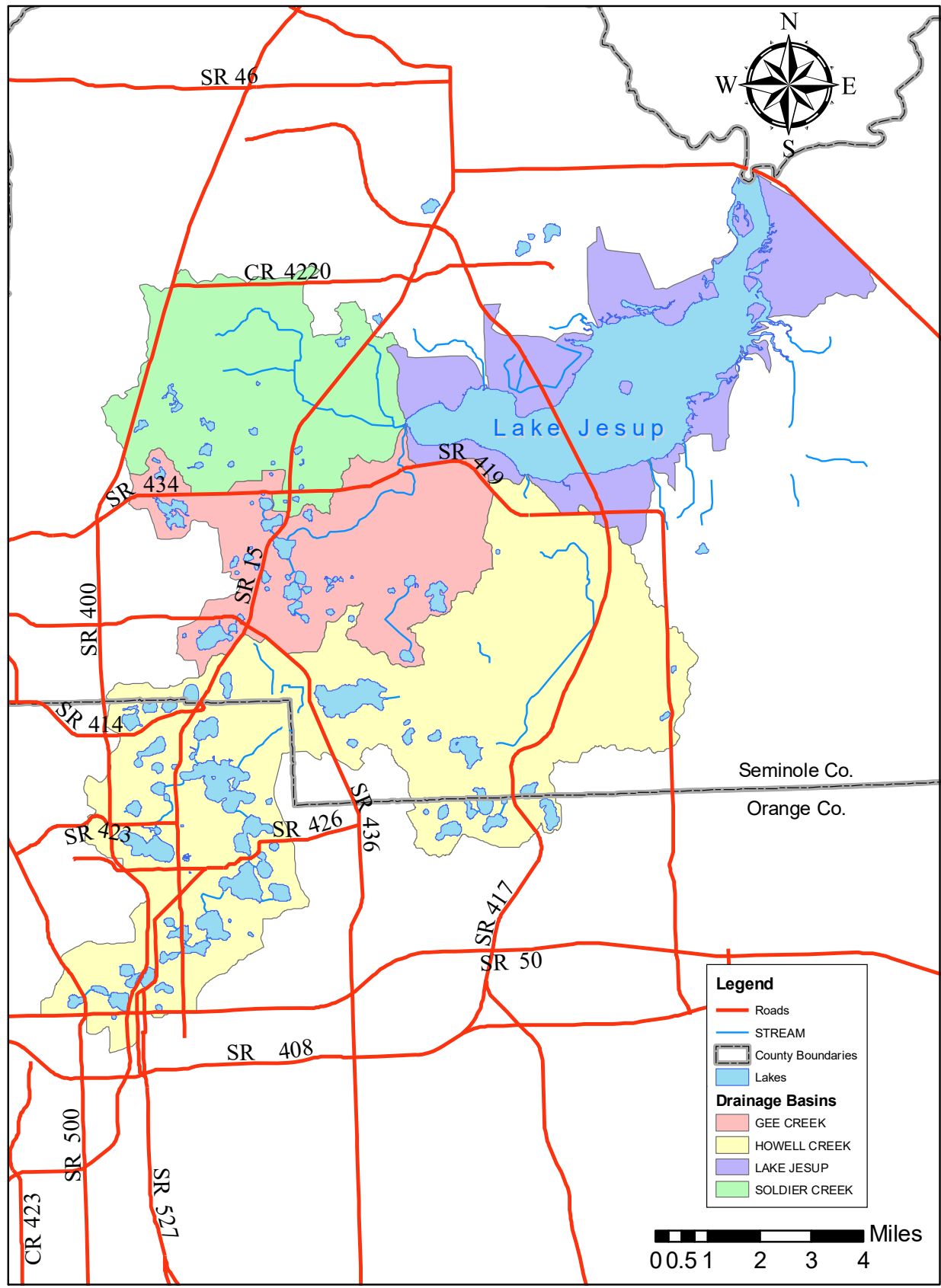


Figure 1-2. Lake Jesup Watershed and Sub-basin Areas.
(SOURCE: Final FDEP TMDL Report, 2006)

According to FDEP, estimates of hydrologic and nutrient loadings from shallow groundwater into Lake Jesup are partially included in the TMDL report. The percentage of the total stream flow that was baseflow, estimated using a hydrograph separation technique based on the measured flow in gauged streams, is also applied to the ungauged areas that are immediately adjacent to the lake, representing the shallow groundwater entering directly into the lake primarily around the perimeter of the lake. Additional nutrient loadings were added to the baseflow by FDEP to reflect loadings from septic tanks within 200 meters of the lake or a tributary. The baseflow loadings calculated using this method include the sum of tributary dry weather flow and seepage around the perimeter of the lake plus septic loadings. According to the TMDL report, the baseflow component contributed an annual average of 17,513 ac-ft/yr of water, 10,400 kg/yr of total nitrogen, and 3,300 kg/yr of total phosphorus to Lake Jesup during the period from 1995-2002.

An independent evaluation of the hydrologic and nutrient loadings from groundwater seepage to Lake Jesup was conducted by ERD from 2009-2010. Groundwater seepage meters were installed at 40 locations within Lake Jesup, and 9 separate monitoring events were conducted at each site over a 14-month field monitoring program from June 2009-August 2010. During each monitoring event, field measurements of seepage volume were conducted at each site, and a filtered water sample was collected for laboratory analysis. The mean measured seepage inflow into Lake Jesup during the field monitoring program was 1.18 liters/m²-day, equivalent to approximately 22,994 ac-ft/yr. This value is substantially greater than the TMDL estimate of the overall annual baseflow inputs to Lake Jesup of 17,513 ac-ft/yr. Groundwater seepage entering Lake Jesup was characterized by elevated levels of both total nitrogen and total phosphorus, with an estimated annual nitrogen influx of 89,183 kg/yr and an estimated annual phosphorus influx of 9,484 kg/yr. Each of these values is also substantially greater than the baseflow loading estimates provided in the TMDL report which includes both the lake and the entire watershed. Questions arose at the time as to the source of the nutrient loadings and whether the elevated nutrient concentrations reflect seepage reaching the lake or if the seepage is impacted by migration through the existing muck sediments.

The previous groundwater seepage study conducted by ERD was designed to determine the significance of groundwater seepage entering Lake Jesup in comparison with the estimated hydrologic and nutrient budgets provided in the TMDL report. However, the ERD study did not address the ultimate source of nutrient loadings entering Lake Jesup through groundwater seepage or the significance of existing sediments in regulating seepage characteristics.

A supplemental evaluation was conducted by ERD from January 2012-March 2013 to further evaluate the impacts of the existing sediments on seepage characteristics entering the lake. The potential impact of sediments on groundwater seepage were evaluated by conducting side-by-side comparisons of seepage meters installed in areas with and without existing sediments. Pairs of seepage meters with and without existing sediments were installed at 6 separate locations throughout Lake Jesup. The results of this study form the basis of this current report. This evaluation provides important information on sediment impacts on groundwater seepage which assists in the general understanding of nutrient dynamics within the lake and provides additional information to evaluate potential impacts of dredging projects within the lake.

1.2 Work Efforts Conducted by ERD

Field monitoring was conducted by ERD over a 15-month period from January 2012-March 2013 to evaluate the impacts of existing sediments on the hydrologic and water quality characteristics of shallow groundwater seepage inflows to Lake Jesup. Side-by-side groundwater seepage meters were installed at 6 locations within Lake Jesup, with one seepage meter in each pair exposed to the existing sediments and one meter installed on the firm lake bottom. Six separate monitoring events were conducted at each monitoring site over the 15-month field monitoring program. During each monitoring event, field measurements of seepage volume were conducted, and a filtered seepage sample was collected for laboratory analyses.

This report has been divided into four separate sections for presentation of the work efforts conducted by ERD. Section 1 contains an introduction to the report, background information on Lake Jesup and phosphorus loadings, and a general overview of the work efforts performed by ERD. A discussion of field and laboratory activities is given in Section 2. Section 3 contains a discussion of the results of the field and laboratory activities. A summary is presented in Section 4. Appendices are also attached which contain technical data and analyses used to support the information contained within the report.

SECTION 2

FIELD AND LABORATORY ACTIVITIES

2.1 Introduction

A schematic of a typical hydrologic cycle illustrating groundwater seepage to surface waters is given on Figure 2-1. Shallow groundwater seepage originates as precipitation which infiltrates into the ground. Water which is not evaporated or transpired by vegetation continues to infiltrate vertically through the ground until reaching the saturated water table zone. At this point, the groundwater begins to move laterally, down-gradient, until reaching the nearest waterbody.

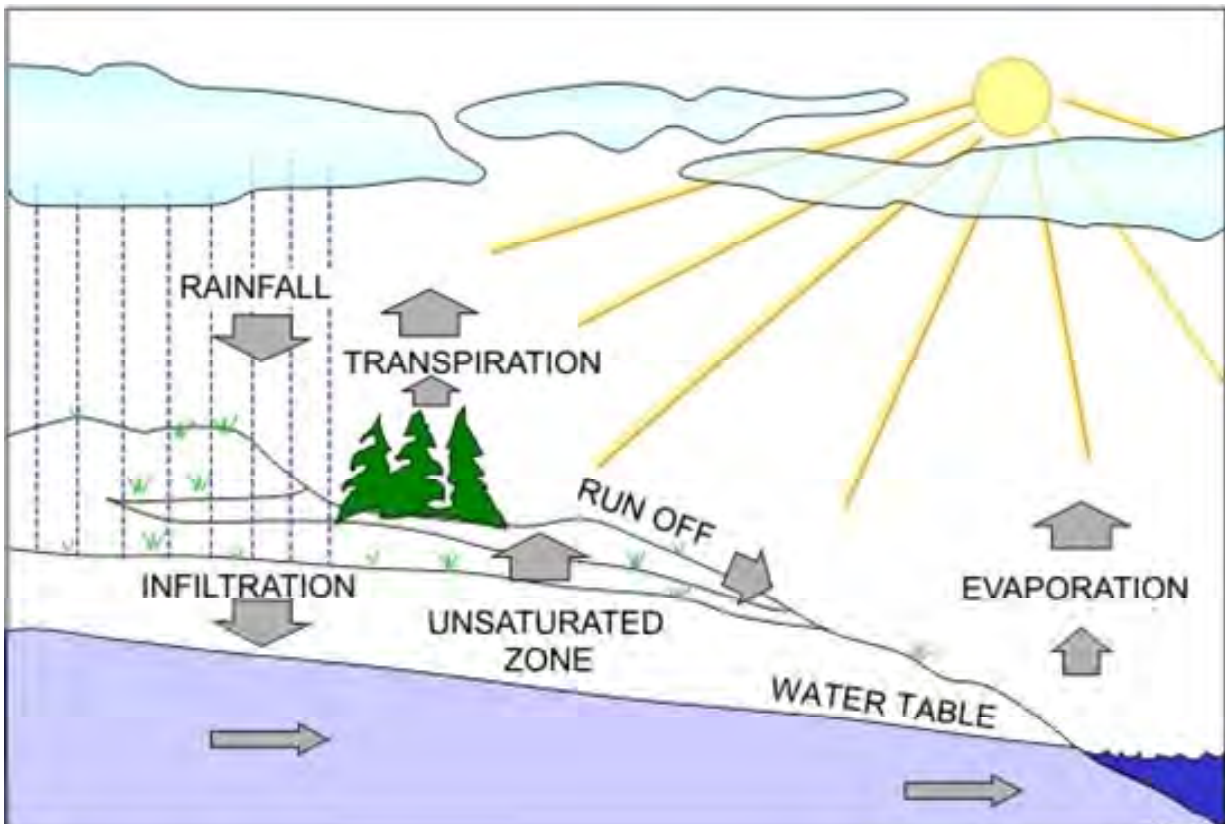


Figure 2-1. Hydrologic Cycle Illustrating Groundwater Seepage to Surface Waters.

The chemical characteristics of the groundwater seepage are impacted by a variety of factors, including: land cover; soil characteristics; travel distance through the soil; and other groundwater inputs from septic tanks, fertilizers, agricultural activities, wastewater disposal, and industrial activities. Many hydrologic models and TMDL evaluations incorrectly assume that groundwater seepage originates exclusively as a result of inputs from septic tanks which are adjacent to the receiving waterbody, and groundwater inputs are routinely under-estimated in terms of both volume and nutrient loadings.

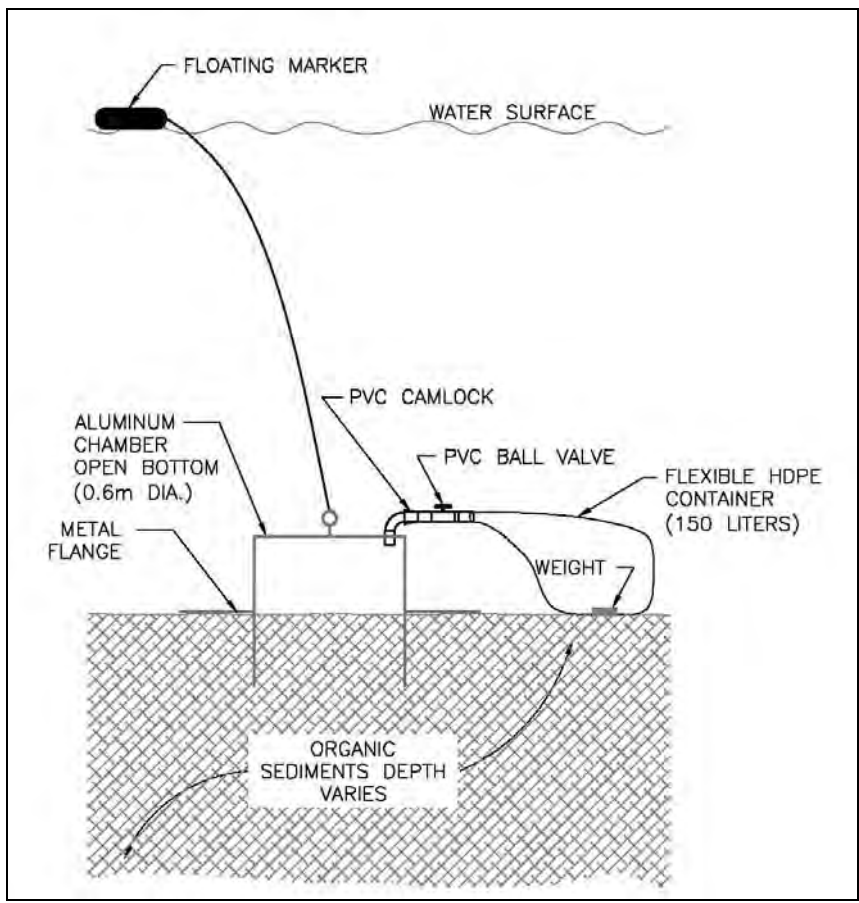
Field investigations were performed by ERD to evaluate the impacts of existing sediments on the quantity and quality of shallow groundwater seepage entering Lake Jesup. Seepage inflow into the lake in areas with and without existing sediments was quantified using pairs of underwater seepage meters installed at 6 locations throughout the lake. Seepage meters provide a mechanism for direct measurement of groundwater inflow into a lake by isolating a portion of the lake bottom so that groundwater seeping up through the bottom sediments into the lake can be collected and characterized. Use of the direct seepage meter measurement technique avoids errors, assumptions, and extensive input data required when indirect techniques are used, such as the Gross Water Budget or Subtraction Method, as well as computer modeling and flow net analyses.

With installation of adequate numbers and proper placement, seepage meters can be a very effective tool to estimate groundwater-surface water interactions. Seepage inflow is generally greatest along the perimeter of a waterbody, and the majority of seepage meters are typically placed in shallow shoreline areas. Seepage inflow generally decreases with distance from the shoreline, and fewer seepage meters are placed in central portions of a lake. Placement of seepage meters should also consider variability in upland land uses, topography, and sewage disposal techniques to properly characterize groundwater inflows to a lake. The seepage meter technique has been recommended by the U.S. Environmental Protection Agency (EPA) and has been established as an accurate and reliable technique in field and tank test studies (Lee, 1977; Erickson, 1981; Cherkauer and McBride, 1988; Belanger and Montgomery, 1992). One distinct advantage of seepage meters is that seepage meters can provide estimates of both water quantity and quality entering a waterbody, whereas estimated or modeling-based methods can only provide information on water quantity. ERD has conducted seepage monitoring in over 40 lakes within the State of Florida.

2.2 Field Activities

2.2.1 Seepage Meter Construction and Installation

Schematics of typical seepage meter installations used in Lake Jesup to evaluate sediment impacts on seepage are given on Figure 2-2. Seepage meters were constructed from a 2-ft diameter aluminum cylinder with a closed top and open bottom and a height of 36 inches. Each seepage meter isolated a sediment area of approximately 3.14 ft². The seepage meters used in Lake Jesup were also equipped with a 4-ft diameter flange which was welded to the outside of the aluminum cylinder to help stabilize the meters in areas of unconsolidated sediments, particularly in central portions of Lake Jesup, and to minimize settling of the meters over time. A photograph of a typical seepage meter used in Lake Jesup is given in Figure 2-3. The seepage meters were inserted into the lake sediments to the metal flange, resulting in a sediment penetration of approximately 18-24 inches, with approximately 8-12 inches of water trapped inside the seepage meter above the sediments. A large concrete weight (~75 lbs) was placed on top of each seepage meter.



a.
Seepage Meter
Installed on Top of
Existing Sediments

b.
Seepage Meter
Installed in Area
with Muck
Sediment Removed

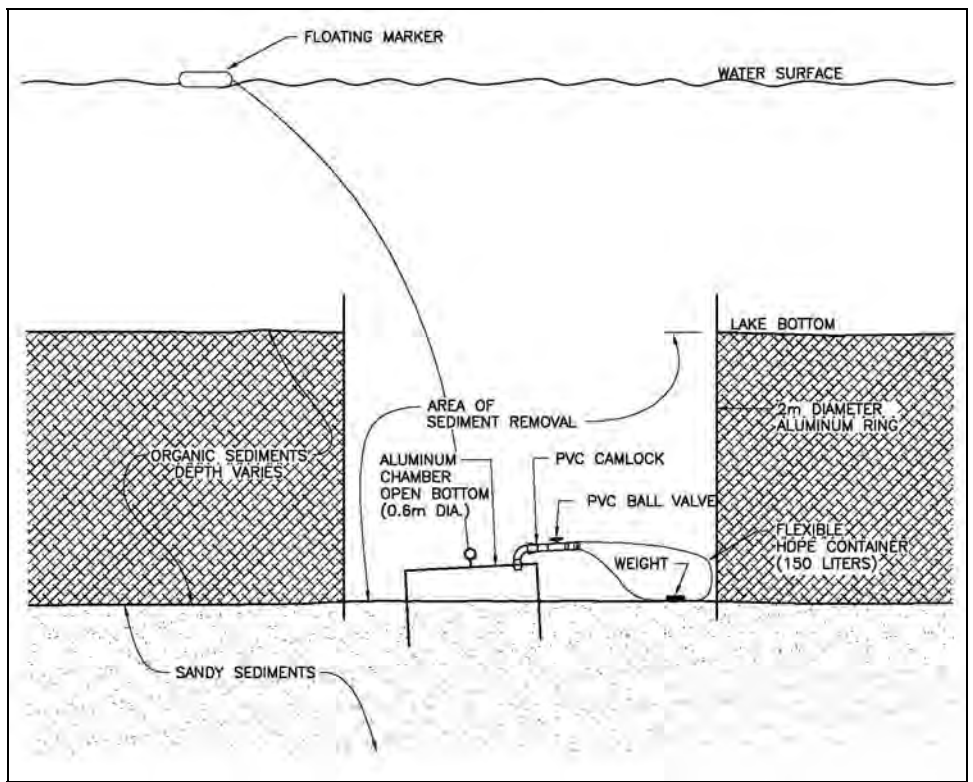


Figure 2-2. Typical Seepage Meter Installation.

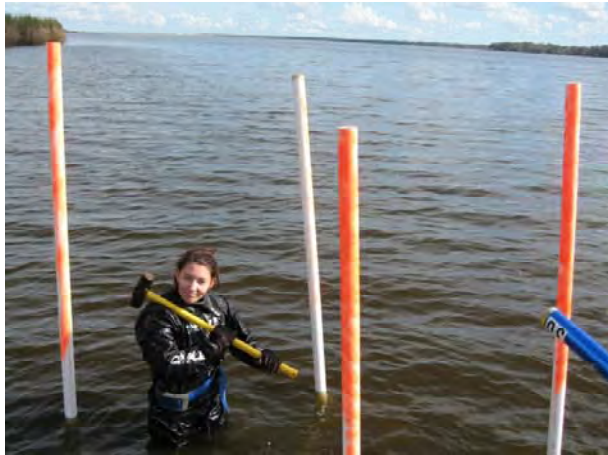


Figure 2-3. Typical Seepage Meter Used in Lake Jesup.

Pairs of seepage meters were installed at 6 locations in Lake Jesup. One of the seepage meters was installed on top of the existing sediments, as illustrated on Figure 2-2a, with the second seepage meter installed adjacent to the first seepage meter in an area where the existing organic sediments had been removed, as illustrated on Figure 2-2b. A 2-meter diameter and 1-meter tall aluminum ring was inserted through the sediments and into the firm sandy bottom of the lake. The organic sediments were pumped from the interior of the cylinder down to the firm sandy sediments using a 3-inch Mudhog-type pump. The seepage meter was then installed inside the chamber on the firm sandy sediments which form the original bottom of Lake Jesup. This protocol allowed a side-by-side comparison of the seepage characteristics collected in areas with and without the existing sediment accumulations.

The parent sediment material in Lake Jesup was primarily sand mixed with organic material. In many areas, the sand was cemented and dense, making it difficult to insert the seepage meter. Areas of blue clay mixed with sand were also observed.

Photographs of the installation process for the aluminum cylinders, including sediment removal, are given on Figure 2-4. The aluminum cylinder was inserted through the existing organic sediments to the firm sand bottom using a sledge hammer. The muck was then pumped from inside the chamber to expose the firm sand bottom of the lake. The organic material which was pumped from the cylinder consisted primarily of very fine flocculent particles which required a considerable amount of time to settle from the water column back into the sediment layer. When the installation was completed, each of the aluminum cylinders was marked using three to four 2-inch PVC posts to warn boaters of the potential hazard and to assist in locating the sites for collection of groundwater samples.



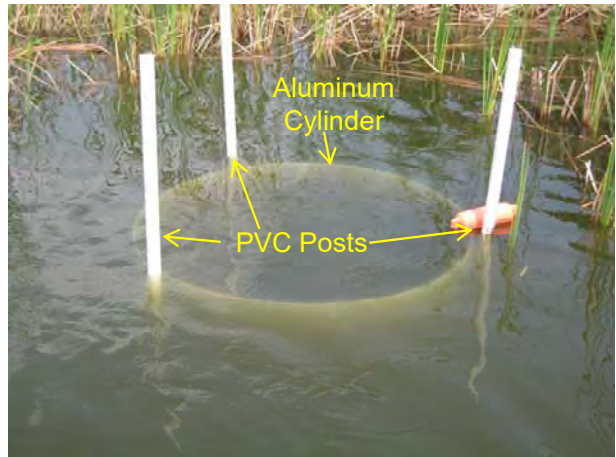
Cylinder inserted into sediments using sledge hammer



Muck is pumped from cylinder to firm bottom



Muck impacts on lake water



Completed installed chamber

Figure 2-4. Photographs of Installation of the Aluminum Cylinders and Sediment Removal.

In general, seepage meter pairs were installed primarily around the perimeter of the lake since seepage is most significant in shoreline areas. The seepage meters installed on the existing muck sediments were inserted through the unconsolidated sediment layer into the consolidated sediments. The seepage meters were inserted by repeatedly pounding around the perimeter of the meter using a 20-pound hammer weight until the seepage meter met significant resistance from the sediment material, and no additional movement of the meter was observed. Seepage meters installed in these areas were extremely stable, and additional settling of the seepage meters during the monitoring program is unlikely.

In central portions of the lake where the muck accumulations were deeper, the seepage meters were inserted through the surficial unconsolidated sediments into the layer of consolidated sediments. If possible, the flange was extended to the top of the consolidated sediment layer to achieve maximum stability for the seepage meter. The seepage meter installed on muck sediments in central portions of the lake was less stable than the shoreline meters since the parent bottom

material could not be reached. The meter penetrated into the consolidated sediment layer, which provided a relatively stable platform since the outer flange was resting on top of the consolidated layer. However, further limited settling of this meter over time cannot be ruled out.

A 0.75-inch PVC fitting was threaded into the top of each seepage cylinder. The 0.75-inch PVC fitting was attached to a female quick-disconnect PVC camlock fitting. A flexible polyethylene bag, with an approximate useable volume of 40 gallons (150 liters), was attached to the seepage meters using a quick-disconnect PVC male camlock fitting with a terminal ball valve. Each of the collection bags was constructed of 3-mil black polyethylene to prevent light penetration into the bag which could potentially stimulate photosynthetic activity within the sample prior to collection and result in an alteration of the chemical characteristics of the sample.

Prior to attachment to the seepage meter, all air was removed from inside the polyethylene collection bag, and the PVC ball valve was closed so that lake water would not enter the collection bag prior to attachment to the seepage meter. A diver then connected the collection bag to the seepage meter using the PVC camlock fitting. After attaching the collection bag to the seepage meter, the PVC ball valve was then opened, allowing seepage to enter the bag. Groundwater influx into the open bottom of the seepage meter is collected inside the flexible polyethylene bag. Photographs of the seepage sample collection process are given on Figure 2-5.



Diver preparing to retrieve collection bag;
sediment easily disturbed



Diver returning with collection bag
during seepage monitoring event

Figure 2-5. Photographs of the Seepage Sample Collection Process.

Each seepage meter was installed with a slight tilt toward the outlet point so that any gases which may be generated inside the seepage meter would exit into the collection bag, preventing buoyant conditions from developing inside the meter. Two 10-ounce plastic-coated fishing weights were placed inside each of the collection bags to prevent the bags from floating up towards the water surface as a result of trapped gases. The location of each pair of seepage meters was indicated by 2-inch PVC poles inserted around the perimeter of the aluminum cylinder.

Six pairs of seepage meters (12 seepage meters total) were installed in Lake Jesup on January 25 and 31, 2012. Locations for the seepage meters are indicated on Figure 2-6. The majority of the seepage meters were installed around the perimeter of the lake at a water depth of approximately 3 ft. A pair of seepage meters was also installed in a more central portion of the lake.

An expanded location map for seepage monitoring Site 1 is given on Figure 2-7. Site 1 is located on the northern shore of the western lobe of the lake where the inflow from Soldiers Creek enters Lake Jesup. Land use adjacent to seepage monitoring Site 1 includes a combination of wetland and upland forests.

An expanded location map for seepage monitoring Site 2 is given on Figure 2-8. Site 2 is located on the southern side of the western lobe adjacent to a residential community and the mouth of Howell Creek, and is the only seepage monitoring site with significant urbanized activity adjacent to the site. This site also exhibited some of the deepest and most flocculent sediments observed within the lake. The photographs included in Figure 2-5 were taken at this site.

An expanded location map for seepage monitoring Site 3 is given on Figure 2-9. Site 3 is located on the southern side of Lake Jesup slightly west of the inflow for Solary Creek. Watershed areas adjacent to Site 3 consist primarily of wetland and upland forested areas.

An expanded location map for seepage monitoring Site 4 is given on Figure 2-10. Site 4 is located in the northern-central portion of Lake Jesup adjacent to wetland marshes and upland areas used primarily for cattle grazing activities.

An expanded location map for seepage monitoring Site 5 is given on Figure 2-11. Site 5 is located adjacent to an expansive wetland area with upland land use consisting primarily of agricultural activities.

An expanded location map for seepage monitoring Site 6 is given on Figure 2-12. Site 6 is located in the northeastern portion of Lake Jesup adjacent to the inflows from Black Creek and Salt Creek. This site was located near the center portion of the lake to evaluate sediment impacts in areas other than the monitored shoreline areas.

2.2.2 Seepage Meter Monitoring

Polyethylene collection bags were attached to each of the 12 seepage meters at the time of installation. The initial seepage monitoring event was conducted during March 2012, approximately 6 weeks following installation. During this event, the volume of seepage collected at each site was measured and recorded. However, the collected sample was discarded since the initial sample represents a combination of seepage and lake water trapped inside the seepage meter at the time of installation. Beginning with the second monitoring event, samples were retained for laboratory analyses. Each of the 12 seepage meters was monitored on approximately a bi-monthly basis from January 2011-March 2012, with shorter event intervals during wet season conditions and longer event intervals during dry season conditions. Seepage monitoring events were conducted during the months of March, July, August, November, January and March. Five separate seepage monitoring events were conducted for evaluation of quantity and quality at each of the monitoring sites. The seepage meters were removed at the end of the monitoring program.

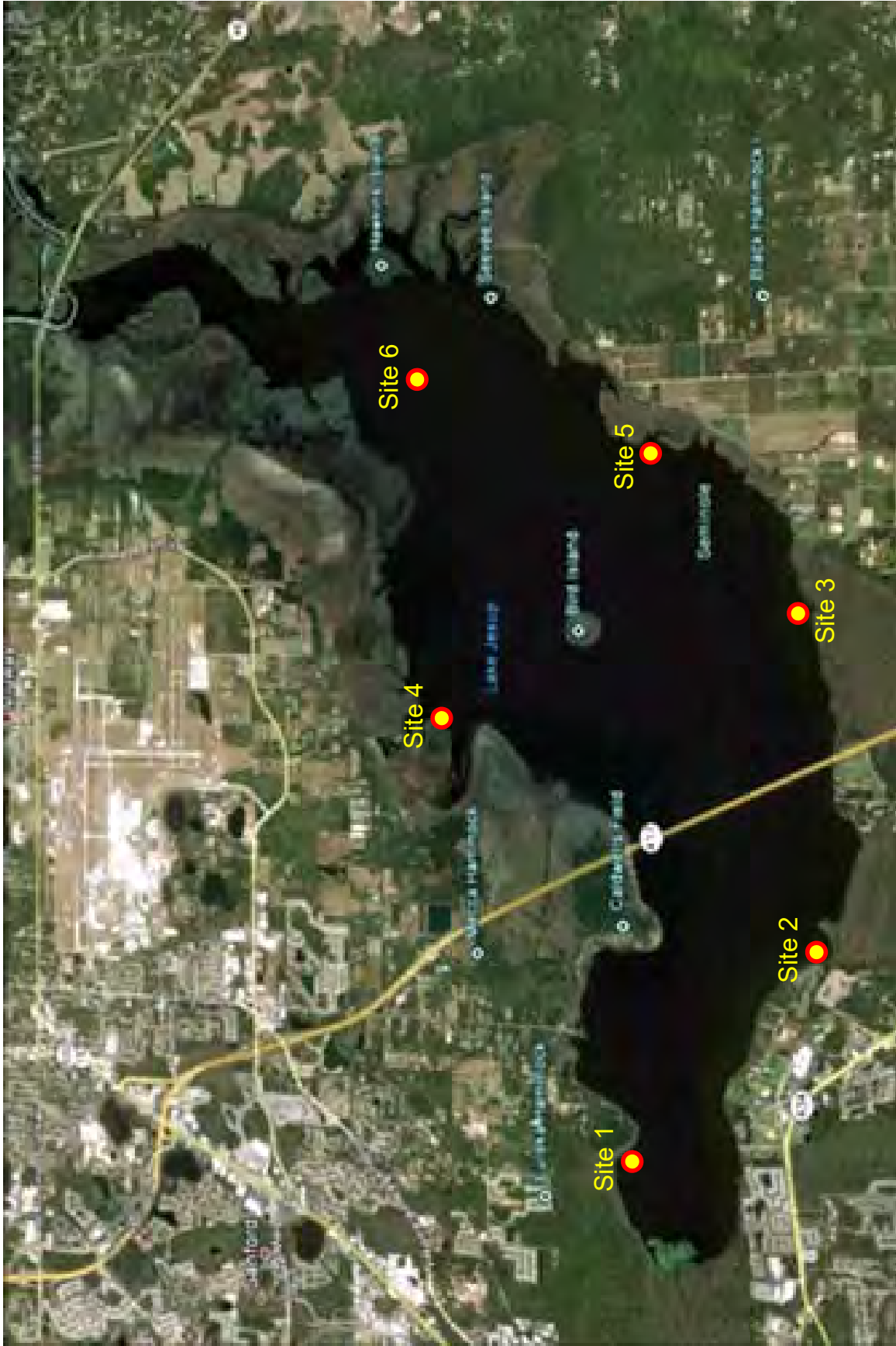


Figure 2-6. Locations for Seepage Meter Pairs Installed in Lake Jesup.

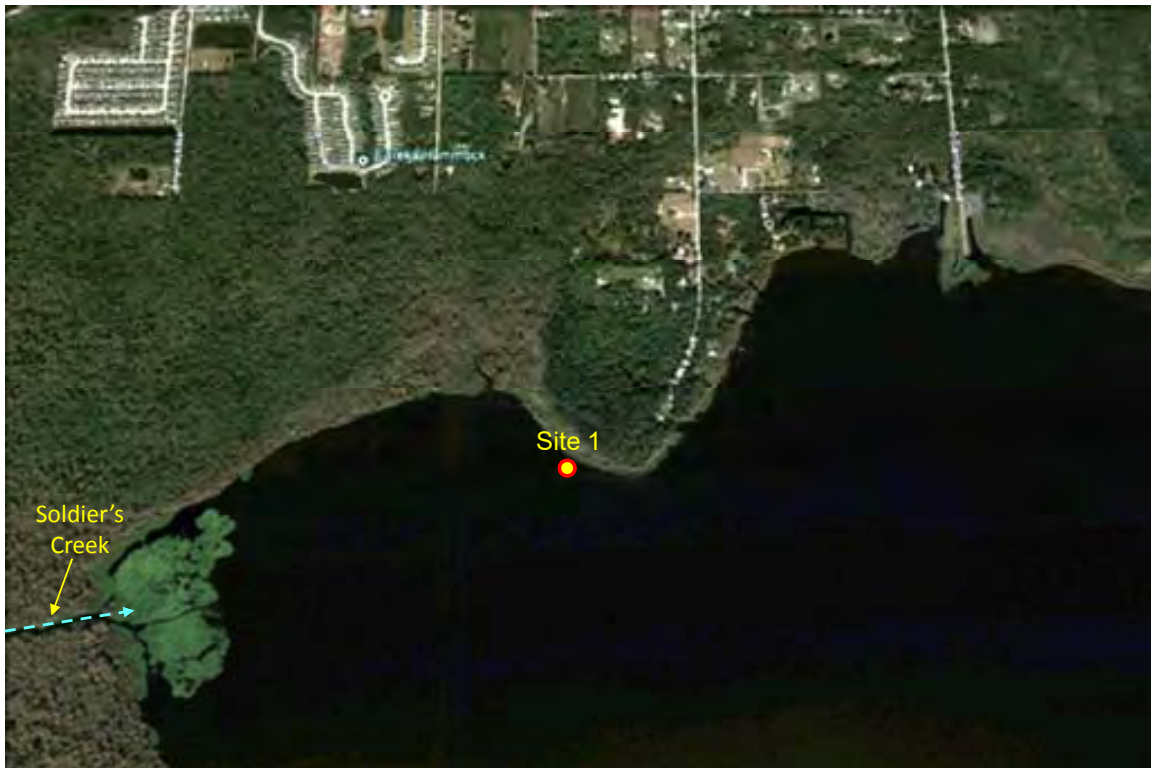


Figure 2-7. Expanded Location Map for Seepage Monitoring Site 1.

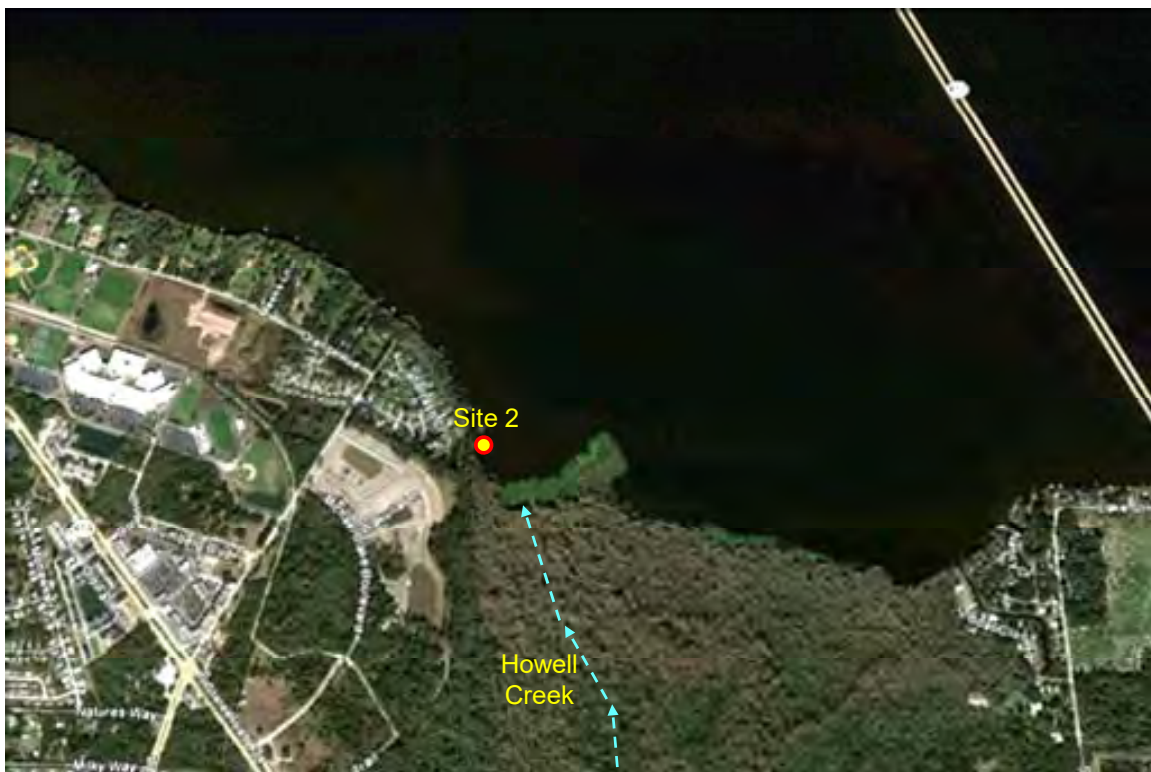


Figure 2-8. Expanded Location Map for Seepage Monitoring Site 2.

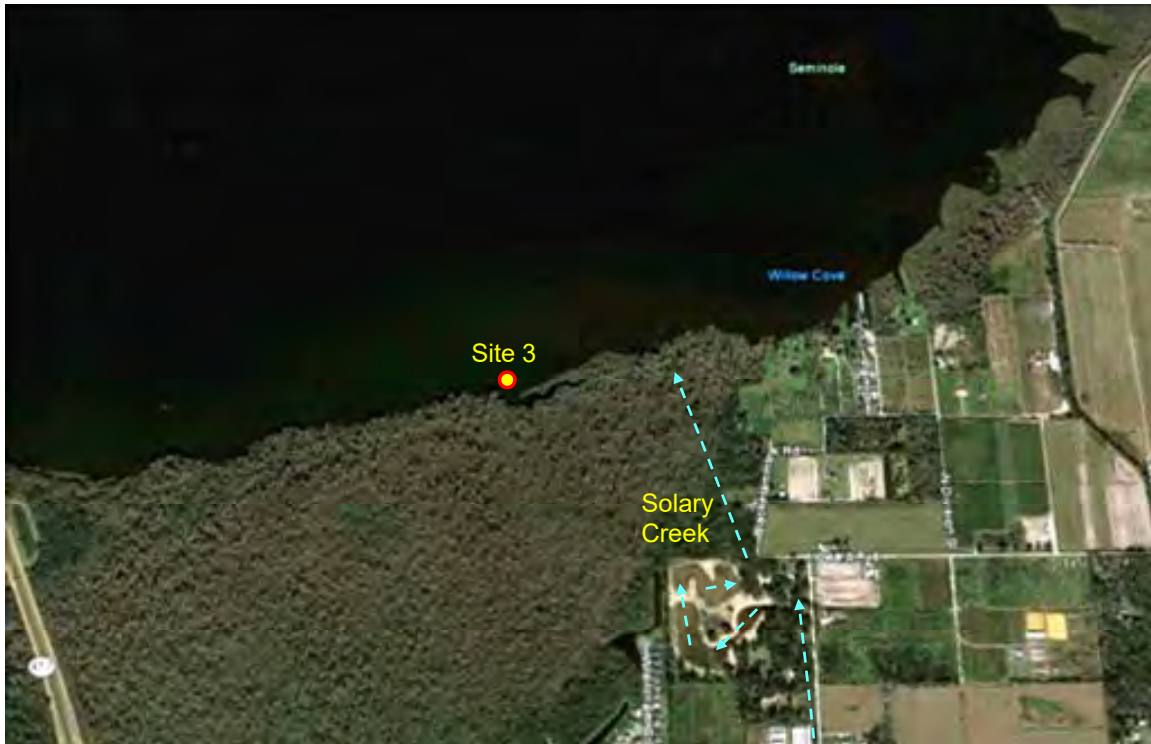


Figure 2-9. Expanded Location Map for Seepage Monitoring Site 3.

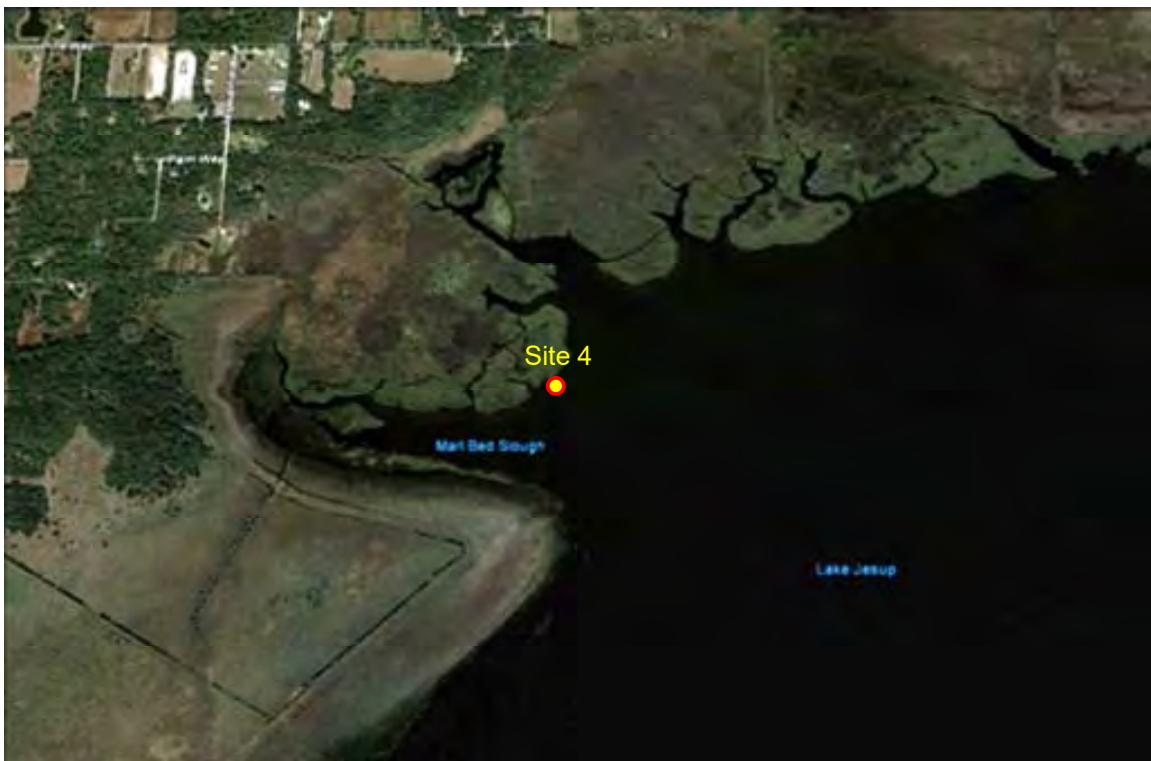


Figure 2-10. Expanded Location Map for Seepage Monitoring Site 4.

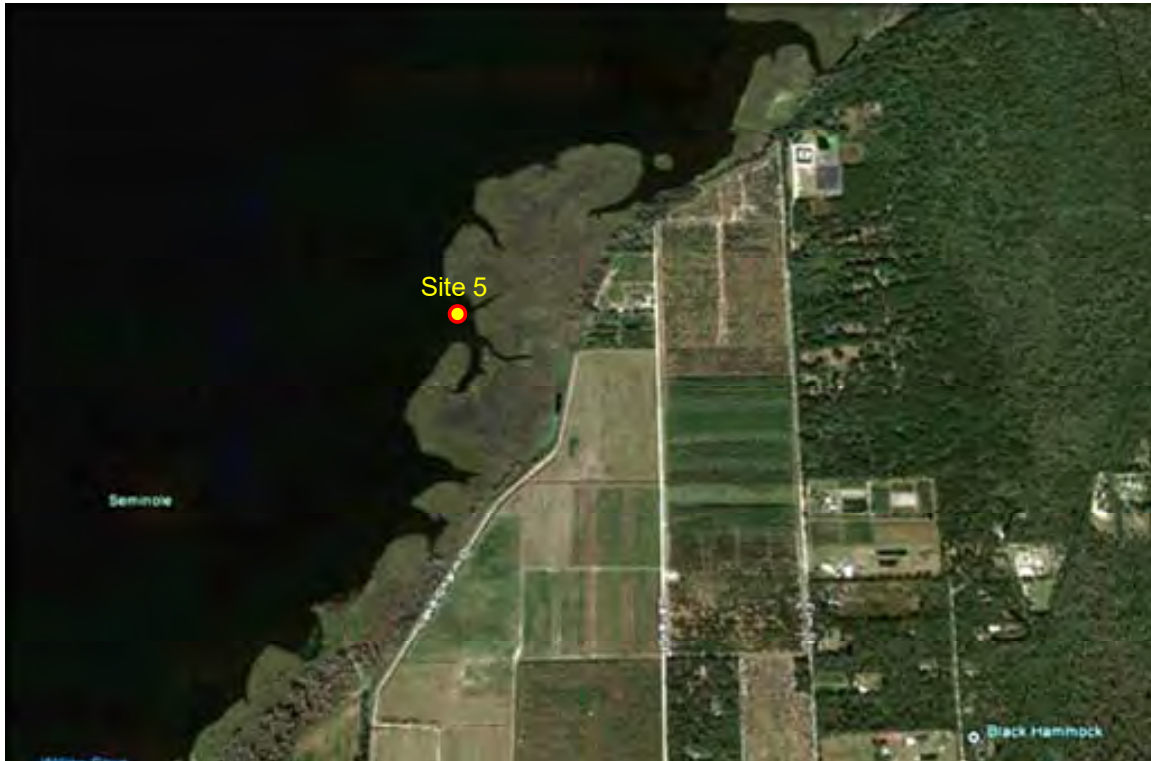


Figure 2-11. Expanded Location Map for Seepage Monitoring Site 5.



Figure 2-12. Expanded Location Map for Seepage Monitoring Site 6.

During the collection process, a diver was used to close the PVC ball valve and remove the collection bag from the seepage meter using the quick-disconnect camlock fitting. The collection bag was placed onto the boat and the contents were emptied into a polyethylene container. The volume of seepage collected in the container was measured using either a 4-liter graduated cylinder or a 20-liter graduated polyethylene bucket, depending on the collected volume.

During some of the initial monitoring events, seepage meter samples were found to contain turbidity or particles originating from the sediments isolated within the seepage meter. Since these suspended contaminants are not part of the seepage flow, all seepage meter samples collected for chemical analyses were field-filtered using a 0.45 micron disposable glass fiber filter typically used for filtration of groundwater samples. A new filter was used for each seepage sample. Seepage samples were filtered immediately following collection using a battery operated peristaltic pump at a flow rate of approximately 0.25 liter/minute. The filtered seepage sample was placed in ice for return to the ERD laboratory for further chemical analyses.

During collection of the seepage samples, information was recorded on the time of sample collection, the total volume of seepage collected at each site, and general observations regarding the condition of the seepage collection bags and replacement/repair details. The seepage flow rate at each location is calculated by dividing the total collected seepage volume (liters) by the area of the seepage meter and the time (days) over which the seepage sample was collected.

2.3 Laboratory Analyses

Each of the collected seepage samples was evaluated in the ERD Laboratory for general parameters and nutrients. A summary of laboratory methods and MDLs for analyses conducted on water samples collected during this project is given in Table 2-1. The ERD Laboratory is NELAC-certified (No. 1031026). Additional details on field operations, laboratory procedures, and quality assurance methodologies are provided in the ERD Comprehensive Quality Assurance Plan.

TABLE 2-1**ANALYTICAL METHODS AND DETECTION
LIMITS FOR LABORATORY ANALYSES**

MEASUREMENT PARAMETER		METHOD	METHOD DETECTION LIMITS (MDLs)¹
General Parameters	Hydrogen Ion (pH)	SM-21, Sec. 4500-H ⁺ B ²	NA
	Specific Conductivity	SM-21, Sec. 2510 B	0.2 µmho/cm
	Alkalinity	SM-21, Sec. 2320 B	0.5 mg/l
Nutrients	Ammonia-N (NH ₃ -N)	SM-21, Sec. 4500-NH ₃ G	0.005 mg/l
	Nitrate + Nitrite (NO _x -N)	SM-21, Sec. 4500-NO ₃ F	0.005 mg/l
	Total Nitrogen	SM-21, Sec. 4500-N C	0.01mg/l
	Orthophosphorus (SRP)	SM-21, Sec. 4500-P F	0.001 mg/l
	Total Phosphorus	SM-21, Sec. 4500-P B.5	0.001 mg/l

1. MDLs are calculated based on the EPA method of determining detection limits
2. Standard Methods for the Examination of Water and Wastewater, 21st Ed., 2005.

SECTION 3

RESULTS

A discussion of field and laboratory activities conducted by ERD to evaluate the impacts of the existing muck sediments on the quantity and quality of shallow groundwater seepage entering Lake Jesup is given in the following sections. These sections include a discussion of rainfall, quantity of data collected, seepage inflow rates, and chemical characteristics of groundwater seepage with and without sediment contact.

3.1 Rainfall Characteristics

Shallow groundwater seepage originates primarily as rainfall which infiltrates into shallow soils and migrates down gradient within a watershed until reaching a surface waterbody, channel, river, or stream. As a result, rainfall has a significant impact on the quantity of shallow groundwater seepage entering the lake.

A review of available rainfall recording stations in the vicinity of Lake Jesup was conducted to identify potential sources for estimation of historical rainfall characteristics in the general area of Lake Jesup as well as measured rainfall during the field monitoring program from January 2012-March 2013. Two separate rainfall recording stations were identified in the general vicinity of Lake Jesup. One site is identified as “Sanford Experimental Station” (NCDC Station No. 87982) which is located south of Lake Monroe, and west of downtown Sanford, approximately 6 miles northwest of Lake Jesup. Rainfall data at this site are available from June 1956-present. A second rainfall recording station, maintained by SJRWMD and identified as Citrus Road (Site No. 09992839), is located approximately 3.2 miles southwest of Lake Jesup and appears to be the closest recording rainfall site to the lake. However, meteorological data at this station are available only from 1995-present.

The purpose of the long-term historical rainfall station is to provide estimates of “normal” monthly rainfall in the vicinity of Lake Jesup. The Sanford Experimental Station is selected as the source of these data so that a longer historical period of record could be included. Monthly rainfall records were obtained for this site over the period from 1971-2000, and these data are used to reflect “normal” rainfall in the general vicinity of Lake Jesup. The location of the Sanford Experimental Station site is indicated on Figure 3-1.

Rainfall characteristics during the field monitoring program from January 2012-March 2013 were obtained from the SJRWMD Citrus Road (Site No. 09992839) recording site due to the closer proximity to Lake Jesup. Daily rainfall records are available at this site over the entire period of the field monitoring program for the seepage evaluation project. Therefore, rainfall recorded at the Citrus Road site is used to reflect actual rainfall in the vicinity of Lake Jesup during the field monitoring program. The location of the Citrus Road site is also given on Figure 3-1.

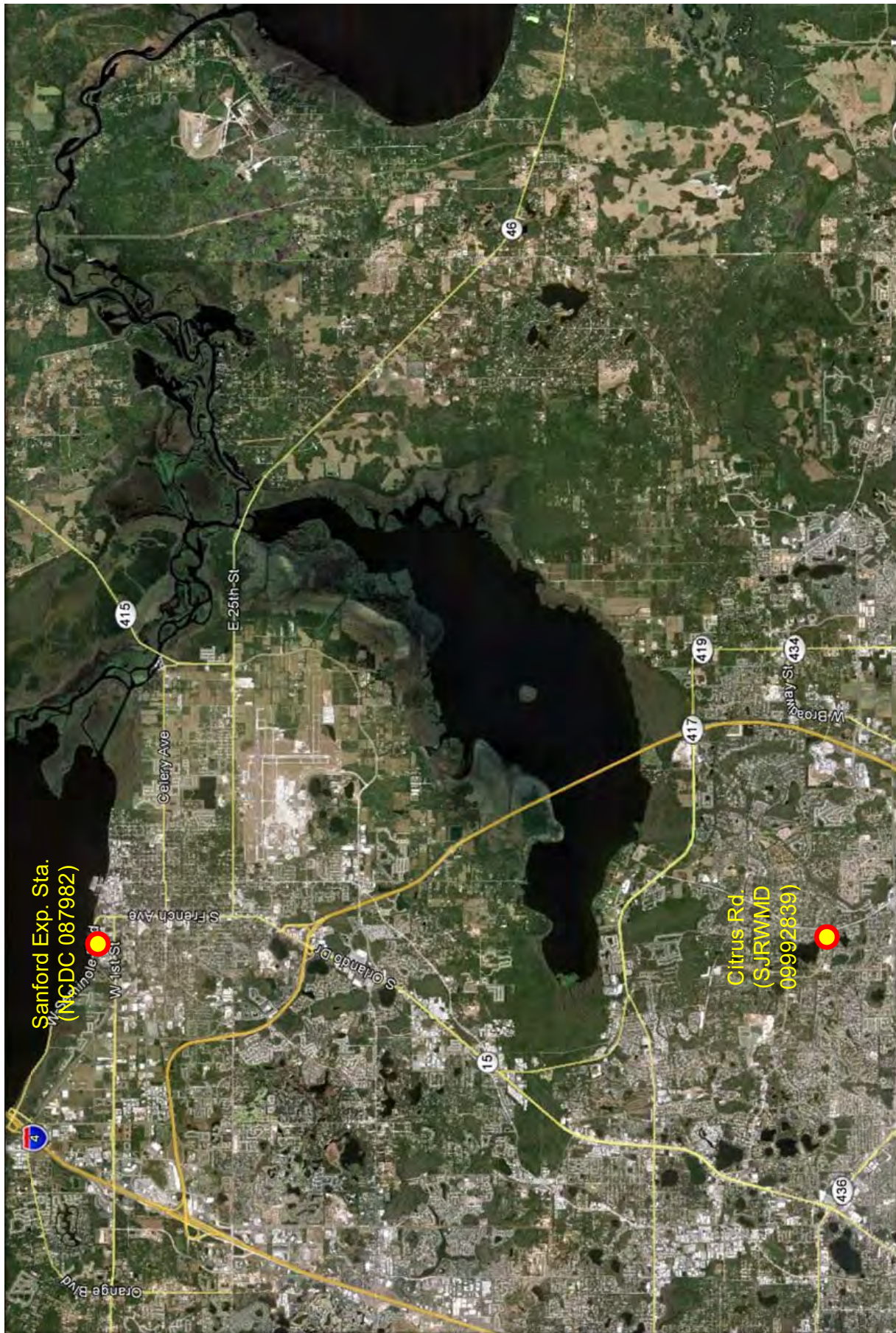


Figure 3-1. Locations of Identified Rainfall Recording Stations in the Vicinity of Lake Jesup.

A comparison of long-term “normal” rainfall in the vicinity of Lake Jesup (based upon the historical data at the Sanford Experimental Station site) and “actual” rainfall during the field monitoring program from January 2012-March 2013 (based upon rainfall records collected at the Citrus Road site) is given in Table 3-1. During the 15-month monitoring program, a total of approximately 59.90 inches of rainfall fell in the general vicinity of Lake Jesup. The long-term historical (normal) rainfall during the 15-month monitoring program is approximately 60.67 inches. The measured rainfall of 59.90 inches during the field monitoring program is approximately 1% less than the long-term annual mean of 60.67 inches.

TABLE 3-1

**SUMMARY OF MEASURED AND HISTORICAL
RAINFALL IN THE VICINITY OF LAKE JESUP**

MONTH		RAINFALL AT THE CITRUS ROAD SITE (January 2012-March 2013) (inches)	MEAN RAINFALL AT THE SANFORD EXPERIMENTAL STATION (87982 NCDC) (1971-2000) (inches)
2012	January	0.11	2.73
	February	1.88	2.93
	March	1.15	3.87
	April	1.29	2.32
	May	3.88	3.28
	June	14.08	6.95
	July	4.61	6.86
	August	10.92	7.75
	September	7.61	6.16
	October	7.09	3.71
	November	0.28	2.23
	December	2.09	2.35
2013	January	1.19	2.73
	February	1.84	2.93
	March	1.88	3.87
TOTALS:		59.90	60.67

A graphical comparison of measured and historical rainfall in the vicinity of Lake Jesup is given on Figure 3-2. Rainfall measured in the vicinity of Lake Jesup at the Citrus Road site during February, May, and December 2012 appears to be approximately normal compared with long-term rainfall characteristics. Substantially lower than normal rainfall occurred in the vicinity of Lake Jesup during January, March-April, July, and November 2012, and January-March 2013. Substantially higher than normal rainfall was observed during June, August, September, and October 2012.

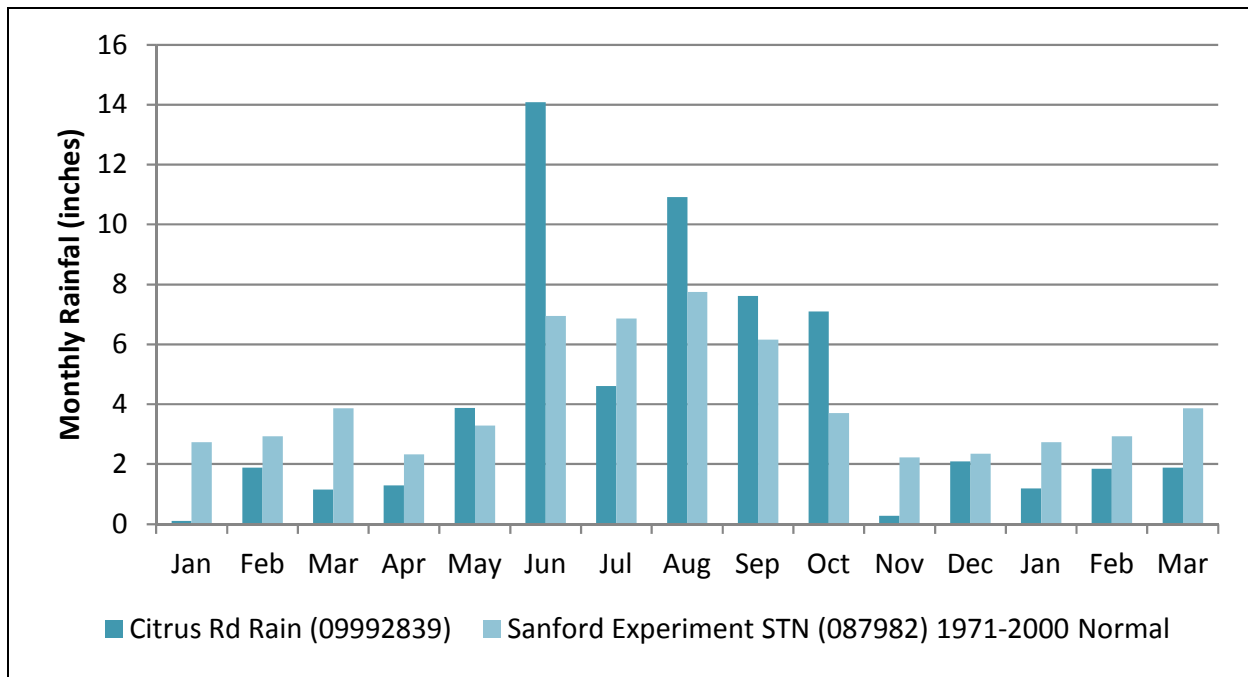


Figure 3-2. Comparison of Measured and Historical Rainfall in the Vicinity of Lake Jesup.

3.2 Hydrologic Inputs

3.2.1 Data Collection

Seepage influx into Lake Jesup was monitored over a 415-day period from January 25, 2012-March 15, 2013. Six separate seepage monitoring events were conducted to evaluate the quantity of shallow seepage entering Lake Jesup, with and without sediment contact, with laboratory analysis of the seepage samples conducted during 5 of the 6 monitoring events.

During the field monitoring program, 65 seepage samples were collected to measure volumetric inflow rates at the 12 monitoring sites. This value represents approximately 90% of the 72 potential seepage samples which would have been generated by conducting 6 monitoring events at each of the 12 sites. A graphical illustration of the number of samples collected at each of the seepage monitoring sites in Lake Jesup is given on Figure 3-3. Nine of the 12 seepage sites had useable inflow data during all 6 of the potential events. Two of the seepage monitoring sites produced useable inflow data during 5 of the 6 monitoring dates, with 1 site (Site 6), located in central portions of the lake where the equipment was most visible, producing useable inflow data during only 1 monitoring event.



Figure 3-3. Number of Useable Groundwater Seepage Inflow Samples Collected at the 6 Monitoring Sites.

The principle causes for the low percentage of useable seepage samples at Site 6 are vandalism of the seepage meters along with damage caused by wildlife. The external seepage meter at this site (with sediment contact) was uprooted from the sediments on multiple occasions, with resulting damage to the seepage meter fittings and collection bags. On most dates, the meter was either repaired or, if the damage was too severe, replaced with a new seepage meter. As a result, only 1 of the 6 potential samples was collected at this site.

The surficial sediments in Lake Jesup are extremely unconsolidated and easily disturbed. The process of retrieving the collected seepage samples using a diver stirred up plumes of flocculent sediment material which created a large area of elevated turbidity near the sampling location. A photograph of sediment resuspension during collection of seepage samples is given in Figure 3-4. These resuspended sediments had no impact on the seepage samples and is mentioned only to illustrate conditions within the lake.



Figure 3-4. Resuspended Sediments During Collection of Seepage Samples.

3.2.2 Seepage Inflow

A complete listing of individual seepage measurements conducted at each of the 12 monitoring sites during each of the monitoring events is given in Appendix A. Information is provided on the date and time of installation for each of the seepage meters, date and times for each of the field monitoring events, volume of seepage collected during each event, and the calculated seepage time and seepage rate. General comments and observations concerning the condition of the seepage meter and sample collection system are also provided.

A summary of measured seepage inflows to Lake Jesup from January 2012-March 2013 at each of the 6 pairs of monitoring sites is given in Table 3-2. Information is provided for the mean seepage inflow measured at each site, the measured minimum and maximum inflow rates, and the number of samples collected at each site. The majority of seepage inflow rates range from approximately 0.2-1.5 liters/m²-day. The mean seepage inflow rates listed on Table 3-2 and in Appendix A reflect weighted inflow rates rather than the mean of the individual measured inflow rates since the monitoring events are not evenly spaced. The mean inflow rate for each site is calculated according to the following equation:

$$\text{Mean Inflow Rate} = \frac{\text{Total Seepage Volume Collected}}{\text{Number of Days Included in Collected Samples}}$$

TABLE 3-2
SUMMARY OF MEASURED SEEPAGE INFLOWS
TO LAKE JESUP FROM JANUARY 2012-MARCH 2013

SITE	WITHOUT SEDIMENTS				WITH SEDIMENTS			
	Number of Samples	Seepage Rate (liters/m ² -day)			Number of Samples	Seepage Rate (liters/m ² -day)		
		Minimum Value	Maximum Value	Mean		Minimum Value	Maximum Value	Mean
1	6	0.36	0.84	0.55	6	0.51	1.08	0.82
2	5	0.34	3.82	2.11	6	0.35	1.38	0.75
3	6	0.34	0.96	0.56	6	0.66	1.10	0.84
4	6	0.01	0.77	0.26	6	0.26	1.19	0.50
5	6	0.20	0.55	0.33	6	0.24	0.97	0.50
6	5	0.11	0.51	0.27	2	0.46	0.55	0.51

A summary of mean seepage inflows at the Lake Jesup monitoring sites, with and without sediment contact, is given in Table 3-3. Mean inflow rates for the seepage meters with sediment contact were higher in value at 5 of the 6 monitoring sites, while only 1 site (Site 2) exhibited higher inflow rates in the seepage meter without sediment contact. The lower seepage inflow rates observed in the seepage meters installed inside the aluminum cylinders with the sediments removed can be at least partially explained by the type and consistency of the parent soil material which lies underneath the accumulated muck layers. As discussed in Section 2, the parent sandy bottom of Lake Jesup consists of a cemented mixture of sand and fine organic matter. It was extremely difficult to insert the seepage meters into this material to obtain a watertight seal. As a result, the lower measured seepage rates inside the aluminum cylinders are likely related to the inability to form a tight seal between the seepage meter and the parent lake bottom material.

TABLE 3-3

**SUMMARY OF MEAN SEEPAGE INFLOWS
AT THE LAKE JESUP MONITORING SITES**

SITE	MEAN SEEPAGE INFLOW (liters/m ² -day)	
	Without Sediments	With Sediments
1	0.55	0.82
2	2.11	0.75
3	0.56	0.84
4	0.26	0.50
5	0.33	0.50
6	0.27	0.51
Mean	0.68	0.65
Geometric Mean	0.50	0.64

Arithmetic mean and geometric mean values are provided at the bottom of Table 3-3 to reflect the overall mean seepage inflow rates for seepage meters with and without sediment contact. The arithmetic mean values are very similar, with a mean of 0.68 liters/m²-day for seepage meters without sediment contact compared with 0.65 liters/m²-day for seepage meters with sediment contact. The geometric mean value is also calculated for the seepage data since virtually all environmental data exhibit log-normal distributions, and a geometric mean may be a more accurate reflection of central tendency than a simple arithmetic mean. The geometric mean for seepage inflow without sediment contact is 0.50 liters/m²-day compared with 0.64 liters/m²-day for seepage collected in areas with sediment contact.

A statistical summary of measured seepage inflow rates at the 6 monitoring sites is given in Figure 3-5. A graphical summary of the monitoring data is presented in the form of Tukey box plots, also often called "box and whisker plots". The bottom of the box portion of each plot represents the lower quartile, with 25% of the data points falling below this value. The upper line of the box represents the 75% upper quartile, with 25% of the data falling above this value. The horizontal line within the box represents the median value, with 50% of the data falling both above and below this value. The vertical lines, also known as "whiskers", represent the 5 and 95 percentiles for the data sets. Individual values which fall outside of the 5-95 percentile range are indicated as **red dots**.

As indicated on Figure 3-5, median values (indicated by the blue horizontal lines in each of the box plots) are higher for Sites 1-5 for seepage meters placed with existing sediments compared with seepage meters installed without sediments. No conclusions can be made regarding relative seepage inflow rates at Site 6 since only one measurement was recorded in the seepage meter installed with sediment contact. A discussion of potential causes for the observed differences in measured seepage inflow rates is given in Section 3.2.4.

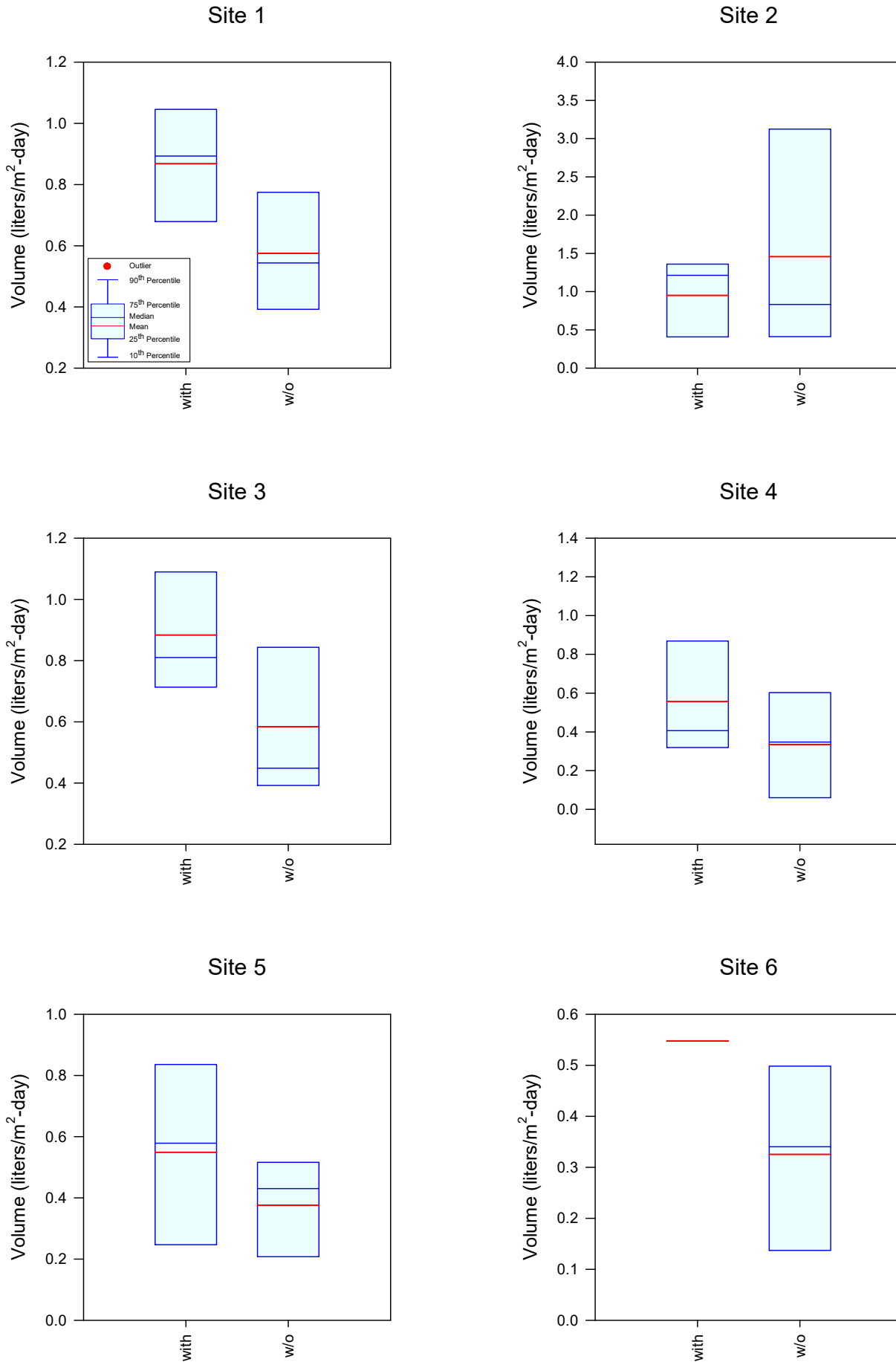


Figure 3-5.
Statistical Comparison of Measured Seepage Inflow Rates at the 6 Monitoring Sites With and Without Sediment Contact.

An analysis was conducted to determine if statistically significant differences exist between seepage inflow rates measured in seepage meters with and without sediment contact. A summary of an analysis of variance (ANOVA) comparison of seepage inflow rates in seepage meters installed in areas with and without sediments is given in Table 3-4. ANOVA comparisons were conducted using the PROC GLM procedure of SAS. The data sets were evaluated for normality and equality of variances prior to testing. The calculated model significance level is provided, with values of 0.05 or less indicating statistically significant differences at the 0.05 level of significance or better, and values in excess of 0.05 indicating a lack of statistical significance. Mean values are provided for seepage meters with and without sediment contact. The results of a Tukey grouping analysis are also provided which identify statistically similar treatment types. Seepage inflow rates are listed from highest to lowest for each treatment type.

TABLE 3-4

**ANOVA COMPARISON OF SEEPAGE INFLOW RATES
IN LAKE JESUP WITH AND WITHOUT SEDIMENT CONTACT**

DATA TREATMENT	MODEL SIGNIFICANCE LEVEL	CONDITION	MEAN VALUE (liters/m²-day)	TUKEY GROUPING
Normal Data	0.2743	Without	0.68	A
		With	0.65	A
Log-Transformed Data	0.0245	With	0.64	A
		Without	0.50	B

As indicated on Table 3-4, no statistically significant difference was detected between seepage inflow rates in Lake Jesup measured in areas with and without sediment contact using the collected data. However, when a log transformation was applied to the inflow data, the inflow rates observed in the chambers with sediment contact were statistically higher in value than inflow rates measured in seepage meters without sediment contact.

3.2.3 Seasonal Variability in Seepage Rates

As discussed in Section 3.1, rainfall in the vicinity of Lake Jesup was approximately normal during the field monitoring program. Since seepage originates from rainfall, seepage inflow to Lake Jesup should be higher during periods of frequent rainfall or following significant rain events.

A summary of mean seepage inflows to Lake Jesup for each of the 6 collection dates is given on Table 3-5. The mean values summarized in this table reflect the log-normal mean value for all seepage inflow data collected on each collection date. The values summarized in Table 3-4 appear to exhibit a slight seasonal pattern, with more elevated seepage inflow rates during wet season conditions and reductions in seepage inflow observed during dry season conditions.

TABLE 3-5

**MEAN SEEPAGE INFLOWS TO
LAKE JESUP BY COLLECTION DATE**

DATE	MEAN SEEPAGE INFLOW (liters/m ² -day)	
	Without Sediments	With Sediments
3/9/12	0.80	0.83
7/13/12	0.87	0.41
8/24/12	0.72	1.06
11/30/12	0.26	0.58
1/25/13	0.62	0.80
3/15/13	0.42	0.89

A graphical comparison of mean event seepage inflow rates to Lake Jesup during the field monitoring program in areas with and without sediment contact is given on Figure 3-6. Measured event rainfall depths from the Citrus Road site are also included for comparison purposes. In general, seepage inflow appears to be loosely correlated with rainfall in the watershed, with stable or increasing seepage values during periods of high rainfall, and decreasing seepage rates during periods of low rainfall.

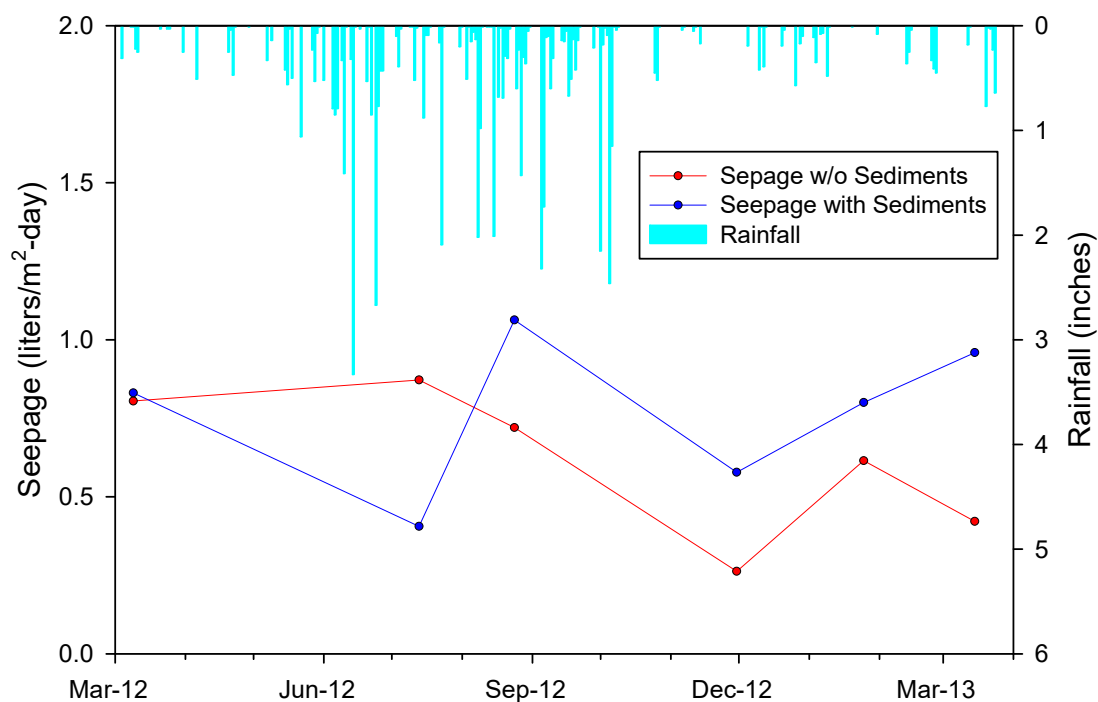


Figure 3-6. Temporal Variability in Mean Seepage Inflow Rates to Lake Jesup During the Field Monitoring Program.

3.2.4 Error Evaluation

Volumetric measurements of seepage inflow using the seepage meter method are subject to several potential sources of error. First, a loss of seepage could occur as a result of an incomplete seal between the perimeter of the seepage meter and the bottom sediments. If this seal is not intact, seepage inflow may escape from the seepage meter into the lake without being collected in the sample bag. This type of error is generally limited to areas with firm sandy sediments, such as those which occurred inside the aluminum cylinders. Consolidated muck sediments, such as those found throughout Lake Jesup, provide an excellent seal with the seepage apparatus. As discussed previously, loss of seepage may have occurred in the seepage meters installed on the sandy bottom.

A second potential for error exists if additional settling of the seepage meters occurs during the field monitoring program. As the seepage meter settles, the displaced water volume is forced into the seepage bag and is included in the seepage field measurements. This phenomenon was highly unlikely in the meters installed on the cemented sand bottom. In muck type sediments, this type of error is generally minimized by inserting the seepage meters until the thick consolidated organic material is reached. This was possible for many of the shoreline seepage meters installed in Lake Jesup, and error from additional settling of the seepage meters is not a significant concern in these portions of the lake. All of the shoreline seepage meters were installed at least into the consolidated sediment layer and were pounded into the sediments until no additional movement of the seepage meter occurred. Although additional settling of the seepage meters cannot be ruled out in these areas, any additional movement should be very minimal. No visual changes in seepage meter profiles were observed by the field crew at any of the monitoring sites.

However, the seepage meter installed in a more central portion of the lake (Site 6) was located in an area with deeper muck accumulations, and it was not possible to insert the seepage meter into the firm organic sediments. The enlarged flange welded onto the seepage meters (Figure 2-3) is intended to both stabilize the seepage meter and minimize settling in unconsolidated sediments. However, errors in seepage measurements created by settling at Site 6 are still possible, but thought to be relatively minimal.

3.3 Chemical Characteristics of Seepage Samples

Seepage samples collected during the final 5 of 6 seepage monitoring events in Lake Jesup were submitted for laboratory analyses. The initial samples were discarded since they reflected a combination of seepage and residual lake water from the seepage meter installation. A complete listing of laboratory measurements conducted on individual seepage samples collected at each of the 12 monitoring sites is given in Appendix B. A total of 54 seepage samples was collected during the field monitoring program for laboratory analyses. This value reflects approximately 90% of the number of potential samples for laboratory analyses which would have been generated by conducting 5 monitoring events at each of the 12 monitoring sites (60 potential seepage samples).

A summary of mean chemical characteristics of seepage samples collected in Lake Jesup from January 2012-March 2013 is given in Table 3-6. The data summarized in this table reflect the volume-weighted mean characteristics for each of the evaluated parameters at each monitoring site.

TABLE 3-6

**MEAN CHARACTERISTICS OF GROUNDWATER
SEEPAGE COLLECTED AT THE LAKE JESUP SEEPAGE
MONITORING SITES FROM JANUARY 2012-MARCH 2013**

SITE	SAMPLE DESCRIPTION	NUMBER OF SAMPLES COLLECTED	pH (s.u.)	ALK. (mg/l)	SPEC. COND. ($\mu\text{mho/cm}$)	NH ₃ -N ($\mu\text{g/l}$)	NO _x -N ($\mu\text{g/l}$)	TOTAL N ($\mu\text{g/l}$)	SRP ($\mu\text{g/l}$)	TOTAL P ($\mu\text{g/l}$)
1	Without	5	7.43	90.0	764	378	2,167	3,761	143	160
	With	5	7.37	89.4	745	894	1,114	3,449	135	159
2	Without	4	7.65	129	361	632	19	766	118	141
	With	5	7.63	126	465	1,330	361	2,022	205	237
3	Without	5	7.55	137	976	1,424	2,209	5,192	416	452
	With	5	7.41	104	899	1,521	249	3,462	177	219
4	Without	5	7.64	163	1,044	991	4,004	6,558	741	790
	With	5	7.47	132	985	1,834	2,360	5,664	582	623
5	Without	5	7.52	152	1,388	3,015	1,211	5,604	303	369
	With	5	7.36	98.1	961	1,231	502	3,103	34	120
6	Without	4	7.47	234	2,081	4,453	2,122	7,934	1,298	1,565
	With	1	7.21	134	1,042	3,038	63	4,649	30	34

In general, groundwater seepage entering Lake Jesup was found to be approximately neutral to slightly alkaline in pH, with measured values ranging from 7.43-7.65 in seepage collected without sediment contact, and values ranging from 7.21-7.63 in samples collected with sediment contact. Seepage entering Lake Jesup was also moderately to well buffered, with the majority of measured alkalinity values in excess of 100 mg/l. Alkalinity values in seepage collected without sediment contact ranged from 90-234 mg/l, while alkalinity values in samples collected with sediment contact ranged from 89.4-134 mg/l. In general, samples collected without sediment contact appear to exhibit somewhat higher alkalinity values than samples collected with sediment contact, suggesting that the sediments may consume alkalinity from the seepage during migration through the sediment layers.

Seepage samples collected in Lake Jesup were also characterized by moderate to elevated levels of specific conductivity. Mean conductivity values in sediments collected without sediment contact ranged from 361-2,081 $\mu\text{mho/cm}$, while conductivity values in samples collected with sediment contact ranged from 465-1,042 $\mu\text{mho/cm}$. The data suggests that the sediments may also be consuming dissolved ions from the seepage during migration through the sediments, resulting in lower conductivity values after sediment contact.

Measured concentrations of ammonia in groundwater seepage were highly variable throughout Lake Jesup in samples collected both with and without sediment contact. Mean ammonia concentrations in samples collected without sediment contact ranged from 378-4,453 $\mu\text{g/l}$, while samples collected with sediment contact ranged from 894-3,038 $\mu\text{g/l}$. Although the data are highly variable, the sediments do not appear to either add or remove ammonia inputs from groundwater seepage.

Measured concentrations of NO_x were also highly variable in seepage samples collected throughout Lake Jesup. Mean NO_x concentrations in seepage samples collected with sediment contact ranged from 19-4,004 $\mu\text{g/l}$, while NO_x concentrations in seepage collected with sediment contact ranged from 63-2,360 $\mu\text{g/l}$. In contrast to ammonia, NO_x concentrations appear to be somewhat different in samples collected with and without sediment contact. In general, seepage samples collected without sediment contact exhibited substantially higher concentrations of NO_x compared with samples collected with sediment contact. These data suggest that denitrification processes may be responsible for removing NO_x during migration through the sediments. Measured concentrations of total nitrogen in groundwater seepage entering Lake Jesup were also highly variable in value.

Measured total nitrogen concentrations in seepage samples collected without sediment contact ranged from 766-7,934 $\mu\text{g/l}$, while total nitrogen concentrations in seepage samples collected with sediment contact ranged from 2,022-5,664 $\mu\text{g/l}$. Overall, total nitrogen concentrations were higher in seepage collected without sediment contact than in samples collected with sediment contact, further suggesting that denitrification processes may be responsible for removing nitrogen in seepage during migration through the organic sediment layers.

Measured concentrations of SRP were both highly variable and high in value in seepage samples collected from Lake Jesup. Mean SRP concentrations in samples collected without sediment contact ranged from 118-1,298 $\mu\text{g/l}$, while mean SRP concentrations in seepage samples collected with sediment contact ranged from 30-582 $\mu\text{g/l}$. Overall, phosphorus concentrations in seepage collected without sediment contact were substantially greater in value than samples collected with sediment contact, suggesting that SRP removal may occur during migration of the seepage through the organic sediment layers.

A similar trend is also apparent for total phosphorus, with mean total phosphorus concentrations in seepage samples collected without sediment contact ranging from 141-1,565 $\mu\text{g/l}$, and total phosphorus concentrations in samples with sediment contact ranging from 34-623 $\mu\text{g/l}$. Overall, the mean total phosphorus concentration in samples collected without sediment contact appears to be much greater in value than total phosphorus concentrations collected in seepage with sediment contact.

As indicated on Figure 3-3, the seepage monitoring sites are numbered in order from west to east, with Site 1 located on the west end of the lake and Site 6 on the east end. As indicated on Table 3-6, a distinct concentration gradient is present in seepage characteristics across Lake Jesup, with increasing concentrations of alkalinity, ammonia, total nitrogen, SRP, and total phosphorus from west to east. This gradient is highly apparent for seepage collected on the sand bottom, which reflects the characteristics of seepage reaching the lake bottom, and is much less apparent for seepage which has migrated through the sediment layer. These data suggest that the sediments may be modifying the characteristics of seepage which results in more uniform seepage characteristics which actually discharge into Lake Jesup.

A statistical comparison of measured seepage pH values in samples collected with and without sediment contact is given on Figure 3-7. Mean seepage pH values appear to be relative similar in samples collected with and without sediment contact at Sites 1, 3, and 4, with slightly more elevated pH measurements observed in samples collected without sediment contact at Sites 2 and 5. No comparison can be made for pH values at Site 6 since only one sample is available which was collected with sediment contact. In general, measured sediment pH values without sediment contact appear to exhibit a higher degree of variability than samples collected with sediment contact for Sites 1, 3, 4, and 5.

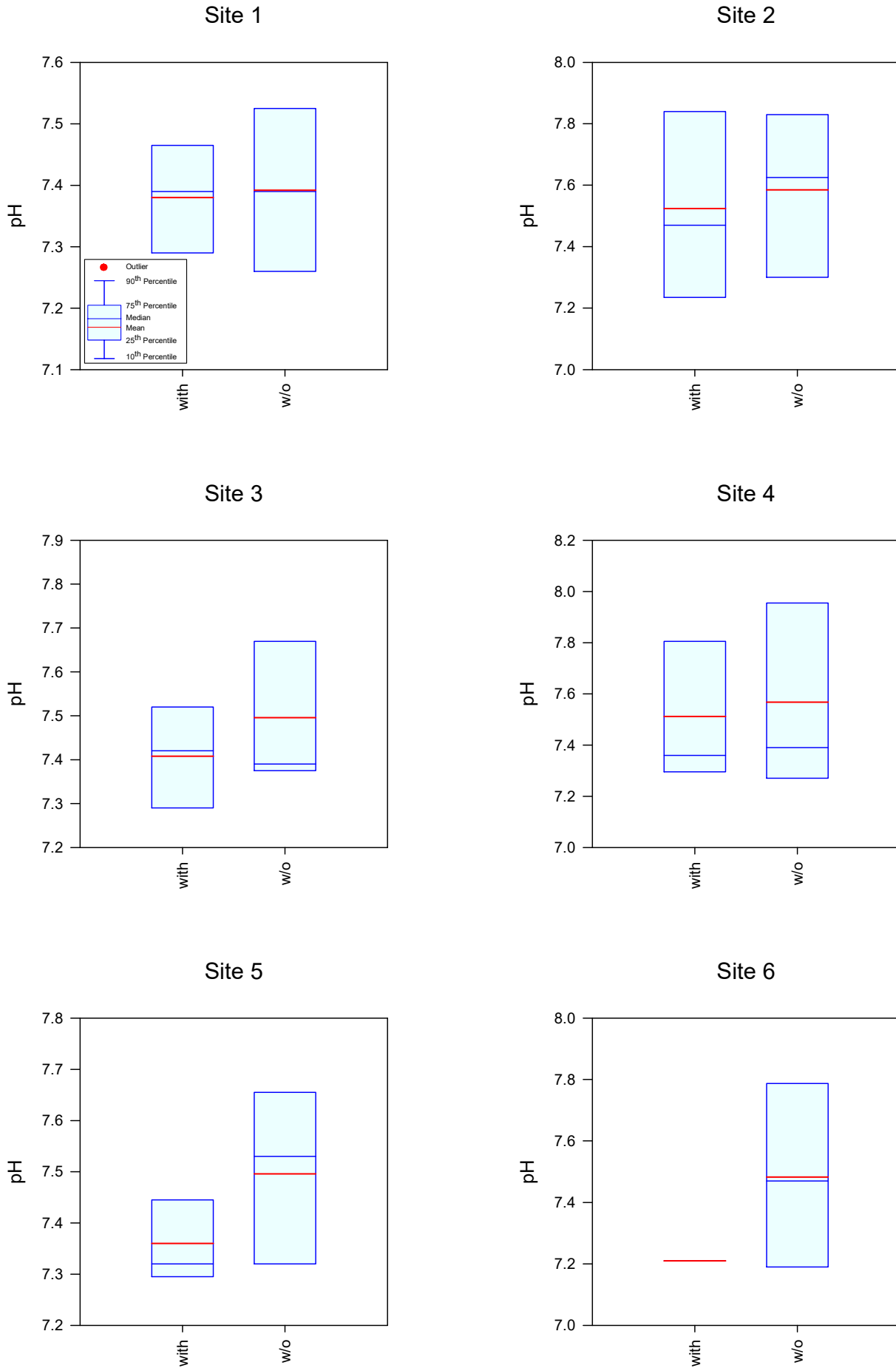


Figure 3-7.
Statistical Comparison of pH Values in Seepage Samples Collected With and Without Sediment Contact.

A statistical comparison of measured seepage alkalinity values in samples collected with and without sediment contact is given on Figure 3-8. Measured alkalinity values exhibited a relatively wide range of variability in concentrations at several of the monitoring sites. In general, more elevated levels of alkalinity were observed in samples collected without sediment contact for Sites 2, 3, and 5, with relatively similar values between samples collected with and without sediments at Site 1 and a more elevated median value observed for samples with sediment contact at Site 4. Measured alkalinity values were also highly variable within the lake, with a general trend of increasing alkalinity from west to east across Lake Jesup.

A statistical comparison of measured conductivity values in seepage samples collected with and without sediment contact is given on Figure 3-9. Median conductivity values at Sites 1 and 3 are relatively similar in samples collected with and without sediment contact. However, measured conductivity values at Sites 4 and 5 appear to be greater in samples collected without sediment contact, suggesting that migration through the sediments may reduce available ions entering the lake through groundwater seepage. The opposite pattern was observed at Site 2 where a higher level of conductivity was observed in samples collected with sediment contact compared to samples collected without sediment contact. Measured conductivity values were also highly variable throughout the lake, with a general trend of increasing conductivity from west to east within Lake Jesup.

A statistical comparison of measured ammonia concentrations in seepage samples collected with and without sediment contact is given on Figure 3-10. Median ammonia concentrations were higher in samples collected with sediment contact at Sites 1, 2, 3, and 4, with relatively similar median values observed at Site 5. Overall, the data suggests that ammonia may be released from the sediments into groundwater seepage although the pattern does not appear to be uniform throughout the lake.

A statistical comparison of measured NO_x concentrations in seepage samples collected with and without sediment contact is given on Figure 3-11. At Sites 1 and 3, samples collected without sediment contact exhibited a much higher median concentration for NO_x. Relatively similar NO_x concentrations were observed between samples collected with and without sediment contact at Sites 4 and 5, with substantially higher NO_x concentrations observed in samples collected with sediment contact at Site 2. These data also suggest that sediments may be impacting NO_x concentrations, although the trend is variable throughout the lake.

A statistical comparison of concentrations of total nitrogen in seepage samples collected with and without sediment contact is given on Figure 3-12. Seepage concentrations of total nitrogen were relatively similar at Site 1 between samples collected with and without sediment contact. Samples with sediment contact exhibited higher median concentrations of total nitrogen at Sites 2 and 4, while the highest total nitrogen concentrations at Sites 3 and 5 occurred in seepage meters without sediment contact. Similar to trends previously observed for NO_x, sediment impacts on seepage characteristics appear to be highly variable throughout Lake Jesup, with sediments in some areas resulting in increases in total nitrogen and sediments in other areas resulting in decreases in total nitrogen.

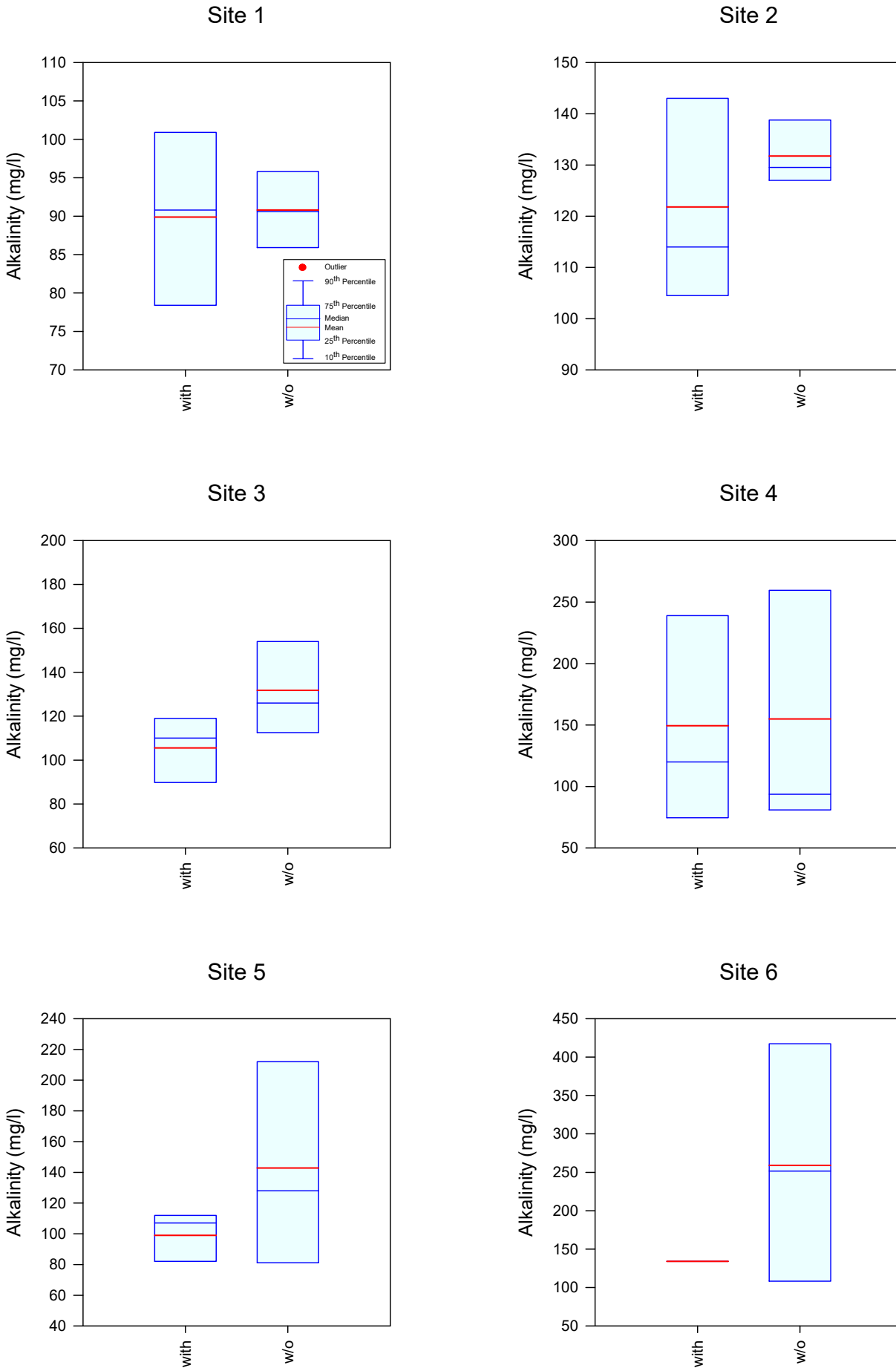


Figure 3-8.

Statistical Comparison of Alkalinity Values in Seepage Samples Collected With and Without Sediment Contact.

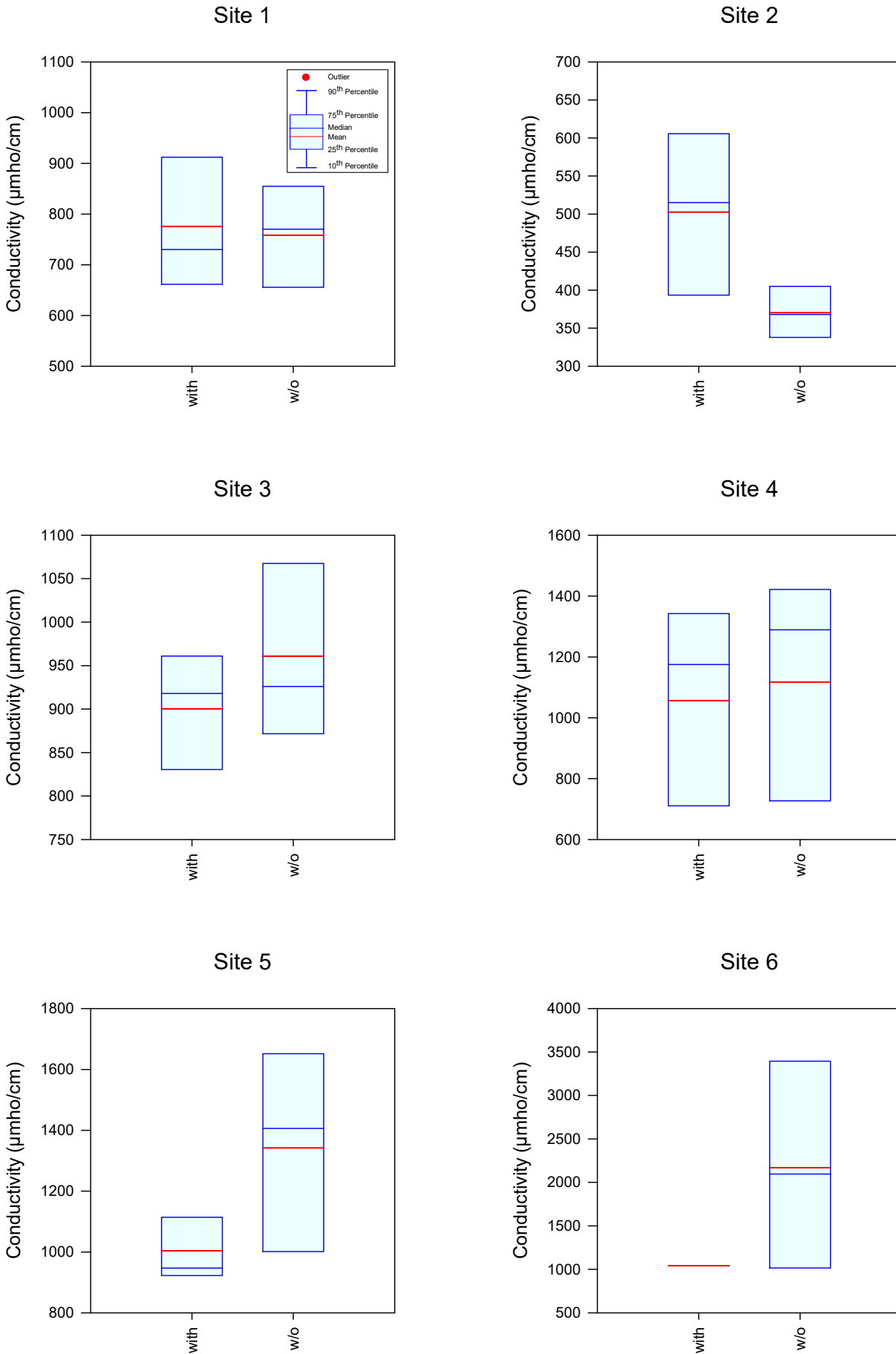


Figure 3-9. Statistical Comparison of Conductivity Values in Seepage Samples Collected With and Without Sediment Contact.

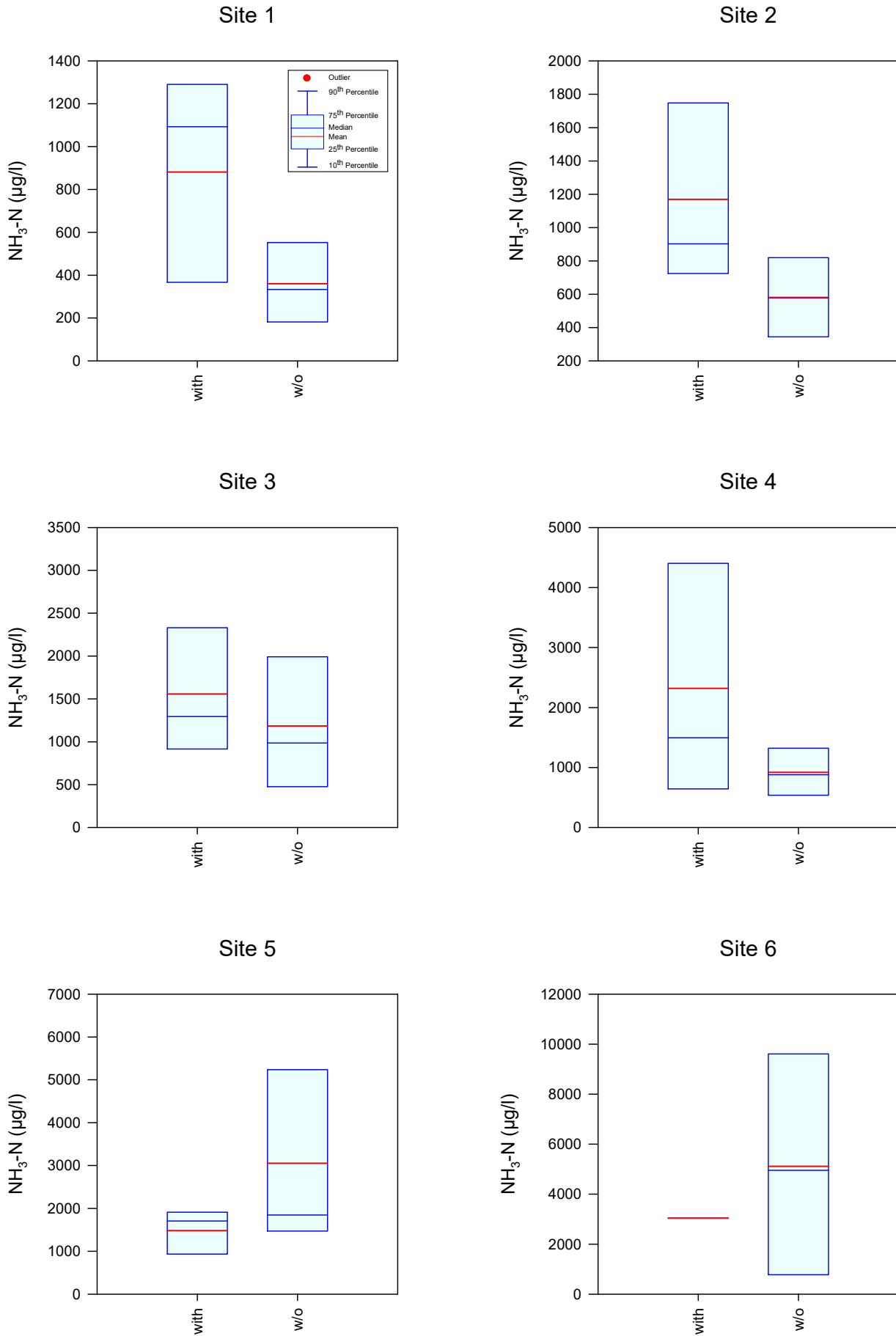


Figure 3-10.

Statistical Comparison of Ammonia Concentrations in Seepage Samples Collected With and Without Sediment Contact.

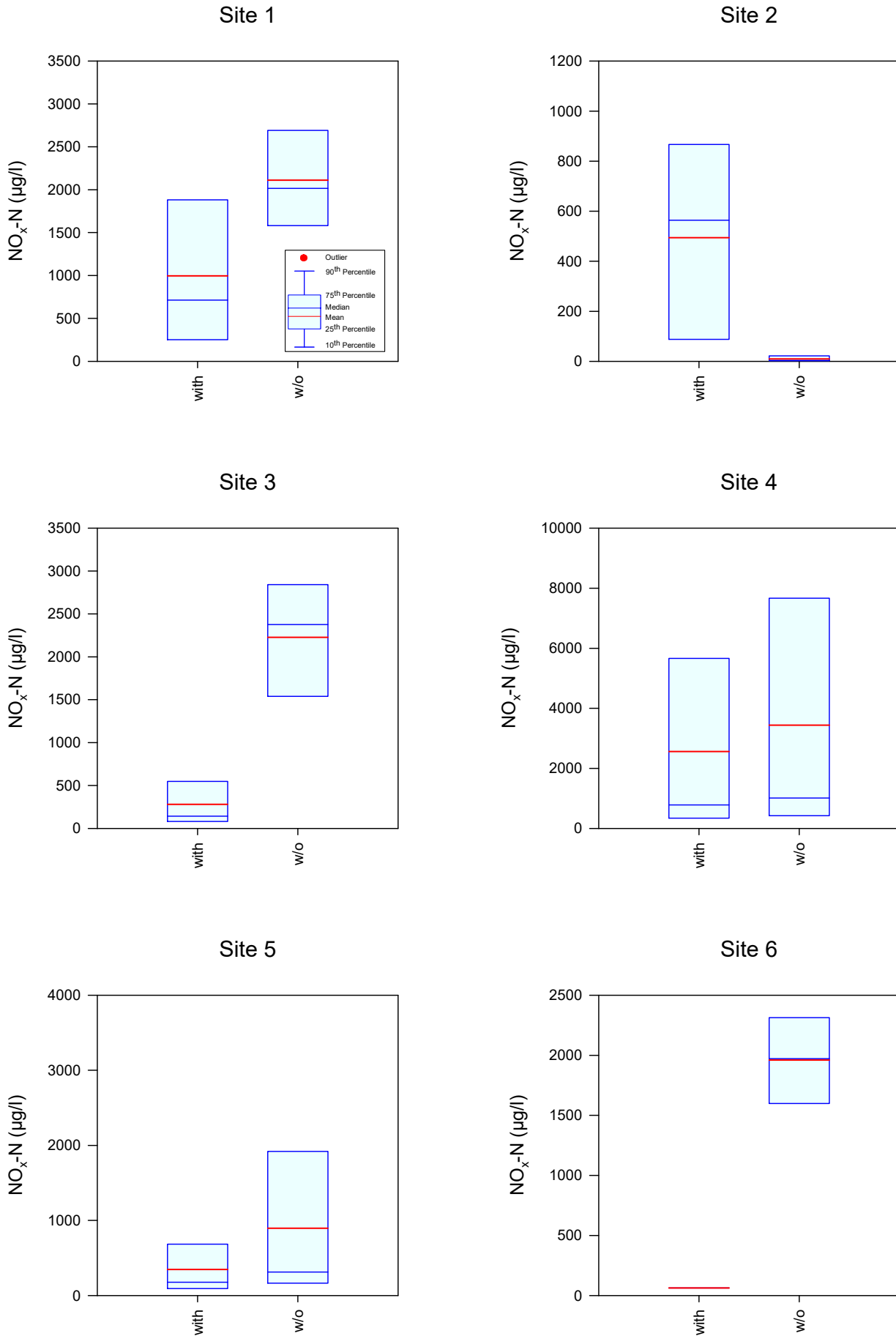


Figure 3-11.

Statistical Comparison of NO_x Concentrations in Seepage Samples Collected With and Without Sediment Contact.

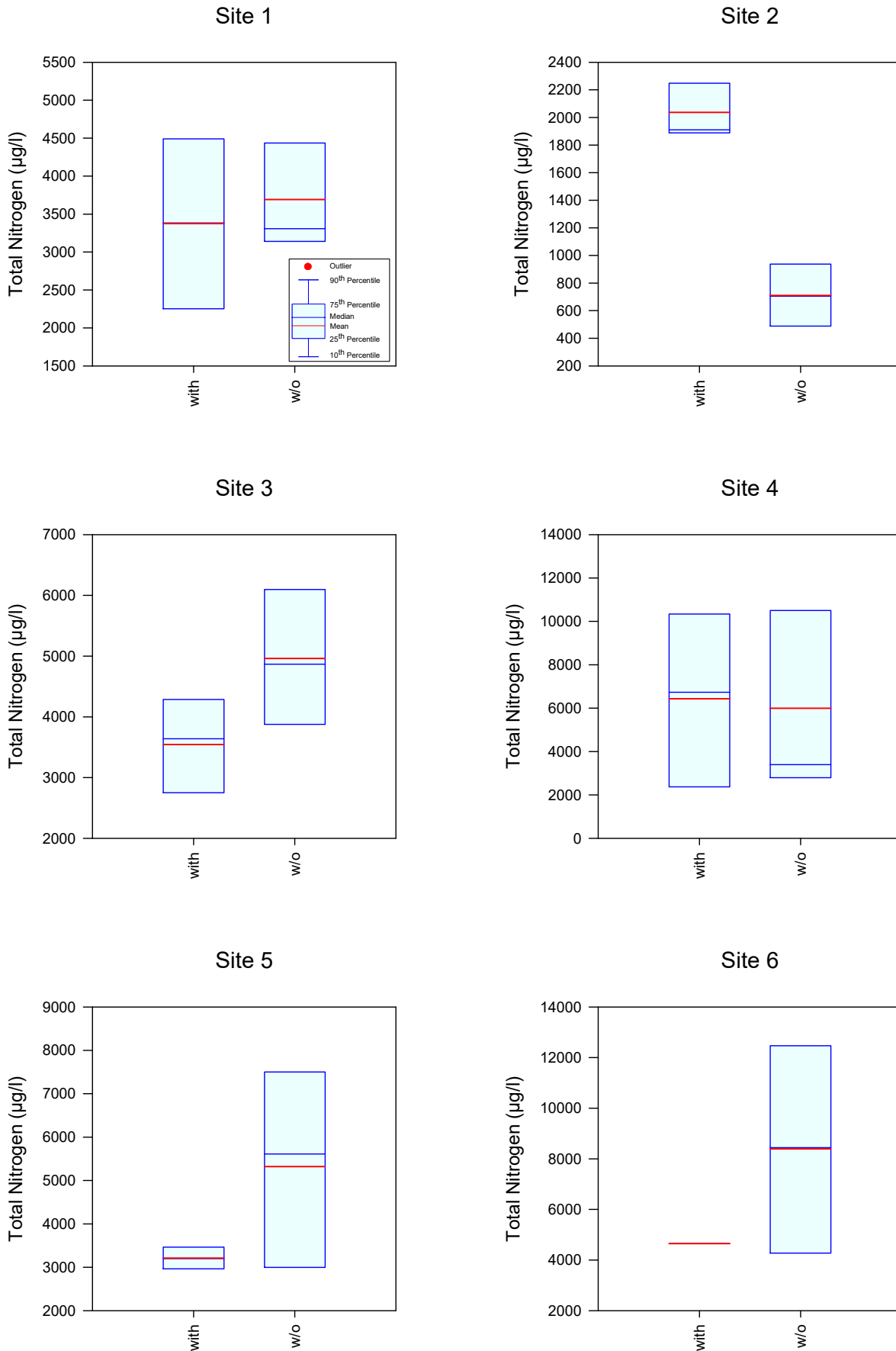


Figure 3-12.

Statistical Comparison of Total Nitrogen Concentrations in Seepage Samples Collected With and Without Sediment Contact.

A statistical comparison of measured SRP concentrations in seepage samples collected with and without sediment contact in Lake Jesup is given on Figure 3-13. Measured SRP concentrations were higher in value in seepage collected without sediment contact at Sites 1, 3, and 5, with higher SRP concentrations observed in chambers with sediment contact at Sites 2 and 4. Similar to the trend observed previously for total nitrogen, impacts to SRP concentrations appear to vary throughout Lake Jesup.

A statistical comparison of measured seepage concentrations of total phosphorus in samples collected with and without sediment contact is given on Figure 3-14. More elevated total phosphorus concentrations were observed in samples collected without sediment contact at Sites 1, 3, and 5, with higher total phosphorus concentrations observed with sediment contact at Sites 2 and 4. Impacts of sediments on seepage characteristics also appears to be variable throughout Lake Jesup.

An ANOVA comparison of seepage characteristics in Lake Jesup with and without existing sediments is given in Table 3-7. This analysis was conducted using a combined data set formed from all of the collected measured seepage characteristics, and the chemical characteristics measured in seepage meters with sediment contact were compared with the characteristics of the combined samples collected without sediment contact. No statistically significant differences were observed in seepage characteristics collected in Lake Jesup with or without existing sediments. However, it is interesting to note that the highest mean concentrations for each of the parameters listed in Table 3-7 occurred in samples collected without sediment contact. Although not statistically significant at the 0.05 level of significance, statistically significant differences would have been recognized for alkalinity, NO_x, and SRP if the analysis had been conducted at a 0.10 level of significance.

An ANOVA comparison of seepage characteristics in Lake Jesup with and without existing sediments, using a log-normal transformation of the data, is given on Table 3-8. A log-normal transformation was conducted to the data since environmental data normally exhibit log-normal distributions. Based upon this analysis, statistically significant differences were observed only for SRP and total phosphorus, with significantly higher concentrations observed in samples collected without sediments than in samples collected with sediments. No statistically significant differences were observed at the 0.05 level of significance for any of the other remaining parameters, although the differences in measured alkalinity concentrations would have been significant at the 0.10 level of significance. Similar to the trend observed for the non-transformed data set summarized in Table 3-7, the highest values for each of the measured parameters were obtained in samples collected without sediment contact, although the differences were only statistically significant for SRP and total phosphorus.

An additional ANOVA comparison was conducted to evaluate seepage characteristics in Lake Jesup with and without existing sediments by individual monitoring site. This analysis was conducted using data collected at a given site for seepage samples with sediment contact which is compared with seepage characteristics collected without sediment contact. A summary of statistically significant differences in seepage characteristics for each of the individual monitoring sites, using the non-transformed data sets, is given in Table 3-9. Parameters which did not have statistically significant differences (0.05 level) are not included in Table 3-9.

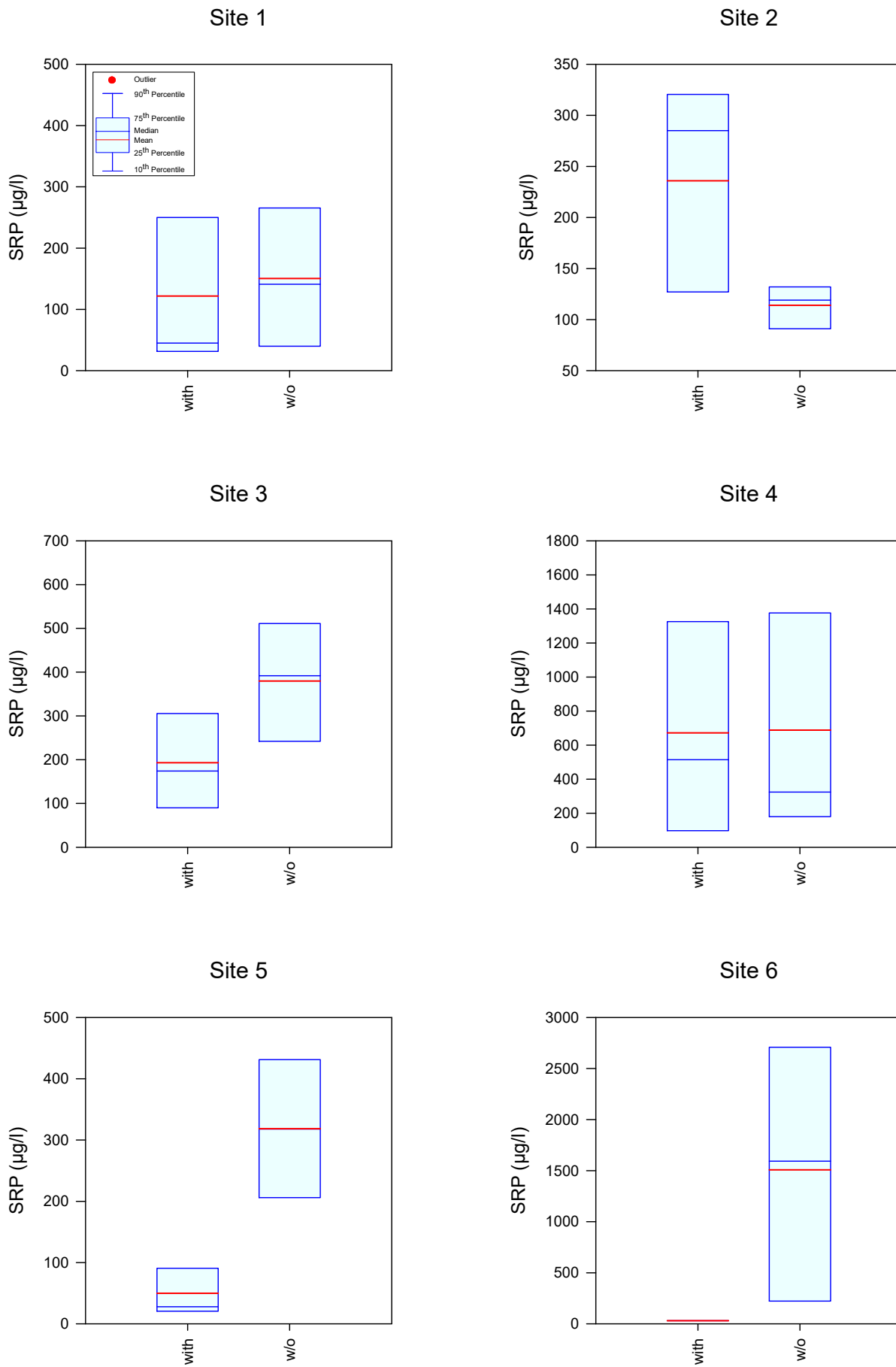


Figure 3-13.

Statistical Comparison of SRP Concentrations in Seepage Samples Collected With and Without Sediment Contact.

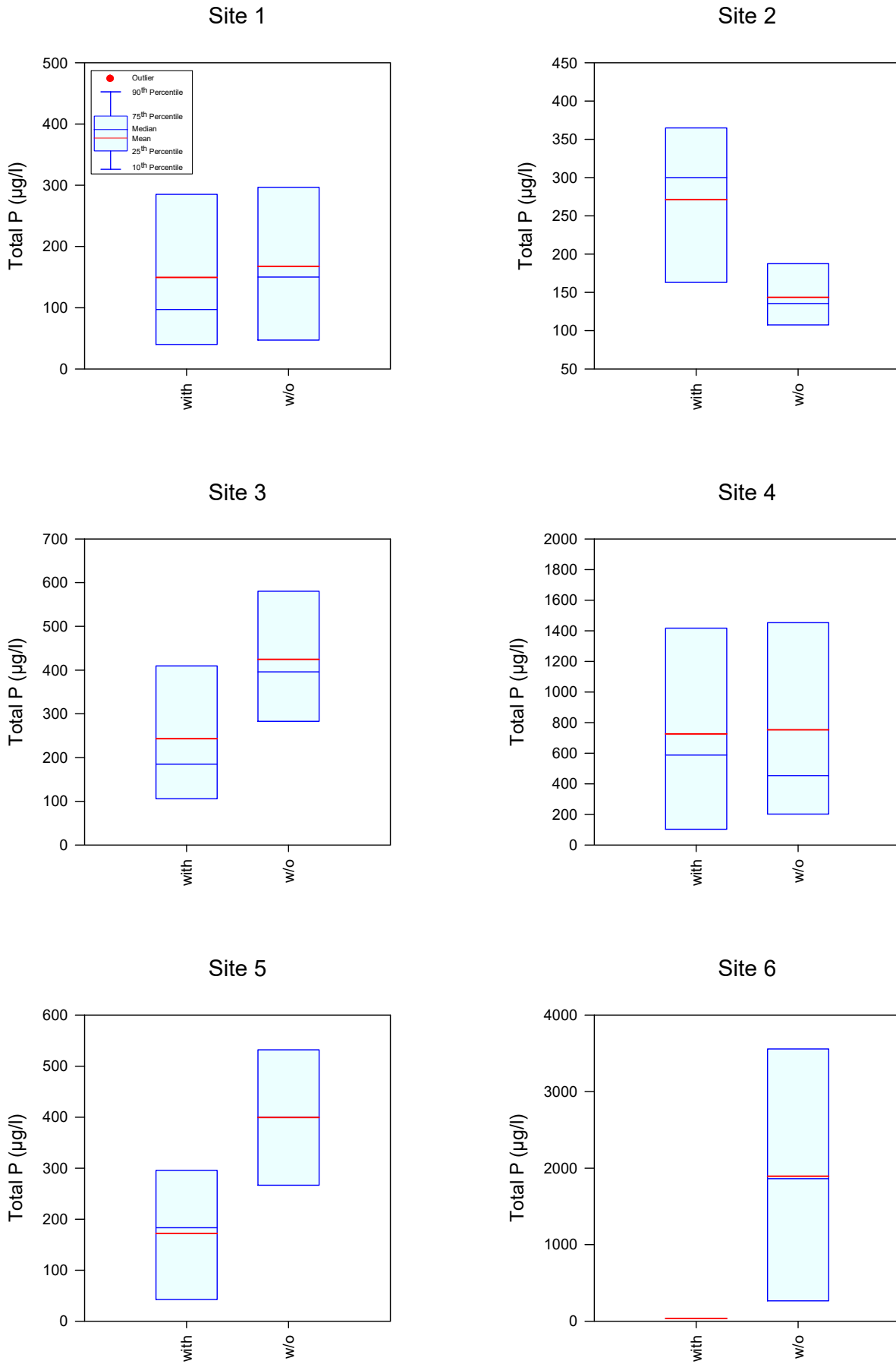


Figure 3-14.

Statistical Comparison of Total Phosphorus Concentrations in Seepage Samples Collected With and Without Sediment Contact.

TABLE 3-7

**ANOVA COMPARISON OF NON-TRANSFORMED
SEEPAGE CHARACTERISTICS IN LAKE JESUP WITH
AND WITHOUT EXISTING SEDIMENTS**

PARAMETER	UNITS	MODEL SIGNIFICANCE LEVEL	CONDITION	MEAN CONCENTRATION	TUKEY GROUPING
pH	s.u.	0.2347	without	7.50	A
			with	7.43	A
Alkalinity	mg/l	0.0759	without	149	A
			with	114	A
Conductivity	μmho/cm	0.94	without	1,109	A
			with	855	A
Ammonia	μg/l	0.6343	without	1,798	A
			with	1,541	A
NO _x	μg/l	0.0749	without	1,830	A
			with	901	A
Total N	μg/l	0.1635	without	4,867	A
			with	3,754	A
SRP	μg/l	0.0951	without	506	A
			with	246	A
Total P	μg/l	0.1083	without	603	A
			with	302	A

TABLE 3-8

**ANOVA COMPARISON OF LOG-TRANSFORMED
SEEPAGE CHARACTERISTICS IN LAKE JESUP WITH
AND WITHOUT EXISTING SEDIMENTS**

PARAMETER	UNITS	MODEL SIGNIFICANCE LEVEL	CONDITION	MEAN CONCENTRATION	TUKEY GROUPING
pH	s.u.	0.2360	without	7.50	A
			with	7.43	A
Alkalinity	mg/l	0.0846	without	131	A
			with	104	A
Conductivity	μmho/cm	0.2346	without	948	A
			with	814	A
Ammonia	μg/l	0.5567	without	1,139	A
			with	970	A
NO _x	μg/l	0.3414	without	567	A
			with	339	A
Total N	μg/l	0.5516	without	3,703	A
			with	3,311	A
SRP	μg/l	0.0095	without	275	A
			with	117	B
Total P	μg/l	0.0324	without	329	A
			with	171	B

TABLE 3-9

**SUMMARY OF SIGNIFICANT DIFFERENCES IN
SEEPAGE CHARACTERISTICS (NON-TRANSFORMED) WITH AND
WITHOUT SEDIMENT CONTACT BY MONITORING SITE**

SITE	PARAMETER	UNITS	MODEL SIGNIFICANCE LEVEL	CONDITION	MEAN CONCENTRATION	TUKEY GROUPING
1	None	--	--	--	--	--
2	Total N	µg/l	0.0001	With Without	2,037 710	A B
3	NO _x	µg/l	0.0003	Without With	2,227 280	A B
4	None	--	--	--	--	--
5	SRP	µg/l	0.0036	Without With	318 50	A B
	Total P	µg/l	0.0357	Without With	399 172	A B
6	NO _x	µg/l	0.0203	Without With	1,961 63	A B

No statistically significant differences were observed for any of the evaluated parameters at monitoring Sites 1 and 4. However, a statistically significant difference in total nitrogen concentrations was observed at Site 2, with higher total nitrogen concentrations observed in samples collected with sediment contact compared with samples collected without sediment contact. The more elevated concentrations of total nitrogen observed in seepage with sediment contact at Site 2 is contrary to the lake-wide trend of higher seepage concentrations without sediment contact. At this site, it appears that migration of seepage through the existing sediments results in an increase in total nitrogen concentrations compared with concentrations entering the lake through the sand bottom layer.

Statistically significant differences were observed at Site 3 for NO_x, at Site 5 for SRP and total phosphorus, and at Site 6 for NO_x between samples collected with and without sediment contact. However, in contrast to the trend observed at Site 2, the statistically significant differences observed at Sites 3, 5, and 6 all indicate more elevated concentrations for each of the significant parameters without sediment contact and lower concentrations with sediment contact. Data collected at these three sites suggest that the sediments act as a sink for various forms of nitrogen and phosphorus which enters Lake Jesup through the bottom sediment layers.

A summary of significant differences in seepage characteristics for samples collected with and without sediment contact using the log-transformed data set is given in Table 3-10. No statistically significant differences were observed between samples collected with and without sediment contact for any of the measured parameters at Site 4. Statistically significant differences were observed for NO_x at Sites 1, 3, and 6 as well as SRP at Site 5, with higher concentrations observed for the indicated parameters in samples collected without sediment contact compared with samples collected with sediment contact, suggesting that the sediments provide uptake for various forms of nitrogen and phosphorus during migration from the parent sandy layer through the existing organic muck sediments.

TABLE 3-10

**SUMMARY OF SIGNIFICANT DIFFERENCES IN
SEEPAGE CHARACTERISTICS (LOG-TRANSFORMED) WITH AND
WITHOUT SEDIMENT CONTACT BY MONITORING SITE**

SITE	PARAMETER	UNITS	MODEL SIGNIFICANCE LEVEL	CONDITION	MEAN CONCENTRATION	TUKEY GROUPING
1	NO _x	µg/l	0.0457	Without With	2,051 659	A B
2	NO _x	µg/l	0.0048	With Without	259 5	A B
	Total N	µg/l	0.0002	With Without	2,028 679	A B
	SRP	µg/l	0.0449	With Without	216 112	A B
3	NO _x	µg/l	0.0010	Without With	2,143 189	A B
4	None	--	--	--	--	--
5	SRP	µg/l	0.0025	Without With	381 37	A B
6	NO _x	µg/l	0.0006	Without With	1,933 65	A B

However, similar to the trend observed for the non-transformed data set, the statistically significant differences observed at Site 2 all indicate higher concentrations of parameters with sediment contact compared with concentrations measured without sediment contact. These data suggest that sediment and seepage characteristics at Site 2 are somehow different than characteristics measured in other parts of the lake since the sediments appear to be a source of nutrients at Site 2 rather than a sink, as observed at each of the remaining sites.

The statistical analyses discussed previously indicate that in most areas of the lake the existing sediments do not significantly enhance concentrations of groundwater seepage entering Lake Jesup. It appears that the existing sediments may result in reductions in concentrations for many parameters as the seepage migrates from the sand bottom through the thick layers of accumulated muck. For parameters such as SRP and total phosphorus, phosphorus concentrations are approximately double in samples collected without sediment contact compared with samples collected with sediment contact. Lesser differences are observed for each of the remaining parameters, although in all cases (with the exception of Site 2), samples collected with sediment contact are lower in value than samples collected without sediment contact.

The field and laboratory data suggest that, in most areas of Lake Jesup, the existing sediments do not currently have a negative impact on water quality characteristics of seepage inputs entering Lake Jesup. The sediments appear to be a sink for virtually all of the measured seepage parameters by removing alkalinity, nitrogen, and phosphorus which enters the lake from groundwater seepage. The field and laboratory data suggest that removal of the existing sediments may increase loadings to Lake Jesup from groundwater seepage, although the magnitude of this additional loading should be compared with the load reduction achieved by removing the nutrient-rich sediments and the associated internal recycling.

Over the past 20 years, ERD has conducted monitoring of groundwater seepage in over 40 lakes within the State of Florida, and ERD maintains a database of measured seepage concentrations for each monitored lake. A statistical comparison of seepage nutrient concentrations in Lake Jesup with and without sediment contact and seepage concentrations measured by ERD in other Central Florida lakes is given on Figure 3-15. The Lake Jesup data reflect all samples collected during the field monitoring program with and without sediment contact. In general, measured concentrations of both total nitrogen and total phosphorus in seepage entering Lake Jesup are greater than median concentrations for groundwater seepage measured by ERD in other Central Florida lakes. Measured concentrations of total nitrogen and total phosphorus in Lake Jesup seepage samples collected without sediment contact are greater in value than median concentrations measured with sediment contact.

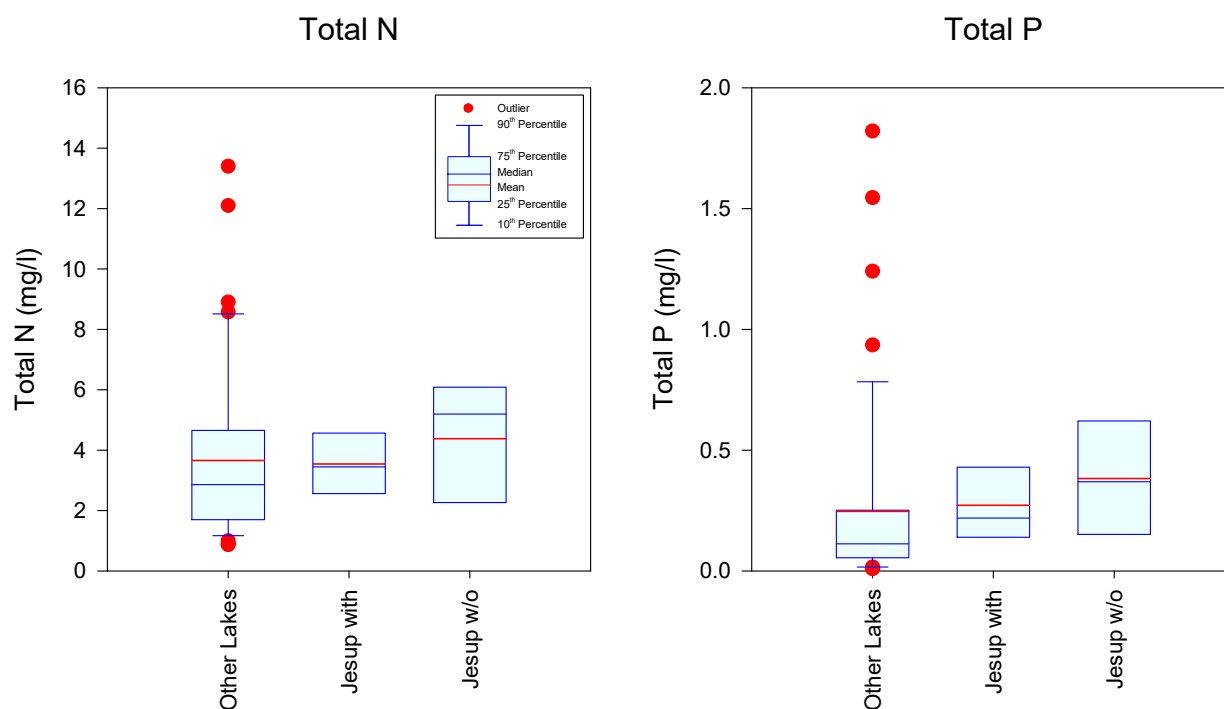


Figure 3-15. Comparison of Seepage Nutrient Concentrations in Lake Jesup With and Without Sediments and Seepage Concentrations Measured in Other Central Florida Lakes.

3.4 Horizontal Variability in Seepage Characteristics

A graphical comparison of flow-weighted mean concentrations of alkalinity in Lake Jesup seepage samples collected with and without sediment contacts is given on Figure 3-16. The mean concentration for samples collected with sediment contact reflects the first number in parentheses underneath each of the site designations, with the mean concentration without sediment contact given as the second value. In general, measured seepage concentrations were relatively similar in samples collected with and without sediment contact in the extreme western portions of Lake Jesup. However, a trend of increasing alkalinity values is apparent in eastern portions of the lake as well as a larger difference between alkalinity measurements conducted in samples collected with and without sediment contact.

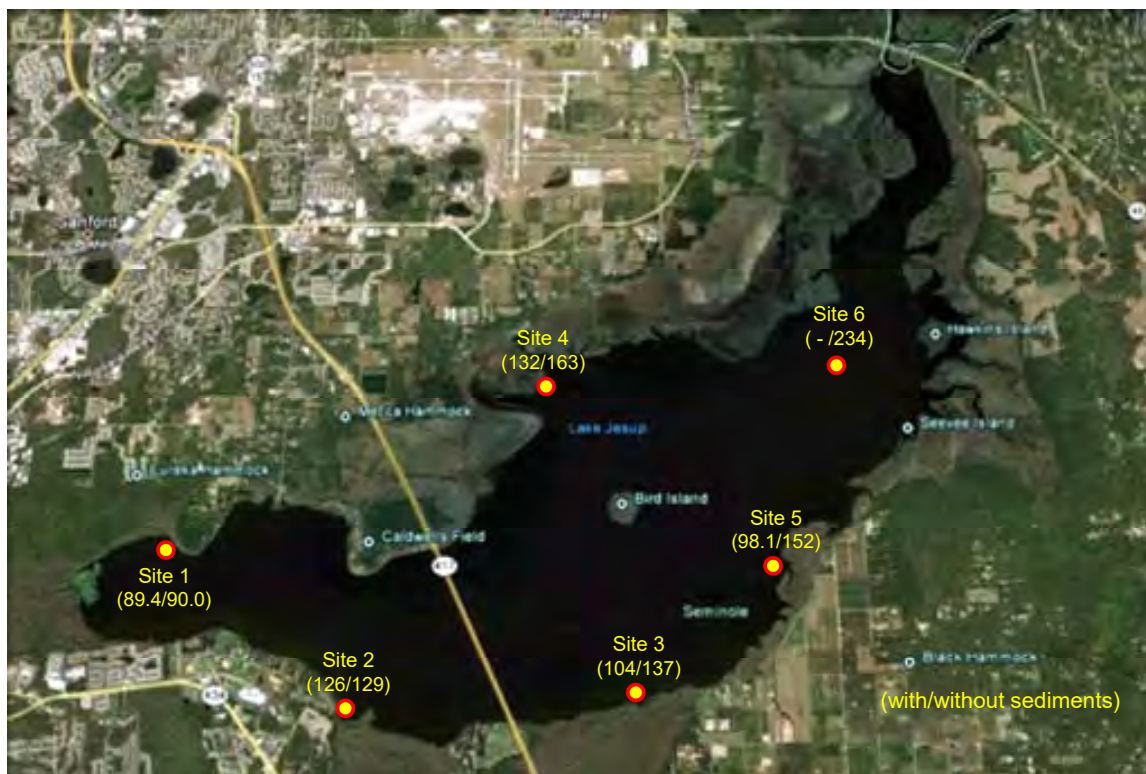


Figure 3-16. Flow-Weighted Mean Concentrations of Alkalinity in Lake Jesup Seepage Samples With and Without Sediment Contact.

A graphical summary of flow-weighted mean concentrations of ammonia in Lake Jesup seepage samples collected with and without sediment contact is given on Figure 3-17. In general, ammonia concentrations in groundwater seepage appear to be lowest in western portions of the lake, with ammonia concentrations in samples collected with sediment contact approximately twice as high as samples collected without sediment contact. A general trend of increasing ammonia seepage concentrations is apparent in eastern portions of the lake, particularly at Sites 5 and 6.

A graphical comparison of flow-weighted mean concentrations of total nitrogen in seepage samples collected in Lake Jesup with and without sediment contact is given on Figure 3-18. Similar to the trends observed for ammonia, the lowest seepage concentrations of total nitrogen appear to occur in western portions of the lake. Seepage concentrations of total nitrogen increase substantially in areas west of SR 417 to values which are approximately 2-3 times greater than concentrations measured west of SR 417. The most elevated seepage total nitrogen concentrations were observed at Sites 4, 5, and 6. At Sites 4 and 5, total nitrogen concentrations with sediments were somewhat lower than concentrations measured without sediments.

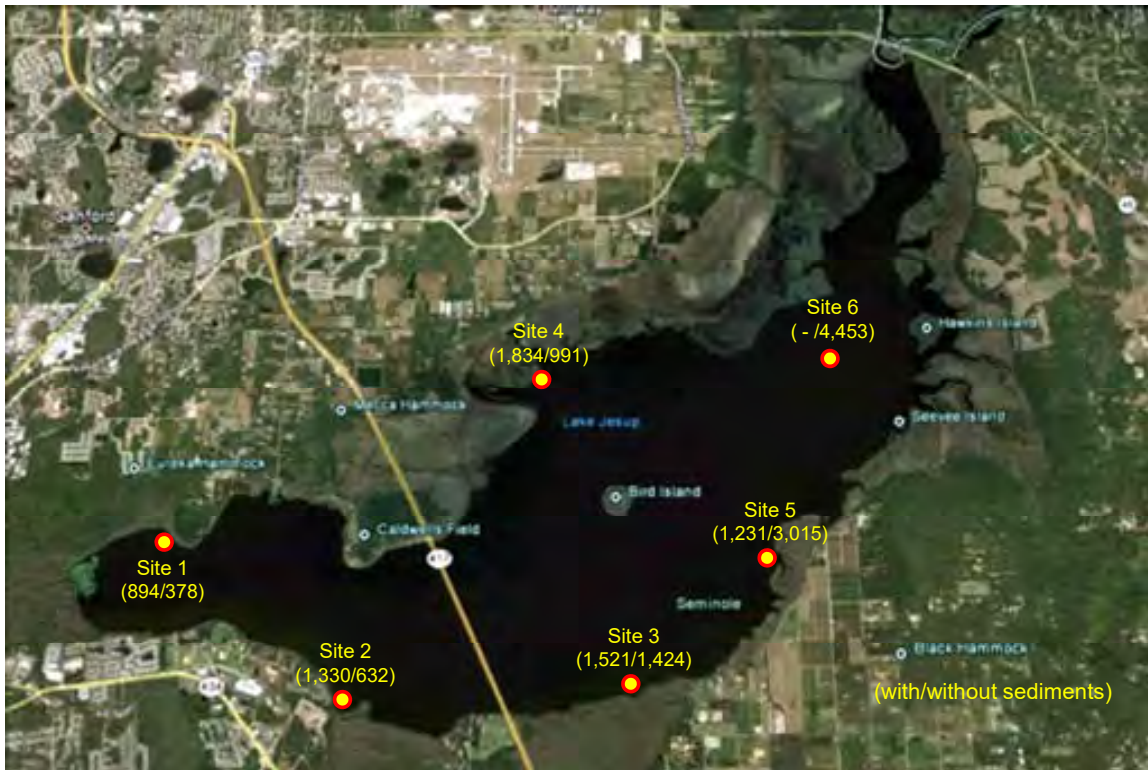


Figure 3-17. Flow-Weighted Mean Concentrations of Ammonia in Lake Jesup Seepage Samples With and Without Sediment Contact.

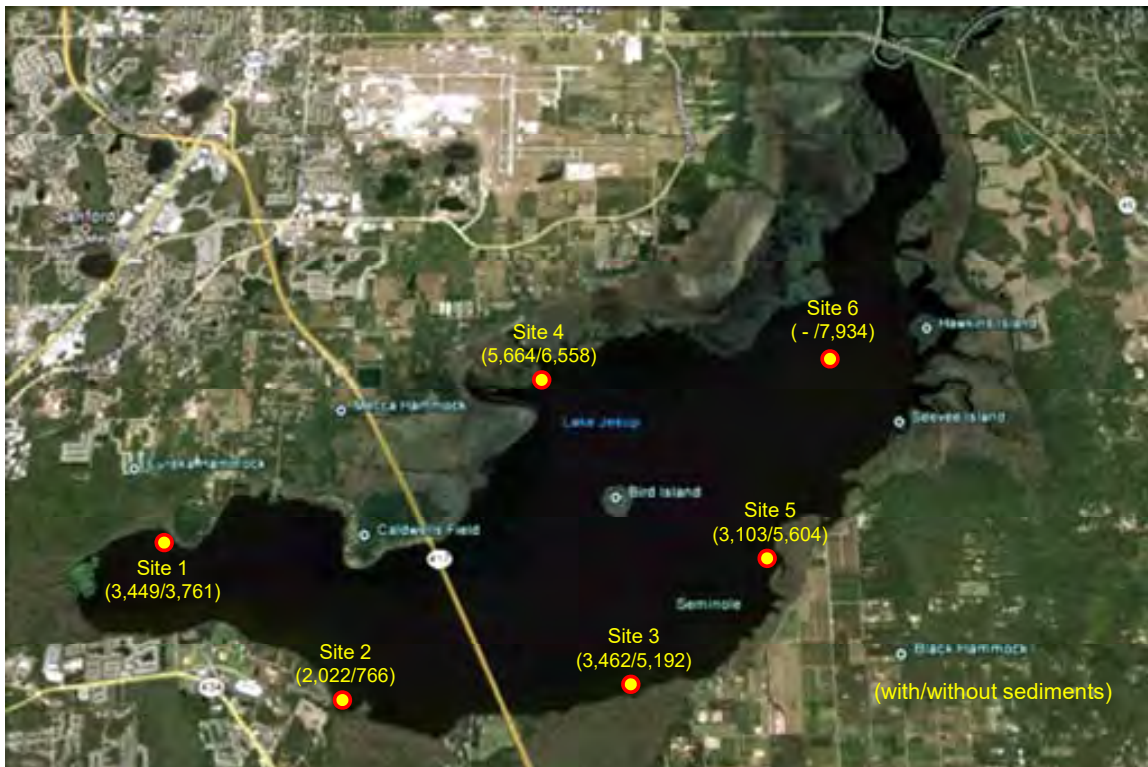


Figure 3-18. Flow-Weighted Mean Concentrations of Total Nitrogen in Lake Jesup Seepage Samples With and Without Sediment Contact.

A graphical comparison of flow-weighted mean concentrations of SRP in seepage samples collected from Lake Jesup with and without sediment contact is given on Figure 3-19. In general, seepage concentrations of SRP were lowest in value in areas west of SR 417, with higher values measured in areas east of SR 417, particularly for samples collected without sediments. Substantially elevated levels of SRP were observed in seepage collected at Sites 3, 4, 5, and particularly at Site 6 in areas where sediments had been removed. The flow-weighted mean SRP concentration at Site 6 of 1,298 $\mu\text{g/l}$ reflects seepage characteristics as it enters Lake Jesup prior to migrating through the organic sediment layer. This value reflects an extremely elevated phosphorus concentration which is input into the lake on a continuous basis.

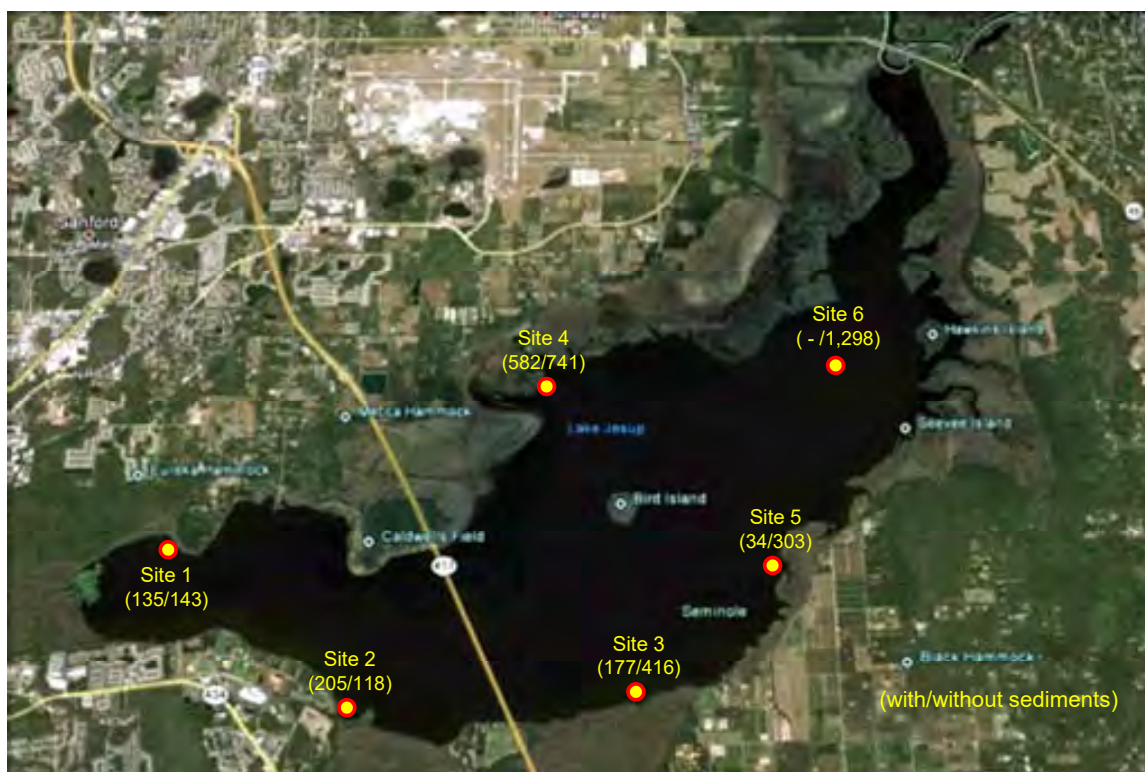


Figure 3-19. Flow-Weighted Mean Concentrations of SRP in Lake Jesup Seepage Samples With and Without Sediment Contact.

A graphical summary of flow-weighted mean concentrations of total phosphorus in seepage samples collected from Lake Jesup with and without sediment contact is given on Figure 3-20. In general, concentrations of total phosphorus exhibit a pattern similar to that discussed previously for SRP. The lowest concentrations of total phosphorus in groundwater seepage generally occur west of SR 417, with substantially higher concentrations observed in areas east of SR 417. Substantially elevated seepage concentrations of total phosphorus were observed at Sites 3, 4, 5, and 6, particularly in samples collected without sediment contact. Phosphorus concentrations entering Lake Jesup in these areas appear to be mitigated to some extent during migration through the sediments. However, extremely elevated levels of total phosphorus appear to be entering Lake Jesup from groundwater seepage, particularly in western portions of the lake.

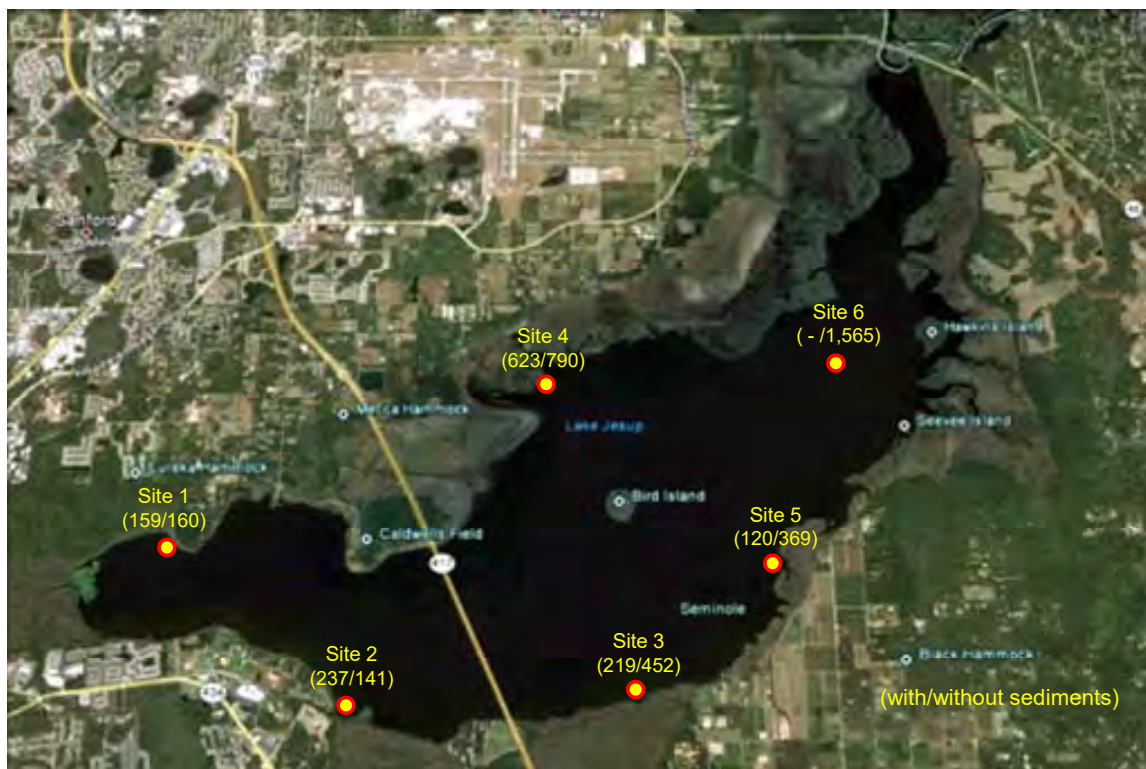


Figure 3-20. Flow-Weighted Mean Concentrations of Total Phosphorus in Lake Jesup Seepage Samples With and Without Sediment Contact.

3.5 Comparison with Previous Studies

As referenced in Section 1, an evaluation of the hydrologic and nutrient loadings from groundwater seepage to Lake Jesup was conducted by ERD from 2009-2010, with a Final Report issued in February 2011. Groundwater seepage meters were installed at 40 locations within Lake Jesup, and nine separate monitoring events were conducted at each site over a 14-month field monitoring program.

A comparison of mean seepage characteristics measured during the 2011 and 2013 seepage evaluations was conducted to evaluate seepage characteristics in similar areas of Lake Jesup measured during the two separate studies. Each of the six monitoring sites used during the 2013 study have a corresponding monitoring site from the 2011 study in relatively close proximity. Since the 2011 study only included seepage meters with sediment contact, only the 2013 seepage samples collected with sediment contact are used for comparison. Monitoring Sites 1-4 from the 2013 study have closely located seepage monitoring sites available from the 2011 study which contained sufficient data for comparison of chemical characteristics. Monitoring Sites 5 and 6 also contain closely located monitoring sites from the 2011 study, but the 2011 monitoring site closest to Site 5 contains only a limited number of data points, while the monitoring Site 6 from the current study contains no useable data for the seepage meters installed with sediment contact. Therefore, comparable monitoring sites are only available for the current monitoring sites designated as Sites 1-4.

A tabular comparison of mean measured seepage characteristics at similar monitoring sites during the 2011 and current 2013 seepage study is given on Table 3-11. Measured seepage pH values are relatively similar in value at each of the four comparable monitoring sites during both the 2011 and 2013 evaluations. Measured alkalinity values also appear to be in relatively close agreement, with the exception of Site 3 which exhibits a somewhat lower alkalinity value during the current study than observed during 2011. Measured conductivity values between the two studies are very similar at each of the four comparable sites.

TABLE 3-11

COMPARISON OF MEAN MEASURED SEEPAGE CHARACTERISTICS AT SIMILAR MONITORING SITES DURING THE 2011 AND CURRENT SEEPAGE STUDY

SITE NUMBER	STUDY REFERENCE	pH (s.u.)	ALKALINITY (mg/l)	CONDUCTIVITY (µmho/cm)	TOTAL N (µg/l)	TOTAL P (µg/l)
1	2013 ¹	7.37	89.1	745	3,449	159
37	2011 ²	7.41	118	673	3,802	386
2	2013 ¹	7.63	126	465	2,022	237
32	2011 ²	7.33	102	564	4,256	600
3	2013 ¹	7.41	104	899	3,462	219
28	2011 ²	7.91	226	996	9,946	1,248
4	2013 ¹	7.47	132	985	5,664	623
22	2011 ²	7.66	151	968	5,557	598

1. Harper, H.H. (April 2013). "Evaluation of Sediment Impacts on Hydrologic and Nutrient Loadings from Groundwater Seepage to Lake Jesup." Draft Final Report.
2. Harper, H.H. (February 2011). "Evaluation of Hydrologic and Nutrient Loadings from Groundwater Seepage to Lake Jesup." Final Report.

Measured concentrations of total nitrogen at Sites 1, 2, and 4 are relatively similar to values measured during the previous 2011 study. However, a relatively large difference was observed in measured nitrogen concentrations at Site 3 between the 2011 and 2013 studies. A similar pattern was also observed for seepage concentrations of total phosphorus, with relatively similar concentrations observed at Sites 1, 2, and 4 and a relatively large difference in measured total phosphorus concentrations at Site 3. Overall, with the exception of Site 3, seepage characteristics are relatively similar between the two monitoring sites at similarly located monitoring sites.

SECTION 4

SUMMARY AND CONCLUSIONS

4.1 Summary

An initial evaluation of the hydrologic and nutrient loadings from groundwater seepage to Lake Jesup was conducted by ERD from 2009-2010, with a Final Report issued in February 2011. Groundwater seepage meters were installed in 40 locations within Lake Jesup, and 9 separate monitoring events were conducted at each site over a 14-month field monitoring program from June 2009-August 2011. Groundwater seepage entering Lake Jesup was characterized by elevated levels of both total nitrogen and total phosphorus in this initial seepage study, and the calculated annual seepage mass loadings were substantially greater than baseflow loading estimates provided in the TMDL report for Lake Jesup. Questions then arose at the time as to the source of the nutrient loadings and whether the elevated seepage nutrient concentrations are impacted by migration through the existing muck sediments.

A supplemental evaluation was conducted by ERD from January 2010-March 2013 to further evaluate the impacts of the existing sediments on seepage characteristics entering the lake. Side-by-side comparisons of seepage meters installed in areas with and without existing sediments were used to evaluate potential impacts of the sediments on seepage inputs. Pairs of seepage meters with and without existing sediments were installed at 6 separate locations throughout Lake Jesup, and field monitoring was conducted by ERD over a 415-day period from January 2012-March 2013 to evaluate the impacts of existing sediments on the hydrologic and water quality characteristics of shallow groundwater seepage inflows to Lake Jesup. Rainfall during the seepage field monitoring program was approximately normal, with an estimated 59.90 inches of rainfall occurring in the vicinity of Lake Jesup during the period from January 2012-March 2013 compared with a long-term “normal” rainfall of 60.67 inches.

Six separate monitoring events were conducted to evaluate the quantity of shallow seepage entering Lake Jesup, with and without sediment contact, with laboratory analyses of the seepage samples conducted during 5 of the 6 monitoring events. Seepage inflow rates into Lake Jesup were relatively similar in meters installed with and without sediment contact, with an arithmetic mean of 0.68 liters/m²-day for seepage meters incubated without sediment contact compared with 0.65 liters/m²-day for meters with sediment contact. Geometric mean values were slightly different, with an overall mean seepage inflow of 0.50 liters/m²-day without sediment contact compared with 0.64 liters/m²-day with sediment contact. Analysis of variance (ANOVA) comparisons were conducted to evaluate whether statistically significant differences exist in measured seepage rates with and without sediment contact. No statistically significant difference was detected using the normal field measured data, although the seepage meters incubated with sediment contact were found to have a statistically higher inflow rate when a log transformation was conducted on the data set.

The slightly lower seepage inflow rate measured in seepage meters inserted on the sand bottom of the lake is thought to be due to the inability to form a tight seal between the seepage meter and the cemented sand bottom, which allowed some of the incoming seepage to bypass the seepage meter collection system. Overall, there appears to be no significant difference in seepage inflow rates in areas with and without sediment contact.

Groundwater seepage entering Lake Jesup was found to be approximately neutral to slightly alkaline in pH, moderately to well buffered, with low to elevated levels of conductivity, depending on location within the lake. Measured nutrient concentrations were highly variable in seepage samples, with a general trend of lower nutrient concentrations in western portions of the lake and higher nutrient concentrations in eastern portions of the lake for seepage samples collected without sediment contact. An ANOVA comparison was conducted to identify statistically significant differences between seepage characteristics collected in Lake Jesup with and without existing sediments. When the combined raw data sets were compared, no statistically significant differences were detected between seepage collected with and without existing sediments, although each of the evaluated parameters exhibited higher values in seepage collected without existing sediments than in seepage collected with existing sediments. When a log transformation was conducted to the data sets, statistically significant differences in seepage characteristics were detected for both SRP and total phosphorus, with higher concentrations for each parameter observed in seepage samples collected without sediment contact compared with seepage samples collected with sediment contact.

A supplemental ANOVA comparison was conducted to identify statistically significant differences between seepage characteristics with and without existing sediments for each of the individual monitoring sites. The comparison conducted using the non-transformed data set indicated statistically significant differences in seepage characteristics for NO_x at Sites 3 and 6, and SRP and total phosphorus at Site 5. Each of these analyses indicated higher concentrations for these parameters in samples collected without sediment contact compared with samples collected with sediment contact. These data suggest that the sediments act as a sink for nutrient loadings entering Lake Jesup through the parent sandy sediment material. However, a statistically significant difference for total nitrogen was observed at Site 2 which indicated higher concentrations with sediment contact than without, suggesting that the sediments may be a source of nutrients to the seepage inflow in the area of Site 2, located near the mouth of Howell Creek.

The ANOVA comparison conducted on the log-transformed data set indicated statistically significant differences for NO_x at Sites 1, 3, and 6, and a statistically significant difference for SRP at Site 5. Each of these differences reflect higher concentrations in seepage without sediment contact than in seepage collected with sediment contact, suggesting that the sediments may remove certain forms of nitrogen and phosphorus which enter Lake Jesup through the parent sandy bottom material. However, similar to the trend observed for the non-transformed data set, statistically significant differences were observed at Site 2 for NO_x , total nitrogen, and SRP, all of which indicate higher concentrations with sediment contact than without, suggesting that the sediments are a source of nutrients to groundwater inflow in the vicinity of Site 2.

The field and laboratory data collected at 5 of the 6 sites suggest that the existing sediments do not currently exert a negative impact on water quality characteristics of seepage inputs entering Lake Jesup. The sediments in Lake Jesup are highly active on a microbial level, as evidenced by the nearly permanent anoxic conditions which exist within the sediments. Therefore, the microbial community appears to be utilizing nutrients and alkalinity from the seepage, resulting in lower concentrations of seepage actually reaching the water column of Lake Jesup compared with seepage which originates from the lake bottom. In contrast, data collected at one of the 6 sites suggest that the sediments may be contributing nutrients to seepage flow.

Based upon the analyses conducted during this study, the primary source of the elevated seepage characteristics appears to be watershed areas adjacent to Lake Jesup. The existing sediments appear to have minimal impact on seepage characteristics in most areas of Lake Jesup, and may, in fact, be reducing seepage concentrations of nutrients and alkalinity to some extent. Further studies are recommended to evaluate why data collected at Site 2 appear to be contrary to data collected in other parts of Lake Jesup.

4.2 Conclusions

Both the 2011 and 2013 seepage studies conducted by ERD confirm that shallow groundwater seepage represents a significant hydraulic and nutrient loading to Lake Jesup which is largely unaccounted for in the TMDL for the lake. The measured seepage inflows to Lake Jesup represent 12% of the total annual hydrologic inputs summarized in the TMDL report, along with 33% of the annual nitrogen loadings and 36% of the annual phosphorus loadings. These additional seepage loadings reduce the significance of runoff as a loading source and impact the water quality benefits which can be achieved through stormwater management projects.

Lake Jesup exhibits a strong horizontal gradient in seepage characteristics from west to east across the lake, the magnitude of which is unprecedented in previous seepage monitoring conducted by ERD. Migration of the seepage through the muck sediments reduces much of the observed variability in raw seepage characteristics which enter the lake through the sand bottom. In some areas, the sediments appear to be providing uptake for some of the seepage constituents, while in other areas the sediments appear to contribute loadings to the seepage inflow.

The role of sediments in regulating seepage characteristics is largely unrelated to the independent role of the sediments in contributing nutrient loadings to the lake through internal recycling. The sediments in Lake Jesup are highly anoxic, regardless of dissolved oxygen concentrations measured in the water column, and although the rate of nutrient recycling has not been fully quantified, the sediments are almost certainly a significant additional source of nutrient loadings to the lake which has also not been included in the TMDL evaluation. There is no question that the seepage loadings to Lake Jesup estimated in the 2011 ERD study include a portion of the internal loading as well, particularly in more central portions of the lake, but separation of these inputs cannot be achieved based on the collected seepage data. Further studies are recommended to quantify nutrient loadings from internal recycling.

APPENDICES

APPENDIX A

**FIELD MEASUREMENTS OF
SEEPAGE INFLOW VOLUMES IN LAKE JESUP
FROM JANUARY 2012 – MARCH 2013**

Seepage Meter Field Measurements

Location: Lake Jesup

Site: 1 - Without Sediments

Date Installed: 1/25/12

Chamber Diameter: 0.58 m

Sediment Area Covered: 0.27 m²

Date	Time Collected	Volume Collected (liters)	Previous Collection Event		Seepage Time (days)	Seepage (liters/m2-day)	Comments / Observations
			Date	Time			
1/25/12	11:05	----	----	----	----	----	Bags Installed
3/9/12	10:15	7.25	1/25/12	11:05	44.0	0.61	Measured volume, no sample collected
7/13/12	10:42	18.5	3/9/12	10:15	126.0	0.54	Sample collected, bag in good condition
8/24/12	10:12	9.5	7/13/12	10:42	42.0	0.84	Sample collected, bag in good condition
11/30/12	11:18	11.25	8/24/12	10:12	98.0	0.42	Sample collected, bag in good condition
1/25/13	11:24	10.75	11/30/12	11:18	56.0	0.71	Sample collected, bag in good condition
3/15/13	10:25	4.75	1/25/13	11:24	49.0	0.36	Sample collected, bag in good condition
Mean Seepage:						0.55	

Seepage Meter Field Measurements

Location: Lake Jesup

Site: 1 - With Sediments

Date Installed: 1/25/12

Chamber Diameter: 0.58 m

Sediment Area Covered: 0.27 m²

Date	Time Collected	Volume Collected (liters)	Previous Collection Event		Seepage Time (days)	Seepage (liters/m2-day)	Comments / Observations
			Date	Time			
1/25/12	11:14	----	----	----	----	----	Bags Installed
3/9/12	10:18	10.5	1/25/12	11:14	44.0	0.88	Measured volume, no sample collected
7/13/12	10:47	17.25	3/9/12	10:18	126.0	0.51	Sample collected, bag in good condition
8/24/12	10:17	12.25	7/13/12	10:47	42.0	1.08	Sample collected, bag in good condition
11/30/12	11:25	26.75	8/24/12	10:17	98.0	1.01	Sample collected, bag in good condition
1/25/13	11:20	13.5	11/30/12	11:25	56.0	0.89	Sample collected, bag in good condition
3/15/13	10:22	11.25	1/25/13	11:20	49.0	0.85	Sample collected, bag in good condition
Mean Seepage:						0.82	

Seepage Meter Field Measurements

Location: Lake Jesup

Site: 2 - Without Sediments

Date Installed: 1/31/12

Chamber Diameter: 0.58 m

Sediment Area Covered: 0.27 m²

Date	Time Collected	Volume Collected (liters)	Previous Collection Event		Seepage Time (days)	Seepage (liters/m2-day)	Comments / Observations
			Date	Time			
1/31/12	14:14	----	----	----	----	----	Bags Installed
3/9/12	10:30	21.5	1/31/12	14:14	37.8	2.10	Measured volume, no sample collected
7/13/12	10:26	130	3/9/12	10:30	126.0	3.82	Sample collected, bag in good condition
8/24/12	10:00	11.75	7/13/12	10:26	42.0	1.04	Sample collected, bag in good condition
11/30/12	10:55	----	8/24/12	10:00	----	----	No sample collected, meter flipped, meter reinstalled
1/25/13	11:05	9.5	11/30/12	10:55	56.0	0.63	Sample collected, bag in good condition
3/15/13	11:00	4.5	1/25/13	11:05	49.0	0.34	Sample collected, bag in good condition
Mean Seepage:						2.11	

Seepage Meter Field Measurements

Location: Lake Jesup

Site: 2 - With Sediments

Date Installed: 1/31/12

Chamber Diameter: 0.58 m

Sediment Area Covered: 0.27 m²

Date	Time Collected	Volume Collected (liters)	Previous Collection Event		Seepage Time (days)	Seepage (liters/m2-day)	Comments / Observations
			Date	Time			
1/31/12	14:26	-----	-----	-----	-----	-----	Bags Installed
3/9/12	10:32	6.25	1/31/12	14:26	37.8	0.61	Measured volume, no sample collected
7/13/12	10:33	11.75	3/9/12	10:32	126.0	0.35	Sample collected, bag in good condition
8/24/12	10:03	13.75	7/13/12	10:33	42.0	1.21	Sample collected, bag replaced
11/30/12	11:00	12.5	8/24/12	10:03	98.0	0.47	Sample collected, bag in good condition
1/25/13	11:09	20.25	11/30/12	11:00	56.0	1.34	Sample collected, bag in good condition
3/15/13	11:08	18.25	1/25/13	11:09	49.0	1.38	Sample collected, bag replaced
Mean Seepage:						0.75	

Seepage Meter Field Measurements

Location: Lake Jesup

Site: 3 - Without Sediments

Date Installed: 1/31/12

Chamber Diameter: 0.58 m

Sediment Area Covered: 0.27 m²

Date	Time Collected	Volume Collected (liters)	Previous Collection Event		Seepage Time (days)	Seepage (liters/m2-day)	Comments / Observations
			Date	Time			
1/31/12	13:55	-----	-----	-----	-----	-----	Bags Installed
3/9/12	10:44	7.5	1/31/12	13:55	37.9	0.73	Measured volume, no sample collected
7/13/12	10:10	15.25	3/9/12	10:44	126.0	0.45	Sample collected, bag replaced
8/24/12	9:44	8.25	7/13/12	10:10	42.0	0.73	Sample collected, bag in good condition
11/30/12	10:42	11.75	8/24/12	9:44	98.0	0.44	Sample collected, bag in good condition
1/25/13	10:42	14.5	11/30/12	10:42	56.0	0.96	Sample collected, bag in good condition
3/15/13	11:45	4.5	1/25/13	10:42	49.0	0.34	Sample collected, bag in good condition
Mean Seepage:						0.56	

Seepage Meter Field Measurements

Location: Lake Jesup

Site: 3 - With Sediments

Date Installed: 1/31/12

Chamber Diameter: 0.58 m

Sediment Area Covered: 0.27 m²

Date	Time Collected	Volume Collected (liters)	Previous Collection Event		Seepage Time (days)	Seepage (liters/m2-day)	Comments / Observations
			Date	Time			
1/31/12	13:40	-----	-----	-----	-----	-----	Bags Installed
3/9/12	10:46	11.25	1/31/12	13:40	37.9	1.10	Measured volume, no sample collected
7/13/12	10:14	22.5	3/9/12	10:46	126.0	0.66	Sample collected, bag in good condition
8/24/12	9:48	12.5	7/13/12	10:14	42.0	1.10	Sample collected, bag in good condition
11/30/12	10:46	20.25	8/24/12	9:48	98.0	0.76	Sample collected, bag replaced
1/25/13	10:46	12.25	11/30/12	10:46	56.0	0.81	Sample collected, bag in good condition
3/15/13	11:50	14.25	1/25/13	10:46	49.0	1.08	Sample collected, bag in good condition
Mean Seepage:						0.84	

Seepage Meter Field Measurements

Location: Lake Jesup

Site: 4 - Without Sediments

Date Installed: 1/31/12

Chamber Diameter: 0.58 m

Sediment Area Covered: 0.27 m²

Date	Time Collected	Volume Collected (liters)	Previous Collection Event		Seepage Time (days)	Seepage (liters/m2-day)	Comments / Observations
			Date	Time			
1/31/12	13:34	-----	-----	-----	-----	-----	Bags Installed
3/9/12	11:02	5.5	1/31/12	13:34	37.9	0.54	Measured volume, no sample collected
7/13/12	9:26	3.75	3/9/12	11:02	125.9	0.11	Sample collected, bag in good condition
8/24/12	9:00	8.75	7/13/12	9:26	42.0	0.77	Sample collected, bag in good condition
11/30/12	9:35	0.25	8/24/12	9:00	98.0	0.01	Sample collected, bag replaced
1/25/13	10:10	5.25	11/30/12	9:35	56.0	0.35	Sample collected, bag in good condition
3/15/13	13:05	5.75	1/25/13	10:10	49.1	0.43	Sample collected, bag in good condition
Mean Seepage:						0.26	

Seepage Meter Field Measurements

Location: Lake Jesup

Site: 4 - With Sediments

Date Installed: 1/31/12

Chamber Diameter: 0.58 m

Sediment Area Covered: 0.27 m²

Date	Time Collected	Volume Collected (liters)	Previous Collection Event		Seepage Time (days)	Seepage (liters/m2-day)	Comments / Observations
			Date	Time			
1/31/12	13:42	-----	-----	-----	-----	-----	Bags Installed
3/9/12	11:04	9.75	1/31/12	13:42	37.9	0.95	Measured volume, no sample collected
7/13/12	9:20	8.75	3/9/12	11:04	125.9	0.26	Sample collected, bag in good condition
8/24/12	9:05	13.5	7/13/12	9:20	42.0	1.19	Sample collected, bag in good condition
11/30/12	9:30	10.75	8/24/12	9:05	98.0	0.41	Sample collected, bag replaced
1/25/13	10:14	5.75	11/30/12	9:30	56.0	0.38	Sample collected, bag in good condition
3/15/13	13:10	7.25	1/25/13	10:14	49.1	0.55	Sample collected, bag replaced
Mean Seepage:						0.50	

Seepage Meter Field Measurements

Location: Lake Jesup

Site: 5 - Without Sediments

Date Installed: 1/25/12

Chamber Diameter: 0.58 m

Sediment Area Covered: 0.27 m²

Date	Time Collected	Volume Collected (liters)	Previous Collection Event		Seepage Time (days)	Seepage (liters/m2-day)	Comments / Observations
			Date	Time			
1/25/12	12:40	-----	-----	-----	-----	-----	Bags Installed
3/9/12	11:18	5.25	1/25/12	12:40	43.9	0.44	Measured volume, no sample collected
7/13/12	9:58	6.75	3/9/12	11:18	125.9	0.20	Sample collected, bag in good condition
8/24/12	9:32	5.5	7/13/12	9:58	42.0	0.49	Sample collected, bag in good condition
11/30/12	10:30	5.75	8/24/12	9:32	98.0	0.22	Sample collected, bag in good condition
1/25/13	10:27	6.5	11/30/12	10:30	56.0	0.43	Sample collected, bag in good condition
3/15/13	12:15	7.25	1/25/13	10:27	49.1	0.55	Sample collected, bag in good condition
Mean Seepage:						0.33	

Seepage Meter Field Measurements

Location: Lake Jesup

Site: 5 - With Sediments

Date Installed: 1/25/12

Chamber Diameter: 0.58 m

Sediment Area Covered: 0.27 m²

Date	Time Collected	Volume Collected (liters)	Previous Collection Event		Seepage Time (days)	Seepage (liters/m ² -day)	Comments / Observations
			Date	Time			
1/25/12	12:52	----	----	----	----	----	Bags Installed
3/9/12	11:21	11.5	1/25/12	12:52	43.9	0.97	Measured volume, no sample collected
7/13/12	10:03	8.75	3/9/12	11:21	125.9	0.26	Sample collected, bag in good condition
8/24/12	9:36	8.25	7/13/12	10:03	42.0	0.73	Sample collected, bag in good condition
11/30/12	10:25	6.25	8/24/12	9:36	98.0	0.24	Sample collected, bag in good condition
1/25/13	10:31	8.75	11/30/12	10:25	56.0	0.58	Sample collected, bag in good condition
3/15/13	12:20	12.5	1/25/13	10:31	49.1	0.94	Sample collected, bag replaced
Mean Seepage:						0.50	

Seepage Meter Field Measurements

Location: Lake Jesup

Site: 6 - Without Sediments

Date Installed: 1/25/12

Chamber Diameter: 0.58 m

Sediment Area Covered: 0.27 m²

Date	Time Collected	Volume Collected (liters)	Previous Collection Event		Seepage Time (days)	Seepage (liters/m ² -day)	Comments / Observations
			Date	Time			
1/25/12	14:05	----	----	----	----	----	Bags Installed
3/9/12	11:34	4.75	1/25/12	14:05	43.9	0.40	Measured volume, no sample collected
7/13/12	9:42	3.75	3/9/12	11:34	125.9	0.11	Sample collected, bag in good condition
8/24/12	9:18	5.25	7/13/12	9:42	42.0	0.46	Sample collected, bag in good condition
11/30/12	10:00	5.75	8/24/12	9:18	98.0	0.22	Sample collected, bag in good condition
1/25/13	11:45	----	11/30/12	10:00	----	----	No sample collected, bag missing, bag replaced
3/15/13	12:40	6.75	1/25/13	11:45	49.0	0.51	Sample collected, bag in good condition
Mean Seepage:						0.27	

Seepage Meter Field Measurements

Location: Lake Jesup

Site: 6 - With Sediments

Date Installed: 1/25/12

Chamber Diameter: 0.58 m

Sediment Area Covered: 0.27 m²

Date	Time Collected	Volume Collected (liters)	Previous Collection Event		Seepage Time (days)	Seepage (liters/m ² -day)	Comments / Observations
			Date	Time			
1/25/12	14:19	----	----	----	----	----	Bags Installed
3/9/12	11:37	5.5	1/25/12	14:19	43.9	0.46	Measured volume, no sample collected
7/13/12	9:40	----	3/9/12	11:37	----	----	No sample collected, bag missing, bag replaced
8/24/12	9:22	----	7/13/12	9:40	----	----	No sample collected, meter flipped, meter reinstalled
11/30/12	10:10	----	8/24/12	9:22	----	----	No sample collected, bag missing, bag replaced
1/25/13	11:50	----	11/30/12	10:10	----	----	No sample collected, bag missing, bag replaced
3/15/13	12:45	7.25	1/25/13	11:50	49.0		Sample collected, bag in good condition
Mean Seepage:						0.51	

APPENDIX B

**CHEMICAL CHARACTERISTICS OF
GROUNDWATER SEEPAGE SAMPLES
COLLECTED IN LAKE JESUP FROM
JANUARY 2012 – MARCH 2013**

Characteristics of Groundwater Seepage Collected in Lake Jesup from January 2012 - March 2013

Sample Description	Date Collected	pH (s.u.)	Alkalinity (mg/L)	Spec. Cond. (µmho/cm)	NH ₃ -N (µg/L)	NO _x -N (µg/L)	Total N (µg/L)	SRP (µg/L)	Total P (µg/L)	Seepage (liters/m ² -day)
SP 1C	7/13/12	7.39	84.4	922	248	2,015	3,307	224	284	0.54
SP 1C	8/24/12	7.51	87.4	787	333	2,871	4,540	141	150	0.84
SP 1C	11/30/12	7.31	101	604	529	2,512	4,331	307	309	0.42
SP 1C	1/25/13	7.54	90.6	707	575	1,501	3,189	37	44	0.71
SP 1C	3/15/13	7.21	90.6	770	115	1,663	3,091	43	50	0.36
Min. Value		7.21	84.4	604	115	1,501	3,091	37	44	0.36
Max. Value		7.54	101	922	575	2,871	4,540	307	309	0.84
Flow-weighted Mean		7.43	90.0	764	378	2,167	3,761	143	160	0.55
SP 1L	7/13/12	7.50	90.8	1,021	1,093	311	3,383	45	119	0.51
SP 1L	8/24/12	7.43	73.8	605	1,254	1,106	3,746	63	97	1.08
SP 1L	11/30/12	7.34	104	730	1,326	2,656	5,236	437	451	1.01
SP 1L	1/25/13	7.39	83.0	718	211	714	2,116	18	24	0.89
SP 1L	3/15/13	7.24	97.8	803	523	191	2,390	45	56	0.85
Min. Value		7.24	73.8	605	211	191	2,116	18	24	0.51
Max. Value		7.50	104	1,021	1,326	2,656	5,236	437	451	1.08
Flow-weighted Mean		7.37	89.4	745	894	1,114	3,449	135	159	0.82
SP 2C	7/13/12	7.74	127	349	717	28	855	123	147	3.82
SP 2C	8/24/12	7.23	132	411	438	3	555	115	124	1.04
SP 2C	1/25/13	7.86	141	334	313	3	465	83	102	0.63
SP 2C	3/15/13	7.51	127	387	854	3	965	135	201	0.34
Min. Value		7.23	127	334	313	3	465	83	102	0.34
Max. Value		7.86	141	411	854	28	965	135	201	3.82
Flow-weighted Mean		7.65	129	361	632	19	766	118	141	2.11

Characteristics of Groundwater Seepage Collected in Lake Jesup from January 2012 - March 2013

Sample Description	Date Collected	pH (s.u.)	Alkalinity (mg/L)	Spec. Cond. (µmho/cm)	NH ₃ -N (µg/L)	NO _x -N (µg/L)	Total N (µg/L)	SRP (µg/L)	Total P (µg/L)	Seepage (liters/m ² -day)
SP 2L	7/13/12	7.39	114	663	902	564	1,911	323	396	0.35
SP 2L	8/24/12	7.77	100	548	775	632	1,906	114	118	1.21
SP 2L	11/30/12	7.08	109	515	674	1,101	2,272	318	334	0.47
SP 2L	1/25/13	7.91	147	362	1,866	156	2,223	285	300	1.34
SP 2L	3/15/13	7.47	139	425	1,629	19	1,871	140	208	1.38
Min. Value		7.08	100	362	674	19	1,871	114	118	0.35
Max. Value		7.91	147	663	1,866	1,101	2,272	323	396	1.38
Flow-weighted Mean		7.63	126	465	1,330	361	2,022	205	237	0.75
SP 3C	7/13/12	7.47	126	1,084	444	3,066	5,485	430	555	0.45
SP 3C	8/24/12	7.37	101	926	511	1,511	3,788	298	315	0.73
SP 3C	11/30/12	7.39	131	860	985	2,617	4,865	392	396	0.44
SP 3C	1/25/13	7.87	177	1,051	2,901	2,376	6,709	592	606	0.96
SP 3C	3/15/13	7.38	124	883	1,082	1,567	3,960	186	251	0.34
Min. Value		7.37	101	860	444	1,511	3,788	186	251	0.34
Max. Value		7.87	177	1,084	2,901	3,066	6,709	592	606	0.96
Flow-weighted Mean		7.55	137	976	1,424	2,209	5,192	416	452	0.56
SP 3L	7/13/12	7.42	97.0	988	1,178	504	3,638	227	382	0.66
SP 3L	8/24/12	7.33	82.6	877	1,833	53	3,729	112	135	1.10
SP 3L	11/30/12	7.25	116	784	2,828	143	4,843	384	437	0.76
SP 3L	1/25/13	7.57	122	918	1,295	594	3,225	174	185	0.81
SP 3L	3/15/13	7.47	110	934	654	107	2,277	68	76	1.08
Min. Value		7.25	82.6	784	654	53	2,277	68	76	0.66
Max. Value		7.57	122	988	2,828	594	4,843	384	437	1.10
Flow-weighted Mean		7.41	104	899	1,521	249	3,462	177	219	0.84

Characteristics of Groundwater Seepage Collected in Lake Jesup from January 2012 - March 2013

Sample Description	Date Collected	pH (s.u.)	Alkalinity (mg/L)	Spec. Cond. (µmho/cm)	NH ₃ -N (µg/L)	NO _x -N (µg/L)	Total N (µg/L)	SRP (µg/L)	Total P (µg/L)	Seepage (liters/m ² -day)
SP 4C	7/13/12	7.31	93.6	1,526	878	19	2,493	324	454	0.11
SP 4C	8/24/12	7.39	75.2	716	652	825	3,092	152	160	0.77
SP 4C	11/30/12	7.23	86.4	738	423	1,011	3,396	208	244	0.01
SP 4C	1/25/13	8.02	244	1,289	1,066	6,926	9,599	1,262	1,330	0.35
SP 4C	3/15/13	7.89	275	1,317	1,575	8,403	11,399	1,491	1,576	0.43
Min. Value		7.23	75	716	423	19	2,493	152	160	0.01
Max. Value		8.02	275	1,526	1,575	8,403	11,399	1,491	1,576	0.77
Flow-weighted Mean		7.64	163	1,044	991	4,004	6,558	741	790	0.26
SP 4L	7/13/12	7.36	120	1,175	4,444	382	6,730	514	588	0.26
SP 4L	8/24/12	7.32	70.0	752	1,222	298	2,794	147	149	1.19
SP 4L	11/30/12	7.27	79.0	669	65	781	1,944	48	56	0.41
SP 4L	1/25/13	7.88	241	1,181	4,362	2,375	8,399	948	1,018	0.38
SP 4L	3/15/13	7.73	237	1,504	1,496	8,945	12,276	1,703	1,817	0.55
Min. Value		7.27	70.0	669	65	298	1,944	48	56	0.26
Max. Value		7.88	241	1,504	4,444	8,945	12,276	1,703	1,817	1.19
Flow-weighted Mean		7.47	132	985	1,834	2,360	5,664	582	623	0.50
SP 5C	7/13/12	7.25	94.4	1,406	3,989	254	5,609	317	569	0.20
SP 5C	8/24/12	7.39	67.8	1,052	1,845	312	3,319	95	181	0.49
SP 5C	11/30/12	7.53	128	950	1,282	74	2,678	398	400	0.22
SP 5C	1/25/13	7.73	225	1,683	6,488	381	8,450	464	495	0.43
SP 5C	3/15/13	7.58	199	1,620	1,659	3,459	6,554	318	352	0.55
Min. Value		7.25	67.8	950	1,282	74	2,678	95	181	0.20
Max. Value		7.73	225	1,683	6,488	3,459	8,450	464	569	0.55
Flow-weighted Mean		7.52	152	1,388	3,015	1,211	5,604	303	369	0.33

Characteristics of Groundwater Seepage Collected in Lake Jesup from January 2012 - March 2013

Sample Description	Date Collected	pH (s.u.)	Alkalinity (mg/L)	Spec. Cond. (µmho/cm)	NH ₃ -N (µg/L)	NO _x -N (µg/L)	Total N (µg/L)	SRP (µg/L)	Total P (µg/L)	Seepage (liters/m ² -day)
SP 5L	7/13/12	7.35	89.6	1,213	1,708	22	3,198	47	183	0.26
SP 5L	8/24/12	7.32	74.4	944	1,584	160	3,200	28	67	0.73
SP 5L	11/30/12	7.27	113	1,015	2,044	194	3,569	134	365	0.24
SP 5L	1/25/13	7.54	111	947	1,781	177	3,361	27	226	0.58
SP 5L	3/15/13	7.32	107	901	288	1,172	2,727	14	18	0.94
Min. Value		7.27	74.4	901	288	22	2,727	14	18	0.24
Max. Value		7.54	113	1,213	2,044	1,172	3,569	134	365	0.94
Flow-weighted Mean		7.36	98.1	961	1,231	502	3,103	34	120	0.50
SP 6C	7/13/12	7.54	428	3,047	9,835	1,549	12,486	2,740	3,726	0.11
SP 6C	8/24/12	7.87	385	3,509	8,923	2,351	12,415	2,608	3,050	0.46
SP 6C	11/30/12	7.40	118	1,148	976	1,746	4,210	578	676	0.22
SP 6C	3/15/13	7.12	105	972	710	2,197	4,466	104	128	0.51
Min. Value		7.12	105	972	710	1,549	4,210	104	128	0.11
Max. Value		7.87	428	3,509	9,835	2,351	12,486	2,740	3,726	0.51
Flow-weighted Mean		7.47	234	2,081	4,453	2,122	7,934	1,298	1,565	0.50
SP 6L	3/15/13	7.21	134	1,042	3,038	63	4,649	30	34	0.55
Min. Value		7.21	134	1,042	3,038	63	4,649	30	34	0.55
Max. Value		7.21	134	1,042	3,038	63	4,649	30	34	0.55
Flow-weighted Mean		7.21	134	1,042	3,038	63	4,649	30	34	0.51

EVALUATION OF PHYSICAL / CHEMICAL CHARACTERISTICS OF SOFT SEDIMENTS IN LAKE JESUP

---Technical Report---

Revised September 29, 2014

Redacted Version
Completed by District Staff
2/23/2015

Prepared For:

St. Johns River Water Management District
Contract No. 27945



Prepared By:

Environmental Research and Design, Inc.
Harvey H. Harper, III, Ph.D., P.E.
3419 Trentwood Blvd., Suite 102
Belle Isle (Orlando), FL 32812-4864
Phone: 407-855-9465



TABLE OF CONTENTS

Section	Page
LIST OF TABLES	LT-1
LIST OF FIGURES	LF-1
1. INTRODUCTION	1
2. FIELD SAMPLING	1
2.1 Sediment Monitoring Sites	1
2.2 Collection Methods	1
2.2.1 Soft Sediment Depth	1
2.2.2 Sediment Sampling Techniques	4
2.2.3 Meteorological Data	4
3. LABORATORY METHODS	4
3.1 Sediment Characterization Methods	4
3.2 Sediment Speciation Techniques	5
4. RESULTS	7
4.1 Meteorological Conditions	7
4.2 Visual Sediment Characteristics	7
4.3 Soft Sediment Accumulation	7
4.4 Physical Sediment Characteristics	7
4.5 Nutrients and Organic Carbon	12
4.6 Sediment Phosphorus Speciation	14
4.7 Isotope Analyses	17
5. SEDIMENT INACTIVATION COST ANALYSIS	17
5.1 Introduction	17
5.2 Chemical Requirements	17
5.3 Cost Analysis	26
5.4 Longevity of Treatment	27

Appendices

- A. Photographs of Sediment Core Samples Collected in Lake Jesup

LIST OF FIGURES

Figure / Description	Page
2-1 Sediment Monitoring Sites in Lake Jesup Used by ERD	2
3-1 Schematic of Chang and Jackson Speciation Procedure for Evaluating Soil Phosphorus Bonding	6
5-1 Isopleths of Saloid-Bound Phosphorus in the Top 10 cm of Lake Jesup Sediments	20
5-2 Isopleths of Iron-Bound Phosphorus in the Top 10 cm of Lake Jesup Sediments	21
5-3 Isopleths of Total Available Phosphorus in the Top 10 cm of Lake Jesup Sediments	22

1. INTRODUCTION

This Technical Report provides a summary of work efforts conducted by Environmental Research & Design, Inc. (ERD) for the St. Johns River Water Management District (District) to evaluate the physical and chemical characteristics of unconsolidated flocculent sediments in Lake Jesup. The primary objective of this project is to measure the current depth and physical/chemical characteristics of the unconsolidated floc layer in Lake Jesup using sample sites from a similar study conducted during 1996 by Cable, et al. (1997).

In addition, isotope analyses were also conducted on supplemental sediment core samples collected at each of the monitoring sites to assess potential sources of soft floc within the lake.

2. FIELD SAMPLING

Evaluation of sediment characteristics was conducted in Lake Jesup at 49 locations used during the 1996 study. Sediment core samples were collected at each of the 49 sites and evaluated for moisture content, organic content, bulk density, total nitrogen, total organic matter, total phosphorus, non-apatite inorganic phosphorus (NAIP), sediment phosphorus speciation, and stable isotopes. A summary of field and laboratory methods used by ERD to accomplish these objectives is summarized in the following sections.

2.1 Sediment Monitoring Sites

Collection of sediment core samples in Lake Jesup was conducted on three consecutive days from August 4-6, 2014, with 14 sediment core samples collected on August 4th, 22 sediment core samples collected on August 5th, and 13 sediment core samples collected on August 6th. Locations of sediment monitoring sites in Lake Jesup used by ERD are illustrated on Figure 2-1. The monitoring sites illustrated on Figure 2-1 are intended to replicate the monitoring sites used during the 1996 study. A tabular comparison of the 1996 and 2014 sediment site coordinates is given on Table 2-1. As requested by the District, the horizontal datum is UTM 1 NAD 83 (90). The relative difference between the 1996 and 2014 sediment monitoring locations is provided in the final column of Table 2-1. Relative differences between the 1996 and 2014 sediment monitoring sites ranged from 1.4-60.2 m, with an overall mean relative difference of 21.2 m (69.5 ft).

2.2 Collection Methods

2.2.1 Soft Sediment Depth

Water depth at each of the 49 sediment monitoring sites was determined by lowering a 20-cm diameter Secchi disk attached to a graduated line until resistance from the sediment layer was encountered. The depth on the graduated line corresponding to the water surface was recorded in the field and is defined as the water depth at each site. After measurement of the water depth at each site, a 1.5-inch diameter graduated aluminum pole was then lowered into the water column and forced into the sediments to the point of refusal. The depth corresponding to the water surface is defined as the depth to the firm lake bottom. The difference between the depth to the firm lake bottom and the water depth at each site is defined as the depth of unconsolidated sediments.

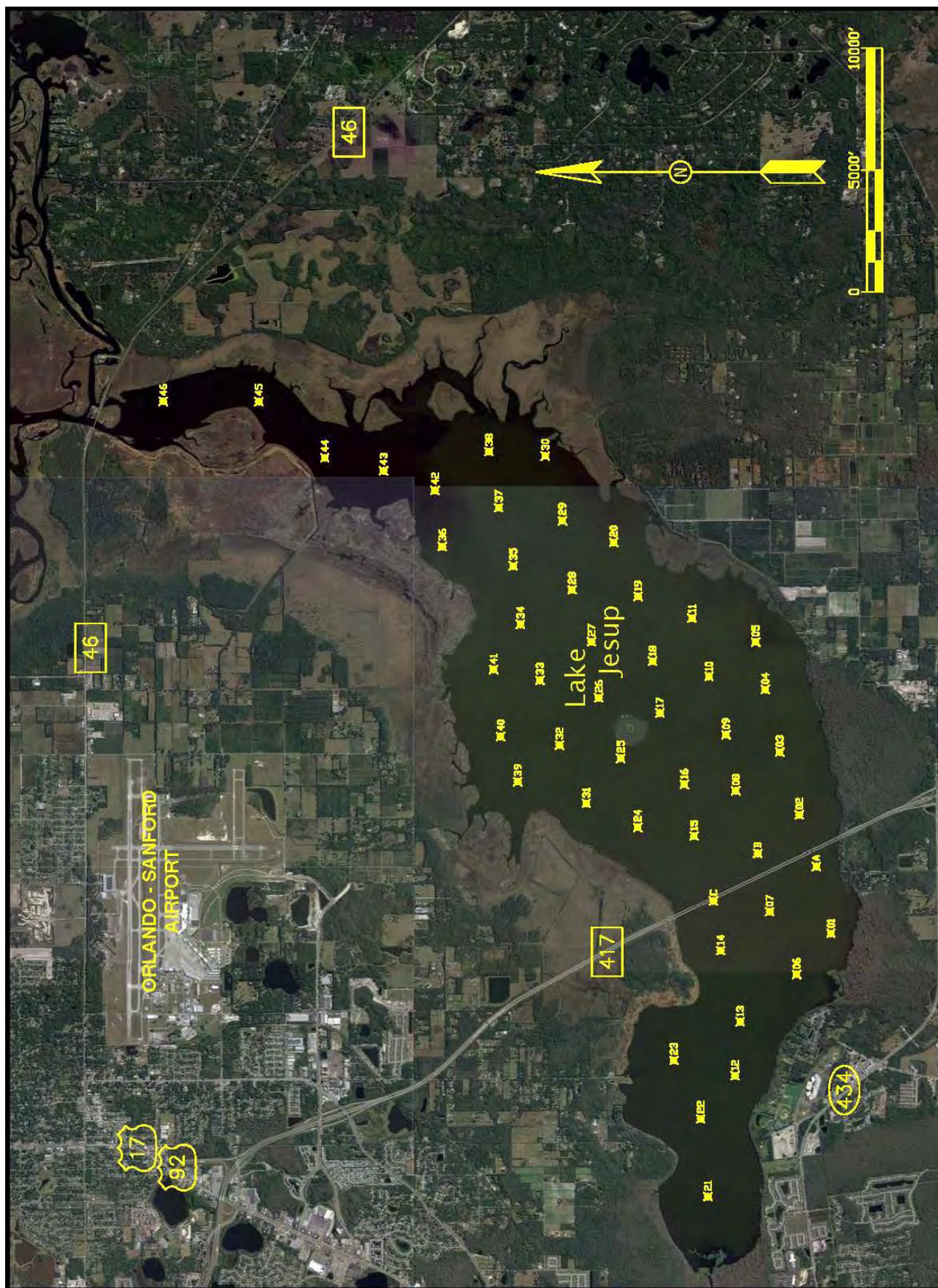


Figure 2-1. Sediment Monitoring Sites in Lake Jesup Used by ERD.

TABLE 2-1
COMPARISON OF 1996 AND 2014 SEDIMENT SITE COORDINATES

SITE	1996 STUDY		2014 STUDY		RELATIVE DIFFERENCE (m)
	Northing	Easting	Northing	Easting	
LJ-1	3175020	476015	3175012	476045	31.1
LJ-2	3175417	477508	3175431	477486	26.1
LJ-3	3175662	478295	3175669	478308	14.8
LJ-4	3175845	479082	3175850	479082	5.0
LJ-5	3175967	479679	3175992	479680	25.0
LJ-6	3175452	475500	3175464	475559	60.2
LJ-7	3175789	476288	3175834	476300	46.6
LJ-8	3176216	477808	3176200	477818	18.9
LJ-9	3176338	478513	3176340	478518	5.4
LJ-10	3176552	479246	3176577	479241	25.5
LJ-11	3176766	479979	3176744	479990	24.6
LJ-12	3176224	474227	3176270	474237	47.1
LJ-13	3176161	474905	3176170	474951	46.9
LJ-14	3176405	475800	3176424	475803	19.2
LJ-15	3176741	477239	3176746	477258	19.7
LJ-16	3176863	477890	3176857	477922	32.6
LJ-17	3177169	478786	3177167	478786	2.0
LJ-18	3177260	479437	3177251	479443	10.8
LJ-19	3177443	480251	3177479	480255	36.2
LJ-20	3177750	480930	3177761	480929	11.1
LJ-21	3176566	472708	3176585	472716	20.6
LJ-22	3176656	473685	3176698	473746	74.1
LJ-23	3176993	474418	3177020	474425	27.9
LJ-24	3177448	477349	3177470	477377	35.6
LJ-25	3177662	478217	3177660	478228	11.2
LJ-26	3177938	478977	3177930	478984	10.6
LJ-27	3178029	479683	3178039	479680	10.4
LJ-28	3178274	480334	3178272	480340	6.3
LJ-29	3178395	481202	3178395	481204	2.0
LJ-30	3178610	482017	3178611	482018	1.4
LJ-31	3178094	477649	3178110	477639	18.9
LJ-32	3178431	478382	3178433	478401	19.1
LJ-33	3178676	479196	3178662	479217	25.2
LJ-34	3178921	479901	3178915	479912	12.5
LJ-35	3179012	480634	3179020	480628	10.0
LJ-36	3179904	480879	3179902	480883	4.5
LJ-37	3179195	481367	3179199	481359	8.9
LJ-38	3179317	482072	3179325	482082	12.8
LJ-39	3178955	477921	3178930	477925	25.3
LJ-40	3179170	478491	3179159	478490	11.1
LJ-41	3179260	479332	3179269	479329	9.5
LJ-42	3179995	481585	3179985	481593	12.8
LJ-43	3180641	481830	3180654	481848	22.2
LJ-44	3181379	481994	3181395	481989	16.8
LJ-45	3182209	482700	3182221	482700	21.2
LJ-46	3183409	482702	3183424	482721	12.0
LJ-A	3175203	476856	3175174	476866	24.2
LJ-B	3175941	477020	3175935	477053	30.7
LJ-C	3176496	476425	3176496	476432	33.5
Mean Relative Difference (m):					21.2

2.2.2 Sediment Sampling Techniques

Sediment samples were collected at each of the 49 monitoring sites using a stainless steel split-spoon core device, which was penetrated into the sediments to the point of refusal. After retrieval of the sediment sample, any overlying water was carefully decanted before the split-spoon device was opened to expose the collected sample. Visual characteristics of each sediment core sample were recorded, the exposed core was photographed, and the 0-10 cm layer was carefully sectioned off and placed into a polyethylene container for transport to the ERD laboratory. Duplicate core samples were collected at each site, and the 0-10 cm layers were combined together to form a single composite sample for each of the sites. The polyethylene containers used for storage of the collected samples were filled completely to eliminate air space in the storage container above the composite sediment sample. Each of the collected samples was stored in ice and returned to the ERD laboratory for physical and chemical characterization.

A supplemental sediment core sample was also collected at each of the 49 monitoring sites for analysis of stable isotopes. These samples were collected using the same methodology outlined above with the exception that the entire muck layer was removed rather than just the 0-10 cm layer. The entire soft muck layer was placed into a stainless steel mixing bowl and thoroughly mixed using a stainless steel spoon. A sub-sample of the mixed sediment layer was placed into a polyethylene container for transport to the ERD Laboratory. The polyethylene containers were filled completely to eliminate air space in the storage container above the composite sediment sample. Each of the samples was stored in ice and returned to the ERD Laboratory.

2.2.3 Meteorological Data

Meteorological characteristics of air temperature and wind speed were measured at each of the 49 monitoring sites using a SpeedTech WindMate Model 350 wind/weather meter. Wind direction was determined using a compass.

3. LABORATORY METHODS

3.1 Sediment Characterization Methods

A summary of methods and analytical procedures for general parameters and nutrients conducted on the Lake Jesup sediment samples is given in Table 3-1. Analyses for moisture content, bulk density, organic content, total nitrogen, total organic carbon, total phosphorus, and NAIP were conducted on the 0-10 cm layer, with analyses conducted by ERD for all parameters except total nitrogen and TOC. The stable nitrogen isotope analyses were conducted by the Colorado Plateau Isotope Laboratory using the composite layer of the soft sediment material. Instructions on preparation and shipping of the sediment samples were provided to ERD by the Isotope Laboratory.

TABLE 3-1
LIST OF GENERAL PARAMETERS AND NUTRIENTS

PARAMETER	METHOD/ PREPARATION	ANALYTICAL PROCEDURE	REFERENCE	SEDIMENT LAYER (cm)	ANALYSIS CONDUCTED BY
Water Content	Dry sub-sample of sediment to a constant weight	70°C for 72 hours	--	0-10	ERD
Bulk Density	Wet weight of sediment divided by volume of wet sediment	--	--	0-10	ERD
Organic Content	Loss on ignition	550°C for 2 hours in muffle furnace	Håkanson & Jansson (1983)	0-10	ERD
Total N and Total Organic C	Combust fine, dried and sieved sediment	Carlo Erba CNS elemental analyzer	--	0-10	Colorado Plateau Isotope Laboratory
Total P	Combust sample in muffle furnace for 2 hours at 550°C and dissolve ash in 6 M HCl	Analyze for TP using EPA Method 365.1	--	0-10	ERD
Non-Apatite Inorganic P (NAIP)	Extract sediment with 0.1 M NaOH for 17 hours at 25°C	Analyze for SRP using EPA Method 365.1	Williams, et al. (1976)	0-10	ERD
Stable Isotope Analysis of N	Dry at 550°, crush and grind, sieve using #20 sieve	--	--	Composite of soft sediment layer	Colorado Plateau Isotope Laboratory

3.2 Sediment Speciation Techniques

In addition to general sediment characterization, a fractionation procedure for inorganic soil phosphorus was conducted on each of the 49 collected sediment samples. A modified version of the Chang and Jackson Procedure, as proposed by Peterson and Corey (1966), was used for phosphorus fractionation. The Chang and Jackson Procedure allows the speciation of sediment phosphorus into saloid-bound phosphorus (defined as the sum of soluble plus easily exchangeable sediment phosphorus), iron-bound phosphorus, and aluminum-bound phosphorus. Although not used in this project, subsequent extractions of the Chang and Jackson procedure also provide calcium-bound and residual fractions.

The Chang and Jackson procedure was originally developed at the University of Wisconsin to evaluate phosphorus bonding in dried agricultural soils. However, drying of wet sediments will significantly impact the phosphorus speciation, particularly the soluble and iron-bound associations. Therefore, the basic Chang and Jackson method was adapted and modified by ERD for wet sediments by adjusting solution concentrations and extraction timing to account for the liquid volume in the wet sediments and the reduced solids mass. This modified method has been used as the basis for all lake sediment inactivation projects which have been conducted in the State of Florida.

Saloid-bound phosphorus is considered to be available under all conditions at all times. Iron-bound phosphorus is relatively stable under aerobic environments, generally characterized by redox potentials greater than 200 mv (E_h), while unstable under anoxic conditions, characterized by redox potential less than 200 mv. Aluminum-bound phosphorus is considered to be stable under all conditions of redox potential and natural pH conditions. A schematic of the Chang and Jackson Speciation Procedure for evaluating soil phosphorus bounding is given in Figure 3-1.

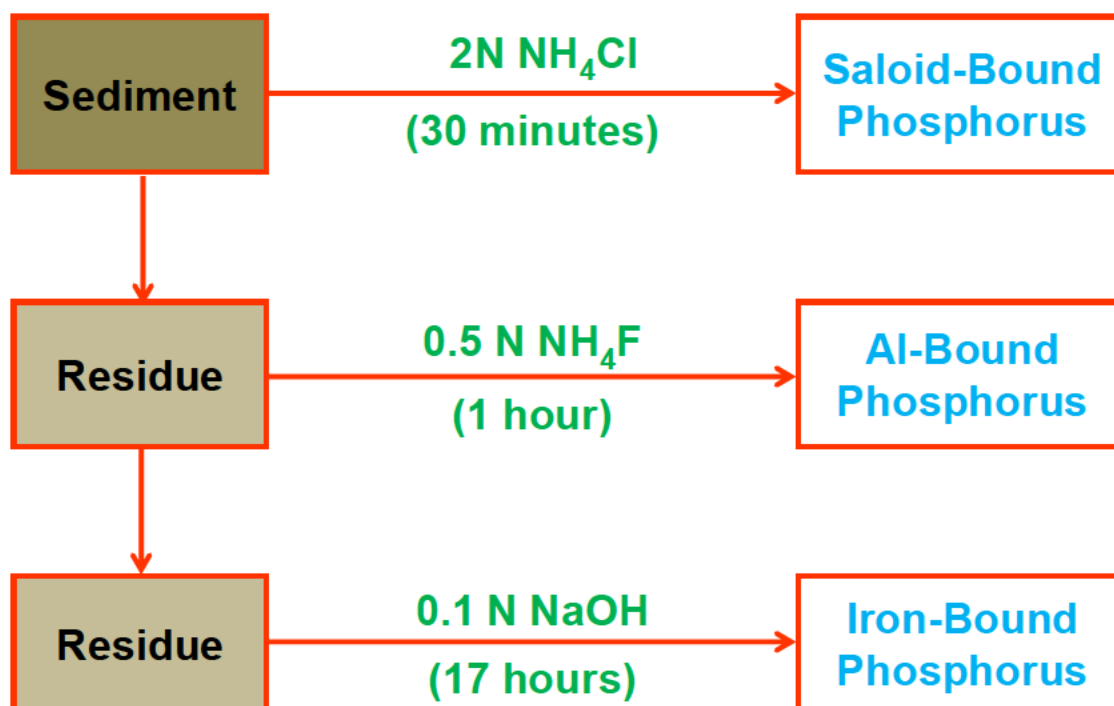


Figure 3-1. Schematic of Chang and Jackson Speciation Procedure for Evaluating Soil Phosphorus Bonding.

For purposes of evaluating release potential, ERD typically assumes that potentially available inorganic phosphorus in soils/sediments, particularly those which exhibit a significant potential to develop reduced conditions below the sediment-water interface, is represented by the sum of the soluble inorganic phosphorus and easily exchangeable phosphorus fractions (collectively termed saloid-bound phosphorus), plus iron-bound phosphorus which can become solubilized under reduced conditions. Aluminum-bound phosphorus is generally considered to be unavailable in the pH range of approximately 5.5-7.5 under a wide range of redox conditions.

4. RESULTS

4.1 Meteorological Conditions

A summary of meteorological conditions during the Lake Jesup sediment monitoring program is given on Table 4-1. Sediment collection was conducted on three consecutive days from August 4-6, 2014. Air temperatures ranged from the low 80s to the low 90s, with low to moderate wind speeds ranging from calm to 7.4 mph. Wind direction was primarily from the west.

4.2 Visual Sediment Characteristics

Visual characteristics of sediment core samples were recorded for each of the 49 sediment samples collected in Lake Jesup. In general, a surficial layer of unconsolidated organic muck was observed at 42 of the 49 monitoring sites, with measured depths ranging from 0-7 cm. This unconsolidated surficial layer is comprised primarily of fresh organic material, such as dead algal cells, and detritus which has recently accumulated onto the bottom of the lake, and this layer is relatively easily disturbed by wind action or boating activities. Beneath the unconsolidated surficial layer, the organic muck becomes more consolidated with a consistency similar to pudding. These layers reflect older organic deposits which are resistant to further degradation and do not resuspend into the water column except during vigorous wind activity on the lake. Several of the monitoring locations were characterized by brown fine sand with no visual muck accumulations. Photographs of sediment characteristics at each of the 49 sites in Lake Jesup are given in Appendix A.

4.3 Soft Sediment

A tabular summary of soft sediment measurements conducted in Lake Jesup by ERD is given on Table 4-2. Estimates of the soft sediment depth are obtained by subtracting the measured water depth from the depth to firm bottom at each monitoring site. Calculated soft sediment depths in Lake Jesup ranged from 0-7.68 ft, with an overall geometric mean of 1.96 ft.

4.4 Physical Sediment Characteristics

Each of the 49 collected sediment core samples was evaluated for moisture content, organic content, and bulk density. In addition, ERD also evaluated sediment pH to support the evaluation of feasibility for an alum treatment to the lake sediments. A tabular summary of physical characteristics of Lake Jesup sediments is given in Table 4-4. Sediment pH values ranged from slightly acidic to slightly alkaline, with an overall geometric mean value of 6.96.

TABLE 4-1

METEOROLOGICAL CONDITIONS DURING LAKE JESUP SEDIMENT MONITORING

SITE	DATE	TIME	AIR TEMPERATURE (°F)	WIND	
				Speed (mph)	Direction
LJ-1	8/4/14	11:08	87.0	1.4	W
LJ-2	8/4/14	13:32	87.5	4.0	W
LJ-3	8/4/14	13:38	87.3	5.0	W
LJ-4	8/5/14	10:20	84.0	6.0	W
LJ-5	8/5/14	10:40	84.4	7.6	W
LJ-6	8/4/14	10:49	86.0	2.5	W
LJ-7	8/4/14	11:27	85.2	4.0	W
LJ-8	8/5/14	9:47	82.8	5.3	W
LJ-9	8/5/14	10:02	81.5	7.4	W
LJ-10	8/5/14	10:59	83.0	1.5	W
LJ-11	8/5/14	11:47	84.6	6.4	W
LJ-12	8/4/14	9:56	86.8	1.6	W
LJ-13	8/4/14	10:33	86.8	1.4	W
LJ-14	8/4/14	11:48	85.1	5.2	W
LJ-15	8/5/14	9:16	82.3	4.4	W
LJ-16	8/5/14	9:32	82.8	5.4	W
LJ-17	8/5/14	11:19	84.4	5.0	W
LJ-18	8/5/14	11:33	85.6	5.3	W
LJ-19	8/5/14	12:04	85.0	6.0	W
LJ-20	8/5/14	12:20	86.3	5.5	W
LJ-21	8/4/14	9:15	83.5	2.0	W
LJ-22	8/4/14	9:38	83.6	3.7	W
LJ-23	8/4/14	10:15	84.1	4.4	W
LJ-24	8/6/14	9:11	84.5	1.8	W
LJ-25	8/6/14	9:26	84.1	3.3	W
LJ-26	8/6/14	9:39	85.0	2.1	W
LJ-27	8/6/14	9:54	85.7	1.1	W
LJ-28	8/6/14	10:07	84.1	1.0	W
LJ-29	8/5/14	12:56	89.0	6.3	W
LJ-30	8/5/14	13:09	86.1	5.8	W
LJ-31	8/6/14	12:32	87.8	1.3	NW
LJ-32	8/6/14	12:15	88.1	1.7	W
LJ-33	8/6/14	12:02	91.0	0.6	W
LJ-34	8/6/14	11:01	88.6	2.3	W
LJ-35	8/6/14	10:28	90.9	4.4	W
LJ-36	8/5/14	15:16	87.4	5.5	SW
LJ-37	8/5/14	13:24	86.8	3.1	W
LJ-38	8/5/14	13:38	86.9	6.5	W
LJ-39	8/6/14	11:45	94.5	Calm	-
LJ-40	8/6/14	11:35	92.1	1.5	W
LJ-41	8/6/14	11:22	87.1	2.3	W
LJ-42	8/5/14	15:03	87.9	3.3	W
LJ-43	8/5/14	13:55	88.0	3.4	W
LJ-44	8/5/14	14:09	91.9	2.1	W
LJ-45	8/5/14	14:27	90.0	4.7	W
LJ-46	8/5/14	14:42	87.5	5.8	W
LJ-A	8/4/14	12:41	86.4	2.7	W
LJ-B	8/4/14	12:24	90.1	3.6	W
LJ-C	8/4/14	12:04	87.7	3.2	W

TABLE 4-2

LAKE JESUP SOFT SEDIMENT MEASUREMENTS

SITE	DATE	WATER DEPTH		DEPTH TO FIRM BOTTOM		SOFT SEDIMENT DEPTH	
		ft	m	ft	m	ft	m
LJ-1	8/4/14	6.40	1.95	10.3	3.14	3.90	1.19
LJ-2	8/4/14	6.89	2.10	10.9	3.32	4.01	1.22
LJ-3	8/4/14	7.22	2.20	10.0	3.05	2.78	0.85
LJ-4	8/5/14	6.89	2.10	11.8	3.60	4.91	1.50
LJ-5	8/5/14	6.23	1.90	10.8	3.29	4.57	1.39
LJ-6	8/4/14	6.89	2.10	13.5	4.12	6.61	2.02
LJ-7	8/4/14	7.22	2.20	14.9	4.54	7.68	2.34
LJ-8	8/5/14	7.54	2.30	12.7	3.87	5.16	1.57
LJ-9	8/5/14	9.51	2.90	10.0	3.05	0.49	0.15
LJ-10	8/5/14	8.86	2.70	11.0	3.35	2.14	0.65
LJ-11	8/5/14	6.89	2.10	10.5	3.20	3.61	1.10
LJ-12	8/4/14	7.90	2.41	13.1	3.99	5.20	1.58
LJ-13	8/4/14	7.94	2.42	9.7	2.96	1.76	0.54
LJ-14	8/4/14	7.90	2.41	9.8	2.99	1.90	0.58
LJ-15	8/5/14	7.38	2.25	12.5	3.81	5.12	1.56
LJ-16	8/5/14	7.54	2.30	13.2	4.02	5.66	1.72
LJ-17	8/5/14	5.48	1.67	5.5	1.68	0.02	0.01
LJ-18	8/5/14	8.53	2.60	9.3	2.84	0.77	0.24
LJ-19	8/5/14	6.23	1.90	10.6	3.23	4.37	1.33
LJ-20	8/5/14	6.23	1.90	9.8	2.99	3.57	1.09
LJ-21	8/4/14	6.56	2.00	11.4	3.48	4.84	1.48
LJ-22	8/4/14	8.04	2.45	10.3	3.14	2.26	0.69
LJ-23	8/4/14	7.05	2.15	8.5	2.59	1.45	0.44
LJ-24	8/6/14	6.89	2.10	11.1	3.38	4.21	1.28
LJ-25	8/6/14	6.89	2.10	7.2	2.20	0.31	0.10
LJ-26	8/6/14	8.69	2.65	9.5	2.90	0.81	0.25
LJ-27	8/6/14	7.54	2.30	9.9	3.02	2.36	0.72
LJ-28	8/6/14	9.18	2.80	10.2	3.11	1.02	0.31
LJ-29	8/5/14	6.89	2.10	10.2	3.11	3.31	1.01
LJ-30	8/5/14	5.90	1.80	10.0	3.05	4.10	1.25
LJ-31	8/6/14	6.89	2.10	8.0	2.44	1.11	0.34
LJ-32	8/6/14	6.43	1.96	8.5	2.59	2.07	0.63
LJ-33	8/6/14	7.05	2.15	9.7	2.96	2.65	0.81
LJ-34	8/6/14	7.87	2.40	8.0	2.44	0.13	0.04
LJ-35	8/6/14	6.56	2.00	9.7	2.96	3.14	0.96
LJ-36	8/5/14	5.90	1.80	9.1	2.77	3.20	0.97
LJ-37	8/5/14	7.54	2.30	9.3	2.84	1.76	0.54
LJ-38	8/5/14	6.23	1.90	9.8	2.99	3.57	1.09
LJ-39	8/6/14	5.90	1.80	9.1	2.77	3.20	0.97
LJ-40	8/6/14	6.49	1.98	9.1	2.77	2.61	0.79
LJ-41	8/6/14	6.00	1.83	6.0	1.83	0.00	0.00
LJ-42	8/5/14	7.22	2.20	9.7	2.96	2.48	0.76
LJ-43	8/5/14	6.23	1.90	8.8	2.68	2.57	0.78
LJ-44	8/5/14	5.90	1.80	8.5	2.59	2.60	0.79
LJ-45	8/5/14	5.90	1.80	8.9	2.71	3.00	0.91
LJ-46	8/5/14	4.59	1.40	9.7	2.96	5.11	1.56
LJ-A	8/4/14	7.54	2.30	9.9	3.02	2.36	0.72
LJ-B	8/4/14	7.22	2.20	11.8	3.60	4.58	1.40
LJ-C	8/4/14	6.89	2.10	9.3	2.84	2.41	0.74
Minimum Value:		4.59	1.40	5.50	1.68	0.00	0.00
Maximum Value:		9.51	2.90	14.90	4.54	7.68	2.34
Geometric Mean:		6.95	2.12	9.87	3.01	1.96	0.61

TABLE 4-4
PHYSICAL CHARACTERISTICS OF LAKE JESUP SEDIMENTS

SITE	SEDIMENT LAYER (cm)	pH (s.u.)	MOISTURE CONTENT (%)	PERCENT SOLIDS (%)	ORGANIC CONTENT (%)	WET DENSITY (g/cm ³)	TOC (% dry wt.)	RATIO TOC/ORGANIC
LJ-1	0-10	6.95	91.1	8.9	31.7	1.09	12.11	0.38
LJ-2	0-10	6.90	92.9	7.1	35.1	1.07	16.30	0.46
LJ-3	0-10	6.74	91.3	8.7	31.7	1.09	14.15	0.45
LJ-4	0-10	6.61	91.2	8.8	28.7	1.09	10.31	0.36
LJ-5	0-10	6.79	91.9	8.1	33.3	1.08	16.04	0.48
LJ-6	0-10	6.89	91.6	8.4	33.3	1.08	13.70	0.41
LJ-7	0-10	6.81	93.2	6.8	34.3	1.07	15.18	0.44
LJ-8	0-10	6.95	90.1	9.9	25.7	1.11	8.86	0.35
LJ-9	0-10	7.13	57.2	42.8	9.0	1.58	6.95	0.77
LJ-10	0-10	7.00	48.1	51.9	7.6	1.72	4.89	0.64
LJ-11	0-10	6.82	92.9	7.1	37.4	1.07	5.28	0.14
LJ-12	0-10	7.01	90.8	9.2	28.2	1.10	13.24	0.47
LJ-13	0-10	6.96	89.8	10.2	26.2	1.11	11.32	0.43
LJ-14	0-10	7.01	91.2	8.8	27.9	1.10	4.78	0.17
LJ-15	0-10	6.99	92.5	7.5	31.9	1.08	13.94	0.44
LJ-16	0-10	6.94	90.1	9.9	26.7	1.11	13.78	0.52
LJ-17	0-10	7.32	24.7	75.3	0.9	2.12	0.47	0.51
LJ-18	0-10	6.54	44.5	55.5	5.1	1.79	3.96	0.78
LJ-19	0-10	6.85	92.2	7.8	33.2	1.08	6.51	0.20
LJ-20	0-10	6.89	90.2	9.8	30.2	1.10	11.88	0.39
LJ-21	0-10	6.86	93.0	7.0	34.2	1.07	15.51	0.45
LJ-22	0-10	6.91	90.2	9.8	22.7	1.11	10.07	0.44
LJ-23	0-10	6.94	90.8	9.2	27.4	1.10	10.81	0.39
LJ-24	0-10	6.99	88.6	11.4	20.8	1.13	13.96	0.67
LJ-25	0-10	7.49	22.8	77.2	0.8	2.15	0.63	0.79
LJ-26	0-10	6.91	46.2	53.8	6.6	1.75	5.90	0.90
LJ-27	0-10	6.90	86.0	14.0	15.9	1.18	9.79	0.62
LJ-28	0-10	6.98	60.4	39.6	12.3	1.54	10.48	0.85
LJ-29	0-10	6.87	92.8	7.2	37.4	1.07	12.55	0.34
LJ-30	0-10	6.81	92.2	7.8	34.9	1.08	14.04	0.40
LJ-31	0-10	7.00	87.9	12.1	22.8	1.14	8.84	0.39
LJ-32	0-10	6.90	90.6	9.4	27.6	1.10	5.27	0.19
LJ-33	0-10	6.93	91.4	8.6	28.4	1.09	5.70	0.20
LJ-34	0-10	8.22	30.3	69.7	3.1	2.01	0.85	0.28
LJ-35	0-10	6.90	88.8	11.2	23.0	1.13	11.43	0.50
LJ-36	0-10	6.83	87.1	12.9	17.7	1.16	7.49	0.42
LJ-37	0-10	6.90	92.0	8.0	31.5	1.08	9.84	0.31
LJ-38	0-10	6.86	94.1	5.9	38.5	1.05	13.28	0.34
LJ-39	0-10	6.89	89.2	10.8	20.7	1.13	7.35	0.36
LJ-40	0-10	7.02	89.4	10.6	22.3	1.12	8.00	0.36
LJ-41	0-10	8.45	26.0	74.0	1.1	2.10	0.37	0.33
LJ-42	0-10	6.91	86.0	14.0	16.5	1.18	11.32	0.68
LJ-43	0-10	6.87	85.9	14.1	19.9	1.17	6.43	0.32
LJ-44	0-10	7.02	90.2	9.8	26.3	1.11	11.05	0.42
LJ-45	0-10	6.80	84.4	15.6	17.4	1.19	13.07	0.75
LJ-46	0-10	6.83	91.4	8.6	30.7	1.09	10.90	0.36
LJ-A	0-10	6.58	90.2	9.8	28.3	1.10	16.92	0.60
LJ-B	0-10	6.85	91.9	8.1	31.0	1.08	15.68	0.51
LJ-C	0-10	6.63	93.9	6.1	38.3	1.06	12.25	0.32
Minimum Value:		6.54	22.8	5.9	0.8	1.05	0.37	0.14
Maximum Value:		8.45	94.1	77.2	38.5	2.15	16.92	0.90
Geometric Mean:		6.96	77.0	12.9	18.8	1.21	7.90	0.42

Measurements of sediment moisture content in Lake Jesup sediments were found to be highly variable throughout the lake. The majority of the sediment core samples are characterized by elevated values of moisture content, suggesting that the sediments consist primarily of organic muck. Twenty-nine (29) of the 49 sediment samples are characterized by moisture contents of 90% or greater, with 40 of the 49 samples exhibiting moisture contents of 85% or greater. Only 7 of the 49 sediment sites are characterized by moisture contents less than 50% which suggests mixtures of sand and organic muck. Sediment moisture contents less than 25%, reflecting primarily sand-type sediments, were observed at 3 of the 49 sites. The overall geometric mean moisture content within the lake is 77%.

Measured sediment organic contents (loss on ignition) in Lake Jesup sediments were also highly variable, ranging from 0.8-38.5%. Thirty-five (35) of the 49 sediment samples are characterized by organic contents of approximately 20% or greater which is primarily associated with organic muck.

Sediment density values in Lake Jesup were also highly variable, ranging from 1.05-2.15 g/cm³. Sediment wet densities of approximately 1.2 g/cm³ or less primarily reflect organic muck-type sediments, with densities of approximately 2 g/cm³ or greater reflecting primarily sand.

Measurements of total organic carbon (TOC) in the Lake Jesup sediments were conducted by the Colorado Plateau Laboratory. TOC concentrations in the sediment samples ranged from 0.37-16.92%, with an overall geometric mean of 7.9%. Calculated ratios of TOC/organic content were relatively consistent among the sediment monitoring sites, with the vast majority of measured values ranging from approximately 0.3-0.5. The overall geometric mean ratio of TOC/organic content is 0.42.

4.5 Nutrients and Organic Carbon

A summary of sediment nutrient concentrations in Lake Jesup is given in Table 4-5. Sediment phosphorus concentrations are provided for ashed sediments based upon the analytical technique requested by the District and for comparison with the previous 1996 analyses which also used ashed sediments. However, phosphorus concentrations measured on ashed sediments have limited value in highly organic liquid sediments similar to those which exist in Lake Jesup, and phosphorus concentrations measured on a wet weight or volumetric basis provide a much better method of comparison. Therefore, calculations are also provided for total phosphorus concentrations on a wet sediment basis as well as concentrations per cm³ of sediment which is perhaps the most useful method of expressing phosphorus concentrations for these type sediments. Total phosphorus concentrations in terms of µg/cm³ of wet sediment ranged from 55-347 µg/cm³, with an overall geometric mean of 126 µg/cm³.

Sediment nitrogen concentrations were measured as a percentage of dry sediment weight to be consistent with the 1996 measurements and the analytical technique used for nitrogen determination. Overall, the sediments in Lake Jesup are approximately 0.58% nitrogen on a dry weight basis. Similar to the comments provided previously for phosphorus, nitrogen concentrations expressed on a dry weight basis have limited value in highly organic liquid sediments similar to those which exist in Lake Jesup due to the relatively small amount of solid matter in the surficial sediments. A more useful method of expressing nitrogen concentrations is on a wet weight or volumetric basis similar to that used for phosphorus. Total nitrogen concentrations in terms of µg/cm³ of wet sediment in Lake Jesup ranged from 232-2,618 µg/cm³, with an overall geometric mean of 904 µg/cm³.

TABLE 4-5

MEASURED SEDIMENT NUTRIENT CONCENTRATIONS IN LAKE JESUP

SITE	SEDIMENT LAYER (cm)	DATE COLLECTED	SEDIMENT PHOSPHORUS CONCENTRATION				SEDIMENT NITROGEN CONCENTRATION			
			µg/g ash wt.	µg/g dry wt.	µg/g wet wt.	µg/cm ³ wet	% dry wt.	mg/g dry	µg/g wet	µg/cm ³ wet
LJ-1	0-10	8/4/14	1,795	1,226	109	119	0.64	6.4	567	618
LJ-2	0-10	8/4/14	2,193	1,424	101	108	1.32	13.2	932	996
LJ-3	0-10	8/4/14	2,053	1,403	122	133	1.10	11.0	957	1,043
LJ-4	0-10	8/5/14	1,537	1,095	96	105	0.82	8.2	720	787
LJ-5	0-10	8/5/14	1,438	959	78	84	1.09	10.9	886	958
LJ-6	0-10	8/4/14	1,211	808	68	73	1.11	11.1	931	1,009
LJ-7	0-10	8/4/14	2,377	1,561	106	113	1.21	12.1	822	878
LJ-8	0-10	8/5/14	1,192	886	88	97	0.69	6.9	687	763
LJ-9	0-10	8/5/14	393	358	153	242	0.36	3.6	1,546	2,448
LJ-10	0-10	8/5/14	157	145	75	129	0.29	2.9	1,523	2,618
LJ-11	0-10	8/5/14	2,186	1,369	97	103	0.43	4.3	304	324
LJ-12	0-10	8/4/14	1,263	907	84	92	1.13	11.3	1,040	1,143
LJ-13	0-10	8/4/14	2,583	1,906	194	216	0.93	9.3	945	1,051
LJ-14	0-10	8/4/14	1,299	937	83	90	0.37	3.7	322	353
LJ-15	0-10	8/5/14	1,144	779	58	63	1.22	12.2	907	976
LJ-16	0-10	8/5/14	1,020	748	74	82	1.14	11.4	1,132	1,256
LJ-17	0-10	8/5/14	197	195	147	311	0.04	0.4	335	711
LJ-18	0-10	8/5/14	324	308	171	306	0.23	2.3	1,280	2,293
LJ-19	0-10	8/5/14	1,707	1,141	90	97	0.50	5.0	392	423
LJ-20	0-10	8/5/14	2,072	1,445	141	156	0.96	9.6	937	1,033
LJ-21	0-10	8/4/14	1,868	1,230	86	92	0.96	9.6	676	723
LJ-22	0-10	8/4/14	2,213	1,711	168	187	0.64	6.4	628	700
LJ-23	0-10	8/4/14	1,837	1,334	122	135	0.89	8.9	815	896
LJ-24	0-10	8/6/14	800	633	72	82	1.19	11.9	1,355	1,538
LJ-25	0-10	8/6/14	211	209	161	347	0.03	0.3	212	457
LJ-26	0-10	8/6/14	93	87	47	82	0.21	2.1	1,122	1,967
LJ-27	0-10	8/6/14	974	819	115	135	0.94	9.4	1,315	1,547
LJ-28	0-10	8/6/14	591	519	205	317	0.34	3.4	1,332	2,057
LJ-29	0-10	8/5/14	1,541	964	69	74	1.03	10.3	739	789
LJ-30	0-10	8/5/14	2,493	1,622	127	136	1.03	10.3	806	867
LJ-31	0-10	8/6/14	1,384	1,068	129	147	0.68	6.8	816	930
LJ-32	0-10	8/6/14	1,527	1,106	103	114	0.23	2.3	211	232
LJ-33	0-10	8/6/14	1,543	1,104	95	103	0.46	4.6	397	433
LJ-34	0-10	8/6/14	205	199	138	279	0.07	0.7	478	961
LJ-35	0-10	8/6/14	1,071	825	92	104	1.05	10.5	1,179	1,331
LJ-36	0-10	8/5/14	673	553	72	83	0.68	6.8	876	1,016
LJ-37	0-10	8/5/14	1,589	1,088	87	94	0.71	7.1	569	615
LJ-38	0-10	8/5/14	1,591	978	58	61	0.89	8.9	527	555
LJ-39	0-10	8/6/14	918	729	79	89	0.59	5.9	644	727
LJ-40	0-10	8/6/14	1,587	1,232	131	147	0.66	6.6	704	791
LJ-41	0-10	8/6/14	145	144	106	223	0.03	0.3	248	521
LJ-42	0-10	8/5/14	1,908	1,592	223	263	0.84	8.4	1,180	1,388
LJ-43	0-10	8/5/14	1,159	928	130	152	0.41	4.1	578	676
LJ-44	0-10	8/5/14	1,268	935	92	101	0.80	8.0	786	871
LJ-45	0-10	8/5/14	1,628	1,346	210	250	1.10	11.0	1,713	2,044
LJ-46	0-10	8/5/14	1,742	1,207	104	113	0.88	8.8	759	827
LJ-A	0-10	8/4/14	1,975	1,415	138	153	1.41	14.1	1,374	1,518
LJ-B	0-10	8/4/14	911	629	51	55	1.32	13.2	1,075	1,165
LJ-C	0-10	8/4/14	2,884	1,780	108	114	1.05	10.5	636	672
Minimum Value:			93	87	47	55	0.03	0.3	211	232
Maximum Value:			2,884	1,906	223	347	1.41	14.1	1,713	2,618
Geometric Mean:			1,069	805	104	126	0.58	5.8	745	904

A tabular summary of sediment characteristics measured by ERD in 25 Central Florida lakes, ranging from oligotrophic to hypereutrophic, is given in Table 4-6 for comparison purposes. Summary statistics are provided at the bottom of Table 4-6, with an overall geometric mean value listed for eutrophic and hypereutrophic lakes. The overall geometric mean phosphorus concentration in Lake Jesup sediments of $126 \mu\text{g}/\text{cm}^3$ is approximately half of the total phosphorus concentration of $260 \mu\text{g}/\text{cm}^3$ measured by ERD in other eutrophic and hypereutrophic Central Florida lakes. The lower phosphorus concentrations in Lake Jesup may suggest that phosphorus in upper portions of the sediment layer may be continuously stripped and recycled from the sediments into the overlying water column, perhaps aided by wind activity, resulting in a relatively low sediment accumulation rate for phosphorus. In addition, the sediments are highly anoxic, as evidenced by the strong hydrogen sulfide smell even in surficial sediment layers, which creates conditions unsuitable for long-term phosphorus retention. The overall total nitrogen concentration in Lake Jesup sediments of $904 \mu\text{g}/\text{cm}^3$ is also slightly lower than the mean value of $1,109 \mu\text{g}/\text{cm}^3$ measured by ERD in other Florida lakes. The slightly lower nitrogen concentration in Lake Jesup sediments may also be related to the anoxic conditions which, combined with the abundance of organic matter, likely supports a significant population of denitrifying bacteria.

4.6 Sediment Phosphorus Speciation

As discussed in Section 3.2, each of the 49 collected sediment samples was fractionated to identify phosphorus bonding mechanisms within the sediments. A summary of sediment phosphorus speciation in Lake Jesup sediments is given in Table 4-7. Soloid-bound phosphorus, reflecting soluble plus easily exchangeable associations, was highly variable in Lake Jesup sediments, ranging from 2.4 - $43.2 \mu\text{g}/\text{cm}^3$ with an overall geometric mean of $15.2 \mu\text{g}/\text{cm}^3$. This value is somewhat greater than commonly observed by ERD in other Central Florida lake sediments.

Concentrations of iron-bound phosphorus in the sediments of Lake Jesup were also highly variable, ranging from 2.7 - $24.4 \mu\text{g}/\text{cm}^3$ with an overall geometric mean of $12.7 \mu\text{g}/\text{cm}^3$. This value is substantially lower than iron-bound phosphorus concentrations commonly observed in other lakes and is likely related to the continuous anoxic conditions within the sediments which limits the ability for iron-phosphorus bonds to form. Overall, the sediments in Lake Jesup contain an average of $29.8 \mu\text{g}/\text{cm}^3$ of available sediment phosphorus.

Measured concentrations of aluminum-bound phosphorus in Lake Jesup sediments range from 4.9 - $62.3 \mu\text{g}/\text{cm}^3$ with an overall geometric mean of $23.4 \mu\text{g}/\text{cm}^3$. Based on an average total phosphorus concentration of $126 \mu\text{g}/\text{cm}^3$, approximately 20% of the sediment phosphorus is bound with aluminum in an unavailable form.

Measured concentrations of NAIP are provided in the final column of Table 4-7 for comparison purposes. NAIP concentrations are highly variable, ranging from 1.8 - $84.3 \mu\text{g}/\text{cm}^3$, with an overall geometric mean of $39.6 \mu\text{g}/\text{cm}^3$. The NAIP fraction appears to over-estimate the total available phosphorus measurement by approximately 33% since it combines multiple bonding mechanisms together.

TABLE 4-6
SEDIMENT CHARACTERISTICS OF CENTRAL
FLORIDA LAKES MONITORED BY ERD

LAKE	DATE COLLECTED	PARAMETER										TROPIC STATUS
		pH (s.u.)	Moisture Content (%)	Organic Content (%)	Wet Density (g/cm ³)	Total N (µg/cm ³)	Total P (µg/cm ³)	Saloid-Bound P (µg/cm ³)	Iron-Bound P (µg/cm ³)	Total Available P (µg/cm ³)	Percent of Sediment P Available (%)	
Asher	9/15/10	5.67	93.6	66.8	1.03	2,874	140	1.2	11	12	9	Hypereutrophic
Cub	11/9/10	6.13	47.7	3.2	1.69	2,022	70	0.1	12	13	19	Mesotrophic
Little Bear	11/9/10	6.21	40.6	1.8	1.85	2,568	66	0.2	9	10	15	Mesotrophic
Bear	12/17/10	6.59	34.7	2.2	1.87	871	115	0.2	10	11	10	Oligotrophic
Booker	7/21/05	6.48	77	25	1.26	527	400	10	59	69	17	Eutrophic
Belair	12/15/11	5.81	47.3	4.2	1.68	668	90	0.2	39	39	43	Eutrophic
Deforest	12/15/11	5.99	70.4	15.8	1.32	329	63	0.7	18	19	30	Mesotrophic
East Crystal	12/15/11	5.97	42.5	3.9	1.77	681	104	0.7	38	39	38	Eutrophic
Amory	12/15/11	5.90	46.3	6.9	1.64	763	86	1.1	36	38	44	Eutrophic
Jesup	7/11/12	6.10	41.9	2.8	1.76	5,043	1,871	0.8	47	51	3	Mesotrophic
Jessamine	12/10/11	6.41	51.2	33.8	1.57	1,653	125	0.4	45	46	37	Mesotrophic
Anderson	1/20/11	6.17	48.8	5.2	1.57	5,390	3,477	3	172	178	8	Eutrophic
Holden	10/8/03	6.59	36.3	2.1	1.81	755	335	9.6	155	167	50	Eutrophic
Killarney	3/24/11	6.39	40.5	3.1	1.74	4,470	923	4	64	72	8	Mesotrophic
Lawne	8/22/11	6.50	44.7	5.0	1.63	5,228	1,365	6	47	56	7	Eutrophic
Pineloch	3/29/06	6.98	92.1	50.4	2.41	5,692	1,198	45	201	216	34	Mesotrophic
Howell	10/16/08	6.7	48.3	10.7	1.75	596	273	14.3	15	29	15	Eutrophic
Bear Gully	10/16/08	6.42	61.5	16.8	1.54	1,320	119	1.1	11	12	11	Eut./Hyp.
Middle Triplet	2/27/13	6.21	68.9	24.1	1.27	1,400	170	2.3	52	56	33	Eutrophic
North Triplet	2/27/13	6.26	55.6	10.4	1.44	904	121	2.6	54	57	48	Mesotrophic
South Triplet	3/3/12	6.10	84.8	52.6	1.16	1,304	132	4.4	38	42	31	Eut./Hyp.
Queens Mirror	3/3/12	5.88	87.8	57.5	1.12	1,126	123	4.0	42	46	37	Eut./Hyp.
Silver	3/28/12	6.49	48.3	6.8	1.58	463	1,164	1.4	50	52	5	Eut./Hyp.
Thonotosassa	4/2/07	7.03	34.2	1.4	1.80	565	226	-	-	-	-	Hypereutrophic
Virginia	2/8/08	6.62	47.4	4.0	1.64	944	220	0.8	13	15	7	Mesotrophic
Minimum Value:		5.67	34.2	1.4	1.03	329	63	0.1	9	10	3	
Maximum Value:		7.03	93.6	66.8	2.41	5,692	3,477	45	201	216	50	
Geometric Mean (Eut./Hyp.):		6.25	55.2	10.2	1.48	1109	260	2.4	40	45	19	

TABLE 4-7

SPECIATION OF SEDIMENT PHOSPHORUS BONDING IN LAKE JESUP SEDIMENTS

SITE	DATE COLLECTED	SEDIMENT P CONC. ($\mu\text{g}/\text{cm}^3$ wet)			Al-Bound P ($\mu\text{g}/\text{cm}^3$ wet)	Total P ($\mu\text{g}/\text{cm}^3$ wet)	Percent Sediment P Available (%)	NAIP ($\mu\text{g}/\text{cm}^3$ wet)
		Saloid-Bound P	Fe-Bound P	Total Available P				
LJ-1	8/4/14	10.3	10.5	20.8	19.1	119	17.4	39.8
LJ-2	8/4/14	26.2	13.4	39.6	25.9	108	36.8	53.3
LJ-3	8/4/14	25.6	12.5	38.1	30.4	133	28.6	47.5
LJ-4	8/5/14	28.2	11.9	40.0	16.4	105	38.1	38.2
LJ-5	8/5/14	29.6	12.9	42.4	25.1	84	50.2	42.3
LJ-6	8/4/14	11.3	9.4	20.7	19.8	73	28.3	61.9
LJ-7	8/4/14	15.8	10.1	26.0	20.1	113	22.9	47.0
LJ-8	8/5/14	8.9	14.1	22.9	31.2	97	23.6	50.2
LJ-9	8/5/14	7.4	20.6	28.0	57.8	242	11.6	84.3
LJ-10	8/5/14	5.4	11.5	16.9	30.4	129	13.1	35.9
LJ-11	8/5/14	15.5	17.1	32.6	25.7	103	31.6	40.4
LJ-12	8/4/14	7.9	12.5	20.4	20.4	92	22.2	50.9
LJ-13	8/4/14	25.4	14.8	40.2	36.7	216	18.6	69.3
LJ-14	8/4/14	7.8	10.5	18.3	17.1	90	20.3	12.3
LJ-15	8/5/14	16.0	12.7	28.7	22.3	63	45.8	38.3
LJ-16	8/5/14	9.8	13.6	23.4	24.8	82	28.4	53.1
LJ-17	8/5/14	2.8	10.0	12.8	4.9	311	4.1	13.8
LJ-18	8/5/14	7.8	17.5	25.3	47.9	306	8.3	51.1
LJ-19	8/5/14	24.7	14.9	39.6	30.6	97	41.0	49.1
LJ-20	8/5/14	29.6	14.6	44.2	62.3	156	28.3	48.3
LJ-21	8/4/14	17.0	11.3	28.3	14.6	92	30.7	53.9
LJ-22	8/4/14	15.1	12.1	27.2	25.5	187	14.5	27.8
LJ-23	8/4/14	26.6	13.0	39.6	32.4	135	29.4	51.4
LJ-24	8/6/14	25.2	2.7	28.0	25.2	82	34.2	57.1
LJ-25	8/6/14	5.4	11.8	17.2	6.4	347	5.0	28.3
LJ-26	8/6/14	8.2	24.4	32.6	33.3	82	39.7	46.2
LJ-27	8/6/14	14.1	6.4	20.5	28.2	135	15.2	40.6
LJ-28	8/6/14	13.4	17.4	30.9	17.1	317	9.7	31.0
LJ-29	8/5/14	17.2	11.9	29.1	24.8	74	39.3	40.9
LJ-30	8/5/14	24.0	11.2	35.2	23.5	136	25.9	40.1
LJ-31	8/6/14	28.1	16.8	44.9	39.5	147	30.5	42.7
LJ-32	8/6/14	17.7	16.3	34.0	45.6	114	29.9	50.7
LJ-33	8/6/14	22.5	13.9	36.4	25.3	103	35.2	46.6
LJ-34	8/6/14	2.4	7.3	9.7	6.1	279	3.5	1.8
LJ-35	8/6/14	28.1	16.1	44.2	25.3	104	42.3	41.8
LJ-36	8/5/14	22.2	11.6	33.8	25.2	83	40.7	55.6
LJ-37	8/5/14	29.3	11.5	40.8	28.1	94	43.3	51.1
LJ-38	8/5/14	17.3	9.2	26.5	16.5	61	43.3	51.7
LJ-39	8/6/14	19.3	12.7	32.0	23.8	89	35.9	47.9
LJ-40	8/6/14	26.7	16.7	43.4	25.1	147	29.6	44.1
LJ-41	8/6/14	2.6	21.3	23.9	6.3	223	10.7	5.8
LJ-42	8/5/14	26.6	15.0	41.7	25.7	263	15.9	53.1
LJ-43	8/5/14	21.3	22.7	44.0	60.0	152	28.8	27.8
LJ-44	8/5/14	24.3	12.7	37.0	19.2	101	36.5	50.2
LJ-45	8/5/14	25.0	14.9	39.9	24.9	250	16.0	49.7
LJ-46	8/5/14	20.6	14.6	35.2	22.7	113	31.1	65.1
LJ-A	8/4/14	43.2	13.9	57.1	30.8	153	37.4	49.8
LJ-B	8/4/14	19.0	9.1	28.1	18.5	55	50.8	44.9
LJ-C	8/4/14	10.1	10.4	20.6	19.5	114	18.1	53.2
Minimum Value:		2.4	2.7	9.7	4.9	55.3	3.5	1.8
Maximum Value:		43.2	24.4	57.1	62.3	347	50.8	84.3
Geometric Mean:		15.2	12.7	29.8	23.4	126	23.6	39.6

4.7 Isotope Analyses

A tabular summary of isotope analyses conducted on Lake Jesup sediments is given on Table 4-8. The results of the isotope analyses will be discussed in a separate report prepared by the Colorado Isotope Laboratory.

5. SEDIMENT INACTIVATION COST ANALYSIS

A supplemental analysis was conducted to prepare a cost estimate for sediment inactivation in Lake Jesup to provide information for comparison of potential lake restoration projects. This analysis is based upon the speciation of phosphorus bonding in Lake Jesup sediments, summarized in Table 4-7. Since seepage flux also migrates through the sediments, the analysis includes both phosphorus loadings from sediments and from groundwater seepage entering Lake Jesup.

5.1 Introduction

Sediment phosphorus inactivation is a lake restoration technique which is designed to reduce sediment phosphorus release by combining available phosphorus in the sediments with a metal salt to form an insoluble inert precipitate, rendering the sediment phosphorus unavailable for release into the overlying water column. Although salts of aluminum, calcium, and iron have been used for sediment inactivation in previous projects, aluminum salts are the clear compounds of choice for this application. Inactivation of sediment phosphorus using aluminum is often a substantially less expensive option for reducing sediment phosphorus release since removal of the existing sediments is not required.

Sediment phosphorus inactivation is most often performed using aluminum sulfate, commonly called alum, which is applied at the surface in a liquid form using a boat or barge. Upon entering the water column, the alum forms an insoluble precipitate of aluminum hydroxide which attracts phosphorus, bacteria, algae, and suspended solids within the water column, settling these constituents into the bottom sediments. Upon reaching the bottom sediments, the residual aluminum binds tightly with phosphorus within the sediments, forming an inert precipitate which will not be re-released under any conceivable condition of pH or redox potential which could occur in a natural lake system. These sediment treatments have been shown to be effective from 5-20 years, depending upon the sediment accumulation rate within the lake from the remaining phosphorus sources.

5.2 Chemical Requirements

Sediment inactivation in Lake Jesup would involve addition of liquid aluminum sulfate at the water surface using an application boat. Upon entering the sediments, the alum will combine with existing phosphorus within the sediments, primarily saloid- and iron-bound associations, forming insoluble inert precipitates which will bind the phosphorus, making it unavailable for release into the overlying water column. It is generally recognized that the top 10 cm layer of the sediments is the most active in terms of release of phosphorus under both aerobic and anoxic conditions. Therefore, the objective of a sediment inactivation project is to provide sufficient alum to bind the saloid- and iron-bound phosphorus associations in the top 10 cm of the sediments.

TABLE 4-8

**RESULTS OF SEDIMENT ISOTOPE ANALYSES
CONDUCTED ON LAKE JESUP SEDIMENTS**

SAMPLE I.D.	SITE	DATE ANALYZED	POSITION	MASS (mg)	CO ₂ Ampl (volts)	N ₂ Ampl (volts)	CO ₂ Area (V/s)	N ₂ Area (V/s)	δ ¹³ C (‰)	δ ¹⁵ N (‰)
S14-273	LJ-1	25-Aug-14	95	19.884	5.69	3.63	142.42	53.94	-17.86	2.08
S14-274	LJ-2	25-Aug-14	6	9.999	4.34	3.67	96.51	56.16	-22.68	1.06
S14-265	LJ-3	25-Aug-14	96	10.391	3.92	3.09	87.01	48.61	-22.46	1.97
S14-305	LJ-4	25-Aug-14	28	20.080	5.19	4.70	122.45	70.26	-21.95	2.08
S14-306	LJ-5	25-Aug-14	12	9.996	4.29	3.03	94.90	46.33	-21.46	1.38
S14-266	LJ-6	25-Aug-14	10	10.091	3.80	3.09	81.83	47.82	-23.04	0.61
S14-270	LJ-7	25-Aug-14	5	9.986	4.08	3.37	89.70	51.50	-21.74	1.34
S14-303	LJ-8	25-Aug-14	11	10.047	2.55	1.84	52.60	29.74	-22.92	1.12
S14-304	LJ-9	25-Aug-14	27	19.955	3.77	1.97	81.79	30.85	-17.84	3.15
S14-307	LJ-10	25-Aug-14	29	19.972	2.75	1.58	57.44	25.10	-23.28	3.56
S14-310	LJ-11	25-Aug-14	30	20.047	2.95	2.32	62.29	36.86	-18.11	2.70
S14-275	LJ-12	25-Aug-14	7	10.051	3.67	3.13	78.72	48.38	-23.14	0.13
S14-267	LJ-13	25-Aug-14	98	10.515	3.30	2.60	70.37	41.58	-22.87	1.58
S14-271	LJ-14	25-Aug-14	21	20.025	2.70	1.98	56.32	31.25	-22.78	1.43
S14-301	LJ-15	25-Aug-14	99	9.989	3.78	3.31	82.40	51.75	-22.61	1.16
S14-302	LJ-16	25-Aug-14	103	9.952	3.73	3.08	81.16	48.42	-22.12	1.82
S14-308	LJ-17	25-Aug-14	53	69.824	0.83	0.77	17.81	13.79	-21.25	1.57
S14-309	LJ-18	25-Aug-14	41	29.977	3.28	1.88	69.78	29.57	-26.58	1.55
S14-311	LJ-19	25-Aug-14	31	20.059	3.58	2.75	76.98	42.77	-19.76	1.89
S14-312	LJ-20	25-Aug-14	110	10.619	3.48	2.73	74.61	43.35	-20.12	1.88
S14-278	LJ-21	25-Aug-14	9	10.119	4.22	2.71	92.87	41.49	-24.12	1.44
S14-276	LJ-22	25-Aug-14	8	10.044	2.86	1.71	59.82	27.40	-24.42	0.68
S14-269	LJ-23	25-Aug-14	104	10.570	3.19	2.50	67.57	40.02	-21.98	2.01
S14-336	LJ-24	25-Aug-14	101	10.108	3.81	3.28	83.51	51.37	-22.06	1.75
S14-337	LJ-25	25-Aug-14	54	69.982	1.16	0.48	24.55	8.62	-12.11	1.38
S14-338	LJ-26	25-Aug-14	48	30.089	4.62	1.72	104.73	26.94	-16.42	2.56
S14-339	LJ-27	25-Aug-14	16	9.957	2.78	2.50	57.64	39.90	-21.27	0.40
S14-340	LJ-28	25-Aug-14	94	10.377	2.98	0.91	64.30	14.91	-7.81	4.37
S14-313	LJ-29	25-Aug-14	14	10.315	3.60	2.90	76.56	45.10	-21.13	1.19
S14-314	LJ-30	25-Aug-14	106	10.409	3.94	2.95	86.46	45.80	-18.41	1.75
S14-348	LJ-31	25-Aug-14	18	9.998	2.52	1.78	52.23	28.78	-20.72	1.93
S14-347	LJ-32	25-Aug-14	58	70.012	7.59	4.70	217.45	67.49	-11.73	2.50
S14-346	LJ-33	25-Aug-14	39	19.983	3.16	2.52	67.18	39.49	-21.59	2.45
S14-342	LJ-34	25-Aug-14	56	70.009	1.64	1.23	33.85	20.98	-19.78	1.59
S14-341	LJ-35	25-Aug-14	100	10.445	3.31	2.94	70.60	46.78	-20.35	1.58
S14-322	LJ-36	25-Aug-14	34	19.953	4.01	3.75	88.18	57.68	-22.04	2.02
S14-315	LJ-37	25-Aug-14	109	10.599	2.94	1.99	61.64	32.11	-18.95	2.15
S14-316	LJ-38	25-Aug-14	108	9.993	3.64	2.40	78.55	37.88	-19.16	2.25
S14-345	LJ-39	25-Aug-14	38	19.922	3.95	3.28	86.44	50.49	-21.45	2.32
S14-344	LJ-40	25-Aug-14	17	9.954	2.29	1.74	47.05	28.20	-21.53	1.28
S14-343	LJ-41	25-Aug-14	57	69.968	0.68	0.58	13.68	10.31	-22.85	2.62
S14-321	LJ-42	25-Aug-14	33	20.025	5.54	4.81	134.01	71.81	-20.34	2.33
S14-317	LJ-43	25-Aug-14	46	30.054	4.94	3.49	113.94	52.82	-18.37	1.70
S14-318	LJ-44	25-Aug-14	107	9.972	3.09	2.13	65.17	34.12	-18.54	1.94
S14-319	LJ-45	25-Aug-14	15	10.044	3.63	3.02	77.64	47.12	-21.32	1.73
S14-320	LJ-46	25-Aug-14	32	19.967	5.38	5.02	128.69	75.12	-20.26	2.35
S14-277	LJ-A	25-Aug-14	102	10.471	4.58	4.12	104.89	62.76	-22.55	1.92
S14-272	LJ-B	25-Aug-14	97	9.849	4.09	3.58	91.43	55.57	-22.29	1.39
S14-268	LJ-C	25-Aug-14	4	10.080	3.43	2.91	73.04	45.11	-23.32	0.26
Minimum Value:					0.68	0.48	13.68	8.62	-26.58	0.13
Maximum Value:					7.59	5.02	217.45	75.12	-7.81	4.37

Isopleths of saloid-bound phosphorus concentrations in the top 10 cm of Lake Jesup sediments were generated using the measured sediment speciation data summarized in Table 4-7. An isopleth map of saloid-bound phosphorus concentrations in Lake Jesup sediments is given on Figure 5-1. In general, areas of highest saloid-bound phosphorus concentrations appear to correspond roughly with areas of the largest muck accumulations. In general, saloid-bound phosphorus concentrations in Lake Jesup are approximately 10 times greater than saloid-bound phosphorus typically measured by ERD in urban lakes.

An isopleth map of iron-bound concentrations in the top 10 cm of Lake Jesup sediments is given in Figure 5-2. Areas of iron-bound phosphorus also correspond roughly with areas of highest sediment accumulations within the lake. In contrast to the substantially elevated concentrations of saloid-bound phosphorus, iron-bound phosphorus concentrations in Lake Jesup sediments are substantially lower in value than commonly observed by ERD in urban lakes.

Total available phosphorus is defined as the sum of saloid-bound and iron-bound phosphorus associations in lake sediments. Isopleths of total available phosphorus in the top 10 cm of Lake Jesup sediments are illustrated on Figure 5-3. Total available phosphorus isopleths range from approximately 20-55 $\mu\text{g}/\text{cm}^3$ throughout the lake. The top 0-10 cm layer of the sediments is considered to be the most active layer with respect to exchange of phosphorus between the sediments and the overlying water column. Inactivation of phosphorus within the 0-10 cm layer is typically sufficient to substantially eliminate sediment release of phosphorus within a lake. Prior research involving sediment inactivation has indicated that an excess of aluminum is required within the sediments to cause phosphorus to preferentially bind with aluminum rather than other available competing agents. Previous sediment inactivation projects performed by ERD have been conducted at molar Al:P ratios of 2, 3, 5, and 10, with most recent sediment inactivation projects performed using a 10:1 ratio which has been demonstrated to reduce available sediment phosphorus by 80-90%.

A summary of estimated total available phosphorus in the sediments of Lake Jesup is given in Table 5-1. On a mass basis, the sediments of Lake Jesup contain approximately 106,126 kg of available phosphorus in the top 10 cm. On a molar basis, this equates to approximately 3,423,415 moles of available phosphorus to be inactivated. A summary of alum requirements for sediment inactivation is also provided in Table 5-1. Using an Al:P ratio of 10:1, sediment inactivation in the Lake Jesup would require approximately 4,168,616 gallons of alum, equivalent to approximately 926 tankers. The equivalent aerial aluminum dose for this application would be 28.3 g Al/m² based on an assumed lake area of 8,068 acres.

Previous alum surface applications performed for inactivation of sediment phosphorus release by ERD have indicated that the greatest degree of improvement in surface water characteristics and the highest degree of inactivation of sediment phosphorus release are achieved when the total recommended alum addition occurs through multiple applications of aluminum to the waterbody spaced at intervals of approximately 3-6 months. Using multiple applications also reduces the applied water column alum dose and can eliminate the need for additional chemicals (such as sodium aluminate) to buffer the water column which can substantially enhance the treatment cost. Each subsequent application results in additional improvements in water column quality and additional aluminum floc added to the sediments for long-term inactivation of sediment phosphorus release.

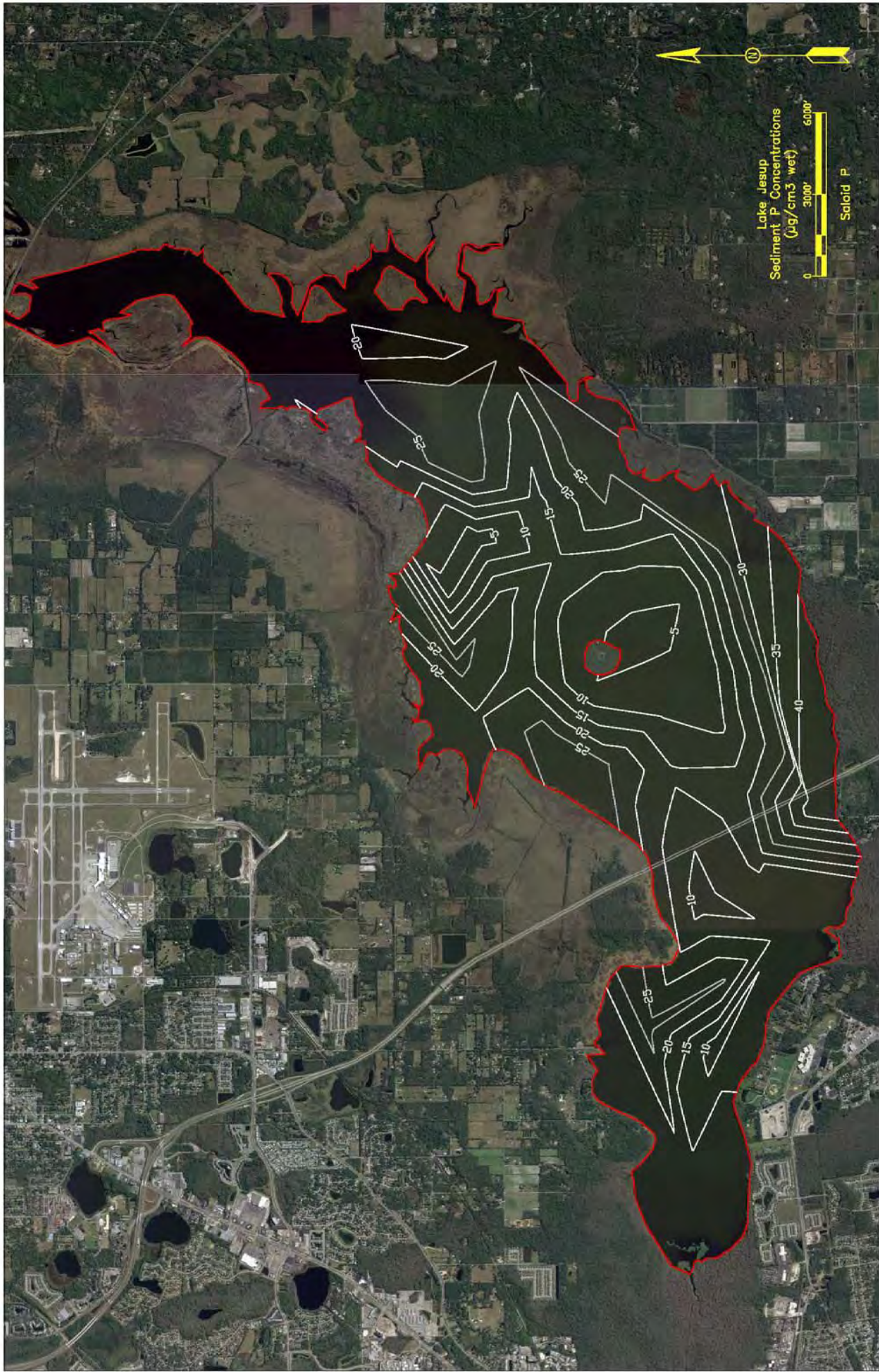


Figure 5-1. Isopleths of Saloid-Bound Phosphorus in the Top 10 cm of Lake Jesup Sediments.

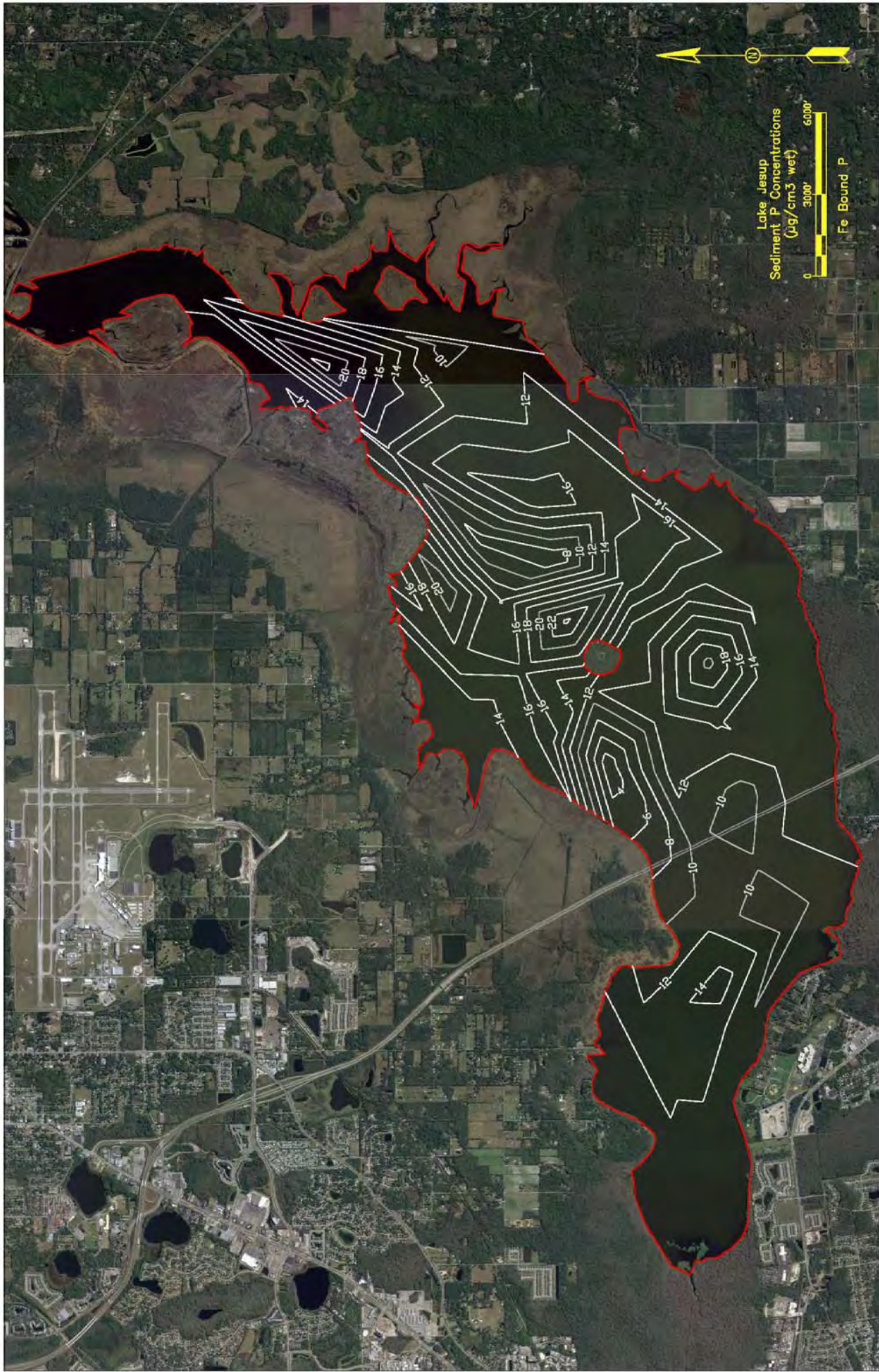


Figure 5-2. Isopleths of Iron-Bound Phosphorus in the Top 10 cm of Lake Jesup Sediments.

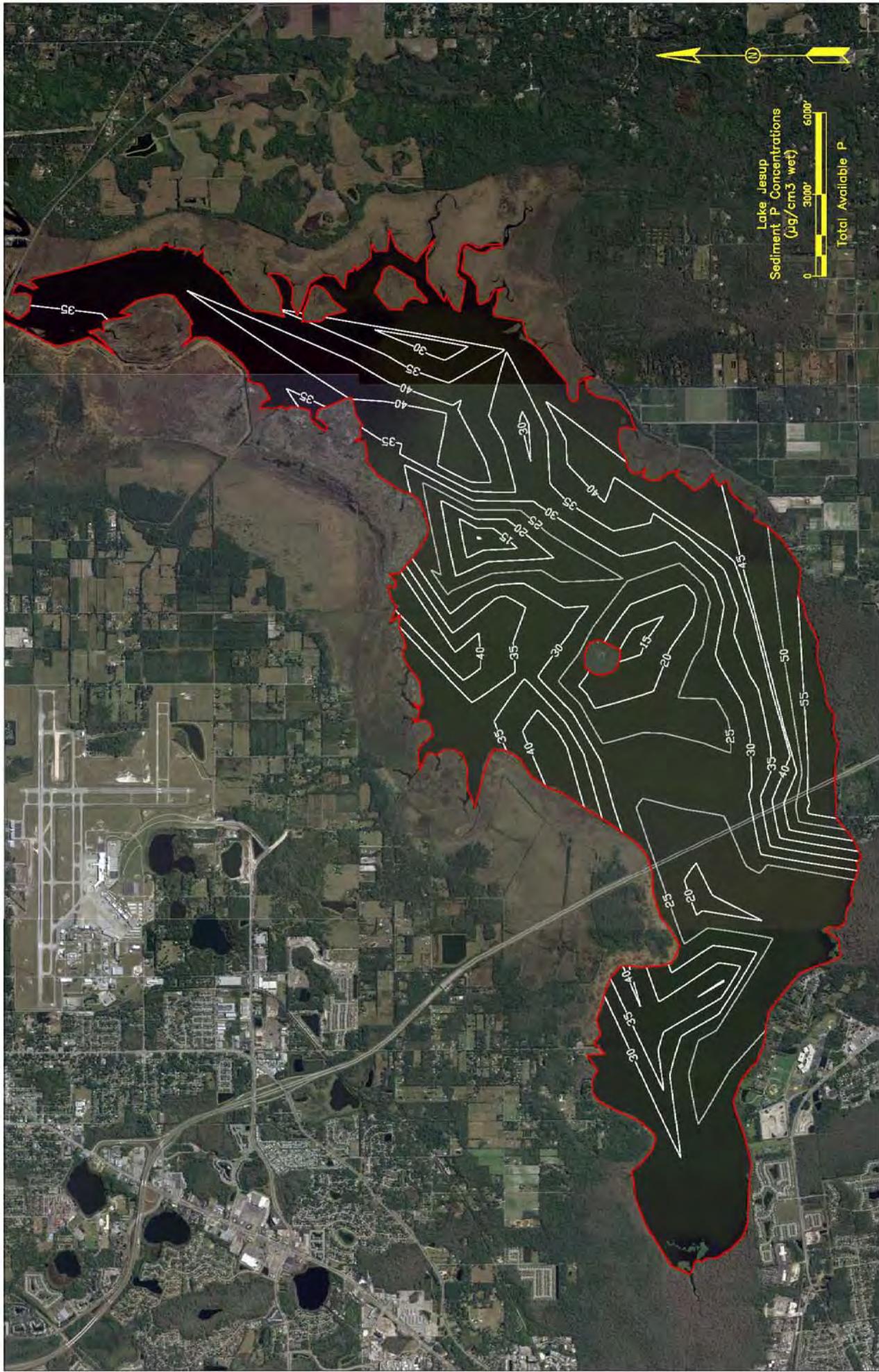


Figure 5-3. Isopleths of Total Available Phosphorus in the Top 10 cm of Lake Jesup Sediments.

TABLE 5-1

**SUMMARY OF SEDIMENT AVAILABLE PHOSPHORUS
AND INACTIVATION REQUIREMENTS FOR LAKE JESUP**

AVAILABLE P CONTOUR INTERVAL ($\mu\text{g}/\text{cm}^3$)	CONTOUR INTERVAL MID-POINT ($\mu\text{g}/\text{cm}^3$)	CONTOUR AREA (acres)	AVAILABLE PHOSPHORUS		ALUM REQUIREMENTS (Al:P Ratio = 10:1)	
			kg	moles	moles Al	gallons alum
< 10	7.5	0.10	0	10	102	12
10-15	12.5	55.8	282	9,112	91,116	11,095
15-20	17.5	317	2,247	72,472	724,719	88,247
20-25	22.5	1,267	11,540	372,273	3,722,733	453,309
25-30	27.5	1,707	19,005	613,074	6,130,740	746,526
30-35	32.5	1,410	18,548	598,320	5,983,200	728,561
35-40	37.5	2,098	31,860	1,027,755	10,277,549	1,251,474
40-45	42.5	704	12,107	390,547	3,905,471	475,560
45-50	47.5	181	3,480	112,245	1,122,449	136,678
50-55	52.5	180	3,834	123,679	1,236,787	150,601
> 55	57.5	138	3,222	103,929	1,039,286	126,552
Overall Totals:		8,058	106,126	3,423,415	34,234,153	4,168,616

Additional aluminum can also be added to the sediments to create an active absorption mechanism for phosphorus inputs into the water column as a result of groundwater seepage. An evaluation of hydrologic and nutrient loadings from groundwater seepage to Lake Jesup was conducted by ERD from 2009-2010. Groundwater seepage meters were installed at 40 locations within Lake Jesup, and 9 separate monitoring events were conducted over a 14-month field monitoring program. Groundwater seepage entering Lake Jesup was characterized by elevated levels of total phosphorus, with an estimated annual phosphorus influx of 9,484 kg/yr from groundwater seepage. A carefully planned application of alum can provide an abundance of aluminum which can intercept groundwater inputs of phosphorus over a period of many years. As a result, alum applications can be used to eliminate phosphorus from the combined inputs resulting from internal recycling as well as groundwater seepage.

A summary of calculations of alum requirements for control of phosphorus loading from groundwater seepage is given in Table 5-2. This analysis is based upon the measured phosphorus seepage loadings to Lake Jesup of 9,484 kg/yr and assumes a control period of 10 years. Over the 10-year control period, approximately 94,840 kg of phosphorus will enter Lake Jesup through groundwater seepage. This is equivalent to approximately 3,059,355 moles of phosphorus to be inactivated.

TABLE 5-2
ALUM REQUIREMENTS FOR SEEPAGE
CONTROL IN LAKE JESUP

	PARAMETER	UNITS	VALUE
Estimated Phosphorus Mass to be Controlled	Seepage Phosphorus Loading	g/m ² -yr	0.234
	Annual Phosphorus Loading from Seepage	kg/yr	9,484
	Desired Length of Control	years	10
	Total Phosphorus Mass to be Inactivated	kg	94,840
	Moles of Phosphorus to be Inactivated	moles	3,059,355
Alum Requirements	Inactivation Al:P Ratio	--	10:1
	Moles of Aluminum Required	moles	30,593,548
	Alum Required	gallons	3,725,307
	Number of Tankers @ 4,500 gallons	--	828
	Mean Water Column Dose	mg Al/liter	20.8

Assuming an inactivation Al:P ratio of 10:1, inactivation of 3,059,355 moles of phosphorus will require 30,593,548 moles of aluminum which is equivalent to approximately 3,725,307 gallons of alum. This volume of alum is equivalent to approximately 828 tankers containing 4,500 gallons each, with an overall mean water column dose of 20.8 mg Al/liter.

In addition to the estimated alum requirements for sediment inactivation and seepage control, additional alum will also be consumed for removal of total phosphorus within the water column of the lake during each proposed alum application. However, the amount of alum required for removal of water column phosphorus is typically minimal in comparison with the volume of alum added for sediment inactivation and seepage control. A summary of alum requirements for removal of water column phosphorus concentrations in Lake Jesup is given in Table 5-3. This analysis assumes a mean water column volume of approximately 32,231 ac-ft and a mean water column total phosphorus concentration of 100 µg/l. The corresponding water column total phosphorus mass is 3,975 kg or 128,224 moles of total phosphorus. For removal of water column phosphorus, an Al:P ratio of 1:1 is assumed. The required alum for removal of water column total phosphorus is approximately 15,613 gallons per application. This value is insignificant in comparison with the alum requirements for sediment inactivation and seepage control. It is assumed that this volume of alum would be required for water column phosphorus removal during each of the proposed applications, even though water column concentrations will likely be reduced from the assumed value of 100 µg/l as the application process progresses.

TABLE 5-3
ALUM REQUIREMENTS FOR WATER COLUMN
TOTAL PHOSPHORUS REMOVAL

PARAMETER		UNITS	VALUE
Estimated Phosphorus Mass in Water Column	Water Column Volume	ac-ft	32,231
	Mean Total Phosphorus Concentration	µg/l	100
	Water Column Total Phosphorus Mass	kg moles	3,975 128,224
Alum Requirements	Applied Al:P Ratio	--	1:1
	Moles of Aluminum Required	moles	128,224
	Alum Required	gallons	15,613
	Number of Tankers @ 4,500 gallons	--	3.5

A summary of chemical requirements for sediment inactivation and seepage control in Lake Jesup is given in Table 5-4. The combined quantity of alum required to inactivate sediment phosphorus release and intercept seepage phosphorus loadings is 7,893,923 gallons of alum, equivalent to 1,754 tankers. The water column dose, if the entire alum volume were to be applied during a single application, would be 44 mg Al/liter, equivalent to an areal dose of 53.7 g Al/m².

TABLE 5-4
CHEMICAL REQUIREMENTS FOR SEDIMENT
INACTIVATION AND SEEPAGE CONTROL IN LAKE JESUP

PARAMETER		UNITS	VALUE
Alum Quantity	Inactivation + Seepage	gallons	7,893,923
	Number of Tankers	--	1,754
	Water Column Dose	mg Al/liter	44.0
	Areal Dose	g Al/m ²	53.7
Chemical Requirements per Treatment	Number of Treatments	--	6
	Alum Required per Treatment ¹	gallons	1,331,267
	Dose per Treatment	mg Al/liter	7.3
	Number of Tankers @ 4,500 gallons	--	296

1. Includes an additional 15,613 gallons for removal of water column total phosphorus

The calculated whole water column dose of 44.0 mg Al/liter far exceeds the buffering capacity within Lake Jesup, and multiple applications will be required to avoid undesirable pH impacts or the use of supplemental buffering compounds. A minimum of six separate applications is recommended for Lake Jesup, with one-sixth of the total aluminum mass added during each treatment. If the overall recommended application were to be divided into six individual applications, the overall mean water column dose would be approximately 7.3 mg Al/liter which could likely be tolerated without significant pH impact. The alum volume added during each application would be 1,315,654 gallons, equivalent to 292 tankers. Each application would cover the entire lake area, with the alum volume of 1,315,654 gallons applied on a weighted basis according to the available phosphorus isopleth map given on Figure 5-3.

5.3 Cost Analysis

A summary of estimated costs for sediment inactivation and seepage control in Lake Jesup is given in Table 5-5, based upon the information and assumptions provided in Table 5-4. Application costs are calculated assuming that six separate applications will be conducted, with approximately 1,331,267 gallons added during each application. Planning and mobilization costs are assumed at \$25,000 per application, and alum costs are based upon a unit contract price of \$0.55/gallon. Costs are also included for field monitoring and laboratory analyses.

TABLE 5-5
ESTIMATED COSTS FOR SEDIMENT INACTIVATION
AND SEEPAGE CONTROL IN LAKE JESUP

PARAMETER		QUANTITY/ TREATMENT	UNITS	UNIT COST (\$)	COST/ TREATMENT	TOTAL COST (\$)
Chemical Costs	Alum	1,331,267	gallons	0.55	732,197	4,393,182
Labor Costs	Planning and Mobilization	1	each	25,000	25,000	150,000
	Chemical Application	296	tankers	1,000	296,000	1,776,000
Monitoring and Lab Testing	Field Monitoring	1	each	500	500	3,000
	Lab Analyses (Pre-/Post-)	16	samples	200	3,200	19,200
TOTAL:					\$ 1,056,897	\$ 6,341,382

The overall estimated cost for each of the six applications is \$1,056,897 or \$6,341,382 for the total project cost. However, since the applications would be spaced approximately six months apart, the overall project cost would be spread out over multiple fiscal years. A summary of calculated phosphorus removal costs for sediment inactivation and seepage control in Lake Jesup is given in Table 5-6 based upon a 10-year cost cycle. The alum addition is expected to reduce loadings from internal recycling and seepage inflow by approximately 80% each, resulting in an overall phosphorus load reduction of approximately 160,772 kg over the 10-year period of analysis. Based upon the estimated overall project cost of \$6,341,382, the calculated phosphorus removal costs are \$39/kg or approximately \$18/pound.

TABLE 5-6
PHOSPHORUS REMOVAL COSTS FOR SEDIMENT
INACTIVATION AND SEEPAGE CONTROL IN LAKE JESUP

PARAMETER		UNITS	VALUE
Existing Total Phosphorus Loadings	Internal Recycling	kg	106,126
	Seepage Inflow	kg	94,840
	Total:	kg/yr	200,966
Removal by Alum Treatment	Internal Recycling	%	80
		kg	84,900
	Seepage Inflow	%	80
		kg	75,872
	Total:	kg	160,772
Alum Treatment Cost	Internal Recycling + Seepage	\$	6,340,405
Total Phosphorus Removal Cost		\$/kg	39
		lb/kg	18

5.4 Longevity of Treatment

After initial application, the alum precipitate will form a visible floc layer on the surface of the sediments within the lake. This floc layer will continue to consolidate for approximately 30-90 days, reaching maximum consolidation during that time. Due to the unconsolidated nature of the sediments in much of the lake, it is anticipated that a large portion of the floc will rapidly migrate into the existing sediments rather than accumulate on the surface as a distinct layer. This process is beneficial since it allows the floc to sorb soluble phosphorus during migration through the surficial sediments. Any floc remaining on the surface will provide a chemical barrier for adsorption of phosphorus which may be released from the sediments.

More than 30 sediment inactivation projects have been conducted in the State of Florida on a wide variety of waterbody sizes, depths, and water quality characteristics. Each of these treatments has resulted in substantial improvements in water quality characteristics. The observed improvements in water quality have lasted from a minimum of 10 years to more than 20 years.

The evaluated alum application to Lake Jesup would be an extremely large project. ERD is not aware of any previous projects which have been conducted on a lake of this size and shallow water depth. Although there are no conceivable reasons why the proposed sediment inactivation would not be effective, it may be prudent to conduct a pilot project on a portion of the lake, perhaps in areas west of the S.R. 417 bridge, to evaluate the success and impacts of an alum treatment prior to implementation of a whole-lake treatment.

APPENDIX A

**PHOTOGRAPHS OF SEDIMENT
CORE SAMPLES COLLECTED
IN LAKE JESUP**

Lake Jesup – Site LJ - 1



Lake Jesup – Site LJ - 2



Lake Jesup – Site LJ - 3



Lake Jesup – Site LJ - 4



Lake Jesup – Site LJ - 5



Lake Jesup – Site LJ - 6



Lake Jesup – Site LJ - 7



Lake Jesup – Site LJ - 8



Lake Jesup – Site LJ - 9



Lake Jesup – Site LJ - 10



Lake Jesup – Site LJ – 11



Lake Jesup – Site LJ – 12



Lake Jesup – Site LJ - 13



Lake Jesup – Site LJ - 14



Lake Jesup – Site LJ - 15



Lake Jesup – Site LJ - 16



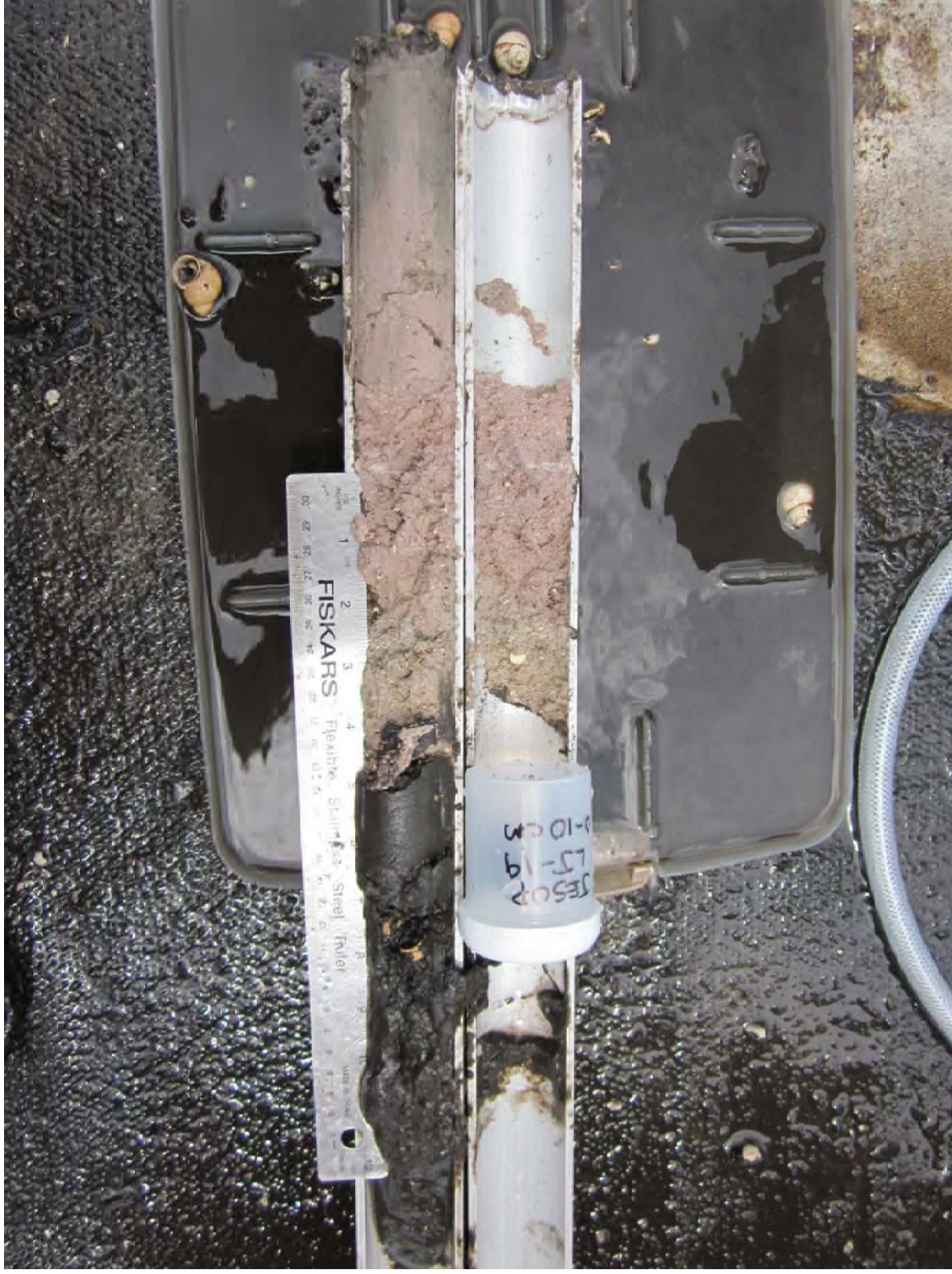
Lake Jesup – Site LJ - 17



Lake Jesup – Site LJ - 18



Lake Jesup – Site LJ - 19



Lake Jesup – Site LJ - 20



Lake Jesup – Site LJ – 21



Lake Jesup – Site LJ – 22



Lake Jesup – Site LJ - 23



Lake Jesup – Site LJ - 24



Lake Jesup – Site LJ - 25



Lake Jesup – Site LJ – 26
(Bottle labeled incorrectly – changed during lab log-in)



Lake Jesup – Site LJ - 27



Lake Jesup – Site LJ - 28



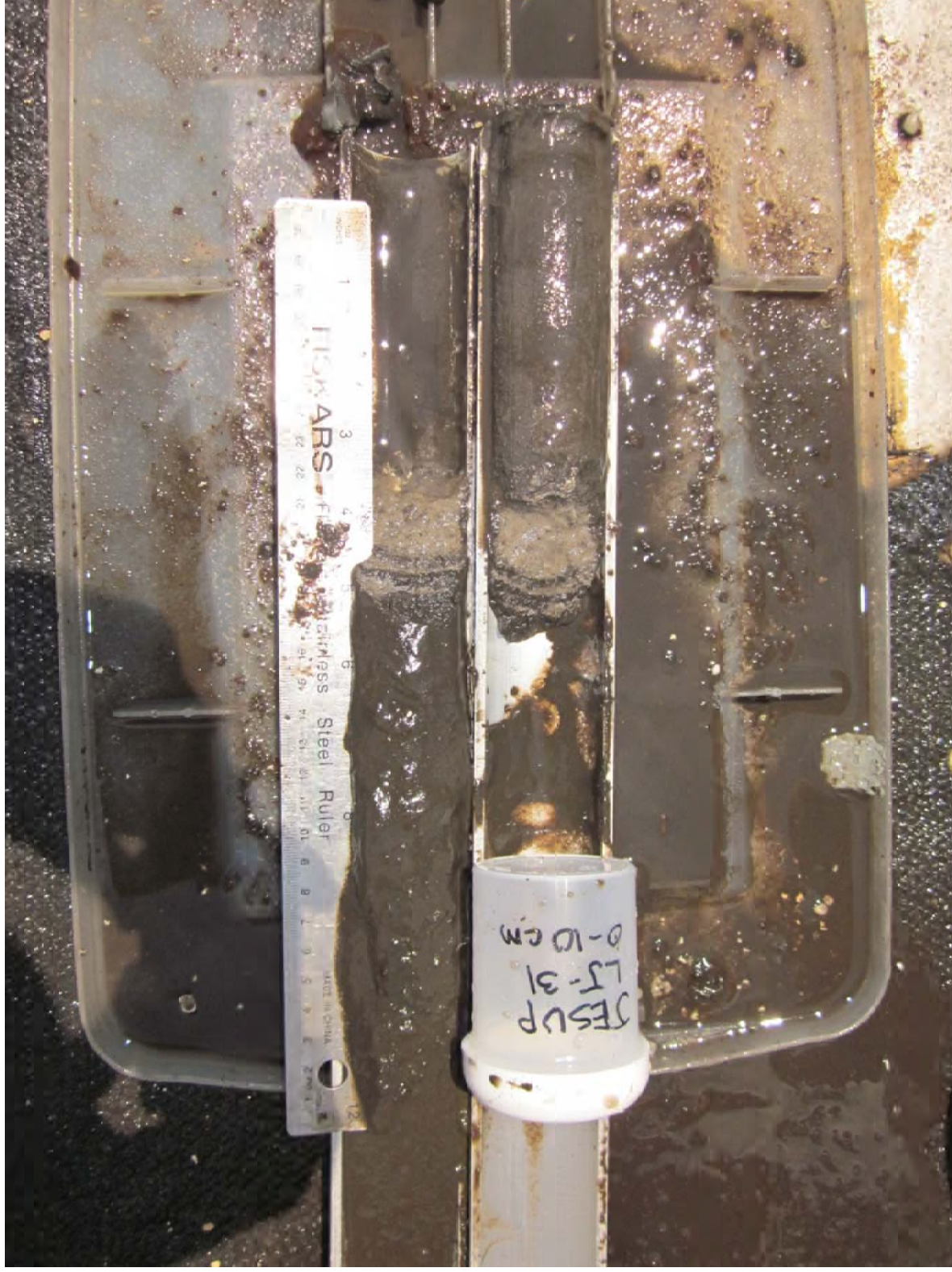
Lake Jesup – Site LJ - 29



Lake Jesup – Site LJ - 30



Lake Jesup – Site LJ - 31



Lake Jesup – Site LJ - 32



Lake Jesup – Site LJ - 33



Lake Jesup – Site LJ - 34



Lake Jesup – Site LJ - 35



Lake Jesup – Site LJ - 36



Lake Jesup – Site LJ - 37



Lake Jesup – Site LJ - 38



Lake Jesup – Site LJ - 39



Lake Jesup – Site LJ - 40



Lake Jesup – Site LJ - 41



Lake Jesup – Site LJ - 42



Lake Jesup – Site LJ - 43



Lake Jesup – Site LJ - 44



Lake Jesup – Site LJ - 45



Lake Jesup – Site LJ - 46



Lake Jesup – Site LJ - A



Lake Jesup – Site LJ - B



Lake Jesup – Site LJ - C

